Digital Data Transmission Over Mobile Radio Channels

by

SAID ATIYA MUHSON
B.Sc., M.Sc.

A Doctoral Thesis

Submitted in partial fulfilment of the

requirements for the award of

Doctor of Philosophy

of the Loughborough University of Technology

February 1987

Supervisors: Dr S. C. BATEMAN
Dr S. D. SMITH

Department of Electronic and Electrical Engineering

To every mother who has lost a son in the Gulf War and to my Mother.

****

CONTENTS

page

ACKNOWLEDGEMENTS

I would like to express my deep gratitude to my supervisors Dr S Bateman and Dr S Smith for their continuous help and advice. Also, I am grateful to Professor A P Clark, the Director of Research for his mosts helpful comments.

I am indebted to the IRAQI GOVERNMENT for granting me the opportunity to carry out this work on a scholarship.

My thanks are also due to Mrs J Brown for typing this thesis and to the Computer Centre staff for their help.

I wish to express my thanks to my parents who suffered too much during my stay in the United Kingdom. Also, I wish to thank my brothers, sisters and friends for their continued support and encouragement.

I cannot thank enough my wife Eiman who has contributed more than most wives; not forgetting my gorgeous daughters Heba and Rusha.

I will never forget the suffering and bravery of the Iraqi soldiers who solidly defend Iraq.

ABSTRACT

The aim of this work is to study data transmission over a microwave digital mobile radio channel at 900 MHz, where the channel is subjected to multipath fading. Besides the fading, the other impairments assumed here are additive noise, co-channel interference and adjacent channel interference. Two modulation techniques are investigated in this work, namely Quadrature-Amplitude-Modulation (QAM) and Quadrature-Phase-Shift-Keying (QPSK). The channel is characterised digitally, assuming multi-path Rayleigh fading in the presence of noise. The detection process studied here are near-maximum likelihood schemes: non-linear equalisation methods are also considered in detail.

The thesis is also concerned with carrier synchronisation and channel estimation under conditions of Rayleigh fading. Since the carrier synchronisation is a most important requirement in mobile radio, a Digital Phase Locked Loop (DPLL) technique has been designed and investigated in the form of a feedback digital synchronisation system. Two types of channel estimation technique, namely feedforward and feedback estimators, are also investigated in this work. The feedback estimator is modified by the addition of a digital control system, in order to reduce its delay, and to cope with rapidly fading signals. Successful carrier synchronisation is demonstrated by the use of space diversity.

The study was completed using models of the component parts of the system, and by the use of extensive computer simulations to analyse the system under various operating conditions.

Important Symbols

These symbols are followed throughout this work unless otherwise stated in the appropriate position

$a(t)$	signal envelope
a_i	real part of a transmitted data symbol s_i
a_i'	detected form of a_i
b_i	imaginary part of s_i
b_i'	detected form of b_i
c_i	sample form of a reference carrier signal, $c(t)$, or a complex-valued correction signal
f_c	carrier frequency
f_o	central frequency of a bandpass filter
f_D	Doppler frequency
$e(t)$	error signal whose z-transform is $E(z)$
$h(t)$	filter impulse response
H_o	the row vector of the nonfading channel impulse response $\{h_\ell\}$
i	time index such that $s_i = s(iT)$
j	$= \sqrt{-1}$
$p(t)$	transmitted signal
P	power reference
$q(t)$	complex-valued Rayleigh fading factor
Q_i	LxL-component diagonal matrix derived from the sampled form of $q(t)$
$r(t)$	the received signal
r_i	the complex-valued sample of $r(t)$ at the output of the demodulator

s_i	the data symbol $s_i = a_i + jb_i$
s'_i	detected data of symbol s_i, $s'_i = a'_i + jb'_i$
t	time
T	duration of a signal element
n(t)	white Gaussian noise
u(t), v(t), w(t)	complex-valued Gaussian noise components
u_i, v_i, w_i	samples form of u(t), v(t), w(t) at t = iT
σ^2	Gaussian noise variance
y(t)	impulse response of the fading channel
Y_i	the row vector of the fading channel impulse response $\{y_{i,\ell}\}$
Y'_i	estimate of Y_i
$\|x_i\|$	absolute value (modulus) of x_i
$\|U_i\|^2$	cost of stored vectors
	Space-diversity symbols
$r_{i,d}$	received signals over two different paths, where d = 1,2
$w_{i,d}$	additive Gaussian noise to each signal received
$Y_{i,d}$	row vectors of the fading channels impulse response
$c_{i,d}$	complex-valued correction signals
BER	Bit Error Rate
SNR	Signal-to-Noise Ratio

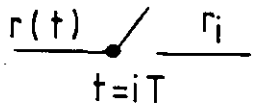

sampler

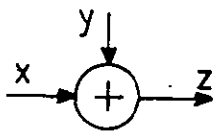

$z = x + y$ adder

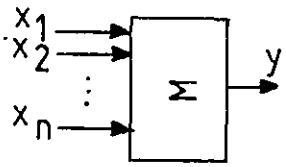

$y = \sum_{i=1}^{n} x_i$ multi-adder

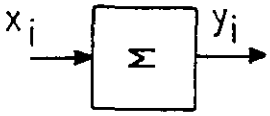

$y_i = y_{i-1} + x_i$ integrator

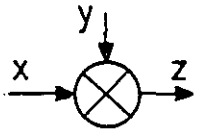

$z = x\,y$ multiplier

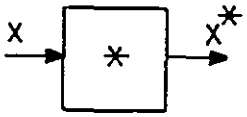

complex conjugate operator

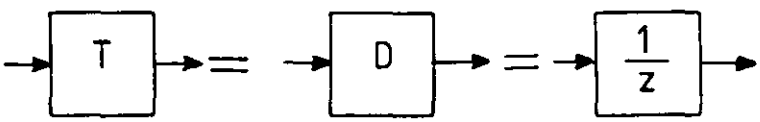

Delay elements

1. INTRODUCTION

This thesis investigates the data transmission of digital data over mobile radio channels, between a base station and a mobile. The work covers the theory and practice of communications applied to modulation, detection and synchronisation methods. Each of the individual parts of the communication system is studied theoretically, followed by comparator simulation tests on suitable models. The systems derived are tested in the presence of idealised noise and distortion. Consequently, the system that has a better simulated performance than any other tested is most likely to be superior in practice.

1.1 Scope of the Work

Conventional modulation techniques, concerning amplitude modulation (AM) and phase modulation (PM), are briefly discussed and compared together with their corresponding demodulation techniques. Multilevel schemes are also considered such as quadrature amplitude modulation (QAM) and multilevel phase-shift-keyed (PSK). Other methods, introduced elsewhere[1-17] are beyond the scope of this study. Conventional differential coding is described for the application in computer simulation studies (see Chapter 2).

Mobile radio channel characterisation in the microwave band of 900 MHz is introduced in Chapter 3. The channel representations are based on the linear modulation and linear demodulation applied to multilevel PSK and QAM signals. The impulse response of the channel is first derived under nonfading conditions. Complex notation has been used since it is much easier to manipulate than the equivalent trigonometric expressions[10,16]. The results obtained here are consistent with those derived in the literature[5,18-21]. After the definition of the multipath phenomena and propagation losses in mobile radio communication, the impulse response of the fading channel is derived. A Rayleigh fading simulator is used as a representative of a multipath fading [10,11,72-99].

A time-invariant channel is discussed and represented by an equivalent lowpass filter under the assumption of a nonfaded signal. By assuming a data rate of 9600 symbols/second, the impulse response of this filter is obtained by using Fourier design methods[102-106,109] as applied to an ideal lowpass filter transfer function with a bandwidth of 4800 Hz satisfying Nyquist sampling theorem, which results in a partial response channel[1,3]. Then, the fading channel is determined when a faded signal is assumed.

The effect of interference from unwanted signals such as co-channel and adjacent-channel interferers, that are occupying the same band and adjacent band respectively, are treated as noise at the receiver[9-11,19 43,112-130]. However, white Gaussian noise is added to the signal at the end of the transmission path.

Spectrum utilisation is very important in cellular mobile radio, hence it is necessary to transmit signal elements at a rate not significantly below the Nyquist rate for the given channel so that the best available tolerance to additive white Gaussian noise can be achieved. Under this condition there is always intersymbol interference[1,3,5,109] in the demodulated and sampled data signal at the receiver. In fact, the intersymbol interference can be reduced by using a wider bandwidth, but this leads to a wasteful spectrum, besides, more noise will pass to the detector. However, cancellation of the intersymbol interference can be accomplished by a technique called channel equalisation[1-5,109, 147-150]. Since the transfer function of a linear equaliser is equal to the inverse of the channel transfer function[1,109,147], only a nonlinear equaliser is used. (The transfer functions of the linear equalisers would tend to infinity, when the channel is subjected to a deep fade, which is most likely in the mobile radio environment.) The nonlinear equaliser can be protected against divergence in such circumstances, in the way described in Chapter 4, with the use of direct cancellation of the intersymbol interference. The nonlinear channel equaliser is conventionally implemented as a linear feedforward transversal filter fed from the output of a nonlinear threshold level detector[109,147]; for this reason it is called nonlinear.

However, a better tolerance to additive noise can be achieved through the application of a maximum likelihood detector instead of the nonlinear equaliser and the corresponding threshold level detector[109,137-147,152]. Unfortunately, the maximum likelihood detector is very complicated and

requires an extremely large number of operations and excessively large storage, even with less severe intersymbol interference[137-142,152,165]. Alternatively, a simpler but somewhat less effective detector, known as near-maximum likelihood detector[147,151-165], can be used.

Since the mobile radio channel is rapidly varying with the time and has a Rayleigh distribution function (see Chapter 3), the synchronisation equipment (data aided digital phase-locked loop, Chapter 5, and channel estimators, Chapter 6) will be much affected by the delay required by the near-maximum likelihood detectors. Hence, it is necessary to use a less dispersive channel and consequently less delay is required. Even so, the performance of a near-maximum likelihood detector will deteriorate under high fading rate conditions (see Chapter 8).

The performance of different multilevel signals in a mobile radio environment is studied in Chapter 4. The study includes 16-level QAM, 8-level PSK, 4-level QAM and QPSK signals (Chapter 2) applied to nonlinear equaliser and near-maximum likelihood detector. The investigation of the detection processes have been performed under the assumptions of coherent demodulation and correct channel estimation.

Coherent demodulation requires the successful regeneration of a reference carrier with a phase and frequency closely matching that of the data carrying signal at the input of the receiver. Unfortunately, it is difficult to simulate a modulated radio frequency signal as a software program unless its frequency is reduced, since the higher frequency signals require longer

execution time by the computer. An example is introduced in Chapter 5, where a binary PSK signal is used. Two carrier recovery systems (CRS1 and CRS2) are investigated with the use of squaring/filtering/frequency dividing by 2 techniques[2,5,12,199]. These two systems fail under fading conditions unless they are used with space diversity (see Chapters 5 and 8).

However, carrier synchronisation is successfully carried out in the base-band region by the use of a digital phase locked loop, DPLL. The DPLL was designed by using some of the rules employed in designing the feedback digital control system[166-170] that are briefly presented in Appendix H. This method offers an opportunity to use any digital filter as a loop filter, while the available DPLL techniques in the literature are restricted to only one filter[171-184,198,199]. The designed DPLL has been tested in the form of first, second and third order systems with application of Butterworth and Chebyshev digital filters. The DPLL design depends on careful selection and implementation of a phase detector, PD, that plays an important part of the entire system. Two types of PD, namely hard limiter/discriminator and tanlock are used and their characteristics are demonstrated (Chapter 5).

The DPLL is tested under nonfading and Rayleigh fading conditions for an unmodulated carrier. Then the work is modified to be used with a suppressed-carrier QPSK (or QAM) signal, in the form of a data aided digital phase locked loop (DA-DPLL). The latter is tested under different fading rates with the use of tanlock-PD only (Chapter 5). The DA-DPLL can cope with a Rayleigh faded signal, but it degrades when erroneous sequences are received. A further disadvantage of DA-DPLL is its weakness caused by the delay when

it is used with a near-maximum likelihood detection scheme under Rayleigh fading conditions.

As mentioned earlier, the sampled impulse response of the channel was assumed to be correctly estimated. Such an assumption is not precisely true, especially in a mobile radio environment. Hence it is necessary, at the receiver, to obtain an estimate of the sampled impulse response of the channel in order to achieve correct detection of the received signal. Two estimators, namely a feedforward channel estimator (FFCE) and a modified feedback channel estimator (MFBCE), are studied in Chapter 6.

The feedback channel estimator (FBCE) techniques available in the literature (203,205,Appendix J) requires a delay. It will be found that the delay degrades the performance of the estimator under Rayleigh fading conditions. The FBCE is modified mathematically in Appendix J in order to eliminate the effect of delay. Moreover, the modified FBCE is further developed, by inserting a digital feedback control system discussed in Appendix H, for use with digital phase-locked loop, to give MFBCE (modified feedback channel estimator).

As mentioned above, the FBCE's available in the literature degrade by the delay, while the FFCE degrades by the existance of the intersymbol interference error signal which is defined in Appendix J. However, these degenerations are eliminated in the MFBCE and better performance is to be expected. Furthermore, the complexity of the MFBCE is identical to the complexity of FFCE without the insertion of the digital control system in MFBCE.

The MFBCE uses the same transversal feedforward filter that can be used in the nonlinear channel equaliser. Hence, it is possible in practice to add only a threshold level detector and to make a collectively adaptive nonlinear channel equalisation and detection scheme[1,5,109,147-150].

Both estimators (FFCE and MFBCE) use the already detected data symbols. But, when the near-maximum likelihood detection scheme is employed, it requires a delay to reach a decision and at the same time, requires to be supplied by the estimated sequence of the sampled impulse response of the channel. The least-square fading-memory prediction method is used since it is a potentially better prediction method[204,206].

(The deep fade occurrence is rare[10,11,117] and of short duration.) However, when it does occur, it will ruin all the built-up synchronisation. Throughout this interval, errors are more likely to occur. Since the chance of having two deep fades from two uncorrelated signals is unusual, then the effect of the fade can be reduced by the application of diversity [9-12,113, 117,123-130,134-136]. Diversity is the technique used to develop the transmitted information from several signals received independently over different fading paths. The objective of a diversity scheme is to combine the multiple signals in order to combat the Rayleigh fading effects. As a result, the diversity scheme can minimize the effect of fading since deep fades rarely occur simultaneously during the same time interval on two or more paths.

Since spectrum utilisation is very important in cellular mobile radio, space diversity is recommended in such an environment[10-12,117,123-130,134-136]

Moreover, a space diversity is achievable in the range of frequencies assumed throughout this work of around 900 MHz, since $\frac{\lambda}{2}$ = 16 cm. Space diversity is introduced in Chapter 7 with use of a combiner identical to the equal-gain combiner[10,11]. Simple tests are carried out in Chapter 7 to show the variations of the signals level before and after combining.

The receiver designed in Chapter 7 has been tested in Chapter 8 to determine its tolerance to additive white Gaussian noise under Rayleigh fading conditions. Only the QPSK signal with differential coding is used. This receiver consists of two sets of demodulators, a two branch combiner and a detector. The two received signals are first demodulated to baseband by the first set of demodulators without removing the frequency offsets or the phase shifts caused by the corresponding paths. Also, the first set of demodulators use the same reference signal whose frequency is equal to the transmitted signal carrier frequency. However, the second set of demodulators, whose functions are to remove any frequency offset and phase shift from the corresponding signals, use two independent correction signals generated by two DA-DPLL's. At the outputs of the second set of demodulators, the signals are now co-phased and can be combined in the way described in Chapter 7. The two signals are combined by simple addition and the resultant signal is fed to a detector which may use a nonlinear equaliser or a near-maximum likelihood scheme. The second set of demodulators and the adder represent the action of equal-gain combiner. The MFBCE is associated with the detector.

The two carrier recovery systems (CRS1 and CRS2) mentioned earlier are employed in receivers with the use of space diversity and the performances of the receivers are also investigated in Chapter 8. Finally, from this investigation, it is found that differential coding and space diversity are essential elements of a digital cellular mobile radio communications system.

2. MODULATION TECHNIQUES

2.1 Introduction

The modulation methods that have been applied in mobile radio systems throughout this work are introduced here. Two conventional modulation techniques are briefly discussed and compared together with their corresponding demodulation techniques. These methods are amplitude modulation (AM) and phase modulation (PM). Multilevel schemes are also considered such as quadrature amplitude modulation (QAM) and quadrature phase-shift-keyed (QPSK). Other methods introduced elsewhere[1-13] are beyond the scope of this study. The ideal channel, which is distortionless channel (with no phase and/or amplitude distortion), is mentioned here for convenience. Of course such a channel does not exist practically, but provides a useful reference for modelling and simulation studies. Because of possible phase ambiguities existing in the recovered carrier[2,5,12] a differential coding (encoding/decoding) scheme is employed in computer simulation studies.

2.2 Modulation and Demodulation Techniques

A continuous wave (CW) sinusoidal signal can be varied by changing its amplitude or phase angle due to specific information that is required to be transmitted over a channel. The general form of a modulated carrier can be represented as

$$m(t) = a(t)\cos(\omega_c t + \phi(t)) \qquad 2.1$$

where $a(t)$ and $\phi(t)$ are the amplitude and phase angle of the modulated

carrier respectively and $\omega_c = 2\pi f_c$, where f_c is the carrier frequency. If $\phi(t)$ is maintained at a constant value and $a(t)$ is made proportional to the information signal $\alpha(t)$, then amplitude modulation (AM) results. Alternatively, the concept of angle modulation is introduced when $a(t)$ is kept constant and $\phi(t)$ is varied in proportion to $\alpha(t)$. This kind of modulation, however, can be described in terms of phase modulation (PM) and frequency modulation (FM). When the instantaneous frequency of $\phi(t)$ (instantaneous frequency = $\frac{1}{2\pi}\frac{d\phi(t)}{dt}$) is linearly related to $\alpha(t)$, then this type of modulation is called FM. PM refers to the change (deviation) of the phase angle $\phi(t)$ according to the information signal, $\alpha(t)$, when the overall carrier frequency is kept constant[1-10].

The modulated signal is now a sine-wave carrier that carries the transmitted data in terms of the amplitude, or phase of this sine wave. If this signal is multiplied by a sine-wave reference carrier having the same frequency, f_c, and phase (relative to the unmodulated carrier) and the resultant is passed thorough a lowpass filter, which removes all high frequency components except in the region of interest without affecting the wanted frequency components, then the transmitted information can be extracted. This is a process of linear demodulation. The linear demodulation of FM modulated carrier requires two coherent detectors of the type described above for AM and PM signals. The reference carrier is frequently regenerated from the received signal.

Since the spectrum utilization is of most importance in cellular mobile radio systems, but the FM systems require wider bandwidth[1-12] therefore they will not be considered throughout this study.

2.3 Binary Modulated Signal

The information that is to be transmitted can be represented by a binary rectangular form[1-11], in which one level represents the binary digit 0 and the other represents the binary digit 1. The duration of each digit element is kept constant at T seconds.

An AM system transmits the digit 0 by the absence of the carrier signal and the digit 1 by the presence of the carrier signal, for the case of ON-OFF Amplitude Shift Keying (ASK). Therefore, Equation 2.1 in this case becomes

$$m(t) = A \cos(\omega_c t) \qquad 2.2$$

where A is either 0 or 1 over an interval T seconds long and $\omega_c = 2\pi f_c$ is the radian frequency of the carrier. The spectrum of an ASK signal depends effectively on the binary rate being transmitted and the carrier frequency f_c Hz. By applying the frequency shift theorem of Fourier transform[2-5, Appendix A], then Equation 2.2 transformed to[1,4]

$$M(f) = \frac{A}{2} \left[F(\omega-\omega_c) + F(\omega+\omega_c) \right] \qquad 2.3$$

where M(f) is the Fourier transform of m(t) and $F(\omega)$ is the Fourier transform of the modulated signal[see Appendix A]. This is the general form of an AM signal[1,3,8,10]. It contains lower and upper sideband symmetrically distributed about the center frequency (carrier frequency). In fact, the transmission bandwidth of the AM signal is twice the baseband signal bandwidth[3].

In the PM signal, the phase of the transmitted signal is interchanged between 0° and 180° (or between 0 and π rad.) in concurrence with the information to be transmitted, while the carrier frequency is kept constant. This type of modulation is called phase-shift-keyed (PSK). Accordingly, for a constant envelope (i.e. a(t) = 1) Equation 2.1 becomes

$$m(t) = \cos(\omega_c t + k_i \pi) \qquad 2.4$$

where k_i is possibly 1 or 0 over an interval of T seconds long, and the suffix i is a time index, such that t = iT. It is also possible to make k_i vary in this form according to a polar NRZ (non-return to zero) signal, when $k_i = (1 + V_i)/2$, where V_i is equally likely to be ± 1. In either case, $m(t) = \pm\cos(\omega_c t)$, which is the same as Equation 2.2 when $A = \pm 1$. The spectrum of the binary PSK signal is the same as that for ASK signal, and hence has a double sideband characteristic (Equation 2.3) and twice the baseband bandwidth, 2B, where B is the baseband bandwidth as shown in Figure 2.1. Therefore, PSK can be considered as a suppressed carrier AM signal[1,3,9]. Yet, both PSK and ASK can successfully be used with sinusoidal roll-off, satisfying Nyquist's vestigial-symmetry theorem, shaping pulses so that it is possible to transmit data at 2B elements per second without intersymbol interference[1,3]. The sinusoidal roll-off shaping is used either by shaping the baseband pulses or by shaping the high-frequency passband pulses. The spectrum of the modulated signal looks like the baseband spectrum shifted up to the carrier frequency, f_c Hz, in the frequency domain and with transmission bandwidth of 2B Hz as shown in Figure 2.2.

The exact frequency and phase of the recieved signal carrier must be known at the receiver for coherent demodulation. Accordingly, the receiver generates from the received signal a reference carrier having the same frequency and phase as the received signal carrier[1-15, see also Chapter 5], for both ASK and PSK. The received signal is multiplied by the reference carrier and the resultant of the product is integrated over each element period, to give at the end of this period a linear estimate of the corresponding modulating waveform, as shown in Figure 2.3. By ignoring the effect of noise, then for the purpose of this discussion only, the received signal can be expressed as

$$r(t) = a'(t) \cos(\omega_c t + k_i \pi + \theta(t)) \qquad 2.5$$

where $\theta(t)$ is assumed to cover all the variation of the received signal phase and/or frequency throughout the whole channel and $a'(t)$ is the envelope of the received signal. Moreover, the receiver bandpass filter has been assumed wide enough to pass the received signal without any distortion or loss. Therefore, the recovered carrier, for use in the demodulation process, can practically be given by

$$c(t) = \cos(\omega_c t + \theta(t)) \qquad 2.6$$

Then, the multiplication of the received signal, $r(t)$ by the recovered carrier signal, $c(t)$ followed by an integrator (or lowpass filter) and threshold level detector, the transmitted information can be detected. Of course the integrator is reset to zero at the start of each element period.

2.4 QAM and QPSK Systems

In the previous section, a binary modulated signal has been discussed on the assumption of an ideal (distortionless) channel. However, if it is required to increase the transmission (information) rate over the same bandwidth (according to Nyquist channel model with no intersymbol-interference), and consequently to increase the bandwidth efficiency, then a multilevel signal must be employed [1-21]. The most general types of multilevel signals are QAM (quadrature amplitude modulation) and QPSK (quadrature phase shift keyed).

The model of a QAM system is shown in Figure 2.4. The binary sequence is Gray coded, in order to reduce the bit error rate, and mapped in such a way to generate the two statistically independent elements a_i and b_i [1,3,10], where i refers to the sampling time index. Appendix C shows how the binary sequence is converted to Gray code and vice versa. The possible value of any a_i and b_i are $\pm 1, \pm 3, \ldots, \pm(L-1)$ where L can have a value of 2, 4, 8, ... to give 4,16, ..., (2^L) points in the QAM system respectively. Table 2.1 and 2.2 show relation between the possible values of a_i and b_i and the corresponding Gray coded binary sequence for 4 and 16 points systems respectively. The a_i is used to modulate the inphase component of the carrier, while b_i modulates the quadrature component. Consequently, the transmitted signal can be given in complex form as

$$p(t) = \sum_i s_i \, h(t-iT) e^{j\omega_c t} \qquad 2.7$$

where $s_i = a_i + jb_i$, h(t) is the Nyquist shaping filter impulse response, $\omega_c = 2\pi f_c$: f_c is the carrier frequency and $j = \sqrt{-1}$. The word "symbol" is used hereafter as reference to s_i. T(in seconds) is the duration of the transmitted symbol. h(t) is the complex-valued filter with a bandwidth of B Hz. Hence according to Nyquist rate the transmission rate is 2B symbols/seconds.

Coherent demodulation is very important in the QAM system[1-11,18,19], as shown in Figure 2.4. Therefore, it is necessary to regenerate the received signal carrier precisely with the correct frequency and phase. Further detection processes will be discussed in Chapter 4.

In a QPSK system, the modulated carrier can take on more than two possible phases. The state of each phase is generated by a unique mapping scheme of consecutive bits that will be called symbols, hereafter. Gray Coded symbols are implied here, as in the QAM signal, in which the adjacent symbols differ by only one bit. Figure 2.5 shows the possible arrangements for the 4 and 8 phases. The duration of each symbol is T sec., where $T = 2T_b$ or $T = 3T_b$ in 4 or 8 phase systems respectively, and T_b is the bit duration (in sec.). Hence, the data (bit) rate that can be transmitted on 4 phase or 8 phase systems is twice or three times the symbol rate respectively, with the same Nyquist bandwidth. However, the relationship between the data rate and symbol rate, for a given Nyquist bandwidth in both QAM and QPSK systems is given by

$$\text{data rate} = \text{symbol rate} \times \log_2(K)$$
$$= 2B \times \log_2(K) \qquad 2.8$$

where K is the possible number of phases in the PSK system (also K is the possible number of points in the QAM system), and B is the baseband bandwidth. The model of QPSK is similar to that of QAM, which is shown in Figure 2.4. The modulated signal can be given, in a complex form, by (2-7,12-14,16)

$$P(t) = \sum_i A\, h(t - iT)\, e^{j(\omega_c t + \phi_i)} \qquad 2.9$$

where A is the constant envelope, and

$$\phi_i = \frac{2\pi k_i}{K} + \lambda_o \qquad 2.10$$

where λ_o is a constant having the value of either 0 or $\frac{\pi}{K}$ and k_i is equally likely to have any of the K possible values that are given by

$$k_i = 0, 1, 2, \ldots, (K-1) \qquad 2.11$$

h(t) is the Nyquist shaping filter impulse response and $\omega_c = 2\pi f_c$: f_c is the carrier frequency. According to the tolerance of the additive white Gaussian noise rules, A is given by[5]

$$A = 1/\sin(\pi/K) \qquad 2.12$$

Therefore $A = \sqrt{2} = 1.414$ for 4 phases system and A = 2.613 for 8 phases system. By comparing Equation 2.9 with Equation 2.7 then the value of the symbol vector is given by

$$\begin{aligned} s_i &= Ae^{j\phi_i} \\ &= A\cos(\phi_i) + jA\sin(\phi_i) \\ &= a_i + jb_i \end{aligned} \qquad 2.13$$

where $j = \sqrt{-1}$. If $\lambda_o = \frac{\pi}{4}$, in 4 phases system, then s_i can have any of the four possible values of $\mp 1 \mp j$. This is exactly the 4-point QAM representation.

As a consequence of the pre-modulation filters, there is a ripple in the envelope of the bandlimited QPSK due to the phase transition, which may lead to zero envelope at the time of transition. So as to maintain a part of the envelope, offset QPSK can be employed. The difference between the conventional QPSK and offset QPSK lies in the data transition between a_i and b_i as they enter the modulators. b_i is offset with respect to a_i by delaying it by an amount equal to half the incoming signal symbol duration, $\frac{T}{2}$ ($\frac{T}{2} = T_b$ in 4-phases and $\frac{T}{2} = 1.5\ T_b$ in 8-phases system), and consequently b_i becomes $b_{i-\frac{1}{2}}$. The variation of the filtered offset QPSK envelope is 3 dB only. After demodulation, however, the demodulated replica of a_i must be delayed by the same amount (T/2) in order to regenerate the transmitted information at the receiver.

The modulated signal at the output of the modulator is normally filtered to limit the radiated spectrum, amplified and then transmitted over the transmission channel (channel characterisation will be discussed in Chapter 3). Since the transmitted signal is in the orthogonal form [2,3,22,24] then the receiver is able to demodulate the signal and separate its components (the replica of a_i and b_i).

2.5 Differential Encoding/Decoding

As mentioned above for coherent demodulation, it is necessary to synchronise the recovered carrier in phase and frequency with respect to the received modulated signal (Equations 2.5 and 2.6). Practically, most of the carrier recovery systems introduce a phase ambiguity into the recovered carrier[2,5,12].

In a binary PSK system, the carrier is recovered by squaring the received modulated signal (taking the second harmonic) and then dividing the frequency by two[2,5,12, Appendix I]. Accordingly, the recovered carrier may be given by

$$c(t) = \cos(\omega_c t + \theta(t) \mp d\pi) \qquad 2.14$$

where d is equally likely to be either 0 or 1. When d = 0 this is exactly Equation 2.6, while when d = 1 the probability of the error is high in the received information. In order to avoid the possibility of high error rate and consequently the phase ambiguity, a simple differential encoder and differential decoder are inserted in the transmitter and receiver, respectively. Figure 2.6 illustrates the possible differential encoding/decoding processes. The output of the differential encoder is given by

$$d_i = \overline{b_i \oplus d_{i-1}} = b_i\, d_{i-1} + \bar{b}_i\, \bar{d}_{i-1} \qquad 2.15$$

where $\oplus$ represents the exlusive-OR operation and $\bar{x}$ is the complement

of x (the complement is the replacement logic 1 by 0 or 0 by 1). Hence, for differentially encoded signal k_i in Equation 2.4 is given by

$$k_i = m_i + k_{i-1} \text{ [MODULO-2]} \qquad 2.16$$

where m_i is either 0 or 1 relative to the information and $k_o = 0$. The MODULO-2 operates as follows:if $k_i > 1$ then $k_i = k_i - 2$ else if $k_i < 0$ then $k_i = k_i + 2$ else $k_i = k_i$. At the receiver, the coherently demodulated signal is differentially decoded to give

$$m_i' = k_i' - k_{i-1}' \text{ [MODULO-2]} \qquad 2.17$$

where k_i', in this case, is the demodulated data, and $k_o' = 0$. Also the MODULO-2 operates on the value of m_i'.

The differentially encoded modulated signal can be demodulated by mutliplying it by a one-bit-duration delayed replica of the same signal and lowpass filtered as shown in Figure 2.6. This is called differentially coherent demodulation[1-6]. In this case m_i' is obtained directly. There is a degradation of 1-2 dB in both coherent and differentially coherent demodulated signals.

The differential coding can be applied in the conventional QPSK and offset QPSK systems in order to avoid the phase ambiguity in the carrier recovery system. Figure 2.7 shows the block diagram of the possible encoding decoding processes for 4-phases PSK system. The output of the encoder is given by

$$A_i = (\overline{P_i \oplus Q_i})(P_i \oplus A_{i-1}) + (P_i \oplus Q_i)(Q_i \oplus B_{i-1}) \qquad 2.18a$$

$$B_i = (\overline{P_i \oplus Q_i})(Q_i \oplus B_{i-1}) + (P_i \oplus Q_i)(P_i \oplus A_{i-1}) \qquad 2.18b$$

where $\oplus$ is exclusive-OR operation and $\overline{(x)}$ is the complement of (x). The values of A_i, B_i, P_i and Q_i either 0 or 1 with duration of T seconds (symbol duration). P_i and Q_i are obtained from the information bit stream via a serial-to-parallel converter. A_i and B_i are mapped by a suitable mapping technique to generate the a_i and b_i elements, that are used to modulate the carrier as shown in Figure 2.4. After demodulation the demodulated elements a_i' and b_i' are mapped back to regenerate A_i' and B_i' and from them the transmitted information can be reconstructed as

$$P_i' = \overline{(A_i' \oplus B_i')}(A_i' \oplus A_{i-1}') + (A_i' \oplus B_i')(B_i' \oplus B_{i-1}') \qquad 2.19a$$

$$Q_i' = \overline{(A_i' \oplus B_i')}(B_i' \oplus B_{i-1}') + (A_i' \oplus B_i')(A_i' \oplus A_{i-1}') \qquad 2.19b$$

where A_i', B_i', P_i' and Q_i' are in one to one correspondence with the values at the transmitter, and all can have either 0 or 1.

The differentially encoded signal at the output of the modulator is the same as that given by Equation 2.9, however, the difference is only in the value of the phase factor in Equation 2.10 which can be given, in this case, by

$$k_i = m_i + k_{i-1} \ [\text{MODULO-K}] \qquad 2.20$$

Where the MODULO-K rule is defined as:

if $k_i < 0$ then $k_i = k_i + K$

if $k_i > (K-1)$ then $k_i = k_i - K$

otherwise $k_i = k_i$

and m_i can equally likely have any of the K possible values as k_i that are given in Equation 2.11. Moreover, m_i is proportional to the transmitted information. Equally, the differential decoding is performed at the receiver as follows:

$$m'_i = k'_i - k'_{i-1} \text{ [MODULO-K]} \qquad 2.21$$

with MODULO-K application to m'_i as:

if $m'_i < 0$ then $m'_i = m'_i + K$

if $m'_i > (K-1)$ then $m'_i = m'_i - K$

othersise $m'_i = m'_i$

From the value of m'_i the transmitted information can be reconstructed. However, when K = 4 (for 4-phases system) Equation 2.20 is the exact approximation to the phase factor of the signal that is modulated by the waveforms obtained from Equation 2.18.

Differentially coherent demodulation may be employed by using the differentially encoded QPSK signal[2]. A typical differentially coherent demodulator for 4-phases differentially encoded QPSK is shown in Figure 2.8.

Differential coding can also be applied to QAM signal[18]. Normally, the bits stream is divided into separate groups of n adjacent digits, where n is the possible number of bits per symbol. Furthermore, the i^{th} group corresponding to i^{th} symbol (s_i) is known as $\alpha_{i,1}, \alpha_{i,2}, \alpha_{i,3}, \cdots \alpha_{i,n}$, where $\alpha_{i,\ell}$ is either 0 or 1. This group is fed to the encoder to give $\beta_{i,1}, \beta_{i,2}, \alpha_{i,3}, \cdots \alpha_{i,n}$ which is the encoded group, where $\beta_{i,1}$ and

$\beta_{i,2}$ are either 0 or 1 and $\alpha_{i,3}$, ... $\alpha_{i,n}$ have the same value as in the original group. At the receiver, the encoded group $\beta'_{i,1}$, $\beta'_{i,2}$, $\alpha'_{i,3}$, ...,$\alpha'_{i,n}$ is decoded to give the received group $\alpha'_{i,1}$, $\alpha'_{i,2}$, $\alpha'_{i,3}$, ... $\alpha'_{i,n}$. The encoding and decoding is performed according to Table 2.3.

2.6 Probability of Error

The modulation and the corresponding demodulation schemes discussed above are applied throughout this work. The ASK, PSK, QAM and QPSK signals are here assumed to be narrow-band with ideal channel (ideal and undistorted waveforms). This has been done to provide a useful reference for modelling the required systems with the minimum mathematical complexity. However, the relative tolerances to additive white Gaussian noise of the different modulated carrier signals apply also in the important case where the conditions of the transmission path is less ideal. There is likely misinterpretation of the received information when the received signal is corrupted by noise. The probability of error may however be found by evaluating the maximum signal-to-noise ratio , when coherent demodulation is employed. Ideally, the received signal element of a binary PSK is given by

$$r(t) = A_o m(t) + n(t) \qquad 2.22$$

where $m(t)$ is given by Equation 2.4, A_o is constant amplitude of the signal envelope, and $n(t)$ is a white Gaussian noise with zero mean and two-sided power spectral density of $\frac{1}{2} N_o$. Since k_i is either 0 or 1 then the received

signal can be rewritten as

$$r(t) = \sqrt{2}\, s \cos(\omega_c t) + n(t) \qquad 2.23$$

where $s = \frac{\mp A_o}{\sqrt{2}}$. Clearly, the term, $s \cos(\omega_c t)$, in Equation 2.23 represents binary ASK suppressed carrier signal. The energy of the transmitted sinal element is given by[1-8]

$$E_o = \int_o^T 2s^2 \cos^2(\omega_c t)\, dt = \bar{s}^2 T \qquad 2.24$$

where $\bar{s}^2$ is the average power per element of the corresponding baseband signal $s(t)$. For coherent demodulation the received signal is multiplied by a reference carrier $c(t) = \sqrt{2} \cos(\omega_c t)$ lowpass filtered and is integrated over an interval O to T seconds, then

$$x(t) = \int_o^T r(t)\, c(t)\, dt$$

$$= s(t) + u(t) \qquad 2.25$$

where $u(t)$ is a Gaussian random process with zero mean and two sided power spectral density of $\frac{1}{2} N_o$. The maximum signal to noise ratio is expressed as the average energy per element of the signal devided by the average noise power. Hence the average noise power is given by

$$P_n = \frac{1}{2} N_o \int_{-\infty}^{\infty} |B(f)|^2\, df$$

$$= \frac{1}{2} N_o \qquad 2.26$$

since $\int_{-\infty}^{\infty} |B(f)|^2\, d(f) = 1$, where $B(f)$ is the transfer function of the receiver bandpass filter and $|x|$ is the modulus (absolute value) of x.

The probability density of Gaussian noise is given by

$$f(u) = \frac{e^{-u^2/2N_o}}{\sqrt{2\pi N_o}} \qquad 2.27$$

However, the function of the receiver is to distinguish between $+\frac{A_o}{\sqrt{2}}$ and $-\frac{A_o}{\sqrt{2}}$ in the presence of the noise. Therefore, the probability of error is given by

$$P_e = \int_{x=y}^{\infty} f(u)\, du = \int_{x=y}^{\infty} \frac{e^{-u^2/2N_o}}{\sqrt{2\pi N_o}}\, du$$

$$= \int_{x=y} \frac{1}{\sqrt{\pi}} e^{-x^2}\, dx$$

$$= \frac{1}{2} Q(y) = \frac{1}{2} Q\left(\frac{2E_o}{N_o}\right)^{\frac{1}{2}} \qquad 2.28$$

where $y = \left(\frac{2s^{-2}}{N_o}\right)^{\frac{1}{2}}$ and Q is error function defined in Appendix C.

Equation 2.28 represents the probability of error in binary PSK and supressed carrier ASK. Consequently, the higher spectral efficiency require higher energy, hence, for multilevel signal the probability of error is given by[1,5]

$$P_c = Q\left(\frac{2E_o}{cN_o}\right)^{\frac{1}{2}} \qquad 2.29$$

where c is the average energy factor of different modulation scheme

and is dimensionless. Equation 2.29 could be deduced exactly in the same way as Equation 2.28 for each of QAM and QPSK signals. The relative tolerance to additive white Gaussian noise is then given by

$$P_{rt} = -10 \log_{10}(c) \qquad 2.30$$

From Equation 2.12 $c = \frac{1}{\sin^2(\pi/K)}$ for QPSK and $c = 2\,\frac{L^2-1}{3}$ for QAM, where $L = \log_2(K)$ and K is the number of points in QAM (also, K in $\sin(\frac{\pi}{K})$ is the number of phases in QPSK).

Generally, the relative tolerance to additive white Gaussian noise is shown in Table 2.4 as calcualted from Equation 2.30.

$\alpha_{i,1}$	$\alpha_{i,2}$	a_i	b_i
0	0	-1	-1
0	1	1	-1
1	1	1	1
1	0	-1	1

Table 2.1: The relation between the elements a_i and b_i and the corresponding Gray coded binary sequence for 4-point QAM

$\alpha_{i,1}$	$\alpha_{i,2}$	$\alpha_{i,3}$	$\alpha_{i,4}$	a_i	b_i
0	0	0	0	-1	-1
0	0	0	1	-1	-3
0	0	1	1	-3	-3
0	0	1	0	-3	-1
1	0	1	0	-3	1
1	0	1	1	-3	3
1	0	0	1	-1	3
1	1	0	1	1	3
1	1	1	1	3	3
1	1	1	0	3	1
0	1	1	0	3	-1
0	1	1	1	3	-3
0	1	0	1	1	-3
0	1	0	0	1	-1
1	1	0	0	1	1
1	0	0	0	-1	1

Table 2.2 The relation between the element a_i and b_i and the corresponding Gray coded binary sequence for 16-point QAM

$\alpha_{n,1}$	$\alpha_{i,2}$	$\beta_{i-1,1}$	$\beta_{i-1,2}$	$\beta_{i,1}$	$\beta_{i,2}$
0	0	0	0	0	0
0	1	0	0	0	1
1	1	0	0	1	1
1	0	0	0	1	0
0	0	0	1	0	1
0	1	0	1	1	1
1	1	0	1	1	0
1	0	0	1	0	0
0	0	1	1	1	1
0	1	1	1	1	0
1	1	1	1	0	0
1	0	1	1	0	1
0	0	1	0	1	0
0	1	1	0	0	0
1	1	1	0	0	1
1	0	1	0	1	1

Table 2.3 Differential encoding/decoding of a binary sequence in QAM

PSK	OOK	QPSK	4-QAM	8- PSK	16-QAM
0	-3	-3	-3	-8	-10

Table 2.4 Tolerance to additive white Gaussian noise nearest 0.5 dB relative to binary PSK with coherent demodulation

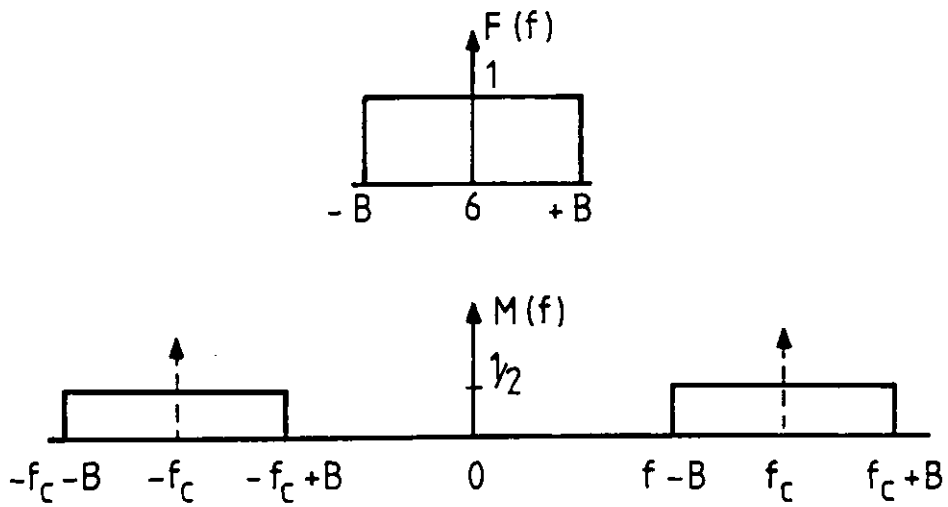

Fig. 2.1. Spectrum of baseband F(f) and passband M(f) signals

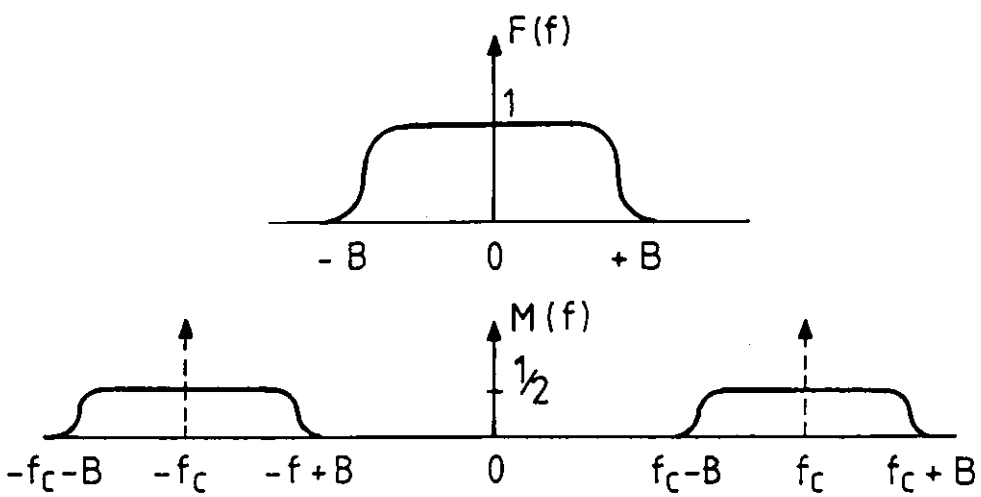

Fig. 2.2 Spectrum of baseband F(f) and passband M(f) signals with roll-off.

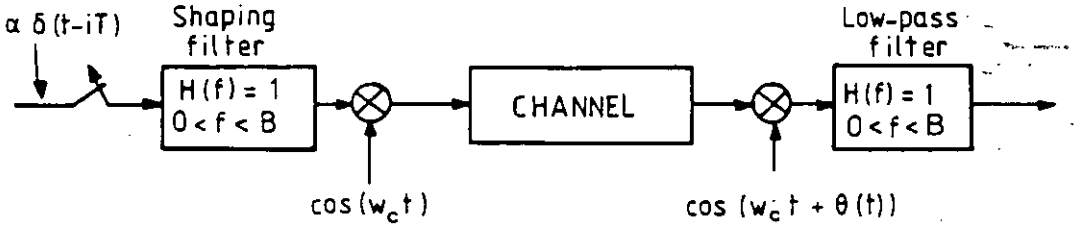

Fig. 2.3 Binary modulation and demodulation techniques for PSK or OOK

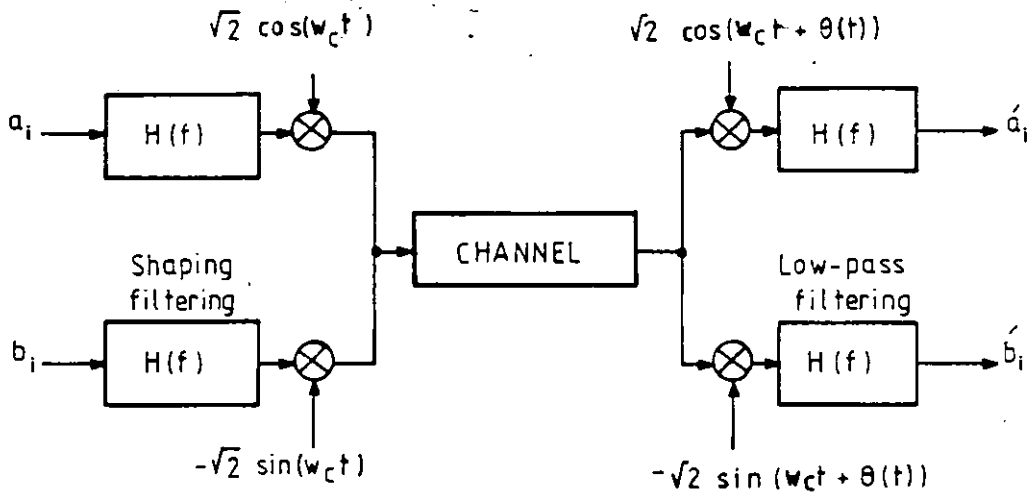

Fig. 2.4 Quantenary modem represents either QAM or QPSK

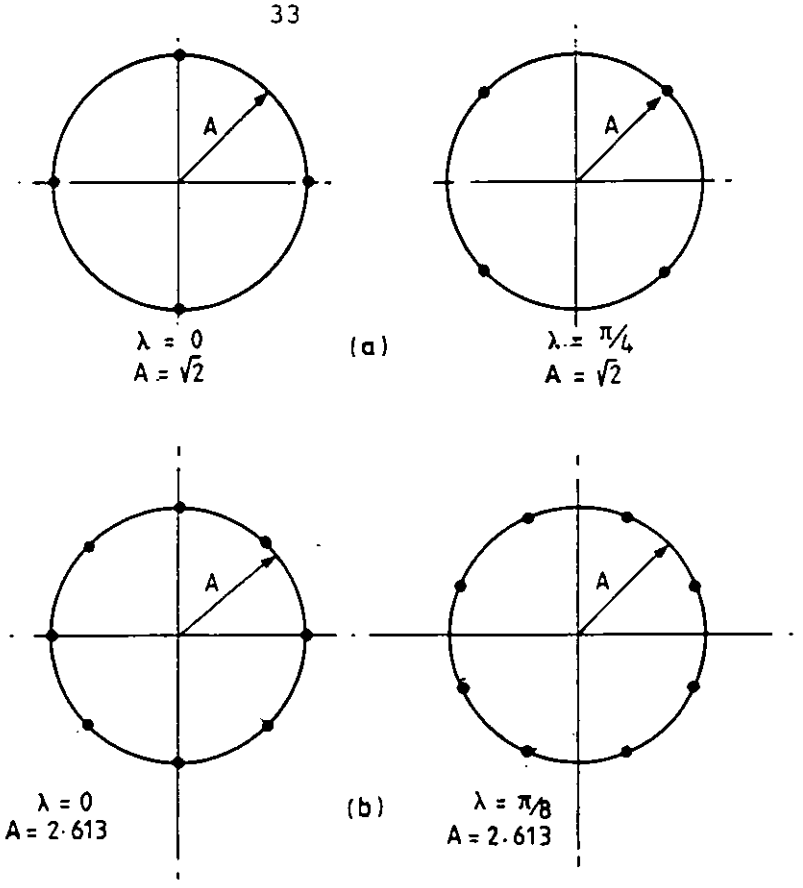

Fig. 2.5 Possible signal vector arrangements for 4 and 8 phases PSK system

a. 4-phases b. 8-phases

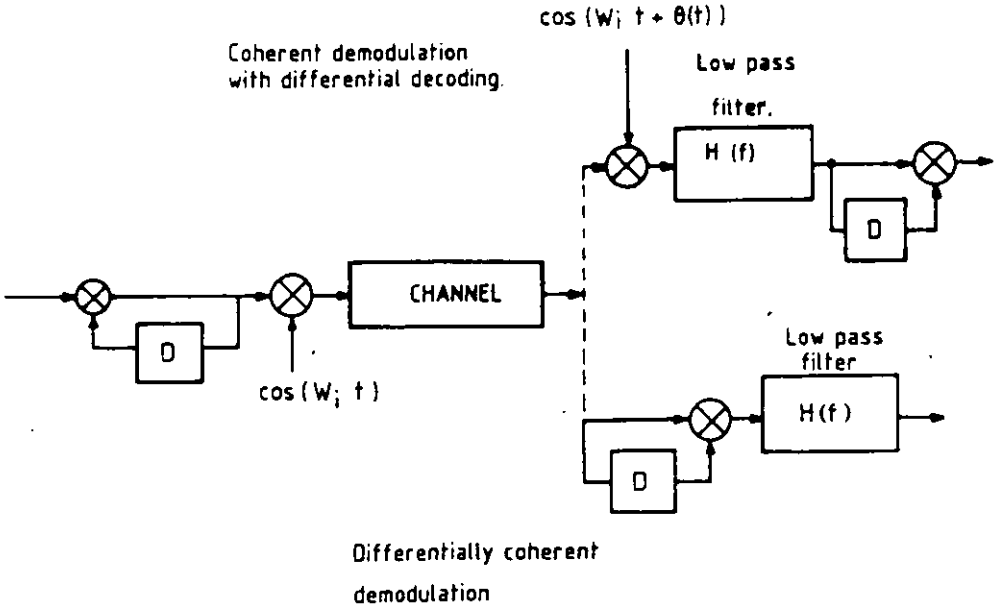

Fig. 2.6 Binary modem using differential coding with either coherent or differentially coherent demodulation

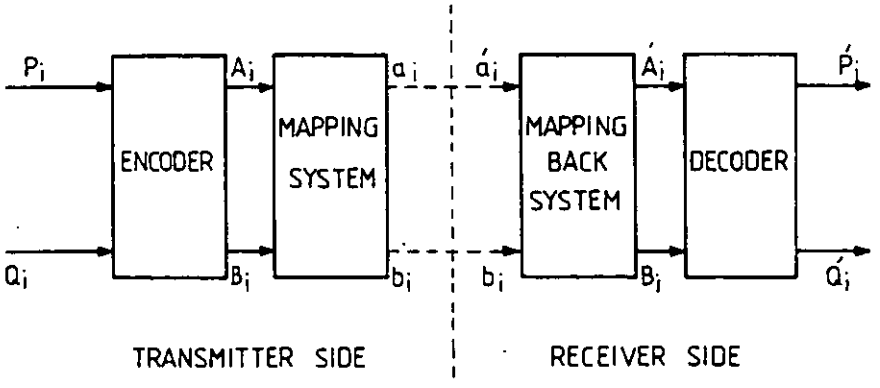

Fig. 2.7. Encoding decoding processes in QPSK system

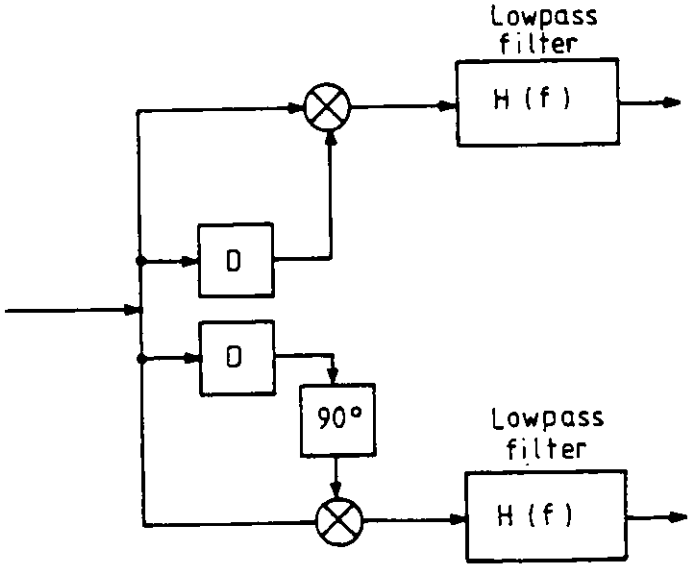

Fig. 2.8. Differentially coherent demodulation for DQPSK signal

3. MOBILE RADIO CHANNEL CHARACTERISATION

3.1 Introduction

The emphasis of this chapter is on land mobile radio channel characterisation in the microwave band. A general representation of a communication channel is introduced here on the basis of linear modulation at the transmitter and linear demodulation at the receiver that are applied to QPSK and QAM system. The impulse response of this channel is first derived, under the assumption of a nonfaded signal, in both passband and baseband regions. The complex notation has been used since it is much easier to manipulate than the equivalent trignometric expression[10]. However, in either method the received baseband signal is derived from the amplitude and phase of the received radio-frequency (RF) signal. The results obtained here are consistent with those derived in the literature[5, 18-20].

Since there is no unique propagation path between the transmitter and the receiver, the field strength fluctuates very rapidly at both the mobile unit and base station with movement of the vehicle carrying the mobile unit. Moreover, the mobile radio channel is subjected not only to the same significant propagation-path losses that are encountered in other types of atmospheric propagation, but is also subjected to path losses that are greatly affected by the general topography of the terrain.

Usually, the mobile antenna height is low which contributes to additional losses. These losses are combined with free-space loss to make up collectively the propagation path-loss which results in reducing the received signal strength not only at the mobile unit, but also at the base station. Nevertheless, there are several methods available in the prediction of the propagation losses, but it is difficult to appraise the difference between them. For this reason, different types of atmospheric propagation losses, that are encountered by a stationary microwave communication system, are explained briefly in Appendix E, to give better understanding of the possible propagation losses in mobile radio communications.

A multipath phenomena is also considered which can cause severe signal fading. This is caused by the presence of many reflectors and scatterers along the propagation path. When the mobile unit is in motion, it passes many different types of local scatterers and reflectors including other vehicles whether in motion or stationary, as it proceeds along its route. The fading characteristic is analyzed statistically in order to look for suitable ways to represent the multipath phenomenon. [Software [10,11,72-82,88-99] and hardware [10,11,81-85,94-98] simulators are introduced as representatives of the multipath fading, but the hardware simulator is recommended and designed to be used throughout this work.] The hardware simulator was given this name because it has been derived from hardware configured simulator and it can be designed as software for the use in computer simulation tests. It will be called in the following chapters a Rayleigh fading simulator for simplicity

A time-invariant channel is discussed and represented by an equivalent lowpass filter under the assumption of nonfaded signal. The impulse response of this filter is obtained by using Fourier design methods as applied to an ideal lowpass transfer function which results in a partial response channel. Then, the faded channel is determined when a faded signal is assumed.

The effects of noise and interference from unwanted signals, that are introduced by the transmission path, are defined briefly. Co-channel and adjacent-channel interferences, which are the interference from signals occupying the same band and adjacent band respectively, are treated as noise at the receiver.

3.2 Channel representation

Generally, the model shown in Figure 3.1 represents the QAM or QPSK system (Chapter 2). The information to be transmitted is carried by the two statistically independent elements a_i and b_i that are in symbol synchronism. The symbol vector is expressed by

$$s_i = a_i + j\, b_i \qquad 3.1$$

where the subscript i is the sampling time index such that $a_i = a(iT)$, $b_i = b(iT)$ and $s_i = s(iT)$, and $j = \sqrt{-1}$. In addition T (in seconds) is the symbol duration. Furthermore, a_i amd b_i are statistically independent and equally likely to have any of the following possible values given by:

For a QAM signal

$$\begin{aligned} a_i = b_i &= \pm 1, \pm 3, \ldots, \pm (m-1) \\ &= 2\,\ell_i - m + 1 \qquad \ell_i = 0, 1, \ldots, (m-1) \end{aligned} \qquad 3.2$$

and for QPSK

$$a_i = \cos\left(\frac{2\pi k_i}{K} + \lambda_o\right) / \sin\left(\frac{\pi}{K}\right) \qquad 3.3a$$

$$b_i = \sin\left(\frac{2\pi k_i}{K} + \lambda_o\right) / \sin\left(\frac{\pi}{K}\right) \qquad 3.3b$$

where $k_i = 0, 1, \ldots, (K-1)$ and K is the possible number of phases in QPSK

system (also K is the possible number of points in the QAM system, and $m = \log_2 K$, see Chapter 2). Moreover, λ_o is constant (either 0 or $\frac{\pi}{K}$) .

3.2.1 Linear passband channel representation

The two elements, a_i and b_i, are fed separately to two Nyquist shaping filters (F_{a_1} and F_{b_1}) with the same transfer function characteristic. The output waveforms from these two filters are used to modulate two carriers at the same frequency, f_c Hz, but in phase quadrature with each other. By assuming linear modulation, the output of the two modulators are added together to form a complex-valued signal given by[16-21]

$$p(t) = \sum_i s_i h_1 (t - iT) e^{j\omega_c t} \qquad 3.4a$$

$$= s_i * h_1(t)\, e^{j\omega_c t} \qquad 3.4b$$

where * means a convolution process, $h_1(t)$ is the complex-valued impulse response of a shaping filter representing the two filters F_{a_1} and F_{b_1} in a complex-form, and $\omega_c = 2\pi f_c$, where f_c is the carrier frequency in Hertz. In fact, the impulse response of each of the two shaping filters separately is real-valued. The combined modulated signal (which represents either QPSK or QAM Equations 3.4a and 3.4b) is normally filtered by the transmitter filter, F_2, to limit the radiated spectrum and is then amplified by a high power amplifier (HPA)[9,19]. (The HPA is assumed here to be a distortionless amplifier which does not affect the channel characteristic,

in any way. However, the radiated signal at the output of the transmitter antenna is given by

$$x(t) = p(t) * h_2(t) \qquad 3.5$$

where $h_2(t)$ is the impulse response of the transmitter bandpass filter. This signal is fed to the transmission path which, generally, must have a frequency characteristic to fit the transmitted signal spectrum without adding significant distortion or loss in the transmitted signal energy. The radio transmission path, however, multiplies the signal by a factor given by

$$q(t) = q_1(t) + jq_2(t) \qquad 3.6$$

where $q_1(t)$ and $q_2(t)$ are the real and imaginary parts of $q(t)$ and $j = \sqrt{-1}$. For an ideal channel $|q(t)| = 1$ ($q_1(t) = 1$ and $q_2(t) = 0$), but for time-invariant-channel $q(t) = e^{j\theta}$, where θ is constant. The behaviour and characteristic of $q(t)$ for the mobile radio environment will be discussed later in Section 3.4. A stationary white Gaussian noise $n(t)$ with a zero mean value and two-sided power spectral density of $\frac{1}{2}$ N_o W/Hz is added to the signal at the end of the transmission path. Hence, the signal at the input of the receiver bandpass filter (F_3) is given by

$$z(t) = x(t).q(t) + n(t) \qquad 3.7$$

The receiver bandpass filter (F_3), whose impulse response is $h_3(t)$, removes as much noise as possible, outside the signal frequency band without distorting the signal itself. The signal at the output of the receiver filter is coherently demodulated by two reference in phase quadrature carriers, that have

the same frequency (f_c) and phase (ϕ) relative to the received signal carrier. The outputs from the two demoulators are then lowpass filtered to remove the high frequency components resulting from the demodulation process. The outputs from the two lowpass filters (F_{a_4} and F_{b_4}) are combined to give a complex signal which is given by:

$$r(t) = z(t) * h_3(t)\, e^{-j(\omega_c t + \phi)} * h_4(t)$$

$$= z(t) * h_3(t) * h_4(t) e^{-j(\omega_c t + \phi)} \qquad 3.8$$

where the $h_4(t)$ represents the complex-valued impulse response of a lowpass filter, that resembles the filtering action of the two real-valued lowpass filtersF_{a_4} and F_{b_4} separately. Moreover $e^{-j(\omega_c t + \phi)}$ is the recovered carrier with appropriate phase shift ϕ, where ϕ is a constant for time-invariant channels. In fact, $\phi = \theta + \psi$ where θ is the phase shift caused by the transmission path and ψ is the phase shift caused by all the filters through which the signal is passed. Therefore Equation 3.8 can be expressed as

$$r(t) = s_i * g(t) + v(t)$$

$$= \sum_i s_i\, g(t - iT) + v(t) \qquad 3.9$$

where g(t) is the overall complex-valued impulse response of the passband channel and v(t) is the resultant complex-valued noise component in the received signal. Furthermore, v(t) is bandlimited Gaussian noise

with zero mean, and is given by

$$v(t) = n(t) * h_3(t) * h_4(t)e^{-j(\omega_c t + \phi)}$$

$$= v_1(t) + jv_2(t) \qquad 3.10$$

where $v_1(t)$ and $v_2(t)$ are statistically independent Gaussian noise sources with zero mean and the same variance.

3.2.2 Linear baseband channel representation

The above analysis emphasizes the impulse response of the linear passband channel that is given by

$$g(t) = h_1(t)e^{j\omega_c t} * (h_2(t)q(t)) * h_3(t)e^{-j(\omega_c t + \phi)} * h_4(t) \qquad 3.11$$

Inevitably, g(t) is said to be nonlinear if one or more of the parameters ($h_1(t)$, $h_2(t)$, $q(t)$, $h_3(t)$ and $h_4(t)$), including the modulator and/or the demodulator, are nonlinear.

The baseband channel impulse response can be deduced in the same way as the impulse response of the passband channel using Fourier transform notation. The waveform at the output of the shaping filters (F_{a_1} and F_{b_1}) is given, in a complex form, by

$$d(t) = \sum_i s_i h_1(t - iT)$$

$$= s_i * h_1(t) \qquad 3.12$$

The Fourier transform of Equation 3.12 is given by (see Appendix A).

$$D(f) = S(f)\, H_1(f) \qquad 3.13$$

where: $D(f) \leftrightarrow d(t)$

$S(f) \leftrightarrow s(iT)$

$H_1(f) \leftrightarrow h_1(t)$

and $\leftrightarrow$ means Fourier transform pairs (direct and inverse). This signal is used to modulate the carrier. The modulation process, however, represents pure translation of the signal spectrum to $\pm f_c$, for linear modulation[2-6, 18-20]. As a result of the linear modulation, the spectrum of the modulated signal is given by

$$P(f) = D(f - f_c) \qquad 3.14$$

P(f) has twice the baseband bandwidth [1,3-6] distributed about the carrier frequency, f_c. Accordingly, the transmitter filter F_2 must fit the transmitted data bandwidth without distortion or loss. Hence the radiated signal is given by

$$X(f) = D(f - f_c)\, H_2(f - f_c) \qquad 3.15$$

where $H_2(f - f_c) \leftrightarrow h_2(t)$. For time-invariant channels, q(t) does not affect the transmitted data spectrum. By ignoring the noise effect (the noise will be treated separately) the received signal at the output of the receiver bandpass filter F_3 is given by

$$Z(f) = X(f)\, H_3(f - f_c)$$

$$= D(f - f_c)H_2(f - f_c)H_3(f - f_c) \qquad 3.16$$

where $H_3(f - f_c) \leftrightarrow h_3(t)$. However, the demodulation process shift the whole spectrum down to baseband centred about zero frequency. The signal, that is given by Equation 3.16, is now ready for demodulation. Consequently, in order to shift down the whole spectrum it is necessary to replace the transmitter and receiver bandpass filters (F_2 and F_3) by the corresponding equivalent lowpass filter[5]. Hence Equation 3.16 becomes

$$Z'(f) = D(f)C_2(f)\ C_3(f) \qquad 3.17$$

where $C_2(f)$ and $C_3(f)$ are the transfer functions of the lowpass filters, that are equivalent to the bandpass filters F_2 amd F_3 in the baseband region respectively. Furthermore, the demodulated signal, that is given by Equation 3.17, is lowpass filtered by the two lowpass filters F_{a_4} and F_{b_4} whose equivalent transfer function $H_4(f)$, where $H_4(f) \leftrightarrow h_4(t)$. Therefore, the received signal spectrum, at the output of the lowpass filters, is given by

$$\begin{aligned} R(f) &= \acute{Z}(f)\ H_4(f) \\ &= D(f)C_2(f)\ C_3(f)H_4(f) \end{aligned} \qquad 3.18$$

Accordingly, by substituting the value of D(f), that is given by Equation 3.13, into Equation 3.18, then the received signal spectrum becomes

$$R(f) = S(f)H_1(f)C_2(f)C_3(f)H_4(f) \qquad 3.19$$

Now, each one of the filters $H_1(f)$, $C_2(f)$, $C_3(f)$ and $H_4(f)$ must agree with Nyquist sampling rate for zero intersymbol-interference[1-5]. This implies

that the minimum bandwidth of each one of them is at least half the data rate ($\frac{1}{2T}$). Eventually, by taking the inverse Fourier transform and reconsidering the noise and the transmission path factor q(t), then the received signal can be expressed by[18-20]

$$r(t) = s_i(t)*(c_2(t)q(t))*c_3(t)*h_4(t) + u(t)$$

$$= \sum_i s_i\, y(t-iT) + u(t) \qquad 3.20$$

where u(t) is the complex-valued noise component in the received signal, and y(t) is the linear baseband channel, which is now given by

$$y(t) = h_1(t)*c_2(t)*c_3(t)*h_4(t).q(t)$$

$$= h_T(t)*h_R(t)\ q(t)$$

$$= h_o(t)\ q(t) \qquad 3.21$$

where $h_T(t) = h_1(t)*c_2(t)$ is the overall transmitter filter

$h_R(t) = c_3(t)*h_4(t)$ is the overall receiver filter

and $h_o(t) = h_T(t)*h_R(t)$ is the baseband time-invariant channel when $|q(t)|$ is constant or equal to unity. It is assumed throughout this work that all the bandpass and lowpass filters in the transmitter and receiver (generally referred to as a modem) have flat frequency responses in the passband. The cascaded frequency response of the above filters in the modem are assumed to satisfy Nyquist's theorem[1-6,9,10,18-20] for zero intersymbol interference. The pulse shaping can yield better performance, when it is divided equally between the transmitter and the

receiver[2,3,10]. Consequently, it is necessary to study the characteristic and behaviour of q(t) before designing the lowpass filter, whose impulse response is equivalent to $h_o(t)$ and satisfies Nyquist's criterion.

It is important to impose hetrodyne principles in the modem under consideration by which the modulation and demodulation take place at relatively low frequencies[9,19]. The modulated signal, with low carrier frequency, is then up-converted to the required frequency at the transmitter and down-converted to appropriate frequency at the receiver by mixers[3-8]. Therefore, the mixer's transfer functions are unavoidable parts of the entire channel. The bandwidth of each mixer can be assumed wide enough to accommodate the new passband signal without distortion, or $H_{mixer}(f) = 1$ over the entire passband region, where $H_{mixer}(f)$ is the transfer function of each mixer. Therefore, the channel transfer function is not affected by the implementation of a hetrodyne system according to the above assumption.

3.2.3 Noise representation

The additive noise, u(t) in Equation 3.20, can be derived by following similar steps that were used to derive the received baseband signal (Equation 3.20). However, in order to avoid unnecessary repetition, it is worth drawing attention to Equation 3.10, from which the noise component in the received signal is now given by

$$\begin{aligned} u(t) &= \acute{n}(t) * c_3(t) * h_4(t) \\ &= \acute{n}(t) * h_R(t) \end{aligned} \qquad 3.22$$

where $n'(t) = n(t)e^{-j(\omega_c t+\phi)}$. Since, by assumption, n(t) is a white Gaussian noise with zero mean and a two-sided power spectral density, the shift-down of its spectrum in the frequency domain does not affect its properties[1-11,18-20]. Consequently, the power spectral density of u(t) is now given by

$$|U(f)|^2 = N_o |H_R(f)|^2 \qquad 3.23$$

where U(f) and $H_R(f)$ are the Fourier transform of u(t) and $h_R(t)$ respectively. The autocorrelation function of u(t) is given, according to the Wiener-Khintchine theorem[22,23, see also Appendix D], by

$$R_u(\tau) = N_o \int_{-\frac{1}{2T}}^{\frac{1}{2T}} |H_R(f)|^2 e^{j\omega\tau} df \qquad 3.24$$

Clearly, when the transfer function of the overall receiver filter, $H_R(f)$, is symmetric about zero frequency, it is also convenient to assume that

$$H_R(f) = \begin{cases} 1 & -\frac{1}{2T} \leq f \leq \frac{1}{2T} \\ 0 & \text{elsewhere} \end{cases} \qquad 3.25$$

which implies that

$$R_u(\tau) = N_o \int_{-\frac{1}{2T}}^{\frac{1}{2T}} e^{j\omega\tau} df$$

$$= \frac{N_o}{T} \text{ sinc } (\frac{\tau}{T}) \qquad 3.26$$

where $\text{sinc}(x) = \sin(\pi x)/\pi x$. This is a real-valued quantity which leads to a conclusion that $u_1(t)$ and $u_2(t)$ are uncorrelated. (Appendix D).

The variance of $u(t)$ is given by

$$\sigma_u^2 = R_u(o) = N_o \int_{-\frac{1}{2T}}^{\frac{1}{2T}} |H_R(f)|^2 \, df$$

$$= \frac{N_o}{T} \qquad 3.27$$

Subsequently, from Appendix D, the variance of $u_1(t)$ or $u_2(t)$ is given by

$$\sigma_{u_1}^2 = \sigma_{u_2}^2 = \frac{N_o}{2T} \qquad 3.28$$

3.3 Transmission path losses in mobile radio

The field strength in the vicinity of a mobile station varies rapidly with the time as long as the vehicle carrying the mobile unit is moving. This leads to a highly variable structure of the received signal because of the existence of multipath between the transmitter and the receiver of the microwave mobile communications. As the vehicle carrying the mobile unit moves through the service area, the received signal envelope, phase and/or frequency fluctuate rapidly due to multipath propagation and interference[9-12,19,21,72-86]. These fluctuations result in a received signal with a Rayleigh probability density[10,11, 72-75]. The multipath fading and interference will be discussed in detail in Sections 3.4 and 3.8 respectively. Nevertheless, in order to understand the path losses in mobile radio communication, the path losses in stationary microwave communication are discussed briefly in Appendix E.

However, the path losses in mobile radio propagation are essentially due to terrain effects and the presence of radio-wave scatterers along the path within the mobile radio environment. The changes in the propagation are caused by the variations in the contour and roughness of the terrain[10,11,27,72-87], including the scatterers, as a result of reflection and diffraction. The line-of-sight condition, in mobile radio communication, can be considered as to have been satisfied when specular and diffuse reflections are present. Also, path losses are inversely proportional to the square of the distance separating the transmitting and receiving antennas.

The specular reflection occurs when radio waves encounter a smooth interface between unlike media and the linear dimensions of the interface are large in comparison with wavelength of the radiated signal. This kind of reflection is analogous to the reflection properties of mirrors as defined by Snell's law, as shown in Figures 3.2 and 3.3.

Diffuse reflection is due to scatterers that are present along the propagation path. The diffuse reflection occurs when radio waves fall upon a rough-textured surface of which the roughness is compatible with the wavelength of the radiated signal. Unlike specular reflection which follows Snell's law, the diffuse reflection scatters the energy so that the reflected waves follow divergent paths. Furthermore, the field intensity of diffusely reflected radio waves is less than that of the specularly reflected waves, since the energy is scattered along the path over a rough surface. Therefore, it is necessary to analyze the reflection properties of the surrounding terrain between the mobile unit and the base station, when considering the mobile radio environment.

Loss due to diffraction of the radio waves occur when the propagation path is obstructed by obstacles in the intervening terrain between the transmitting and receving antennas. The line-of-sight condition is no longer valid, since there are variations in the terrain contour that is obstructing the propagation path. Accordingly, the definition of the line-of-sight condition is different for mobile radio from that discussed in Appendix E for tropospherical propagation. The severity

of signal attenuation depends on whether the obstruction extends through the whole of the first Fresnel zone, along the line-of-sight path, or merely approaches the first Fresnel zone as shown in Figure 3.4. In practice, it is always possible to select the highest point along the propagation path as the ideal location for the base station. Even with good siting of the base station in hilly areas, there will commonly be occasions when the mobile unit is out of sight of the main propagation path.

Different representations of predicting the propagation path loss in mobile radio environment for different situations are helpful in understanding the effect of multipath phenomena on mobile radio signals. Under these circumstances, Equation E.17 is unlikely to be valid. However, the summing of all these effects would introduce so many variables so that a mathematical solution would practically be too complex. Alternatively, combined-techniques of analytical and statistical analysis are recommended. From different measurements, the statistical results can be obtained and analysed according to the criteria that are unique for a particular situation. It is then possible to draw certain analytical conclusions based on electromagnetic theory. The propagation-path loss method is a powerful tool that can produce results closer to the actual path losses from that using either analytical or statistical approaches alone[10]. A number of analytical and statistical models are available for prediction and calculation of the path loss in mobile radio, and it is often difficult to assess the

real difference between them or to determine what conditions have to be applied[10,44-71]. As a result, there is no absolutely complete model, and each one requires the insertion of one or more parameters in order to be fully applicable to the mobile radio channel. Beside this, some of these methods do not actually consider the fading.

3.4 Multipath fading

The major concern in mobile radio studies is multipath fading, which is a common occurrence in the mobile radio environment. The existence of the multipath is independent of the separation distance between base and mobile stations. At any point, the received signal field is made up of a number of waves with random amplitude and different arrival angles for different locations, as shown in Figures 3.5. The relative phases of the received waves are uniformly distributed from $-\pi$ to π. By assuming stationary scatterers and a vehicle carrying mobile unit travelling in the direction shown with velocity v (in miles or km per hour), then the motion introduces a Doppler shift in each wave, that is

$$f_n = \frac{v}{\lambda} \cos(\alpha_n) \qquad 3.29$$

where λ is the wavelength of the transmitted carrier frequency, and α_n is the arrival angle of the n^{th} wave which is the angle between the horizontal plane and the direction line of the n^{th} incident wave on the mobile unit. The field intensity of a vertically polarized signal that can be seen by the mobile antenna is thus given by

$$E_r = E_o \sum_{n=0}^{N-1} \Gamma_n e^{j(\omega_c t + \psi_n)} \qquad 3.30$$

where $\psi_n = \omega_n t + \phi_n$ 3.31a

$$\omega_n = 2\pi f_n = \beta v \cos(\alpha_n) \qquad 3.31b$$

$$\beta = \frac{2\pi}{\lambda} \qquad 3.31c$$

ϕ_n is the random phase angle of the n^{th} wave

and Γ_n is the reflection coefficient of the scatterer which reflects the n^{th} wave. Moreover, E_o is the field intensity of the received signal via a direct path when the vehicle is stationary, also, $\omega_c = 2\pi f_c$ where f_c is the carrier frequency (If N=2, $\psi_o = 0$ and $\Gamma_o = 1$ then Equation 3.30 is identical to Equation E.15 in Appendix E, but in mobile radio environment it is unlikely that $\Gamma_o = 1$).

ϕ_n, for n = 0, 1, ..., N-1, are uniformly distributed from $-\pi$ to $+\pi$. Furthermore, Γ_n, for n = 0, 1, ..., N-1, are normalized such that[10,11]

$$E(\Gamma_n^2) = \frac{1}{N} \sum_{n=0}^{N-1} |\Gamma_n|^2 = 1 \qquad 3.32$$

where E(x) is expected value (Expectation) of x and $|\Gamma_n|$ is the modulus of Γ_n.

Now, E_r may be considered as a narrow band random process[11,72] and as a consequence of the central limit theorem[22], is approximately a Gaussian process for large N. This implies that the mean signal power is constant with time, whereas, in reality it undergoes slow variations as the mobile vehicle moves a few hundreds of yards. However, a Gaussian model gives a successful prediction of the measured statistics of the signal, to good accuracy, in most cases over the ranges of interest for the involved variables[10,11, 72-77]. Nevertheless

Equation 3.30 can be rewritten as[11,72-75]

$$E_r = E_q e^{j \omega_c t} \tag{3.33}$$

where

$$E_q = E_o q(t) \tag{3.34}$$

and

$$q(t) = \sum_{n=0}^{N-1} \Gamma_n e^{j \psi_n} \tag{3.35}$$

Clearly E_q is complex-valued Gaussian random process. By denoting $q_1(t)$ and $q_2(t)$ as the inphase and quadrature components of $q(t)$ respectively, and accordingly $E_{q1} = E_o q_1(t)$ and $E_{q2} = E_o q_2(t)$ are the inphase and quadrature components of E_q respectively. Consequently, E_{q_1} and E_{q_2} have zero mean and equal variance, or

$$E(E_{q_1}) = E(E_{q_2}) = 0 \tag{3.36}$$

and

$$E(E_{q_1}^2) = E(E_{q_2}^2) = \sigma^2 \tag{3.37}$$

where σ^2 is the variance of E_{q_1} or E_{q_2}. Also, E_{q_1} and E_{q_2} are uncorrelated, then

$$E(E_{q_1} E_{q_2}) = 0 \tag{3.38}$$

where $E(x)$ is the expectation of x. As a result, $q_1(t)$ and $q_2(t)$ are uncorrelated with zero mean and equal variance, so[10]

$$E(q_1(t)) = E(q_2(t)) = 0 \tag{3.39}$$

$$E(q_1^2(t)) = E(q_2^2(t)) = 1 \tag{3.40}$$

$$E(q_1(t)\ q_2(t)) = 0 \tag{3.41}$$

Since E_{q_1} and E_{q_2} are Gaussian, then each one of them has a probability density of the form[10,11,22,23]

$$p(y) = \frac{1}{\sqrt{2\pi}\ \sigma}\ e^{-y^2/2\sigma^2} \tag{3.42}$$

where y is either E_{q_1} or E_{q_2}. The probability density of E_q is given by[11,72-75]

$$p(E_q) = \begin{cases} \frac{E_q}{\sigma^2}\, e^{-E_q^2/2\sigma^2} & E_q \geq 0 \\ 0 & E_q < 0 \end{cases} \tag{3.43}$$

which is the Rayleigh density formula[22]. The Rayleigh and Gaussian densities are illustrated in Figure 3.6. The distribution function of E_{q_1} or E_{q_2} is given by

$$P(y \geq Y) = \int_Y^\infty p(y)\,dy$$

$$= \frac{1}{2}\left[1 + Q\left(\frac{Y}{\sqrt{2}\ \sigma}\right)\right] \tag{3.44}$$

where Q(x) is the error function of x (Appendix C). Similarly

$$P\ (E_q \geq E_e) = \int_{E_e}^{\infty} p(E_q)\,dE_q$$

$$= 1 - e^{-E_e^2/\sigma^2} \qquad 3.45$$

This is the simple model of a Rayleigh fading process. The random process $q_1(t)$ and $q_2(t)$ defined by the above will form the basis for the statistical analysis of the received signal throughout this study.

Throughout this discussion, the assumption was made for a mobile unit, but while the mobile is in motion there are three possibilities which must be considered. These are:

the complete absence of paths (including the sky wave[9]),the presence of a single path, and the presence of many paths.
In accordance with the above possibilies, the deep fade may happen in the absence of paths and even with presence of many paths, since the addition of the individual waves may cancel each other. There are situations where multipath fading phenomena exist to give the same result as in Equation 3.30. These situations are[10] :-

i) Where the mobile unit and nearby scatterers are stationary

ii) Where the mobile unit is stationary while the nearby scatterers are moving (passing cars and trucks)

iii) Where the mobile and nearby scatterers are all moving.

It is only in the first situation that q(t), in Equation 3.35, is constant as long as the mobile unit and nearby scatterers are stationary.

3.5 Rayleigh fading simulators

A large number of radio-propagation models deal with prediction of the amplitude and phase of a received signal throughout a mobile channel[10,11,72-82, 84,85,88-98]. All of these models are based on the analyses of the statistics of the faded signal due to the effect of multipath. Furthermore, these models are classified in either software[10,11,72-82,88-97], hardware[10,11,81-85,94-98] or a combination of hardware and software. The software simulator can be represented according to Equation 3.35, with predetermined conditions concerning its parameters[10]. While, in a hardware simulator, $q_1(t)$ and $q_2(t)$ are generated from two separate white Gaussian noise generators according to the conditions given by Equations 3.39 to 3.41, where $q_1(t)$ and $q_2(t)$ are the inphase and quadrature components of $q(t)$, in Equation 3.35, respectively. Furthermore, the field measurement results agree very well with the results obtained from the hardware simulator[81,82,84,85,94-96], therefore the hardware simulator is recommended throughout this work, and will be called the Rayleigh simulator in the following chapters for simplicity. Figure 3.7 shows the Rayleigh multipath fading (hardware) simulator (RMFS) which consists of two white Gaussian noise generators (WGNG), two variable lowpass filters (VLPF) and two balanced mixers (BM). The selection of the cutoff frequency of the lowpass filter depends on the Doppler frequency, which is $|f_D| = \frac{v}{\lambda}$, and depends consequently on the speed of the vehicle, v, where λ is the carrier wavelength and $|f_D|$ is the absolute value of f_D[10-12] (see also Equation 3.29).

The output of the simulator represents the envlope and phase of a Rayleigh faded signal, and the impulse response of the channel is modified by the simulator output as in Equation 3.21.

3.5.1 Design of Rayleigh Fading Simulator

Since it is difficult to achieve variable lowpass filters in computer simulation tests, it is worth while to assume that the mobile unit vehicle moves with speed ν = 75 miles/hr. and the frequency of the radiated carrier is 900 MHz. This leads to a constant Doppler frequency, f_D, of 100 Hz, where $|f_D| = \frac{\nu}{\lambda}$ and λ is the carrier frequency wavelength.

The white Gaussian noise generators,that are shown in Figure 3.7, generate the noise components $n_1(t)$ and $n_2(t)$ that are random process with zero mean, Gaussian probability functions and equal variance, thus

$$q_1(t) = n_1(t) * h_B(t) \qquad 3.46a$$

$$q_2(t) = n2(t) * h_B(t) \qquad 3.46b$$

where $h_B(t)$ is the impulse response of the required lowpass filters, and * means a convolution process. Also $n_1(t)$ and $n_2(t)$ are to be independent (uncorrelated) in order to satisfy the conditions of Equations 3.39-3.41. Therefore, $q_1(t)$ and $q_2(t)$ have the same properties of $n_1(t)$ and $n_2(t)$ so each must process a zero mean, Gaussian probability density function and equal variance. Of course, the variance of $n_1(t)$ and $n_2(t)$ may differ from the variance of $q_1(t)$ and $q_2(t)$ because of the filtering process. Since the power spectra of $q_1(t)$ and $q_2(t)$ are Gaussian shaped with the same root-mean-square (rms) frequency, as illustrated in Figure 3.8, then[18,99]

$$|Q_1(f)|^2 = |Q_2(f)|^2 = \exp(-\frac{f^2}{2 f_{rms}^2}) \quad 3.47$$

where $Q_1(f)$ and $Q_2(f)$ are the spectra of $q_1(t)$ and $q_2(t)$ respectively and f_{rms} is the root mean square value of the maximum input signals ($n_1(t)$ and $n_2(t)$) frequency, which is defined by[100]

$$f_{rms} = \frac{\text{fading}}{1.475} \quad 3.48$$

The frequency spread, f_{sp}, introduced by each of $q_1(t)$ and $q_2(t)$ into the carrier signal waveform is given by

$$f_{sp} = 2f_{rms} = 1.356 \times \text{fading rate} \quad 3.49$$

Note that the term f_D used in sunsequent chapters refers to frequency spread, f_{sp}.

This means that 1 Hz of frequency spread corresponds to 44.25 fades per minute. Let the transfer function of each of the lowpass filters be $H_B(f)$ and let $h_B(t)$ be the inverse Fourier transform of $H_B(f)$ then $H_B(f)$ and $h_B(f)$ can be given by[18,99,101]

$$H_B(f) = \exp(-\frac{f^2}{4 f_{rms}^2}) \quad 3.50a$$

$$h_B(t) = \frac{1}{\sqrt{2\pi}\, t_1} \exp(-\frac{t^2}{4t_1^2}) \quad 3.50b$$

where $t_1 = \frac{1}{2\pi f_{rms}}$. So, the output from the two filters ($q_1(t)$ and $q_2(t)$) satisfy the required properties. From Equation 3.47 the cutoff (3 dB) frequency of each filter is

$$f_{ct} = f_{rms} \left(-2\ell n(0.5) \right)^{\frac{1}{2}}$$

$$= 1.17741\ f_{rms} = 0.588705\ f_{sp} \qquad 3.51$$

where $\ell n(.)$ is the Natural Logarithm. The filter characterized by the above may be approximted by a 5th order Bessel filter[18,102]. The transfer function of the Bessel filter is given by[103-105]

$$H_L(s) = \frac{B_o}{\sum_{k=0}^{L} B_k s^k} \qquad 3.52$$

where

$$B_k = \frac{(2L-k)!}{2^{L-k}\, k!(L-k)!} \qquad 3.53$$

and L is the order of the filter. In this case L = 5 for 5th-order Bessel filter, thus

$$H_5(s) = \frac{945}{945 + 945s + 420s^2 + 105s^3 + 15s^4 + s^5} \qquad 3.54$$

The poles of $H_5(s)$ are

$$P_1 = -3.64674 \qquad 3.55a$$

$$P_{2,3} = -3.35196 \pm j1.74266 \qquad 3.55b$$

$$P_{4,5} = -2.32467 \pm j3.57103 \qquad 3.55c$$

where $j = \sqrt{-1}$. To calculate the cut-off frequency of the 5^{th} order Bessel filter, let $s = j\Omega$ in Equation 3.54. Then Ω_3 is calculated, when $H_5(j\Omega_3) = 0.707$ (3 dB), as

$$\Omega_3 = 2.4274 \quad \text{rad/sec} \tag{3.56}$$

By normalizing the cutoff frequency of $H_5(s)$ (given in Equation 3.54) to 1 Hz, so that it is possible to change the cutoff frequency to any required value, thus

$$c_f = \frac{\omega_3}{\Omega_3} = \frac{2\pi f_3}{2.4274} = 2.58844\ f_3 \tag{3.57}$$

where f_3 is the required cutoff frequency. However, from Equation 3.51, the cutoff frequency is $f_3 = 58.8705$ Hz when f = 100Hz, therefore $c_f = 152.383$. The values of the poles are now given by

$$p'_k = c_f\, p_k \tag{3.58}$$

or

$$p'_1 = -555.7 \tag{3.58a}$$

$$p'_{2,3} = -510.7 \pm j265.55 \tag{3.58b}$$

$$p'_{4,5} = -354.24 \pm j544.16 \tag{3.58c}$$

The required filter must be implemented digitally in order to be used in computer simulation tests. The transfer function of this filter $H_5(z)$ in z-domain is obtained by applying the invariant-impulse response

design method[103-107] to the filter transfer function $H_5(s)$ in s-domain, then

$$H_5(z) = \frac{a_o + a_1 z^{-1} + a_2 z^{-2} + a_3 z^{-3} + a_4 z^{-4}}{1 + b_1 z^{-1} + b_2 z^{-2} + b_3 z^{-3} + b_4 z^{-4} + b_5 z^{-5}} \qquad 3.59$$

where a_ℓ and $b_{\ell+1}$, for $\ell = 0$ to 4, are the coefficients of the filter. The coefficients are obtained by assuming a sampling rate of 250 samples/second for the original waveform. The difference equation of this filter is given by[103-107]

$$q'_{I,k} = \sum_{\ell=0}^{4} (a_\ell \, n_{I,k-\ell} - b_{\ell+1} \, q'_{I,k-\ell-1}) \qquad 3.60$$

where I is either 1 or 2, $n_{I,k}$ and $q'_{I,k}$ are the k^{th} values of the sampled input and output Gaussian process signals respectively, such that $n_{I,k} = n_I(kT')$ and $q'_{I,k} = q'_I(kT')$, where T' is the sampling period. a_ℓ and $b_{\ell+1}$, for $\ell = 0$ to 4 are the filter coefficient as is evident from Equation 3.59. Table 3.1 shows the values of the lowpass filter coefficients, a_ℓ and $b_{\ell+1}$ for $\ell = 0$ to 4. The filter can,practically, be implemented as shown in Figure 3.9 (see Appendix B) where

$$u_{I,k} = n_{I,k} - \sum_{\ell=0}^{4} b_{\ell+1} \, u_{I,k-\ell-1} \qquad 3.61$$

and

$$q'_{I,k} = \sum_{\ell=0}^{4} a_\ell \, u_{I,k-\ell} \qquad 3.62$$

3.6 Time-invariant channel

The impulse response of the baseband channel as seen from Equations 3.20 and 3.21 consists of two parameters $h_o(t)$ and $q(t)$. The term $q(t)$ has been introduced in Section 3.5 which has a Rayleigh probability density function, and represents the random change in the envelope and phase of the received signal. However, $h_o(t)$, formed by the linear modulator, linear demodulator and the transmitter and receiver filters (Equation 3.21), will be studied in this section, for unfaded channels (when $|q(t)| = 1$).

The data rate that can be transmitted over a channel with a bandwidth of B Hz is 2B symbols/second[1,3,4,108,109]. This is called the Nyquist rate, and is obviously related to the Nyquist sampling theorem[108]. As mentioned above, all the transmitter and receiver filters are considered as parts of this channel. Also, the channel is very much affected by the transmission path[109] (see also Sections 3.4 and 3.5). Therefore, the system filtering action and the effect of the transmission path cause the pulses that are to be transmitted on this channel, to spread out as they traverse the system and overlap into the adjacent pulse time slots. The signal overlapping into the adjacent time slot may, if it is too strong, result in an erroneous decision at the receiver. This phenomenon of pulse overlap is termed intersymbol interference. In order to minimize this interference the transmission bandwidth may be widened as much as desired. This is unnecessarily wasteful of the spectrum, and if carried too far, may introduce excessive noise into the system. Instead, the transmitter and receiver

filters must be compromisingly designed with as small a ba... possible such as to eliminate the interference and minimize the noise effects. Obviously, the best waveshape is the signal that is maximum at the decision instant and zero at all other adjacent sampling points. This ideally provides zero intersymbol interference. However, there are practical difficulties with this particular waveshape, which include;

i) The ideal channel is physically unrealisable, and very difficult to approximate in practice because of the sharp cutoff in its amplitude spectrum at the cutoff frequency.

ii) Precise synchronisation is essential when such waveshapes are used. If the timing, at the receiver, differs somewhat from the exact synchronisation, then zero intersymbol interference is no longer obtained.

To overcome the above two difficulties, it is possible to derive from the ideal form the related channel with controllable levels of intersymbol interference[3,109]. Besides, in this channel a higher transmission rate over a given bandwidth is permitted. The resultant channel is known as a partial-response channel[1,9,109]. This channel is much simpler to obtain in practice and the effect of timing jitter may be minimized by careful design[1]. The intersymbol interference introduced by this channel can be compensated for by either suitable signal coding at the transmitter or appropriate detection process at the receiver. However, two models of channels are going to be

introduced hereinafter with a rectangular and raised-cosine spectra, that can be approximated by using Fourier transforms[1,3,109].

The attenuation, A(dB), and group-delay, τ, characteristics for an ideal rectangular channel, as shown in Figures 3.10 and 3.11 respectively, can be given, over the range of frequencies of interest, by

$$A = -20 \log_{10} |H_o(f)| \quad \text{dB} \qquad 3.63$$

$$\tau = -\frac{1}{2\pi}\frac{d\theta(f)}{df} \quad \text{seconds} \qquad 3.64$$

where $H_o(f)$ is the Fourier transform of $h_o(t)$, $\theta(f)$ is the phase of $H_o(f)$ and $|x|$ is the modulus of x. $H_o(f)$ can be calculated by substituting the values of A and τ, that can be measured from the graph of Figures 3.10 and 3.11, into Equations 3.63 and 3.64. The calculated $H_o(f) = |H_o(f)| \exp(j\theta(f))$ is shifted down to the baseband frequency centred about zero Hz, giving the result shown in Figure 3.12.

Alternatively, it has been shown elsewhere[3,109,110] that it is convenient to assume the same transfer function for the transmitter and receiver filters in order to minimize the effect of noise and intersymbol-interference. Hence

$$H_T(f) = H_R(f) = |\alpha(f)| e^{j\Psi(f)} \qquad 3.65$$

where $H_T(f)$ and $H_R(f)$ are the transfer function of the transmitter and receiver filters respectively. But when $|q(t)| = 1$ in Equation 3.21 then

$$H_o(f) = H_T(f)H_R(f) \qquad 3.66a$$

$$= |\alpha(f)|^2 e^{j2\psi(f)} \qquad 3.66b$$

$$= |H_o(f)| e^{j\theta(f)} \qquad 3.66c$$

Therefore

$$|\alpha(f)| = |H_o(f)|^{\frac{1}{2}} \qquad 3.67a$$

$$\psi(f) = \frac{1}{2}\theta(f) \qquad 3.67b$$

However, for a rectangular shaped transfer function, let

$$\alpha(f) = \begin{cases} 1\ e^{j\psi(f)} & -B < f < B \\ 0 & \text{elsewhere} \end{cases} \qquad 3.68$$

then the resultant channel transfer function is given by

$$H_o(f) = \begin{cases} 1\ e^{j\theta(f)} & -B < f < B \\ 0 & \text{elsewhere} \end{cases} \qquad 3.69$$

where B is the baseband bandwidth. However $H_o(f)$ may be obtained either from Equations 3.63 and 3.64 or from Equation 3.69 and is shown in Figure 3.12. Likewise, for the raised-cosine function that is shown in Figure 3.13, it is possible to assume

$$\alpha(f) = \begin{cases} \cos(\frac{\pi}{2} fT)\ e^{j\psi(f)} & -2B < f < 2B \\ 0 & \text{elsewhere} \end{cases} \qquad 3.70$$

The transfer function of the channel is given by

$$H_o(f) = \begin{cases} \frac{1}{2}(1 + \cos(\pi fT))e^{j\theta(f)} & -2B < f \leq 2B \\ 0 & \text{elsewhere} \end{cases} \qquad 3.71$$

where B, as before, is the baseband bandwidth, and T is the sampling period. Also $T = \frac{1}{2B}$ for a Nyquist channel. Both $\alpha(f)$ and $H_o(f)$ are an even function of f in both cases.

★ The impulse response of channel $h_o(t)$ is obtained by applying the inverse Fourier transform to $H_o(f)$, whilst the sampled impulse response of the channel is obtained by applying a discrete Fourier transform (DFT) or fast Fourier transform (FFT) [19,103-107].

The baseband bandwidth is assumed to be 4800 Hz which implies a transmitting symbol rate of 9600 symbols/second. The spectrum of $H_o(f)$ is samples over N samples as shown in Figure 3.14. f_s in Figure 3.14, is the sampling frequency of the periodic response, $H_o(f)$, which may be given by

$$f_s = 2.5 \times \begin{cases} B & \text{for rectangular} \\ 2B & \text{for raised-cosine} \end{cases} \qquad 3.72$$

to satisfy the Nyquist sampling theorem[1-8, 99, 103-109]. The discrete sequence of the periodic response $H_o(f)$ and the corresponding sampled impulse response sequence are linked by the Fourier pair as folllows:-

$$H_m = \sum_{n=0}^{N-1} h_n \, e^{-j2\pi \frac{mn}{N}} \qquad \text{for } m = 0,1,\ldots,N-1 \qquad 3.73$$

$$h_n = \frac{1}{N} \sum_{m=0}^{N-1} H_m \, e^{j2\pi \frac{mn}{N}} \qquad \text{for } n = 0,1,\ldots,N-1 \qquad 3.74$$

where $H_m = H_o(mF)$, $F = \frac{f_s}{N}$, h_n is the sampled impulse response of $H_o(f)$, and $j = \sqrt{-1}$. Tables 3.2 and 3.3 show the complex-valued samples of $H_o(f)$ when N = 32, for rectangular and raised cosine spectra, respectively. The sampled impulse response of $H_o(f)$ is truncated by using a Hamming window[103-105] which is given by

$$\omega(n) = 0.54 + 0.46 \cos\left(\frac{2\pi n}{L}\right) \qquad \text{for } n = 0, 1, \ldots, L-1 \qquad 3.75$$

where L is a constant integer. The resulting sequence of the channel transfer function is given by the z-transform,

$$H_o(z) = h_o + h_1 z^{-1} + \ldots h_{L-1} z^{-L+1} \qquad 3.76$$

The roots of this polynomial are required to be inside the unit circle of the z-plane for minimum phase response[1,109]. Therefore it is necessary to investigate the roots of the polynomial, and if one or more roots are found outside the unit circle of the z-plane they must be replaced by the reciprocal of their complex conjugates[109] in order to achieve the condition of the minimum phase response. The available computer program (see Appendix K) that calculates the roots of the

given polynomial, looks for the roots outside the unit circle and modifies the polynomial by replacing the roots that are outside the unit circle by the reciprocal of their complex conjugates. Tables 3.4 and 3.5 show the roots of Equation 3.76 and their coefficients $\{h_n\}$ after modification for rectangular and raised-cosine shaped channels. Finally, the sampled impulse response sequence of the nonfaded channel is defined by

$$H_o = [\, h_o \; h_1 \; \ldots \; h_{L-1} \,] \qquad 3.77$$

which is a complex-valued sequence.

3.7 A faded digital channel

The assumed data transmission system is shown in Fig. 3.1. The data symbols $\{s_i\}$ are taken to be statistically independent, and equally likely to have values as defined by Equations 3.1. These symbols are used to modulate two carriers in phase quadrature to each other and the modulated signal, which is now either QPSK or QAM, is filtered by the transmitter filter to limit the radiated spectrum. The resulting signal is transmitted over a mobile radio channel which is subjected to Rayleigh fading due to multipath effect. The assumed noise is a white Gaussian noise with zero mean and frequency independent power spectral density which is added to the signal at the output of the transmission link. At the receiving equipment, the spectrum of the received signal is shifted back to the baseband by a process of linear coherent demodulation. The received signal, which is now either QPSK or QAM, is being first filtered to remove as much noise as possible without unduly distorting the data. The reference carriers used for demodulation are adaptively adjusted to the same instantaneous frequency as the received signal carrier, thus eliminating the random frequency offset of the Doppler shift caused by the movement of the mobile units (Section 3.4). This leads to the conclusion that the receiver bandpass filter bandwidth must be made as wide as $2(B + f_{Dm})$ centred about the carrier frequency of the transmitted signal in order to pass the randomly offset signal without distortion[86], where B is the baseband bandwidth and f_{Dm} is the maximum expected Doppler shift. The demodulation process cannot remove the

time-varying distortion (fading) introduced by the mobile radio channel.

The demodulated signal as given by Equation 3.20 is sampled once per received signal symbol at time instant {iT} to give received samples $\{r_i\}$ which are complex-valued, thus

$$r_i = \sum_{\ell=0}^{L-1} s_{i-\ell}\, y_{i,\ell} + u_i \qquad 3.78$$

where $\{s_i\}$ is the data sequence and u_i is the sampled bandlimited waveform of the white Gaussian noise with zero mean and two sided power spectral density of $\frac{1}{2} N_o$. The real and imaginary parts of r_i correspond to the components received over the inphase and quadrature channels respectively. The sampled impulse response of the Rayleigh faded baseband channel is given at time t = iT by

$$Y_i = [\, y_{i,0}\, y_{i,1} \cdots y_{i,L-1} \,] \qquad 3.79$$

The sequence Y_i is complex-valued formed by the linear modulator, transmitter filter, mobile radio link (which consists of mutlipath), receiver filter and linear demodulator. From Equation 3.21 the sequence Y_i may be given by

$$Y_i = H_o\, Q_i \qquad 3.80$$

where H_o is the sequence of the nonfaded linear baseband channel, that has been given by Equation 3.77, and Q_i is (LxL) diagonal matrix of the sequence $\{q_i\}$ which can be obtained from Equation 3.60 or 3.62 by linear or ideal lowpass filter interpolation[8,18], because of the sampling difference. Hence

$$Q_i = \begin{bmatrix} q_i & 0 & 0 & \cdots & 0 \\ 0 & q_{i-1} & 0 & \cdots & 0 \\ 0 & 0 & q_{i-2} & \cdots & 0 \\ 0 & 0 & 0 & \cdots & q_{i-L+1} \end{bmatrix} \qquad 3.81$$

where $q_i = q_{1,i} + j\, q_{2,i}$ and $j = \sqrt{-1}$.

Since $q'_{I,k}$, in Equation 3.60 or 3.62 where I = 1 or 2 and k is the sampling time index of $q'_{I,k}$, is sampled at a rate of 250 samples/second, while the received signal is sampled at data (symbol) rate which is 9600 samples/second, there are about M data samples between two adjacent samples of $q'_{I,k}$, where M is the nearest integer given by $M = \frac{9600}{250} = 38$.

The linear interpolation, however, is performed by connecting each of the two adjacent points of $q'_{I,k}$ (such as $q'_{I,k}$ and $q'_{I,k-1}$) by a straight line as illustrated in Figure 3.15. This line is sampled to give the sequence of the required $\{q_i\}$. such that

$$q_{I,i} = q'_{I,k-1} + i\Delta_{I,k} \qquad 3.82$$

where

$$\Delta_{I,k} = -(q'_{I,k-1} - q'_{I,k})/M \qquad 3.83$$

I is either 1 or 2, k is sampling time index of $q'_{I,k}$ and i is the sampling time index of the received signal. Alternatively, $q_{I,i}$ can be given, as a result of ideal lowpass filter interpolation, by

$$q_{I,i} = \sum_{m=-D}^{D} q'_{I,k+m} \operatorname{sinc}\left(\frac{i-1-m(M-1)}{M-1}\right) \qquad i \leq M \qquad 3.84$$

where I,k,i are as in Equation 3.82, M = 38 and $\operatorname{sinc}(x) = \frac{\sin(\pi x)}{\pi x}$.

Figures 3.16 and 3.17 show the waveform of the real and imaginary parts of q_i that are $q_{1,i}$ and $q_{2,i}$, respectively, when D = 3 and 7. These waveforms were obtained from computer simulation tests for linear and ideal lowpass filter interpolations. The test shows insignificant difference between the two types of interpolations. Therefore linear interpolation is recommended to be used here, since it requires less execution time in computer simulations than the corresponding ideal lowpass filter interpolation.

3.8 Co-channel and Adjacent-channel Interference

The ideas behind frequency planning is effectively to utilize the total frequency band allocated for mobile radio communications. This imposes the use of the same spectrum in some other close service areas (or cells) under a technique of frequency reuse. The factor which limits the frequency reuse is Co-channel Interference[9-11,19,112-122]. Therefore, the co-channel interference depends on the separating distance between the cells using the same frequency range. Moreover, the co-channel interference exists even for reasonable separating distance[112] in a mobile radio environment.

The channels that occupy the frequency range adjacent to the wanted channel spectrum may interfere with wanted signal resulting in Adjacent-channel Interference[9-11,19,43,113-117,123-129]. Also, there is a necessity to increase the cell capacity, but at the same time the adjacent-channel interference has to be kept within desirable limits which requires to separate adjacent channels by a reasonable frequency difference under the concept of channel spacing[125-127,129,130]. Therefore, the adjacent-channel interference depends on the channel spacing in the frequency domain and on the filtering techniques where the deep cutoff results in less interference. Also, adjacent-channel interference can occur even with reasonably large frequency spacing (f_i = 30 kHz) in a mobile radio system.

The effect of both cochannel and adjacent channel interferences can be reduced, and consequently higher capacity may be achieved, by

applying space diversity and/or coding [19,113-120,125-136]. The coding is beyond the scope of this study, whereas space diversity will be considered further in Chapter 7.

However, with cochannel interference it is possible to assume that the interfering signal is given by[10,11,113,116]

$$i_c(t) = p_c(t)e^{j(\omega_c t + \phi_c(t) + \theta_c)} \qquad 3.85$$

where $\phi_c(t)$ is the phase due to modulation, θ_c is the phase difference between the required signal and the interfering signal, $p_c(t)$ is the envelope of the interfering signal which is complex-valued, $\omega_c = 2\pi f_c$, f_c is the carrier frequency. Since the interfering signal $i_c(t)$ is unknown, has random process with zero mean, and occupies the whole spectrum as the spectrum occupied by the wanted signal, therefore it can be treated as noise[9-11,19,43,112-130].

Similarly, in adjacent channel inteference, the interfering signal is assumed to be

$$i_a(t) = a(t) \quad e^{j((\omega_c + \omega_i)t + \phi_a(t) + \theta_a)}$$

$$= p_a(t)\ e^{j(\omega_c t + \phi_a(t) + \theta_a)} \qquad 3.86$$

where $p_a(t) = a(t)e^{j\omega_i t}$, $a(t)$ is the envelope of the interfering signal, $\omega_i = 2\pi f_i$, f_i is the channel spacing (in Hz), $\phi_a(t)$ is the phase due to

modulation, θ_a is the phse diference between the wanted signal and the interfering signal, $\omega_c = 2\pi f_c$, and f_c is the carrier frequency. Hence, Equation 3.86 is identical to Equation 3.85 and both the co-channel and the adjacent channel interferences, have the same properties. Consequently they can be treated as Gaussian noise with zero mean and flat power spectral density over the whole frequency band of interest [9-11,112-125], for the above reason. Therefore, the cochannel and adjacent-channel interferences will be considered as noise in the computer simulation tests implicitly.

ℓ	a_ℓ	$b_{\ell+1}$
0	0.9590	0.7502
1	-0.5740	-0.6302
2	0.3620	0.2844
3	-0.1054	-0.0654
4	0.0131	6.24×10^{-3}

Table 3.1 The coefficients of the 5th order Bessel lowpass digital filter

frequency Hz	real part	imaginary part
0.0	1.0000000000000	0.0000000000000
375.0	0.9927088740290	0.1205366808243
750.0	0.9709418171517	0.2393156654005
1125.0	0.9350162420757	0.3546048886503
1500.0	0.8854560245878	0.4647231740738
1875.0	0.8229838642657	0.5680647490896
2250.0	0.7485107458907	0.6631226608149
2625.0	0.6631226552377	0.7485107508316
3000.0	0.5680647429576	0.8229838684983
3375.0	0.4647231674763	0.8854560280504
3750.0	0.3546048816835	0.9350162447178
4125.0	0.2393156581661	0.9709418189349
4500.0	0.1205366734277	0.9927088749271
4875.0	0.0000000000000	0.0000000000000
5250.0	0.0000000000000	0.0000000000000
5625.0	0.0000000000000	0.0000000000000
6000.0	0.0000000000000	0.0000000000000
6375.0	0.0000000000000	0.0000000000000
6750.0	0.0000000000000	0.0000000000000
7125.0	0.0000000000000	0.0000000000000
7500.0	0.1205366734277	0.9927088749271
7875.0	0.2393156581661	0.9709418189349
8250.0	0.3546048816835	0.9350162447178
8625.0	0.4647231674763	0.8854560280504
9000.0	0.5680647429576	0.8229838684983
9375.0	0.6631226552377	0.7485107508316
9750.0	0.7485107458907	0.6631226608149
10125.0	0.8229838642657	0.5680647490896
10500.0	0.8854560245878	0.4647231740738
10875.0	0.9350162420757	0.3546048886503
11625.0	0.9709418171517	0.2393156654005
12000.0	0.9927088740290	0.1205366808243

Table 3.2 Frequency response samples of a rectangular shaped channel

frequency Hz	real part	imaginary part
0.0	1.0000000000000	0.0000000000000
750.0	0.9782857160406	0.1187853923686
1500.0	0.9153340493365	0.2256095815539
2250.0	0.8174429734258	0.3100152291752
3000.0	0.6942261867978	0.3643580122502
3750.0	0.5574089800405	0.3847516411146
4500.0	0.4193668706126	0.3715266302120
5250.0	0.2915960232456	0.3291438719143
6000.0	0.1833131020387	0.2655748798575
6750.0	0.1003651575490	0.1912298331082
7500.0	0.0445896568470	0.1175732643623
8250.0	0.0137060826037	0.0556077645554
9000.0	0.0017512881333	0.0144231562312
9750.0	0.0000000000000	0.0000000000000
10500.0	0.0000000000000	0.0000000000000
11250.0	0.0000000000000	0.0000000000000
12000.0	0.0000000000000	0.0000000000000
12750.0	0.0000000000000	0.0000000000000
13500.0	0.0000000000000	0.0000000000000
14250.0	0.0000000000000	0.0000000000000
15000.0	0.0017512881333	0.0144231562312
15750.0	0.0137060826037	0.0556077645554
16500.0	0.0445896568470	0.1175723643623
17250.0	0.1003651575490	0.1912298331082
18000.0	0.1833131020387	0.2655748798575
18750.0	0.2915960232456	0.3291438719143
19500.0	0.4193668706126	0.3715266302120
20250.0	0.5574089800405	0.3847516411146
21000.0	0.6942261867978	0.3643580122502
21750.0	0.8174429734258	0.3100152291752
22500.0	0.9153340493365	0.2256095815539
24000.0	0.9782857160406	0.1187853923686

Table 3.3 Frequency response samples of a raised-cosine channel

Rectangular results

Polynomial order 3

Coefficients of polynomial

Real part	Imaginary part
0.516624E+00	0.485374E+00
0.221125E+00	-0.493380E-02
-0.963370E-02	-0.104515E+00
-0.356200E-03	0.595200E-02

Roots of polynomial

Real part	Imaginary part	Modulus
0.578382E-01	0.737297E-03	0.578429E-01
0.200452E+00	0.226371E+00	0.302365E+00
-0.480870E+00	-0.844231E-02	0.480944E+00

The polynomial after modification

Real part	Imaginary part
0.100000E+01	0.000000E+00
0.222579E+00	-0.218666E+00
-0.110860E+00	-0.981492E-01
0.538306E-02	0.646351E-02

Table 3.4 Root test result for a rectangular shaped channel impulse response

Raised-Cosine results

Polynomial order 3

Coefficients of polynomial

Real part	Imaginary part
0.344837E+00	0.171787E+00
0.208211E+00	0.598284E-01
0.365648E-01	-0.250927E-01
0.140800E-03	-0.369750E-02

Roots of polynomial

Real part	Imaginary part	Modulus
0.240616E-01	0.143450E+00	0.145454E+00
-0.125027E+00	0.673627E-01	0.142019E+00
-0.452025E+00	-0.108827E+00	0.464941E+00

The polynomial after modification

Real part	Imaginary part
0.100000E+01	0.000000E+00
0.552991E+00	-0.101986E+00
0.559095E-01	-0.100619E+00
-0.395242E-02	-0.875349E-02

Table 3.5 Root test result for a raised-cosine shaped channel impulse response

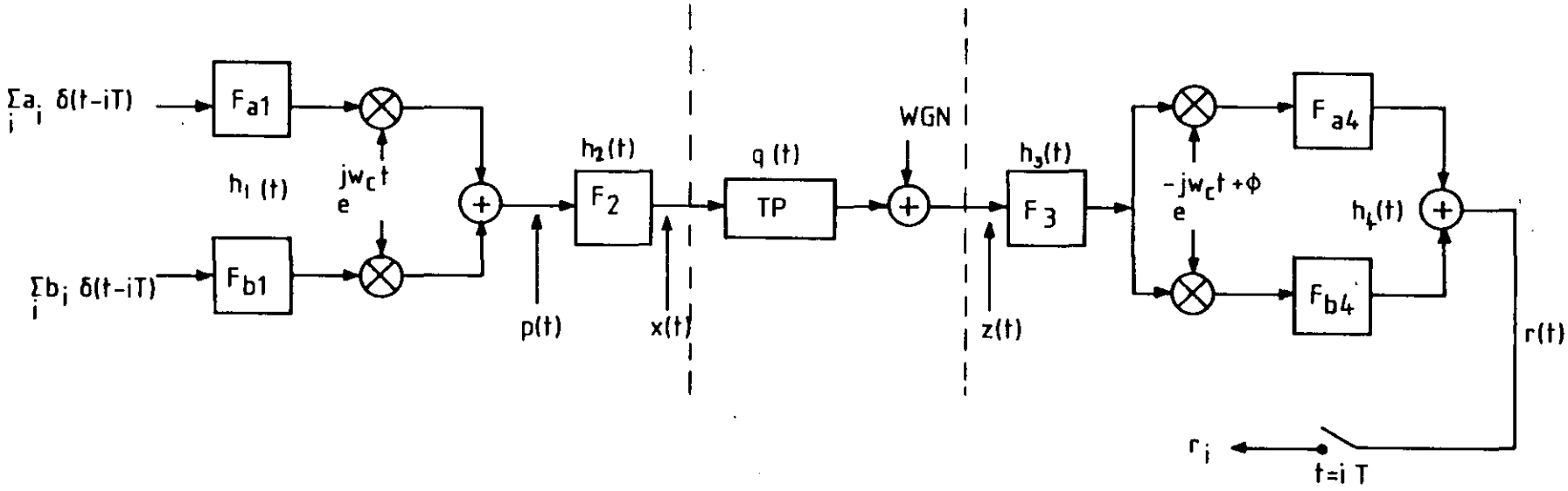

Fig. 3.1. GENERAL MODEL REPRESENTING A QAM or QPSK SYSTEM
WGN: WHITE GAUSSIAN NOISE, TP: TRANSMISSION PATH.

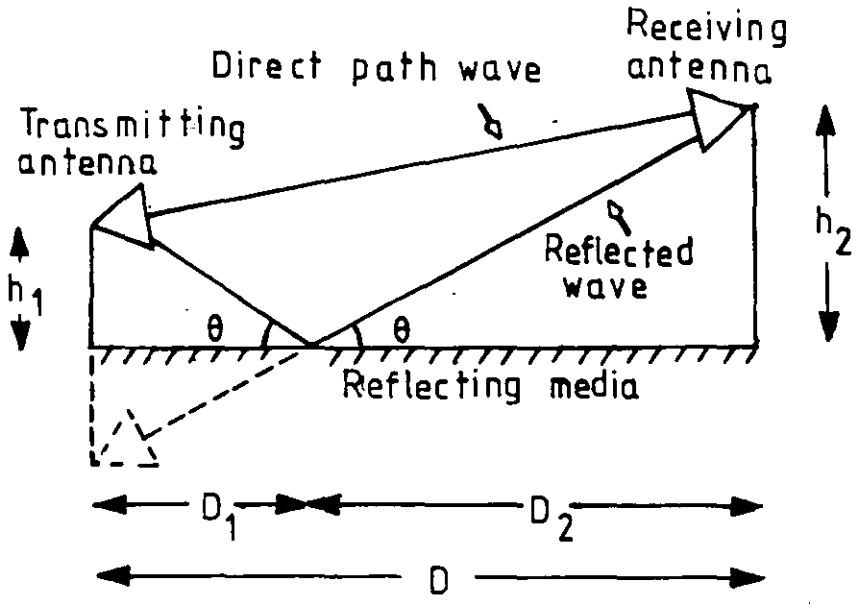

Fig. 3.2 Reflection phenomena

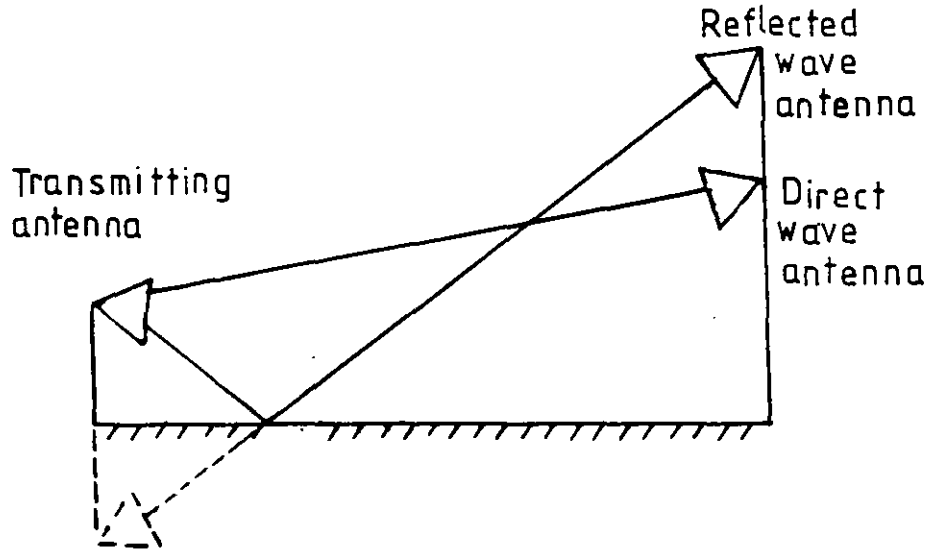

Fig. 3.3 Space diversity

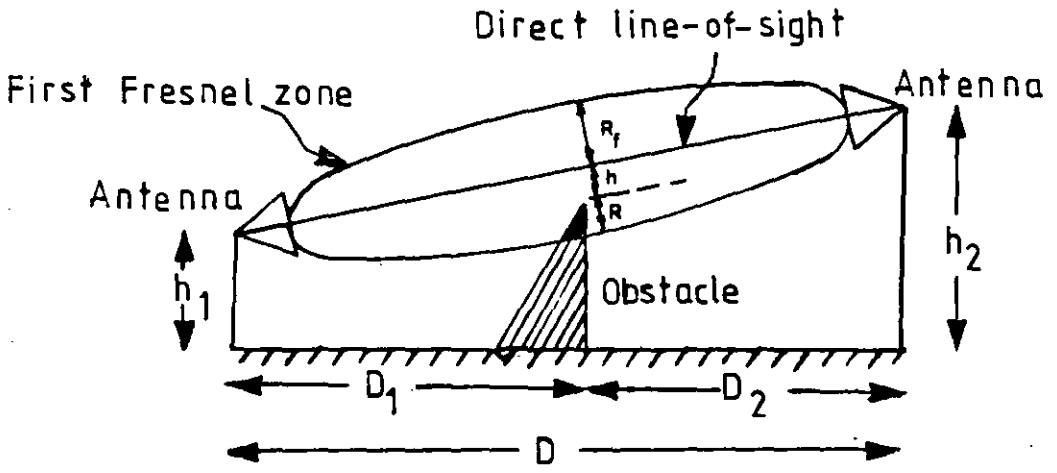

Fig. 3.4 Line-of-sight communication

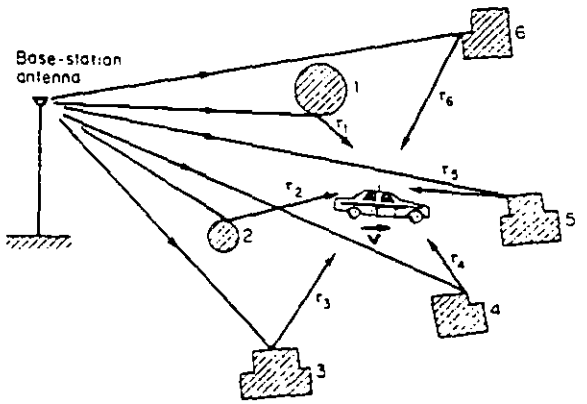

Fig. 3.5 Multipath phenomena in mobile radio communication

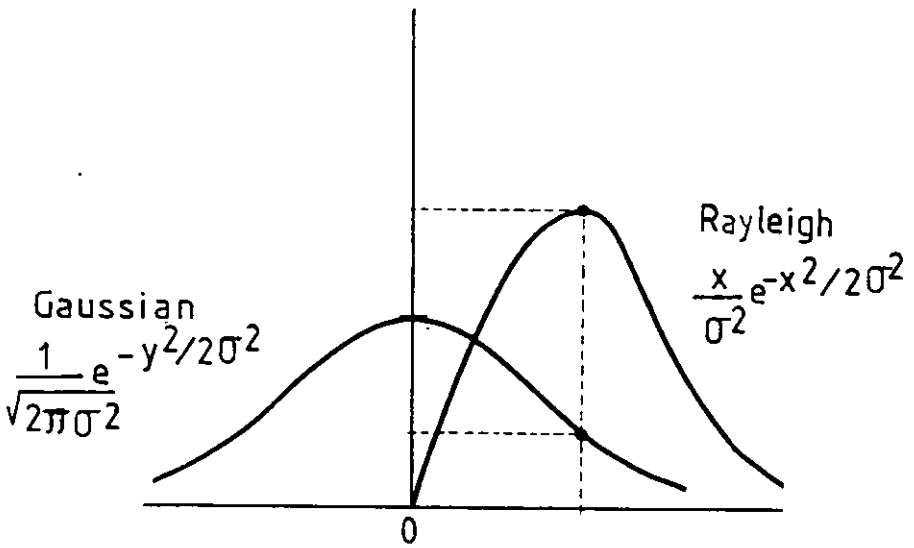

Fig. 3.6 Rayleigh and Gaussian densities

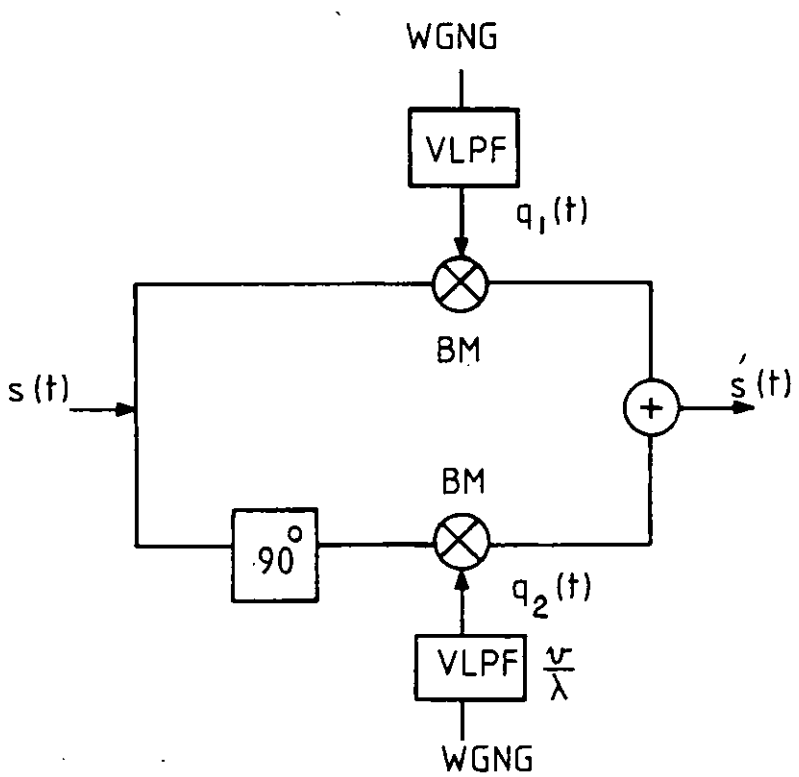

Fig. 3.7 Rayleigh multipath fading simulator

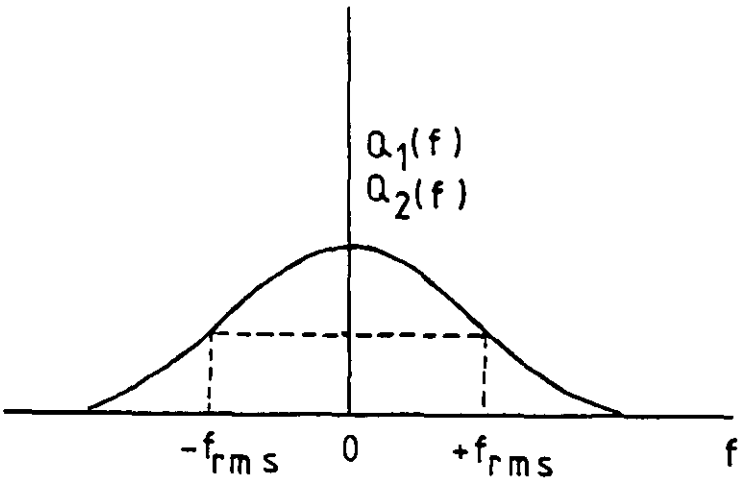

Fig. 3.8 Spectrum of $q_1(t)$ and $q_2(t)$

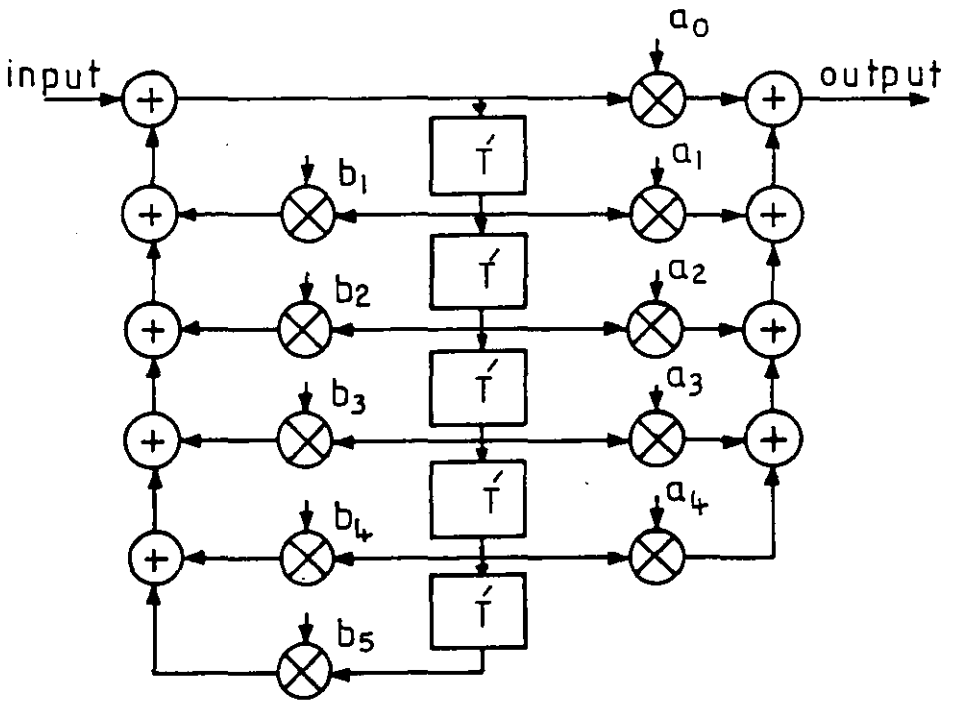

Fig. 3.9 The 5th order Bessel digital lowpass filter used in RMFS

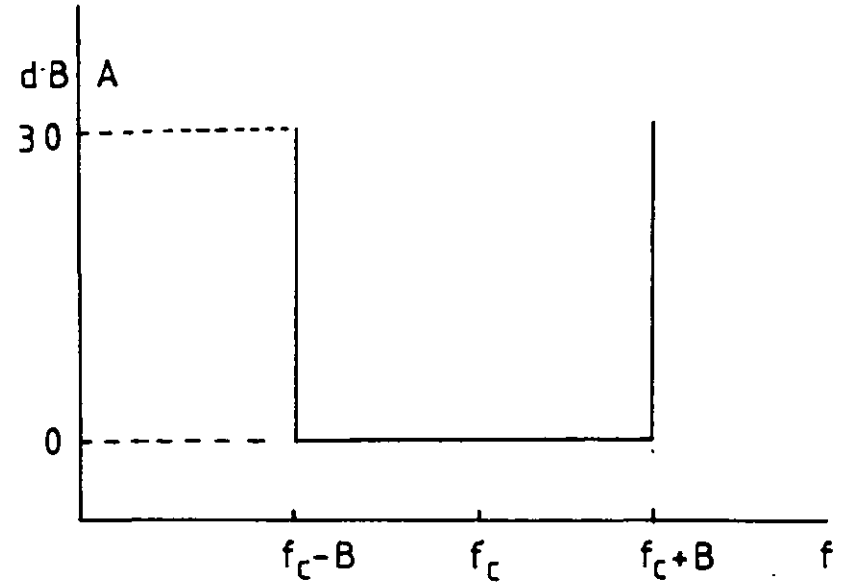

Fig. 3.10 Attenuation characteristic for an ideal channel

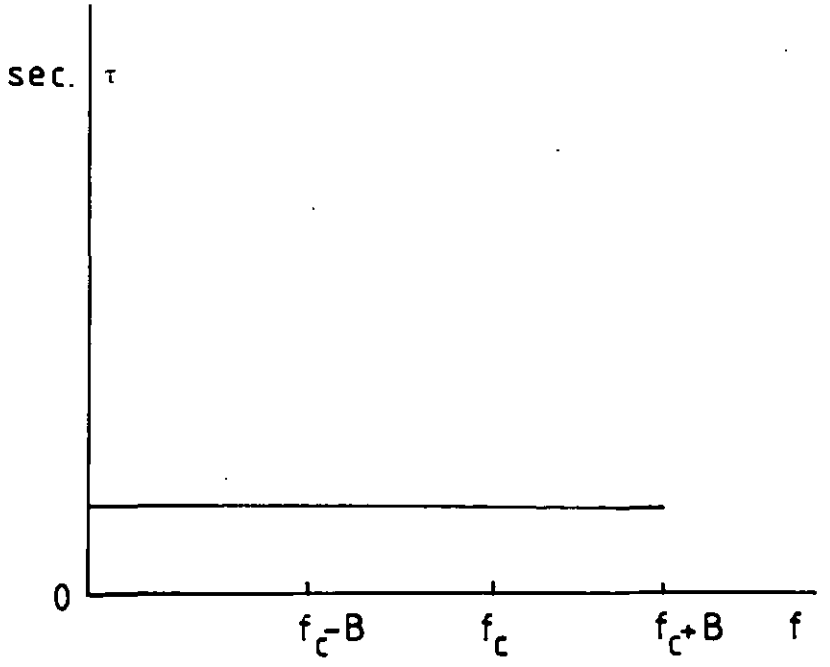

Fig. 3.11 Group-delay characteristic for an ideal channel

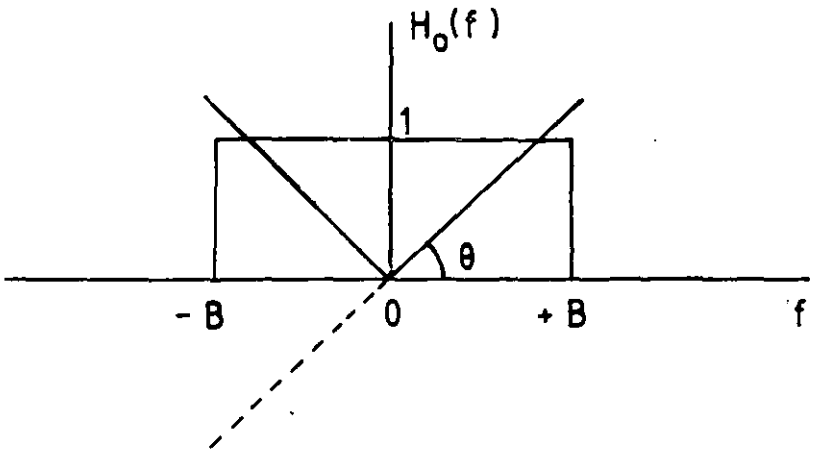

Fig. 3.12 An ideal channel transfer function with rectangular shape and linear phase

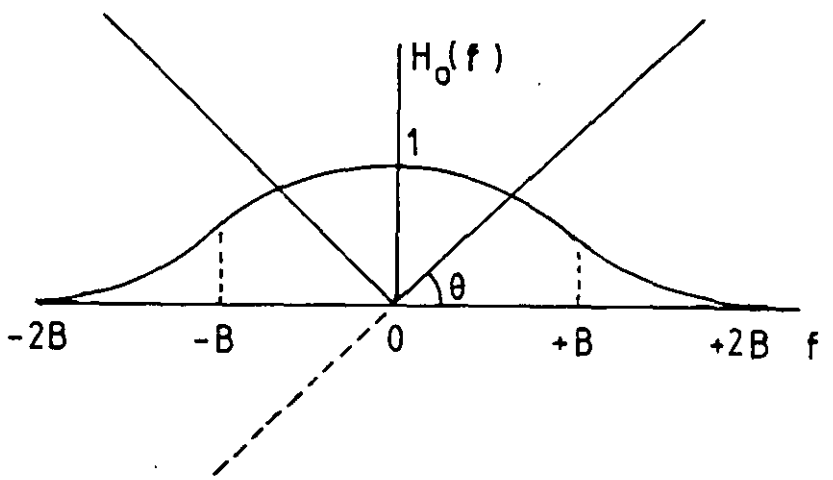

Fig. 3.13 A raised-cosine shaped channel with linear phase

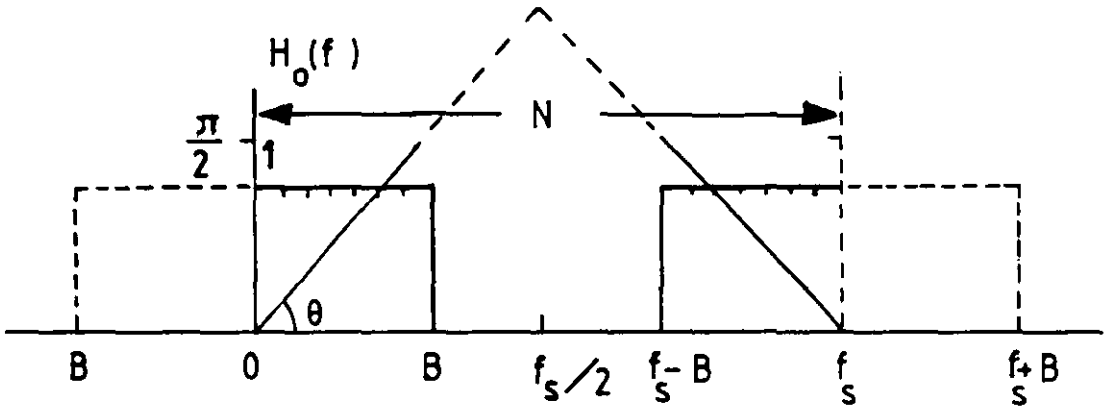

$B = 4800$

$f_s = 12000$ slope of $\theta = \frac{\pi}{2B}$

$N = 32$

Fig. 3.14 The illustration of sampling of $H_o(f)$ spectrum.

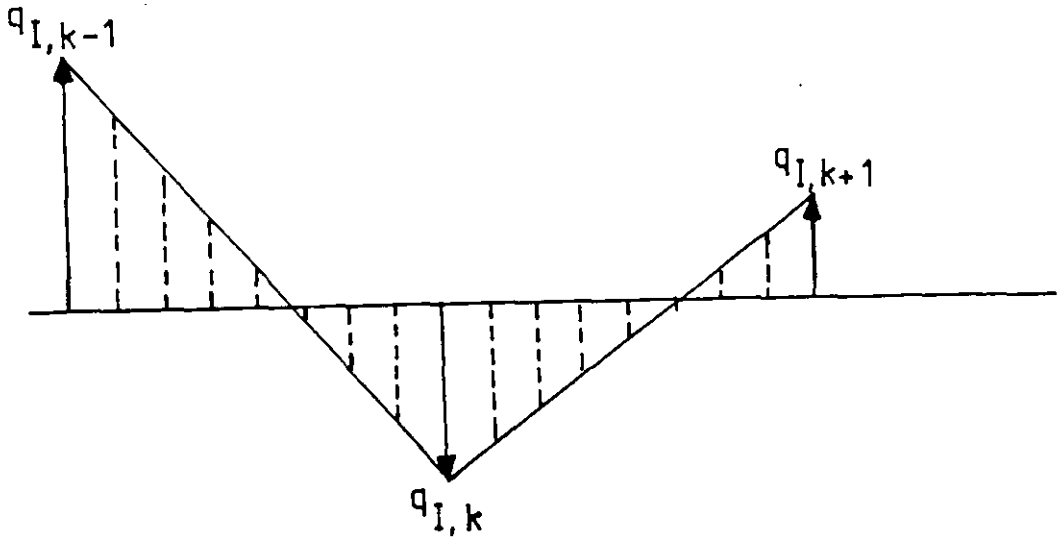

Fig. 3.15 Linear interpolation

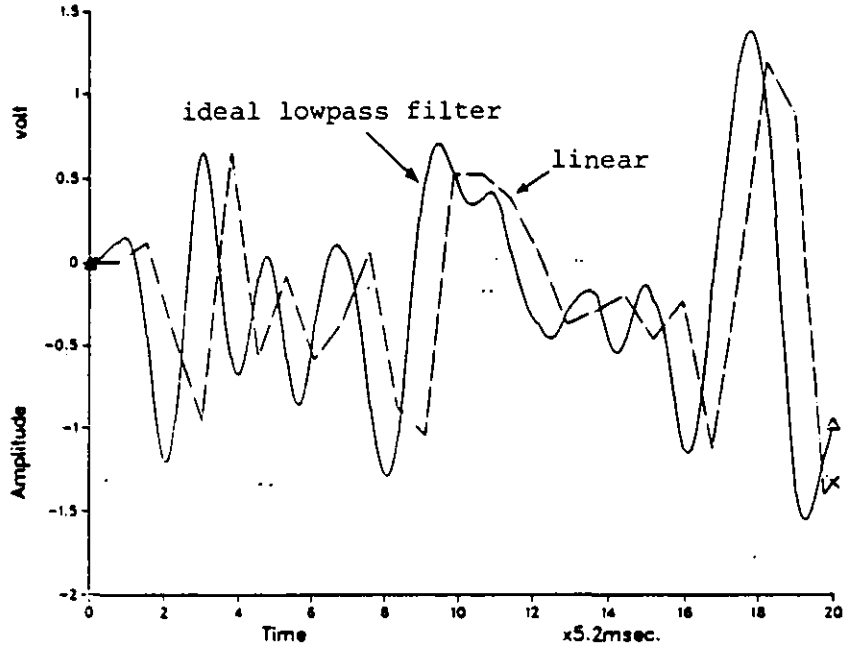

a) Real parts

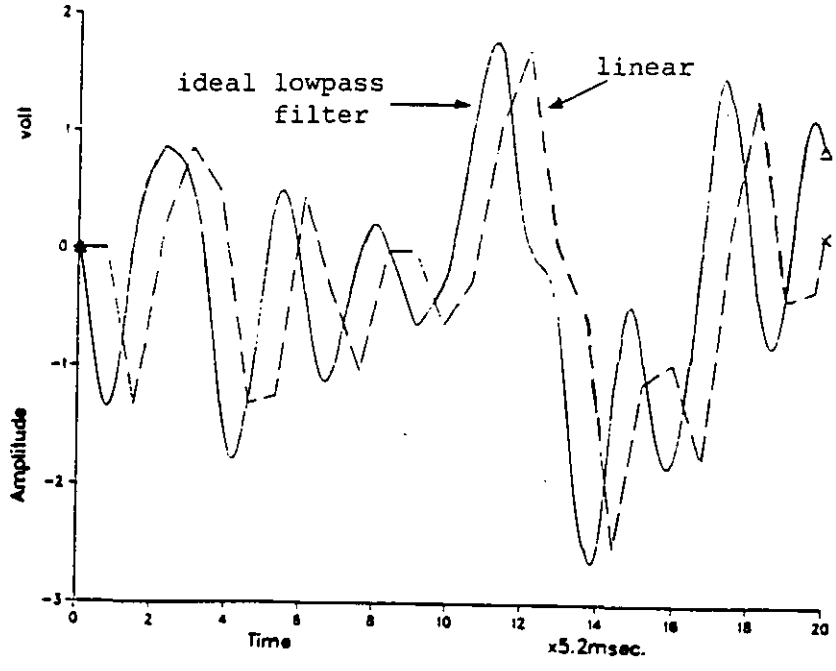

b) imaginary parts

Fig. 3.16 Comparison on linear and ideal lowpass filter interpolation when D = 3

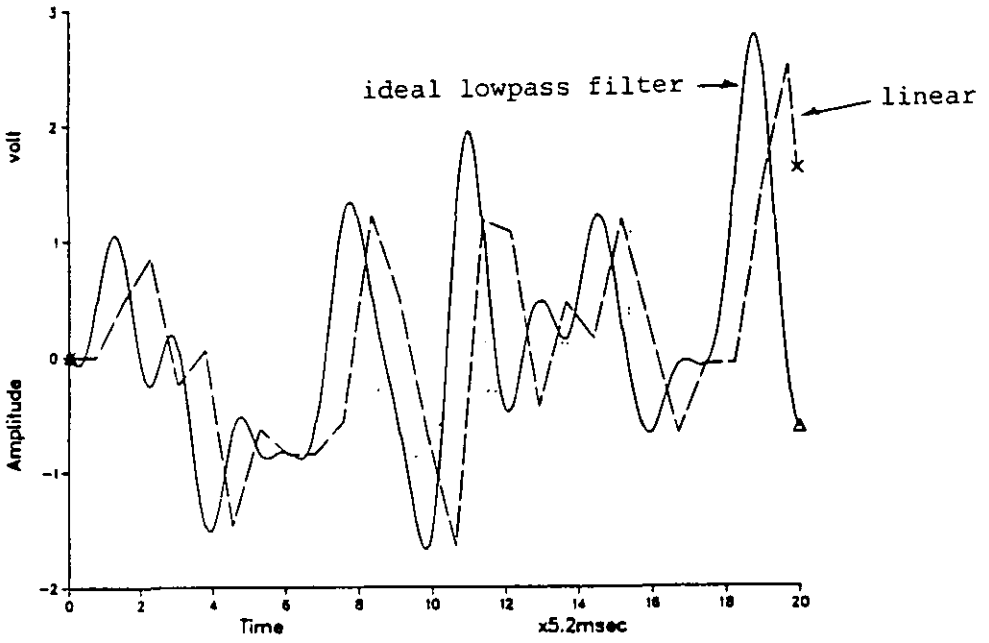

a) Real part

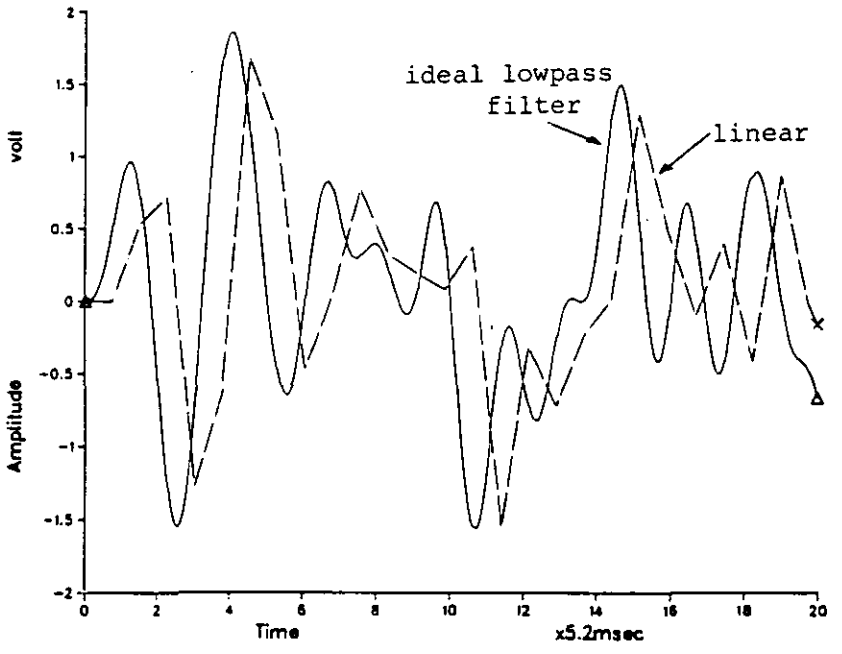

b) Imaginary part

Fig. 3.17 Comparison of linear and ideal lowpass filter interpolation when D = 7.

4. DATA DETECTION

4.1 Introduction

Spectrum utilisation is very important in cellular mobile radio, therefore it is necessary to transmit signal elements at a rate not significantly below the Nyquist rate for the given channel in order to achieve the best available tolerance to additive white Gaussian noise. Under this condition there is always intersymbol interference[1,3,5,109] in the demodulated and sampled data signal at the receiver. In fact, the intersymbol interference can be reduced by using wider bandwidth, but this leads to a wasteful spectrum, besides, more noise will pass through to the detector. However, cancellation of the intersymbol interference can be achieved by a technique called channel equalisation[109,147-150]. Since the transfer function of a linear equaliser is equal to the inverse of the channel transfer function[1,109,147], only nonlinear equaliser is presented here. Because the channel transfer function may have a zero value, when the channel is subjected to a deep fade, which is most likely in mobile radio communications, and subsequently the transfer function of the linear equaliser would tend to infinity. However, the nonlinear equaliser can be protected against divergence in such circumstances in the way described here. The nonlinear channel equaliser is conventionally implemented as a linear feedforward transversal filter fed from the output of a nonlinear threshold level detector[109,147], that is why it is called the nonlinear equalizer.

However, a better tolerance to additive noise can be achieved through the application of a maximum likelihood detector instead of the nonlinear

equaliser and the threshold level detector[109,137-147,152]. Unfortunately, the maximum likelihood detector is very complicated and requires an extremely large number of operations and excessively large storage, even with less severe intersymbol interference[137-142,152,165]. Alternatively, a simpler but somewhat less effective detector, known as near-maximum likelihood detector[151-165], can be used.

Nevertheless, in most of the recent years research, where a near maximum likelihood detector is very widely employed[151-155, 159-165], a channel, which is time-invariant or otherwise very slowly varying with time, is assumed and computer simulation tests have shown that advantages of 3 dB or more can be achieved over the application of conventional nonlinear equalisers[148-155, 157-164]. Furthermore, under the conditions of a time-invariant channel, the near maximum likelihood detector is much less seriously affected (than the conventional nonlinear equaliser), by the use of a suboptimum carrier synchronisation technique and imperfections in channel estimation, even when a poor channel is used[158]. Moreover, the increase in equipment complexity of a modem (modulator-demodulator) using a near-maximum likelihood detector over the corresponding modem using a nonlinear equaliser is not very significant and surprisingly small[158]. Finally, the performance of synchronisation equipments (carrier phase control and channel estimator) are not too much affected by the delay required by the detection process of the near maximum likelihood detector, when the channel is very slowly varying with time.

The situation in mobile radio is, however, quite different, since the channel is rapidly varying with the time and hence the synchronisation

equipment will be much affected by the delay required by a near maximum likelihood detector. Therefore, it is necessary to use less dispersive channel and consequently less delay is required by the near maximum likelihood detector, or otherwise to use other means by which the delay can be reduced such as an adaptive filter[137,147,161]. Only the former method is investigated, here.

The aim of this chapter is to study the performance of different multi-level signals in a mobile radio environment. Four signals are studied here; 16-level QAM, 8-level PSK, 4-level QAM and QPSK (see Chapter 2), by employing both nonlinear equalisers and near maximum likelihood detectors. The investigations of the detection processes have been performed under the assumption of coherent demodulation and correct channel estimation, and the model used here is based on the model described in Chapter 3, which is shown in Figure 4.1. The effect of Rayleigh fading is investigated on the individual systems under different fading rates in the presence of white Gaussian noise. The tests themselves were performed by extensive use of computer simulation methods (Appendix K).

4.2 Basic Assumptions

The model of the mobile channel (based on the model descrined in Chapter 3, Figure 3.1) is shown in Figure 4.1. The information to be transmitted is a sequence of binary digits $\{\alpha_i\}$, where

$$\alpha_i = 0 \text{ or } 1 \qquad 4.1$$

The bit rate and the corresponding multilevel signals for the signals designated as S_1, S_2, S_3 and S_4 are shown in Table 4.1. $\{\alpha_i\}$ are statistically independent and equally likely to have either binary values given in Equation 4.1. Also $\{\alpha_i\}$ are mapped by a suitable mapping technique as shown in Figure 4.2, to generate a sequence of data symbols $\{s_i\}$ that are given by

$$s_i = a_i + j\ b_i \qquad 4.2$$

where $j = \sqrt{-1}$. The values of a_i and b_i are given in Table 4.2 for each individual system. These values are obtained by assuming the same error rate performance[5], for the multilevel signals.

It is assumed that $s_i = 0$ for $i \leq 0$, so that s_i is the i^{th} transmitted data symbol. Also, for $i > 0$, the $\{s_i\}$ are statistically independent and equally likely to have any of their possible values given by Equation 4.2. The basic structure of the modulator and demodulator has been described briefly in Chapter 2. The signals transmitted over the inphase channel of the system are represented by real-valued quantities, and the signals transmitted over the quadrature channel by imaginary-valued quantities, to give a resultant complex-valued baseband signal at both the input and

output of the transmission path, as shown in Figure 4.1. The lowpass filter and linear modulator at the transmitter, the transmission path (which is represented here by a multipath Rayleigh fading simulator (MRFS), as discussed in Chapter 3 for mobile radio communications), and the linear demodulator with lowpass filter at the receiver together form a linear baseband channel (Figure 4.1). The complex-valued impulse response of the channel, y(t), has a finite duration for practical pruposes. Also, y(t) is time variant with a Rayleigh distribution function such that

$$y(t - mT) \neq y(t - nT) \qquad 4.3$$

where both y(t - mT) and y(t - nT) are time shifted versions of y(t) for any integers $m \neq n$. The relationship between the resultant linear baseband channel and the passband channel is considered in Chapter 3.

It is assumed that the interfering noise, including co-channel interference and adjacent channel interference introduced during the transmission is statationary white Gaussian noise, which is added to the data signal at the output of the transmission path, to give a complex-valued baseband noise waveform w(t) at the output of the receiver filter (Chapter 3). The resulting waveform at the output of this filter is, therefore, the complex-valued baseband signal

$$r(t) = \sum_i s_i \, y(t - iT) + w(t) \qquad 4.4$$

The received waveform, r(t), has a bandwidth extending from -B to +B, where B = 4800 Hz, and is sampled once per data symbol at time instants t = iT, to give the received samples

$$r_i = \sum_{\ell=0}^{L-1} s_{i-\ell} y_{i,\ell} + w_i \qquad 4.5$$

where $r_i = r(iT)$, $y_{i,\ell} = y_\ell(iT)$ and $w_i = w(iT)$. The sampling rate is, of course, close to the Nyquist rate, which is 9600 samples/second. The real and imaginary parts of the noise components $\{w_i\}$ in the received sample $\{r_i\}$ are statistically independent Gaussian random variables with zero mean and have the same variance.

The sampled impulse response of the linear baseband channel (Figure 4.1) is given by the L-component row vector (Equation 3.79)

$$Y_i = [y_{i,0}, y_{i,1} \cdots, y_{i,L-1}] \qquad 4.6$$

where $\{y_i\}$ for $\ell = 0$ to L-1, are complex-valued time variant quantities exhibiting a Rayleigh distribution function, that is given by (Equation 3.80)

$$Y_i = H_o Q_i \qquad 4.7$$

H_o (see Equation 3.77) is the sampled impulse response of the unfaded channel, that is given by the L-component row vector

$$H_o = [h_0, h_1, \cdots, h_{L-1}] \qquad 4.8$$

which are complex-valued and formed from the linear modulator, transmitter filter, linear demodulator and receiver filter, by assuming a perfect transmission path (Chapter 3). Q_i is an (LxL) diagonal matrix that is given by (Equation 3.81)

$$Q_i = \begin{vmatrix} q_i & 0 & \cdot & \cdot & \cdot & 0 \\ 0 & q_{i-1} & \cdot & \cdot & \cdot & 0 \\ \cdot & & & & & \cdot \\ \cdot & & & & & \cdot \\ \cdot & & & & & 0 \\ 0 & \cdot & \cdot & \cdot & 0 & q_{i-L+1} \end{vmatrix} \qquad 4.9$$

The real and imaginary parts of $\{q_i\}$ are statistically independent zero mean Gaussian random variables with equal variance, and are obtained by linear interpolation from the original waveform because of the difference between the sampling frequency used for the original waveform and data symbol rate (Chapter 3). Hence,

$$y_{i,\ell} = h_\ell \, q_{i-\ell} \qquad \text{for } \ell = 0 \text{ to } L-1 \qquad 4.10$$

H_o has been derived from an ideal lowpass filter transfer function by using a Fourier approximation and is arranged in such a way so that $h_o = 1$. The z-transform of the sampled impulse response of the linear non-faded baseband channel is given by

$$H_o(z) = h_o + h_1 z^{-1} + \ldots + h_{L-1} z^{-L+1} \qquad 4.11$$

All the roots (zeros) of $H_o(z)$ are chosen, here, to be inside the unit circle of the z-plane, therefore, no adaptive filter is required to minimize phase distortion[109,161]. Consequently, the z-transform of the fading channel is given by

$$Y_i(z) = y_{i,0} + y_{i,1} z^{-1} + \ldots + y_{i,L-1} z^{-L+1} \qquad 4.12$$

which might have roots outside the unit circle of the z-plane due to the effect of fading at some time during the transmission. However, no attempt has been made here to replace the roots that lie outside the unit circle by the complex conjugate of their reciptorcals, as that has been done elsewhere[109,161], in order to minimize the phase distortion. Coherent demodulation and correct estimation of Y_i are assumed here. The delay in the transmission over the baseband channel other than that involved in the time dispersion of the received signal is, for convenience, neglected so $y_{i,\ell} = 0$ for $\ell < 0$ and $\ell > L-1$.

4.3 Non-linear Equalizer (NLEQ)

The detector which uses a non-linear equalizer is called a decision-feedback-detector or decision-directed-cancellation of intersymbol interference. The name "non-linear" comes from the insertion of a non-linear detector in the feedback path of the equalizer[109, 147], as shown in Figure 4.3. However, the received sample that is given by Equation 4.5 can be rewritten as

$$r_i = s_i\, y_{i,0} + \sum_{\ell=1}^{L-1} s_{i-\ell} y_{i,\ell} + w_i \qquad 4.13$$

where $s_i\, y_{i,0}$ is the wanted signal, $\sum_{\ell=1}^{L-1} s_{i-\ell} y_{i,\ell}$ is intersymbol-interference, and w_i is the noise component. It is assumed that the receiver has complete prior knowledge of sampled impulse response of the channel (Equation 4.6), but it does not know anything about either the sequence $\{s_i\}$ actually transmitted, nor the value of w_i. It does, however, know all possible values of s_i.

Figure 4.3 shows the conventional way of implementing the non-linear equalizer[109,147]. The signal at the output of the filter is subtracted from the corresponding received sample at the output of the multplier to give an input signal to the detector. The intersymbol-interference is removed from the detector input signal by quantized feedback correction.

However, in a mobile radio environment, the channel is time varying with a Rayleigh distribution function. So, $y_{i,0}$ might have zero value when the received signal is subjected to a deep fade. Accordingly, each

component of the sampled impulse response of the channel might have a zero value at the same time; this is why a linear equalizer is not recommended for use, since the transfer function is equal to the inverse of the channel transfer function[109,147].

However, the non-linear equalizer can be realized as shown in Figure 4.4, in which a comparator with -40 dB threshold is introduced in the system as a guard controller. When the absolute value of $y_{i,0}$ decrease beyond -40 dB, the comparator injects in a signal with -40 dB. The short term fading may last for up to five data symbol periods through which the result of wrong decision is most likely and consequently, the probability of error will be high. Nevertheless, the taps gain of linear-feedforward filters have the same values as $y_{i,\ell}$, for ℓ=1,2, ..., L-1, as shown in Figure 4.5. The signals shown are those at time instants t = iT, and s'_i can have all the possible values of s_i. The detector input signal is given by

$$d_i = (r_i - z_i)/y'_{i,0} \qquad 4.14$$

where $y'_{i,0} = y_{i,0}$ or, otherwise, $y'_{i,0}$ = (-40 dB)

$$\text{and} \qquad z_i = \sum_{\ell=1}^{L-1} s'_{i-\ell} y_{i,\ell} \qquad 4.15$$

is the output signal from transversal filter. s'_i is the detected value of s_i. It is assumed that the $\{s'_{i-\ell}\}$ for ℓ=1,2, ..., L-1, have been correctly detected so that $s'_{i-\ell} = s_{i-\ell}$ for each value of ℓ. Then z_i is equal to the intersymbol interference in r_i, and hence

$$d_i = s'_i + w_i/y'_{i,0} \qquad 4.16$$

where s'_i is the wanted signal and $w_i/y'_{i,0}$ is the noise component. Therefore, the nonlinear equalizer removes the intersymbol interference without changing the signal-to-noise ratio[109,147]. Now the detector compares d_i with the appropriate level or levels depending upon which type of signal is being transmitted. If s'_i is correctly detected, then the receiver knows z_{i+1} which will be used to cancel the intersymbol interference from the r_{i+1} at time instant $t = (i+1)T$ to give

$$d_{i+1} = s'_{i+1} + w_{i+1}/y'_{i+1,0} \qquad 4.17$$

It is clear that so long as the received signal-elements are correctly detected, their intersymbol interference in the following elements is eliminated and consequently the channel is correctly equalized.

To start the process of non-linear equalisation, a known sequence of more than L $\{s_i\}$ is transmitted and the intersymbol interference introduced by the received signal-elements is cancelled automatically, without the detection of the corresponding $\{s'_i\}$. The channel is now correctly equalized, and the receiver is ready to detect the following signal elements by cancelling the intersymbol interference and using a threshold level detector. An alternative method of implementing the non-linear equalizer will be referred to in Section 4.5, which deals with near-maximum likelihood detectors.

4.4 Viterbi Algorithm Detector (VAD)

Let R_g, S_g and W_g be the g-components row vectors whose i^{th} components are r_i, s_i and w_i respectively, for i=1, 2, ..., g. Also, let X_g, Z_g and U_g be the g-components row vectors whose i^{th} components are x_i, z_i and u_i respectively, for i=1, 2, ..., g, where x_i can have any one of the K possible value of s_i and z_i is given by

$$z_i = \sum_{\ell=0}^{L-1} x_{i-\ell} \, y_{i,\ell} \qquad 4.18$$

Consequently, u_i is the possible value of w_i satisfying

$$r_i = z_i + u_i \qquad 4.19$$

S_g is equally likely to have any of its K^g possible values and X_g is the maximum likelihood sequence that minimizes $|U_g|^2$,which is given by

$$|U_g|^2 = |u_1|^2 + |u_2|^2 + \ldots + |u_g|^2 \qquad 4.20$$

where $|u_i|$ is the absolute value of u_i.

The receiver, which uses a VAD, holds in its memory K^L maximum-likelihood vectors $\{X_i\}$ corresponding to the K^L different possible combinations of $x_{g-\ell+1}$, $x_{g-\ell+2}$, ..., x_g, bearing in mind that g>>L. The receiver also stores with each stored vector X_g the corresponding value of $|U_g|^2$ that satisfies Equation 4.20. The true maximum-likelihood vector X_g is the one

of the stored vectors $\{X_g\}$ for which $|U_g|^2$ is minimum[136,137,156].

On the receipt of the sample r_{g+1}, each of the stored vectors $\{X_g\}$ forms a common part of K vectors $\{X_{g+1}\}$, which have been obtained by expansion of each of the stored vectors $\{X_g\}$. Furthermore, each of the $\{X_{g+1}\}$ that are originated from the corresponding $\{X_g\}$, have different possible values of x_{g+1}. Then each value of $|U_{g+1}|^2$ is calculated as

$$|U_{g+1}|^2 = |U_g|^2 + |(r_{g+1} - z_{g+1})|^2 \qquad 4.21$$

using the appropriate stored value of $|U_g|^2$.

The VAD now selects the K^L vectors $\{x_{g+1}\}$ that are associated with the smallest value of $|U_{g+1}|^2$, from all K^L possible combinations of vectors of x_{g-L+2}, x_{g-L+3}, ..., x_{g+1}, and stores them together with the value of $|U_{g+1}|^2$. One of the vectors is the true maximum-likelihood vector X_{g+1}. The process continues in this way.

Of course, no decision can take place on the value of s_i, when all $\{s_i\}$ are detected simultaneously from R_g, until the whole message has been received. Practically, as much delay as possible is introduced before an effective decision is made on the value of any of s_i and s_{g-n+1} is now detected as the value of x_{g-n+1} in the true maximum-likelihood sequence X_g, that is associated with the minimum $|U_g|^2$, where n is a large enough integer such as $n>>3L$[152]. When the receiver detects the signal element s_{g-n+1}, it does not reconsider the values of x_{g-n}, x_{g-n-1}, ..., and so on.

Hence in this case, the receiver stores the corresponding K^L n-component vectors $\{Q_g\}$ instead of storing K^L g-component vectors $\{X_g\}$ [152,156], where

$$Q_g = [x_{g-n+1} \quad x_{g-n+2} \cdots\cdots x_g] \qquad 4.22$$

so that Q_g is formed from the last n components of the corresponding X_g.

Clearly, the receiver keeps in its memory K^L n-component vectors$\{Q_g\}$ and K^L values$\{|U_g|^2\}$and performs K^{L+1} squaring operations in order to detect each of the received signal elements. The terms $\{x_{g-\ell}y_{g,\ell}\}$ that are involved in the evaluation of $\{|U_g|^2\}$ and, consequently, the selection of the $\{Q_g\}$, have already been determined and kept in the store. The sampled impulse response of the channel must, of course, be updated regularly, which further increases complexity. Also, when L>>1, both the amount of storage required and the number of operations per received signal-element become excessively large. Alternatively, various techniques known as near-maximum-likelihood techniques[151,165] have recently been developed for considerably reducing the number of operations, as well as the amount of storage involved in the detection process. Two of these methods of near-maximum-likelihood detection will be discussed here and applied to the four multilevel signals introduced earlier.

4.5 Near Maximum Likelihood Detectors

This section deals with detection processes using near maximum likelihood detectors, that are designated as D1, D2 and D3. These detectors are arranged such that:-

i) Detector D1 is employed with signals S1 and S4, and the corresponding systems are abbreviated as S1D1 and S4D1, respectively.

ii) Detector D2 is employed with signal S4 and the corresponding system is abbreviated as S4D2.

iii) Detector D3 is employed with signals S2 and S3 and the corresponding systems are abbreviated as S2D3 and S3D3, respectively.

The detector D3 resembled detector D1 in its operations, but it deals with the phase factor of the maximum likelihood vector as well as with the vectors themselves.

4.5.1 Detector D1

Just prior to the receipt of the sample r_g, the detector holds in its store m different n-component vectors $\{Q_{g-1}\}$, where

$$Q_{g-1} = [x_{g-n-1} \; x_{g-n} \; \ldots \; x_{g-1}] \qquad 4.23$$

and x_i can take on any of K possible values of s_i, where K = 4 for signal

S1 and K = 16 for signal S4. Moreover, it is assumed here that $n \geq L$. Each vector, Q_{g-1}, is formed by the last n-component of the corresponding (g-1)-component vector

$$X_{g-1} = [x_1 \; x_2 \; . \; . \; . \; . \; x_{g-1}] \tag{4.24}$$

which represents a possible received sequence of the data-symbols $\{s_i\}$. Associated with each vector X_{g-1}, is the corresponding $|U_g|^2$, which is called hereinafter the "cost" associated with X_{g-1}, such that

$$|U_{g-1}|^2 = \sum_{i=1}^{g-1} |u_i|^2 \tag{4.25}$$

where

$$u_i = r_i - z_i \tag{4.26}$$

$$z_i = \sum_{\ell=0}^{L-1} x_{i-\ell} y_{i,\ell} \tag{4.27}$$

$x_i = 0$ for $i \leq 0$ and $|u_i|$ is the absolute value (modulus) of u_i. $|U_{g-1}|^2$ is also taken to be the cost of the corresponding vector Q_{g-1}. Under the assumed conditions and for the given received sequence of $\{r_i\}$, it can be shown that the sequence X_{g-1}, that associated with the smallest cost (the value of $|U_{g-1}|^2$), is the more likely to be correct, over all the combinations of the possible value of $\{x_i\}$ (151-155, 157-165).

On the receipt of r_g, each of the m stored vectors $\{Q_{g-1}\}$ is expanded into K (n+1)-component vector $\{P_g\}$, where

$$P_g = [x_{g-n-1} \quad x_{g-n} \ldots x_g] \qquad 4.28$$

The first n-component of the mK vectors $\{P_g\}$, that are derived from the corresponding m vectors $\{Q_{g-1}\}$, are as in the original Q_{g-1} and the last component x_g takes on the K different values, as given in Table 4.2 and shown in Figure 4.2a and 4.2b for signals S1 and S4 respectively. The cost of each vector P_g is calculated as[156]

$$|U_g|^2 = |U_{g-1}|^2 + |r_g - z_g|^2 \qquad 4.29$$

From the mK vectors $\{P_g\}$, originating from m vectors $\{Q_{g-1}\}$ with the smallest costs, the detector selects the vector P_g with smallest cost $|U_g|^2$ and takes the value of the first component x_{g-n-1} of this vector as the detected value, s'_{g-n-1}, of the data symbol s_{g-n-1}. Also, from the remaining (mK-1) vectors $\{P_g\}$, the detector next selects (m-1) vectors, $\{P_g\}$, with the next successive smallest cost $\{|U_g|^2\}$ to give a total of m selected vectors $\{P_g\}$. Of course, no vector is selected more than once in order to ensure that no two or more of them can subsequently become the same. All the non-selected vectors $\{P_g\}$ are now discarded, and the first component, x_{g-n-1}, of each of the remaining m vectors $\{P_g\}$ (including that with the most smallest cost) is omitted, to give the corresponding m n-component vectors $\{Q_g\}$.

The detector has a total of m n-component vectors, which are stored together with their costs$\{|U_g|^2\}$ and is ready, on the receipt of the received sample r_{g+1}, to repeat the procedure just described.

To start off transmission, a known sequence of length more than n must be sent from which the detector generates m n-component vectors, $\{Q_o\}$. Accordingly, m different n-component vectors, $\{Q_o\}$, have been assumed to start up the procdure, one of them is the most likely to be correct with zero cost ($|U_o|^2 = 0$) and the remaining (m-1) vectors, $\{Q_o\}$, with very high cost values.

4.5.2 Detector D2

This detector is a development of detector D1, with double expansion technique applied in signal S4, to give an arrangement involving less storage and a smaller number of operations per received sample[155,160].

On the receipt of r_g, each of the m different n-component vectors $\{Q_{g-1}\}$ is expanded into 4m (n+1)-component vectors $\{P_g\}$. The fist n-components of the four $\{P_g\}$, that are derived from any one of Q_{g-1}, are as in the original $\{Q_{g-1}\}$ and the last component x_g takes on the four different values $\pm 2 \pm j2$[155,160], where $j = \sqrt{-1}$. The cost of each vector P_g is now evaluated as

$$c_g = |U_{g-1}|^2 + |r_g - z_g|^2 \qquad 4.30$$

where z_g is obtained according to Equation 4.27. From the 4m vectors $\{P_g\}$, originating from the m vectors $\{Q_{g-1}\}$ with the smallest costs, the detector selects m vectors $\{P_g\}$ with the smallest costs, c_g and different values of the last component, x_g. The detector next expands each of the selected m vectors $\{P_g\}$ into four $\{P_g\}$, whose first n components are again as in the original vector Q_{g-1}, and to the given value of the last component x_g (which is now one of the four values $\pm 2 \pm j2$) the detector adds the four different values $\pm 1 \pm j$. The cost of each of the expanded vectors is evaluated as

$$|U_g|^2 = |U_{g-1}|^2 + |r_g - z_g|^2 \qquad 4.31$$

x_g can now have any of the 16 different possible values of s_g. The detector next selects one of the 4m vectors $\{P_g\}$ with the smallest cost $|U_g|^2$ and takes the value of the first component, x_{g-n-1}, of this vector as the detected value, s'_{g-n-1}, of the data symbol s_{g-n-1}. Also, from the remaining (4m-1) vectors $\{P_g\}$, the detector selects (m-1) vectors $\{P_g\}$ with the next successive smallest costs $\{|U_g|^2\}$ to give a total of m selected vectors, $\{P_g\}$. Of course, no vector is selected more than once to prevent merging (becoming the same). All the non-selected vectors are now discarded, and the first component x_{g-n-1} of each of the remaining (selected) m vectors $\{P_g\}$ (including that with the most smallest cost) is omitted, to give the corresponding m different n-component vectors $\{Q_g\}$. The detector stores these vectors together with their costs $\{|U_g|^2\}$ and is ready to detect the following samples. The initialisation procedure is identical to that discussed for detector D1.

4.5.3 Detector D3

This detector, which is employed with the PSK signals S2 and S3, is identical to detector D1 and similar assumptions may be used. Since in signals S2 and S3, the information is carried by the phase angle of received signal, the data symbol and phase factor (which is defined in Chapter 2) will be treated here as a one to one correspondence. The arrangement of the detector is as follows:-

Just prior to the receipt of the sample r_g, the detector stores in its memory (store) m different n-component vectors $\{Q_{g-1}\}$, each one of them is defined according to Equation 4.23 and is corresponding to a phase factor sequence.

$$\phi_{g-1} = [\phi_{g-n-1} \quad \phi_{g-n} \cdots \quad \phi_{g-1}] \tag{4.32}$$

where ϕ_i can take on any of K possible values of k_i that are given by

$$k_i = 0, 1, \ldots, K-1 \tag{4.33}$$

(see also Chapter 2). The value of x_i, for each vector, is given by[5]

$$x_i = A(\cos(\frac{2\pi\phi_i}{K} + \lambda_o) + j \sin(\frac{2\pi\phi_i}{K} + \lambda_o)) \tag{4.34}$$

Hence x_i can take any one of the possible values of s_i such as

$$s_i = A(\cos(\frac{2\pi k_i}{K} + \lambda_o) + j \sin(\frac{2\pi k_i}{K} + \lambda_o)) \tag{4.35}$$

when K = 4, $A = \sqrt{2} = 1.414$ and $\lambda_o = \frac{\pi}{K}$ for signal S2, and when K = 8,

$A = 2.613\ \lambda_o = 0$ for signal S3 (see also Table 4.2). As in detector D1, each vector is formed by the last n components of the corresponding (g-1)-component vector X_{g-1} (that is also defined by Equation 4.24), which is corresponding to a phase factor sequence

$$\Xi_{g-1} = [\phi_1\ \phi_2\ \cdots\ \phi_{g-1}] \qquad 4.36$$

On the receipt of r_g, each of the m stored vectors $\{Q_{g-1}\}$, whose corresponding phase factors are ϕ_{g-1}, is expanded into K (n+1)-component vectors $\{P_g\}$, where each one of them corresponds to a phase factor sequence

$$\Psi_g = [\phi_{g-n-1}\ \phi_{g-n}\ \cdots\ \phi_g] \qquad 4.37$$

The first n-components of the mK vectors, that are derived from the corresponding m vectors $\{Q_{g-1}\}$, are as in the original and the last component is x_g, whose phase factor, ϕ_g, takes on K different values. The cost of each vector P_g is evaluated according to Equation 4.29, bearing in mind now all x_g are calculated according to Equation 4.34, at i = g. Also, z_i is calculated according to Equation 4.27.

From the mK vectors, $\{P_g\}$, originating from m vectors, $\{Q_{g-1}\}$, with the smallest costs, the detector selects the vector P_g with the smallest cost, $|U_g|^2$, and takes the value of the first component, x_{g-n-1}, whose phase factor is ϕ_{g-n-1}, as the detected data symbol from which the received information is regenerated. Also, from the remaining (mK-1) vectors, $\{P_g\}$, the detector next selects (m-1) vectors, $\{P_g\}$, with the next smallest

costs, $\{|U_g|^2\}$, to give a total of m selected vectors, $\{P_g\}$. No vector is selected more than once, and all of the non-selected vectors are discarded. The first component x_{g-n-1} with the corresponding phase factor of each of the remaining m vectors, $\{P_g\}$, (including that with the smallest cost) are omitted to give the corresponding m n-component vectors $\{Q_g\}$. The detector now stores these vectors together with their costs, $\{|U_g|^2\}$, and is ready to detect the next received sample. The start of transmission procedure is identical to that of detector D1.

All of the above near maximum likelihood detectors (D1, D2 and D3) become nonlinear equalisers when m = 1 and n = 0, where m is the number of stored vectors n is the required delay.

4.6 Computer Simulation Tests and Results

Computer simulation tests have been carried out on the different arrangements described here, to compare between different systems in a mobile radio environment in the presence of a white Gaussian noise. Any adjacent channel interference and co-channel interference are assumed to be included in the white Gaussian noise function (for more detail see Chapter 3). The two channels used here are derived from an ideal filter transfer function with rectangular and raised-cosine shapes by Fourier approximation methods. (Chapter 3). The two channels are subjected to Rayleigh fading, as discussed earlier.

Before generating the data sequence, two Gaussian random variables, ($q'_{1,N}$ and $q'_{2,N}$) with zero mean and the same variance, are generated and lowpass filtered by a 5th order Bessel digital filter in order to use them in the Rayleigh fading simulator (Figure 3.7, Chapter 3), which is the representation of the transmission path. The variance of these two variables are chosen such that the average signal power at the output of the transmission path is equal to its average input power when a very long sequence (say about 50000 symbols) is used for such tests. Also, these two variables are sampled at a rate of 250 samples/s while the input signal frequency (Doppler frequency) f_D is selected to be 100, 75, 50 and 25 Hz. The received signal, Figure 4.1, is sampled once per data symbol that is 9600 symbol/s. Since the difference between the two sampling frequencies (250 and 9600) is large, the values of $\{q_i = q_{1,i} + j\, q_{2,i}\}$ are obtained from the original two variables $q'_{1,N}$ and $q'_{2,N}$, just described (see also

Chapter 3), by linear interpolation, where $q_{1,i}$ and $q_{2,i}$ are the real and imaginary part of q_i, $j = \sqrt{-1}$, and $q'_{1,N}$ and $q'_{2,N}$ are the real and imaginary parts of the complex-valued sequence q'_N obtained from the output of the lowpass filters, used in the Rayleigh fading simulator. A group of data symbols sequences are incorporated in-between two adjacent variables, q'_N and q'_{N+1}, in the form of a block, as shown in Figure 4.6. Each block contains a sequence of $[s_1, s_2, \ldots\ldots, s_I]$ which must be initialised by a sequence $[s_{-n+1}, s_{-n+2}, \ldots, s_0]$ where I = 38 (=9600/250) and n is the maximum delay required by the corresponding detector, and $L \leq n < 38$. L is the number of components of the sampled impulse response of the channel, in Equation 4.6. However, at the end of each block q'_{N+1} is shifted down to replace q'_N and the new sample q'_{N+2} is created to replace q'_{N+1}. At the same time the sequence $[s_1, s_2, \ldots, s_I]$ is shifted down such that the last n-components are used to replace $[s_{-n+1}, s_{-n+2}, \ldots, s_o]$ which will be used to initialize the new sequence. The shifting procedure takes place as $s_{-\ell} = s_{I-\ell}$, for $\ell = 0, 1, \ldots, n-1$. Furthermore, a new symbol sequence is generated, by mapping the bit-information to be transmitted using a suitable mapping technique (Section 4.2), to replace the old sequence $[s_1, s_2, \ldots, s_I]$, and the test completed in this way for each value of signal to noise ratio (SNR).

In order to calculate the signal to noise ratio, the average signal and noise powers are calculated as follows:-

Average signal power,

$$P_s = \frac{1}{K} \sum_{i=1}^{K} |s_i \, q_i|^2 \qquad 4.38$$

and average noise power (from Equation 4.5)

$$P_n = \frac{1}{K} \sum_{i=1}^{K} |w_i|^2 \qquad 4.39$$

where K = 50000 and $|x|$ is the modulus of x. Therefore, the signal to noise ratio is given by

$$SNR = 10 \log_{10} (P_s/P_n) \quad dB \qquad 4.40$$

while the bit error rate is given by

$$BER = \frac{B_e}{B_t} \qquad 4.41$$

where B_e is the number of error bits in the received signal and B_t is the total number of transmitted bits. The received bit-information is obtained by mapping back the detected symbols by the same mapping technique used at the transmitter (Section 4.2, Chapter 2).

The nonlinear equaliser and near-maximum likelihood detectors are tested according to the algorithms described here, for different multilevel signals in a mobile radio environment. Also, the number of vectors m, used in the near maximum-likelihood detectors, has been chosen as 4, because when m = 1 the near-maximum likelihood becomes a nonlinear equaliser and for m > 4 the improvement, of near-maximum likelihood over the nonlinear equaliser in a less dispersive channel, becomes insignificant.

The computer simulation programs are listed in Appendix K.

The computer simulation test results are shown in Figures 4.7 to 4.20. Figure 4.7 shows the comparison between the four signals (4-level QAM and QPSK, 8-level PSK and 16-level QAM) where a nonlinear equaliser and near maximum likelihood detector used in perfect and nonfaded channel conditions (idle channel condition), and with channel-r (rectangular shaped channel). The abbreviations used refer to the systems described in Section 4.3 and 4.5, with more details when the nonlinear equaliser is used. Differential coding is used in 4- and 8-level PSK signals. Since the channel used is derived from an ideal lowpass filter, the enhancements of near-maximum likelihood upon the nonlinear equaliser are 0.5 dB in 4-level QAM and PSK, 0.8 dB in 8-level PSK and 1 dB in 16-level QAM.

Figures 4.8 and 4.9 show the performances of the 4-level QAM, with SlDl and NLEQ systems, where the channel is subjected to Rayleigh fading with different fading rates. In these two figures and in the following figures the abbreviations, C = r and C = rc refer to rectangular and raised-cosine shaped channels, respectively. Also, f_D refers to the Doppler frequency, in Hz.

The same procedure has been followed to test the other systems under Rayleigh fading conditions with different fading rates, and the results are shown as follows:-

i) For 4-level PSK in Figures 4.10 and 4.11

ii) For 8-level PSK in Figures 4.12 and 4.13

iii) For 16-level QAM in Figures 4.14 and 4.15.

Table 4.3 lists the advantages of using the near maximum likelihood detector over the nonlinear equaliser, for the two channels (rectangular and raised-cosine).

Figures 4.16 and 4.17 compare between different systems under Rayleigh fading conditions when f_D = 100 Hz for the two channels, rectangular and raised-cosine shaped, respectively. The performances of S4D1 and S4D2 in ideal channel conditions are identical, as shown in Figure 4.7. Whereas under Rayleigh fading conditions, system S4D2 degrades, in comparison with S4D1, by 1 dB when a rectangular shaped channel is used (C=r) and by 1.5 dB when raised-cosine shaped channel is used (C=rc),(comparison made at a bit error rate of 10^{-4}) , as shown in Figures 4.14 to 4.17.

Since the aim of this chapter is to study the performances of different systems in a mobile radio environment, differential coding has not been used in Figures 4.8 to 4.17. But, it is possible to use differential coding and an identical performance can be obtained. However, in order to avoid unnecessary repetition, the tests carried out in Figures 4.16 and 4.17 have been only repeated with differential coding as shown in Figures 4.18 and 4.19. The differential coding has been described in detail in Chapter 2. Figure 4.20 compares between systems S1D1, S2D3, S3D3, S4D1 and S4D2 with and without differential coding under the same fading rate (f_D = 100 Hz) when the rectangular shaped

channel is used. In Figure 4.20 DIF=0 refers to the condition when the differential coding is not used whereas DIF=1 when the differential coding is employed. As is evident from Figure 4.20, the differential coding degrades the performances of the systems by 4 dB when compared at a bit error rate of 10^{-4}. Also, from Figures 4.16 to 4.19, it is possible to conclude that the detector employing a nonlinear equaliser degrades by 4 dB with differential coding.

In the nonlinear equaliser, a threshold level detector is used in the system employing QAM signal throughout the above tests, whilst with the system employing PSK signal, a $\tan^{-1}(.)$ function is used to detect the received signal phase and to compare it with all possible phases of the corresponding signal, Figure 4.2c and d.

This chapter leads to the following conclusions:-

i) As expected, there is no advantage in using near-maximum likelihood over nonlinear equaliser over an ideal (distortionless) channel. But as the distortion becomes more prominent, the near-maximum likelihood detector has better performance over the nonlinear equaliser. Since the assumed channels are less dispersive with minimum distortion, use of near maximum likelihood detectors are not expected to give improved performance over the nonlinear equaliser.

ii) Under the assumed Rayleigh fading conditions, the performances of all systems studied here degrades by 20 dB in comparison with nonfading conditions.

iii) Only the near-maximum likelihood detectors are recommended to be used with the systems employing 16-level QAM signal while both the near-maximum likelihood and nonlinear equaliser detectors can be used with 4-level PSK, QAM and 8-level PSK signals.

iv) The near-maximum likelihood detector with the double expansion technique is deteriorated by the Rayleigh fading in comparison to the single expansion technique.

v) Differential coding is essential in carrier-recovery techniques in order to avoid phase ambiguity. However, the differential coding causes a degradation of 4 dB in the corresponding system performances. It may be mentioned here that with no differential coding there is a likelihood of interchange of inphase and quadrature channels creating more complications.

signal	Bit rate bit/s	Symbol rate bauds	modulation scheme	signal levels
s_1	19200	9600	QAM	4
s_2	19200	9600	PSK	4
s_3	28800	9600	PSK	8
s_4	38400	9600	QAM	16

Table 4.1 The different signals used, and the relationships between information rate, symbol rate and signal levels.

signal	a_i	b_i	modulation scheme
s_1	± 1	± 1	QAM
s_2	± 1	± 1	PSK
s_3	± 2.613	0	PSK
	± 1.847	± 1.847	
	0	± 2.613	
s_4	±1, ±3	±1, ±3	QAM

Table 4.2 The possible values of a_i, b_i for given signals

System	Rectangular shaped channel dB	Raised-cosine shaped channel dB
S1D1	0.5	1.0
S2D3	0.5	1.0
S3D3	0.4	0.6
S4D1	indefinite	indefinite
S4D2		

Table 4.3 The enhancements, in dB, of using near maximum likelihood over the nonlinear equaliser under Rayleigh fading conditions for the given channels.

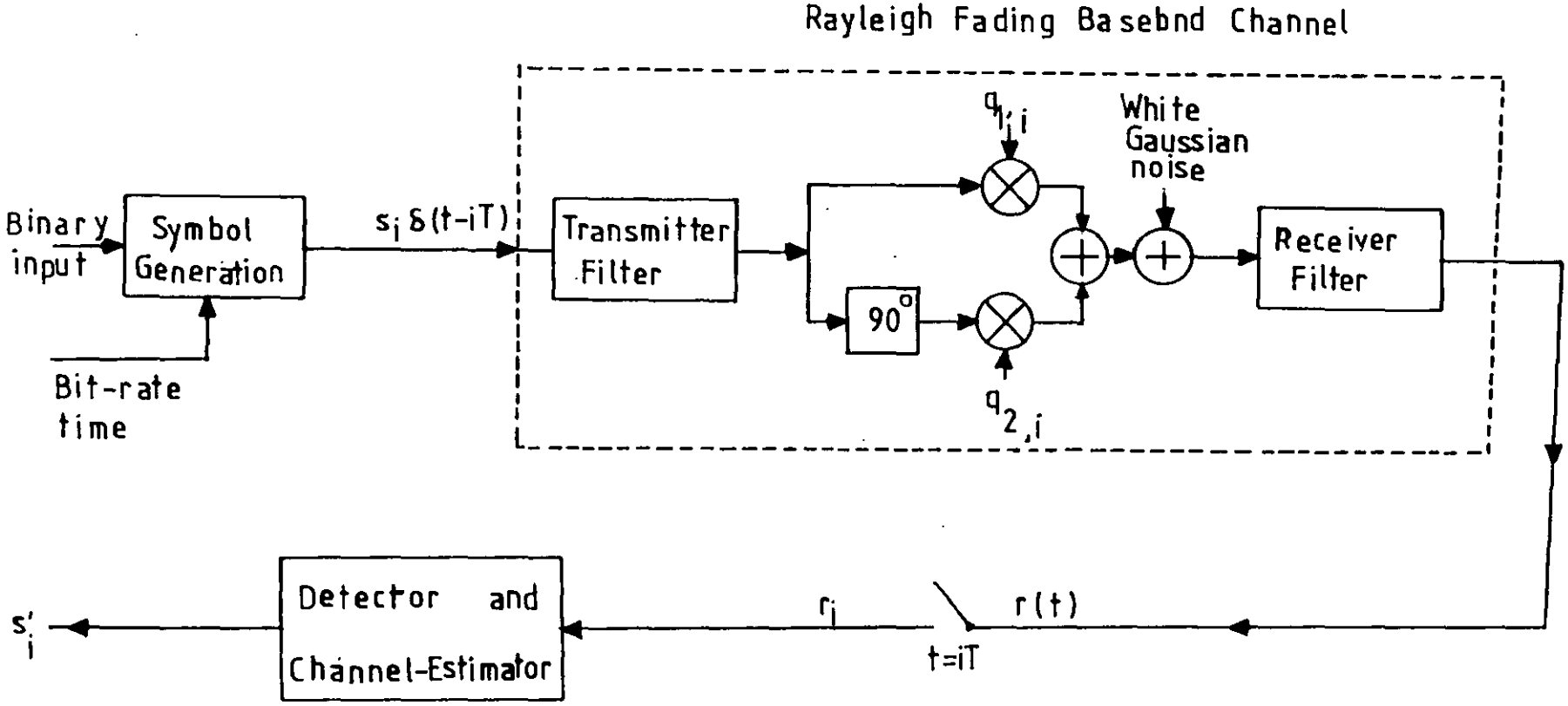

Fig. 4.1 Model of data transmission over mobile radio channel

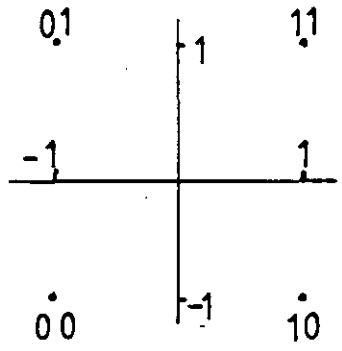

a. 4-QAM

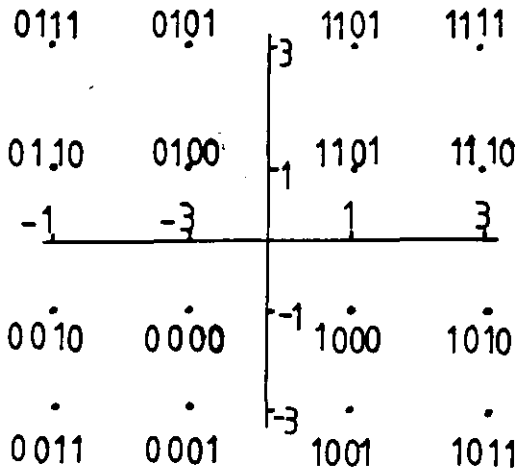

b. 16-QAM

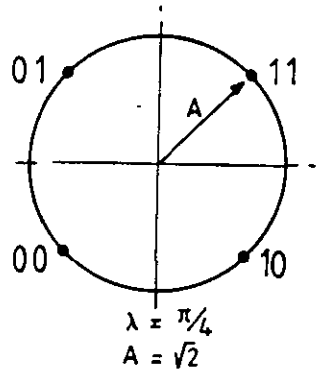

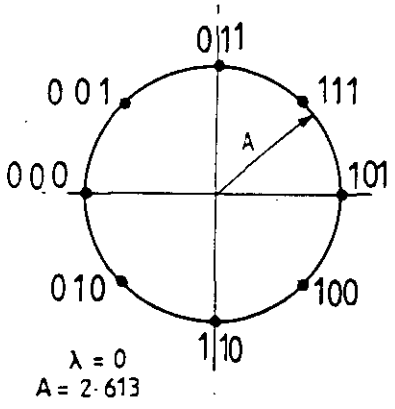

c. QPSK, A = $\sqrt{2}$, $\lambda = 45^{\circ}$ d. 8-phases PSK A = 2.613, $\lambda_o = 0$

Fig. 4.2 Data mapping

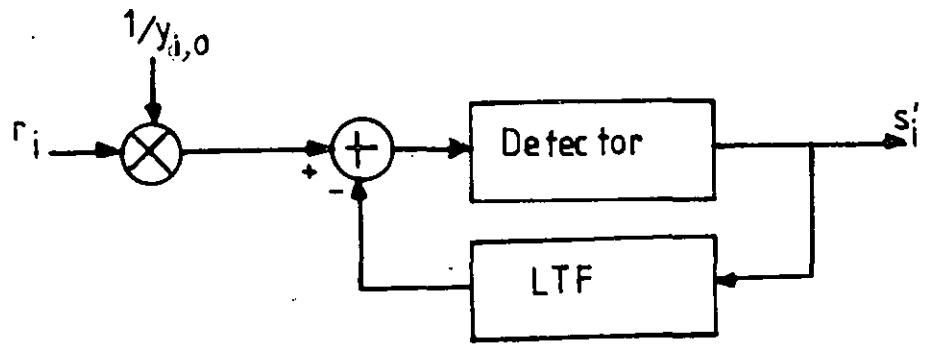

Fig. 4.3 Conventional implementation of a nonlinear equalizer. LTF = Linear Transversal Filter

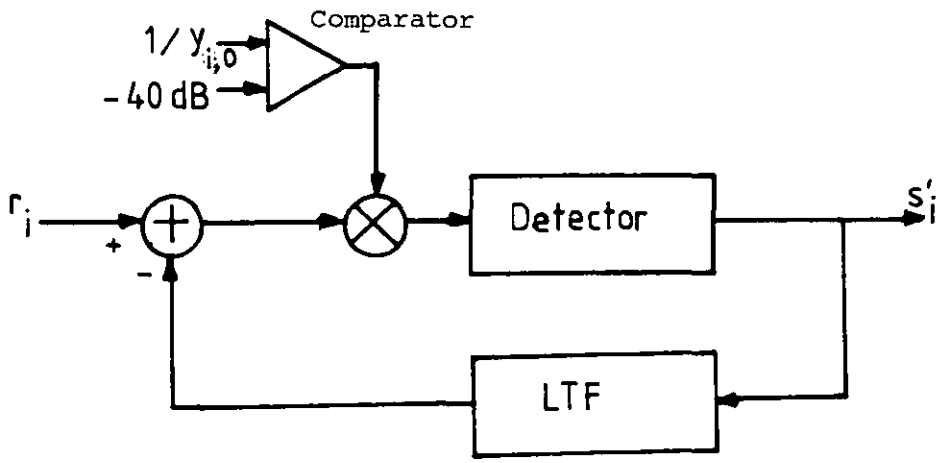

Fig. 4.4 Modified nonlinear equaliser of Figure 4.3 for mobile radio application. LTF = Linear Transversal Filter

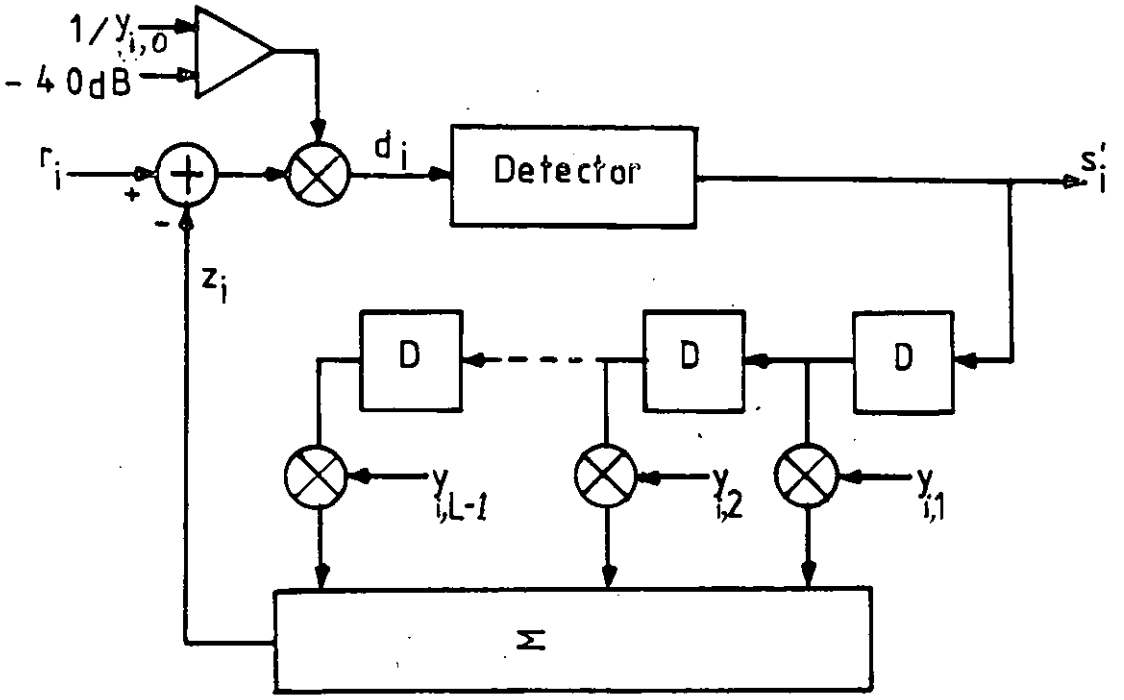

Fig. 4.5 Detail of nonlinear equaliser of Figure 4.4 where D is a delay element of one symbol period

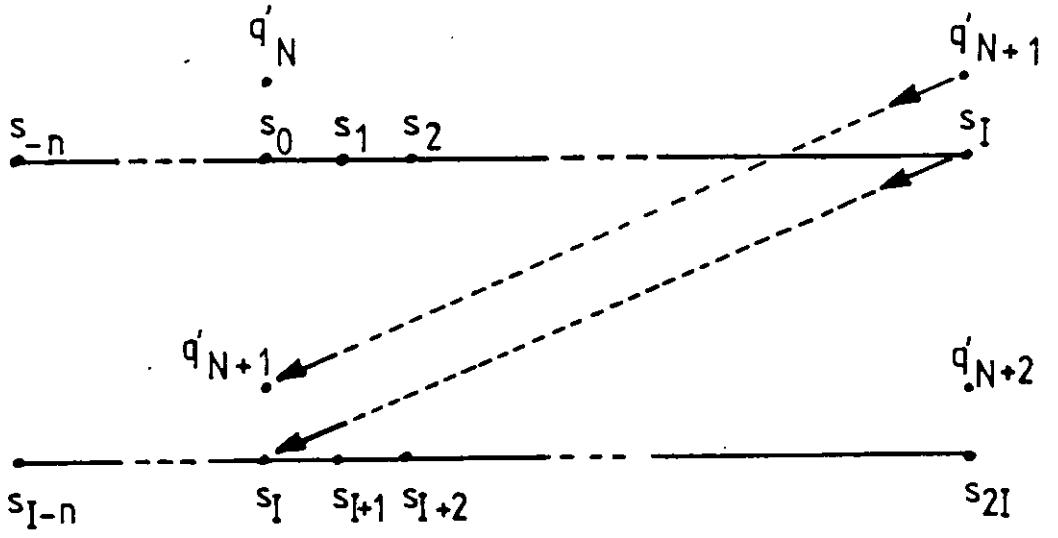

Fig. 4.6 Data arrangement as block for computer simulation

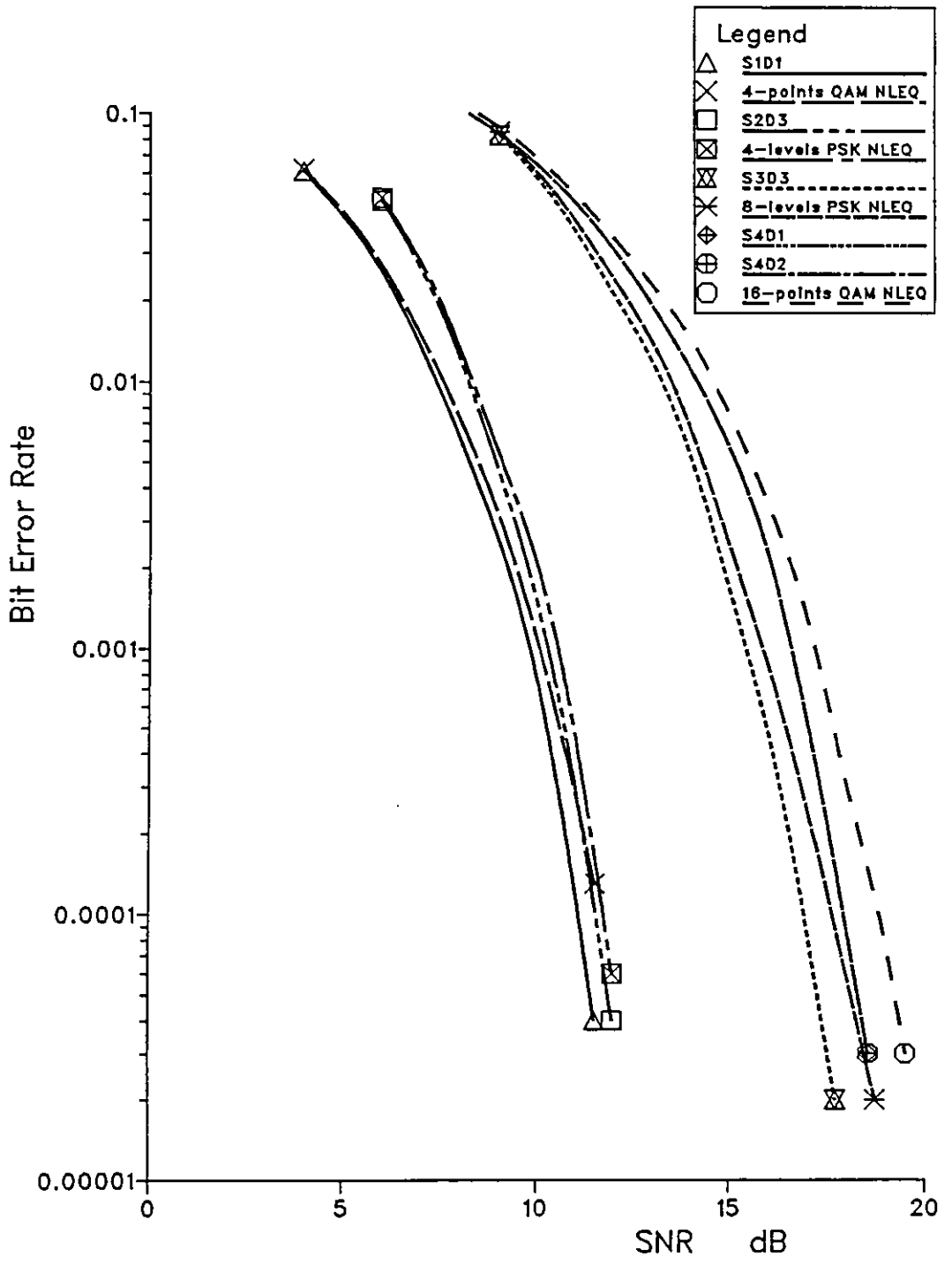

Fig. 4.7 Comparison of different systems performances under idle channel condition.

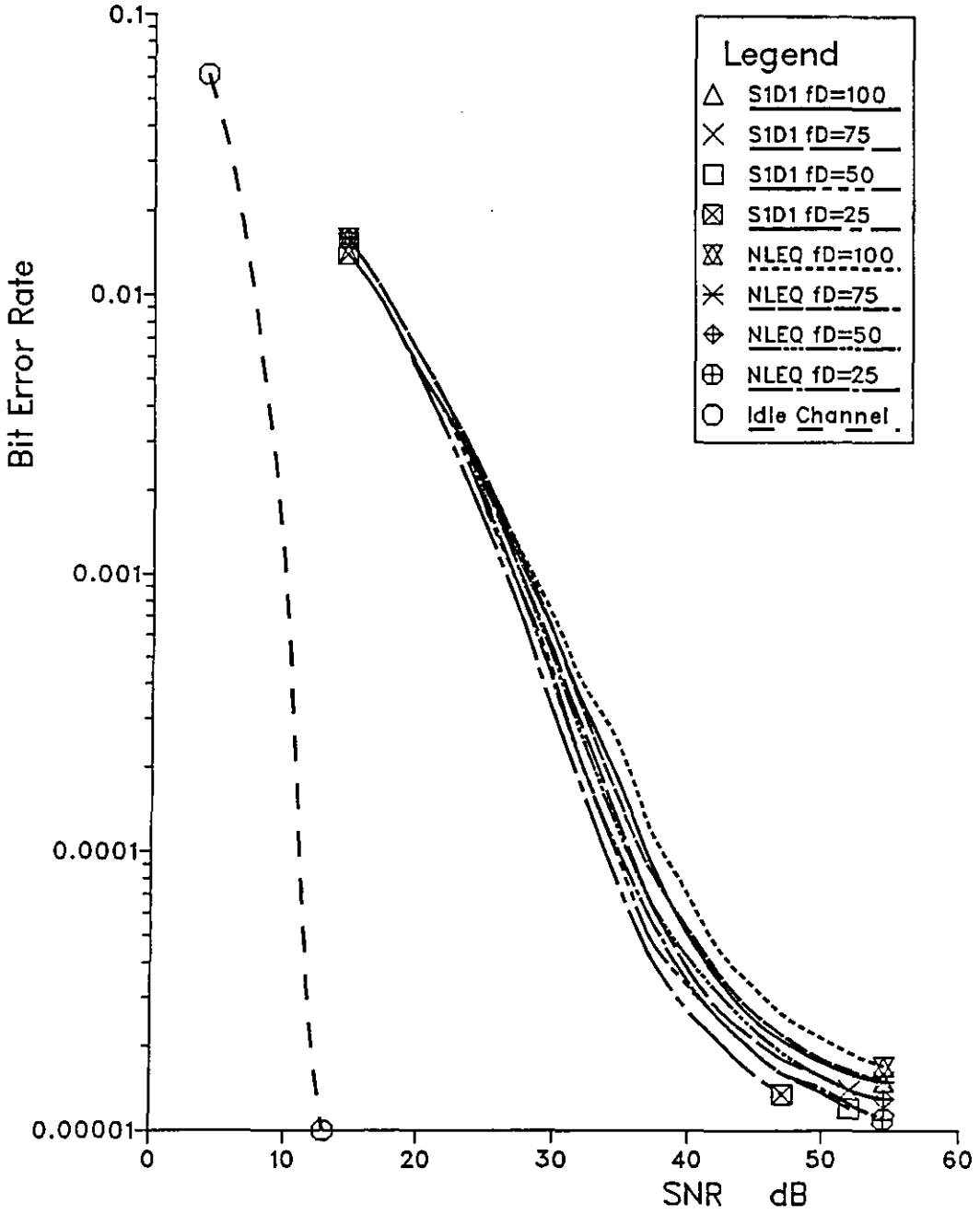

Fig. 4.8 Performances of the S1D1 and NLEQ for different fading rate ;C=r

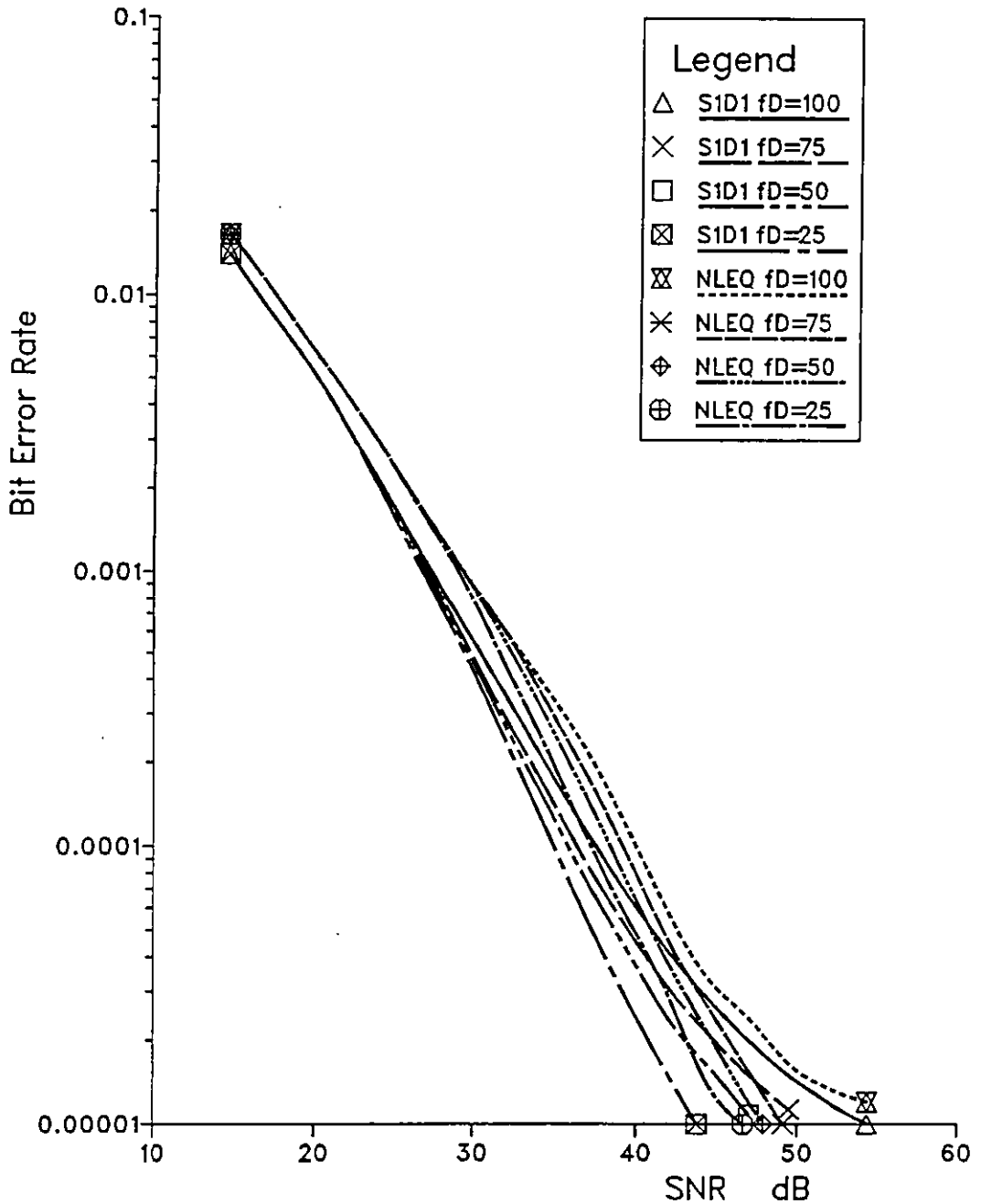

Fig. 4.9 Performances of the S1D1 and NLEQ for different fading rate ; when C=rc.

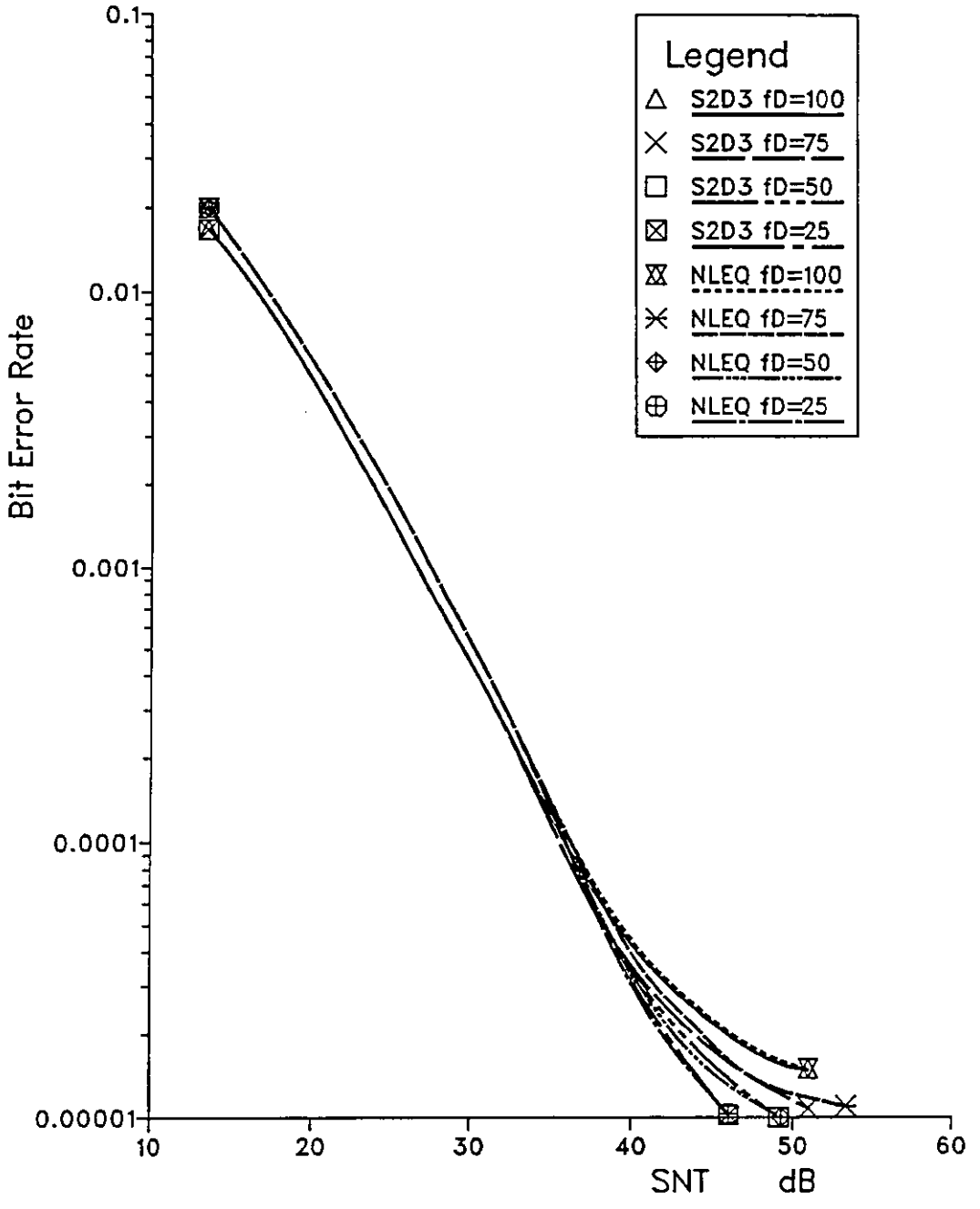

Fig. 4.10 Performances of the S2D3 and NLEQ for different fading rate ; when C=r.

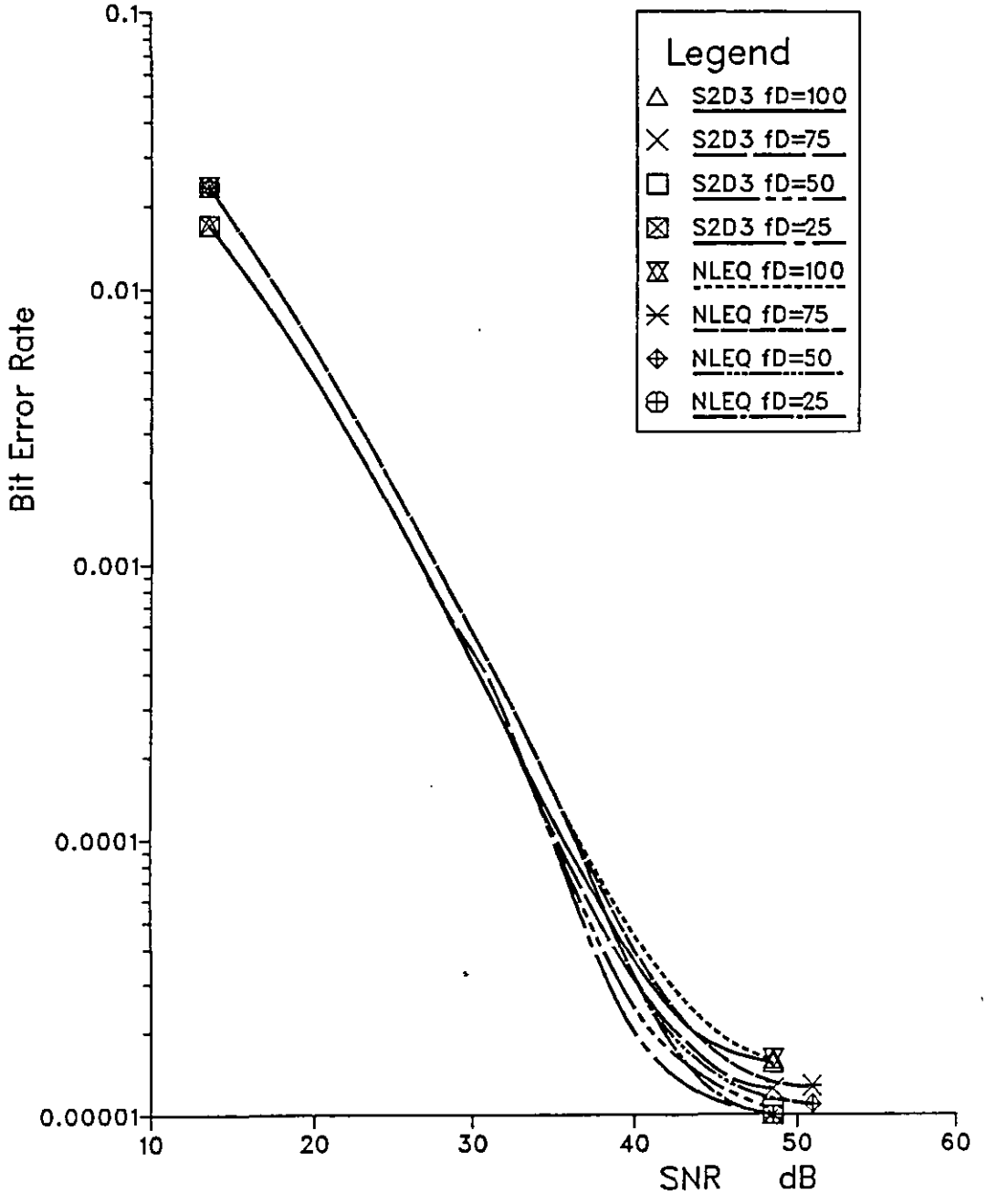

Fig. 4.11 Performances of the S2D3 and NLEQ for different fading rate ; when C=rc.

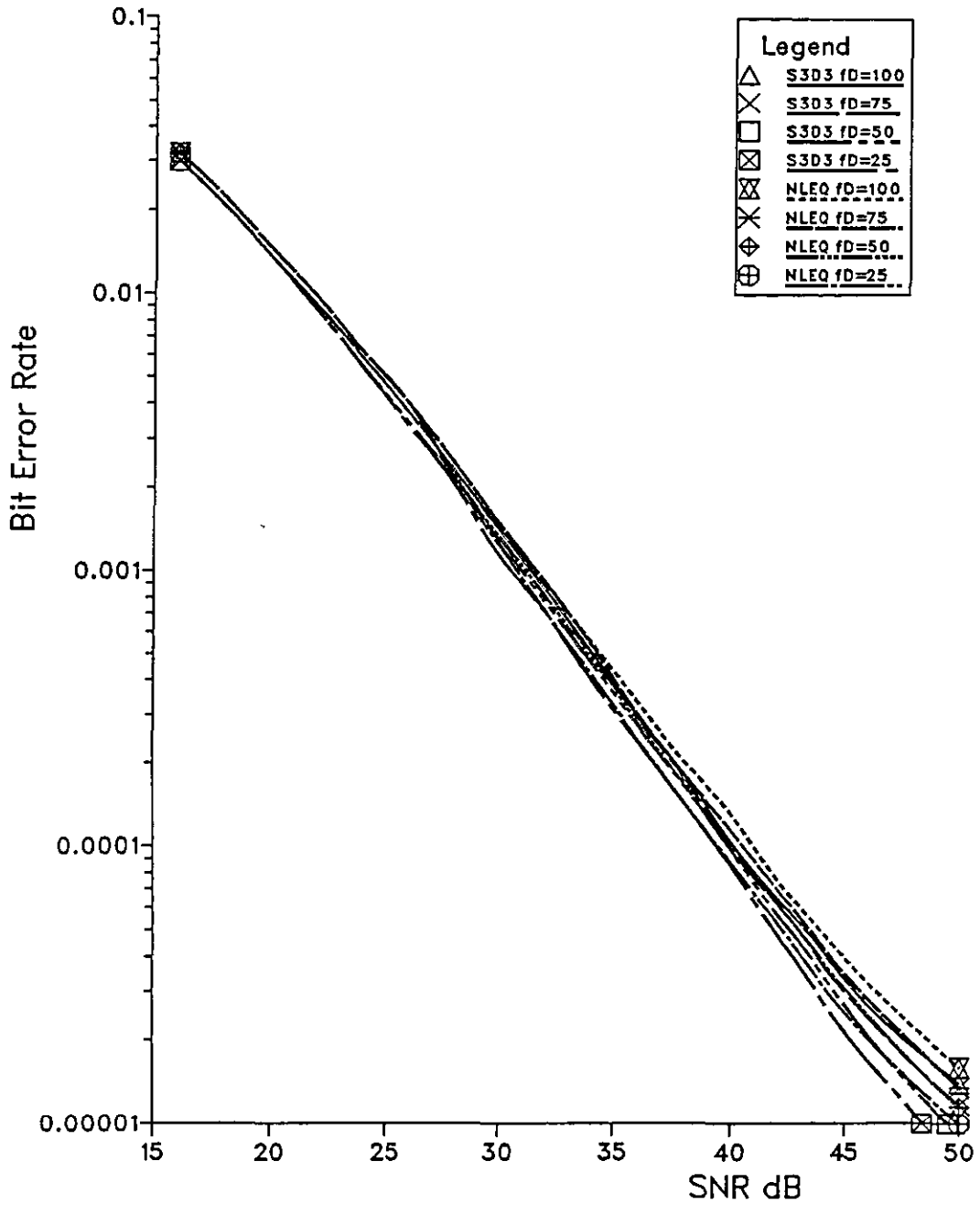

Fig. 4.12 Performances of the S3D3 and NLEQ for different fading rate ; when C=r.

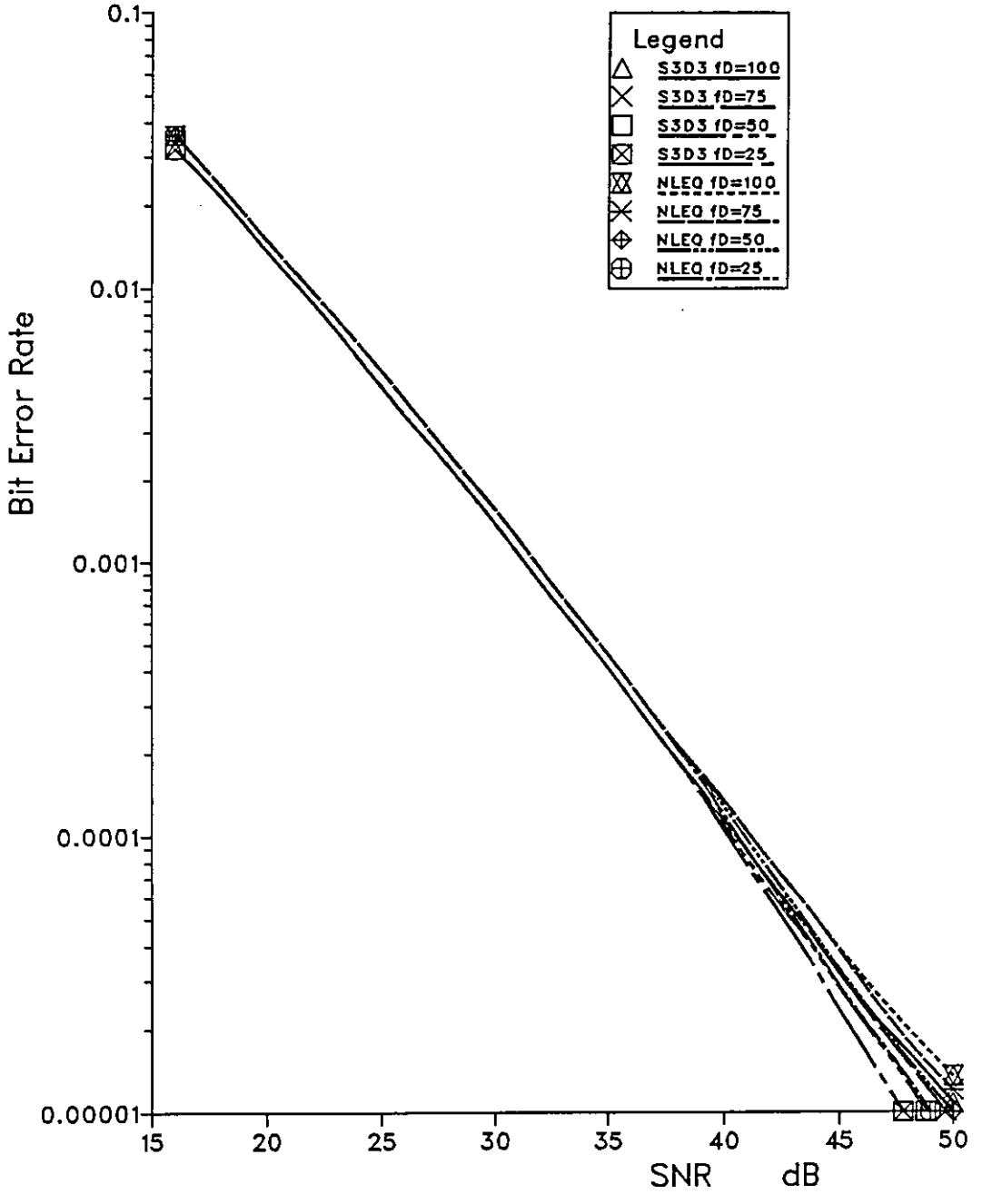

Fig. 4.13 Performances of the S3D3 and NLEQ for different fading rate ; when C=rc.

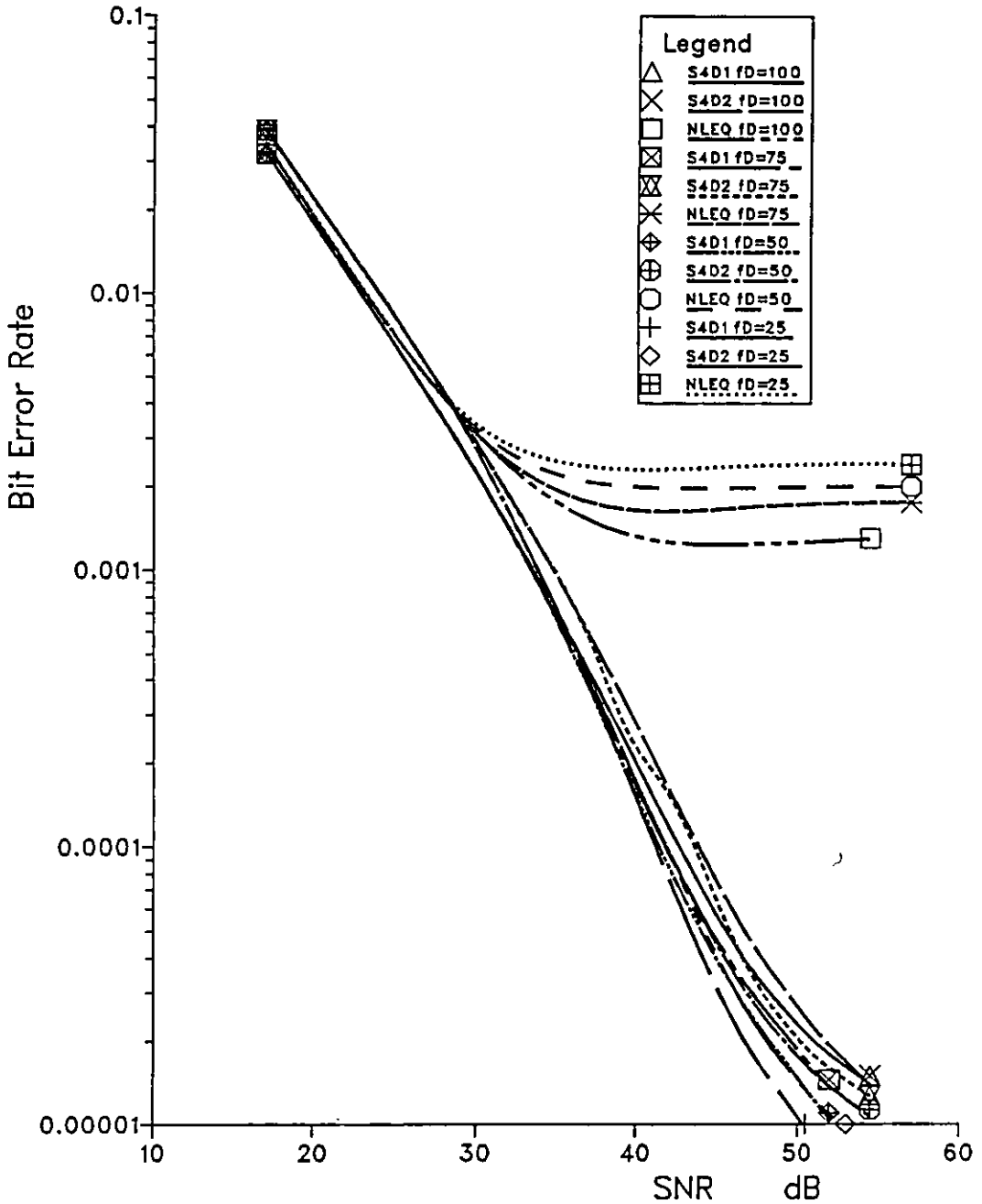

Fig. 4.14 Performances of the S4D1, S4D2 and NLEQ for different fading rate ; when C=r.

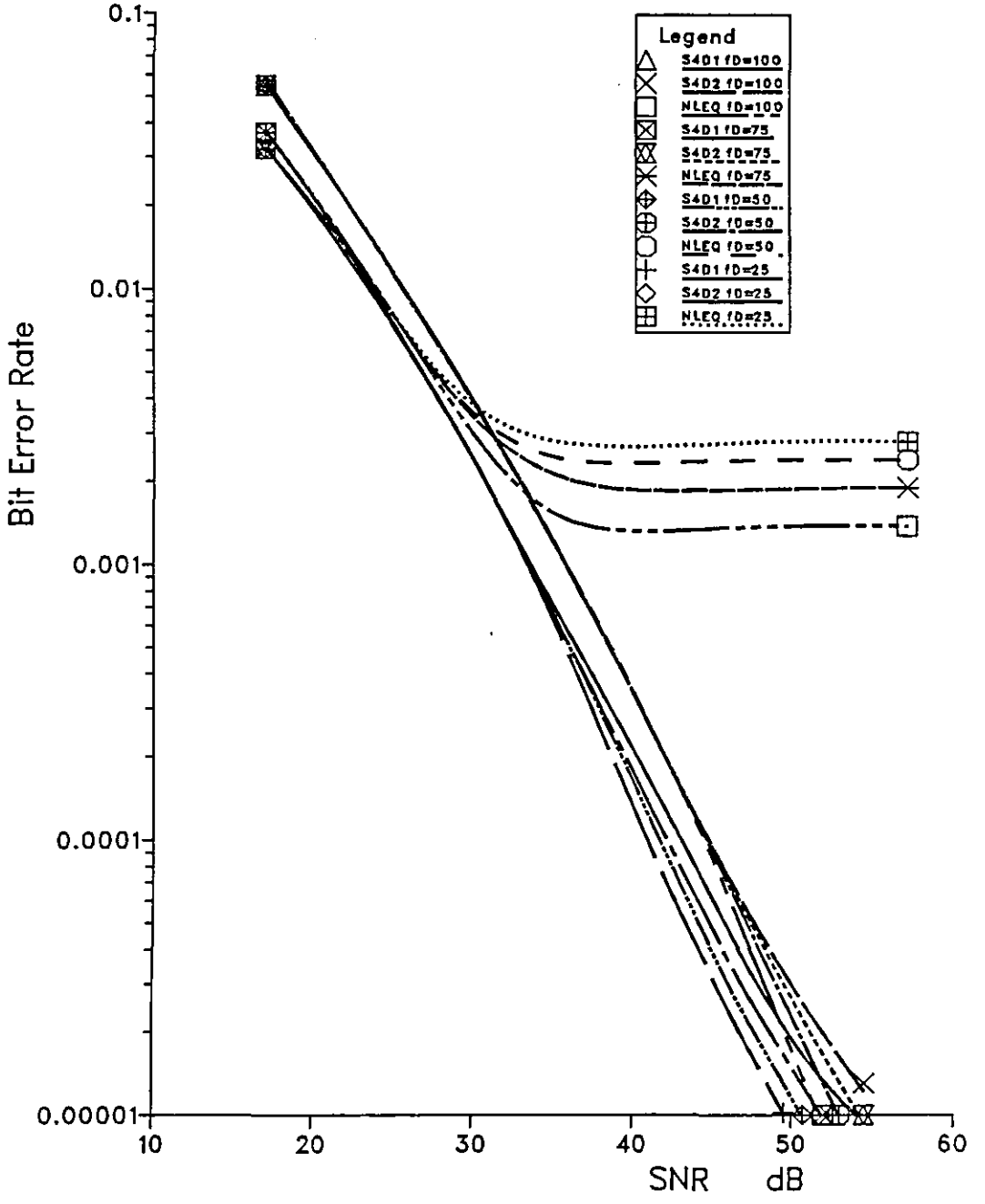

Fig. 4.15 Performances of the S4D1, S4D2 and NLEQ for different fading rate ; C=rc.

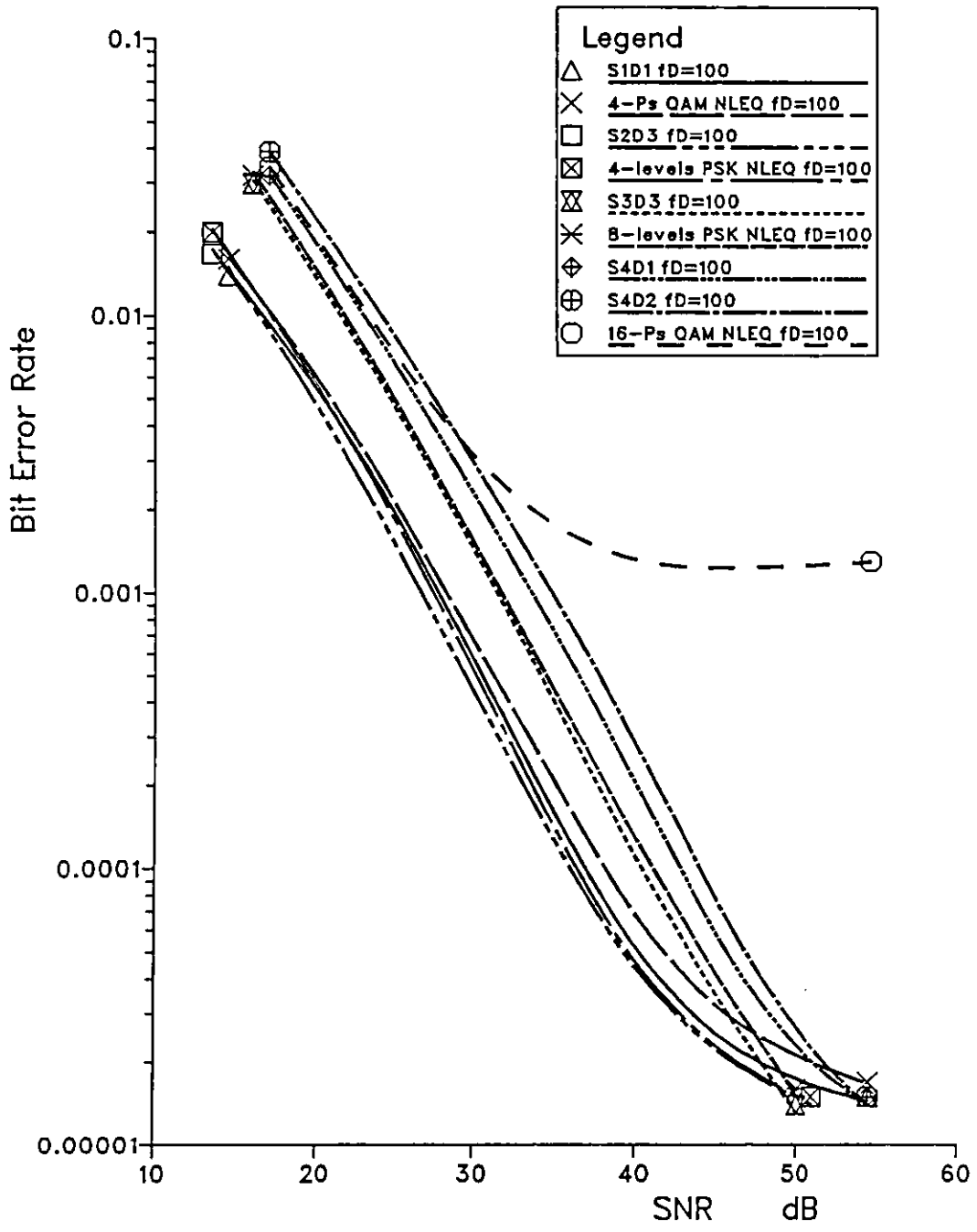

Fig. 4.16 Comparison between different systems performances under Rayleigh fading conditions with fD=100 Hz ; when C=r.

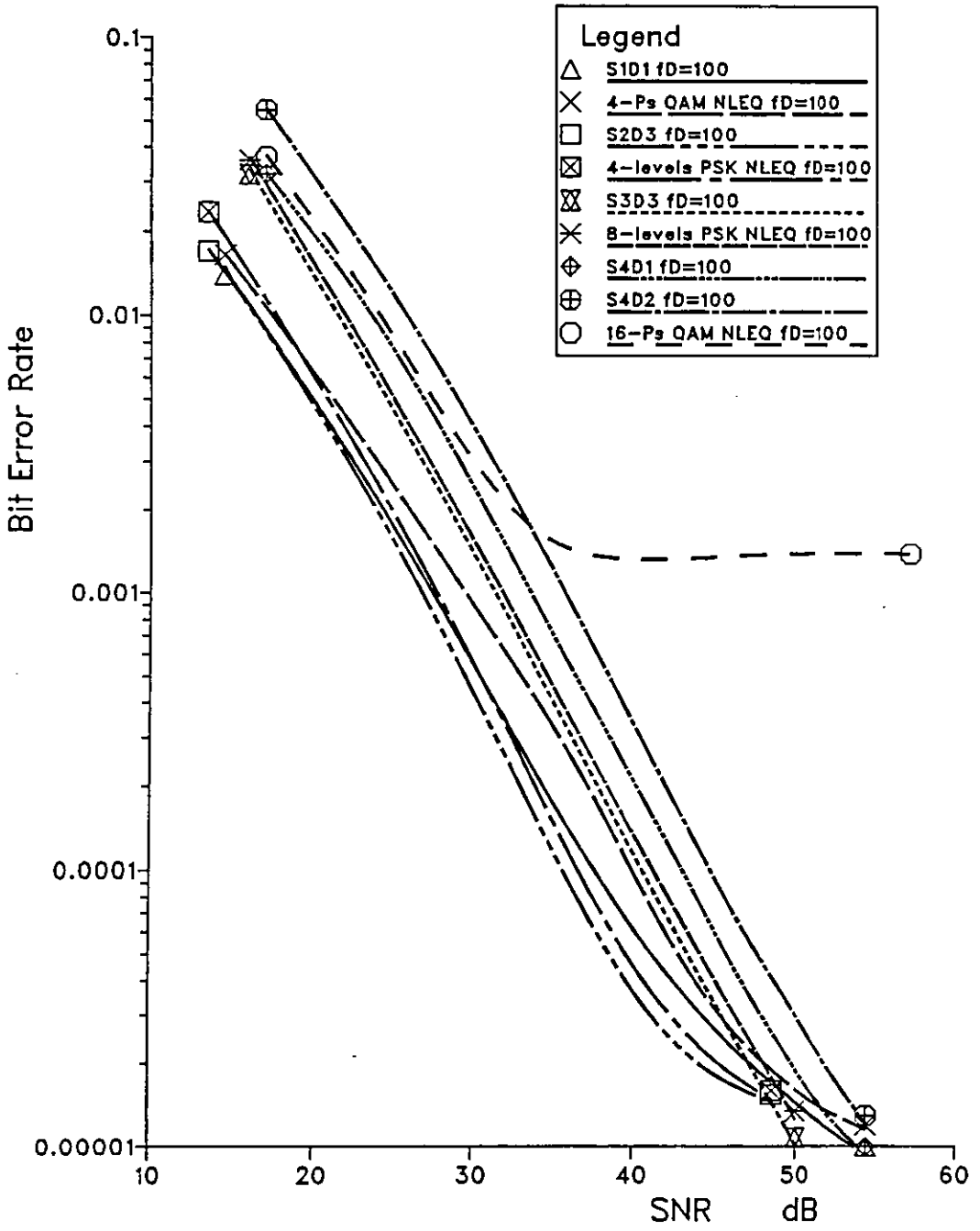

Fig. 4 17 Comparison between different systems performances under Rayleigh fading conditions with fD=100 Hz , when C=rc.

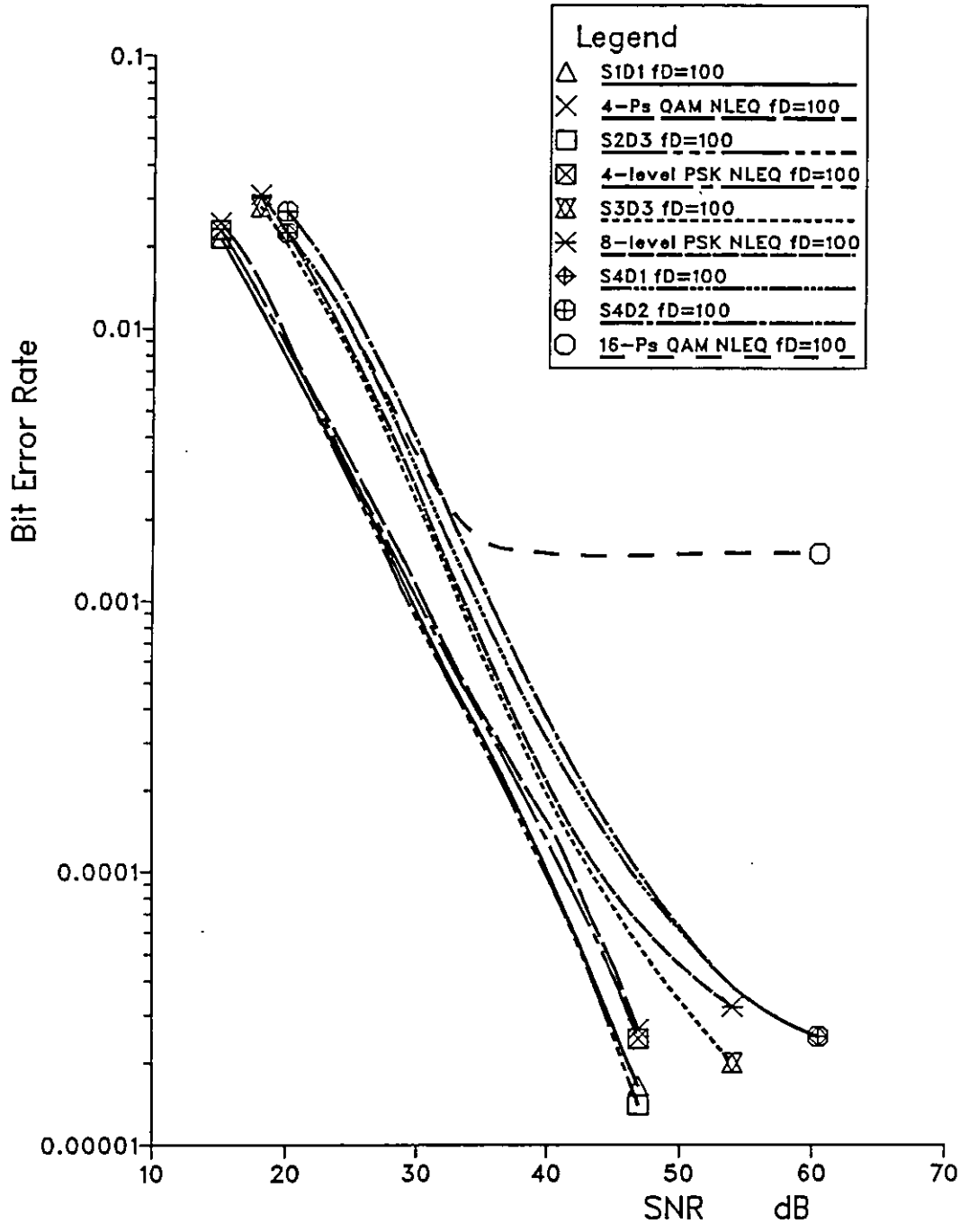

Fig. 4.18 Comparison between different systems performances with differential coding under Rayleigh fading conditions ; fD=100 Hz, when C=r

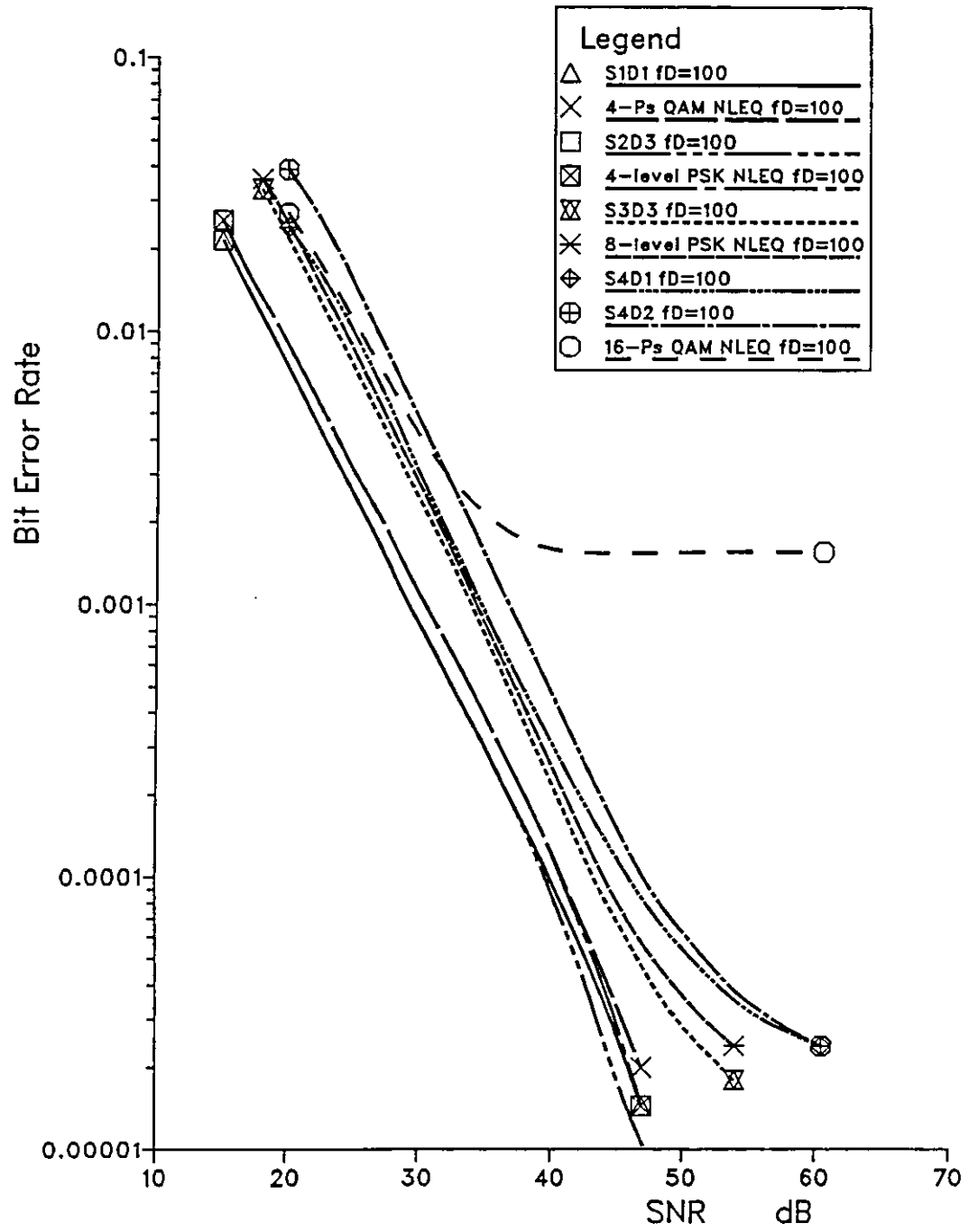

Fig. 4.19 Comparison between different systems performances with differential coding under Rayleigh fading conditions ; fD=100 Hz, when C=rc

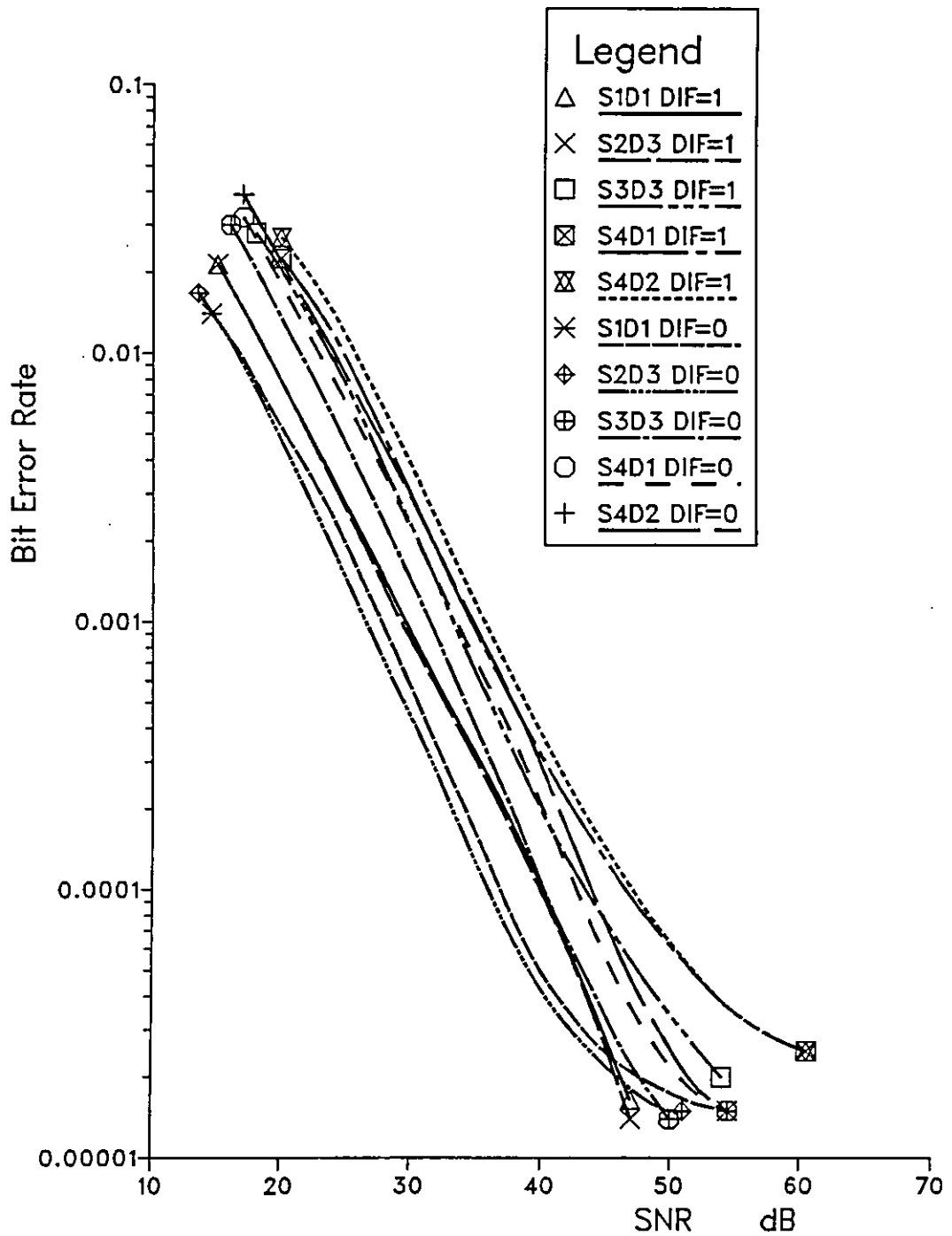

Fig. 4.20 Comparison between different systems performances with and without differential coding under Rayleigh fading conditions ; fD=100 Hz, when C=r

5. CARRIER SYNCHRONISATION

5.1 Introduction

Chapter 4 has dealt with data detection techniques, using the assumption of coherent demodulation. Coherent demodulation requires the successful regeneration of a reference carrier with a phase and frequency closely matching that of the data carrying signal, which is the objective of this Chapter.

Unfortunately, it is difficult to simulate a modulated radio frequency signal as a software program, since it needs a very high sampling rate (higher than the carrier frequency). Of course, a simulation with such a high sampling frequency cannot be achieved in the allowable execution time by the computer. For example, a signal with a carrier frequency, as assumed, of 900 MHz requires a sampling frequency of at least $2 \times 9 \times 10^8 = 18 \times 10^8$ c/s and, subsequently, if the calculation time of each cycle is 1 μsec, then half an hour will be necessary to access the system function for only one symbol duration. One attempt, at normalized radio frequency, is performed in Section 5.5, where a binary PSK (Phase-Shift-Keyed, see also Chapter 2) signal is employed. This simulation, as well, requires an incredibly long execution time. Moreover, the two systems CRS1 and CRS2 (Carrier Recovery Systrem 1 and 2) discussed in Section 5.5 fail under condition of Rayleigh fading and require the followng techniques to enable them to operate under such conditions:-

i) Differential coding (encoding/decoding)

ii) Space diversity

Whether these systems are under fading or non-fading conditions, differential coding is essential in order to reduce the phase ambiguity in the recovered carrier [2,5,12, Chapter 2]. Neither differential coding nor high signal-to-noise ratio (high power signal) can remove the fading effect from the received signal in a mobile radio environment. However, this problem can be resolved by the use of space diversity, where the signals from two antennas can be used to correct the phase of each other. Also, the variance of the phase jitter of CRS1 and CRS2 has not been measured, since it is difficult to calculate $\theta(t)$ from a signal of the form $\{a(t)\cos(\theta(t))\}$ unless $a(t)$ is known. The only tests carried out on these two systems was to measure the bit error rate with variations of signal to noise ratio. This measurement is deferred to Chapter 8, since the problems concerning the space diversity is introduced in Chapter 7.

The carrier synchronisation is successfully carried out in a baseband region by the use of a digital phaselocked loop, DPLL. This DPLL was designed by using some of the rules employed in designing the feedback digital control system that are presented in Appendix H. This method offers an opportunity to use any digital filter as a loop filter, while the available DPLL techniques in the literature are restricted to only one type of filter[171-184,198, 199, Appendix G].

The designed DPLL has been tested in the form of first, second and third order systems with application of Butterworth and Chebyshev digital filters, under nonfading and Rayleigh fading conditions for an unmodulated carrier.

The DPLL design depends on careful selection and implementation of the phase detector, PD, which plays an important part of the whole system. Two types of PD, namely hard limiter/discriminator and tanlock are used and their characteristics are demonstrated.

A data aided DPLL is accomplished here, by also applying the same DPLL introduced in the case of unmodulated carrier, as a carrier recovery system for a modulated signal. This system is tested under different fading rates with the use of a tanlock - PD only. The prementioned systems degrade severely with the delay, when employed with near maximum likelihood detection schemes since these schemes introduce a delay in detection of the data symbols [Chapter 4].

The performance of the DPLL, that has been used here, is investigated in the mobile radio environment, where the channel is subjected to Rayleigh fading under noisy conditons, by extensive computer simulation tests.

5.2 Digital Phase Locked Loop (DPLL)

In Appendix H a feedback digital control system has been designed and its stability has been investigated, whereas this chapter shows the way of employing it as a digital phase locked loop (DPLL). Likewise, the phase locked loop (in both categories, analogue and digital) is, in general, a feedback system which compares the inherent phase of the output signal with the phase of the incoming signal and generates an error signal with which it can control its output signal. The method, which is about to be introduced here, is straightforward and gives more freedom in selecting the loop filter. This filter plays an important part in the system and defines system characteristics, while the DPLL technique in the literature uses only one type of filter[171-183,198,199] as that introduced in Appendix G.

5.2.1 Digital Phase Locked Loop Transfer Function

As in the case of analogue PLL[170,199], the conventional digital PLL consists of a phase detector (PD), loop filter (LF) and voltage controlled oscillator (VCO), as shown in Figure 5.1. An additional delay element, whose significance will be discussed later, is also included in the feedback path.

The tracking performance of the digital (as well as analogue) PLL is based on the assumption that the phase error is sufficiently small, and the phase detector (PD) has a linear characteristic in the range of its operation[170,198].

By assuming that the sampled input signal has a sampled phase $\theta_i = \theta(iT)$ and the sampled output signal has a sampled phase $\phi_i = \phi(iT)$, then the PD output is given by

$$\eta_i = K_d (\theta_i - \phi_{i/i-1}) \qquad 5.1$$

where $\eta_i = \eta(iT)$ and $\phi_{i/i-1}$ is the predicted value of the output signal sampled phase ϕ at time $t = iT$ from the information received at time $t = (i-1)T$. K_d is constant and is called the phase detector gain factor.

The output sequence from the loop filter (LF) is a function of the error measurement sequence $[\eta_i, \eta_{i-1}, \ldots, \eta_{i-n}]$ and, perhaps, of the past values of the filter output sequence $[\delta_{i-1}, \delta_{i-2}, \ldots, \delta_{i-m}]$, where $m \geq n$ (for physical realisability of the filter) and both are intergers. This can be written mathematically as

$$\delta_i = f(\eta_i, \eta_{i-1}, \ldots, \eta_{i-n} : \delta_{i-1}, \delta_{i-2}, \ldots, \delta_{i-m}) \qquad 5.2$$

In fact, there are many possible ways by which the m+n+1 values of the right hand side can be combined to form δ_i. It is more interesting if the right hand side can be combined to form a linear difference equation such as

$$\delta_i = (\alpha_o \eta_i + \alpha_1 \eta_{i-1} + \ldots + \alpha_n \eta_{i-n}) - (\beta_1 \delta_{i-1} + \beta_2 \delta_{i-2} + \ldots + \beta_m \delta_{i-m})$$

$$= \sum_{k=0}^{n} \alpha_k \eta_{i-k} - \sum_{k=1}^{m} \beta_k \delta_{i-k} \qquad 5.3$$

were $\{\alpha_k\}$ and $\{\beta_k\}$ are the loop filter coefficients, that are time-invariant and independent of each other.

The voltage controlled oscillator (VCO) is to determine the phase (and/or frequency) from the measured error signal and the past values of the output signal phase. The VCO can be regarded as a digital integrator. However, the output signal phase can be given by

$$\phi_i = \phi_{i-1} + K_o \quad \delta_i \qquad 5.4$$

where K_o is the gain factor of the VCO. The above algorithm is in the form of linear difference equations. Therefore, the complete system can be represented by a z-domain transfer function.

Since the transfer functions of the LF and VCO are considered to have unique and unavoidable parts of the closed loop transfer function, then the predictor transfer function must also have such a relationship. The transfer function of the predictor should not have an adverse effect either on stability or on the system bandwidth. Furthermore, the entire system's transfer function may become nonlinear if the predictor's transfer function itself is non-linear. In order to avoid this complexity, implicit and simple prediction is assumed. Therefore, the transfer function of the predictor is considered as $\frac{1}{z}$, which is represented by a delay element in the feedback path of the closed loop. Hence, $\phi_{i/i-1}$ in Equation 5.1 becomes ϕ_{i-1} and consequently Equation 5.1 can be transformed to:-

$$\eta(z) = K_d(\theta(z) - z^{-1}\,\phi(z)) \qquad 5.5$$

The transfer function of the VCO can be determined from Equation 5.4 as:-

$$G(z) = \frac{\phi(z)}{\delta(z)} = \frac{K_o z}{z-1} \qquad 5.6$$

Now, let the transfer function of the LF be F(z) (see Figure 5.1), then the output from the filter is given by

$$\begin{aligned} \delta(z) &= \eta(z)F(z) \\ &= K_d(\theta(z) - z^{-1}\phi(z))F(z) \end{aligned} \qquad 5.7$$

The phase of the output signal is obtained from Equations 5.6 and 5.7 as follows:-

$$\begin{aligned} \phi(z) &= \delta(z)G(z) \\ &= K_d(\theta(z) - z^{-1}\phi(z))F(z)G(z) \end{aligned} \qquad 5.8$$

Therefore, the transfer function of a linear DPLL is given by

$$P(z) = \frac{\theta(z)}{\phi(z)} = \frac{K_d F(z)G(z)}{1 + K_d z^{-1} F(z)G(z)} \qquad 5.9$$

The roots of the Characteristic Equation ($1 + K_d z^{-1}F(z)G(z)=0$) in the z-plane must lie inside the unit circle, for stability considerations of the DPPL[167-169, Appendix H]. If one or more of these roots lies outside the unit circle, the system will be unstable. Consequently, the time and frequency responses must be investigated for stability considerations.

5.2.2 Digital Phase Locked Loop Design

The transfer functions of the DPLL and VCO have been deduced as that given by Equations 5.9 and 5.6 respectively. Now, if P(z) can be designed as a stable system and satisfies the bandwidth requirements with the appropriate sampling frequency, bearing in mind it is necessary to avoid aliasing, then the transfer function of the loop filter can be determined as:-

$$F(z) = \frac{1}{G(z)} \quad \frac{zP(z)}{z - P(z)} \qquad 5.10$$

However, in Appendix H, a digital feedback system has been designed and stabilised by using a damping factor. Furthermore, a unity loop gain has been implied in the system throughout the design procedure. From Equation H.5, the transfer function of the digital (feedback) control system can be rewritten as

$$M(z) = \frac{D(z)\ G(z)}{1 + D(z)G(z)} \qquad 5.11$$

The same transfer function has been given to G(z) in both cases (DPLL and digital feedback control system) and used for integration. However, if P(z) and M(z) have the same loop gain, the same bandwidth and the same sampling frequency, then it is possible to say

$$P(z) = M(z) \qquad 5.12$$

By using this result and by substituting Equation 5.12 into Equation 5.10, then,

$$F(z) = \frac{1}{G(z)} \frac{zM(z)}{z - M(z)} \qquad 5.13$$

Moreover, substituting Equation 5.11 into Equation 5.13, then

$$F(z) = \frac{D(z)}{1 + (1 - z^{-1}) G(z) D(z)} \qquad 5.14$$

Since the digital control system has been designed(in Appendix H) under the assumption of unity gain, the unity gain must be also implied in the DPLL. Accordingly, this means $K_d = 1$ in Equation 5.5 and $K_o = 1$ in Equation 5.6 and subsequently $K = K_d K_o = 1$, where K is the overall loop gain. Hence, Equation 5.6 becomes

$$G(z) = \frac{z}{z - 1} = (1 - z^{-1})^{-1} \qquad 5.15$$

Therefore, Equation 5.14 reduces to

$$F(z) = \frac{D(z)}{1 + D(z)} \qquad 5.16$$

If, however, it is required to include a loop gain other than unity gain (or when $K = K_d K_o \neq 1$), then D(z) can include the overall loop gain such that $D(z) = KD(z)$. Also, D(z) may be any digital filter that can be designed by any digitisation method. Furthermore, the filter D(z) has been designed by involving a new damping factor in order to stabilize

the digital feedback system [Appendix H] and consequently the DPLL. The transfer function of theis filter has been given as:

$$D(z) = g_u \frac{\alpha_o + \varepsilon\alpha_1 z^{-1} + \varepsilon\alpha_2 z^{-2}}{1 + \varepsilon\beta_1 z^{-1} + \varepsilon\beta_2 z^{-2}} \qquad 5.17$$

where ε is the new damping factor, g_u is the unit gain factor, α_o, α_1, α_2, β_1 and β_2 are the filter coefficients (Table H.1). Nevertheless, the transfer function of the DPLL loop filter (Equation 5.16) can be rewritten, in general, as

$$F(z) = \frac{c_o + c_1 z^{-1} + c_2 z^{-2} + \ldots + c_n z^{-n}}{1 + d_1 z^{-1} + d_2 z^{-2} + \ldots + d_m z^{-m}} \qquad 5.18$$

where c_i, for i = 0 to n, and d_j, for j = 1 to m, are the loop filter coefficients. Also, $m \geq n$ for physical realisability, and both integers. F(z) has the same order as D(z) and the relationship between their parameters, for a second order filter, can be found as follows (see also Table H.2)

$$c_o = \frac{g_u\alpha_o}{e} \quad , \quad c_1 = \varepsilon\frac{g_u\alpha_1}{e} \quad , \quad c_2 = \varepsilon\frac{g_u\alpha_2}{e}$$

$$d_1 = \varepsilon\frac{1 + g_u\alpha_1}{e} \qquad d_2 = \varepsilon\frac{2 + g_u\alpha_2}{e} \qquad e = 1 + g_u\alpha_o$$

Ultimately, P(z) is regarded as a stable system as long as M(z) is stable.

5.2.2.1 First order DPLL

The first order DPLL can be obtained when $D_o(z) = 1$, or when non-unity loop gain is required to be involved then

$$D_o(z) = K \tag{5.19}$$

where K is the overall gain. Hence, the loop filter becomes

$$F_o(z) = c_o \tag{5.20}$$

where $c_o = K/(1 + K)$. By substituting Equations 5.15 and 5.20 into Equation 5.9 (since D(z) includes the loop gain then $K_d = 1$), then

$$P_o(z) = \frac{c_o z}{z - (1 - c_o)} \tag{5.21}$$

The frequency response is obtained by making

$$z = \exp(j\omega T) = \cos(\omega T) + j\sin(\omega T) \tag{5.22}$$

and substituting in Equation 5.21, then

$$P_o(f) = \frac{c_o(\cos(\omega T) + j\ \sin(\omega T)}{(\cos(\omega T) - (1 - c_o)) + j\ \sin(\omega T)} \tag{5.23}$$

where $T = 1/f_s$, f_s is the sampling frequency, ω is the angular frequency and $j = \sqrt{-1}$. Figure 5.2 shows the frequency response of the

first order DPLL as a function of frequency, when K = 1. The relationship between the bandwidth of the closed loop (B_o) and the open loop gain (K) for a constant (same) sampling frequency is given in Table 5.1.

As it has been mentioned before[170] in case of first order analogue PLL, the larger the value of K, the better the performance of the system. This conclusion is true in the case of the first order DPLL. Unfortunately, there are two major problems. The first concerns the bandwidth, where the larger the value of K the wider the bandwidth and subsequently more noise power will be injected into the loop. The second, on the other hand, concerns the adjacent signal interference [Chapter 3]. It is probable that the DPLL (including higher order) could be locked to an unwanted signal that has greater amplitude than the wanted signal and can pass through the wider bandwidth.

The narrow bandwidth and good tracking performance are also incompatible in the first order DPLL, which has the same characteristic as for the first order analogue PLL.

5.2.2.2 Second and Third order DPLL's

The first order DPLL has a bandwidth defined mainly by the bandwidth of the VCO, since its loop filter can be considered as an allpass (an infinite bandwidth) filter. It has been found, however, that the entire system bandwidth can be minimized by the reduction of the loop gain, but at the expense of the stability. Therefore, in order to achieve a narrow bandwidth and stable DPLL with good tracking performance, a narrower bandwidth digital loop filter can be employed.

The second and third order DPLL's are obtained by using first and second order digital filters, as the loop-filter, respectively. The transfer function of the required digital filter is given by [Appendix H]

$$D_k(z) = \frac{a_o + a_1 z^{-1} + a_2 z^{-2}}{1 + b_1 z^{-1} + b_2 z^{-2}}$$

$$= g_u \frac{\alpha_o + \varepsilon\alpha_1 z^{-1} + \varepsilon\alpha_2 z^{-2}}{1 + \varepsilon\beta_1 z^{-1} + \varepsilon\beta_2 z^{-2}} \qquad 5.24$$

where ε and g_u are the new damping and unity gain factors respectively. Moreover, the values of α_i, for i = i = O to 2, and β_j, for j = 1, 2, are given in Table H.1, and k = 1, 2, 3, [Appendix H]. $D_1(z)$ and $D_2(z)$ have been designed by using the bilinear z-transform method applied to first and second order Butterworth lowpass filters respectively, for a bandwidth of 100 Hz and sampling frequency of 9600 sample/second (102-106, Appendix H). Also $D_3(z)$ has been designed by using the Impulse-invariant z-transform method applied to a second order Chebyshev lowpass filter for the same bandwidth and sampling frequency. Table 5.2 shows the coefficient values of the filters $\{D_k(z)\}$ and the corresponding value of g_u when ε= O.5. By substituting Equation 5.24 into Equation 5.16, then the transfer function of the corresponding three loop filters are obtained as

$$F_k(z) = \frac{c_o + c_1 z^{-1} + c_2 z^{-2}}{1 + d_1 z^{-1} + d_2 z^{-2}} \qquad 5.25$$

The values of c_i, for i = 0 to 2, and d_j, for j = 1, 2, are given in Table 5.3, bearing in mind $D_k(z)$ and $F_k(z)$, for k = 1, 2 and 3, have one to one correspondence according to their subscripts.

Consequently, the transfer functions of the corresponding DPLL's are given by

$$P_k(z) = \frac{e_o + e_1 z^{-1} + e_1 z^{-2} + e_3 z^{-3}}{1 + f_1 z^{-1} + f_2 z^{-2} + f_3 z^{-3}} \qquad 5.26$$

where e_i, for i = 0 to 3, and f_j. for j = 1 to 3, are given in Table 5.4. Also, $F_k(z)$ correspond to $P_k(z)$ according to their subscripts. The roots of the characteristic equations are given in table H.3.

The frequency responses of $P_k(f)$, $F_k(f)$ and $D_k(f)$ are obtained by substituting the value of z, given by Equation 5.22, into the corresponding transfer function and the results are shown in Figures 5.3-5.5. The 6 dB attenuation, appearing in the loop filters $\{F_k(f)\}$ amplitude responses, results from Equation 5.16. When the system is already designed as stable, then this attenuation must not be adjusted, otherwise the system can become unstable. In fact, this attenuation depends on the overall loop gain. As the loop gain approaches infinity the attenuation approaches zero dB, but on the other hand the bandwidth becomes flat. Nevertheless, a unity gain has been implied throughout the design procedure and if any adjustment is necessary, the system should be redesigned.

5.3 Non-modulated Carrier Recovery System

The receiving end of a model, in which a linear DPLL is used as a carrier recovery system for an unmodulated carrier, is shown in Figure 5.6. This model is based on the model described in Chapter 3. It is unlikely to use DPLL for carrier recovery directly from the radio frequency (RF) signal, since it requires a very high sampling frequency to do so. However, it is possible to use a nonlinear combination of analogue and digital systems, which is beyond the scope of this study (for more detail see Ref. 199). Alternatively, the RF signal must be transformed down to baseband so that the DPLL can be applied directly.

In order to resemble the action of the unmodulated carrier in the model assumed throughout this work, it is necessary to transmit a signal modulated by a constant valued data symbol. This symbol can be given by

$$s_i = s(iT) = 1 + j \qquad 5.27$$

where $j = \sqrt{-1}$. It is assumed that $s_i = 0$ for $i \leq 0$, so that s_i is the i^{th} transmitted symbol. The assumed baseband channel (Chapter 3) is formed by the transmitter filter, the transmission path and the receiver filter. Of course, the transmission path is represented by a multipath Rayleigh fading simulator [see Chapters 3 and 4]. The impulse response of this channel is a complex-valued function, $y(t)$, and has a finite duration, for practical purposes. The signal generator at the transmitter, and the mixer at the receiver are also included

in the baseband channel. Now, it is clear that the i^{th} received signal element at the output of the baseband channel is $s_i y(t - iT)$.

It is assumed that the noise, which includes the co-channel interference and adjacent channel interference, is stationary white Gaussian noise with zero mean and a flat (frequency independent) power spectral density. This noise is added to the signal at the output of the transmission path to give the complex-valued Gaussian waveform v'(t). The resulting waveform at the output of the baseband channel is, therefore, a complex-valued signal and is given by

$$r(t) = \sum_i s_i \, y(t-iT) + w(t) \qquad 5.28$$

where w(t) is the narrowband complex-valued Gaussian noise, which is the transform version of v'(t), with zero mean and uniform spectral density over the system bandwidth.

The waveform r(t) is sampled at a rate of 9600 sample/s and r_i, from which the carrier must be regenerated at the receiver, is the received sample at time t = iT. Hence the sampled waveform, which is the input to the DPLL, becomes

$$r_i = \sum_{\ell=0}^{L-1} s_{i-\ell} \, y_{i,\ell} + w_i \qquad 5.29$$

where $y_{i,\ell}$ is the time-varying sampled impulse response of the channel with a Rayleigh distribution function. $w_i = w(iT)$ is the sampled form of the additive noise w(t). Equation 5.29 can be rewritten in polar form as

$$r_i = a_i e^{j\theta_i} \tag{5.30}$$

where $j = \sqrt{-1}$,

$$a_i = a(iT) = (r_{i,1}^2 + r_{i,2}^2)^{\frac{1}{2}} \tag{5.31}$$

is the amplitude of the received signal,

$$\theta_i = \tan^{-1} (r_{i,2}/r_{i,1}) \tag{5.32}$$

covers all the phase and frequency variations throughout the channel, $r_{i,1}$ and $r_{i,2}$ are the real and imaginary parts of the received signal, and are given by $r_{i,1} = a_i \cos(\theta_i)$ and $r_{2,i} = a_i \sin(\theta_i)$.

The received signal, r_i, is multiplied by a correction signal, which is given by

$$c_i = b_i e^{-j\theta'_{i/i-1}} \tag{5.33}$$

where b_i is the amplitude and $\theta'_{i/i-1}$ is the predicted phase of θ' at time instant $t = iT$ from the information received at time $t = (i-1)\,T$. As it has been assumed before, in Section 5.2, for simple and implicit predictions, $\theta'_{i/i-1} = \phi_{i-1}$. Then the multiplication result given by

$$\begin{aligned} e_i &= r_i c_i = e_{i,1} + j\, e_{i,2} \\ &= a_i b_i e^{j(\theta_i - \phi_{i-1})} \end{aligned} \tag{5.34}$$

The phase detector (PD) of the analogue PLL has been well defined elsewhere [170]. A similar characteristic is also required in the case of a DPLL. In both cases however, the phase detector is sensitive to envelope varitions. But the received signal in a mobile radio system suffers from Rayleigh fading and, hence, it has random envelope as well as random phase. Under such circumstances, it is necessary to achieve a constant envelope signal to the PD. Two techniques are going to be introduced here, by which it is possible to achieve effective phase detection:-

i) Hard limiter/discriminator; through which the phase error can be determined as

$$\eta_i = \mathrm{Im}\left(\frac{e_i}{|e_i|} \right)$$

$$\cong \theta_i - \phi_{i-1} \qquad 5.35$$

where $|e_i| = a_i\, b_i$ is the modulus of e_i, and Im(x) stands for imaginary part of x. Also it is possible to use a technique similar to Feed-Forward Automatic Gain Control (FFAFC) [8,180], or Feed-Forward Signal Regeneration (FFSR) [191-194]. The reference signal amplitude can be estimated such that

$$b_i = \frac{1}{a_i} \qquad 5.36$$

under the condition of $a_i \geq -40$ dB. Hence, the error signal, Equation 5.34, becomes

$$e_i = e^{j(\theta_i - \phi_{i-1})} \qquad 5.37$$

and

$$\eta_i \cong \mathrm{Im}(e_i)$$

$$= \theta_i - \phi_{i-1} \qquad 5.38$$

ii) Tanlock technique[181,182]; which is based on the $\tan^{-1}$ function such as, from Equation 5.34,

$$\eta_i = \tan^{-1}(e_{i,2}/e_{i,1})$$

$$= \theta_i - \phi_{i-1} \qquad 5.39$$

As a result of using this function, the characteristics of the phase detctor (PD) is linear in modulo $\frac{\pi}{2}$.

The general form of the loop filter transfer function, that is given in Equation 5.25, represents also a zero order loop filter transfer function, which is defined by Equation 5.20, when all the coefficients are equal to zero except c_o. Moreover, k = 0, in this case. The input sequence, η_i, to the loop filter can be generally calculated according to either Equation 5.35 or 5.39. Hence, the output signal of this filter can be found as

$$\delta_i = \sum_{j=0}^{2} c_j \eta_{i-j} - \sum_{j=1}^{2} d_j \delta_{i-j} \qquad 5.40$$

The phase of the VCO output signal is given by

$$\phi_i = \phi_{i-1} + \delta_i \qquad 5.41$$

In order to calculate the variance of the phase jitter (mean square error of the phase or, simply, the phase variance), let the actual phase of the received signal be $\psi_i = \psi(iT)$. Hence, the phase variance, for each value of the signal-to-noise ratio, is given by

$$P_{var} = \frac{1}{K} \sum_{i=1}^{K} (\psi_i - \phi_{i-1})^2 \qquad 5.42$$

where K is a very large integer, i.e. $K \geq 25000$, and $\phi_o = 0$. Now, suppose that the actual value of the received signal, before the addition of the noise, is given by

$$x_i = \sum_{\ell=0}^{L-1} s_{i-\ell} y_{i,\ell}$$

$$= x_{1,i} + j x_{2,i}$$

$$= a'_i e^{j\psi_i} \qquad 5.43$$

where $a'_i = |x_i|$ is the modulus of x_i, $x_{1,i} = a' \cos(\psi_i)$ and $x_{2,i} = a' \sin(\psi_i)$ are the real and imaginary parts of x_i respectively, and $j = \sqrt{-1}$. Then, the phase variance can be determined by taking the imaginary part of the resultant that is obtained from the multiplication Equation 5.43 by the modified form of the regenerated signal. This signal may be given by

$$c_i = e^{-j\phi_{i-1}}$$

$$= c_{1,i} + j\, c_{2,i} \qquad 5.44$$

where $c_{1,i} = \cos(\phi_{i-1})$ and $c_{2,i} = -\sin(\phi_{i-1})$ are the real and imaginary parts of c_i. Thus

$$P_{var} = \frac{1}{K} \sum_{i=1}^{K} u_i^2 \qquad 5.45$$

where $u_i = (x_{1,i}\ c_{2,i} + x_{2,i}\ c_{1,i})/a_i'$. The phase variance in dB is given, from Equation 5.45, by

$$P_{var} = 10 \log_{10} (P_{var}) \qquad 5.46$$

5.4 Data Aided Digital Phase-Locked-Loop (DA-DPLL)

Since there is intersymbol interference in the received signal of the data transmission system[1,109,Chapter 3], the reference carrier at the receiver cannot be easily regenerated from a suppressed carrier modulated signal, even with small intersymbol interference, when a multilevel signal (such as 4-level QAM or PSK) is employed. The DA-DPLL uses the detected data to excite the digital phase-locked loop (DPLL) which is used as a carrier recovery system in the presence of intersymbol interference and noise. Hence, this system is sometimes referred to as Decision-Feedback-Carrier-Recovery-Loops (DFCRL)[183], that is analogous to remodulated analogue carrier recovery systems[170].

The received signal, in this system is first roughly demodulated by mutliplying it by a signal whose frequency is equal to the carrier frequency at the transmitter followed by lowpass filtering, regardless of the frequency offset and phase shift that are caused by the transmission path. The resulting signal is then demodulated again by a second demodulator which multiplies it by a regenerated correction signal from the output of the VCO to remove any frequency offset and/or phase shift. The resultant signal is then fed to a detector which may be a non-linear equalizer or a near-maximum liklihood detector, where the latter introduces a delay of n data symbols, where n is an appropriate integer. The output signal from the detector, which is the received data symbol

and is assumed correctly detected, is fed to a feedforward transversal filter whose impulse response resembles the channel impulse response. The output signal from the second demodulator is multiplied, with appropriate delay, by the complex-conjugate of transversal filter output signal and the multiplication result is fed to a phase detector of the DPLL. This system is illustrated in Figure 5.7, and the required algorithm will be discussed in detail as follows:-

The received baseband signal at the output of the first demodulator is given, as before, by Equation 5.28 which may be a 4-level PSK or QAM signal (see Chapters 3 and 4), where in this case

$$s_i = a_i + j\, b_i \qquad 5.47$$

is the data symbol at time $t = iT$, $j = \sqrt{-1}$. The baseband channel $y(t)$ is now formed by the linear modulator, linear demodulator, transmission path and all associated filters of the transmitter and receiver. Also, it is assumed here that $s_i = 0$ for $i \leq 0$ so that s_i is i^{th} transmitted data symbol which is equally likely to have any of the four possible values given by Equation5.47 where $a = \pm 1$ and $b_i = \pm 1$.

The received signal $r(t)$ is sampled once per data symbol at instants $t = iT$ to give the received samples $\{r_i\}$ given by Equation 5.29 from which the carrier must be reconstructed at the receiver. This signal can be rewritten as

$$r_i = p_i e^{j\theta_i} \qquad 5.48a$$

$$= r_{1,i} + j\, r_{2,i} \qquad 5.48b$$

where $r_{1,i}$ and $r_{2,i}$ are the real and imaginary parts of r_i respectively,

$$p_i = (r_{1,i}^2 + r_{2,i}^2)^{1/2} \qquad 5.49a$$

is the modulus of r_i, and

$$\theta_i = \tan^{-1}(r_{2,i}/r_{1,i}) \qquad 5.49b$$

is its phase. This signal is demodulated again to remove any frequency offset or phase shift, caused by the transmission path, by multiplying it by the correction signal. This signal is taken from the output of the voltage controlled oscillator (VCO), which may be given, in the case of using a nonlinear equaliser as a detector (n = 0 in Figure 5.7), by

$$c_i = e^{-j\phi_{i/i-1}} \qquad 5.50a$$

where $c_i = c(iT)$ (correction signal)and $\phi_{i/i-1}$ is the frequency and/or phase shift that has been estimated at time t = (i-1)T to be used at time t = iT. Inevitably, it is assumed here that $\phi_{i/i-1} = \phi_{i-1}$ for simple prediction techniques (Section 5.2). Therefore, equation 5.50a becomes

$$c_i = e^{-j\phi_{i-1}} \qquad 5.50b$$

The received signal is multiplied by the correction signal, c_i, and the resultant signal is given by

$$r'_i = r_i c_i$$

$$= p_i e^{j(\theta_i - \phi_{i-1})} \qquad 5.51$$

This signal is further multiplied by, r''_i, from the output of transversal filter and the multiplication resultant is given by

$$e_i = r'_i (r''_i)^* \qquad 5.52$$

where $e_i = e(iT)$ and $(r''_i)^*$ is the complex-conjugate of $r''_i = r''(iT)$. r''_i may also be obtained from the channel estimator [Chapter 6, Appendix J], thus

$$r''_i = \sum_{\ell=0}^{L-1} s'_{i-\ell}\, y'_{i-1,\ell} \qquad 5.53$$

where s'_i is the detected data value of the symbol s_i and $y'_{i-1,\ell}$ is the estimated sampled impulse response of the baseband channel at time $t = iT$ from the information received at time $t = (i-1)T$. This signal can be also rewritten as

$$r''_i = p'_i e^{j\psi_i} \qquad 5.54$$

where p'_i is the envelope of the estimated signal r''_i and ψ_i is its phase. Hence, the error signal now becomes

$$e_i = p_i p'_i e^{j(\theta_i - \phi_{i-1} - \psi_i)} \qquad 5.55a$$

$$= e_{1,i} + j\, e_{2,i} \qquad 5.55b$$

where $e_{1,i}$ and $e_{2,i}$ are the real and imaginary parts of e_i, respectively. The phase detector used here is a tanlock detector[181,182, see also Section 5.3] but it is possible to use a limiter/discriminator. Accordingly, the signal at the output of the phase detector is given by

$$\eta_i = \tan^{-1}(e_{2,i}/e_{1,i}) \qquad 5.56$$

where $\eta_i = \eta(iT)$. This signal is fed to the loop filter of DPLL, which is a lowpass filter (Equation 5.25), whose output is given by

$$\delta_i = \sum_{k=0}^{2} c_k \eta_{i-k} - \sum_{k=1}^{2} d_k \delta_{i-k} \qquad 5.57$$

where c_k, for k = 0 to 2, and d_k, for k = 1,2 are the filter coefficients, that are given in Table 5.3 and Section 5.2. Finally, this signal is used to excite the VCO and the result will be

$$\phi_i = \phi_{i-1} + \delta_i \qquad 5.58$$

This represents the phase of the correction signal, Equation 5.50b, which must be used to demodulate the next received sample.

In order to calculate the variance of the phase jitter, for each value of signal-to-noise ratio (SNR), it is necesssary to know the actual shift in the received signal phase and/or frequency, caused by the

transmission path. Since the transmission is represented by the Rayleigh fading simulator [Chapter 3], then the phase variance can be given by

$$P_{var} = \frac{1}{N} \sum_{i=1}^{N} (\phi_{i-1} - \phi_{q,i})^2$$

$$= 10 \log_{10} \left(\frac{1}{N} \sum_{i=1}^{N} (\phi_{i-1} - \phi_{q,i})^2\right) \quad \text{dB} \qquad 5.59$$

where $\phi_{q,i}$ is the actual phase of the received signal. $\phi_{q,i}$ can be obtained from the Rayleigh fading simulator as:

$$\phi_{q,i} = \tan^{-1}(q_{2,i}/q_{1,i}) \qquad 5.60$$

where $q_{1,i}$ and $q_{2,i}$ are the real and imaginary parts of q_i that is given by Equation 3.81 (see also Equation 5.64). In Equation 5.59 N = 5.0000.

5.5 Radio-frequency Signal Representation

The model of a binary data-transmission, that employs PSK modulation techniques [Chapter 2], is shown in Figure 5.8. This is a synchronous serial digital system in which the receiver is held synchronised in time with the received stream of the data element. Also, the information is assumed a binary rectangular signal in which level (-1) represents the digit 0 and the level (+1) represents the digit 1. The baseband data rate is 9.6 kbits/s, therefore the signal $\alpha(t)$ bearing this information is used to modulate the carrier ($\cos(\omega_c(t))$ by using a phase modulation (PM) scheme. The PM signal uses the same carrier frequency for the two binary elements, but with a phase of 0° corresponding to binary digit 0 and 180° corresponding to binary digit 1, while the envelope is kept constant. The resultant signal is called phase-shift-keyed, PSK. This is also a suppressed carrier amplitude modulated (AM) signal, whose two binary elements are antipodal[1, see also Chapter 2].

The radio-frequency (RF) signal at the output of transmitter bandpass filter is given by

$$s(t) = \cos(\omega_c t + \phi_s(t)) \qquad 5.61$$

where $\phi_s(t) = \pi(1 - \alpha_i)$, $\alpha_i = \alpha(iT)$ is the sampled data sequence at time $t = iT$, T is the period of the data symbol ($T = 1/9600$ seconds), $\omega_c = 2\pi f_c$, and f_c is the carrier frequency. The carrier frequency, f_c,

has been assumed to be 900 MHz, but such high frequencies cannot be represented by a software program, hence it has been normalized to 19.2 kHz.

In a mobile radio environment, the transmitted signal is subjected to multipath fading that can be represented by a fading simulator such as that discussed in Chapter 3. At the end of the transmission path a white Gaussian noise has been added to the signal, so that the received RF signal becomes

$$r(t) = a(t)\cos(\omega_c t + \phi_s(t) + \phi_q(t) + \theta_o) + \omega(t) \qquad 5.62$$

where

$$a(t) = (q_1^2(t) + q_2^2(t))^{\frac{1}{2}} \qquad 5.63$$

is the envelope of the received signal,

$$\phi_q(t) = \tan^{-1}(q_2(t)/q_1(t)) \qquad 5.64$$

is a random phase shift that is caused by the transmission path, θ_o is a constant phase shift, and

$$\omega(t) = \omega_1(t)\cos(\omega_c t) - \omega_2(t)\sin(\omega_c t) \qquad 5.65$$

The noise components $\omega_1(t)$ and $\omega_2(t)$ are two-sided white Gaussian noise with zero mean and the same variance σ^2 [Appendix D]. Furthermore, $q_1(t)$ and $q_2(t)$ are real-valued statistically independent Gaussian random variables with zero mean and the same variance, that are achieved

from narrowband Gaussian noise by passing the noise through a lowpass filter with a maximum bandwidth of 100 Hz (Chapter 3). Moreover, $q_1(t)$ and $q_2(t)$ are obtained by linear interpolation because of the difference between their sampling frequency and the data samples [Chapters 3 and 4].

The received RF signal is sampled at a rate of $16f_c$ sample/second, and is assumed to be in synchhonism with the sampler at the transmitter. The signal-to-noise ratio can be calculated at the input of the receiver as follows:-

Let a_i be the sampled value of the received signal envelope, a(t), at time $t = iT$ and w_i be the sampled value of the additive white Gaussian noise, $\omega(t)$, at the same time, where $T_s = 1/f_s = 1/(16f_c)$. Therefore, the average signal power is given by

$$P_s = \frac{1}{K} \sum_{i=1}^{K} a_i^2 \qquad 5.66$$

and, similarly, the average noise power can be obtained as

$$P_n = \frac{1}{K} \sum_{i=1}^{K} w_i^2 \qquad 5.67$$

where K is a very large integer. Thus, the signal-to-noise ratio, ψ, is given by

$$\psi = 10 \log_{10} (P_s/P_n) = 10 \log_{10} \left(\sum_{i=1}^{K} a_i^2 / \sum_{i=1}^{K} w_i^2 \right) \qquad 5.68$$

The filter designated as F_1 is used as the receiver filter as shown in Figure 5.9. F_1 is feedforward bandpass filter and has a bandwidth that

is governed primarily by the data rate and the Doppler frequency centered at the carrier frequency, where the bandwidth of filter F_1 is given by

$$B_{F1} = 1/T + 2\ f_D \qquad 5.69$$

T is the symbol period(T = 1/9600 seconds) and f_D is the Doppler frequency. The filter, F_1, is designed by using Fourier approximation method[103-106] applied to a rectangular shaped ideal bandpass filter, according to the specification described above with the use of a Hamming window function (103-106, see also Appendix B). The number of taps has been chosen as 43 for relatively high stopband attenuation[103]. The delay of this filter is ignored here, but it will be considered in error calculations.

Two systems, that are using squaring techniques to generate a coherent reference carrier from the RF-signals, will be discussed here (see also Appendix I).

5.5.1 Carrier Recovery System 1 (CRS1)

The output from the receiver filter (F_1) is squared and bandpass filtered by filter F_2. The filter, F_2, is also designed by the same method used to design filter F_1, and has the same bandwidth, but centered at twice the carrier frequency. The same sampling frequency is used. In fact this filter (F_2) should be designed in much lower bandwidth or as wide as 4 x maximum Doppler frequency[12]. Unfortunately it is found, however, difficult to achieve such a narrowband filter at such high sampling frequencies. Despite the fact that a large number of

taps is required for relatively high stopband attenuation[103], and consequently longer computer execution time is needed. For these reasons, the same bandwidth as that for filter F_1 is used for filter F_2, which may lead to the disadvantage of wider bandwidth and subsequently more noise will pass through to the frequency divider.

The signal at the output of the filter F_2 is converted from a sinusoidal waveform to a square waveform by a zero threshold comparator[201,202, Appendix I] (which represents a hard limiter), and by using D-type flip-flops to divide the frequency by 2; this system is depicted in Figure 5.9.

The output from the frequency divider is converted back to sinusoidal form by passing it through a bandpass filter. The filter used for this purpose has the same specification as that of filter F_1 (in practice, it is not necessary to use such a wide bandwidth filter, since the signal at the output of the divider needs much less bandwidth or a bandwidth of $2 \times f_D$ Hz).

Finally, providing the system with a hard limiter followed by a bandpass filter is to achieve a constant envelope, which is, however, necessary for the system. The complete block daigram of system CRS1 is shown in Figure 5.9.

However, by assuming $\theta = 0$ in Equation 5.62, then the sampled form of the received RF-signal can be given by

$$r_i = a_i \cos(\omega_c iT_s + \phi_{s,i} + \phi_{q,i}) + w_i \qquad 5.70$$

at time $t = iT_s$, where $T_s = T/32$, $r_i = r(iT)$, $a_i = a(iT_s)$ $\phi_{s,i} = \phi_s(iT_s)$. $\phi_{q,i} = \phi_q(iT_s)$ and $w_i = w(iT_s)$. Correspondingly, the regenerated carrier signal can be determined at the same time $t = iT_s$ as

$$c_i = \cos(\omega_c\, iT_s + \phi'_{q,i}) \qquad 5.71$$

where $\phi'_{q,i} = \phi'_q\,(iT_s)$ covers the variation of the phase and frequency throughout the transmission path. The conherent demodulation must be carried out as described in Chapter 2 (see Chapter 8).

5.5.2 Carrier Recovery System 2 (CRS2)

The format of system CRS2 resembles that of system CRS1 but with addition of a mixer. The mixer consists of local oscillator, a balanced modulator and a bandpass filter as shown in Figure 5.10. Let the output signal of the local oscillator be

$$L_i = \cos(\omega_L\, iT_s) \qquad 5.72$$

Where $\omega_L = 2\pi f_L$ and f_L is the local oscillator frequency. The f_L is assumed here to be equal to $2f_c$. Hence, the signal at the output of the mixer is obtained by the multiplication of r_i and L_i, and by bandpass filtering the resultant, then

$$r'_i = a_i\cos((\omega_c - \omega_L)\, iT_s + \phi_{s,i} + \phi_{q,i}) + \omega'_i \qquad 5.73$$

where r_i is given by Equation 5.70, and ω'_i is the resultant of the noise component at the output of the mixer. Of course, ω'_i has the same

properties as ω_i but with a frequency transformation. Now, this signal is passed through the same operations as the corresponding signal in system CRS1, or the signal passes via limiter, squarer, frequency divider and all the associated filters. Hence, the regenerated carrier can now be given by

$$c_i = \cos((\omega_c - \omega_L)\ iT_s + \phi'_{q,i}) \qquad 5.74$$

where $\Phi'_{q,i}$ covers the frequency and/or phase difference throughout the transmission path. The difference between Equation 5.74 and Equation 5.71 is the existence of ω_L, the local oscillator angular frequency, in Equation 5.74. Hence, multiplying the regenerated carrier, Equation 5.74, by the received signal, Equation 5.70, and bandpass filtering it, will not result in a baseband signal, but will give the following result:

$$r_{L,i} = a_i \cos(\omega_L\ iT_s + \phi_{s,i}) + \omega''_i \qquad 5.75$$

where ω''_i is the additive Gaussian noise that has passed through all the frequency conversion processes as the signal. To demodulate this signal (Equation 5.75), it has to be multiplied by the local oscillator signal (Equation 5.72) and lowpass filters, as illustrated in Figure 5.10.

Indeed, in both systems, CRS1 and CRS2, it is necessary to consider the delay caused by all filters used in the receiver, knowing that all the transmitter filters are assumed ideal.

Unfortunately, there is always a phase ambiguity in the recovered carrier signal. This ambiguity is caused by the squaring technique which results

either inphase or 180° out of phase. Therefore, differential coding must be used to remove this ambiguity. Also, both systems are unstable in the mobile radio environment, where the received signal is subjected to multipath Rayleigh fading. Since each of them collapses, particularly, in a deep fade unless resynchronisation is adopted by, for example, using a retraining signal or otherwise by any other means. A more promising technique used here is space diversity, where the signals received by two antennas separated by a distance of $k\lambda/2$ [10,11,131-136] can be used to correct the phase of each other, where λ is the carrier wavelength and k is integer such that $k \geq 1$. This matter will be discussed further in Chapters 7 and 8. Moreover, the variances of the phase jitter of CRS1 and CRS2 have not been calcualted because of the technical difficulties. Only bit error rate has been calculated for these two systems with the use of differential coding and space diversity, and the results are postponed to Chapter 8.

5.6 Computer Simulation Tests and Results

5.6.1 Testing the CRS1 and CRS2

It has been found difficult to carry out tests concerning the variance of the phase jitter of CRS1 and CRS2. The only tests carried out on these two systems are to measure the bit error rate versus the signal to noise ratio that are presented in Chapter 8. These systems have not collapsed with the use of space diversity, where the signals received via two antennas correct the phase of each other, throughout a run of 15000 symbols (bits) for each signal-to-noise ratio (SNR) tested, where binary PSK signal was assumed. It is reasonable to conclude that CRS1 and CRS2 are capable of tracking and regenerating the carrier in the way described here.

5.6.2 Unmodulated carrier recovery system tests

The tests are carried out mainly to test the performances of the different arrangements of digital phase locked loop, DPLL, whose models are shown in Figure 5.6. The systems tested here are:-

i) DPLL1: which is a first order DPLL

ii) DPLL2B: which is a second order DPLL

iii) DPLL3B and DPLL3C which are third order DPLL's

The letters B, in DPLL2B and DPLL3B, and C in DPLL3C, refer to Butterworth and Chebyshev lowpass filters that are involved in the design of the corresponding systems. The phase detectors, PD, are

configured into two categories, namely hard limiter/discriminator, HLD, and tanlock, TAN, that are described in Section 5.3. Furthermore, the tests are performed under two conditions, these are:-

i) Rayleigh fading conditions with a maximum Doppler frequency of 100 Hz (f_D = 100 Hz), the results are shown in Figures 5.11 and 5.12.

ii) Non-fading condition when the received signal has a constant envelope and random frequency, where the frequency is normally distributed with zero mean and standard deviation of 100 Hz. The results are shown in Figures 5.13 and 5.14.

It is clear from Figures 5.11 to 5.14 that the first DPLL1 has the highest phase variance and DPLL2B and DPLL3C are the best. DPLL3C has a little wider bandwidth, as shown in Figure 5.5, but at the same time has a quicker time response performance (Figure H.4, Appendix H). For these two reasons it has higher phase variance than DPLL2B at low signal to noise ratio, while it has the lower phase variance at high signal to noise ratio as shown in Figures 5.11 to 5.14. The system performances degrade with fading conditions, which is evident from Figure 5.15. Also, the application of the tanlock phase detector (TAN-PD) gives a better performance than the use of hard limiter/discriminator, which is clear from Figure 5.15 (see also Figures 5.22 and 5.23).

5.6.3 Data aided carrier recovery system tests

All of the above four systems, DPLL1, DPLL2B, DPLL3B and DPLL3C are also used as DA-DPLL for carrier recovery, but with the use of a

tanlock phase detector, TAN-PD, only. The systems were tested under Rayleigh fading conditions, with different fading rates when the Doppler frequency, f_D = 100, 50, 25 and 10 Hz. The results are shown in Figures 5.16 to 5.19. As the fading rate decreases all the pre-mentioned systems give a better performance. But DPLL1 shows much better performance at low signal to noise ratio as the fading rate decreases.

The DA-DPLL might be used with near-maximum likelihood detection schemes, that require a delay to reach a decision, and since the DA-DPLL uses the already detected data to excite the DPLL, then the error signal would also have the same delay. The delay degrades the performance of all the abovementioned systems as shown in Figures 5.20 and 5.21 when the signal to noise ratio is 15 and 30 dB respectively.

5.6.4 Phase-Detector Characteristic

It is possible to measure the phase detector PD charactreristic, under nonfading conditions with relatively high signal to noise ratio (say 30 dB) by making the phase of the received signal vary from $-\theta$ to $+\theta$ and taking the output from the loop filter without correcting the phase of the received signal. This means taking δ_i in either case (modulated and unmodulated signal, see Figures 5.6 and 5.7) without feeding it to the voltage controlled oscillator (VCO). The results, that are shown in Figures 5.22 and 5.23, indicate better linearity in the case of the tan-lock-PD than that of hard limiter/discriminator PD. That is why the phase variance in case of using tanlock-PD is

low as shown in Figure 5.15. But, in both cases, the phase detector is linear around zero phase error. The DPLL2B, DPLL3B and DPLL3C have same PD characteristic (coincide with each other), as is clearly shown in Figure 5.22 and 5.23. This means that the higher order systems have characteristics, which give higher error signal, whilst the first order system has a characteristic, which gives less error signal. For this reason, the first order system DPLL1, cannot cope with rapidly varying phase signal. This is clear from Figures 5.16 to 5.19. Of course, in a severe fade the phase error, θ, may be higher than 60°, or higher then what are shown in Figures 5.22 and 5.23.

It can be concluded from this chapter that:-

i) The first order digital phase-locked loop (DPLL) with large loop gain has better tracking performance but has a wide bandwidth and, consequently, more noise will be injected into the loop. Hence, the narrow bandwidth and good tracking performance are incompatible in first order digital phaselocked loop.

ii) The loop filter of first order DPLL is zero order and has an infinite bandwidth. Therefore, it is possible to use a higher order digital filter with narrower bandwidth in order to achieve narrow bandwidth and good tracking performance. The second and third order DPLL's are designed here for narrow bandwidth achievement.

iii) A new method has been developed here to design the second and third order DPLL by using some of the rules employed in designing a

feedback digital control system. This method offers an opportunity to use any digital filter as a loop filter, while the available DPLL techniques in the literature are restricted to only one type of filter. The second and third order DPLL's (DPLL2B and DPLL3B) have been designed using first and second order Butterworth digital lowpass filters, respectively. Also a third order DPLL (DPLL3C) has been designed by using a second order Chebyshev digital lowpass filter. All of the above systems show good tracking performance in a mobile radio environment, where the channel is subjected to a Rayleigh fading and hence the received signal has a rapidly varying envelope and phase. At high signal-to-noise ratio and at the same rate of phase change, the tracking ability is the same for these systems under fading and nonfading conditions.

iv) The most important part of the DPLL is the phase detector (PD). Two types of phase detector, namely hard limiter/discriminator and tanlock, are used. The DPLL system employing tanlock-PD gives 2 dB tolerance to additive noise over the DPLL system employing a hard limiter/discriminator.

v) Stability is crucial when designing a digital phaselocked loop system. A system with the quickest time response has best stability, on the other hand this system has the widest bandwidth. Hence its performance deteriorates at low signal-to-noise ratio and gradually improves as the signal-to-noise ratio increases. An example of such characteristic is illustrated by the behaviour of the DPLL3C.

iv) Since the employment of the tanlock-PD has led to a system with a better performance, hence,the tanlock-PD is employed in data aided digital

phaselocked loop (DA-DPLL). The DA-DPLL performs reasonably well with a fading channel, but its disadvantage is the inability to sustain the same performance when erroneous sequences are received.

vii) The DA-DPLL's have a further disadvantage when they are used with the near maximum likelihood detection scheme, since they deteriorate with the delay.

viii) Squaring/filtering/frequency dividing by 2 carrier recovery system is used with a binary modulated PSK radio frequency signal. It has been found difficult to simulate such a signal, with a carrier frequency of 900 MHz, in a software program. Alternatively, the high frequency is normalized to a much lower frequency. The simulation is carried out on two systems (CRS1 and CRS2) only to measure the bit error rate using space diversity. The results are deferred to Chapter 8, since the space diversity concept will be discussed in Chapter 7. The phase of each of the two signals is corrected by the other signal, in a way which will be described in Chapter 8, when the former one has suffered a deep fade. From the above argument, it can be concluded that the received signal carrier can be regenerated by the two systems (CRS1 and CRS2), since the results of probability of error measurements of receivers, where they are used, are reasonably good (see Chapter 8).

K rad/sec	0.0	6.94×10^{-2}	0.139	0.276	0.54	1.0	$\sqrt{2}$
B Hz	0.0	$f_s/64$	$f_s/32$	$f_s/16$	$f_s/8$	$f_s/4$	$f_s/2$

Table 5.1 The relationship betweenthe loop gain, K, and the Bandwidth of the first order DPLL, where f_s is the sampling frequency.

k	a_o	a_1	a_2	b_1	b_2	g_u
1	0.3545	0.1773	0.0	-0.4683	0.0	25.87
2	0.2044	0.2044	0.1022	-0.954	0.456	196.263
3	1.0076	-0.501	0.0	-0.9944	0.4972	0.9926

Table 5.2 The coefficients of the digital filter $D_k(z)$ when $\varepsilon = 0.5$, and the value of the corresponding unity gain factor

k	c_o	c_1	c_2	d_1	d_2
1	0.2617	0.131	0.0	-0.2149	0.0
2	0.167	0.167	0.0835	-0.627	0.4632
3	0.502	-0.25	0.0	-0.743	0.247

Table 5.3 The coefficients of the loop filter $F_k(z)$ when $\varepsilon = 0.5$.

k	e_o	e_1	e_2	f_1	f_2	f_3
1	0.2617	0.131	0.0	-0.9532	0.3459	0.0
2	0.2044	0.2044	0.1022	-0.954	1.41	-0.456
3	1.0076	-0.501	0.0	-1.9944	1.4916	-0.4972

Table 5.4 The coefficients of the DPLL's whose transfer functions are $P_k(z)$, when $\epsilon = 0.5$

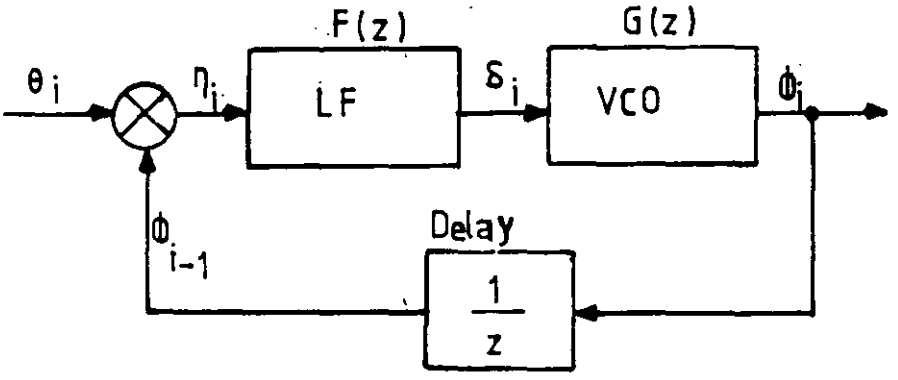

Fig. 5.1 Block diagram of a conventional digital phase-locked loop (DPLL)

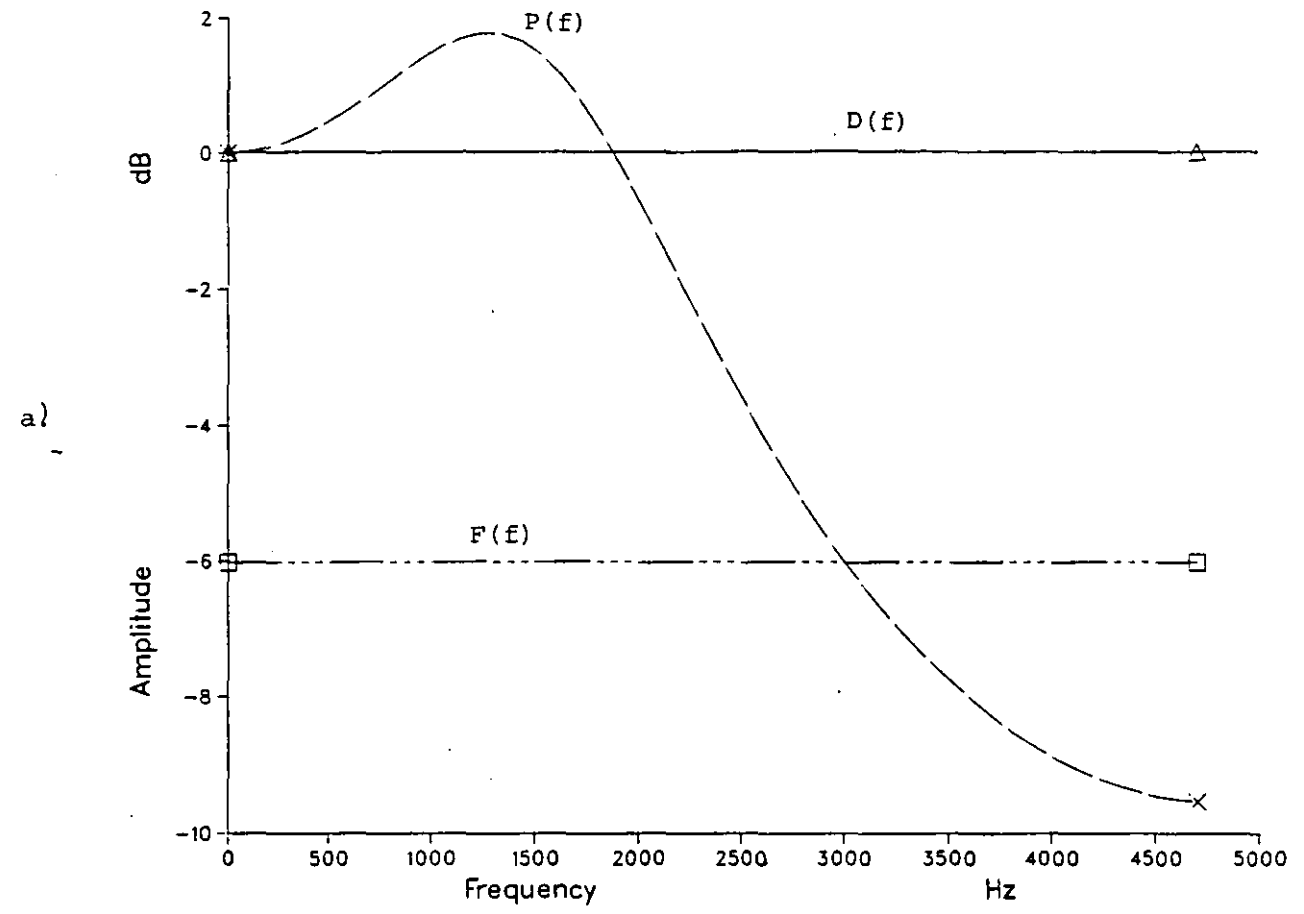

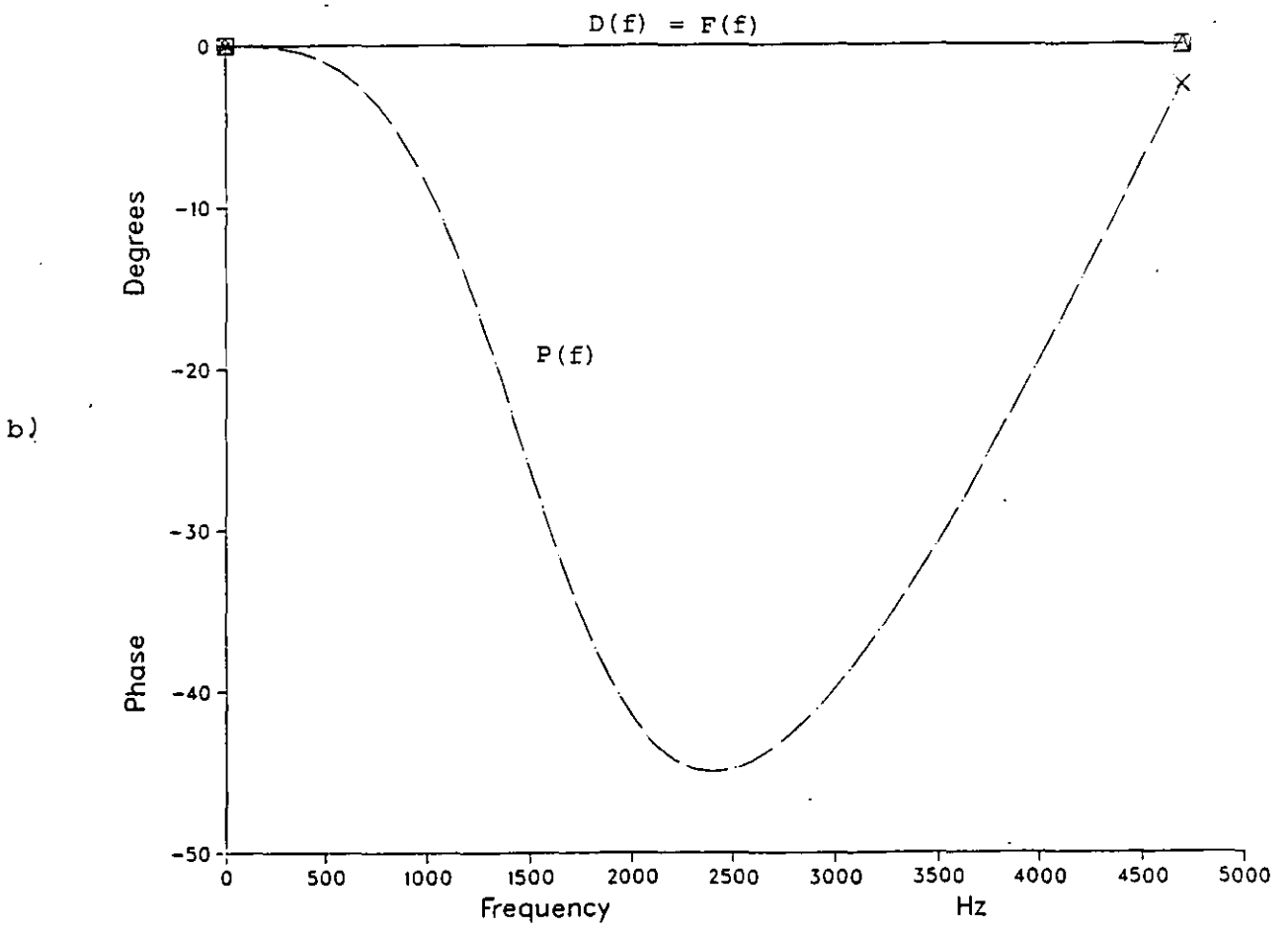

Fig. 5.2 Frequency response of first order DPLL; a) Amplitude; b) phase

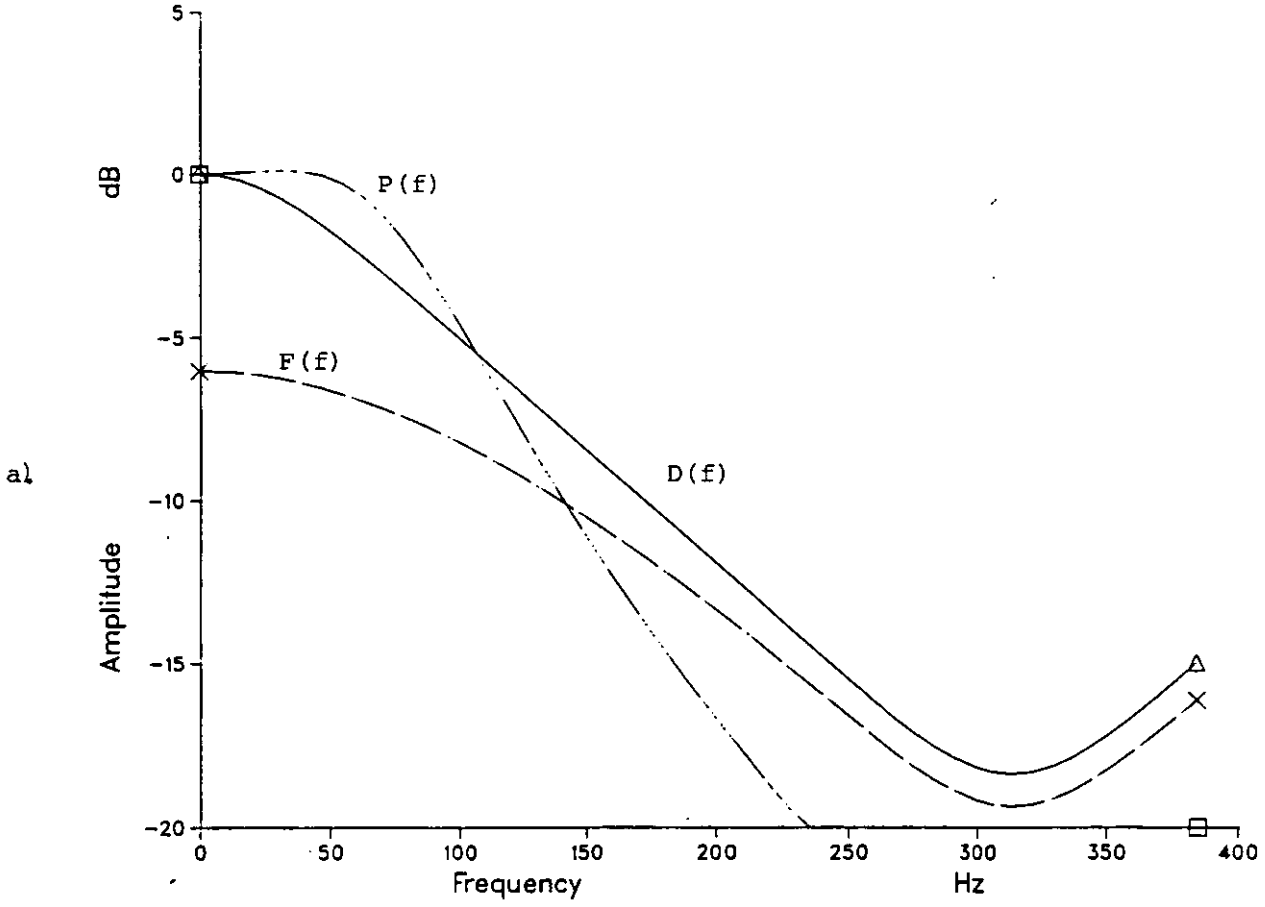

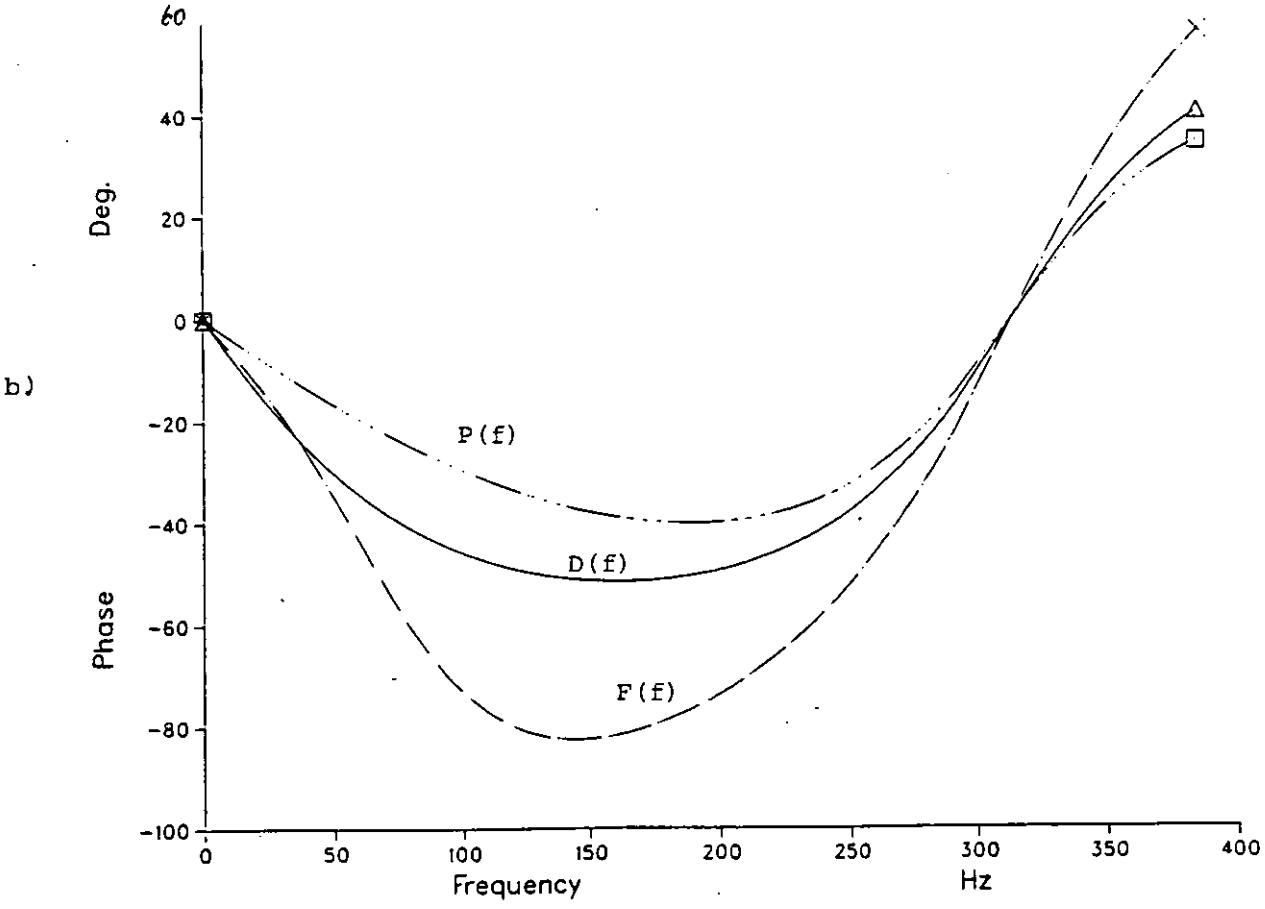

Fig. 5.3 Frequency response of second order DPLL; a) Amplitude; b) phase

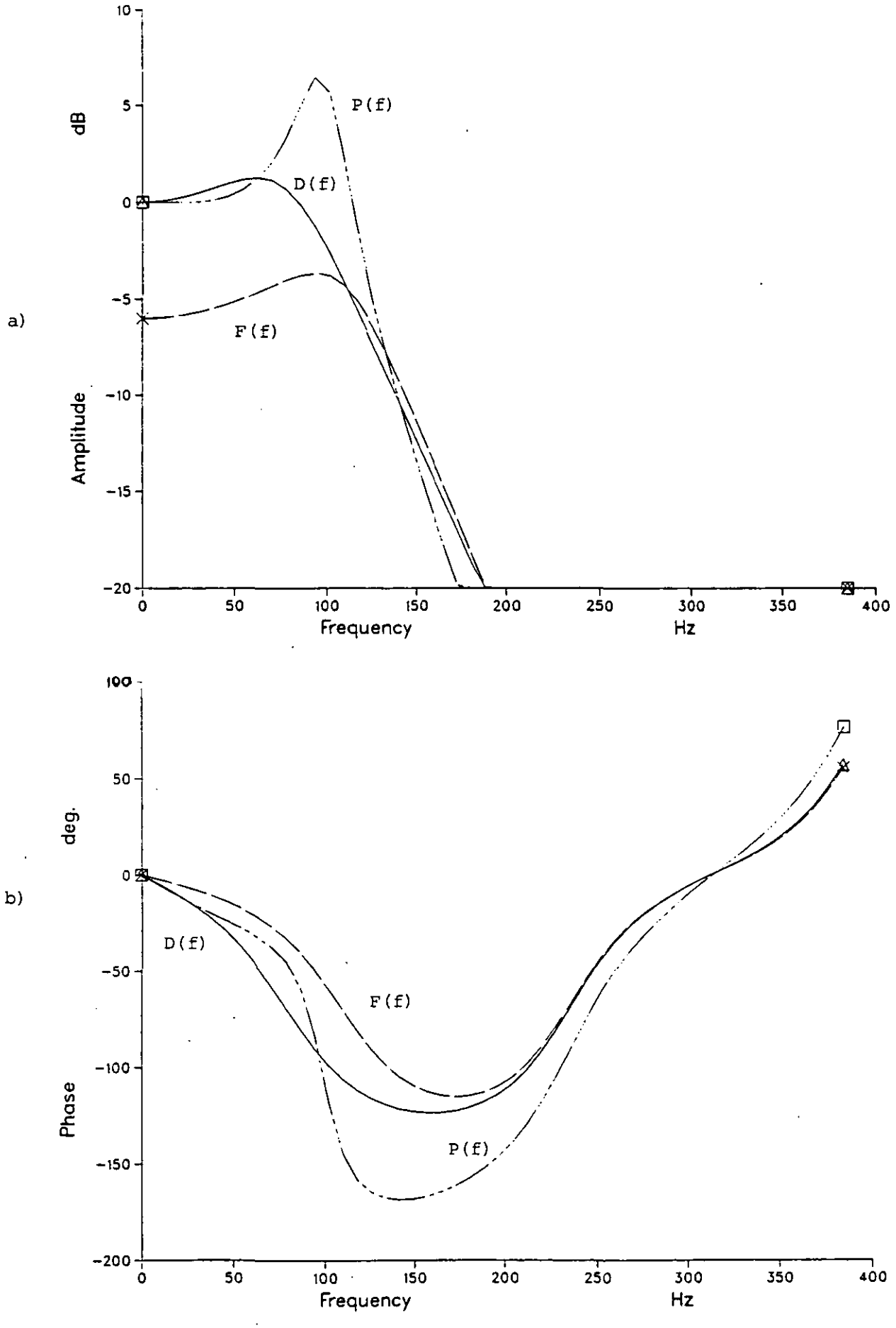

Fig. 5.4 Frequency response for 3rd order DPLL with Butterworth digital filter. a) Amplitude; b) phase

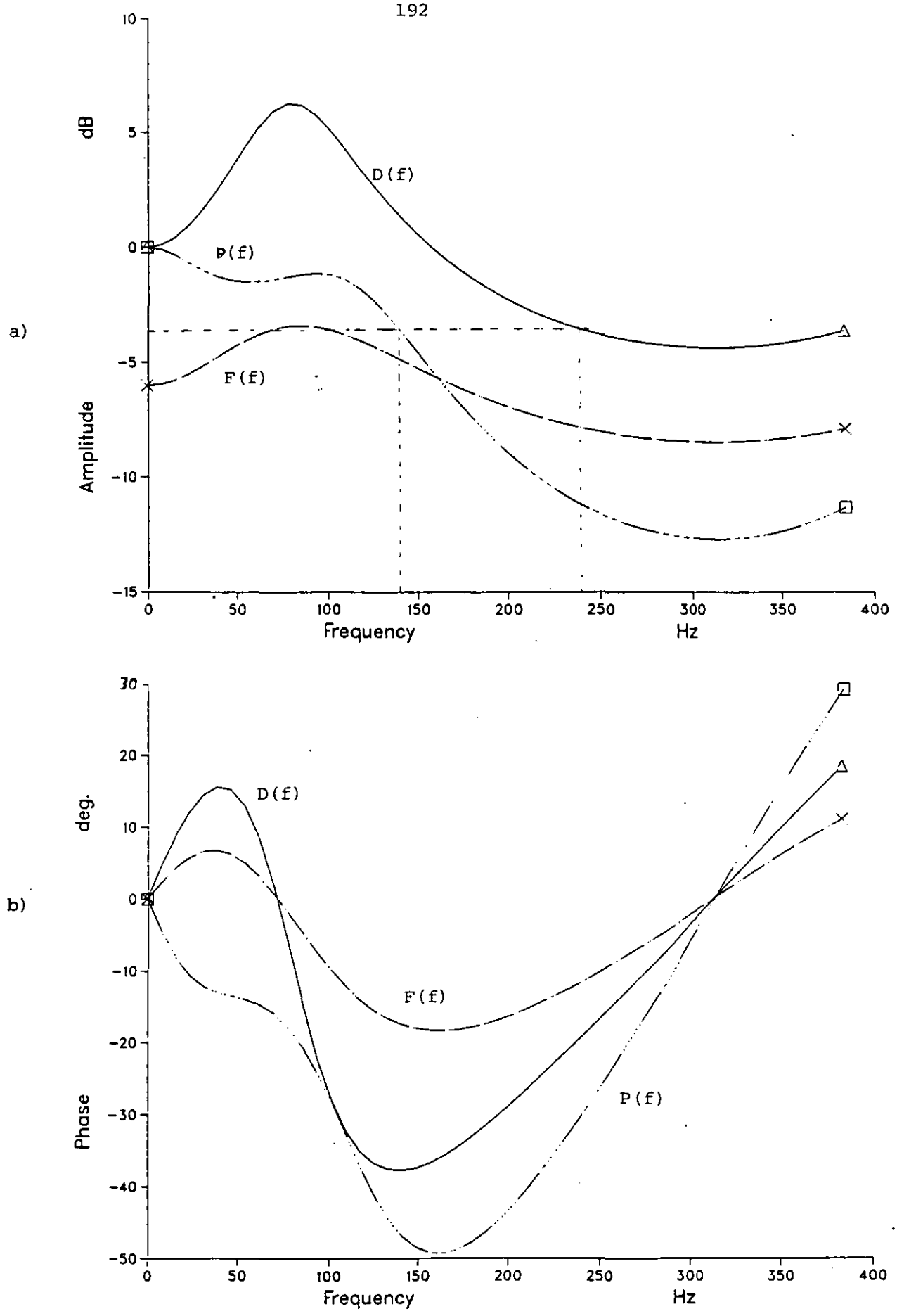

Fig. 5.5 Frequency response for 3rd order DPLL with Chebyshev digital filter. a) Amplitude; b) phase

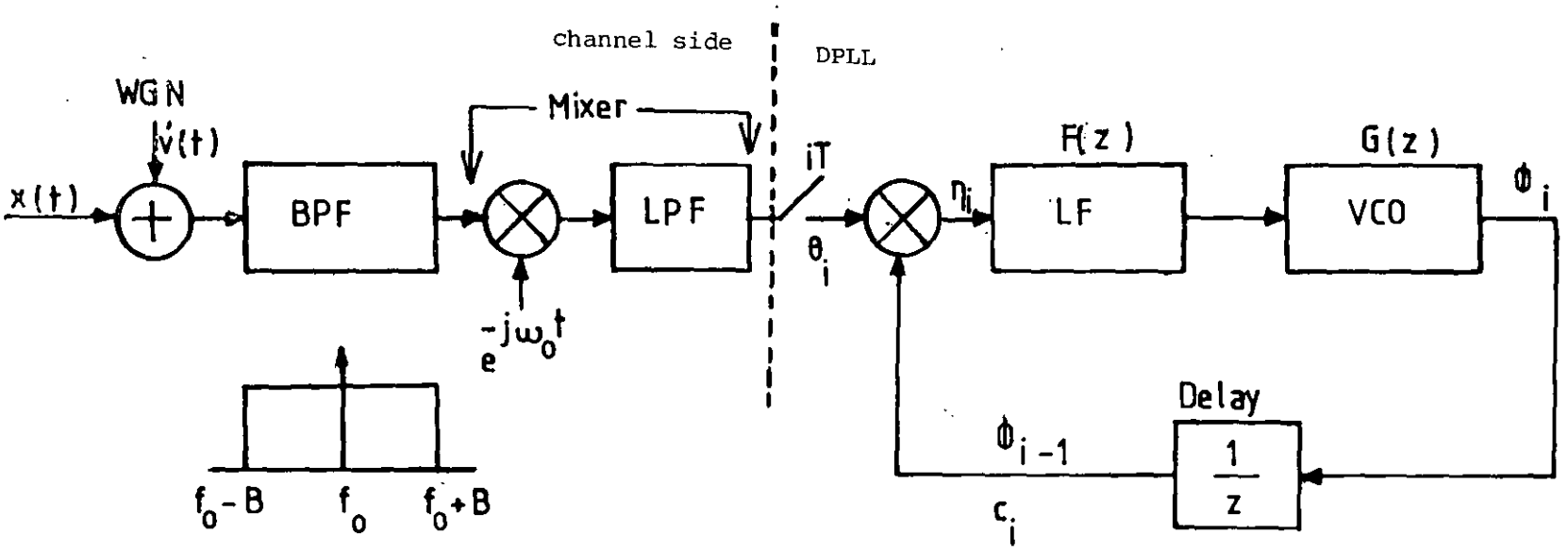

Fig. 5.6 Model of DPLL as carrier recovery

BPF; is the receiver bandpass filter

LPF: is a lowpass filter

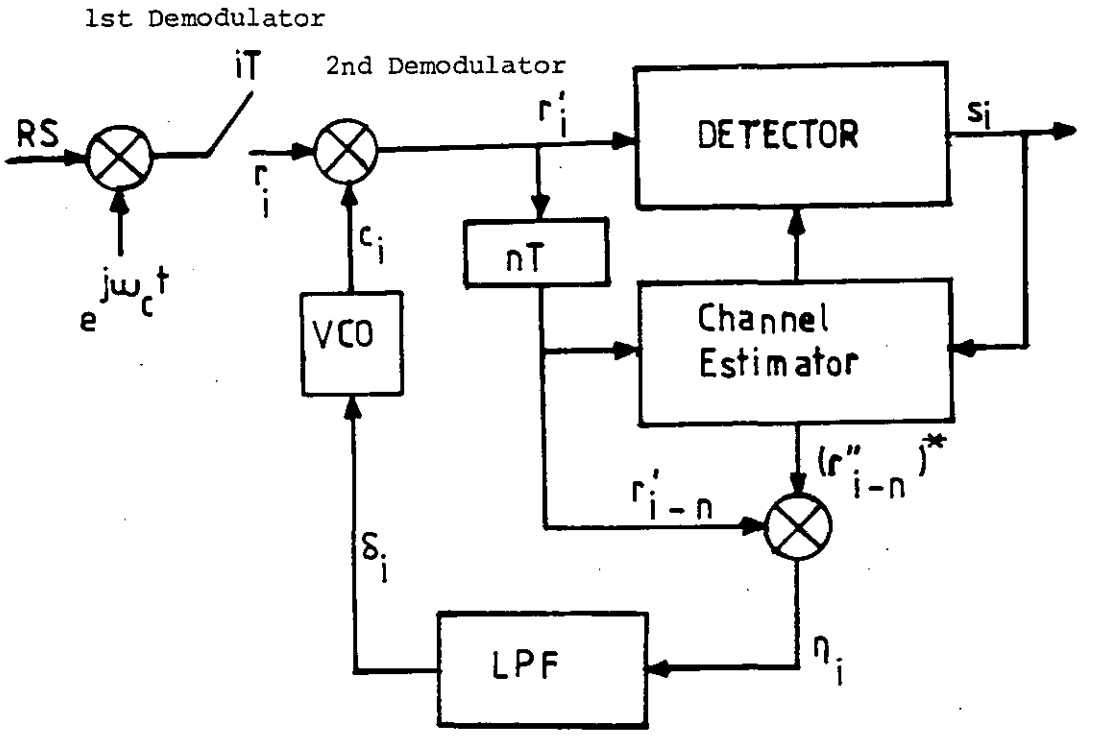

Fig. 5.7 Data Aided Carrier Recovery System employing DPLL, where

RS : Received signal

VCO : Voltage Control Oscillator

LPF : Lowpass Filter

nT : A delay element of nT

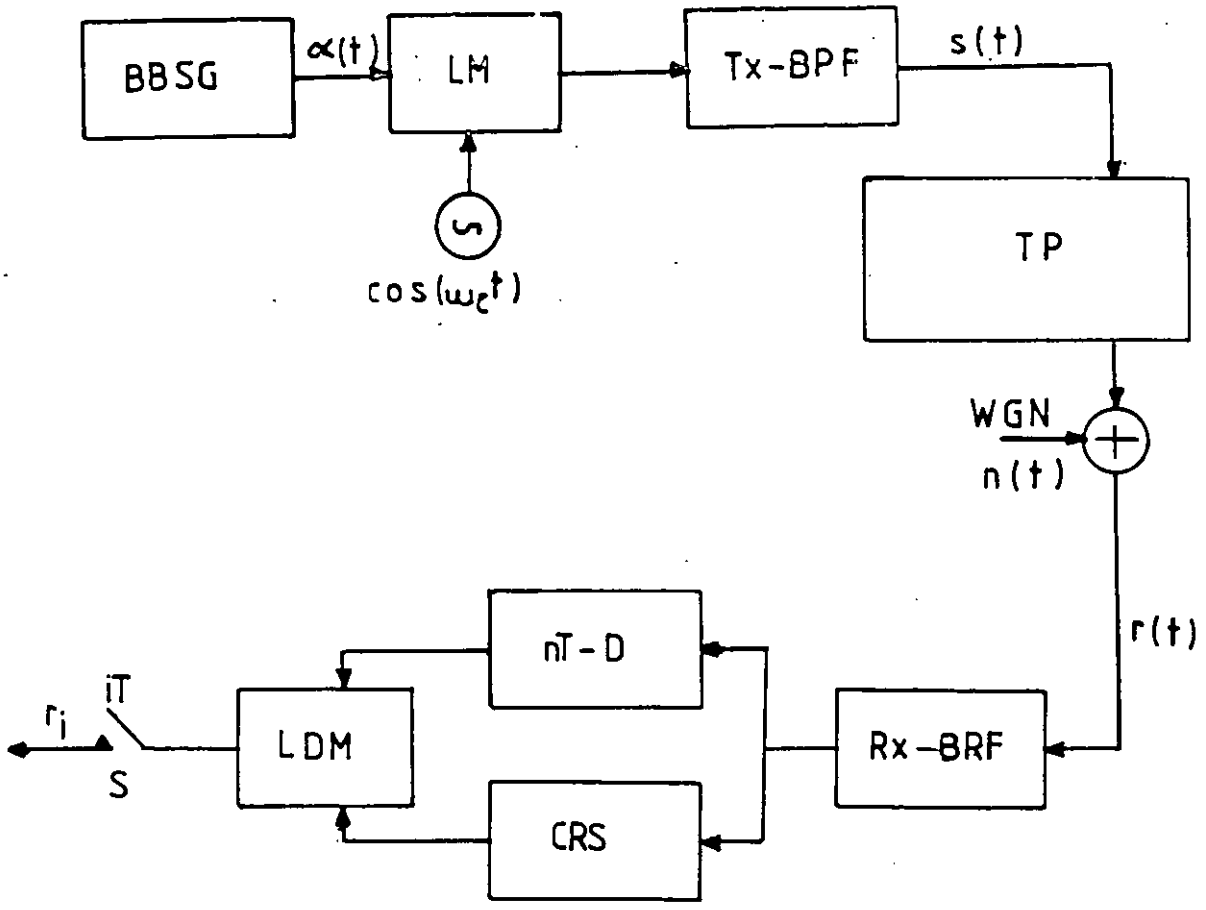

Fig. 5.8 Data Transmission Model with Carrier Recovery System, where

BBSG : Baseband Signal Generator
LM : Linear Modulator
Tx-BPF: Transmitter Bandpass Filter
Rx-BPF: Receiver Bandpass Filter
CRS : Carrier Recovery System
nT-D : A Delay Circuit of nT
LDM : Linear demodulator
s : Sampler
WGN : White Gaussian Noise
TP : Transmission Path

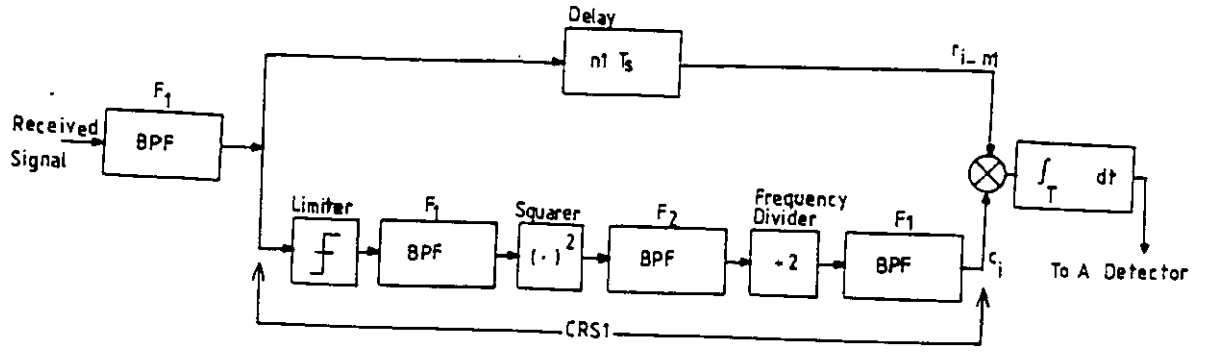

Fig. 5.9 A Receiver with Complete Carrier Recovery System CRS1

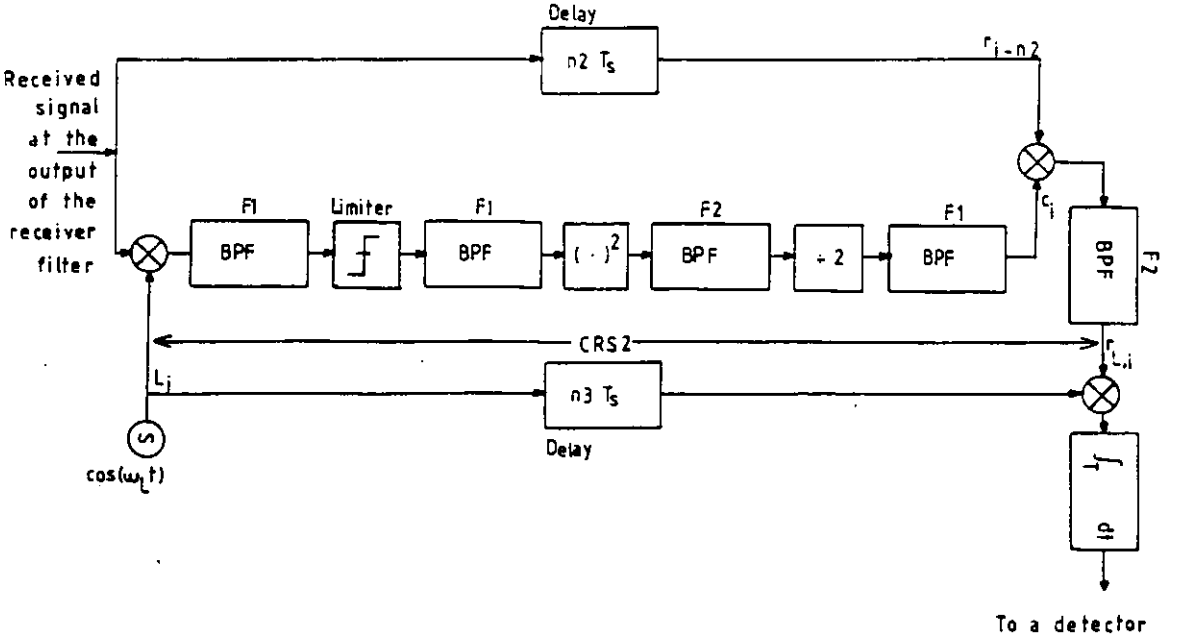

Fig. 5.10 A Receiver with Carrier Recovery System CRS2

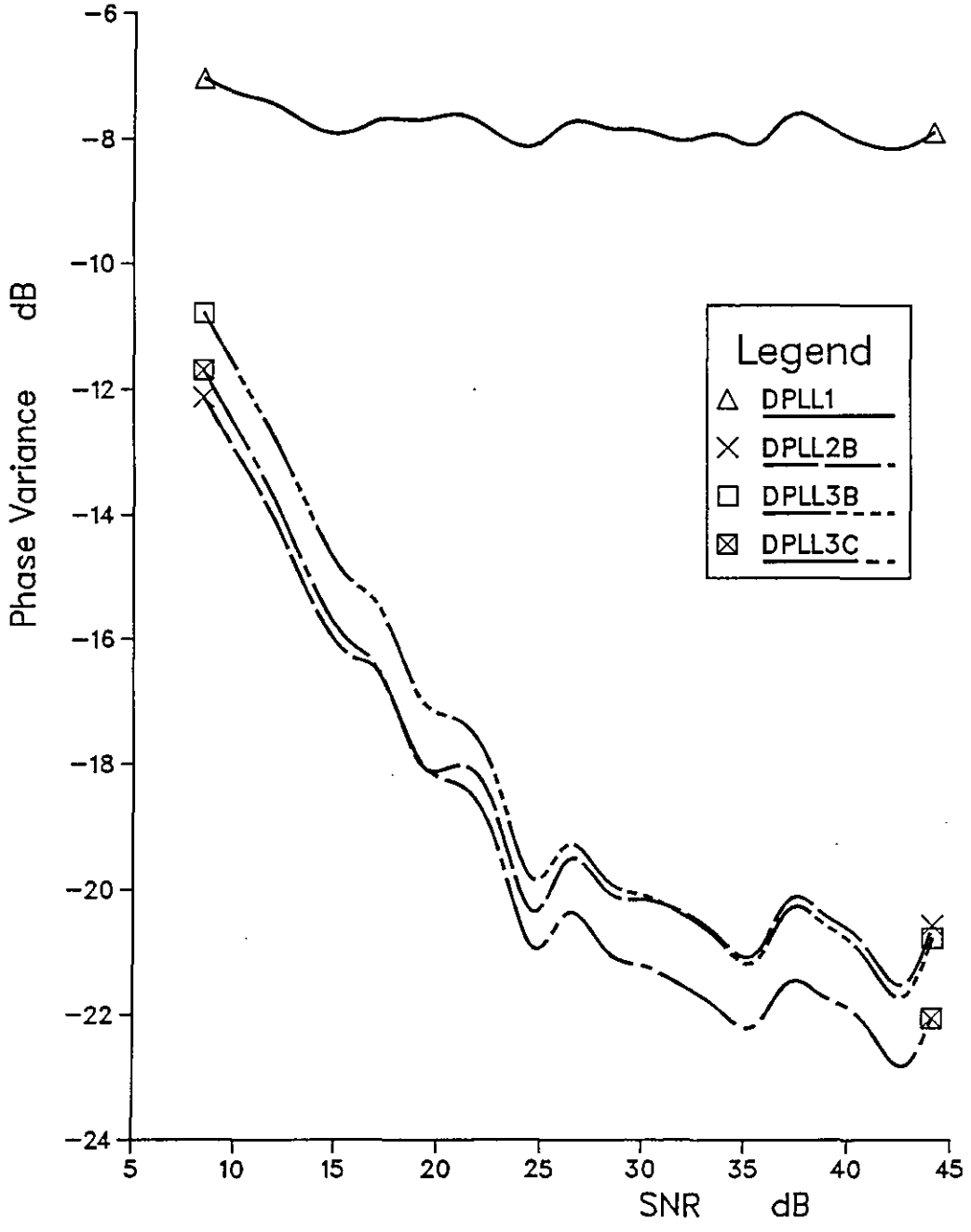

Fig. 5.11 Performances of different arrangements of DPLL's with hard limiter/discriminator under Rayleigh fading conditions, when f_D=100 Hz .

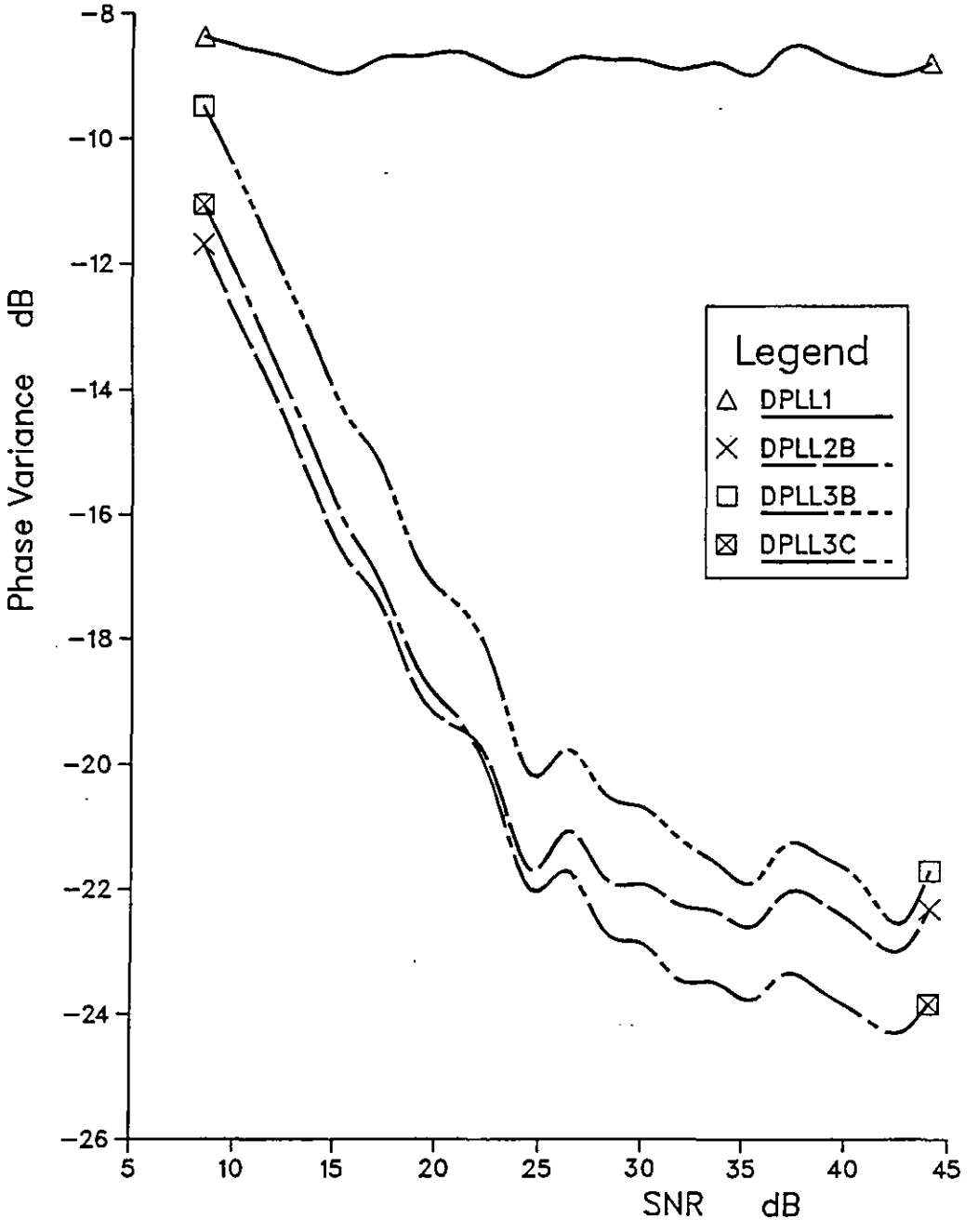

Fig. 5.12 Performances of different arrangements of DPLL's with tanlock PD under Rayleigh fading conditions, when f_D=100 Hz .

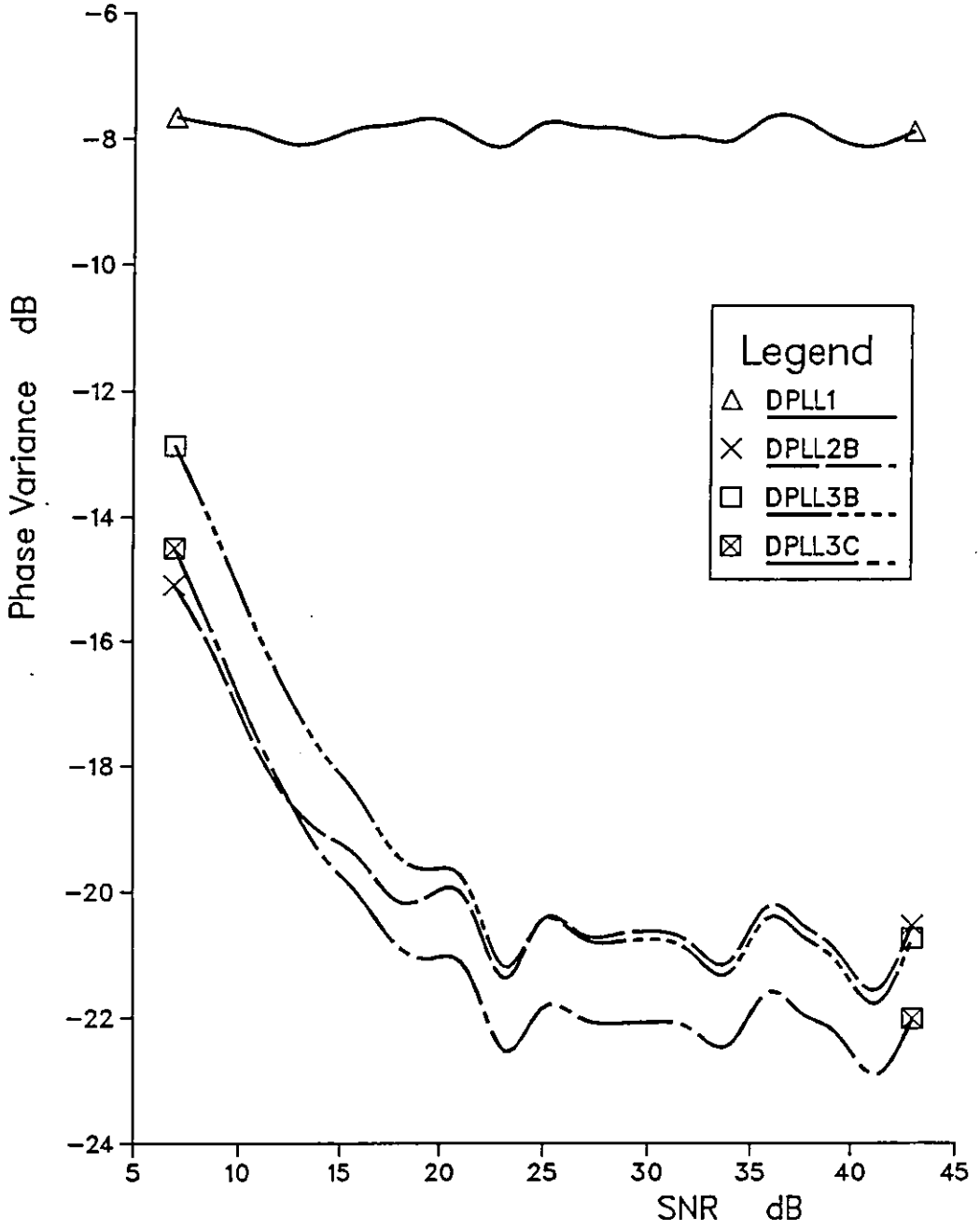

Fig. 5.13 Performances of different arrangements of DPLL's with hard limiter/discriminator when the received signal has a constant envelope and random frequency.

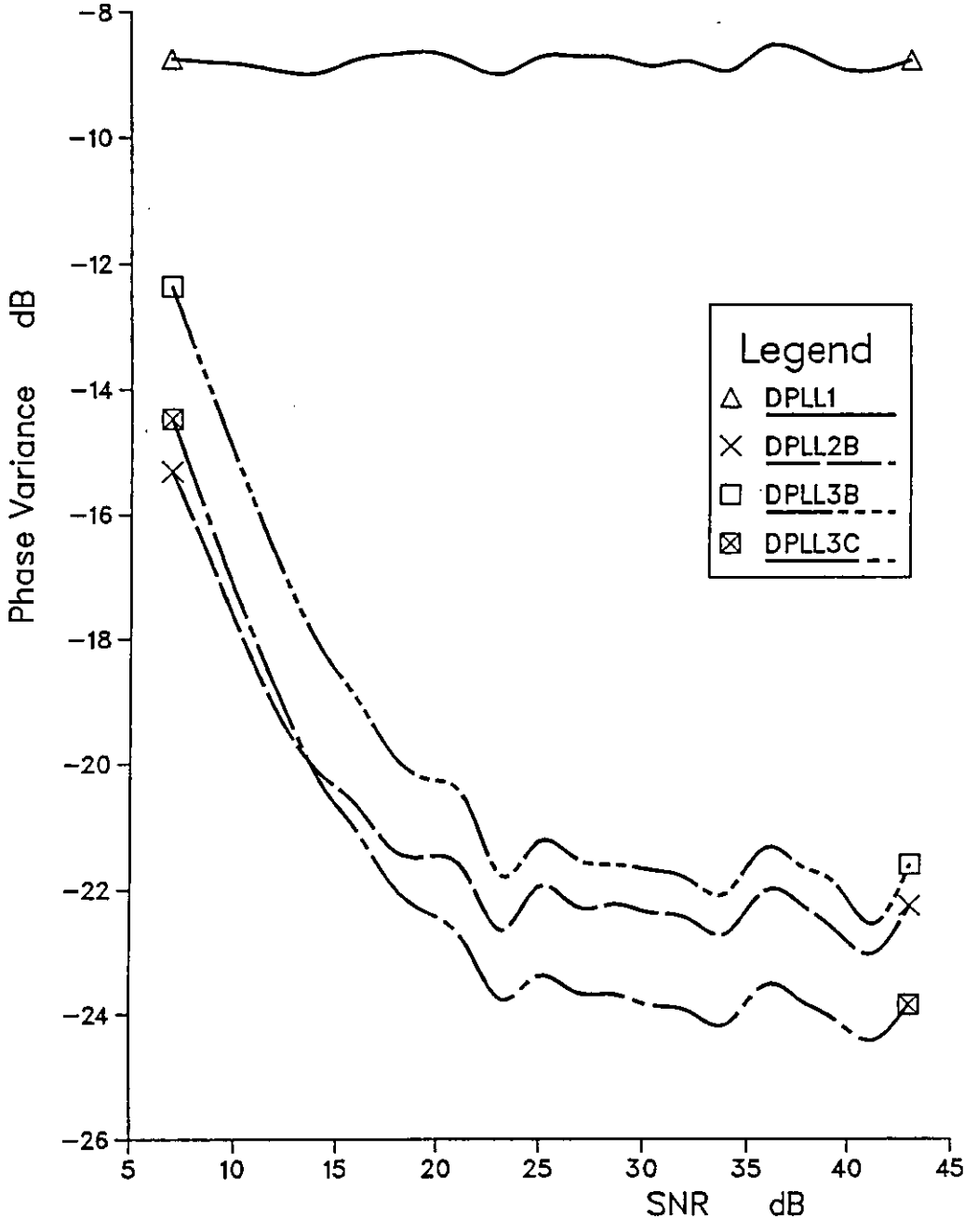

Fig. 5.14 Performances of different arrangements of DPLL's with tanlock PD. when the received signal has a constant envelope and random frequency.

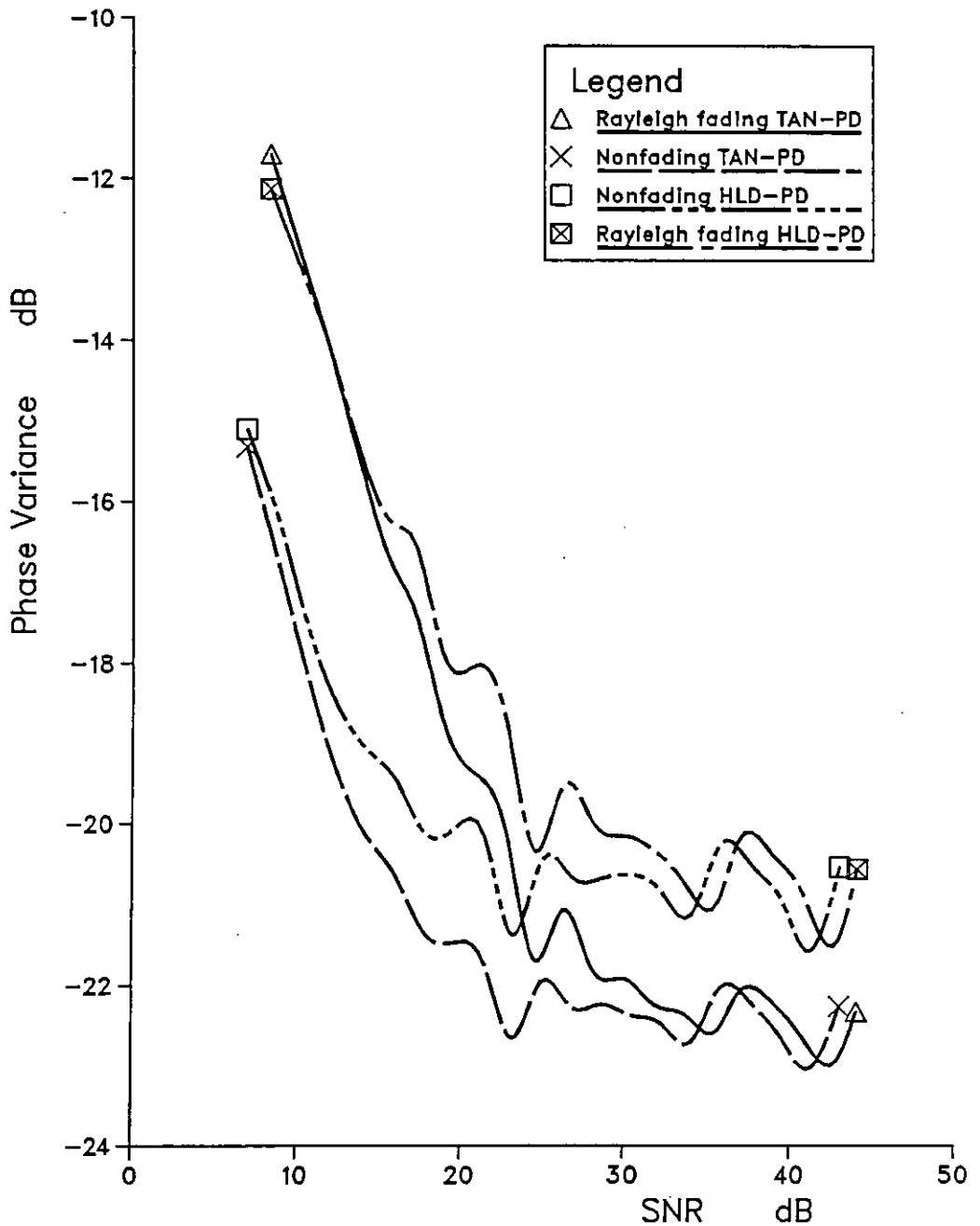

Fig. 5.15 Performance of DPLL2B under fading and nonfading conditions with Tanlock 'TAN' and hard/limiter discriminator 'HLD' as PD's.

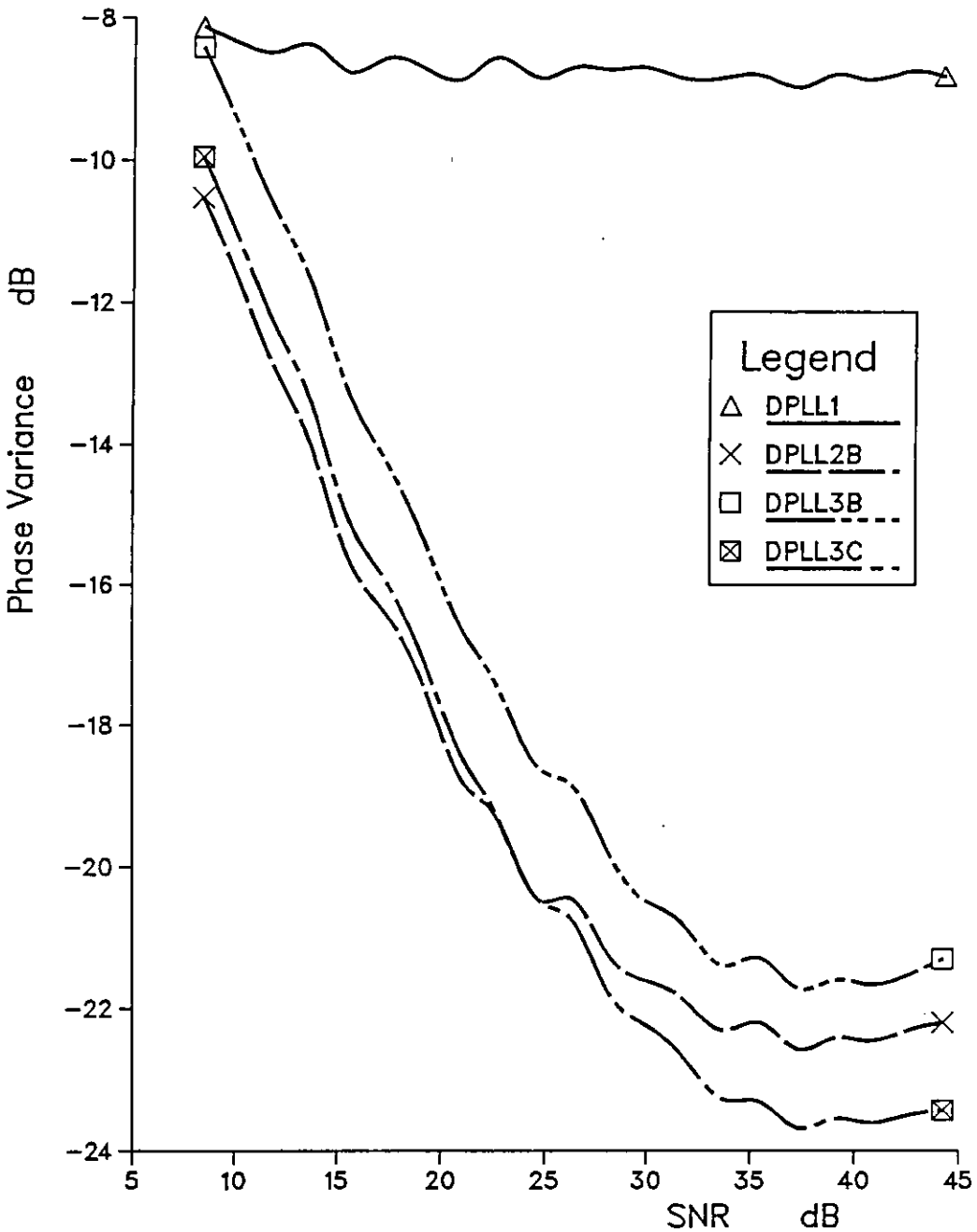

Fig. 5.16 Performances of different arrangements of DA–DPLL's with Tanlock–PD under Rayleigh fading conditions when fD=100 Hz.

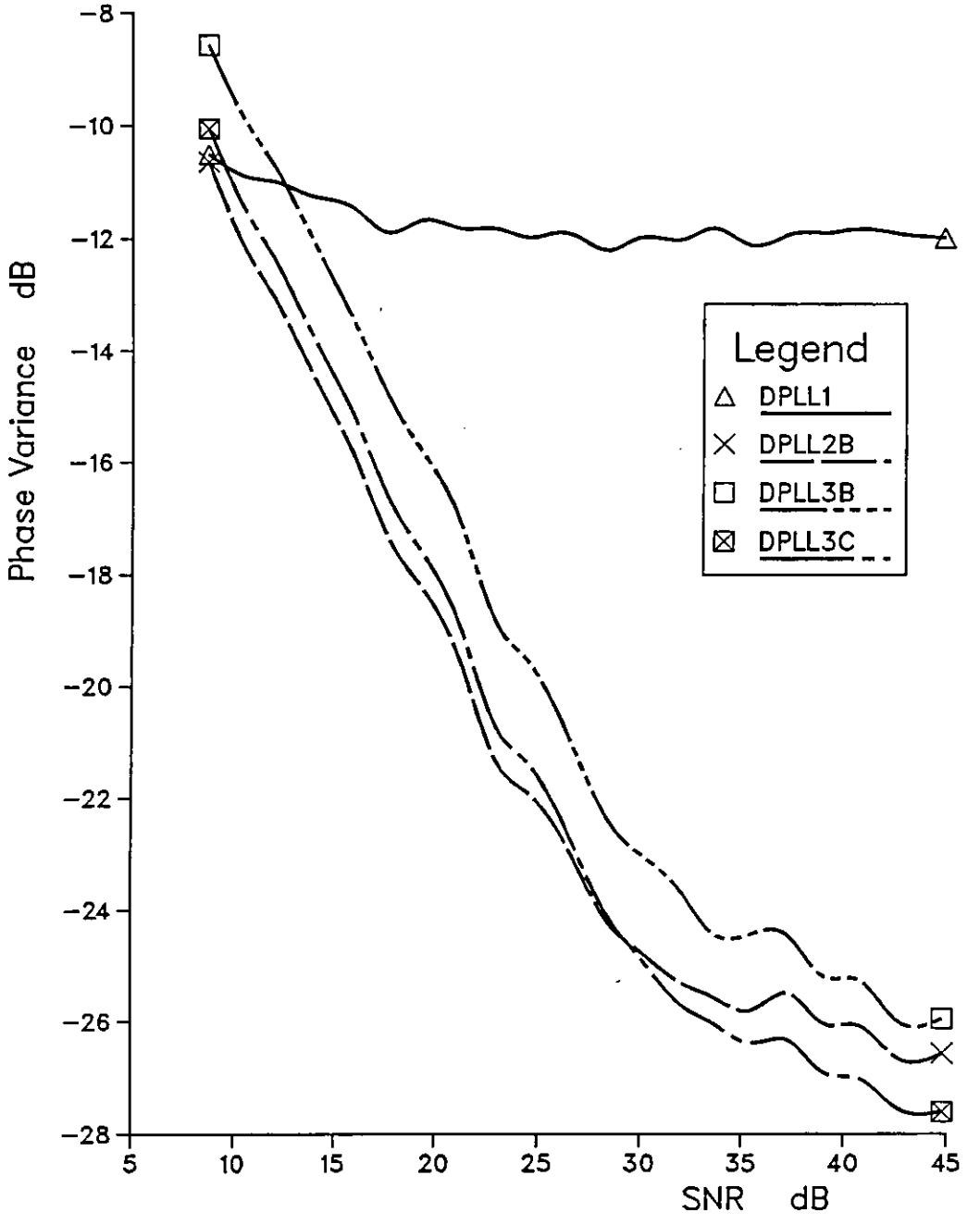

Fig. 5.17 Performances of different arrangements of DA−DPLL's with Tanlock−PD under Rayleigh fading conditions when fD=50 Hz.

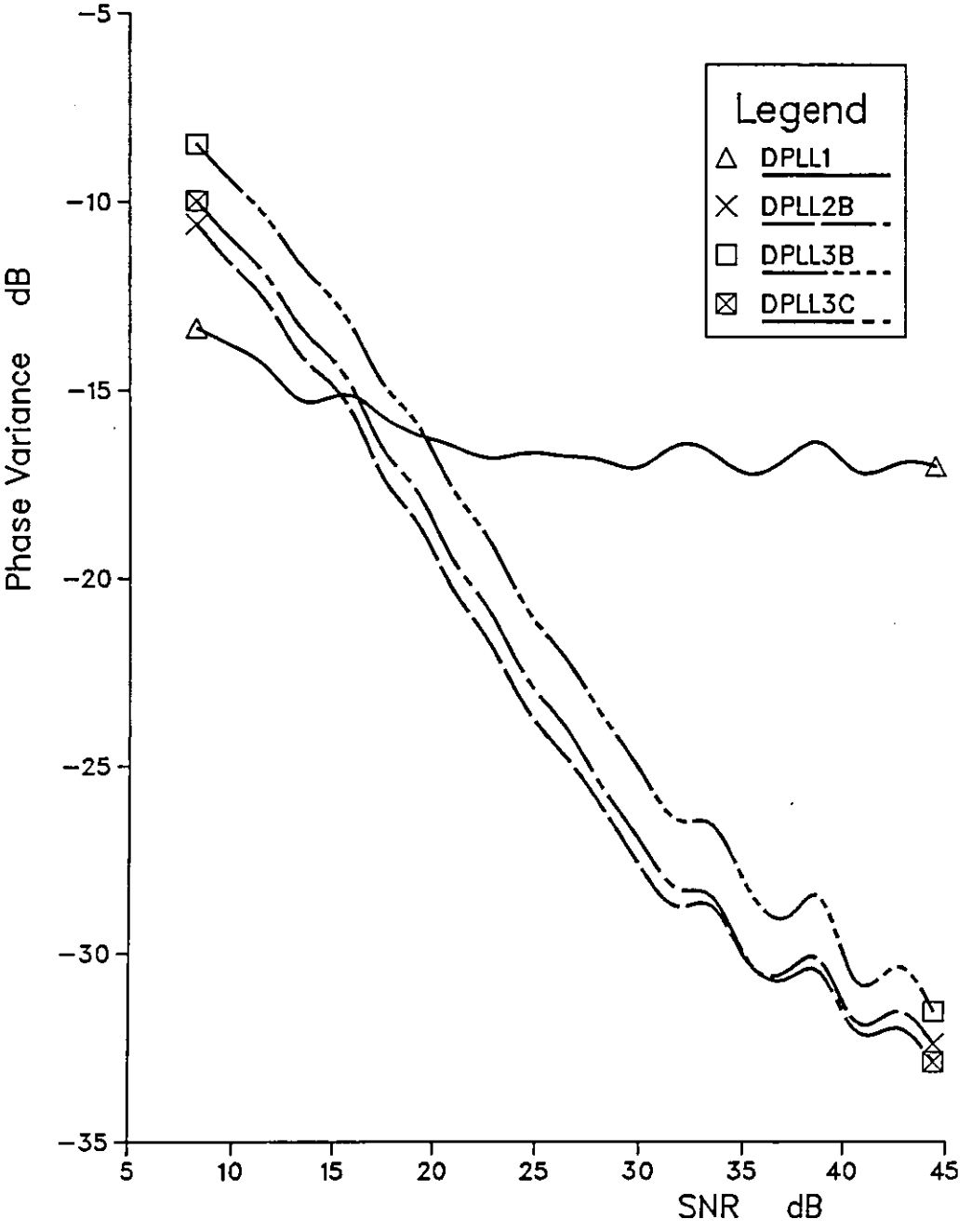

Fig. 5.18 Performances of different arrangements of DA–DPLL's with Tanlock–PD under Rayleigh fading conditions when fD=25 Hz.

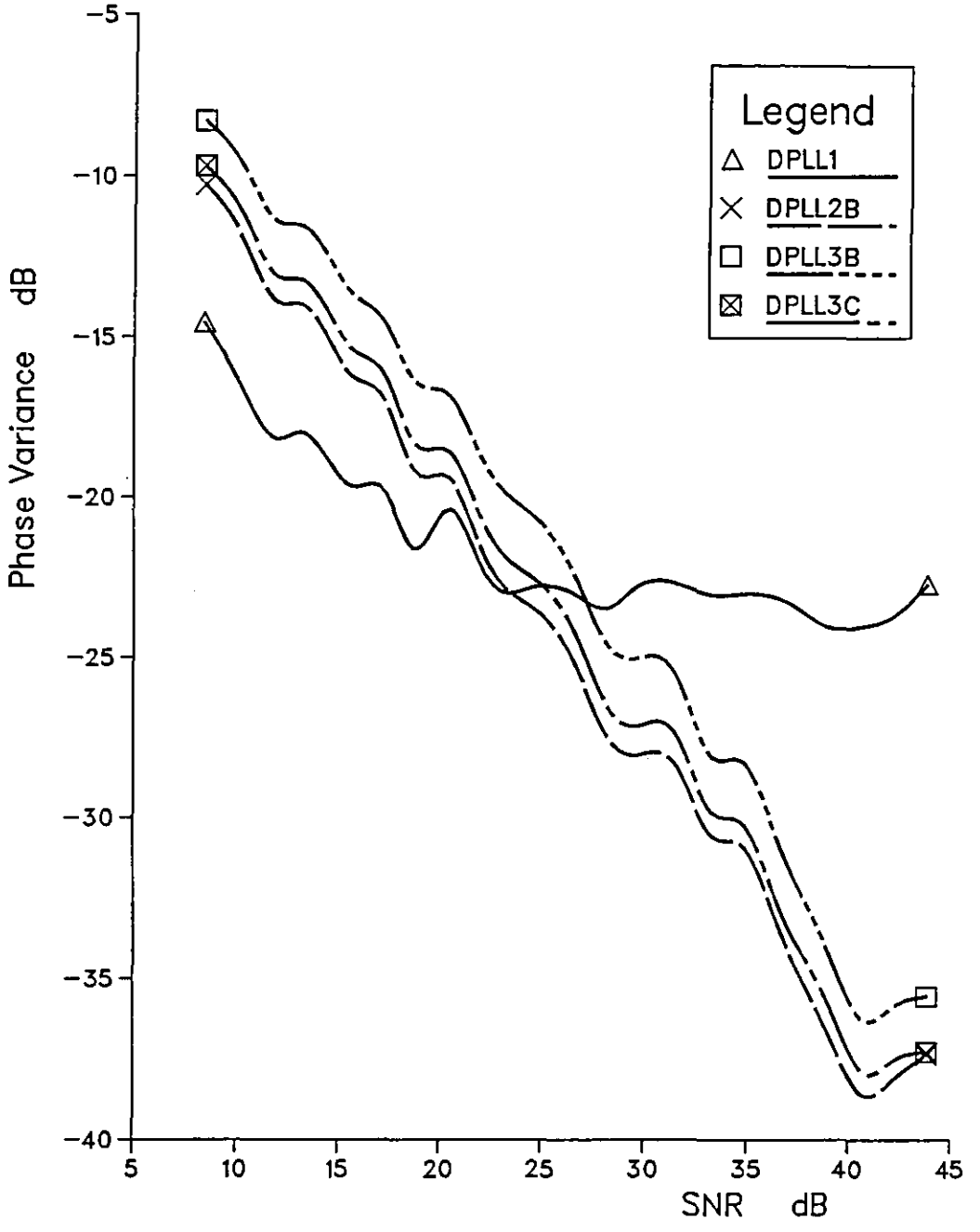

Fig. 5.19 Performances of different arrangements of DA–DPLL's with Tanlock–PD under Rayleigh fading conditions when fD=10 Hz.

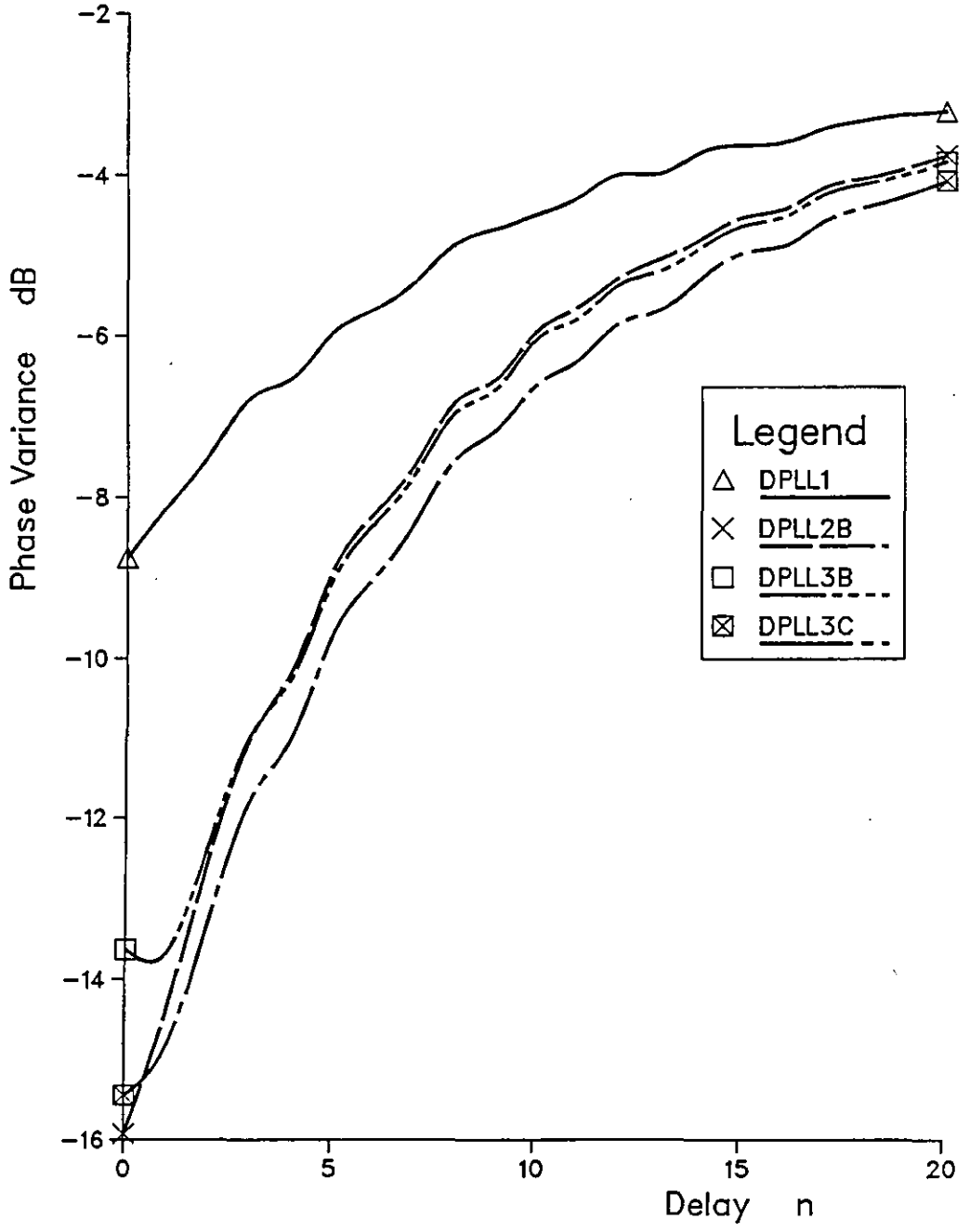

Fig. 5.20 Delay effects on the performances of DA–DPLL's with Tanlock–PD under Rayleigh fading conditions when SNR=15 dB and fD=100 Hz.

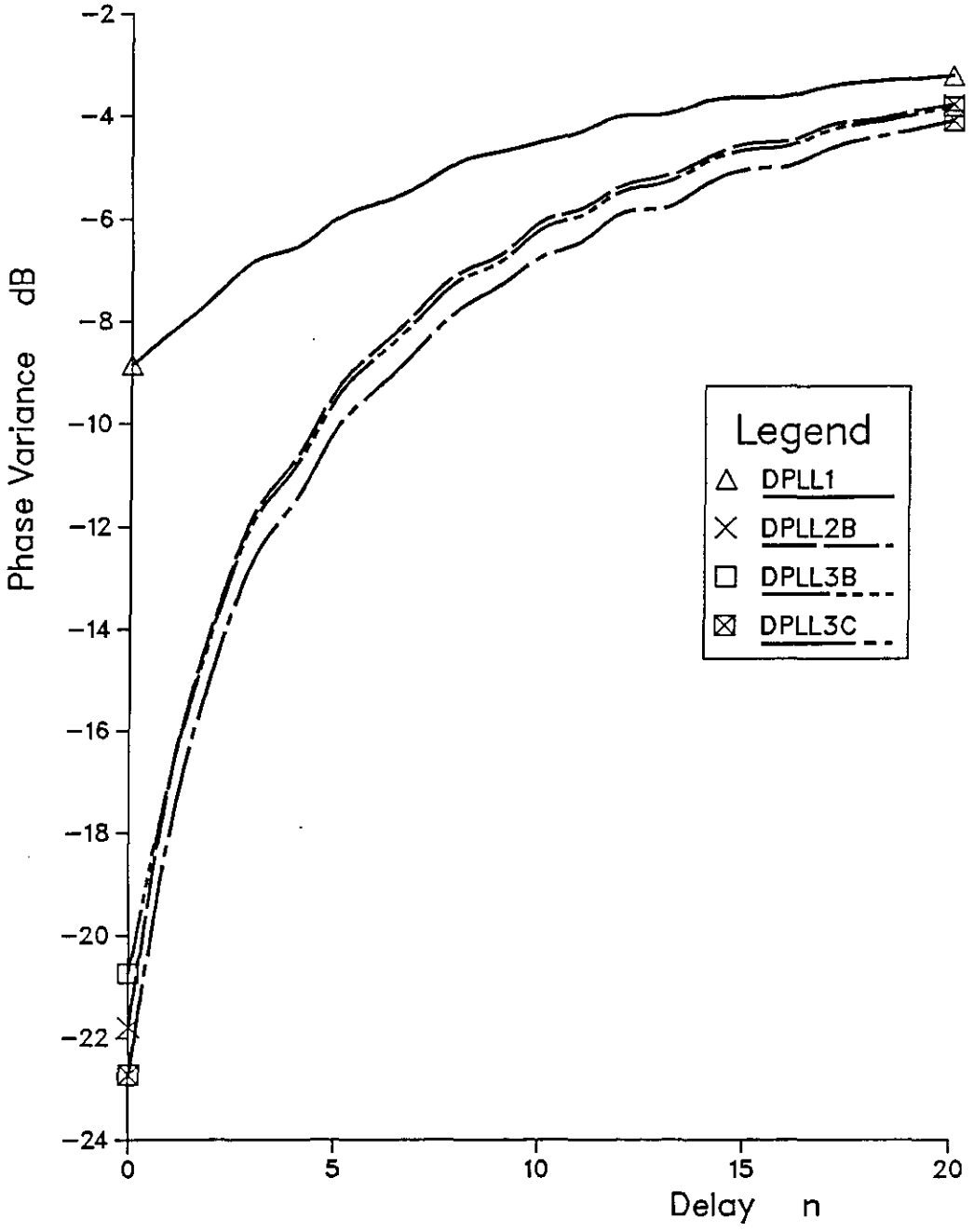

Fig. 5.21 Delay effects on the performances of DA–DPLL's with Tanlock–PD under Rayleigh fading conditions when SNR=30 dB and fD=100 Hz.

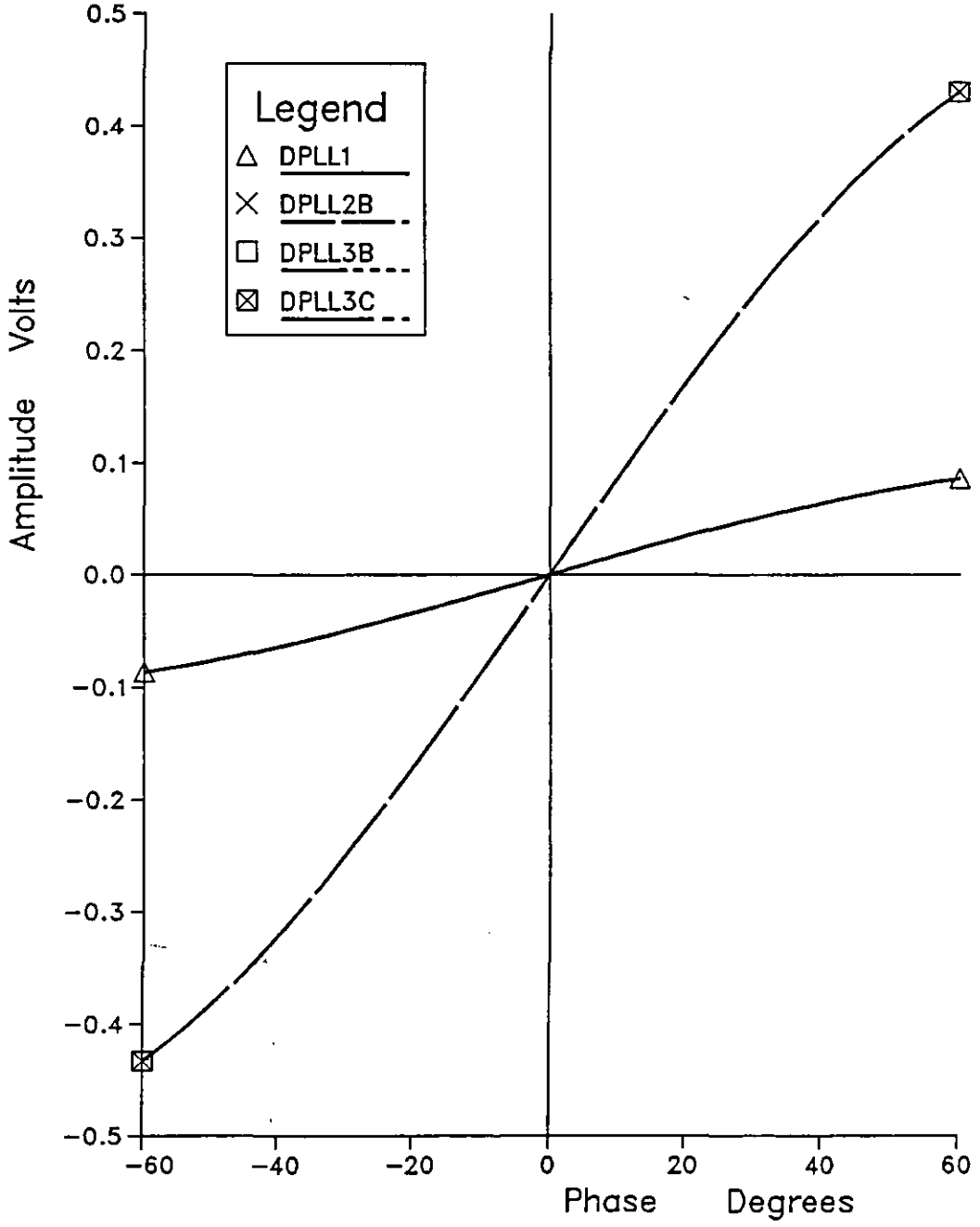

Fig. 5.22 Phase Detector Characteristic of different DPLL's under perfect codition {No Fading} with HLD–PD when SNR=30 dB.

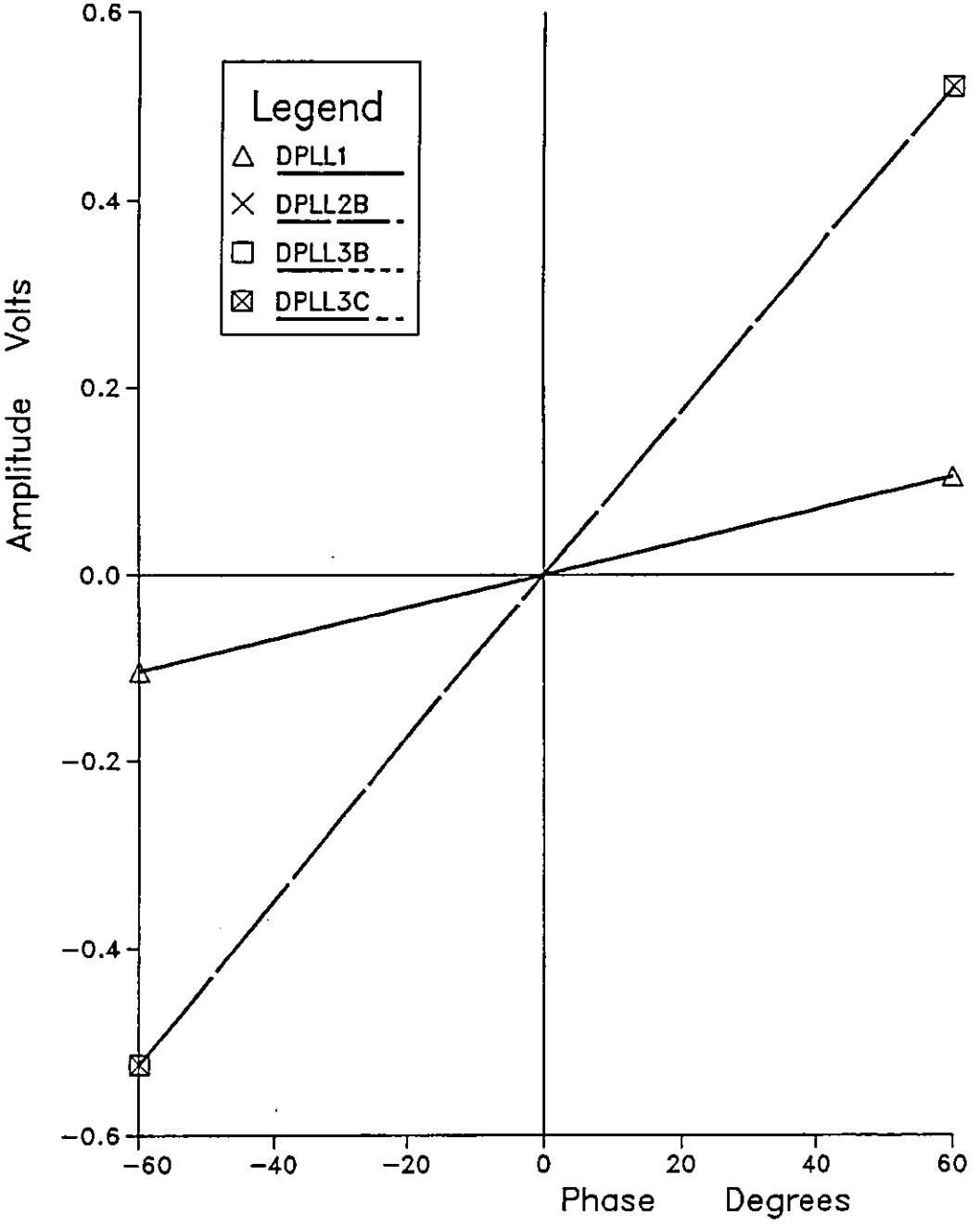

Fig. 5.23 Phase Detector Characteristic of different DPLL's under perfect codition {No Fading} with Tanlock–PD when SNR=30 dB.

6. CHANNEL ESTIMATION

6.1 Introduction

In the preceding chapters, the sampled impulse response of the channel was assumed correctly estimated. This assumption is not precisely true, especially in a mobile radio environment. Hence, it is necessary, at the receiver, to obtain an estimate of the sampled impulse response of the channel in order to achieve correct detection of the received signal. Two estimators are studied here, namely a feedforward channel estimator (FFCE) and a modified feedback channel estimator (MFBCE).

The feedback channel estimator techniques available in the literature (203,205,Appendix J), requires a delay of LT seconds, where L is the number of samples in the sampled impulse response and T is the symbol duration. It will be found that this delay degrades the performance of the estimator. Therefore, the feedback channel estimator is modified mathematially in Appendix J, in order to eliminate the effect of delay. Moreover, the modified feedback channel estimator used here is further developed by inserting a digital feedback control system, described in Appendix H, for the use with digital phaselocked loop techniques (Chapter 5).

The feedback channel estimators available in the literature, as prementioned, degrade by the delay, while the feedforward channel estimator degrades by the existence of the intersymbol interference error signal, which is defined in Appendix J. These degradations are eliminated in the modified feedback channel estimator (MFBCE) and better performance

is to be expected. Furthermore, the complexity of the MFBCE is identical to the complexity of FFCE, without the insertion of the digital control system in MFBCE.

The MFBCE uses the same transversal feedforward filter (called here dynamic filter) that has been used by the non-linear channel equaliser (Figure 4.5). Hence, it is possible in practice to add only a threshold level detector and to make a collectively adaptive nonlinear channel equalisation[5,109,147] and detections scheme.

Both estimators (FFCE and MFBCE) use the already detected data symbol. But, when the near-maximum likelihood detection scheme is employed, it requires a delay to reach a decision and at the same time requires to be supplied by the estimated sequence of the sampled impulse response of the channel. Therefore, the least-square fading-memory prediction method is used here, since it is a potentially better prediction method[204,206].

The two estimators studied here (FFCE and MFBCE) are tested separately under noisy and Rayleigh fading conditions, by extensive computer simulations. This measurement covers the optimisation tests, tolerance to additive noise tests, effect of delay tests, and convergence tests. All these tests are carried out in a mobile radio environment, represented by Rayleigh fading simulators.

6.2 Basic Assumptions

The data transmission model is shown in Figure 6.1, which is based on the model described in Chapters 3 and 4. The signal at the input of the baseband channel is a sequence of impulsed data symbol $s_i\delta(t - iT)$ where s_i are assumed statistically independent and equally likely to have any of K possible values (Chapters 2 and 4).

In mobile radio environment, the channel is subjected to multipath fading with Rayleigh distribution function. Therefore, the transmission path is represented by the multipath Rayleigh fading simulator defined and designed in Chapter 3. The transmission path (Rayleigh fading simulator) multiplies the impulse response of the channel by the factor q(t) which introduces the random phase/frequency fluctuations and fading (see Chapter 3, Equation 3.21). Hence, the baseband channel impulse response y(t), with an effective duration of LT seconds, is time varying with a Rayleigh distribution function, where L is a positive integer and T is the duration of the symbol in seconds. The noise introduced by the channel is white Gaussian noise, that is added to the signal at the output of the transmission path. Also, the noise is assumed here to include co-channel interference and adjacent channel interference. The noise becomes band-limited Gaussian noise at the output of the receiver filter.

At the output of the Rayleigh fading baseband channel, the received signal r(t) is sampled once per data element at time t=iT to give the received signal samples

$$r_i = \sum_{\ell=0}^{L-1} s_{i-\ell}\, y_{i,\ell} + w_i \qquad 6.1$$

where $w_i = w(iT)$ is the complex-valued samples waveform of the additive band-limited noise with zero mean and power spectral density of $\frac{1}{2} N_o$. The complex-valued sampled impulse response of the channel is given by (Equations 3.79 and 3.80)

$$\begin{aligned} Y_i &= [y_{i,0}\ y_{i,1} \cdots y_{i,L-1}] \\ &= H_o Q_i \end{aligned} \qquad 6.2$$

where

$$H_o = [H_o\ h_1 \ldots h_{L-1}] \qquad 6.3$$

is the linear (nonfading) baseband channel impulse response (Equation 3.77) and

$$Q_i = \begin{vmatrix} q_i & 0 & \cdots & 0 \\ 0 & q_{i-1} & \cdots & 0 \\ \vdots & \vdots & & \vdots \\ 0 & 0 & & q_{i-L+1} \end{vmatrix} \qquad 6.4$$

is (LxL) diagonal matrix derived from the Rayleigh fading simulator (Equation 3.81). The linear modulator, linear demodulator, the transmitter and receiver filters all together form H_o (for more detail see Chapter 3). The delay (which is the relative mean of all paths delay in case of multipath propagation[10,11]) other than dispertion is neglected here so that $y_{i,\ell} = 0$ for $\ell < 0$ and $\ell > L-1$.

The detected replica of $\{s_i\}$ designated as $\{s'_i\}$ which are, for reasonable purposes, assumed correctly detected[5,200,203-206]. Thus $s'_i = s_i$ for all values of i. The signals r_{i-n} and s'_{i-n} are fed to the channel estimator to give an estimate Y'_i of Y_i at time $t = iT$, where n is an appropriate integer, that represents the number of samples by which the detector delayed the detected element, when a near-maximum likelihood detector is used, and

$$Y'_i = [y'_{i,0} \quad y'_{i,1} \cdots y'_{i,L-1}] \tag{6.5}$$

is the estimated sampled impulse response of the channel.

6.3 Feedforward Channel Estimator (FFCE)

The FFCE based on the feedforward tranversal filter is shown in Figure 6.2. The mathematical analysis, for deriving the stepsize that is used to update the estimate Y_i' of Y_i, is introduced in Appendix J. On the receipt of r_i, the estimator holds in its stores the detected data symbol $\{s_i'\}$ of $\{s_i\}$, which are assumed correctly detrected[5,109,200,203-206]. Also, the delay required by the detector (in case of using near maximum likelihood detection schemes) is neglected here for the purpose of this discussion. Hence, the estimate Y_i' of Y_i is given by[5,220,203-205]

$$Y_i' = Y_{i-1}' + b\, P_i \qquad 6.6$$

where b is a small positive constant that controls the rate of convergence of the estimator and P_i is an L-component vector given by

$$P_i = e_i[(s_i')^* \ (s_{i-1}')^* \ (s_{i-2}')^* \ \ldots \ (s_{i-L+1}')^*] \qquad 6.7$$

$(s_i')^*$ is the complex-conjugate of s_i' and e_i is the error signal obtained from the subtraction of the estimated signal r_i' from the received signal r_i, or

$$e_i = r_i - r_i' \qquad 6.8$$

where r_i is defined by Equation 6.1 and

$$r_i' = \sum_{\ell=0}^{L-1} s_{i-\ell}'\, Y_{i-1,\ell}' \qquad 6.9$$

Hence, the ℓ^{th} component of Y'_i is given by

$$y'_{i,\ell} = y'_{i-1,\ell} + b\, e_i\, (s'_{i-\ell})^* \qquad 6.10$$

It has been found in Appendix J, that the major impairments in the FFCE are the noise and intersymbol interference error signal components which cannot be easily compensated for especially in rapidly varying and noisy channels. Also, for multilevel QAM-signals, it is necessary to multiply by the reciptocal of $s'_{i-\ell}$, in Equation 6.10, and not by $(s'_{i-\ell})^*$ in order to reduce the noise and intersymbol interference error signal components (Appendix J). Moreover, the values of the intersymbol interference error signal components cannot be assumed to be equal to zero, in mobile radio communications: such assumptions may be possible in conditions where the channel is slowly varying with time.

6.4 Modified Feedback Channel Estimator (MFBCE)

The operation of the feedback channel estimator (FBCE) is based on the feedback filter shown in Figure 6.3, and its mathematical analysis is presented in Appendix J. The FBCE gives Y_i' the estimate of Y_i on the receipt of $r_{i+L}^{(109,203,205)}$, and hence, there is a delay of LT seconds, where L is an appropriate integer and T (in seconds) is the symbol duration. As in the case of FFCE, the FBCE must also use the already detected data symbols to generate an error signal by which it can control its output. Hence, the detection process has to be delayed by the same period, even with a zero delay detector such as the nonlinear equaliser. This delay, however, does not only degrade the performance of FBCE, but degrades the performance of the detector as well.

The FBCE is modified mathematically in order to overcome the discrepancy caused by the delay (Appendix J). The modification led to a further development by which the practical implementation is easier. The developed system consists of:-

i) A dynamic feedforward transversal filter

ii) A feedback digital control system

iii) A static feedforward transversal filter

Figure 6.4 illustrates the arrangement of the MFBCE which operates as follows:-

i) The dynamic filter takes its coefficients from the estimated impulse response of the channel by feedback loops (not shown in Figure 6.4).

It detects any changes in the channel and feeds its output after multiplication by $(s_i')^{-1}$ to the digital control system. Hence, the signal at the input of the digital control system is given by

$$\phi_i = (r_i - \sum_{\ell=1}^{L-1} s'_{i-\ell} y'_{i-1,\ell})(s'_i)^{-1}$$

$$= y_{i,0} + (s'_i)^{-1} \sum_{\ell=1}^{L-1} (s_{i-\ell}\, y_{i,\ell} - s'_{i-\ell}\, y'_{i-1,\ell})$$

$$+ w_i (s'_i)^{-1} \qquad 6.11$$

ii) The feedback digital control system employed here is second order that has been designed and tested previously (Appendix H, Chapter 5). It has two important facilities since it acts as a noise filter and a controller. It compares its input and output to generate an error signal that is given by

$$e_i = \phi_i - q'_{i-1} \qquad 6.12$$

This signal is fed to the loop filter of the feedback control system and the filter output is found to be

$$\delta_i = \sum_{k=0}^{2} c_k\, e_{i-k} - \sum_{k=1}^{2} d_k\, \delta_{i-k} \qquad 6.13$$

where c_k , for k=0 to 2, and d_k, for k=1,2 are the filter coefficients

defined in Chapter 5, in the case of digital phase-locked loop (DPLL2B). Subsequently, this signal is fed to an integrator to give

$$q'_i = q'_{i-1} + \delta_i \qquad 6.14$$

The signal from the output of the digital control is passed to the static filter.

iii) The static feedforward filter has constant coefficients, that are given by Equation 3.77, and the step-size factor b, which is a constant parameter (Equation J.33). This filter gives L different components representing the sequence Y'_i the estimate of Y_i. An individual component is given by

$$y'_{i,\ell} = (b-1)y'_{i-1,\ell} + bq'_{i-\ell}\, h_\ell \quad \text{for } \ell = 0,1, \ldots, L-1 \qquad 6.15$$

where $\{h_\ell\}$ are given by Equation 3.77. Clearly, the names dynamic and static have been given to those two filters according to the behaviour of their coefficients.

The sequence $\{q'_i\}$ can be arranged in a diagonal matrix such as (Equation J.46)

$$Q'_i = \begin{vmatrix} q'_i & 0 & 0 & \ldots & 0 \\ 0 & q'_{i-1} & 0 & \ldots & 0 \\ 0 & 0 & q'_{i-2} & \ldots & 0 \\ \vdots & \vdots & \vdots & & \vdots \\ 0 & 0 & 0 & & q'_{i-L+1} \end{vmatrix}, \qquad 6.16$$

Then the row estimate ψ_i, whose components are used to update Y'_{i-1}, is given by (Equation J.47)

$$\psi_i = H_o Q'_i \qquad 6.17$$

Hence, the estimate Y'_i of Y_i is obtained according to Equation J.40, such as

$$Y'_i = (1-b)\, Y'_{i-1} + b\, \psi_i$$

$$= Y'_{i-1} + b(\psi_i - Y'_{i-1})$$

$$= Y'_{i-1} + b(H_o Q'_i - Y'_{i-1}) \qquad 6.18$$

The components of Y'_i are used by the detector for detection of the next data symbol without any delay.

6.5 Least-Square Fading-Memory Prediction

The application of a near-maximum likelihood detection scheme requires a delay of n sampling interval in order to detect s'_i, after the reception of r_{i+n} (151-165, Chapter 4), where n is an appropriate integer and r_{i+n} is given by Equation 6.1. Clearly, the estimators described above give an estimate Y'_i of Y_i, when r_i is received. Also, the estimators use r'_i, the estimated signal which is obtained from the detected sequence, S'_i, and the estimated sampled impulse response of the channel, Y'_{i-1}, in their estimation processes. While the near-maximum likelihood detector needs to use Y'_{i+n}, Y'_{i+n-1}, Y'_{i+n-2}, ..., Y'_{i-1} to be able to carry out the detection procedure described in Chapter 4. Accordingly, the components of the sequences $(Y'_{i+n}, Y'_{i+n-1}, Y'_{i+n-2}, \ldots)$ must be provided by using one of the prediction methods (203,204). Moreover, the received signal sequence $[r_{i+n}, r_{i+n-1}, r_{i+n-2}, \ldots, r_i]$ has to be kept in store for subsequent detection and estimation processes. The predicted value of Y'_{i+n} from the information received at time t=iT (seconds) is designated as $Y'_{i+n/i}$. Different methods for predicting the value of $Y'_{i+1/i}$ or $Y'_{i+n/i}$ from the estimate Y'_i, Y'_{i-1}, ... of Y_i, Y_{i-1}, ... have been studied elsewhere (200,203,204); the least-square fading-memory prediction is recommended for use here (204,206). Subsequently, a degree 1 polynomial is only used here which is given by

$$(Y'_{i+1/i})' = (Y'_{i/i-1})' + (1 - \theta)^2 E_i \qquad 6.19$$

$$Y'_{i+1/i} = Y'_{i/i-1} + (Y'_{i+1/i})' + (1 - \theta^2) E_i \qquad 6.20$$

$$Y'_{i+n/i} = Y'_{i+1/i} + (n+1)(Y'_{i+1/i})' \qquad 6.21$$

where $(Y'_{i+1/i})'$ is a function of the first differential of $Y'_{i+1/i}$ with respect to time and

$$E_i = Y'_i - Y'_{i/i-1} \qquad 6.22$$

θ is a real constant in the range 0 to 1.

$(Y'_{i+1/i})'$ appears essentially as a dummy variable in the algorithm but its function is to assist in determining the required prediction and it is not necessary to be considered in further detail[203]. Furthermore, the values of individual components of $(Y'_{i+1/i})'$ may be zero when no changes occur in the channel. However, the polynomial is initialized as follows

$$Y'_{1/O} = Y'_O = H_o$$

$$(Y'_{1/O})' = O \qquad 6.23$$

Clearly, increasing the value of θ towards 1, the weight factor decreases in the prediction process.

6.6 Computer Simulation Tests and Results

The performances of the FFCE and MFBCE are studied here by computer simulation tests in the presence of additive noise and Rayleigh fading conditions.

The two systems have two not well valued parameters since the value of each is between zero and one. These parameters are:-

i) The convergence constant, b.

ii) The prediction weighting factor, θ.

Therefore, it is necessary to select the values of these two parameters (b and θ) such that each of the estimators gives optimum performance in noisy conditions and in possible fading rates. The optimisation tests can be carried out by selecting either the value of θ as near as possible to 1 or the value of b as close as possible to zero and making the value of the other parameter vary from zero up to one, with relatively low signal-to-noise ratio, according to the following steps:-

1st step. Let $\theta = 0.9$ and making the value of b vary from zero toward 1. The value of b (say $b = b_1$) at which the estimator gives minimum mean square error (minimum MSE) is taken for the use in the next step.

2nd step. is performed by letting the value of θ vary, say from 0.1 by suitable steps up to the value of 1, with $b = b_1$ and by taking θ_1 the value of θ at which the estimator gives minimum mean square error.

3rd step. This step is the reptition of 1st step, but now with $\theta = \theta_1$. b_2 the value of b, at which the estimator gives minimum mean square error, is selected.

4th step. If $b_2 \neq b_1$, Step 2 must be repeated, but with $b = b_2$, and $\theta = \theta_2$ is recorded. Moreover, if $b_2 = b_1$ then b_2 and θ_1 will be used as the system optimising values. The 1st and 2nd steps are repeated in the way described in the 3rd and 4th steps until either the values of $b_\ell = b_{\ell-1}$ or $\theta_\ell = \theta_{\ell-1}$. The last values of b and θ are kept as the optimised values, at the satisfaction of the above conditions (see Tables 6.1 and 6.2).

The mean square error for the optimisation test only is given by

$$MSE = 10 \log_{10} \left(\frac{1}{(M-N)2L} \sum_{i=N}^{M} |Y_i' - Y_i|^2\right) \quad dB \qquad 6.24$$

where Y_i is the actual sampled impulse response of the channel, N = 1000 and M = 50000. The factor of 2L, used here, is only to increase the range of operation. The optimisation tests were carried out under different Rayleigh fading rate conditions with signal-to-noise ratio of 10 dB calculated as $10 \log_{10} (1/\sigma^2)$, where σ^2 is the noise variance. The results of MSE versus b for different selected values of θ for optimum performance are shown in Figure 6.5 for FFCE and Figure 6.6 for MFBCE. While Figures 6.7 and 6.8 show MSE versus θ for different selected values of b at which the estimators became optimum for FFCE and MFBCE respectively. Tables 6.1 and 6.2 give the values of b and θ for the corresponding Doppler frequency.

The values of b and θ, obtained for optimum systems tested above when only f_D = 100 Hz, are used in the following tests. Figures 6.9 and 6.10 show the variation of MSE with signal-to-noise ratio (SNR) for FFCE when a rectangular shaped channel (C=r) and a raised-cosine shaped channel (C=rc) are used respectively. Also, Figures 6.11 and 6.12 show the variation of MSE with SNR for MFBCE when C=r and C=rc respectively. The MSE and SNR are calculated here as follows:-

$$MSE = 10 \log_{10} \left(\frac{1}{M-N} \sum_{i=N}^{M} |Y_i' - Y_i|^2\right) \quad \text{dB} \qquad 6.25$$

$$P_s = \text{average signal power} = \frac{1}{M-N} \sum_{i=N}^{M} |s_i\ q_i|^2 \quad \text{power units} \qquad 6.26$$

$$P_n = \text{average noise power} = \frac{1}{M-N} \sum_{i=N}^{M} |w_i|^2 \quad \text{power units} \qquad 6.27$$

$$SNR = 10 \log_{10} (P_s/P_n) \quad \text{dB} \qquad 6.28$$

where $\{s_i\}$ are the transmitted sequence, $\{q_i\}$ are obtained from Equation 6.4, $\{w_i\}$ are the additive noise components seen in Equation 6.1, and $|x|$ is the modulus of x.

The above tests are carried out for single prediction step, when n=1 in Equation 6.21, and such prediction is only applicable in the case of using channel equalisation technique. Clearly, both estimators are using the already detected data symbol in their estimation processes. But, the near-maximum likelihood detection scheme requires a delay of n symbols to reach a decision. Therefore, it is necessary to study the

effect of the delay on the performances of the estimators. Figures 6.13 to 6.20 show such effects, when SNR = 10 or 38 dB, on the performances of FFCE and MFBCE with the application of the two channels. Both estimators performance diverge as the delay (represented by n symbols)increases, but the divergence at high SNR is much slower. Table 6.3 gives the values of n at which the MSE = 0 dB when the Doppler frequency f_D = 100 Hz. Clearly, FFCE diverges a little faster than MFBCE as the delay increases. Moreover, both systems diverge faster, when the raised-cosine shaped channel is used than is the case when the rectangular shape is used.

Further comparisons between the performances of FFCE and MFBCE can be assessed to compare between their tolerance to additive noise at f_D = 50 and 100 Hz as shown in Figure 6.21 and 6.22 for rectangular and raised-cosine shaped channels respectively, where (in these two figures) FF refers to FFCE and FB refers to MFBCE. Also, table 6.4 compares the value of MSE at 38 dB signal-to-noise ratio (SNR) obtained from Figures 6.21, 6.22 and also from 6.9 to 6.12 for the two systems under different fading rates. Clearly, MFBCE gives an advantage of 7 to 13 dB in performance over FFCE for the same SNR (= 38 dB). Moreover, there is insignificant difference in the application of the two channels used here when FFCE is used at high fading rate and no difference when MFBCE is used.

All of the above tests were carried out on the assumption that all the required sequences are initialized according to Equation 6.23. But in the case when the estimator does not know the values of these sequences or $Y'_{1/0} = Y'_0=0$ and $(Y'_{1/0})'=0$, then it is necessary to send a retraining

signal with a relatively long well known sequence to the receiver and letting the estimator build up its initialisation. The question is how long the sequence must be. Figures 6.23 to 6.26 show the variation of the square error (SE) with time of n symbols (required to make the system converge). The SE is given by

$$SE = 10 \log_{10} (\cdot |Y'_n - Y_n|^2) \quad dB \qquad 6.29$$

Clearly from Figures 6.23 to 6.26 both systems converge rapidly.

It is possible to conclude from the work presented by this chapter that:-

i) The feedback channel estimator introduced in Appendix J requires a delay of LT seconds, where L is the number of samples in the sampled impulse response of the channel and T is the symbol duration. The feedback estimator is modified mathematically in order to overcome the above delay. Also, a further development is brought forward by the insertion of a digital feedback control system in the modified feedback channel estimator. The insertion of a digital feedback control system may eliminate as much noise as possible outside its bandwidth (100 Hz). Also, from Appendix J, the modified feedback channel estimator, MFBCE, (as well as the feedback channel estimator) can subtract the intersymbol interference error signal components, while the feedforward channel estimator cannot. For the above reasons the MFBCE shows surprisingly much better performance in the above tests over the feedforward channel estimator, FFCE.

ii) It has been found in Appendix J that it is necessary to mutliply by the reciprocal of the data symbol value to obtain a better estimate

of the sampled impulse response of the channel and not by the complex-conjugate of the data symbol value, when the FFCE is used with a multi-level QAM signal.

iii) The values of b and θ, that optimise the estimators under Rayleigh fading condition with Doppler frequency of 100 Hz, were used in all of the above tests of course excluding the optimisation tests. The idea behind that is to design an estimator that can cope with highest possible fading rate. This has led to a high jittering at lower fading rate. Therefore, it is necessary to make the values of b and θ vary in a sense such to optimise the estimator according to the fading rate. Consequently b and θ must not be constants.

iv) Both estimators studied here are highly sensitive to delay.

v) Also both estimators, FFCE and MFBCE, converge quickly, since their convergence constants, b, are relatively large in comparison with results obtained elsewhere[207-206]. Furthermore, the larger the value of b the more susceptible to the noise is the estimator. The values of θ, used here, might also influence the convergence of the two estimators.

vi) At lower fading rates, both estimators are more tolerant to noise, which indicates that both estimators have very narrow bandwidths.

b	θ	f_D Hz
0.09	0.7	100
0.08	0.85	50
0.07	0.7	25
0.05	0.85	10

Table 6.1 Optimum values of b and θ under different fading rates for the feedforward channel estimator.

b	θ	f_D Hz
0.5	0.80	100
0.45	0.85	50
0.175	0.90	25
0.125	0.95	10

Table 6.2 Optimum values of b and θ under different fading rates for the modified feedback channel estimator.

SNR dB	Channel C =	n in FFCE	n in MFBCE
10	r	14	16
10	rc	13	15
38	r	17	18
38	rc	16	17

Table 6.3 The values of delay n when MSE = 0 under a Rayleigh fading with Doppler frequency f_D = 100 for 10, 38 dB signal-to-noise ratio

f_D Hz	MSE in dB for FFCE		MSE in DB for MFBCE	
	C = r	C = rc	C = r	C = rc
100	-11.0	-10.6	-17.0	-17.0
50	-13.6	-13.2	-23.0	-23.0
25	-18.0	-17.7	-32.0	-32.0
10	-25.0	-25.0	-38.0	-38.0

Table 6.4 Mean square error (MSE) measured at 38 dB signal-to-noise ratio (SNR) for FFCE and MFBCE under different Rayleigh fading rates, when rectangular shaped (C=r) and raised-cosine shaped (C=rc) are used.

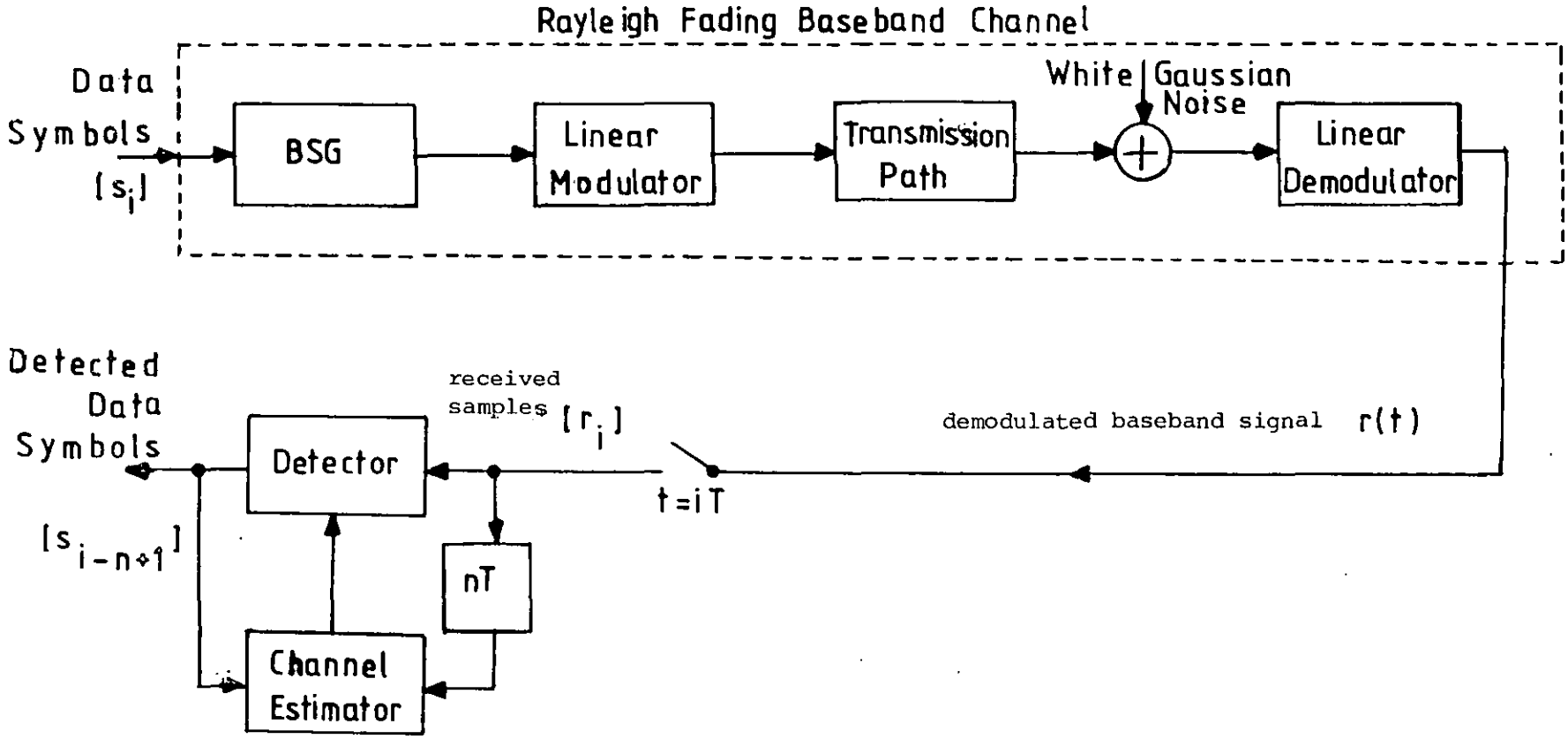

Fig. 6.1 Model of data transmission system

BSG : Baseband signal generator

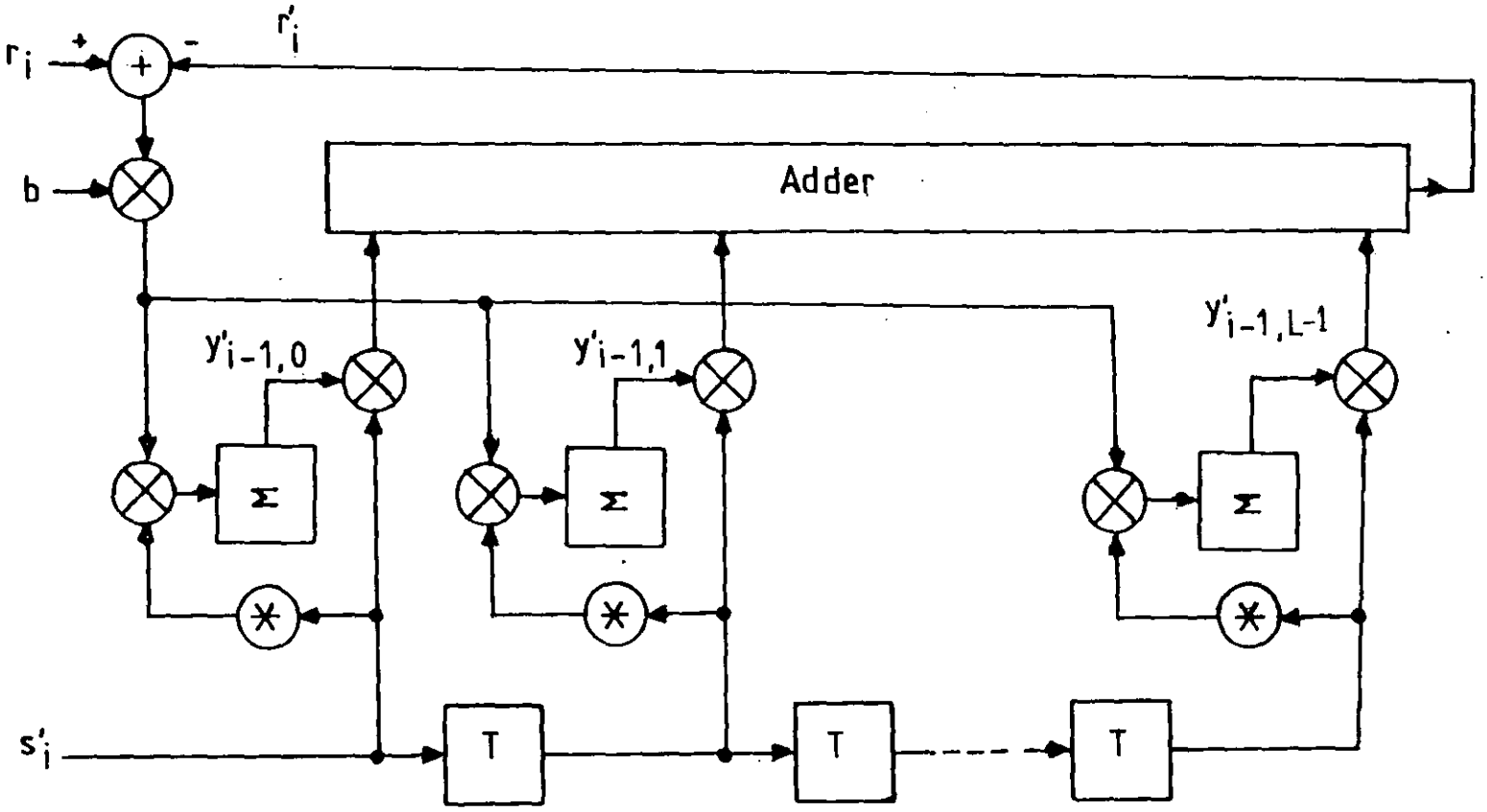

Fig. 6.2 Feedforward channel estimator

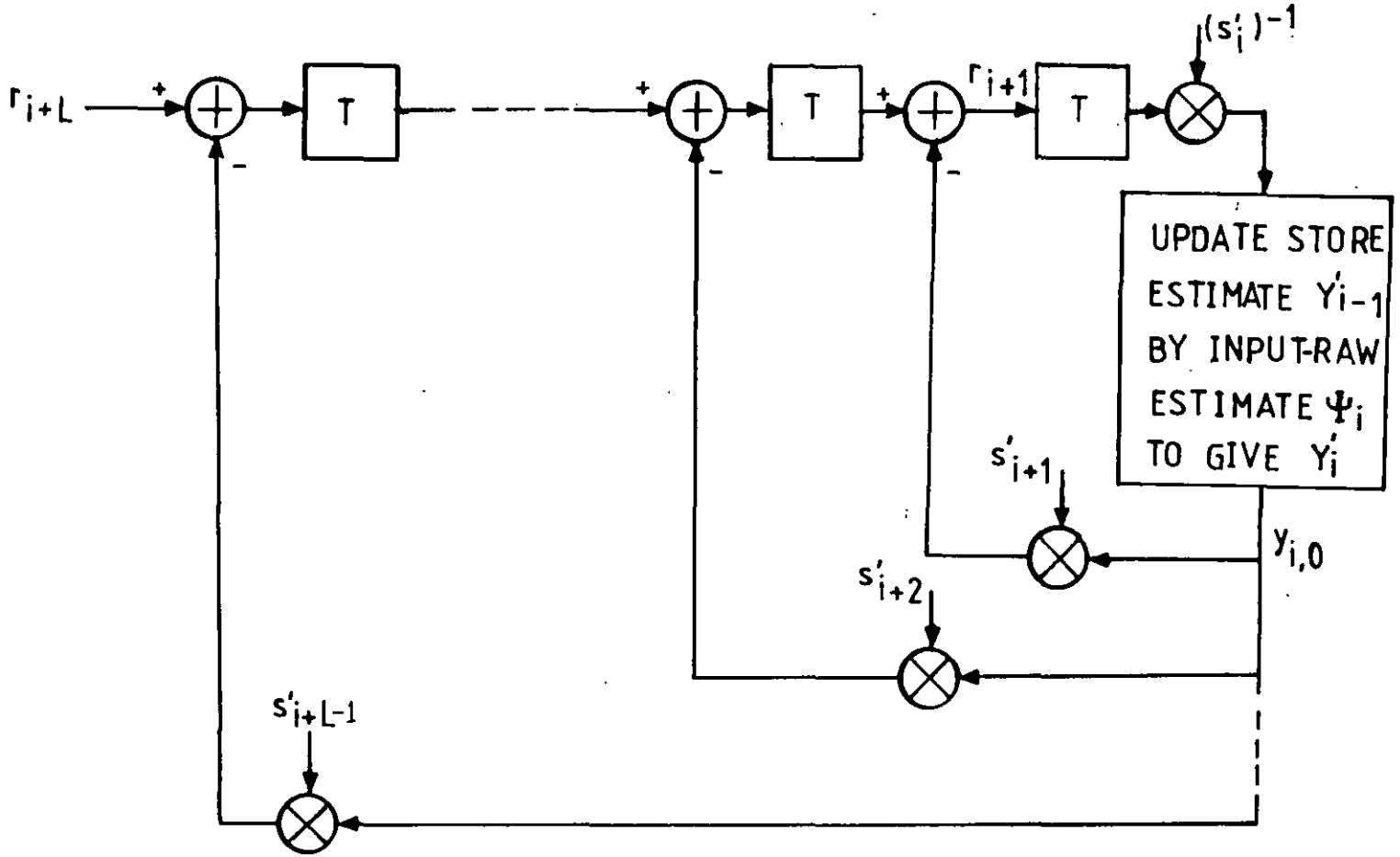

Fig. 6.3 Feedback channel estimator

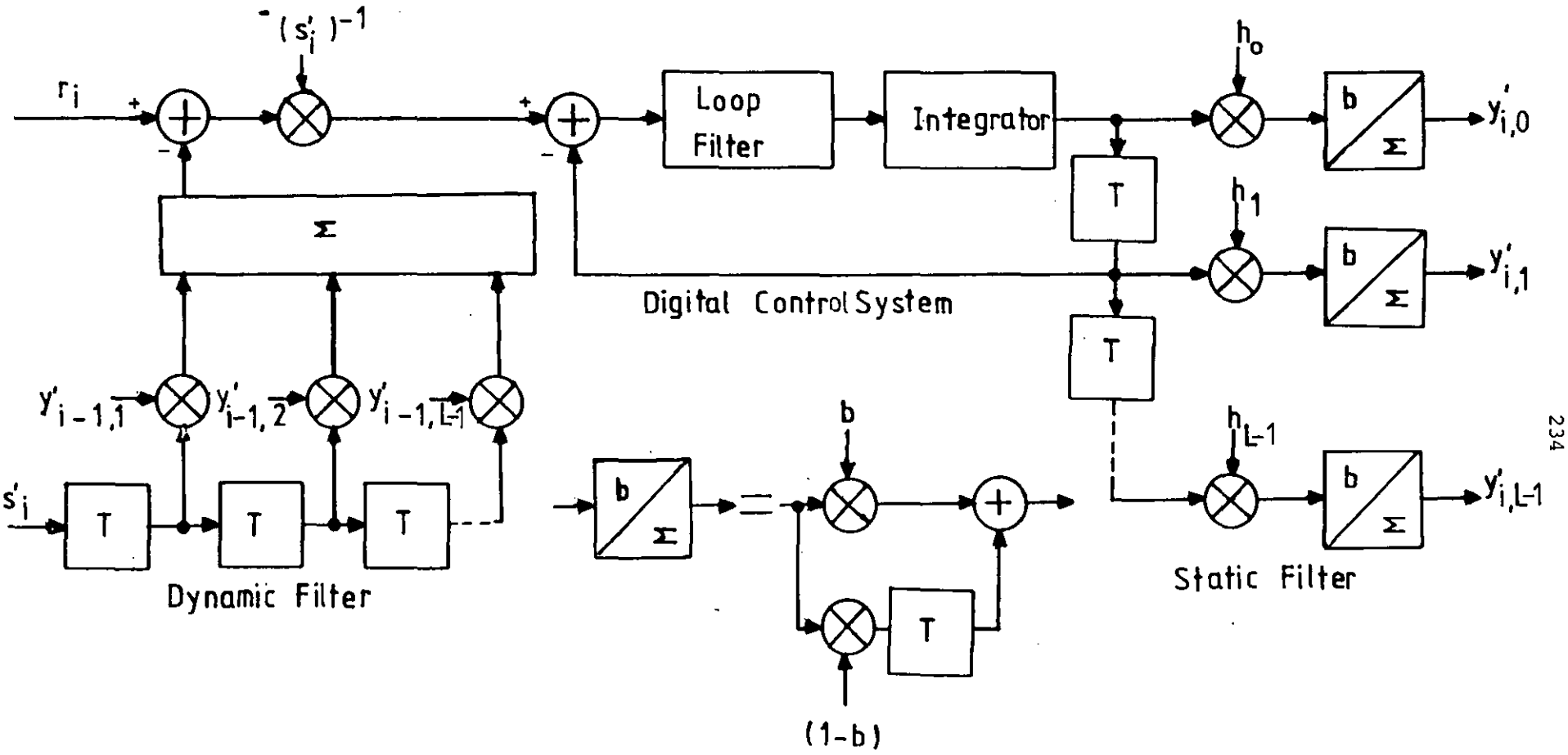

Fig. 6.4 Modified feedback channel estimator

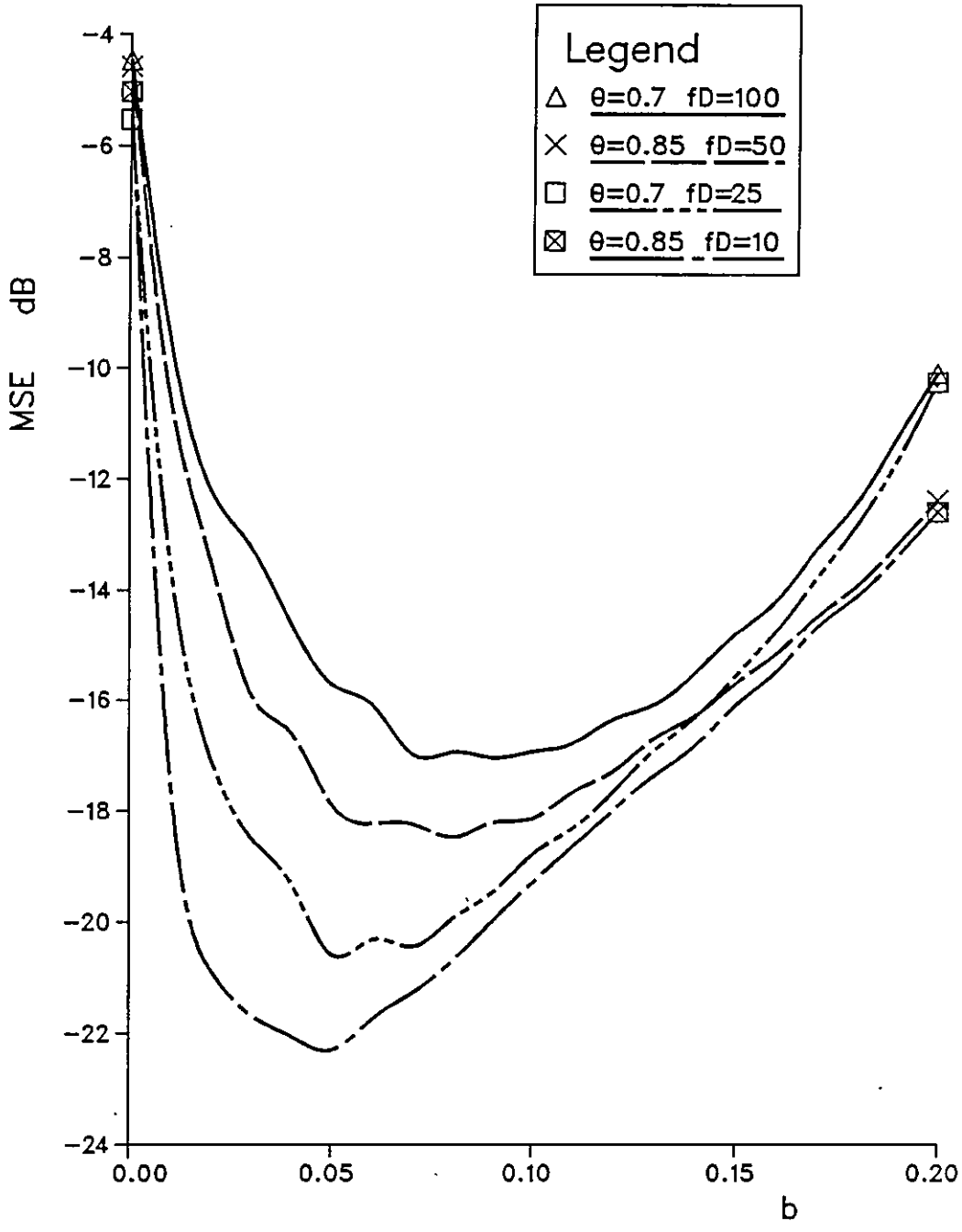

Fig. 6.5 FFCE optimisation tests for different fading rates and different values of θ; SNR=10 dB.
MSE: Mean Square Error

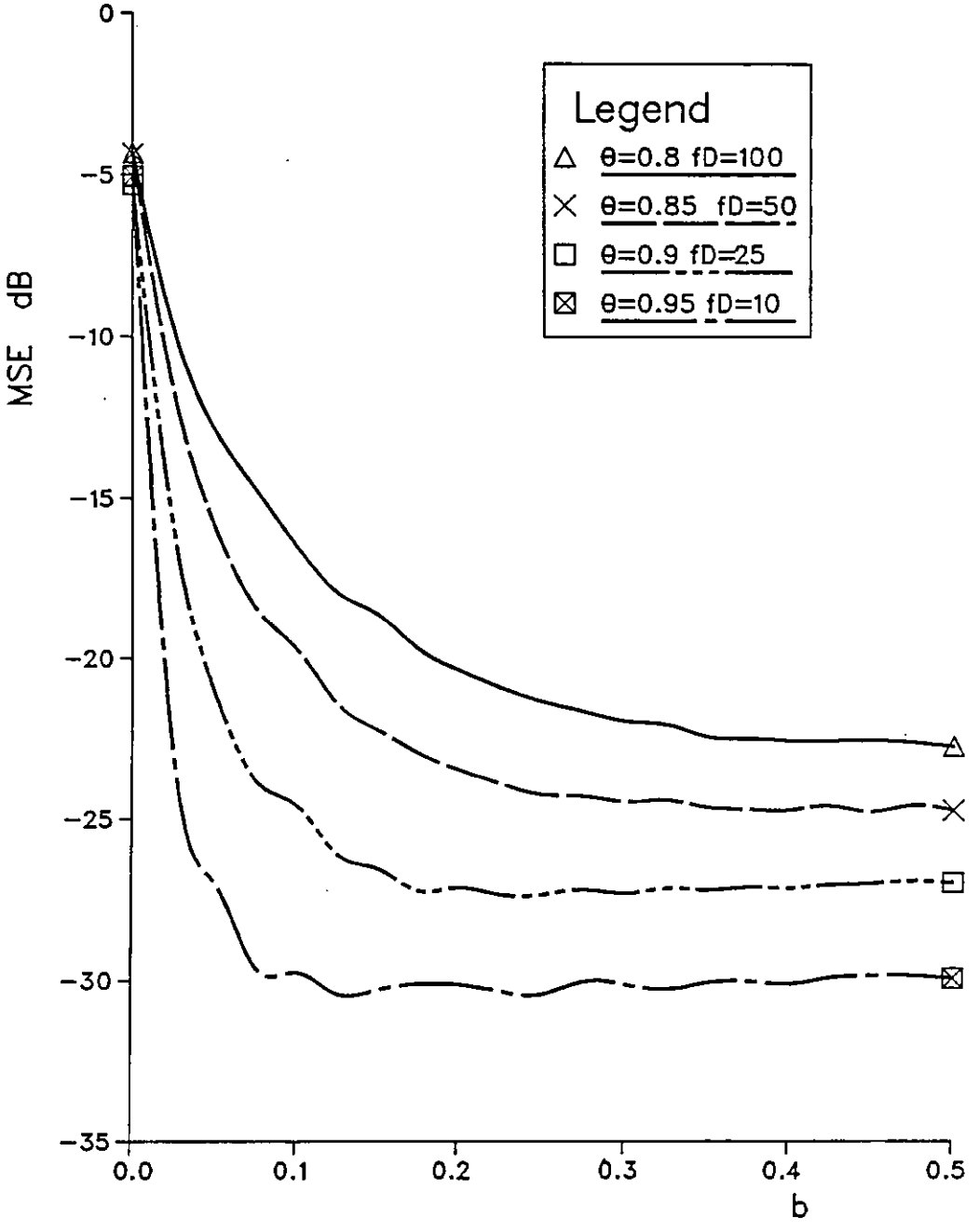

Fig. 6.6 MFBCE optimisation tests for different fading rates and different values of θ; SNR=10 dB.
MSE: Mean Square Error

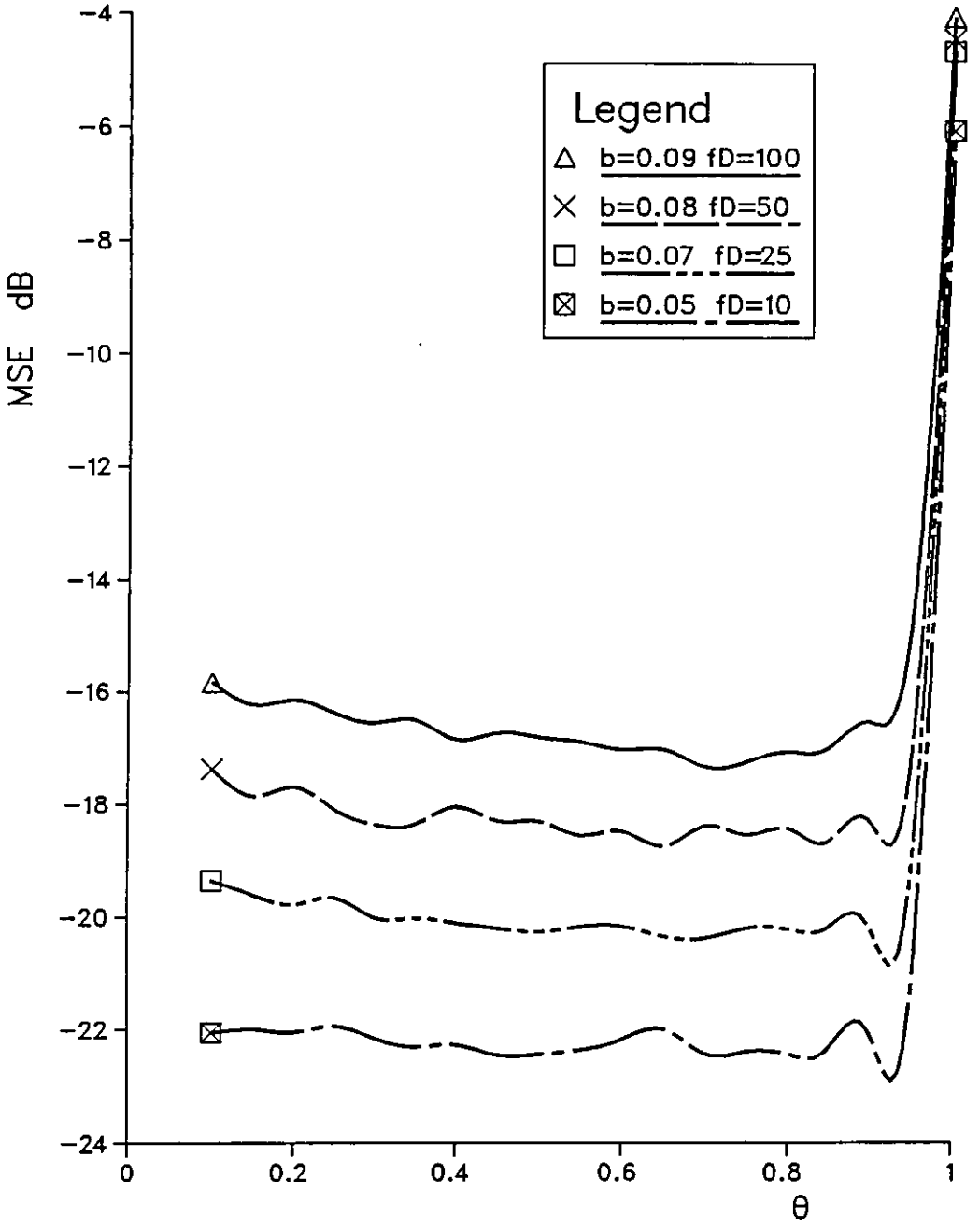

Fig. 6.7 FFCE optimisation tests for different fading rates and different values of b; SNR=10 dB.
MSE: Mean Square Error

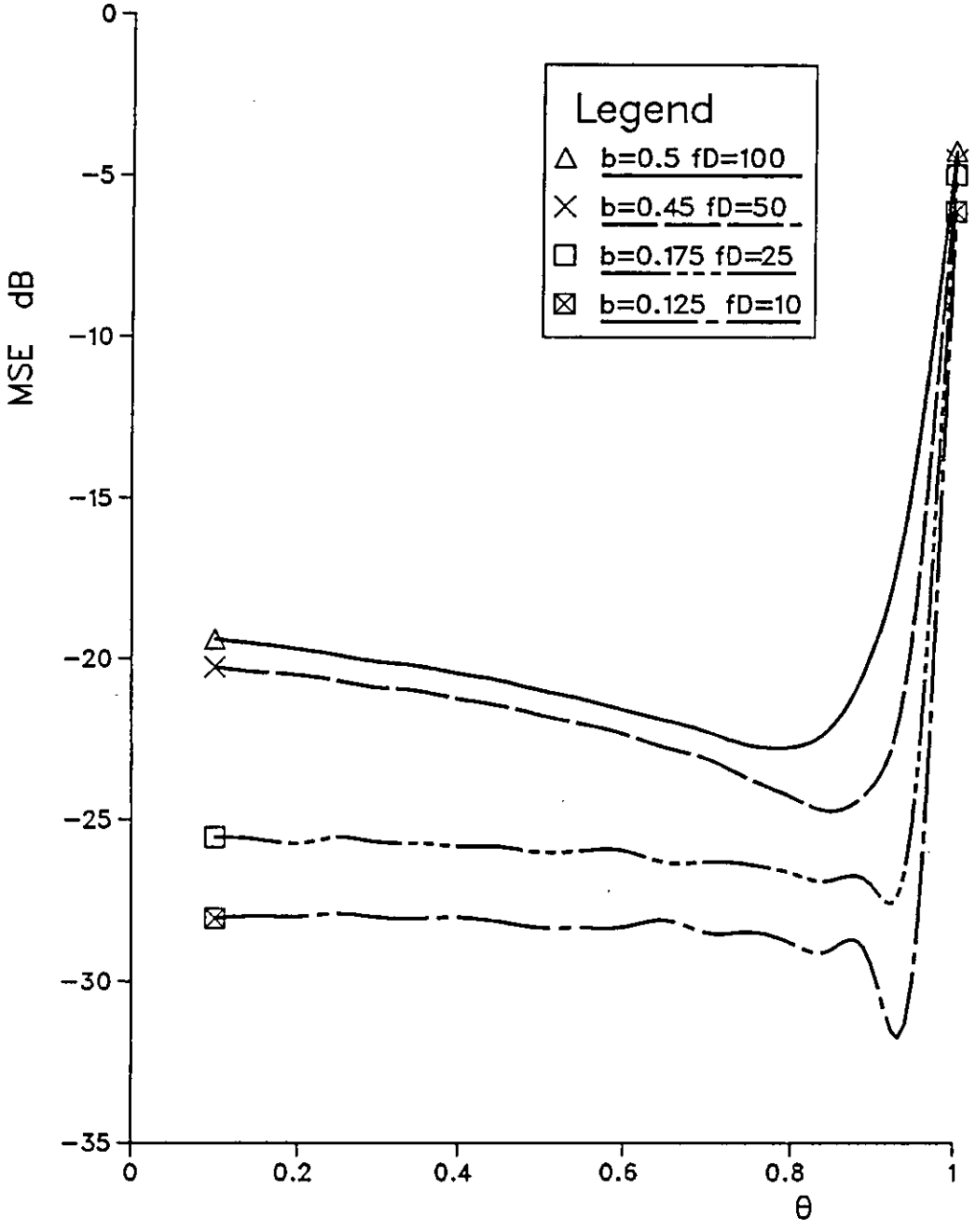

Fig. 6.8 MFBCE optimisation tests for different fading rates and different values of b; SNR=10 dB.
MSE: Mean Square Error

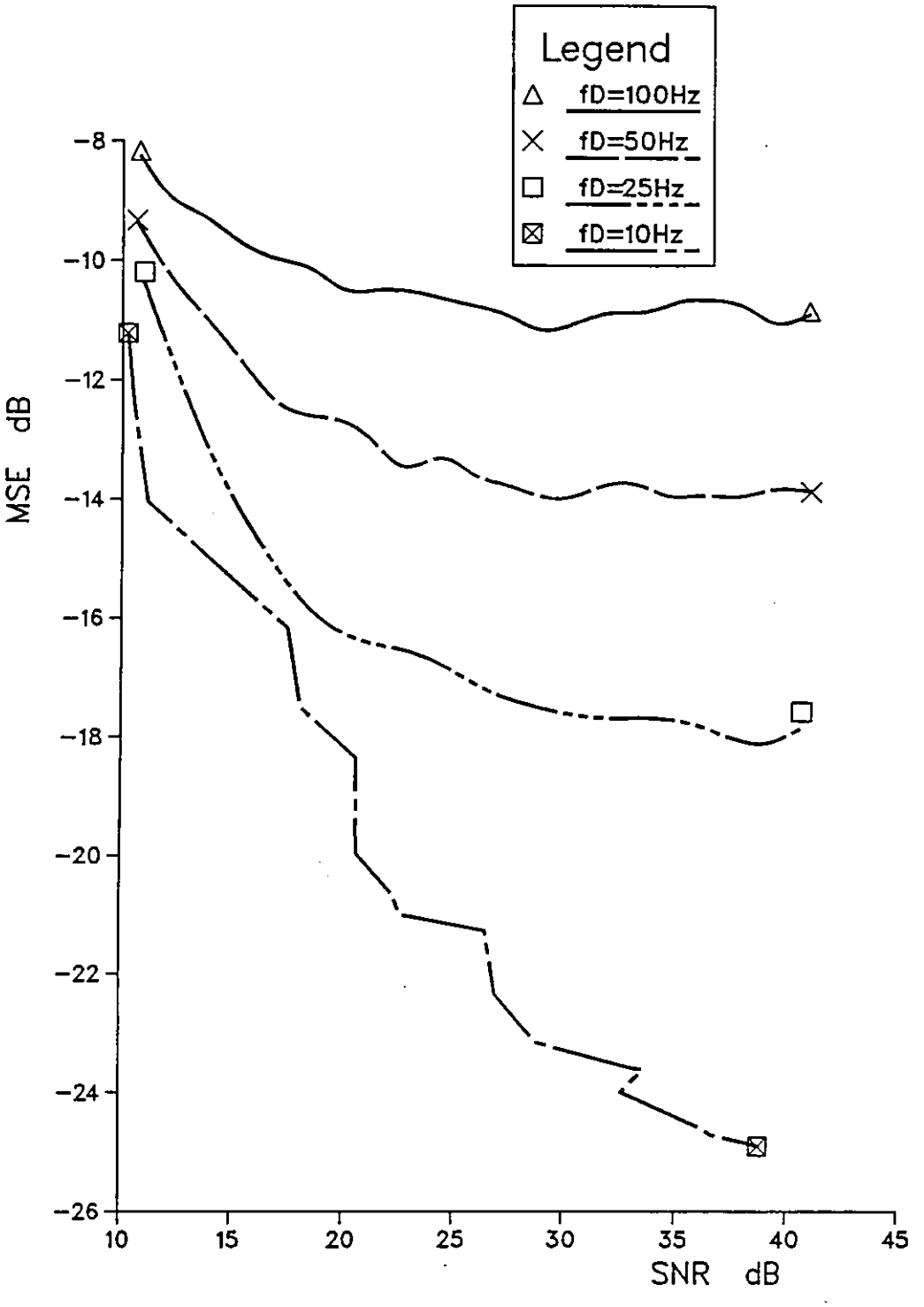

Fig 6.9 Performance of FFCE in additive noise for different fading rates when C=r, θ=0.7 and b=0.09.
MSE: Mean Square Error

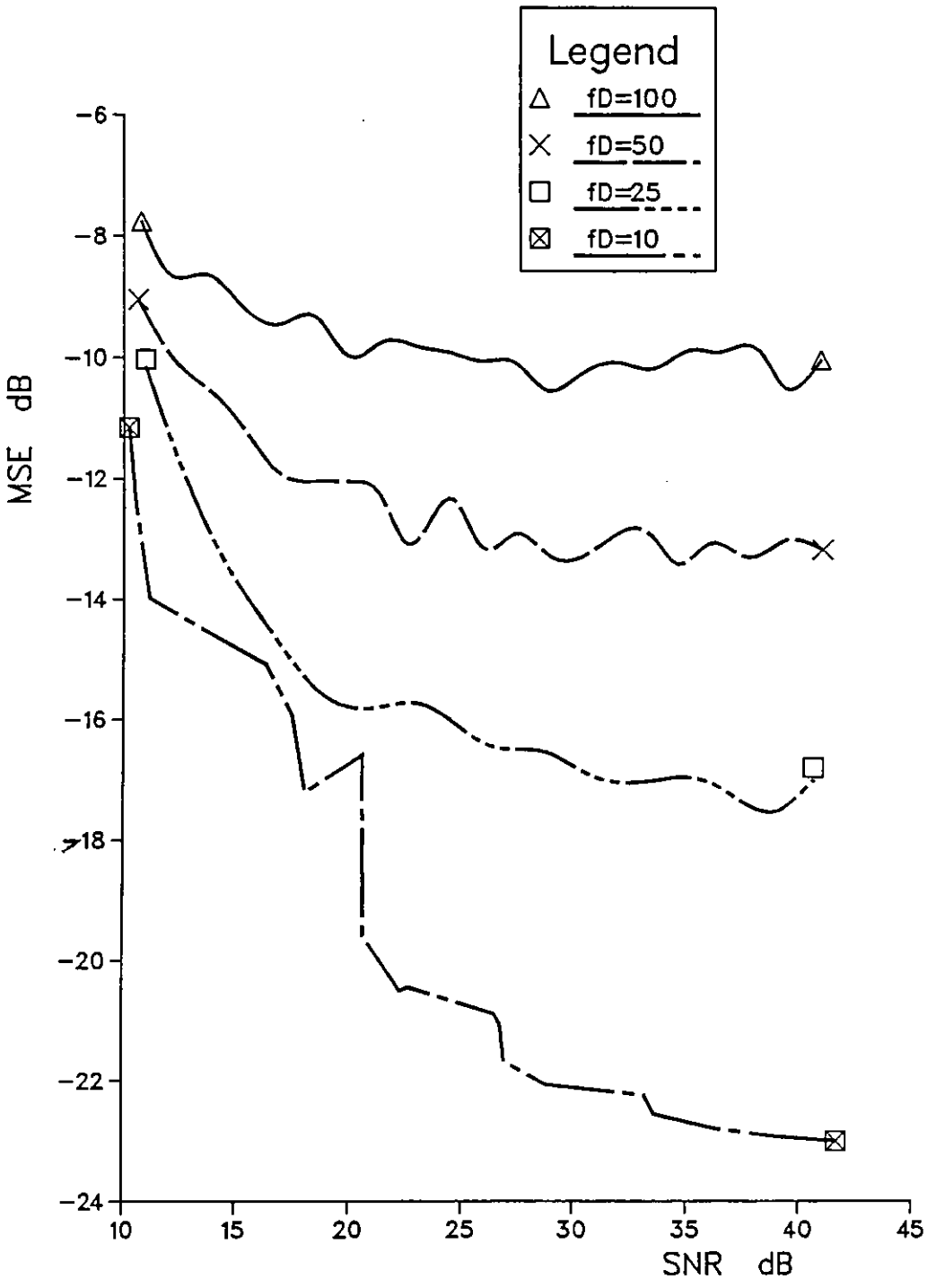

Fig 6.10 Performance of FFCE in additive noise for different fading rates when C=rc, θ=0.7 and b=0.09.
MSE: Mean Square Error

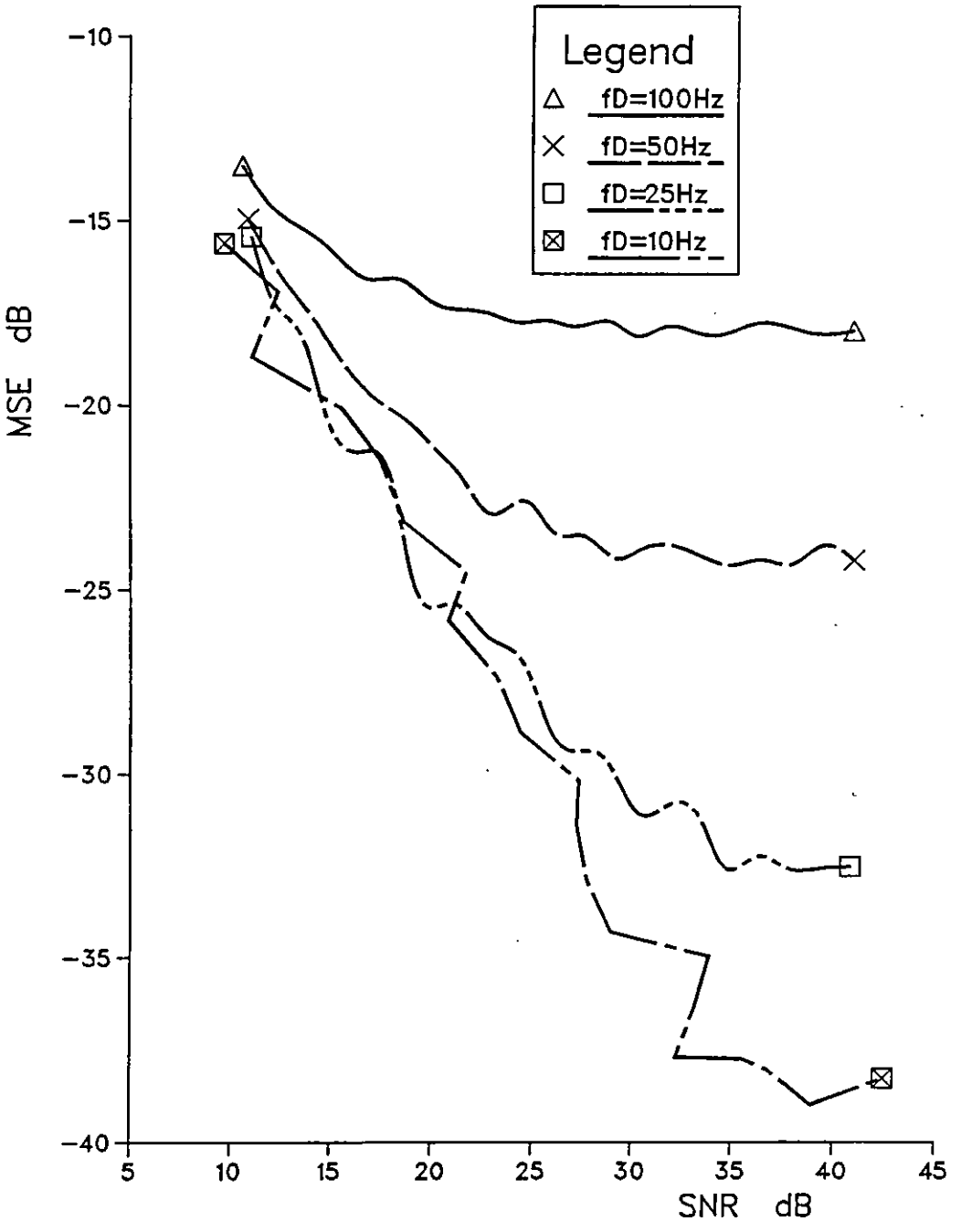

Fig 6.11 Performance of MFBCE in additive noise for different fading rates when C=r, θ=0.8 and b=0.5.
MSE: Mean Square Error

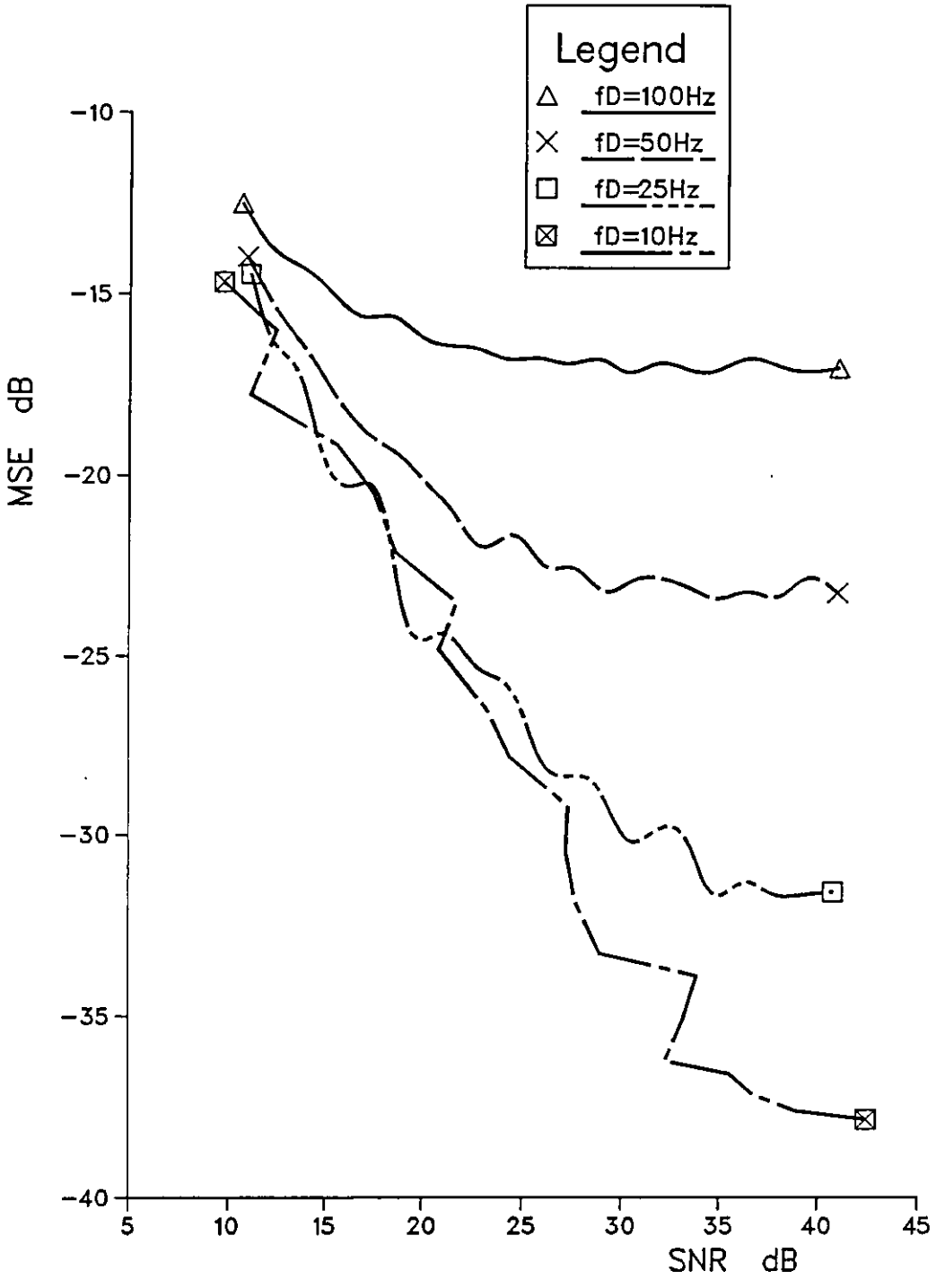

Fig 6.12 Performance of MFBCE in additive noise for different fading rates when C=rc, θ=0.8 and b=0.5.
MSE: Mean Square Error

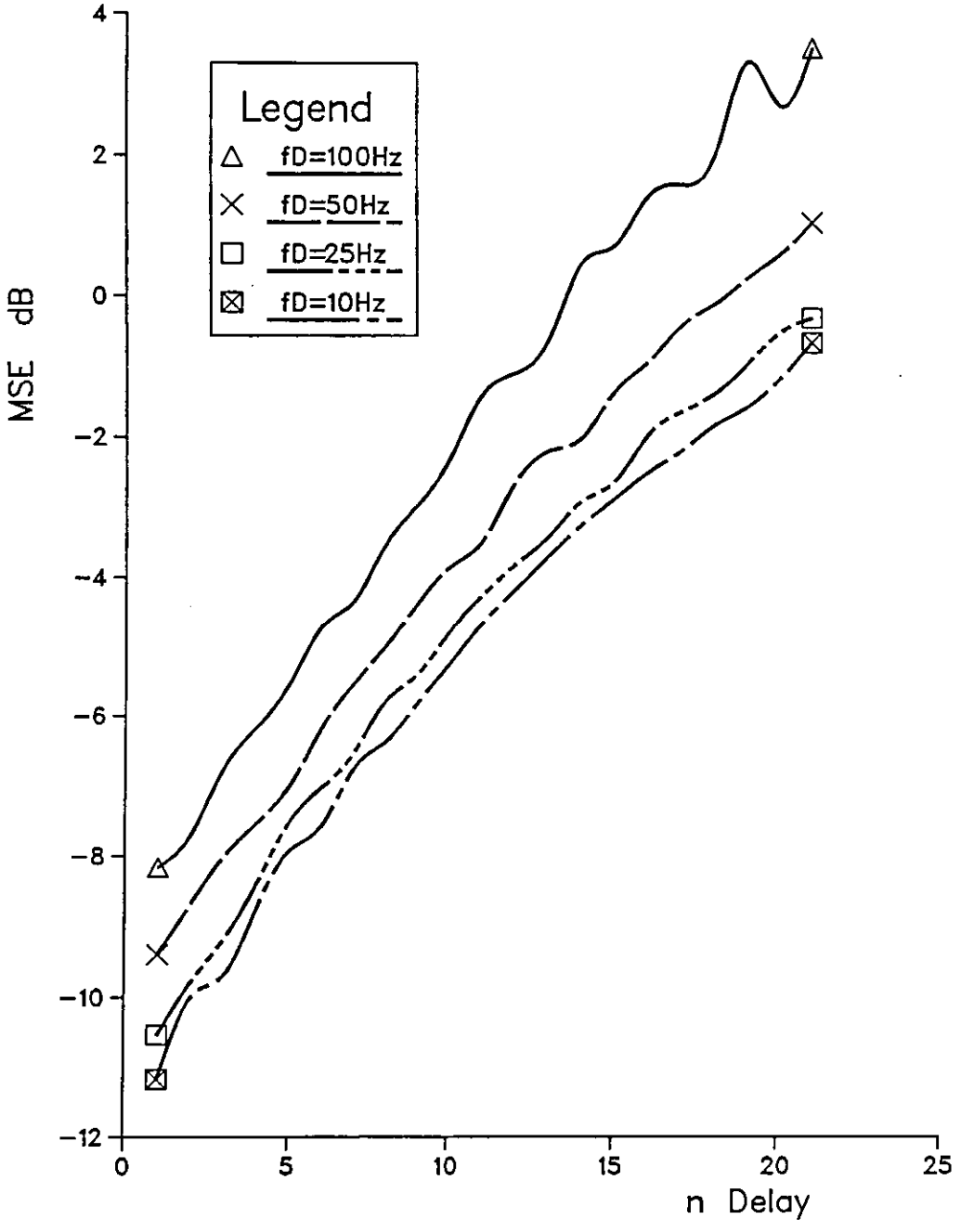

Fig. 6.13 Effect of delay on FFCE performace for different fading rates when SNR=10 dB, C=r, θ=0.7 and b=0.09. MSE: Mean Square Error

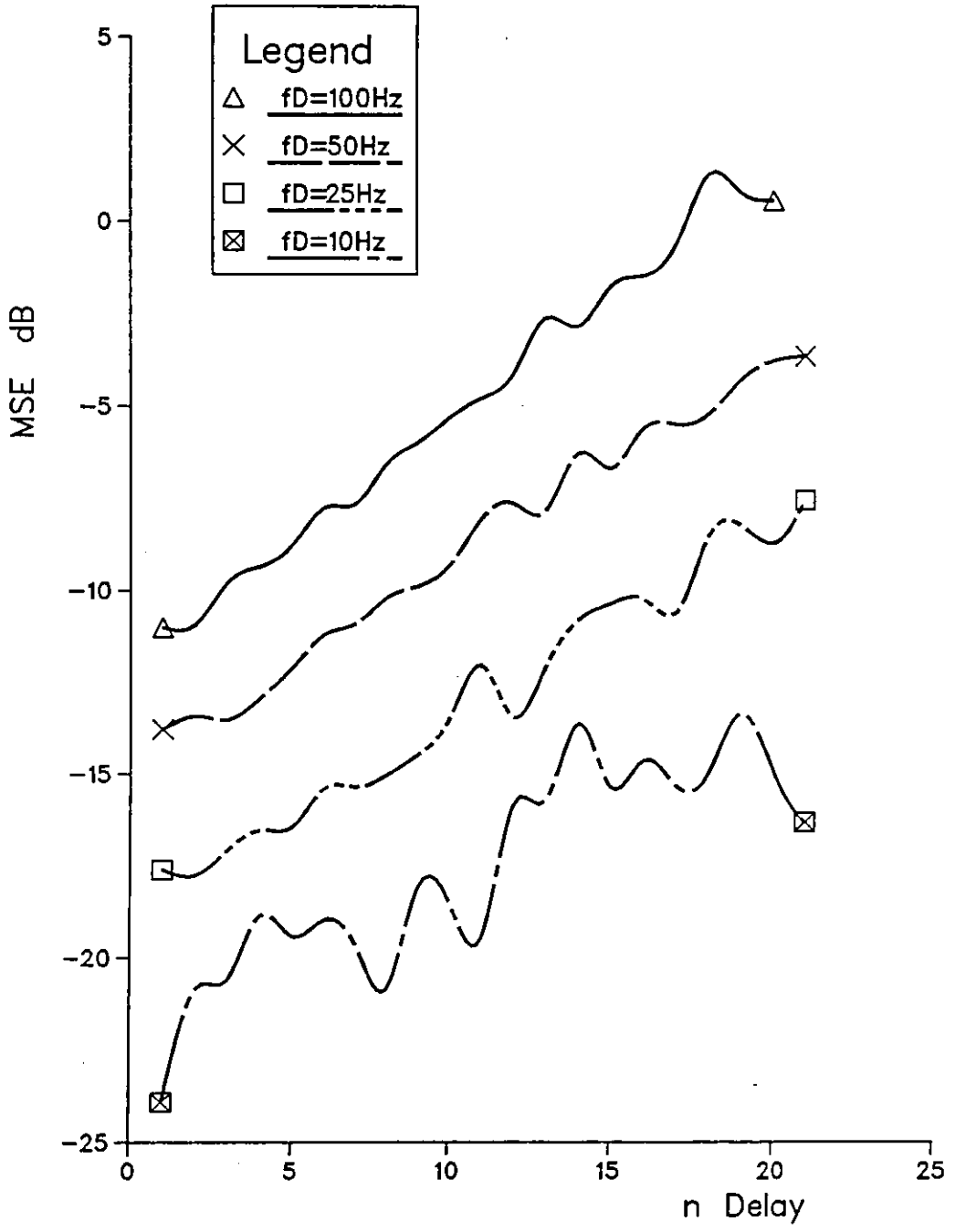

Fig. 6.14 Effect of delay on FFCE performace for different fading rates when SNR=38 dB, C=r, θ=0.7 and b=0.09. MSE: Mean Square Error

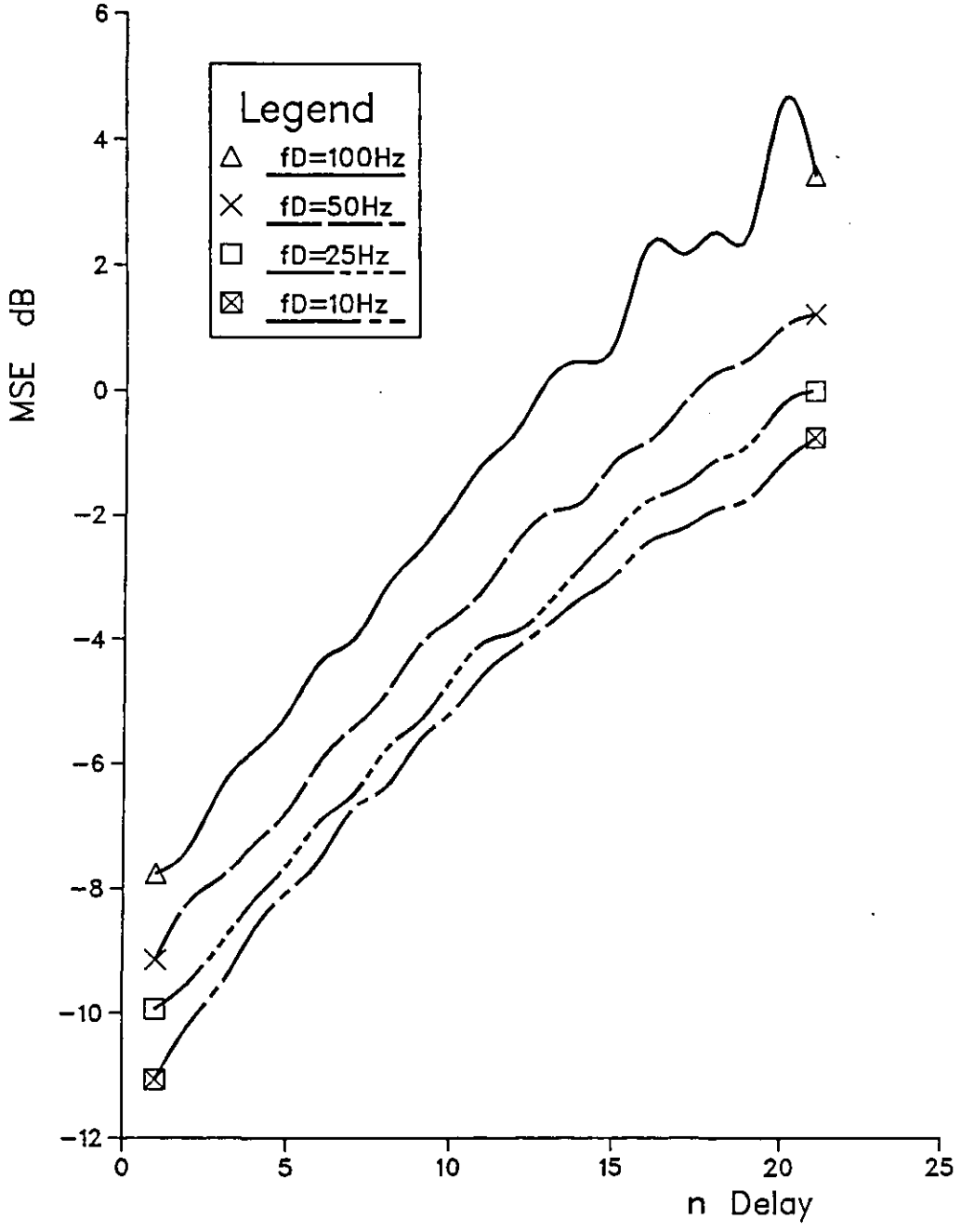

Fig. 6.15 Effect of delay on FFCE performace for different fading rates when SNR=10 dB, C=rc, θ=0.7 and b=0.09. MSE: Mean Square Error

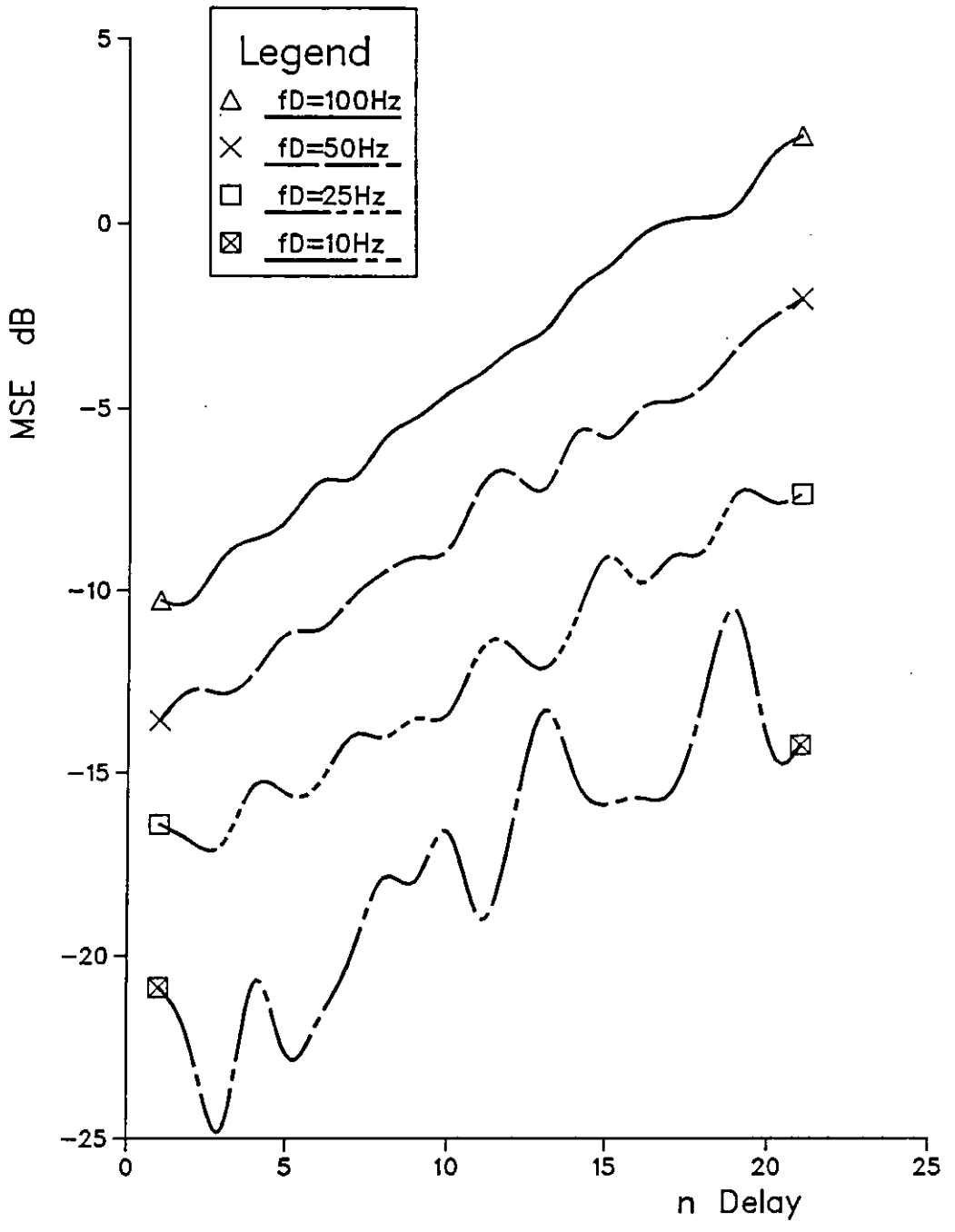

Fig. 6.16 Effect of delay on FFCE performace for different fading rates when SNR=38 dB, C=rc, θ=0.7 and b=0.09. MSE: Mean Square Error

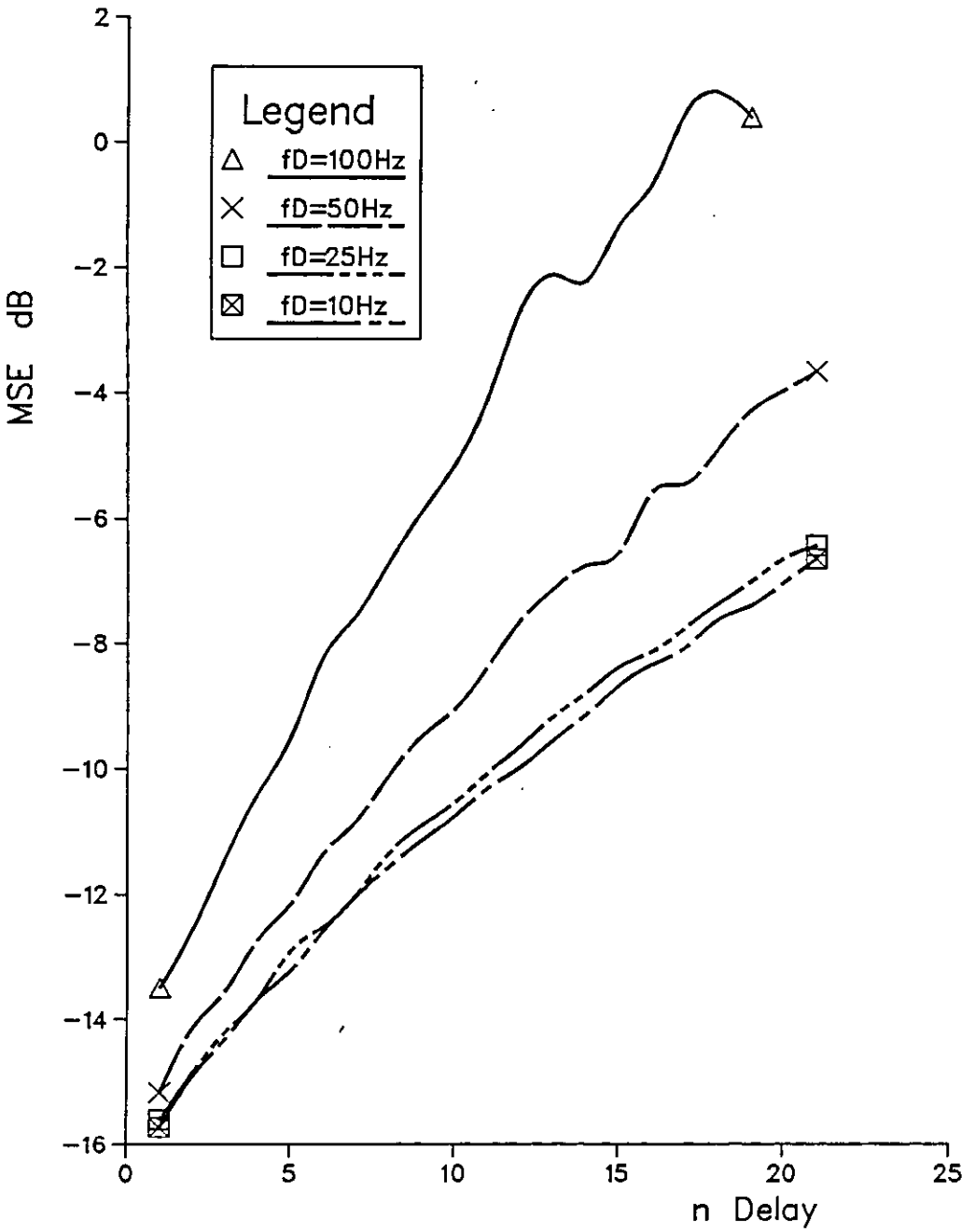

Fig. 6.17 Effect of delay on MFBCE performace for different fading rates when SNR=10 dB, C=r, θ=0.8 and b=0.5. MSE: Mean Square Error

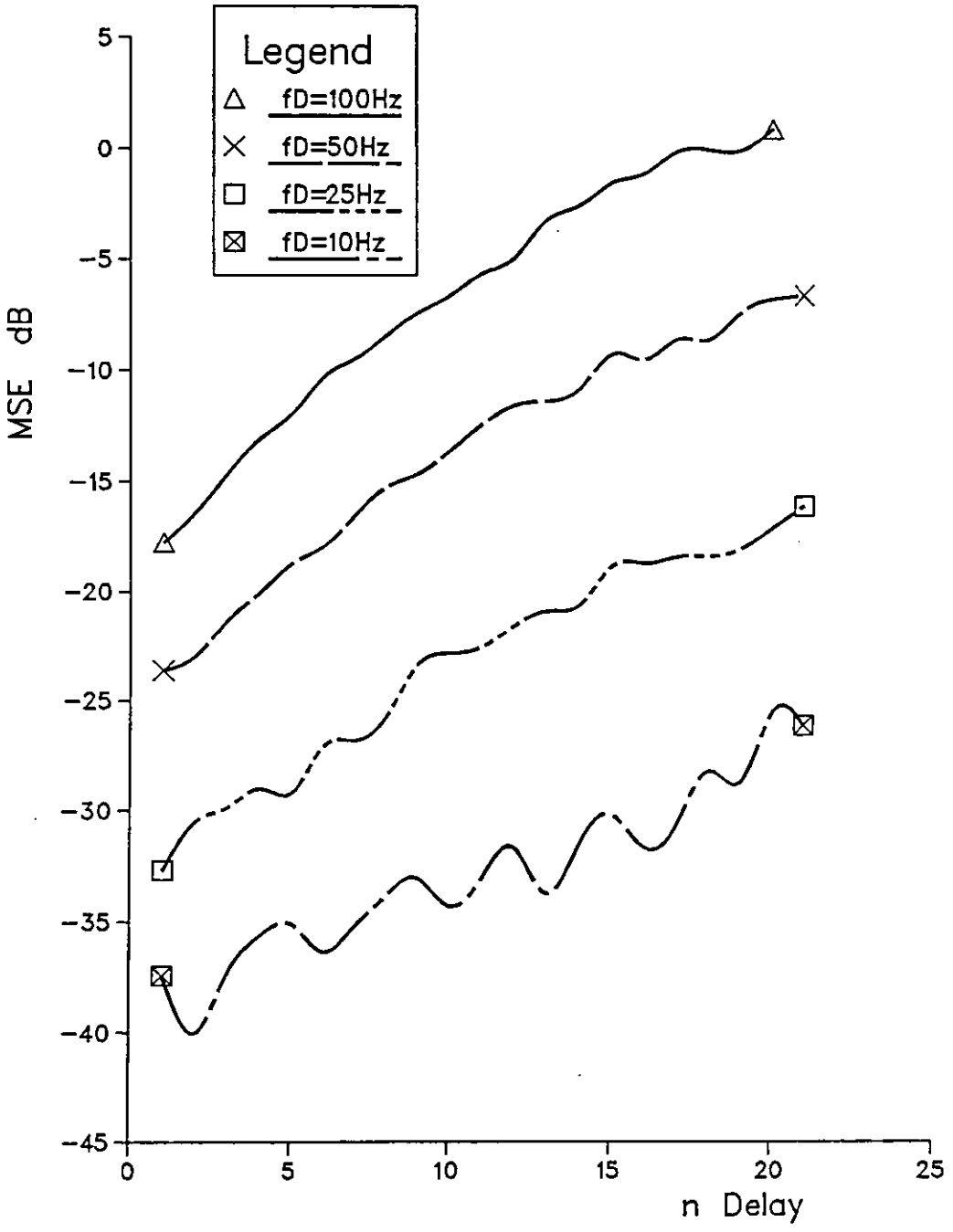

Fig. 6.18 Effect of delay on MFBCE performace for different fading rates when SNR=38 dB, C=r, θ=0.8 and b=0.5. MSE: Mean Square Error

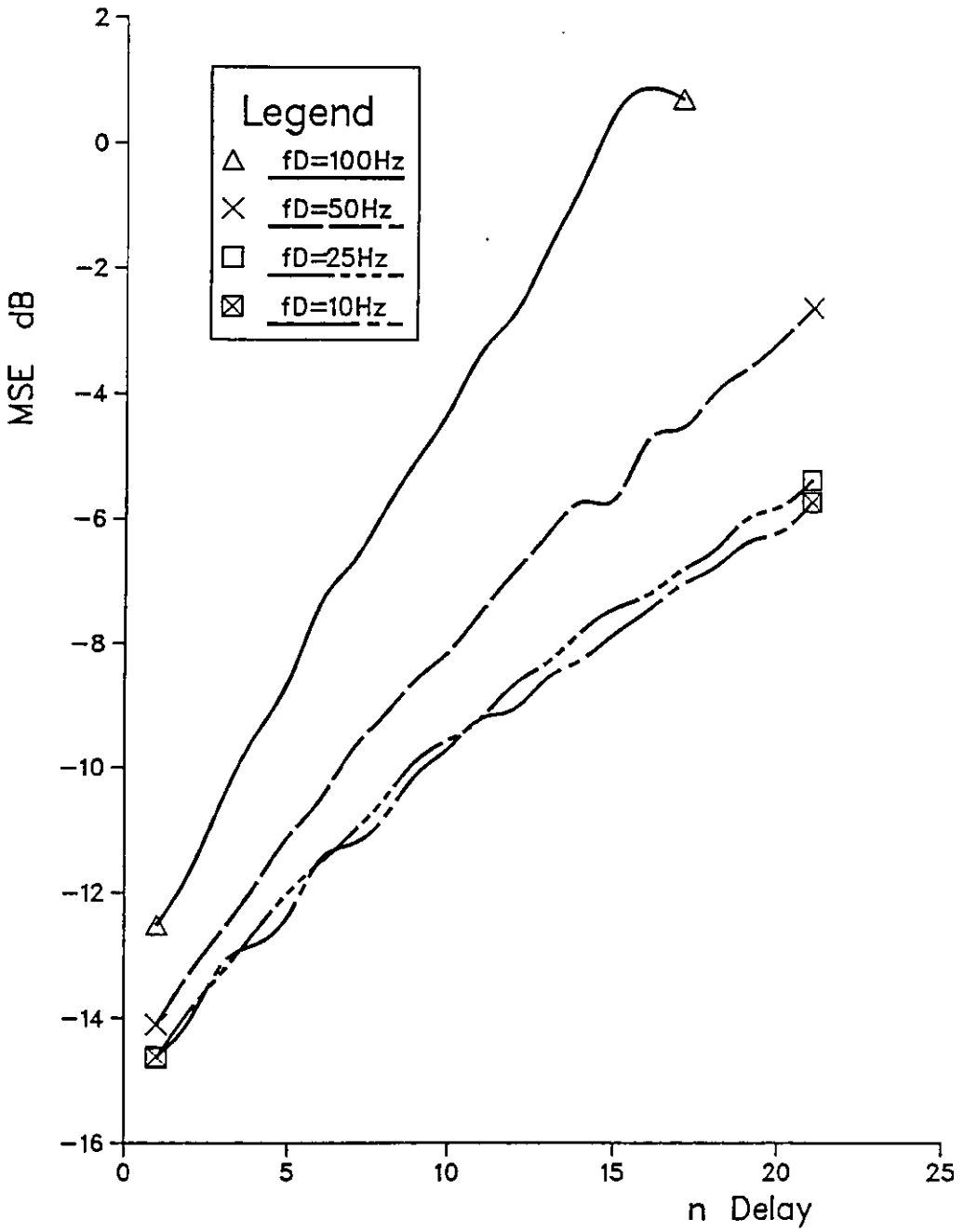

Fig. 6.19 Effect of delay on MFBCE performace for different fading rates when SNR=10 dB, C=rc, θ=0.8 and b=0.5. MSER: Mean Square Error

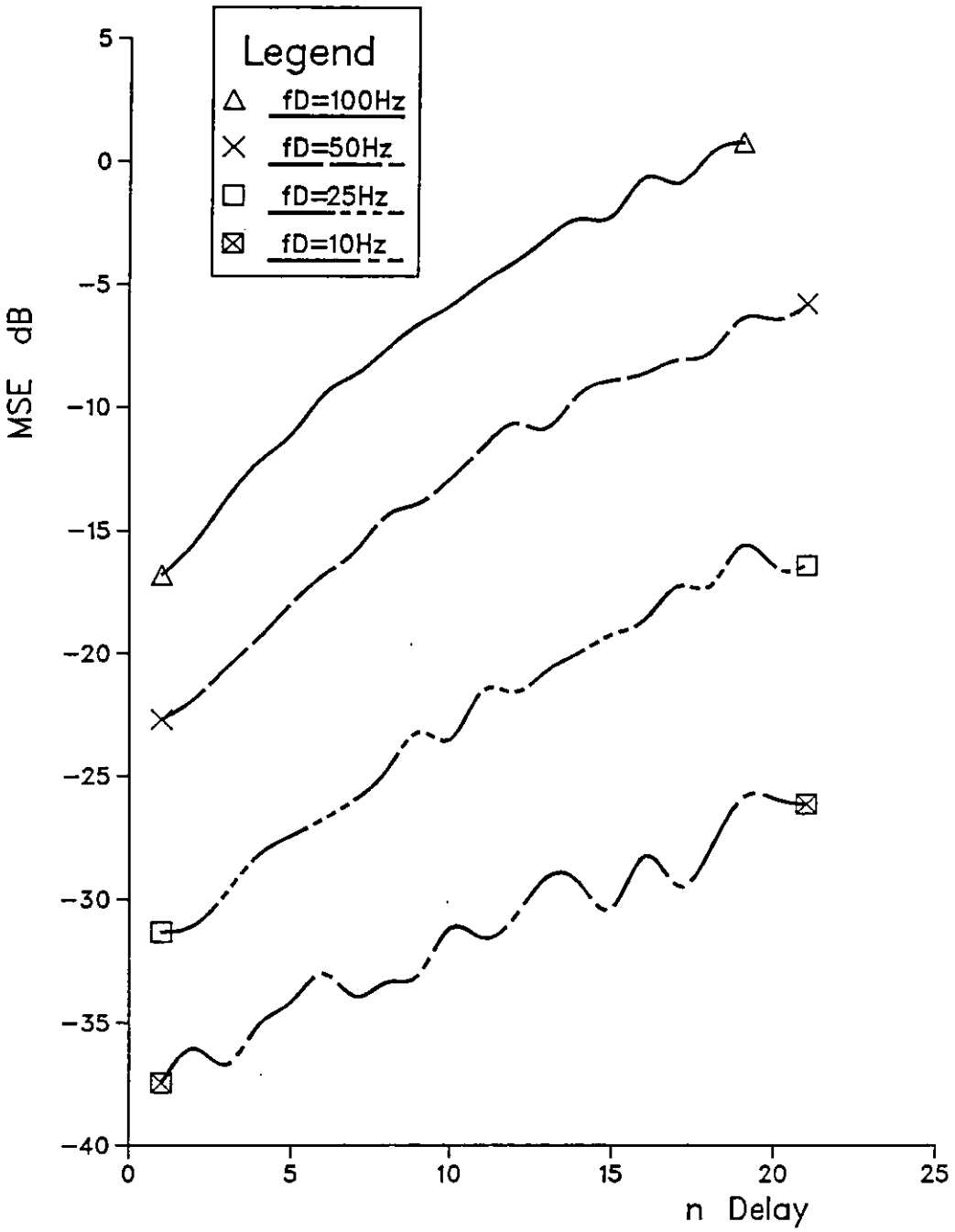

Fig. 6.20 Effect of delay on MFBCE performace for different fading rates when SNR=38 dB, C=rc, θ=0.8 and b=0.5. MSE: Mean Square Error

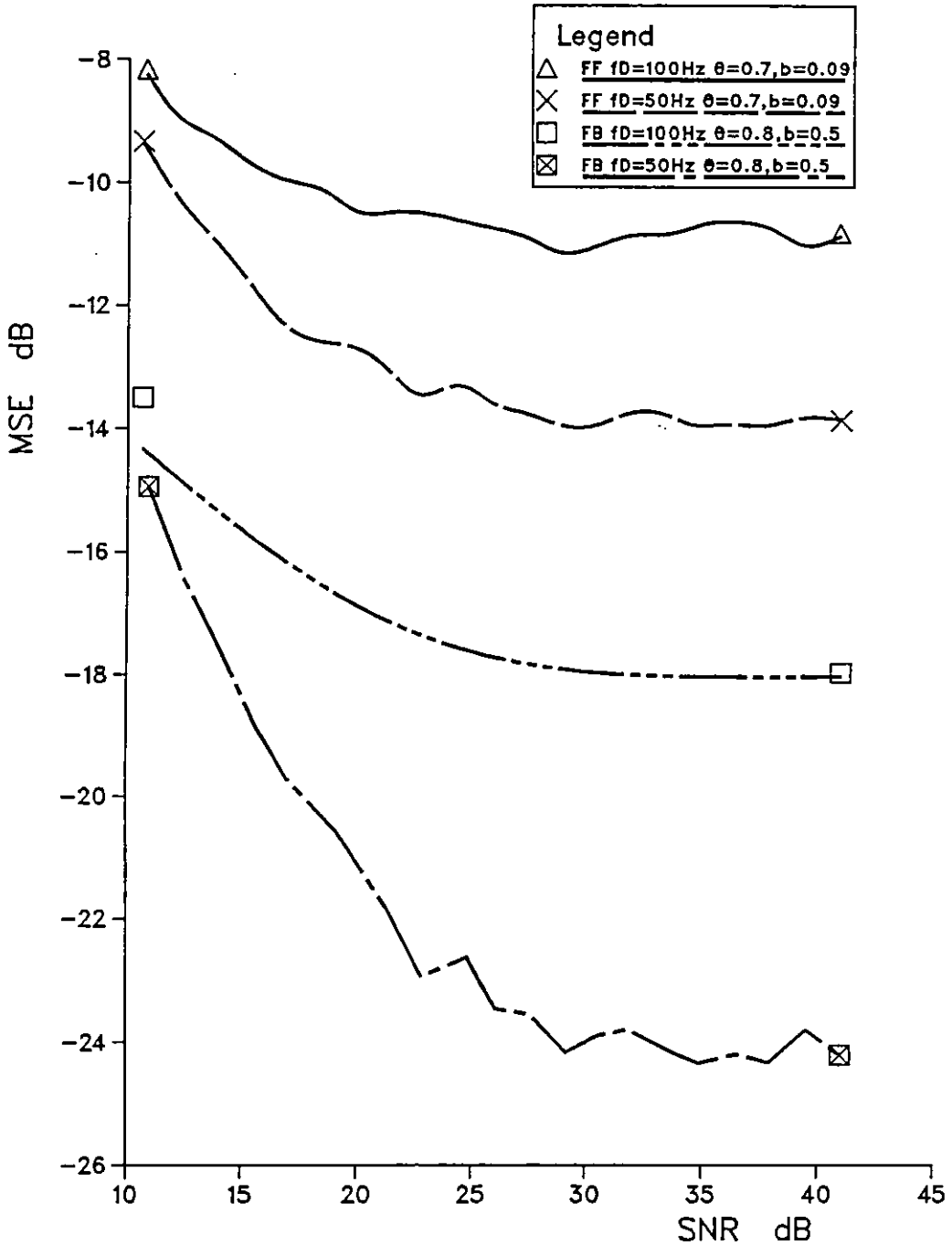

Fig.6.21 Comparison between the performances of FFCE and MFBCE when fD=100 and 50 Hz with C=r.
MSE: Mean Square Error

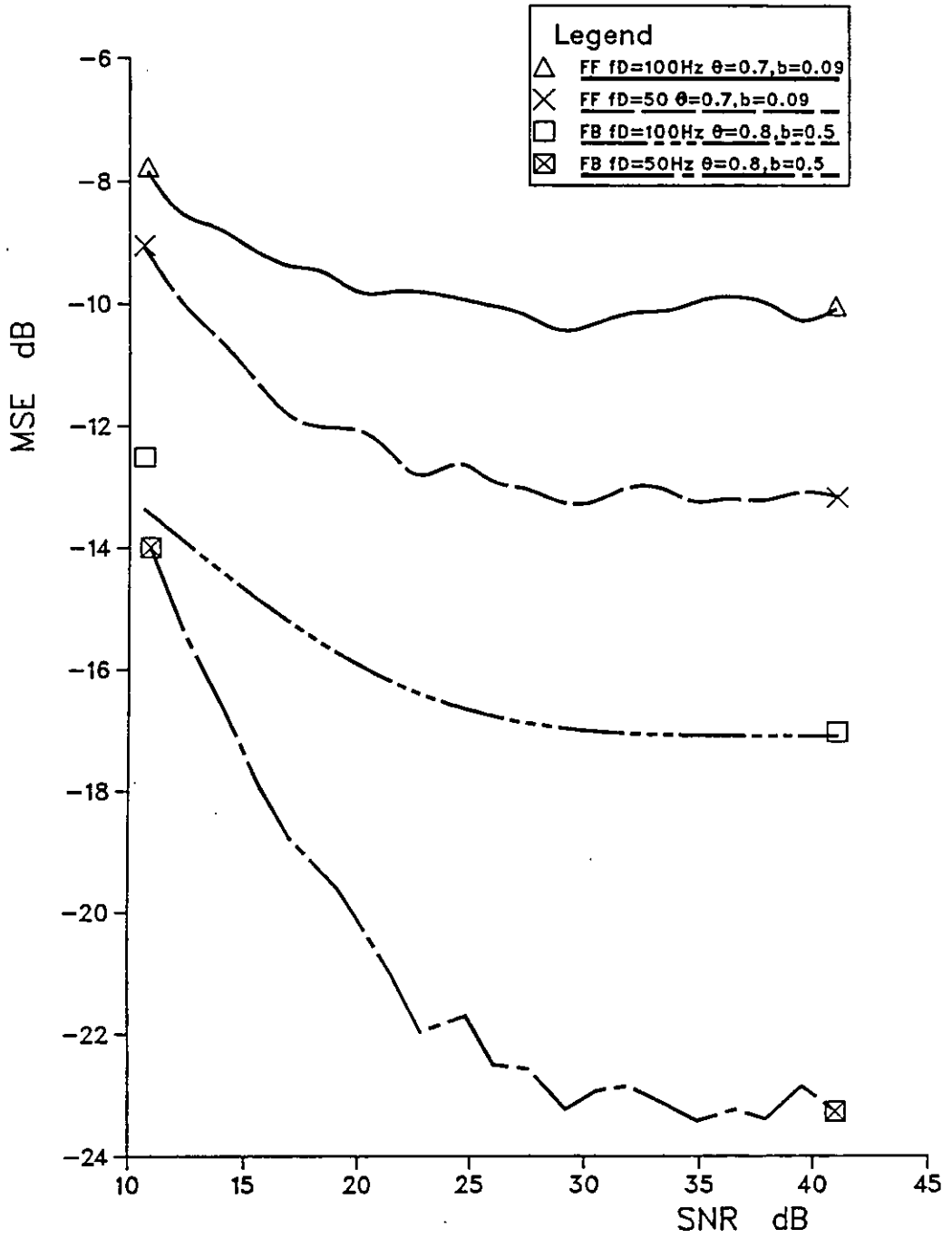

Fig.6.22 Comparison between the performances of FFCE and MFBCE when fD=100 and 50 Hz with C=rc.
MSE: Mean Square Error

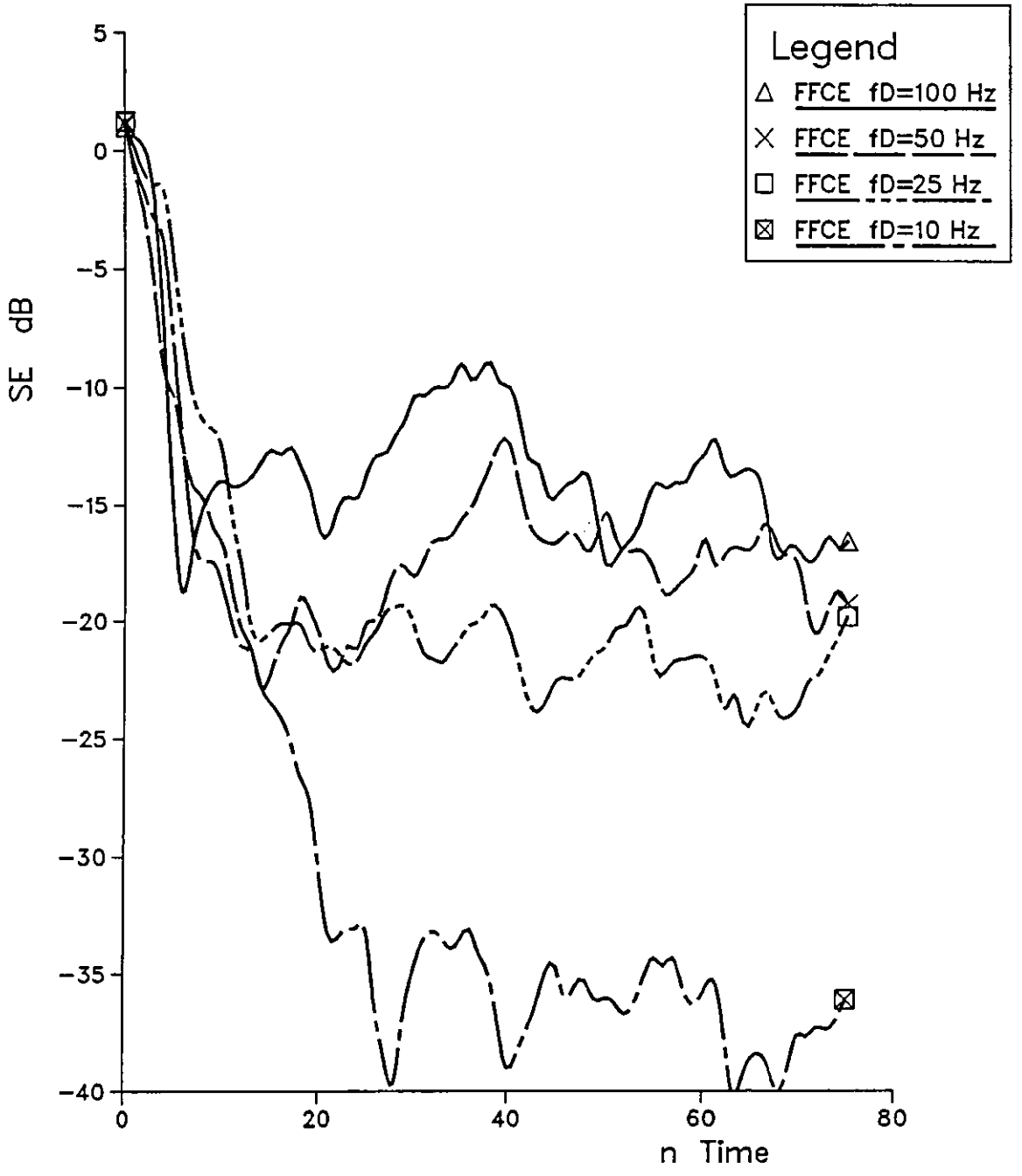

Fig. 6.23 Convegence tests for FFCE under different fading rates when SNR=38 dB, C=rc, θ=0.7 and b=0.09. SE: Square Error

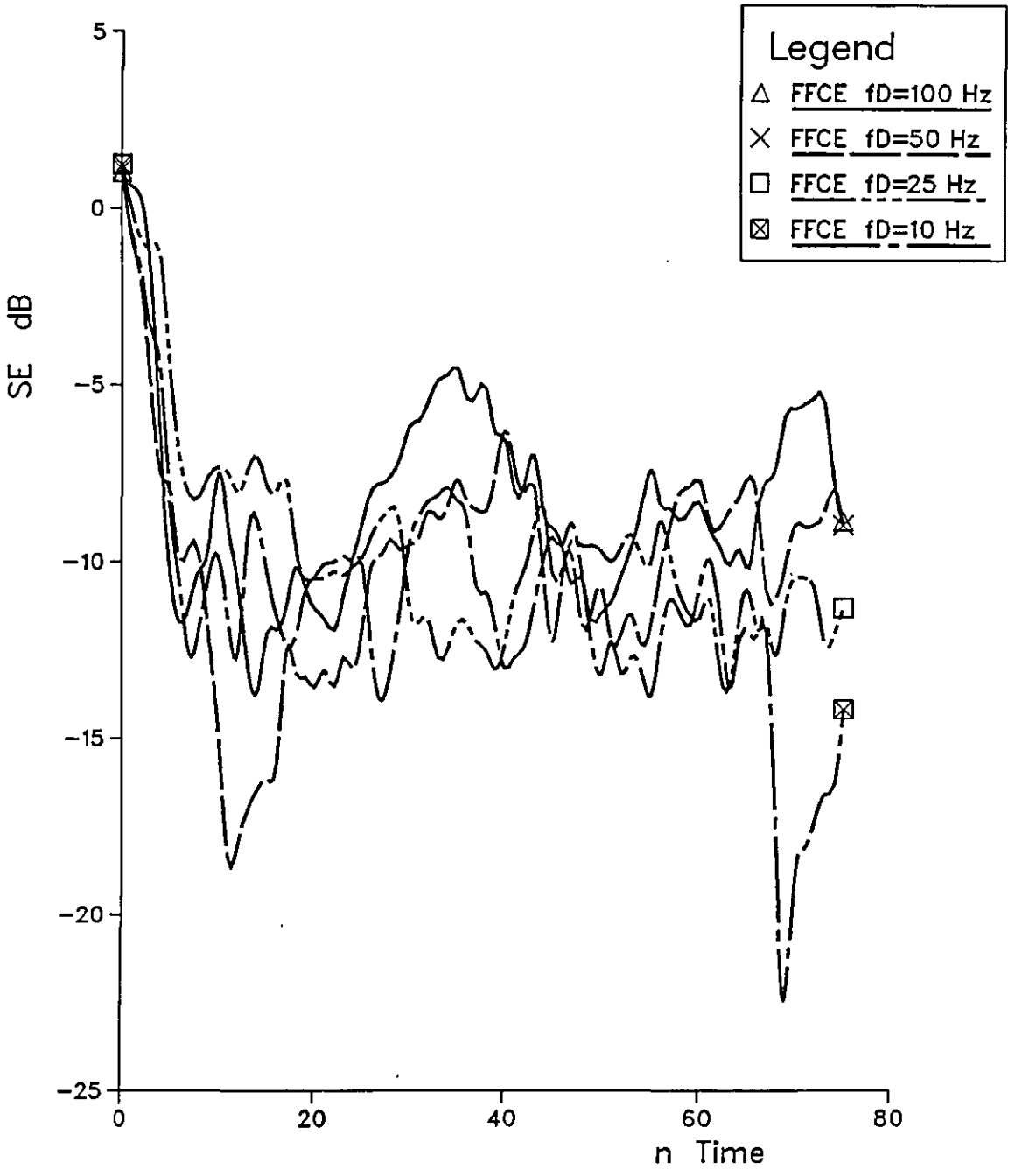

Fig. 6.24 Convegence tests for FFCE under different fading rates when SNR=10 dB, C=rc, θ=0.7 and b=0.09.
SE: Square Error

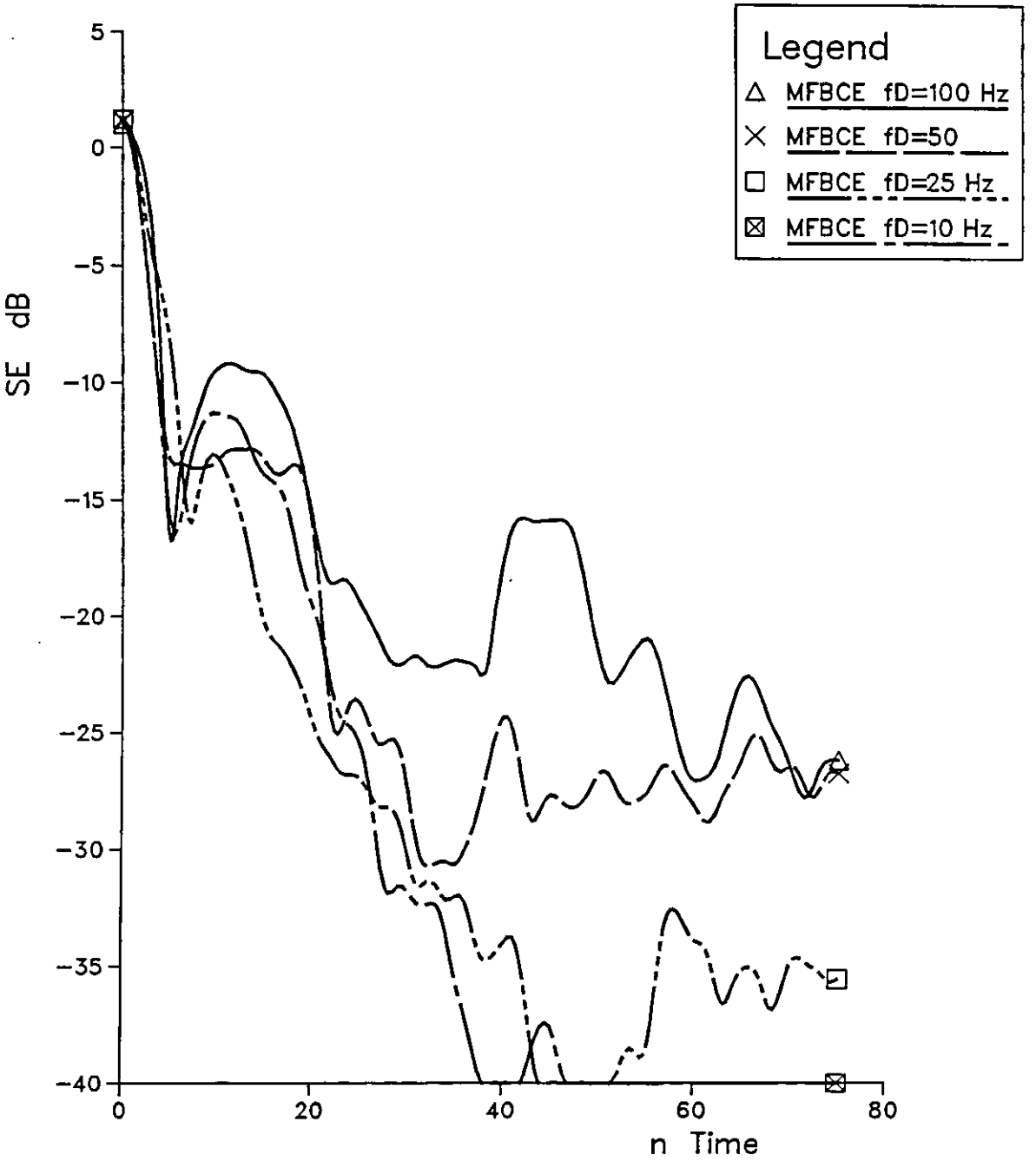

Fig. 6.25 Convegence tests for MFBCE under different fading rates when SNR=38 dB, C=rc, θ=0.8 and b=0.5.
SE: Square Error

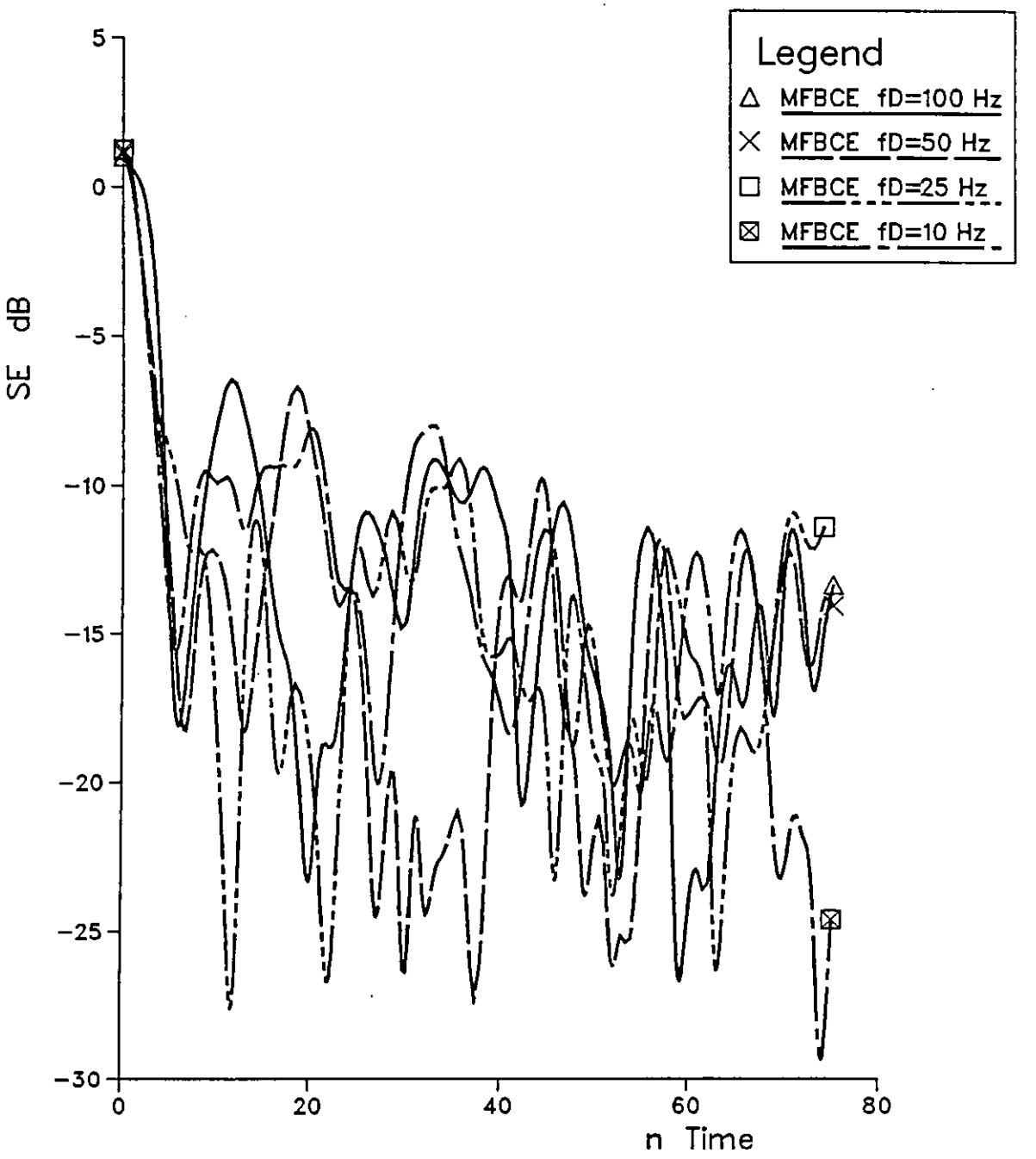

Fig. 6.26 Convegence tests for MFBCE under different fading rates when SNR=10 dB, C=rc, θ=0.8 and b=0.5.
SE: Square Error

7. SPACE DIVERSITY

7.1 Introduction

It is believed, from the preceeding Chapters, that the deep fade occurrence is rare[10,11,117], and of a short duration. However, when it does occur, it will ruin all the built-up synchronisation. Also, throughout this interval, errors are more likely to occur. Since the chance of having two deep fades from two uncorrrelated signals at any instant is unusual, then the effect of the fade can be reduced by the application of diversity[10,11]. Diversity is the technique used to develop the transmitted information from several signals received independently over different fading paths. The objective of a diversity scheme is to combine the multiple signals in order to combat the effects of Rayleigh fading. As a result, the diversity scheme can minimize the effect of fading since deep fades rarely occur simultaneously during the same time interval on two or more paths. The following definitions are used in diversity schemes:-

i) Coherent bandwidth: is the channel (frequency) spacing between two signals with a correlation coefficient of les than 0.5[117]. The coherence bandwidth is typically from 30 kHz to 1 MHz. The frequency selective properties of mobile radio makes it possible for some system plans to employ frequency diversity in order to combat the effect of fading[10,11,117].

ii) Coherent Time: is the difference in time between two samples of signal with a correlation coefficient of less than 0.5[117]. The typical value of coherent time is 1.3 ms or more. The frequency dispersive properties of the channel can be utilized in a time diversity scheme to combat the effect of fading[10,11, 113,117].

iii) Coherent distance: is the minimum distance between two points at which the signals correlation is less than 0.5[11,117]. The typical coherence distance is $n\frac{\lambda}{2}$ in an urban location, where λ is radiated frquency wavelength and n is an integer, $n \geq 1$. This property enables the use of space diversity.

Since the spectrum utilisation isvery important in cellular mobile radio, space diversity is recommended in such an environment[10-12,117, 123-130, 134-175]. Hence, the objective of this chapter is to define the space diversity and to discuss briefly the combining methods. According to the above definitions, space diversity is achievable in the range of frequencies used here, of around 900 MHz since $\frac{\lambda}{2}$ = 16 cm. Simple tests are carried out here to show the variations of the signals level before and after combining, for the case of an unmodulated carrier.

7.2 The significance of space diversity

Space diversity is relatively simple to implement in comparison with the other diversity schemes and does not require any additional frequency spectrum. Moreover, space diversity is strongly considered in mobile radio communication for the above and the following merits[10-12, 117, 123-136]. According to the definition of coherence distance, the basic requirement is to choose space between the antennas at the receiving side or at both sides (transmitting and receiving) such that the individual signals are uncorrelated. The practical spacing is found to be $\frac{\lambda}{2}$ at mobile stations[10,11,117,131,133] and 11λ to 13λ at base stations[10,11,130]. The diversity array can be located either at mobile unit, the base station, or both depending on the successful design of a combining technique and the degree of required enhancement of the signal. Each of the M antennas in the diversity array must provide an independent signal to an M-branch diversity combiner. Then, the combiner operates on the assemblage of signals to produce a favourable result. In principle, there is no limitation on M, the number of array elements, but the amount of improvement realized in the fading condition decreases as M becomes large[11]. When M=2 the improvement is 11.5 dB with 99% reliable signal level and when M=4 the improvement is only 19 dB[11,117]. Furthermore, the acceptable amount of correlation is found ≤ 0.7 with good signal performance[130]. Also, it has been proved elsewhere[125] that the channel spacing can be reduced to half by the use of space diversity under similar co-channel interference conditions.

7.3 Combining Techniques

Since this chapter, as titled, deals with space diversity, therefore it is unnecessary to discuss combining techniques used with other diversity schemes. The following combiners used with space diversity schemes are discussed in detail elsewhere[10,11], and they are briefly presented here:-

i) Selective combiner: The function of this combiner is to select the signal with the highest signal-to-noise-ratio amongst all of the received array. Of course, the system cannot calculate the signal-to-noise ratio but it selects logically the signal with highest level. However, this combiner is an impractical technique for mobile radio since it is very difficult to implement, due to the requirement of a floating threshold level[10].

ii) Switch combiner: This combiner depends on a switch-and-stay strategy. In this technique, the signal is switched to the receiver (demodulator) and stays on until its envelope drops below a predetermined threshold, and then the combiner looks for a signal from the M branches with highest level to switch it on to the receiver.

iii) Maximal-ratio combiner: In this combiner, the M signals are weighted for optimum performance and are co-phased before being combined. The maximal-ratio-combiner can be applied with pre-demodulation or post-demodulation techniques, where the co-phased signals are combined before or after demodulation respectively.

iv) Equal-gain Combiner: uses a simple phase-locked summing circuit to sum all of the M signals. Also, it provides incoherent summing of the various noise elements, but at the same time it provides coherent summing of all the individual signal branches.

However, it is difficult to combine two or more signals with different phases relative to each other, in mobile radio communication, whatever the difference between their amplitudes. The combiner used here is similar to the equal-gain combiner.

7.4 Algorithm for Space Diversity

The requirements of the space diversity technique at the receiving end are two antennas and a two branch combiner, where, in this case M=2. A model of a receiver representing such a technique is illustrated in Figure 7.1. This arrangement at the receiver does not depend on the arrangement of the transmitter, whether the transmitter has a single antenna or more used in a space diversity configuration. However, the two received signals are received over two different paths, each subjected to different Rayleigh fading. The receiver, Figure 7.1, consists of two sets of demodulators,combiner and detector. The two received signals are roughly demodulated, by the first set of demodulators, to give complex-valued baseband waveforms given by

$$r(t,d) = \sum_i s_i \, y(t - iT,d) + w(t,d) \qquad 7.1$$

where, $\{y(t,d)\}$, for d=1,2, are the impulse responses of the channel seen through the two paths and $\{w(t,d)\}$ are the additive bandlimited Gaussian noise components (see Chapters 3 and 4). Of course, both received signals carry the same information s_i. It is assumed that $s_i = 0$ for $i \leq 0$, so that s_i is the i^{th} transmitted data symbol. Also, for $i > 0$, the $\{s_i\}$ are statistically independent and equally likely to have any of K possible values defined in Chapters 2 to 4 for multilevel signals.

The received signals, Equation 7.1, are sampled once per data symbol at the same instant t = iT to give the received samples

$$r_{i,d} = \sum_{\ell=0}^{L-1} s_{i-\ell}\, y_{i,\ell,d} + w_{i,d} \qquad 7.2$$

where $\{y_{i,\ell,d}\}$ are the sampled impulse responses of the two baseband channels seen from the two branches and $w_{i,d} = w(iT,d)$ are the bandlimited Gaussian noise components with zero mean and the same variance. Knowing that each of $\{y_{i,\ell,d}\}$, $\{w_{i,d}\}$, $\{r_{i,d}\}$ and s_i is complex-valued. Of course, the two signals $\{r_{i,d}\}$, for d = 1,2, are uncorrelated according to the definition of coherent distance[10,11,117], therefore

$$E(r_{i,1}\, r^*_{i,2}) = 0 \qquad 7.3$$

where E(x) is the expectation of x, and subsequently

$$E(y_{i,\ell,1}\ \ y^*_{i,\ell,2}) = 0 \qquad \text{for } \ell = 0,1, \ldots, L-1 \qquad 7.4$$

$$E(w_{i,1}\ \ w^*_{i,2}) = 0 \qquad 7.5$$

Clearly, each of $\{y_{i,\ell,d}\}$ has common basis as described in Chapter 3 and the following chapters. Furthermore, each of them has a finite duration for practical purposes.

The second set of demodulators is used to remove separately, any frequency offset and/or phase shift, caused by the transmission paths, from the corresponding signal, so that they can be easily combined. The

combination is performed irrespective of the signals fading. The disadvantage of this combining technique is when any one of the received signals suffers a deep fade,more noise, in comparison with combined signal level, will go through to the detector. But it is still better than selective and switch combiners in regarding the performances of the synchronisation systems which cannot cope easily with sudden jumps between different level signals and will subsequently affect the performance of the detector (Chapter 6), with the assumption that all combiners are using co-phased signals. The second set of demodulators uses a data aided digital phase locked loop (DA-DPLL) (Chapter 5) to generate correction signals that are used for the demodulation processes. The correction signals are given by

$$c_{i,d} = e^{-j\phi_{i,d}} \qquad \text{for } d=1,2 \qquad 7.6$$

where each one of $\{\phi_{i,d}\}$ covers the phase and/or frequency shift caused by the corresponding path and $j = \sqrt{-1}$. Moreover, each of DA-DPLL's is a second order system and has two inputs, the estimated signal that can be obtained from the channel estimator and the demodulated received signal of the corresponding path (Chapters 5,6), as shown in Figure 7.1. The tanlock phase detector is used in each of the DA-DPLL to detect the phase difference between the two input signals to the DA-DPLL (Chapter 5).

The impulse response of the channel corresponding to either path, ($\{y_{i,\ell,1}\}$ or $\{y_{i,\ell,2}\}$), is now formed by the linear modulator, transmitter filter (by assuming single transmitting antenna), the corresponding transmission path, the corresponding linear demodulator and the corresponding receiver filter. Hence, from Equations 3.79 and 3.80, it is possible to obtain

$$Y_{i,d} = H_o Q_{i,d}$$

$$= [y_{i,0,d} \quad y_{i,1,d} \quad y_{i,2,d} \cdots \quad y_{i,L-1,d}] \qquad 7.7$$

where (from Equation 3.77)

$$H_o = [h_o \; h_1 \; h_2 \cdots h_{L-1}] \qquad 7.8$$

is the nonfading channel impulse response and (from Equation 3.81)

$$Q_{i,d} = \begin{vmatrix} q_{i,d} & 0 & 0 & \cdots & 0 \\ 0 & q_{i-1,d} & 0 & \cdots & 0 \\ 0 & 0 & q_{i-2,d} & \cdots & 0 \\ \vdots & \vdots & \vdots & & \vdots \\ 0 & 0 & 0 & & q_{i-L+1,d} \end{vmatrix} \qquad 7.9$$

which are obtained from the Rayleigh fading simulators for the two paths. Of course, the same demodulators and receiver filters are used in the two branches at the receiving end. The modulator and the transmitter filter at the transmitting end, and the demodulator and the receiver filter at the receiving end together form the nonfading channel impulse response, H_o.

The two transmission paths are represented by two Rayleigh fading simulators designed in the same way as described in Chapter 3. The four noise components are obtained from four different noise sources. Also, the four noise components are uncorrelated Gaussian random variables with zero mean and the same fixed variance. Hence, $\{Q_{i,d}\}$ are uncorrelated random

variables with a Rayleigh distribution function to satisfy the condition of space diversity[10,11,117,130].

Equation 7.2 can be rewritten as

$$r_{i,d} = \sum_{\ell=0}^{L-1} s_{i-\ell}\, y'_{i,\ell,d}\, e^{j\phi i,d} + w_{i,d} \qquad 7.10$$

where

$$y_{i,\ell,d} = h_\ell |q_{i-\ell,d}| e^{j\phi i,d} \qquad \text{for } \ell=0,1, \ldots, L-1$$

$$= y'_{i,\ell,d}\, e^{j\phi_{i,d}} \qquad 7.11$$

and $\{\phi_{i,d}\}$ are the phase shifts caused by the two transmission paths and $|q_{i,d}|$ is the modulus of $q_{i,d}$. As a comparison between Equation 7.11 and Equation 7.6, the generated correction signal phases are the same as the received signal phases. Ideally, this is required for such situations, but is not true practically. The two received signals are co-phased by the second set of demodulators as fulfilment of a successful combining method. The signal at the output of the combiner is given by adding the results of multiplying Equation 7.6 by Equation 7.10

$$r'_i = r_{i,1}\, c_{i,1} + r_{i,2}\, c_{i,2}$$

$$= \sum_{\ell=0}^{L-1} s_{i-\ell}\, h'_{i,\ell} + v_i \qquad 7.12$$

where

$$h'_{i,\ell} = h_\ell(|q_{i-\ell,1}| + |q_{i-\ell,2}|) \qquad \text{for } \ell = 0,1, \ldots, L-1$$

$$= h_\ell \, p_{i-\ell} \tag{7.13}$$

$$p_i = |q_{i,1}| + |q_{i,2}| \tag{7.14}$$

and

$$v_i = w_{i,1} \; c_{i,1} + w_{i,2} \; c_{i,2} \tag{7.15}$$

Clearly $\{h'_{i,\ell}\}$ are the components of the resultant channel impulse response that are now given by

$$H'_i = H_o \, P_i$$

$$= [h'_{i;0} \; h'_{i;1} \; h'_{i,2} \cdots h'_{i,L-1}] \tag{7.16}$$

where H_o is given by Equation 7.8 and P_i is $L \times L$ -diagonal matrix such as

$$P_i = \begin{vmatrix} p_i & 0 & 0 & \cdots & 0 \\ 0 & p_{i-1} & 0 & \cdots & 0 \\ 0 & 0 & p_{i-2} & \cdots & 0 \\ \cdot & \cdot & \cdot & & \cdot \\ \cdot & \cdot & \cdot & & \cdot \\ \cdot & \cdot & \cdot & & \cdot \\ 0 & 0 & 0 & \cdots & p_{i-L+1} \end{vmatrix} \tag{7.17}$$

Now, all the components of P_i are real valued representing the resultant of the fading caused by the two transmission paths. v_i is a complex-valued noise component, whose real and imaginary parts are statistically independent Gaussian noise with zero mean and same variance.

The detector must have prior knowledge of H_i' in order to be able to detect the received data symbols s_i' . s_i' can have all possible values of s_i. Furthermore, H_i' is assumed here to be correctly estimated by the channel estimator (Chapter 6). The performance of channel estimator in space diversity will be further considered in Chapter 8. The carrier recovery systems using DA-DPLL are briefly presented here but will also be discussed concisely in Chapter 8. The estimated signal, that can be obtained from the channel estimator, can be given by:

$$z_i = \sum_{\ell=0}^{L-1} s'_{i-\ell}\, h'_{i,\ell} \qquad 7.18$$

The signals at the output of the phase detectors of the DA-DPLL's are given by

$$\theta_{i,d} = \tan^{-1}\left(\frac{I_m(z_i\, r_{i,d})}{R_e(z_i r_{i,d})}\right) \qquad 7.19$$

where $I_m(x)$ and $R_e(x)$ refer to imaginary and real parts of the variable x. These signals are used as inputs to the loop filters of the DA-DPLL's and their output signals are employed to excite the voltage controlled oscillators (VCO's). Let the transfer function of the loop filters and

and VCO's in series form be X(f) whose inverse Fourier Transform is x(t) The generated correction signal phases are now given by

$$\phi_{i,d} = \theta_{i,d} * x(t) \qquad 7.20$$

where * means the convolution process. Since $r_{i,1}$ and $r_{i,2}$ are uncorrelated, then the correction signals, $c_{i,1}$ and $c_{i,2}$, that are obtained from the DA-DPLL's, (Equation 7.6 and 7.20), are also uncorrelated.

7.5 Computer Simulation Tests and Results

Simple tests have been carried out to observe the variation in signals level, in the mobile radio environment. The tests are performed under the assumption of an unmodulated carrier, where, in this case, $s_i = 1 + j1$ and $j = \sqrt{-1}$ (see Chapter 5). The reason behind such tests is to enable close observation to the signal levels and phases before and after combination. Of course, the test can be carried out on a modulated carrier, but it is difficult to observe the phase, since the phase of a phase-modulated carrier is a function of the modulating signal and of the phase shift caused by the transmission paths. As mentioned earlier, the chance of having two deep fades from two uncorrelated signals at the same time is rare. Such a situation is shown in Figure 7.2 as a result of the first test that is consistent with the result obtained elsewhere[10,11]. The results of these tests are shown in Figures 7.2 to 7.6. The two received signals level seen at the output of the first set of demodulators, Figure 7.1 are plotted for a short interval of time in Figure 7.2. The signal level is calculated as:

$$\text{signal level} = 20 \log_{10}\left(\frac{|\text{fading signal envelope}|}{|\text{nonfading signal envelope}|}\right) \quad \text{dB}$$

$$= 20 \log_{10}\left(\frac{|r_{i,d}|}{|f_i|}\right) \quad \text{dB} \qquad 7.21$$

where d is either 1 or 2, $\{r_{i,d}\}$ are the two received fading signals as were given by Equation 7.2, $|x|$ is the modulus of x and

$$f_i = \sum_{\ell=0}^{L-1} s_{i-\ell} h_\ell \qquad 7.22$$

is the actual nonfading received signal. Bearing in mind that $\{h_\ell\}$ are the impulse response components of the nonfading channel given by Equation 7.8. Figure 7.3 shows the signal level at the output of the combiner. Clearly, most of the time the level of the combined signal is above zero dB. However, Figure 7.4 compares between the levels of the two received signals and the combined signal, those are shown in Figure 7.2 and 7.3.

The comparison between the two received signals phase at the output of the first set of demodulators and the phase of combined signal is shown in Figure 7.5. The phase of, for example, the received signals are calculated as:-

$$\text{phase of } (r_{i,d}) = \tan^{-1} \left(\frac{I_m (r_{i,d})}{R_e (r_{i,d})}\right) \quad \text{degrees} \qquad 7.23$$

Clearly, the phase of the signal at the output of the combiner is constant (or it is a function of the modulating signal phase only in case of using a modulated signal). Figure 7.6 (an expanded form of Figure 7.5) is presented to give a clearer view of how the phase of the received combined signal is varying.

The performance of a 4-level PSK system emnploying space diversity will be studied further in Chapter 8.

From this chapter, it is possible to conclude that the effect of the fade can be reduced by the application of space diversity, since the chance of having

two deep fades from two uncorrelated (or with small correlation coefficient) signals is small. Moreover, the space diversity is recommended for use in cellular mobile radio communications, because spectrum utilisation is a very important factor of the overall system design.

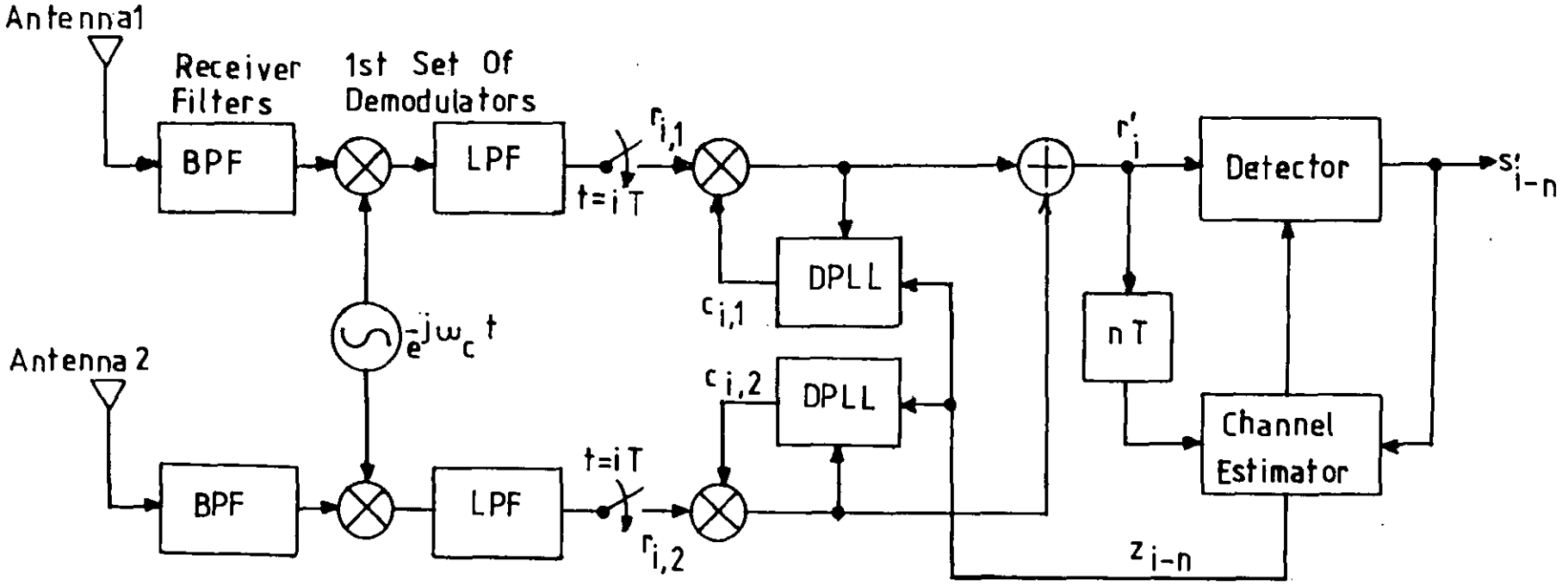

Fig. 7.1 A model of data transmission receiver employing space diversity

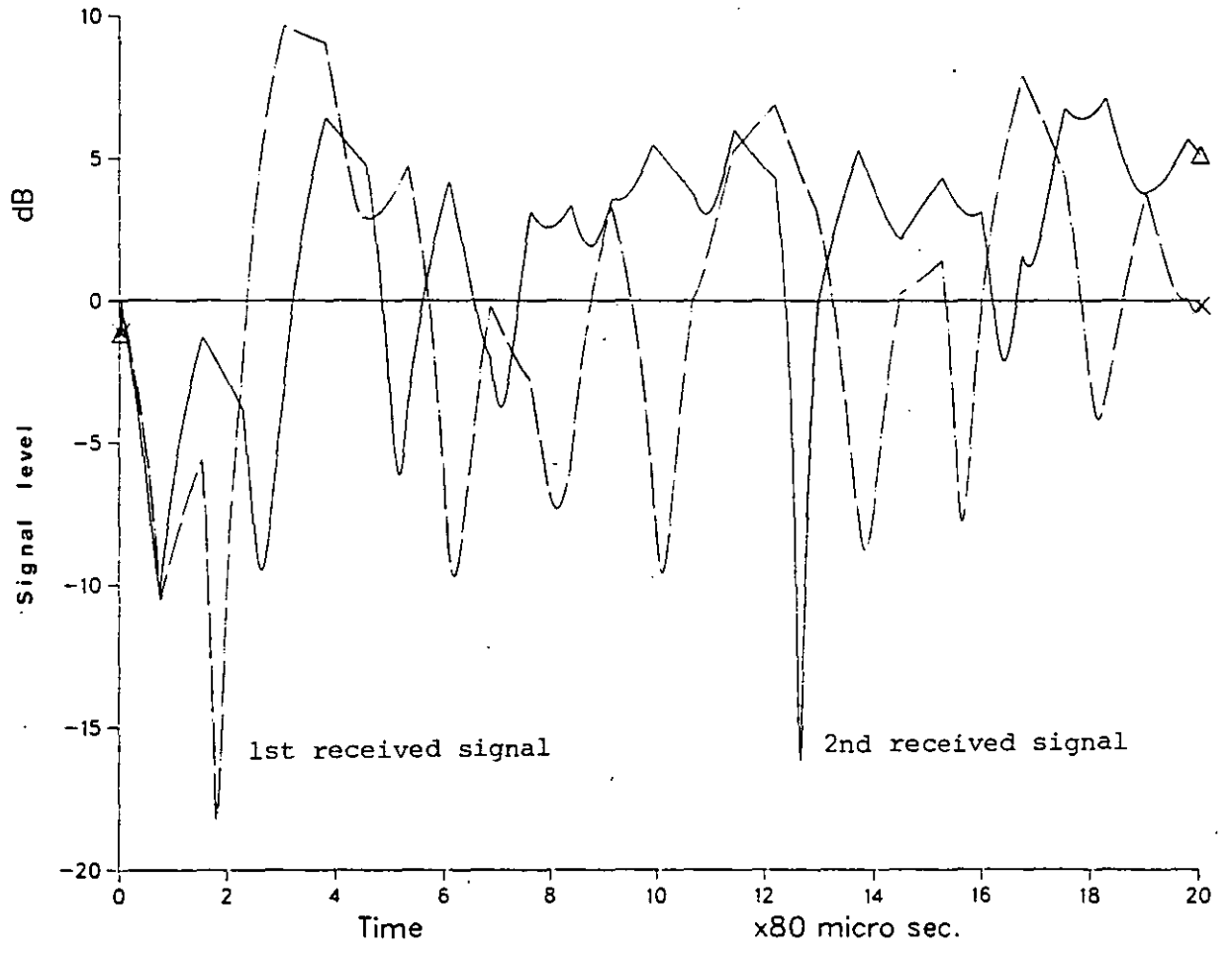

Fig. 7.2 Signals level, in dB, received via two antennas with space diversity technique

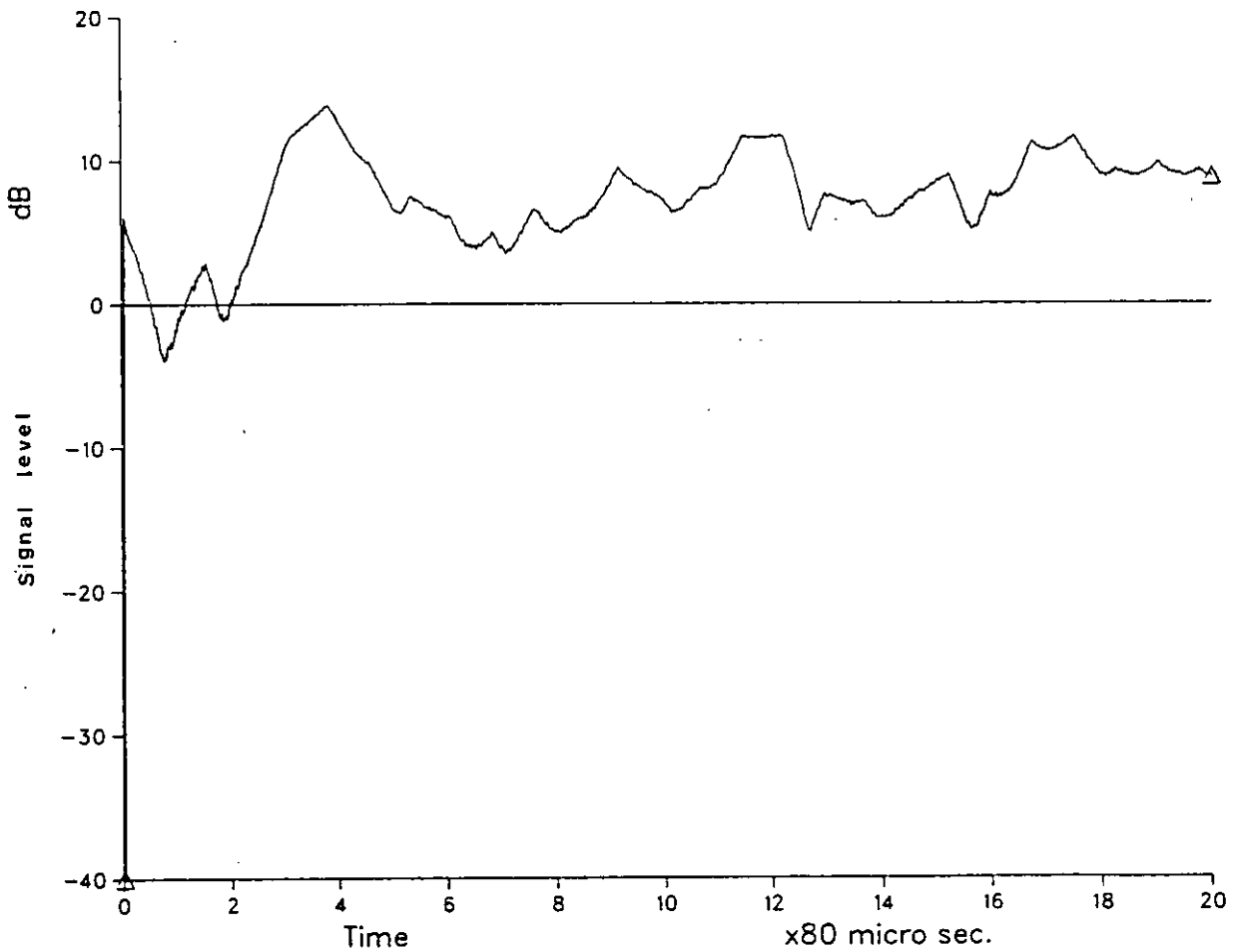

Fig. 7.3 Signal level at the output of the combiner

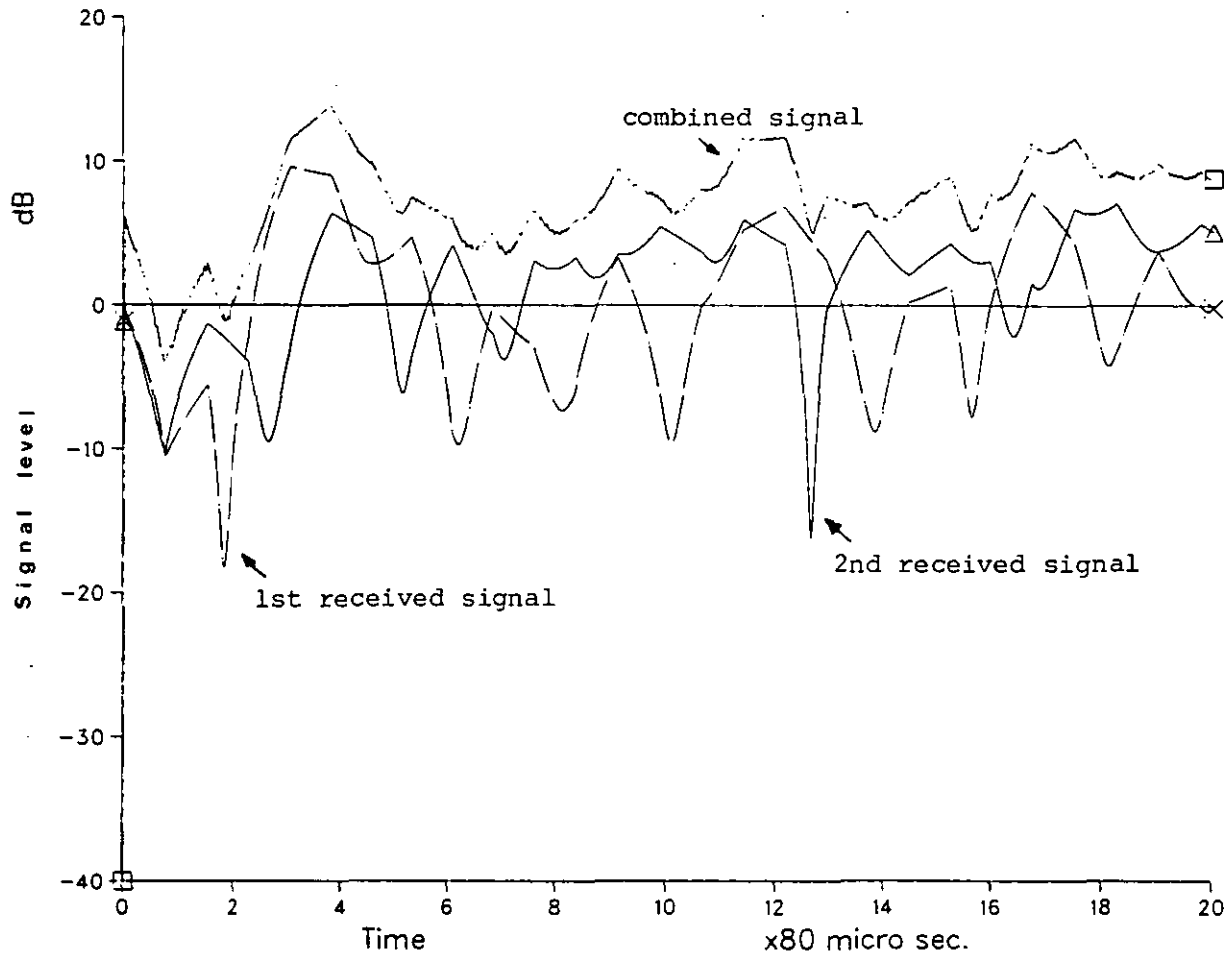

Fig. 7.4 Comparison between the received signals level and the signal level at the output of the combiner

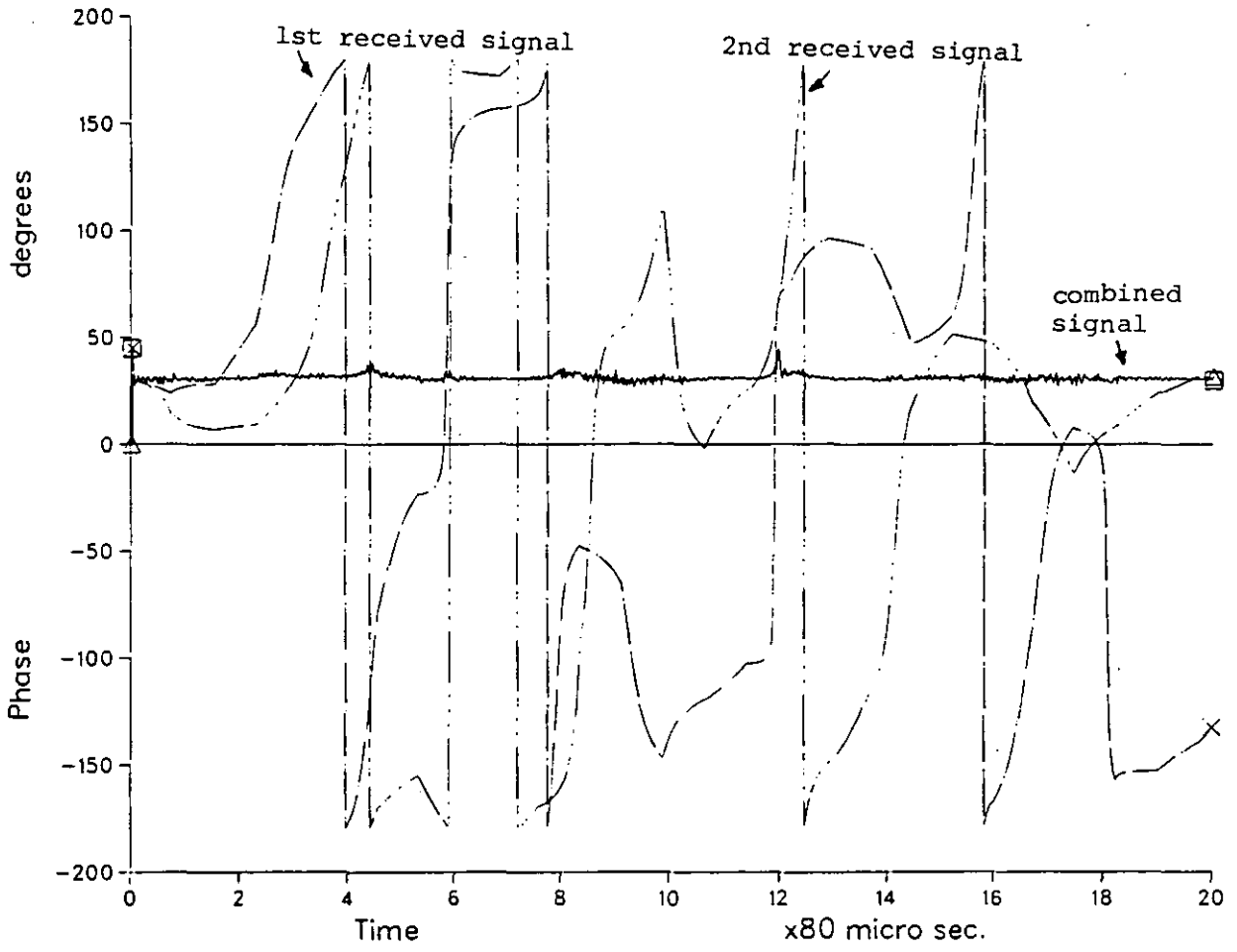

Fig. 7.5 Phase comparison of the two received signals and the signal at the output of the combiner

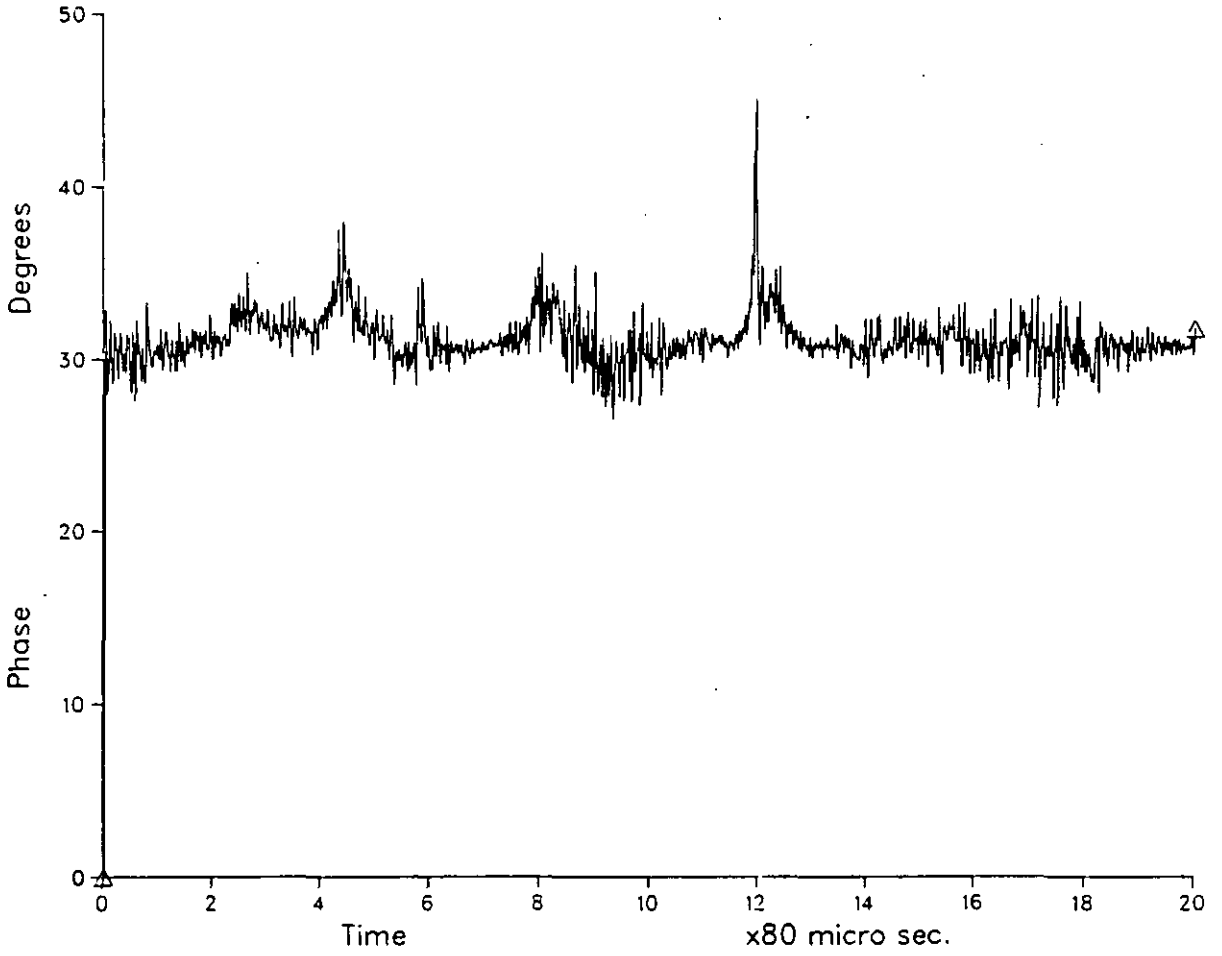

Fig. 7.6 Phase jitter at the output of the combiner

8. OVERALL PERFORMANCE

8.1 Introduction

In Chapter 7 a space diversity technique has been introduced and simple tests were carried out to study the combined signal level and phase with the use of a co-phased combiner. However, it is necessary to determine the tolerance to additive white Gaussian noise of a receiver employing space diversity, which is the objective of this chapter.

A 4-level PSK (phase-shift-keyed) signal with differential coding is the only multilevel signal used here (Chapter 2). The assumed receiver uses two sets of demodulators, a two branch combiner and a detector (see Figure 7.1). The two received signals are first demodulated to baseband by the first set of demodulators without removing the frequency offsets or the phase shifts caused by the corresponding paths. Also, the first set of demodulators use the same reference signal, whose frequency is equal to the transmitted signal carrier frequency. The second set of demodulators, whose functions are to remove any frequency offset and phase shift from the corresponding signals, use two independent correction signals generated by two DA-DLL's. At the output of the second set of demodulators, the signals are co-phased and can be combined (Chapter 7). The resultant signal from the combiner is fed to a detector. A non-linear equaliser, NLEQ, and a near-maximum likelihood, S2D3, detector are used and their performances are compared (Chapter 4). Moreover, the modified feedback channel estimator, MFBCE, is associated with the detector (Chapter 6). All the above equipment is described briefly here,

whilst their details can be seen from the corresponding chapter.

The carrier recovery systems (CRS1 and CRS2) described in detail in Chapter 5 are employed in receivers with the use of space diversity. Also, the co-phased combining method is used. The combined signal is fed to a threshold level detector.

All the systems mentioned above are tested by computer simulation tests (Appendix K).

8.2 Model description

Figure 8.1 shows the model of data transmission channel in the mobile radio environment. This model depends on the models described in Chapters 3 and 4 (Figures 3.1 and 4.1) and has the basic structure of a receiver model employing space diversity that has been described in Chapter 7 (Figure 7.1). Also this model may employ a near maximum likelihood detector or a nonlinear equaliser applied to a QPSK signal, that are described in Chapter 4 as system S2D3 and NELQ, respectively. Furthermore, this model uses the second-order data aided-digital phase loked loop (DA-DPLL) and the modified feedback channel estiamator (MFBCE) which are discussed in detail in Chapters 5 and 6 respetively. The way of realizing these systems in the model is shown in Figure 7.1.

By assuming single transmitting antenna, there is only one linear modulator and one transmitter filter. The signals are received via two antennas corresponding to two independent paths. Consequently, each antenna feeds the corresponding receiver filter and the linear demodulator. Each of the transmission paths is represented by a multipath Rayleigh fading simulator separately, so that the received singals are uncorrelated. Hence,each transmission path and the corresponding demodulator and lowpass filter (which is equivalent to the receiver filter, see Chapter 3) together with linear modulator and lowpass filter (equivalent to the transmitter filter) form the corresponding baseband channel. Accordingly, the two baseband channels are uncorrelated, with Rayleigh distribution functions. The complex-valued impulse response of the two channels, $y(t,d)$, have a finite duration for practical purposes, where $d = 1,2$.

Besides the fading, the other impairment is additive noise that may include co-channel interference and adjacent channel interference. However, the assumed noise is stationary white Gaussian noise, which is added to the information bearing signal at the output of each transmission path. The two complex-valued noise weveforms {w(t,d)} at the output of the two receiver filters are obtained from two different noise sources and, hence, they are uncorrelated. The resulting received signal at the output of the receiver filters are then complex-valued baseband signals given by Equation 7.1. Each of the received waveforms has a bandwidth extending from -B to +B, where B = 4800 Hz, and both are sampled at the same time instant, t = iT, once per data symbol to give the received samples,

$$r_{i,d} = \sum_{\ell=0}^{L-1} s_{i-\ell}\, y_{i,\ell,d} + w_{i,d} \qquad 8.1$$

where $r_{i,d} = r(iT,d)$, $y_{i,\ell,d} = y(iT,d)$ and $w_{i,d} = w(iT,d)$. The sampling rate is close to the Nyquist rate, which is 9600 sample/second. The real and imaginary parts of the noise components $\{w_{i,d}\}$ in the received signals $\{r_{i,d}\}$ are statistically independent Gaussian random variables with zero mean and have the same variance. The sampled impulse response of the linear baseband channels are given by Equation 7.7.

The frequency and/or phase offsets are not yet removed from the received signals, Equation 8.1, and removing them requires the generation of two correction signals, having the same frequency and/or phase offset of the corresponding signal. The system used to solve this problem is the

data aided digital phase locked loop (DA-DPLL) described in Chapter 5. At the output of the second set of demodulators, the demodulated and sampled signals are combined according to Equation 7.12, since they are now co-phased. The resultant signal is fed to a detector which may be a nonlinear channel equaliser with a threshold level detector or a near-maximum likelihood detector, where both are described in detail in Chapter 4 as systems S2D3 and NLEQ.

Since the modified feedback channel estimator (MFBCE) has shown a considerable improvement over the feedforward channel estimator (FFCE), the former is used here. The estimator was described in Chapter 6. The MFBCE uses the same feedforward transversal filter as that used by the nonlinear equaliser. Such an arrangement (of NLEQ and MFBCE) reduces the whole systems complexity.

8.3 Radio-frequency Signal Representation

This section is a continuation of Section 5.5, where the two carrier recovery systems, CRS1 and CRS2, are explained briefly, in order to avoid unnecessary repetition, with use of space diversity. The corresponding demodulation processes are described and detection is performed by using a simple threshold level detector. A post-demoulation combining method is used to combine the two demodulated signals (see Figures 8.2 and 8.3). From Equation 5.70, the two received signals are given by

$$r_{i,d} = a_{i,d} \cos(w_c\, iT + \phi_{s,i} + \phi_{q,i,d}) + w_{i,d} \qquad 8.2$$

where $a_{i,d}$, for d = 1,2, are the envelopes of the two received signals $\{r_{i,d}\}$ via two different paths.

$w_c = 2\pi f_c$; f_c is the carrier frequency,

i is the time index,

$T_s = T/32$; T is the signal element duration (in seconds)

$f_s = 1/T_s$; is the sampling frequency

$\phi_{s,i} = \frac{\pi}{2}(1 + \alpha_i)$; $\alpha_i = \pm 1$ is the sampled data sequence,

$\{\phi_{q,i,d}\}$ are the random phase shifts caused by two different transmission paths (from Equation 5.64) and $\{w_{i,d}\}$ are the additive band limited noise components. The modulation technique used here is binary PSK (phase-shift-keyed) and carrier frequency is reduced to 19.2 kHz for the use of software program simulation. The baseband data rate is 9.6 kbit/s.

The two received signals $\{r_{i,d}\}$ are assumed uncorrelated and hence $\{\phi_{q,i,d}\}$ and $\{w_{i,d}\}$ are uncorrelated (Chapter 7). α_i is equally likely to have any of the two possible values. The noise components, $\{w_{i,d}\}$ are Gaussian with zero mean and same variance. The signal-to-noise ratio is given by (from Equation 5.68)

$$SNR = 10 \log_{10} \sum_{d=1}^{2} \left(\sum_{i=1}^{15000} (a_{i,d})^2 / \sum_{i=1}^{15000} (w_{i,d})^2 \right) \qquad 8.3$$

8.3.1 System 1

The complete block diagram of a receiver employing CRS1 with the use of space diversity is shown in Figure 8.2. The two regenerated carrier signals, that are generated by squaring/filtering/frequency dividing by 2 method from the corresponding received signals, are given by (from Equation 5.71)

$$c_{i,d} = \cos(w_c i T_s + \phi'_{q,i,d}) \qquad \text{for } d = 1,2 \qquad 8.4$$

where $\{\phi'_{q,i,d}\}$ are the estimate of $\{\phi_{q,i,d,}\}$ generated at time $t=(i-1)T_s$. For linear demodulation, each of the received signals is multiplied by the corresponding regenerated carrier signals and the resultant is fed to an integrator circuit (or a lowpass filter) to form a time integral from 0 to T as shown in Figure 8.2. The signal at the output of each integrator is given by

$$g_{\ell,d} = \frac{1}{K} \sum_{k=0}^{K-1} c_{i-K+k+1,d} \; r_{i-K+k+1,d} \qquad 8.5$$

where d = 1,2, $K = T/T_s = 32$, T is the data element duration, T_s is the sampling period and ℓ is the time index of the data element such that $g_{\ell,d} = g_d(\ell T)$. Of course, the integrator should be reset to zero at the end of each integration period. Now, the two signals are combined by direct addition and the result is given by

$$g'_\ell = g_{\ell,1} + g_{\ell,2} \qquad 8.6$$

The threshold level detector, at this stage, compares g'_ℓ with zero threshold and makes a decision on which element has been received, as follows:-

$$\begin{aligned} \alpha'_\ell &= 1 \qquad \text{when } g'_\ell > 0 \\ \alpha'_\ell &= -1 \qquad \text{when } g'_\ell < 0 \end{aligned} \qquad 8.7$$

where α' is the detected data element.

The differential coding is essential in order to overcome the phase ambiguity in the recovered carrier signal phase caused by the squaring processes. In a mobile radio environment, with or without differential coding, there is always phase ambiguity in the recovered carrier signal due to Rayleigh fading. Therefore, space diversity has been used here. Since it is unlikely that the two signals will suffer a deep fade at the same instant (Chapter 7), it is possible to use the stronger signal to correct the regenerated carrier corresponding to the weaker signal. The demodulated signals $g_{\ell,1}$ and $g_{\ell,2}$ suppose to have the same polarity and

consequently their multiplication, $G_\ell = g_{\ell,1}\ g_{\ell 2}$, is always positive An observer can be assumed and operates according to the following procedure:

$If_1 \quad G_\ell < 0 \qquad$ then

$b_\ell = b_{\ell-1} + 1$

Look for the weaker signal (who suffered deep fade)

$If_2 \quad b_\ell > 5 \qquad$ then

Shift the corresponding regenerated carrier signal phase by 180^o (or multiply the corresponding regenerated carrier signal $\{c_{i,d}\}$ by -1)

$End\ if_2$

Else

$b_\ell = 0$

$End\ if_1$

This procedure enables the two regenerated carrier signals to resume their correct phase, throughout the test.

8.3.2 System 2

Figure 8.3 illustrates the block diagram of a receiver in which CRS2 is employed with use of space diversity. Also, the format of CRS2 resembles that of CRS1 with addition of a mixer. The two regenerated reference signals are given in this case by

$$c_{i,d} = \cos((w_c - w_L)\, iT_s + \phi'_{q,i,d}) \qquad \text{for } d = 1,2 \qquad 8.8$$

where $\{\phi'_{q,i,d}\}$ are the estimates of $\phi_{q,i,d}$ generated at time $t = (i-1)T_s$, and $w_L = 2\pi f_L$, f_L is the local oscillator frequency (see Equation 5.74). These signals are obtained by passing the output signals from the two mixers through limiters, squarers, frequency dividers and all associated filters (see Chapter 5). To demodulate the two received signals, (Equation 8.2) they are first multiplied by the two regenerated reference signals and bandpass filtered them. Then, the resultants are second multiplied by the local oscillator signal and the multiplication results are fed to the corresponding time integral circuits. The output of each integrator is given by

$$g_{\ell,d} = \frac{1}{K} \sum_{k=0}^{K-1} L_{i-K+k+1}\, r'_{i-K+k+1,d} \qquad \text{for } d = 1,2 \qquad 8.9$$

where $K = 32$, L_1 is the local oscillator signal (from Equation 5.72)

$$L_i = \cos(w_L\, iT_s) \qquad 8.10$$

and $\{r'_{i,d}\}$ are obtained from mutliplying the two received signals, $\{r_{i,d}\}$, and by the corresponding regenerated reference signals, Equation 8.8, and bandpass filtering them (see Equation 5.75), or

$$r_{i,d} = a_{i,d} \cos(w_L iT + \phi_{s,i}) + w'_{i,d} \qquad 8.11$$

where $w'_{i,d}$ is the additive noise components.

An identical procedure is used to correct the phase of the reference signal corresponding to the signal which is suffering a deep fade, as that used in case of employing CRS1. Furthermore, the identical detection method is used, as that described by Equations 8.6 and 8.7.

8.4 Computer Simulation Tests and Results

8.4.1 Baseband QPSK signal

Computer simulation tests have been carried out on systems S2D3, using near-maximum likelihood detection schemes, and NLEQ, using nonlinear equaliser, to determine their tolerance to aditive white Gaussian noise. Both systems employ 4-level PSK signals with differential coding (encoding/decoding). Also, these tests are carried out using space diversity at the receiving end as an array of two antennas. The enhancement of space diversity is studied with or without the adaptation of channel estimation and phase correction. Two channels are used here with Rayleigh distribution functions. The nonfading channels are derived from the corresponding ideal lowpass filters with rectangular and raised-cosine shapes (see Chapter 3). The signal-to-noise ratio is given by (from Equation 4.40)

$$SNR = 10 \log_{10} (P_s/P_n) \quad \text{dB} \tag{8.12}$$

where (from Equation 4.38)

$$P_s = \frac{1}{2} \sum_{d=1}^{2} \left(\frac{1}{K} \sum_{i=1}^{K} |s_i \, q_{i,d}|^2 \right) \tag{8.13}$$

is the signal average power, (from Equation 4,39)

$$P_n = \frac{1}{2} \sum_{d=1}^{2} \left(\frac{1}{K} \sum_{i=1}^{K} |w_{i,d}|^2 \right) \tag{8.14}$$

is the noise average power and K = 50,000. While the bit error rate is given by (from Equation 4.41)

$$BER = \frac{B_e}{B_t} \qquad 8.15$$

where B_e is the number of error bits in the received signal and B_t is the total number of transmitted bits. The computer simulation tests have been carried over the given channels according to the following sets of tests:-

i) Set 1:

In Chapter 4, the tests have been carried out according to the following assumptions:-

A) Coherent demodulation

B) Correct estimation of sampled impulse response of the channel.

C) The sampled impulse response of the channel performs the Rayleigh fading with appropriate fading rate throughout the channel.

D) According to assumption C, the sampled impulse response carried the Doppler frequency offset with rapidly fluctuating phase, caused by the multipath propagation.

The tests carried out in Chapter 4 show about 20 dB degradation in such an environment.

However, space diversity is used here in order to achieve better performance, since it is unlikely that the two signals suffer deep fade at the same time (Chapter 7). This set of tests is carried out with the above assumptions. The results are shown in Figures 8.4 and 8.5, for different fading rates, where CCA means Coherent demodulation and Correct channel estimation are Assumed. Figures 8.6 and 8.7 compare between these results with the use of space diversity (SD) when the Doppler frequency of 100 Hz

(f_D = 100 Hz) is used, and the corresponding results obtained from Chapter 4 without space diversity. C = r and C = rc mean rectangular and raised-cosine shaped channels respectively. However, the application of space diversity gives, on either channel, 1.5 dB enhancement only, which is much less than that expected. It is difficult to assess the causes now unless all the sets are completed.

ii) Set 2:

In this set, coherent demodulation is also assumed and the sampled impulse response of the channel is estimated by using MFBCE (modified feedback channel estimator). The results are shown in Figures 8.8 and 8.9, where CHE means only CHannel sampled impulse response is Estimated. The results obtained in Set 1 at f_D = 100 Hz for two systems, S2D3 and NLEQ, are used as a reference for this and the following sets of tests for comparison. It is evident from Figures 8.8 and 8.9 that the probability of error decreases as the fading rate decreases, since the mean square error (MSE) of the MFBCE decreases with decreasing of the fading rate as that is tangibly visible in Chapter 6. Also, these results are worse than expected.

iii) Set 3:

As mentioned earlier (in Chapter 6), the MFBCE has a narrow bandwidth and consequently cannot cope with rapidly fluctuating sampled impulse response of the channels. If it is possible to remove the frequency offset and phase shift caused by the transmission paths, the system's tolerance to additive noise may become better.

In Set 1 and Set 2, coherent demodulation has been assumed throughout the tests. This assumption is not exactly true, since all the frequency offset

and phase shift, caused by the transmission paths, have not been removed entirely from the demodulated and sampled received signals. The linear demodulation assumed in the preceding chapters was performed by simple frequency transformation from the passband region to the baseband region by using a signal having the same frequency as the transmitted carrier, but in phase quadrature to each other, as reference signal. Whilst the required reference signal must cover all the frequency offset and phase shift so as to match the received signal phase and frequency[12]. In Chapter 7, the demodulation was carried out by two sets of demodulators for frequency transformation and phase correction to resemble the action of coherent demodulation. This method is used here. As a result all the components of the sampled impulse response now have zero frequency and consequently narrow bandwidth can be accomplished. Figure 8.10 and 8.11 show the results of such tests. Clearly a much better performance can be obtained as the fading rate decreases, where in Figures 8.10 and 8.11 BG means Both channel impulse responses and phase correcting signals are Generated. Table 8.1 gives the enhancement of using space diversity when the sampled impulse response of the channel is estimated and phase correction signals are generated without delay. The results listed in Table 8.1 are measured, from Figure 8.10 and 8.11, at bit error rate of 10^{-4}.

iv) Set 4:

The tests in this set are identical to the corresponding tests in Set 3 but with phase correction signals are only generated and the sampled impulse rsponse of the channel is assumed correctly estimated (CHA.CG). The

results are illustrated in Figures 8.12 and 8.13. Clearly, identical results are obtained as in Set 3 but with much better improvement as shown in Table 8.2.

v) Set 5:

In Sets 3 and 4 the sampled impulse response of the channel is supplied to both detectors used here without a delay. The near-maximum likelihood detector, S2D3, required a delay. However, the phase correction signals are generated without delay, as in Set 4 while the sampled impulse response of the channel is supplied to the nonlinear equaliser detector, NLEQ, without delay and to the near-maximum likelihood detector, S2D3, with a delay by using least-square fading-memory prediction method. The results are shown in Figure 8.14 and 8.15. Evidently, the delay degrades the performance of the near-maximum likelihood detector severely at high fading rate and the degradations gradually diminish as the fading rate decreases.

8.4.2 Passband binary PSK signal

Computer simulation tests have been carried out on the two receivers employing either CRS1 or CRS2 (carrier recovery system 1 or 2) with a threshold level detector to determine their tolerance to additive white Gaussian noise under Rayleigh fading conditions. Both systems use binary PSK (phase-shift-keyed) signal with differential coding and space diversity technique. The signal-to-noise ratio is calculated according to Equation 8.3 . The results of the tests are shown in Figure 8.16. Clearly, the receiver employing CRS2 gives about 3.5 dB better performance over the receiver employing CRS1.

From the above results it is possible to conclude that:

i) The application of space diversity leads to more than 10 dB tolerance to additive noise in a mobile radio environment, depending on the fading rate.

ii) The nonlinear equaliser and near-maximum-likelihood detectors deteriorate with rapidly varying phase of the impulse response of the channel (Set 1). Therefore, it is recommended to remove any phase shift and frequency offset caused by the transmission path from the received signal and subsequently from the impulse response of the channel, in order to achieve better performance.

iii) The channel estimator is also sensitive to the phase fluctuation of the channel impulse response and consequently its deterioration degrades the performance of the corresponding detector (Set 2).

iv) Since the delay degrades the performances of the data aided digital phase locked loop and the channel estimator (see Chapters 5 and 6) these degradations affect the performance of the near-maximum likelihood dectors, even with less dispersive channels as those which were used here, but the performance of near-maximum likelihood is improved gradually as fading rate decreases.

v) The receivers in which the CRS1 and CRS2 (carrier recovery systems 1 and 2) show better tolerance to additive noise under Rayleigh fading condition. Consequently, both CRS1 and CRS2 are capable of tracking and generating the received signal carrier, of course, with the provision of the phase correction logic described here. Moreover, the receiver employing the CRS2 gives 3.5 dB better performance over the receiver employing

the CRS1, since in the former the demodulation takes place using a stable frequency for the local oscillator.

f_D in Hz	Rectangular shaped channel C = r in dB	Raised-cosine shaped channel C = rc in dB
100	indefinite	indefinite
50	12	11.35
25	16.5	15.2

Table 8.1 Improvement of using space diversity when the channel impulse response and the correction signals are all generated.

f_D in Hz	Rectangular shaped channel C = r in dB	Raised-cosine shaped channel C = rc in dB
100	12.1	8.5
50	15.1	13.8
25	17.8	17.25

Table 8.2 Improvement of using space diversity when the correction signals are generated and the channel impulse response is assumed correctly estimated.

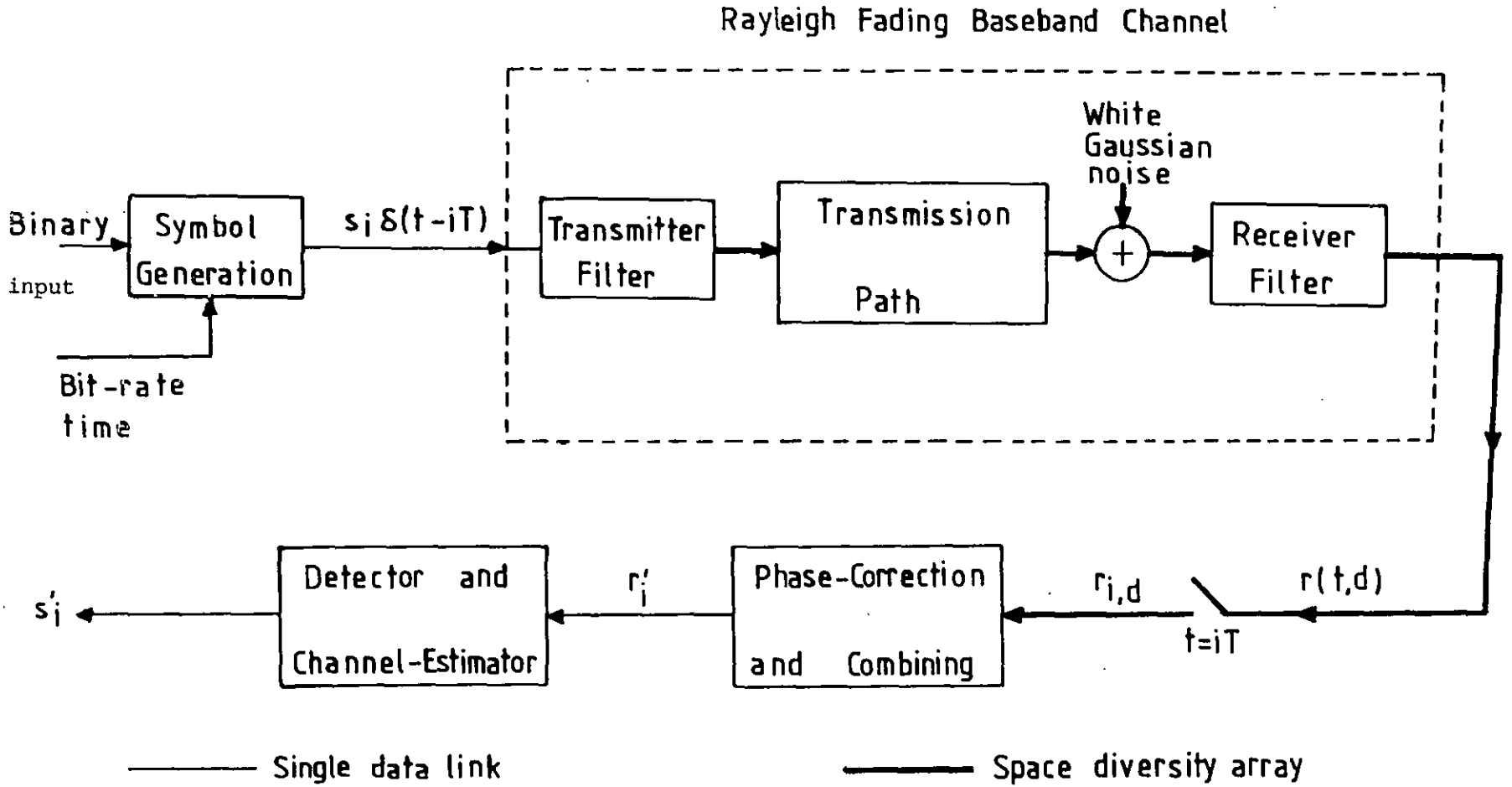

Fig. 8.1 Model of data transmission over mobile radio channel with space diversity technique

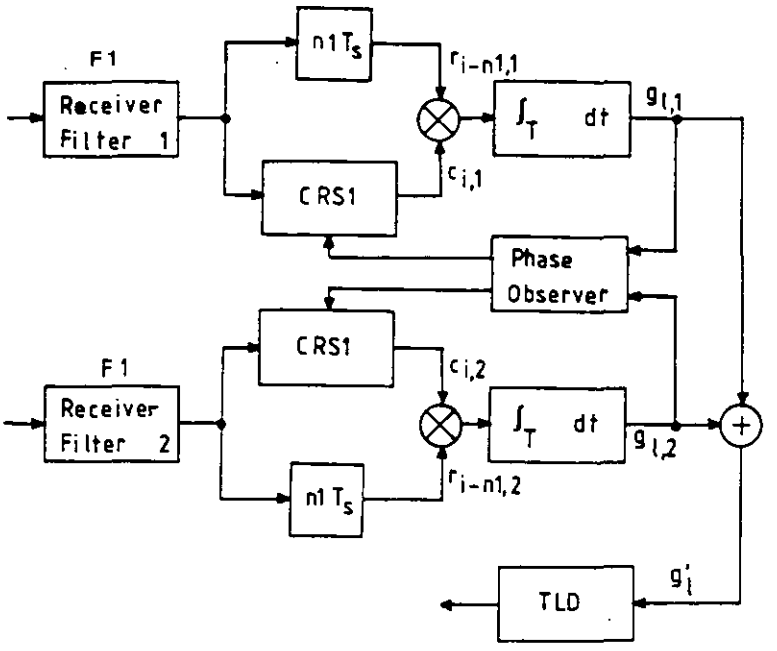

Fig. 8.2 A receiver using CRS1 with space diversity

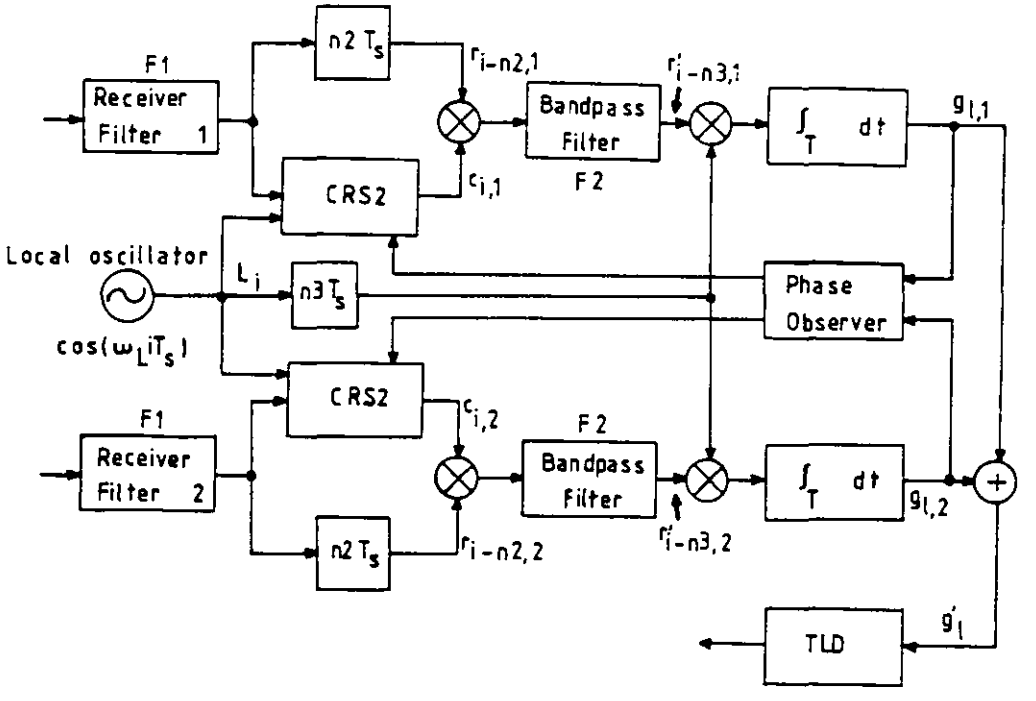

Fig. 8.3 A receiver using CRS2 with space diversity

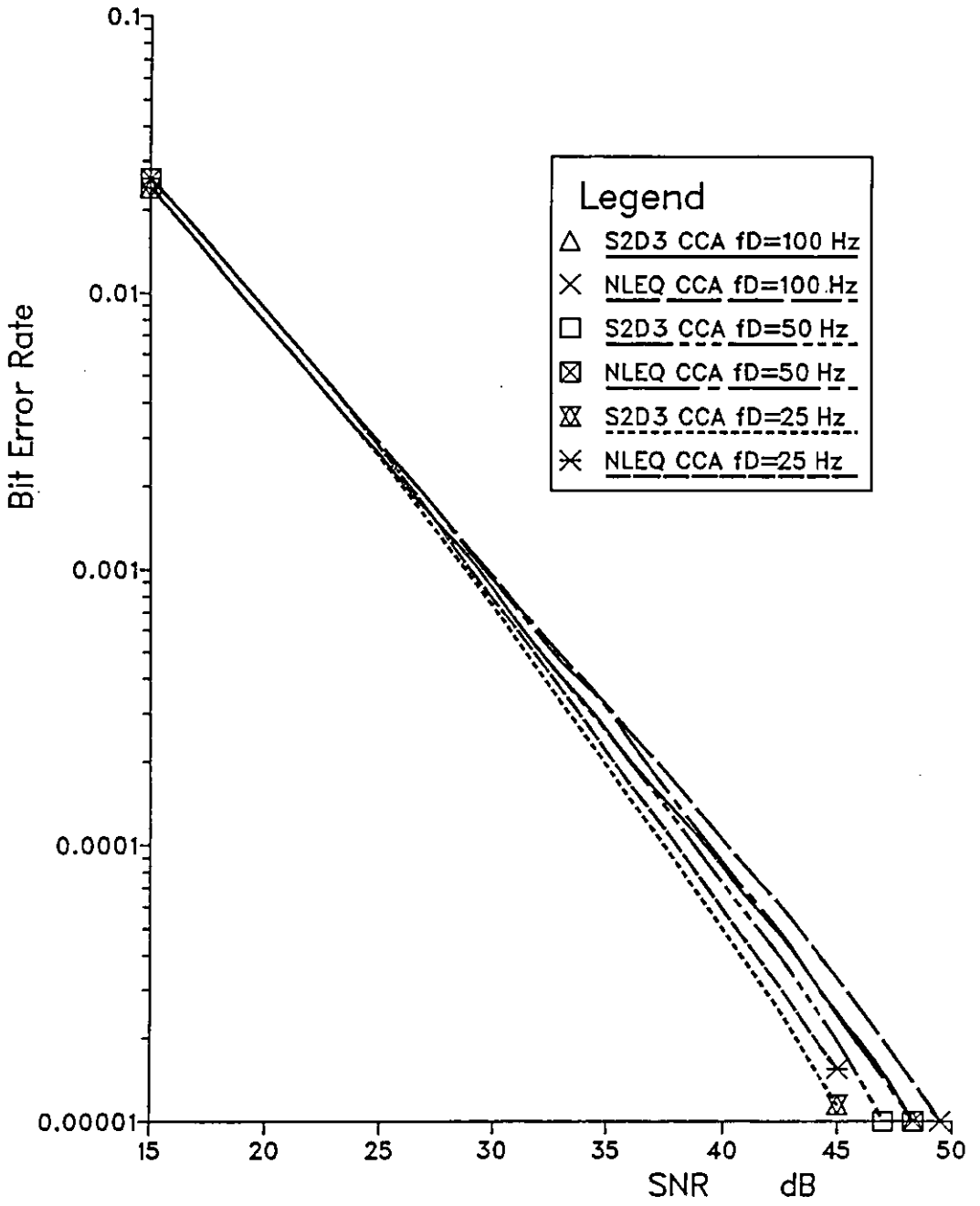

Fig. 8.4 Performances of different systems under different Rayleigh fading rates with use of space diversity by assuming correct impulse response of the channel and linear demodulation when C=r.

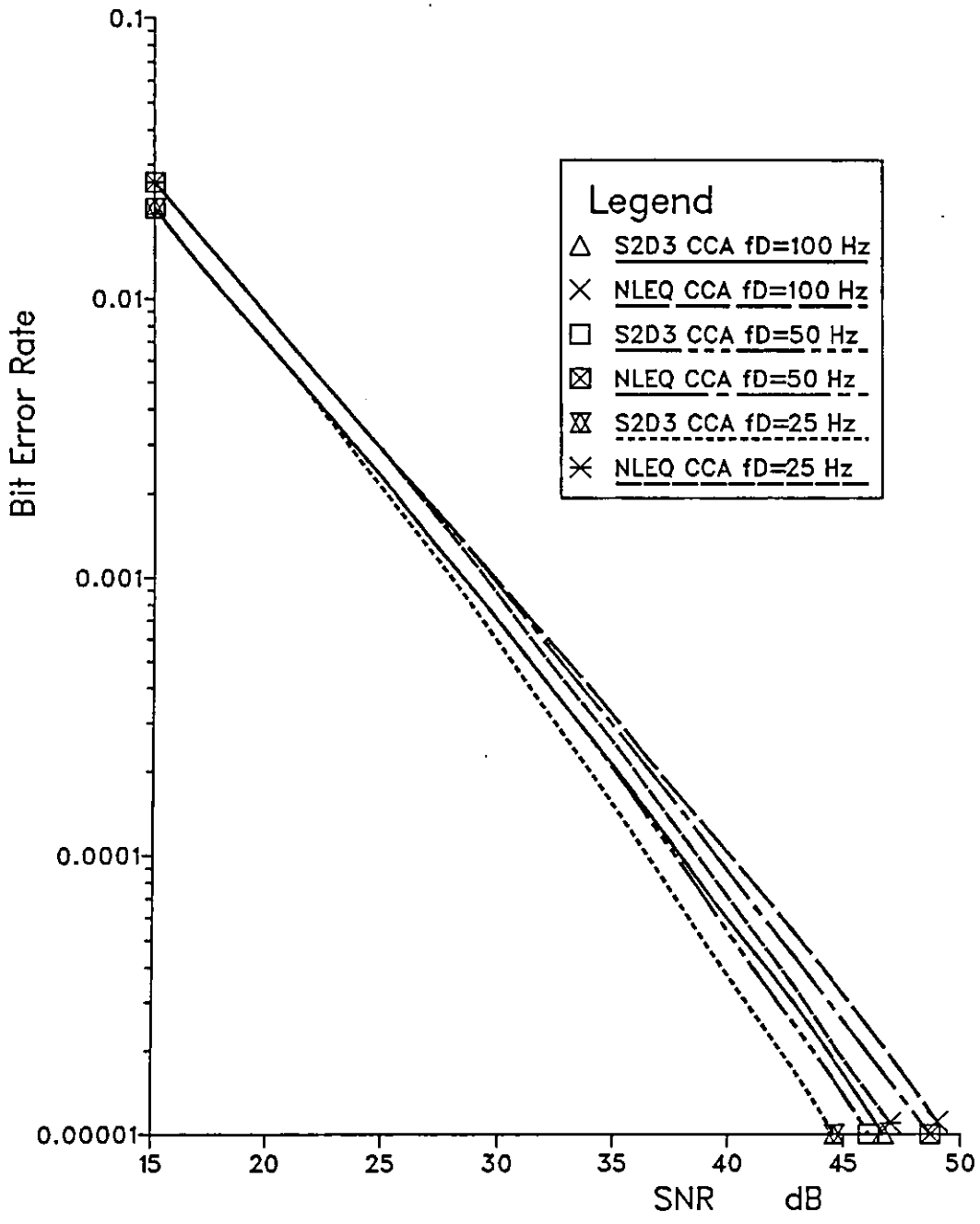

Fig. 8.5 Performances of different systems under different Rayleigh fading rates with use of space diversity by assuming correct impulse response of the channel and linear demodulation when C=rc.

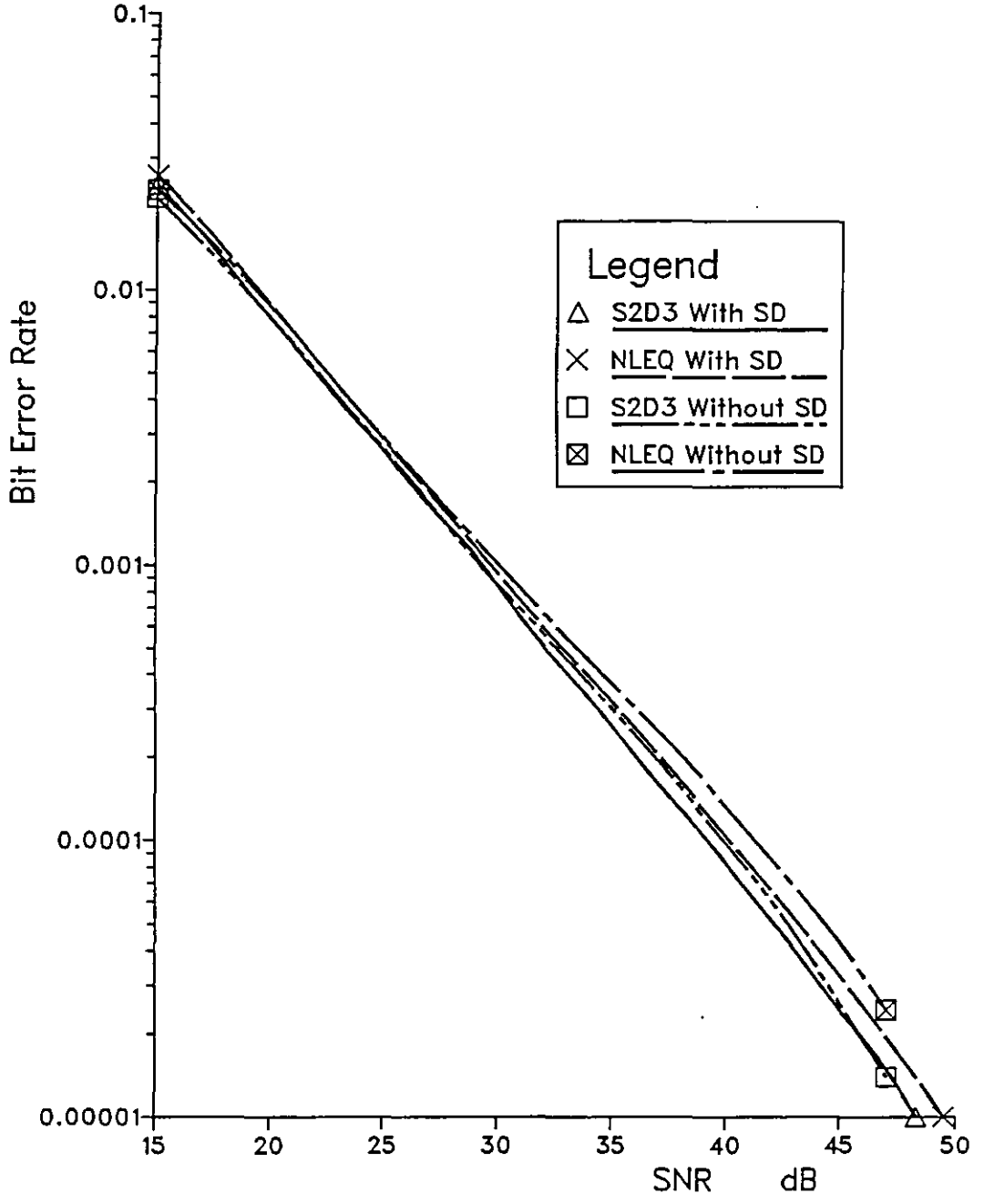

Fig. 8.6 Comparison between systems performances with and without space diversity under Rayleigh fading conditions, when fD=100 Hz and C=r.

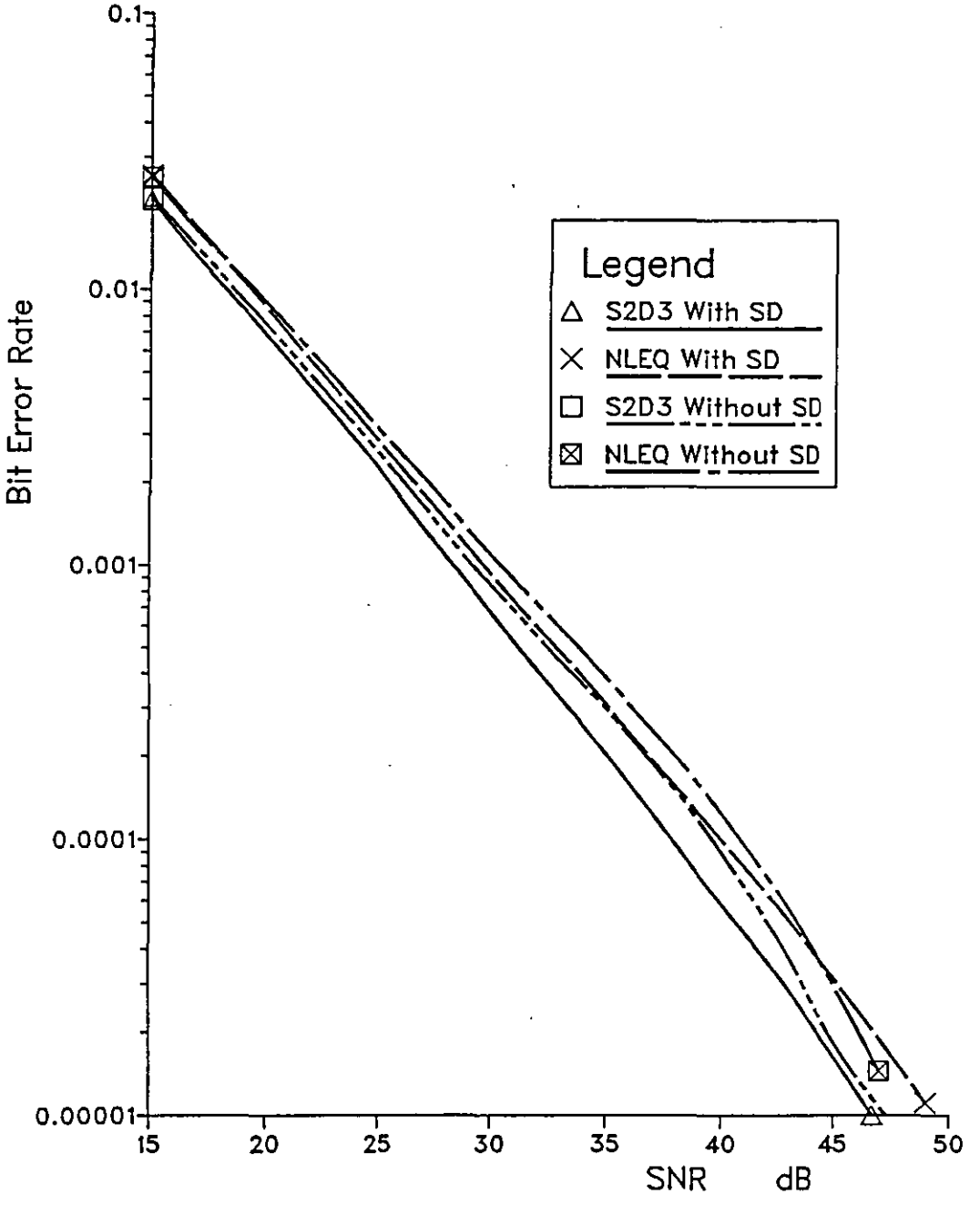

Fig. 8.7 Comparison between systems performances with and without space diversity under Rayleigh fading condition, when fD=100 Hz and C=rc.

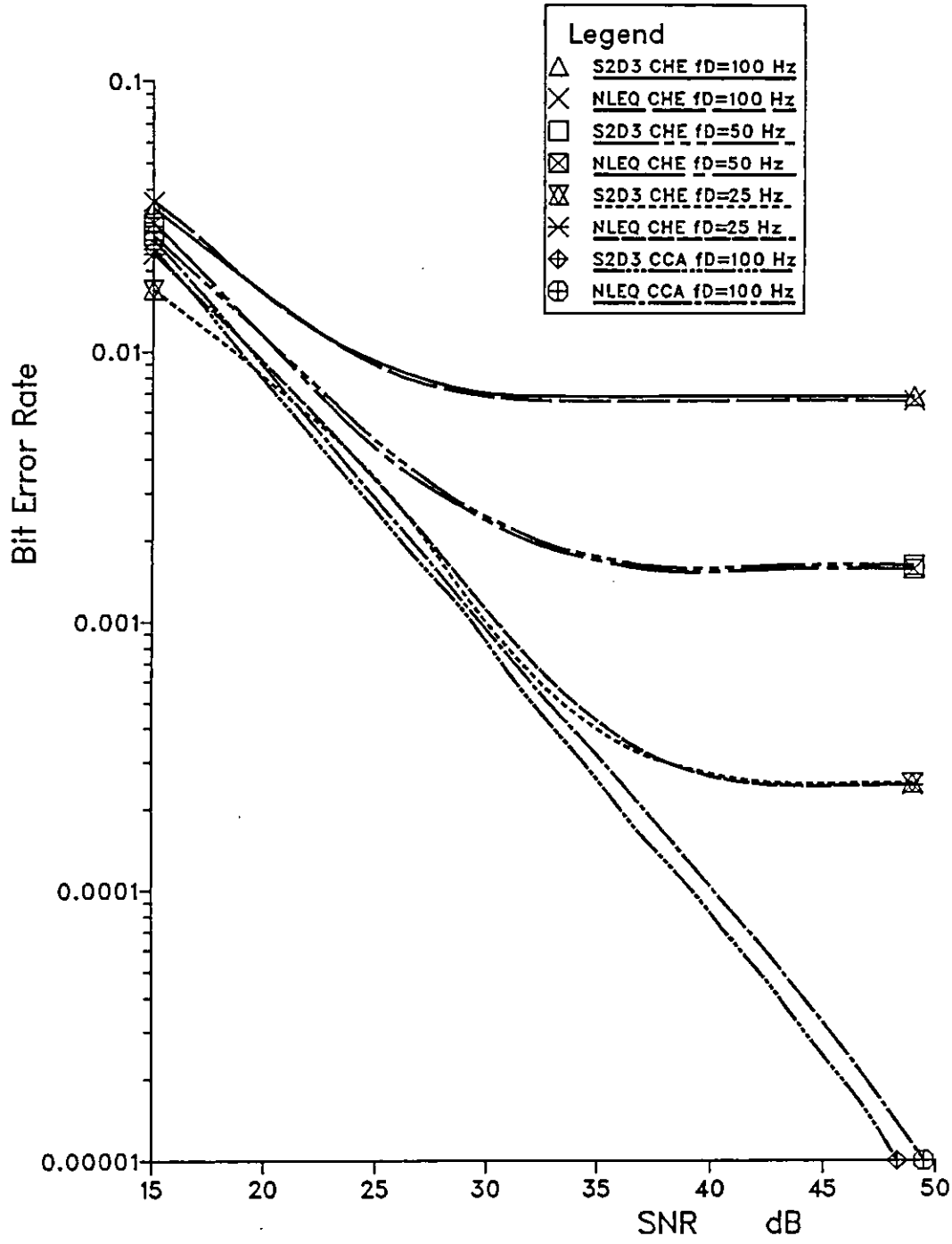

Fig. 8.8 Performances of different systems under different Rayleigh fading rates with use of space diversity by estimating the impulse response of the channel and by assuming linear demodulation; C=r.

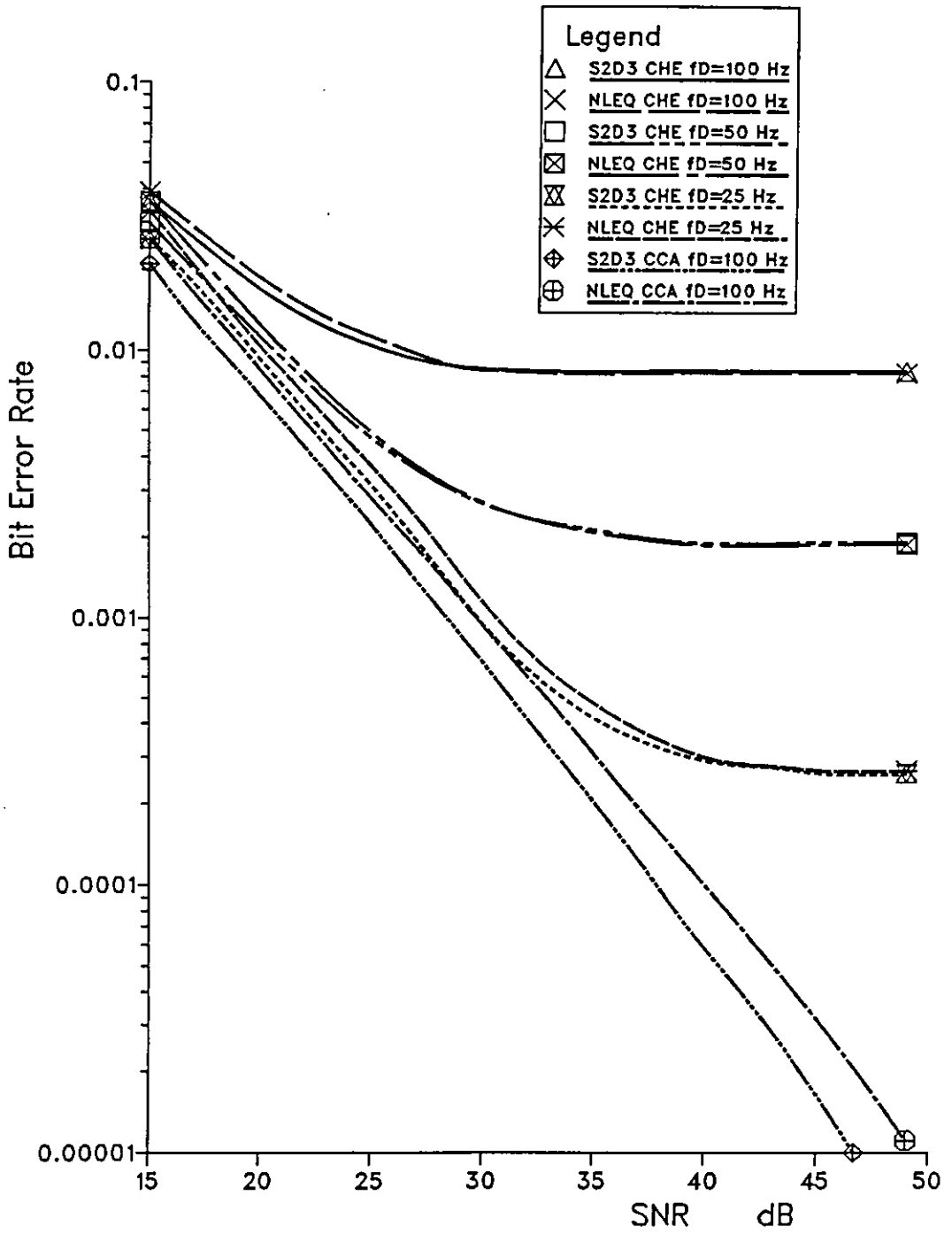

Fig. 8.9 Performances of different systems under different Rayleigh fading rates with use of space diversity by estimating the impulse response of the channel and by assuming linear demodulation; C=rc.

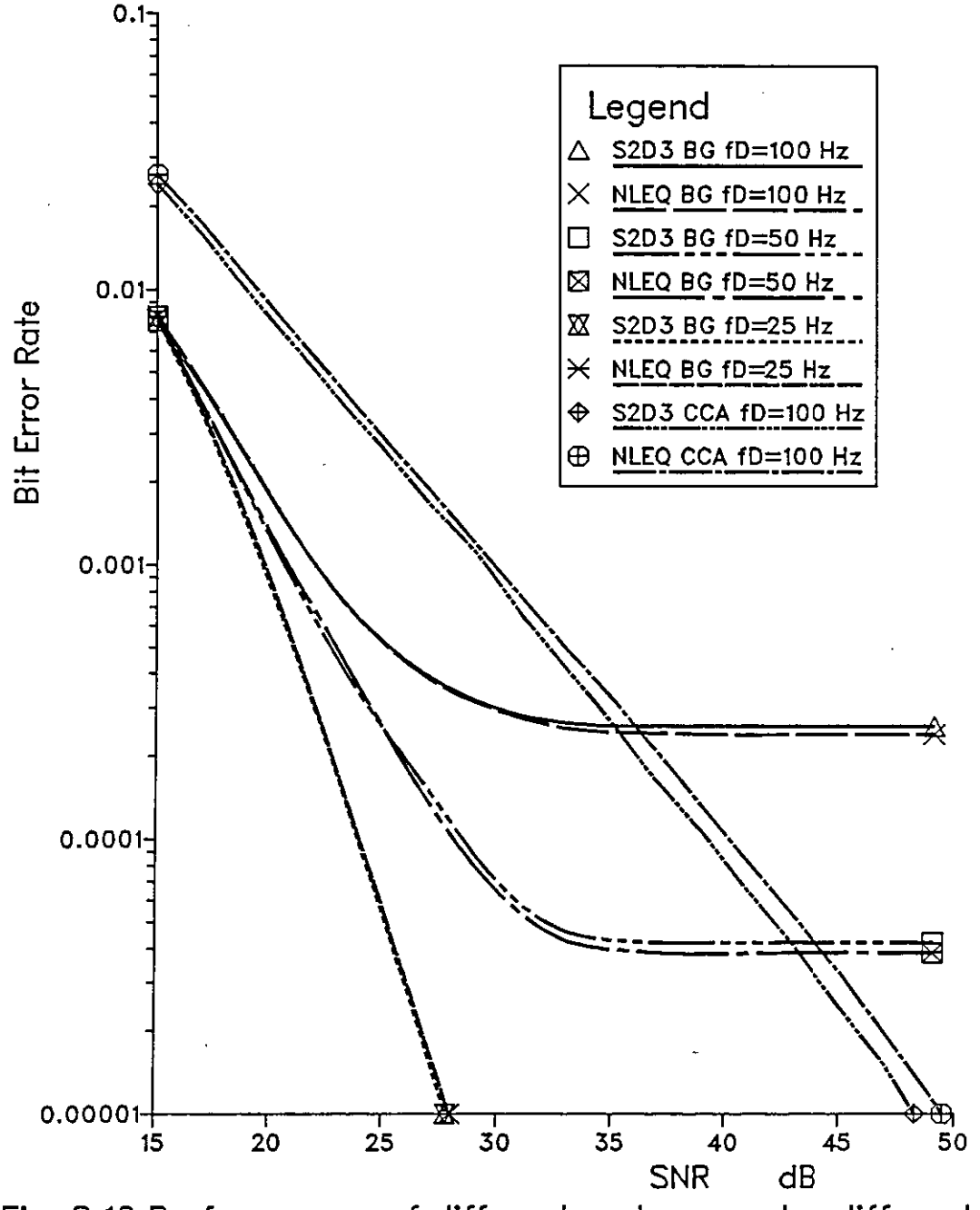

Fig. 8.10 Performances of different systems under different Rayleigh fading rates with use of space diversity by estimating the impulse response of the channel and correcting the phase of the received signals; C=r.

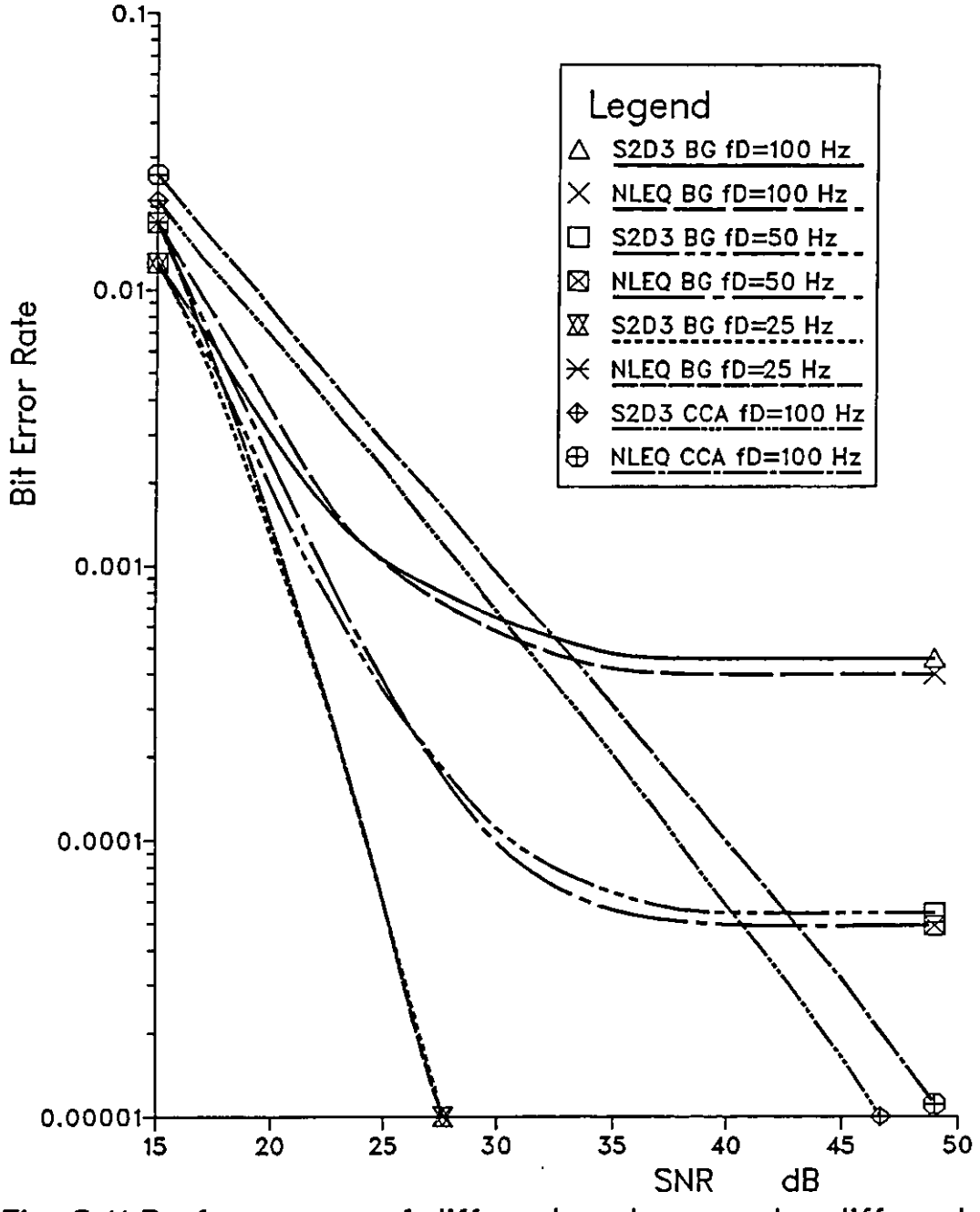

Fig. 8.11 Performances of different systems under different Rayleigh fading rates with use of space diversity by estimating the impulse response of the channel and correcting the phase of the received signals; C=rc.

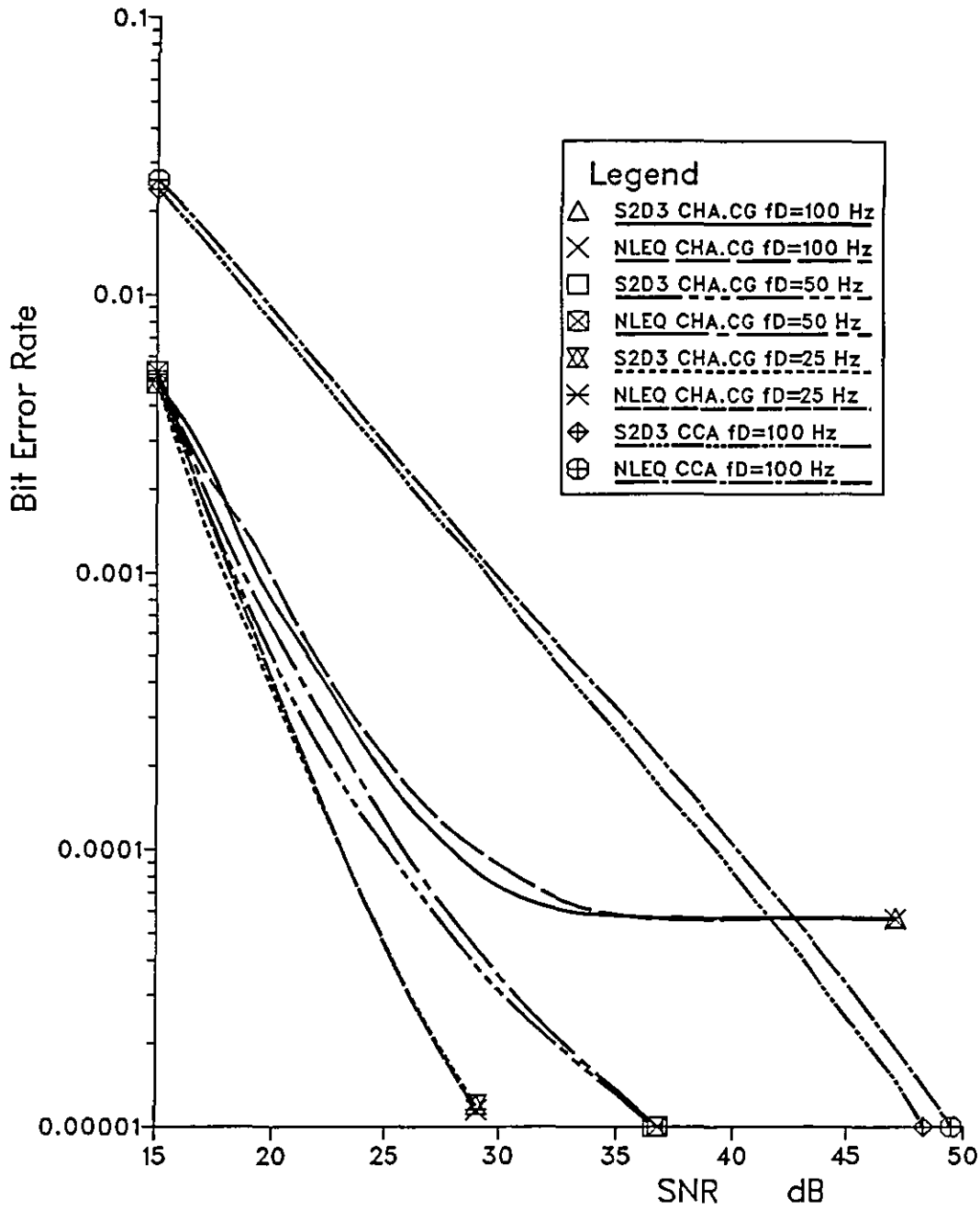

Fig. 8.12 Performances of different systems under different Rayleigh fading rates with use of space diversity by correcting only the phase and assuming correct channel impulse response when C=r.

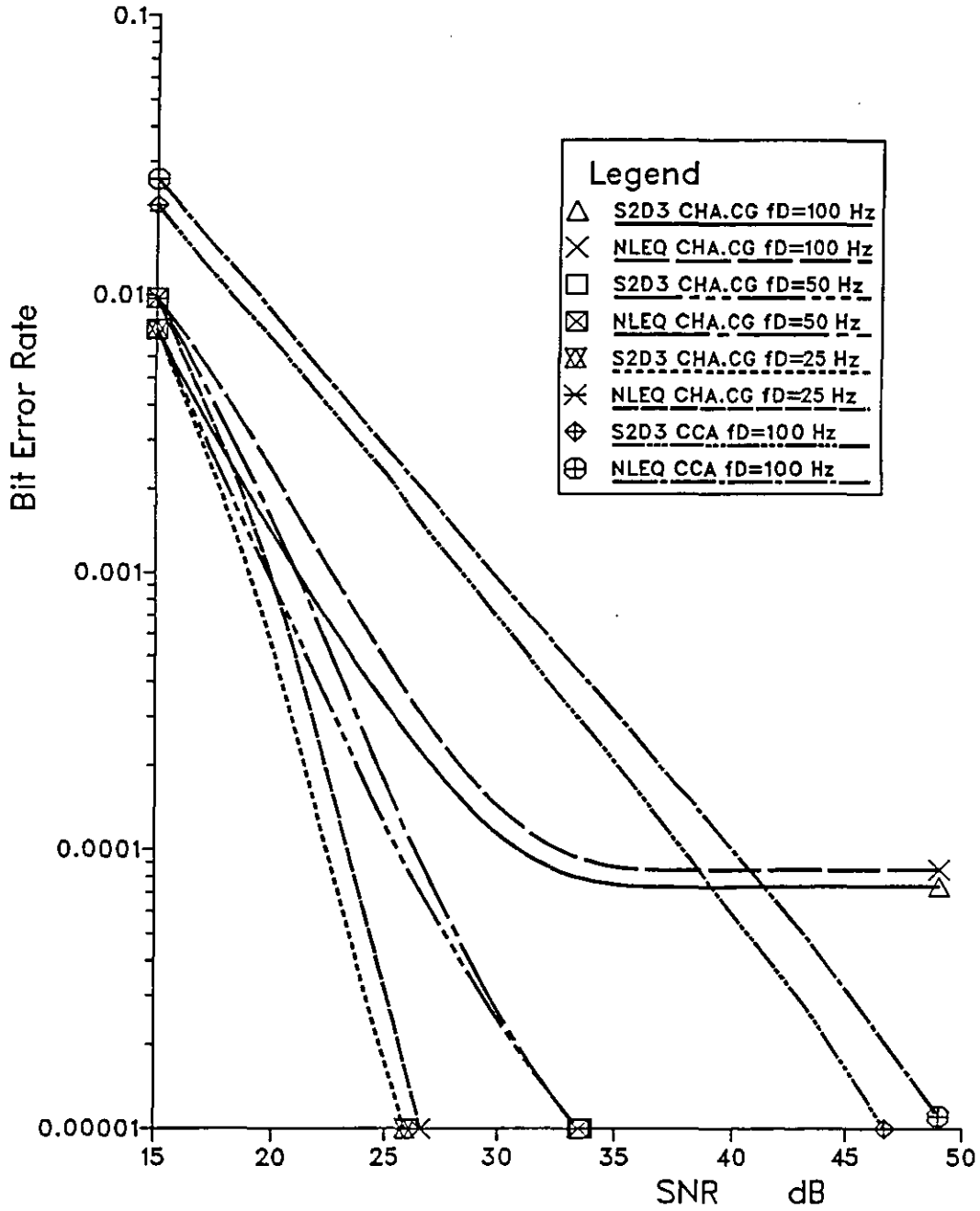

Fig. 8.13 Performances of different systems under different Rayleigh fading rates with use of space diversity by correcting only the phase and assuming correct channel impulse response when C=rc.

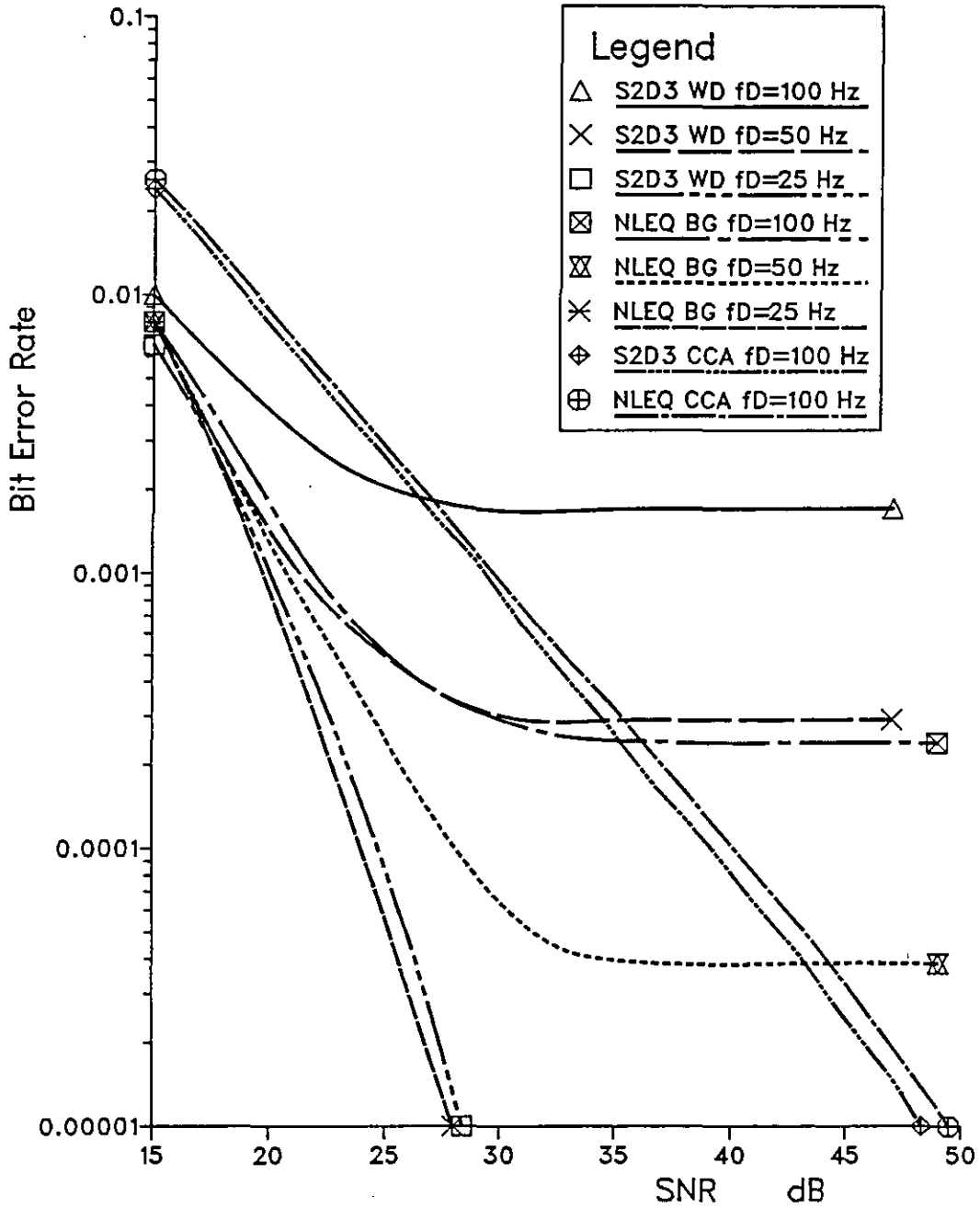

Fig. 8.14 Effect of the delay on the performance of S2D3 under Rayleigh fading conditions when the impulse response of the channel is estimated before nT sec. with prediction, and comparing it with the performance of NLEQ; C=r.

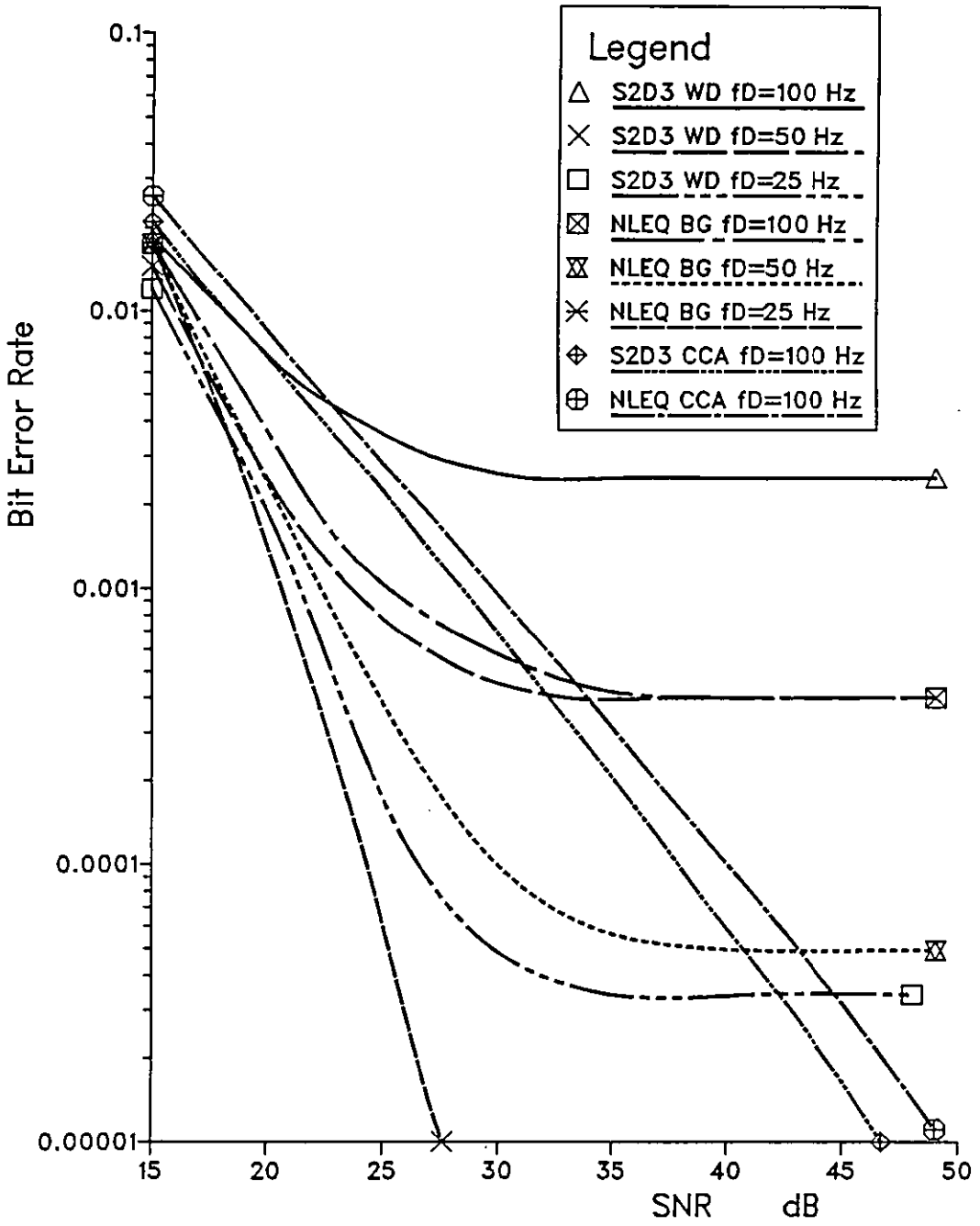

Fig. 8.15 Effect of the delay on the performance of S2D3 under Rayleigh fading conditions when the impulse response of the channel is estimated before nT sec. with prediction, and comparing it with the performance of NLEQ; C=rc.

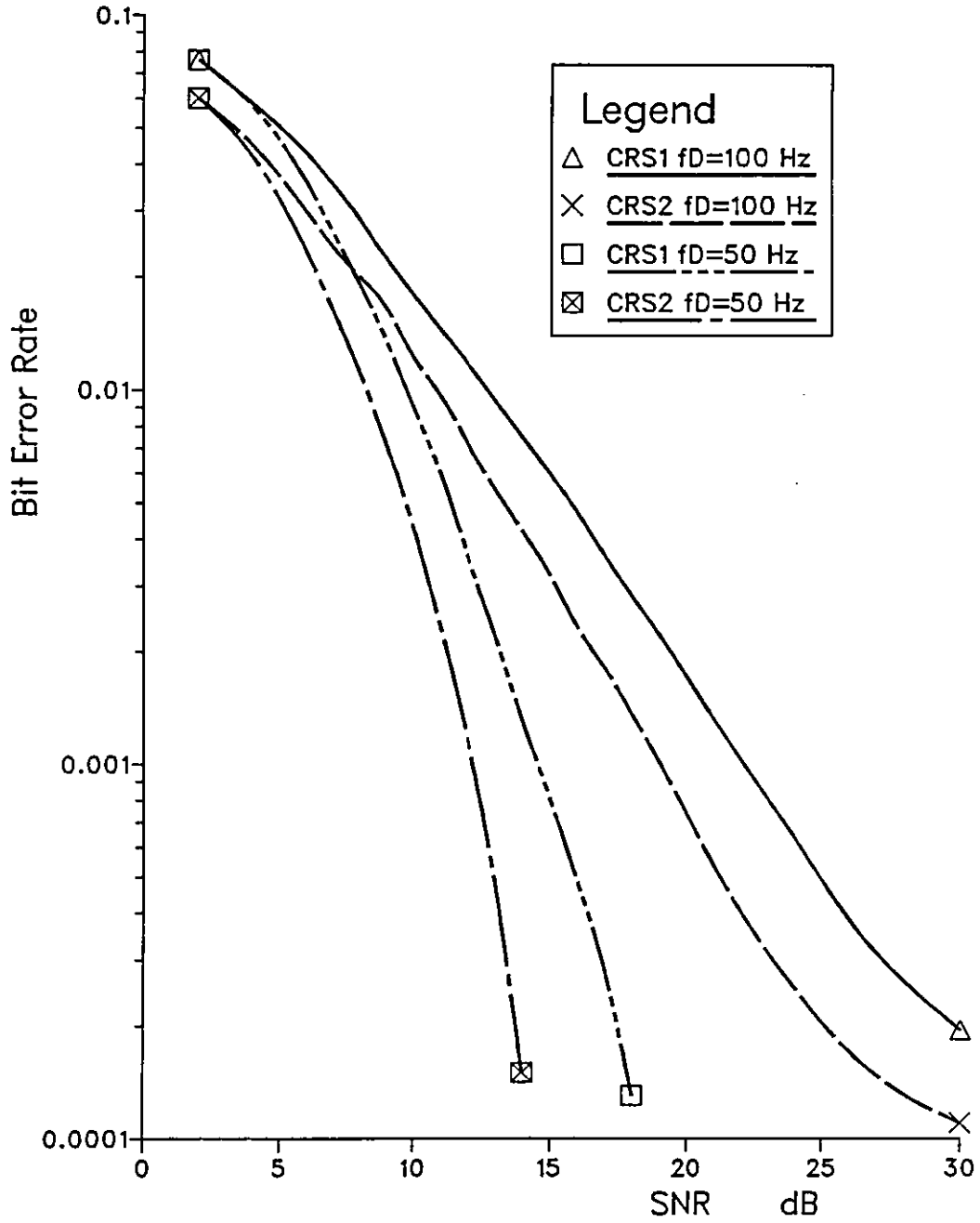

Fig. 8.16 Comparison between performances of receivers employing CRS1 and CRS2 under Rayleigh fading conditions.

9. CONCLUSIONS AND RECOMMENDATIONS

9.1 Conclusions

Since the given channels are not severely dispersive, the improvement when using near-maximum likelihood detection, compared with the corresponding nonlinear equaliser under the same conditions, is not very large. The Rayleigh fading and noisy conditions have been found to degrade the performance of the used detectors, by some 20 dB, in comparison with nonfading conditions. Also, under Rayleigh fading conditions, differential coding degrades the detectors by 4 dB. However, the effect of the fade can be reduced by the application of space diversity, since the chance of having two deep fades from two uncorrelated (or with small correlation coefficient) signals is rare. It is possible to obtain about 10 dB or more tolerance to additive noise in a mobile radio environment depending on the fading rate, by the application of space diversity with co-phased combining techniques, since the given detectors deteriorate with rapidly varying phase of the channel impulse response. Therefore, it is recommended to remove any phase shift or frequency offset caused by the transmission path from the received signal and subsequently from the impulse response of the channel. Only near-maximum likelihood detectors are recommended to be used with 16-level QAM signals under Rayleigh fading conditions.

The narrow bandwidth and a good tracking performance are incompatible in the first order digital phase locked loop (DPLL). However, it is

possible to achieve a narrow bandwidth and good tracking performance with the use of second or third DPLL's. A new method has been developed to design second or third order DPLL by using some of the rules employed in designing a feedback digital control system. This method offers an opportunity to use any digital filter as a loop filter, while the available DPLL techniques in the literature are restricted to only one type of filter. All the DPLL's designed by this method show good tracking performance in mobile radio environment, where the received signal has a rapidly varying envelope and phase. The data aided digital phase locked loop (DA-DPLL) performs reasonably well with the Rayleigh fading channel, but its disadvantage is the inability to sustain the same performance when erroneous sequences are received. A further disadvantage of DA-DPLL is its severe deterioriation with delay, when used with a near-maximum likelihood detector.

The modified feedback channel estimator (MFBCE) has shown surprisingly much better performance over the feedforward channel estimator (FFCE), since the former can subtract the intersymbol interference error signal components and does not require a delay. The selection of convergence constant (b) and the prediction weighting factor (θ) at high fading rate has led to a high jittering at low fading rate. As a result, b and θ must not be constant. Both estimators, FFCE and MFBCE are highly sensitive to delay under Rayleigh fading conditions. Also, both estimators converge quickly, since their convergence constants (b) are relatively large. Furthermore, the larger the value of b the more susceptible the

estimator will be to the noise. At lower fading rates, both estimators are more tolerant to noise which indicates that both, FFCE and MFBCE have very narrow bandwidths. It has been found mathematically necessary to multiply by the reciprocal of the data symbol value in order to achieve a better estimate of the sampled impulse response of the channel, when the FFCE is used with a multilevel QAM signal, with high order level such as 16-level or more.

As mentioned above, the channel estimator has a very narrow bandwidth and hence the discrepancy caused by the phase fluctuation of the channel impulse response degrades not only the estimator itself but the corresponding detector too. The degradations, in the performance of the DA-DPLL and the used estimators due to the delay, affect the performance of the near-maximum likelihood detector even with a less dispersive channel. Therefore, it is possible to accept less improvement from the near-maximum likelihood detector by generating the phase correction and estimating the channel impulse response without delay. Moreover, at relatively low signal-to-noise ratio the near-maximum likelihood detector gives better tolerance than the nonlinear equaliser but they have the same tolerance at high signal-to-noise ratio. The raised-cosine shaped channel has a little wider bandwidth and hence more noise can pass to the detector, estimator or DPLL.

Throughout the investigation of carrier recovery systems (CRS1 and CRS2) with the use of squaring/filtering/frequency dividing by 2 methods are applied to a binary PSK signal; differential coding and space diversity techniques are found essential to regenerate the received signal carrier under Rayleigh fading conditions. Consequently, their tests indicate

that both CRS1 and CRS2 are capable of tracking and regenerating the received signal carrier, of course with the provision of the phase correction logic (described in Chapter 8). Moreover, the receiver employing the CRS2 gives 3.5 dB better performance over the receiver employing the CRS1 under Rayleigh fading conditions, since in the former, the demodulation takes place using a constant and stable frequency from a local oscillator.

9.2 Recommendations for Further Investigations

Throughout this work less dispersive channels are assumed. These channels are derived from ideal lowpass filters by using Fourier design methods. It is necessary, however, to carry out a work similar to that described in Chapter 4 with the use of a practical channel obtained from equipment used for an identical purpose and the same range of frequencies.

The digital phase locked loop described in Chapter 5 has been designed on the assumption of unity overall loop gain. But it is necessary to investigate other values of the loop gain in order to determine to what degree the relevant system might give better tolerance to additive white Gaussian noise in a mobile radio environment.

The data aided digital phase locked loop deteriorates severely with delay, where a simple prediction method has been used. Probably, a better performance might be obtained with the use of much better prediction methods (such as least-square fading-memory, see Chapter 6). However, the insertion of a predictor might have an adverse effect on the system stability. Hence such a matter requires further study.

The modified feedback channel estimator (MFBCE) has been designed with insertion of a feedback digital control system and tested in a mobile radio environment. It is necessary to investigate the performance of this estimator in a high frequency (HF) radio link, with and without the insertion of the feedback digital control system.

A high jittering obtained at low fading rates, since both the FFCE (feedforward channel estimator) and the MFBCE are designed at high possible fading rate by choosing the values of the convergence constant (b) and the prediction weighting factor (θ). It is necessary to investigate that either one or both of b and θ must vary in a sense such as to optimise the corresponding system.

Also, it is necessary to investigate the performance of both the FFCE and MFBCE when any frequency offset and phase shift are removed completely from the received signal by adaptive phase correction methods or by other means.

The receiver, in which space diversity is used, employs 4-level PSK signal only. Therefore, it is necessary to test 8-level PSK or 16-level QAM in an identical receiver.

Appendices

APPENDIX A

SIGNAL ANALYSIS

A.1 Fourier Transform

Fourier transform is the interpretation of signal (or communication system) transfer function. Let f(t) be a periodic function then its Fourier transform is given by

$$F(w) = \int_{-\infty}^{\infty} f(t)\, e^{-jwt}\, dt \qquad A.1$$

Also f(t) is said to be the inverse Fourier transform that may be given by

$$f(t) = \int_{-\infty}^{\infty} \frac{1}{2\pi} F(w) e^{jwt}\, dw \qquad A.2$$

This is called a Fourier transform pair which may be represented by

$$f(t) \leftrightarrow F(w) \qquad A.3$$

This transformation is proved elsewhere[1-8,99,101-107, 109,111]. Table A.1 shows some properties of Fourier transform. However, it is necessary to explain briefly the modulation and frequency shift theorems used in Chapters 2 and 3.

If f(t) is used to modulate $\cos(w_o t)$, then

$$f(t)\cos(w_o t) \leftrightarrow \frac{1}{2}\,[F(w - w_o) + F(w + w_o)] \qquad A.4$$

is the modulated signal Fourier transform pair as given by Equation 2.3 (see also Figures 2.1 and 2.2). In order to shift f(t) somewhere in the frequency domain it has to be multiplied by a shifting signal $e^{jw_o t}$, hence

$$f(t)e^{jw_o t} \leftrightarrow F(w - w_o) \qquad A.5$$

is applied to in Chapter 3 (see Equation 3.4a, 3.4b, 3.8, 3.14,3.17).

A.2 s-z-Transforms

Laplace transform (s-transform) is important in network theory not only because it simplified the solution of the network equations, but mainly because it leads to the concept of the system function. The basic properties of Laplace transform can be found elsewhere[2-7,24,102-107 111,166-170]. For a given function f(t) the Laplace transform is

$$F(s) = \int_o^\infty f(t)e^{-st}\,dt \qquad A.6$$

The notation

$$f(t) \leftrightarrow F(s) \qquad A.7$$

means the Laplace transform pair.

The Laplace transform is used to represent an analogue signal (system). While the digital signal can be represented by z-transform[102-107,109 111,167-169]. The function f(t) has predetermine values, at the sampling instant t = iT, f(i), then

$$F(z) = \sum_{i=0}^{\infty} f(i)\, z^{-i} \qquad A.8$$

Also the notation

$$F(z) \leftrightarrow f(i) \qquad A.9$$

means z-transform pair. Table A.2 shows some of the relationships between f(t), F(s) and F(z). The properties of z-transform can be found elsewhere[102-107,109,111,167-169].

$F(w) = \int_{\infty}^{\infty} f(t)e^{-jwt}dt$		$f(t) = \frac{1}{2\pi}\int_{-\infty}^{\infty} F(w)e^{jwt}\,dw$
$F(t)$	$\leftrightarrow$	$F(w)$
$f^*(-t)$	$\leftrightarrow$	$F^*(w)$
$f(t)\cos(w_o t)$	$\leftrightarrow$	$\frac{1}{2}F(w-w_o) + \frac{1}{2}F(w-w_o)$
$f(t)e^{jw_o}$	$\leftrightarrow$	$F(w-w_o)$
$\int_{-\infty}^{\infty} f_1(x)f_2(t-x)dx$	$\leftrightarrow$	$F_1(w)F_2(w)$
$f_1(t)f_2(t)$	$\leftrightarrow$	$\frac{1}{2\pi}\int_{-\infty}^{\infty} F_1(y)\,F_2(w-y)dy$
$f(t) = \begin{cases} 1 & -B \leq f \leq B \\ 0 & \text{elsewhere} \end{cases}$	$\leftrightarrow$	$2\frac{\sin Bw}{w}$

Table A.1 Some useful properties of Fourier transform

Time Function $f(t) > 0$	Laplace Transform $F(s)$	z-Transform
$u_s(t)$	$\frac{1}{s}$	$\frac{z}{z - 1}$
t	$\frac{1}{s^2}$	$\frac{T_s}{(z - 1)^2}$
e^{-at}	$\frac{1}{s + a}$	$\frac{z}{z - e^{-aT}}$
$\frac{1}{(b - a)}(a^{-at} - e^{bt})$	$\frac{1}{(s + A)(s + b)}$	$\frac{1}{(b - a)}\left[\frac{z}{z - e^{-aT}} - \frac{z}{z - e^{-bT}}\right]$
te^{-at}	$\frac{1}{(s + a)^2}$	$\frac{Tze^{-aT}}{(z - e^{-aT})^2}$
$\sin wt$	$\frac{w}{s^2 + w^2}$	$\frac{z \sin wT}{z^2 - 2z \cos wT + 1}$
$\cos wt$	$\frac{s}{s^2 + w^2}$	$\frac{z(z \cos wT)}{z^2 - 2z \cos wT + 1}$

Table A.2 Useful Laplace and z-transformations

APPENDIX B

DIGITAL FILTER DESIGN

This appendix deals with design of Recursive and Non-recursive filters used throughout this work.

B.1 Recursive digital filter

The output of a recursive digital filter depends on the current input and previous inputs and outputs. Different design methods can be applied to one of the approxmation techniques[102-107,111]. Four filters, first and second Butterworth lowpass filters, second Chebyshev low pass filter, and fifth order Bessel lowpass filter, are designed here. The first three filters are used to design digital phase locked loop (DPLL) (Appendix H, Chapter 5), while the last is used in the Rayleigh fading simulator (Chapter 3).

B.1.1 Butterworth lowpass digital filter

The first and second order analogue (prototype) Butterworth lowpass filters tansfer functions are given by[102-107,111]

$$G_1(s) = \frac{w}{s + w} \qquad \text{B.1}$$

$$G_1(s) = \frac{w^2}{s^2 + \sqrt{2}\, ws + w^2} \qquad \text{B.2}$$

To realise these filters digitally, for computer simulation use, they have to be transformed to z-plane by using the appropriate z-transform methods. Bilinear z-transform is selected to be used with these two filters by substituting

$$s = \frac{2}{T} \left[\frac{z - 1}{z + 1}\right] \qquad \text{B.3}$$

in Equations B.1 and B.2[102-107], where

$$T = \frac{1}{9600} = 0.10416 \quad \text{ms} \qquad \text{B.4}$$

The required filters must be designed so as to accommodate the maximum possible frequency shift of the received signal carrier that may be caused by the transmission path in mobile radio communication. Hence, the expected maximum Doppler frequency shift is 100 Hz when the vehicle carrying the mobile unit is moving with a speed of 75 mph. Thus

$$w = 2\pi f_D = 200\pi = 628.3185 \quad \text{rad./sec.} \qquad \text{B.5}$$

Also, by substituting the values of T and w into the resulting equations of Equations B.1 to B.3, then the general form can be written as (Equation H.8)

$$D_k(z) = \frac{\alpha_o + \alpha_1^{-1} + \alpha_2^{-2}}{1 + \beta_1 z^{-1} \beta_2 z^{-2}} \qquad \text{B.6}$$

The values of α_o, α_1, β_2, β_1 and β_2 are given in Table H.1, when $k = 1,2$.

B.1.2 Chebyshev lowpass digital filter

It is necessary to compare a DPLL with other types of filter such as the Chenyshev lowpass filter. The details of the design of a Chebyshev lowpass filter can be seen elsewhere[102-107,111], here only a brief description is introduced. Let the maximum allowable ripple amplitude α = 0.05 dB, therefore the passband ripple = α + 1 = 1.05 dB. Then

$$1.05 = 10 \log_{10} (1 + \varepsilon^2)$$

and hence

$$\varepsilon = 0.523 \qquad \text{B.7}$$

From the following formula[102-107] the order of (n) of the required filter can be obtained by assuming stopband attenuation of -25 dB

$$25 = 20 \log_{10} \varepsilon + 6(n-1) + 20n \log_{10} w_c$$

where $w_c = 2\pi f_c$ and f_c is the normalised cutoff frequency. Then, by assuming f_c = 1.1 Hz,

$$n = 1.37$$

and hnece

$$n \cong 2 \qquad \text{B.8}$$

Now, the stopband attenuation, $-x_{sp}$, can be calculated as

$$x_{sp} = 20 \log_{10}(0.523) + 6(2-1) + 40 \log_{10} (2.2\pi)$$

$$= 33.953 \text{ dB}$$

Having obtained the values of ε and n the second order Chebyshev can be approximated, by using Equation B.2 according to the procedure described elsewhere[102-107], as

$$G_3(s) = \frac{100.267}{s + 53.8 + j88.85} + \frac{100.267}{s + 53.8 - j88.85} \qquad B.9$$

By using impulse-invariant design method[102-107,111] and according to Table A.2 with use of Equations B.4 and B.5, the transfer function of this filter can be obtained in z-transform as in Equation B.6 and the corresponding coefficient are listed in Table H.1, when $k = 3$.

B.1.3 Bessel lowpass digital filter

In order to avoid unnecessary duplication, the modified values of 5th order lowpass analogue Bessel filter poles are given by Equation 3.58. Since the maximum expected Doppler shift is 100 Hz then it is possible to choose sampling frequency f=250 sample/sec. so as to avoid aliasing errors. From Table A.2 the z-transform of the first pole Equation 3.58a $p_1' = -555.7$ is given by

$$H'_{p_1}(z) = \frac{0.7675z}{z-0.2325} \qquad B.10$$

while for Equation 3.58b is given by

$$H'_{p_{2,3}}(z) = \frac{0.835(z - 0.2)}{z^2 - 0.4z + 0.068} \qquad B.11$$

and that for Equation 3.58.c is given by

$$H'_{p_{4,5}}(z) = \frac{1.1033(z - 0.059)}{z^2 - 0.118z + 0.395} \qquad B.12$$

Then the overall filter transfer function can be given by

$$H_5(z) = H'_{p_1}(z) + H'_{p_{2,3}}(z) + H'_{p_{4,5}}(z) \qquad B.13$$

$$= \frac{0.959 - 0.574z^{-1} + 0.362z^{-2} - 0.1054z^{-3} - 0.0131z^{-4}}{1-0.7502z^{-1} + 0.6302z^{-2} - 0.2844z^{-3} + 0.0654z^{-4} - 6.24\times10^{-3}z^{-5}} \qquad B.13$$

This transfer function can be written in general form like Equation 3.59. Moreover, this filter can also be realised as

$$H_5(z) = H_{B5}(z)\, H_{A5}(z) \qquad B.14$$

where

$$H_{B5}(z) = \frac{1}{1+b_1z^{-1} + b_2z^{-2} + b_3z^{-3} + b_4z^{-4} + b_5z^{-5}} \qquad B.15$$

$$H_{A5}(z) = a_o + a_1 z^{-1} + a_2 z^{-2} + a_3 z^{-3} + a_4 z^{-4} \qquad B.16$$

and the values of a_ℓ, $b_{\ell+1}$, for $\ell = 0$ to 4, are listed in Table 3.1. The two parts of the filter can be represented in series as shown in Figure 3.9.

B.2 Nonrecursive Digital Filter

Two filters designated as F1 and F2 used in the receivers employing carrier recovery systems (CRS1 and CRS2) that are described in Chapters 5 and 8. Both filters are designed by using Fourier design method[102-107], since the frequency response of a nonrecursive filter is a periodic function of w with periods w_s, it can be represented as a Fourier series, $w_s = \frac{2\pi}{NT}$, N is integer and T is the sampling period. The discrete Fourier transform (DFT) of the filter impulse response is given by

$$H_m = \sum_{n=o}^{N-1} h_n \, e^{-j2\pi mn/N} \qquad \text{for } m=0,1,\ldots,N-1 \qquad \text{B.16}$$

where H_m and h_n are complex-valued. Also, h_n can be determined by the application of the inverse discrete Fourier transform (IDFT) such as (see also Equations A.1 and A.2)

$$h_n = \frac{1}{N} \sum_{m=0}^{N-1} H_m \, e^{j2\pi nm/N} \qquad \text{for } n=0,1,\ldots,N-1 \qquad \text{B.17}$$

If H_m for m=0,1,...,N-1 are known then $\{h_n\}$ can be obtained. The next step in the design process involves the modification of impulse response of $\{h_n\}$ by multiplying it with a suitable window function such as a Hamming window function that is given by[102-107]

$$W_i = 0.54 + 0.46 \cos(\pi i/I) \qquad \text{for } i=0,1,\ldots,I-1 \qquad \text{B.18}$$

The impulse response of the used nonfading channels Equation 3.77 have been designed by this method according to the information given in Chapter 3.

However, the transfer function of the required filter can be now given by

$$H(z) = z^{-(I-1)}\left[h_0 W_0 + \sum_{i=1}^{I-1} W_i (h_{-i}\, z^{i} + h_i z^{-i})\right] \qquad \text{B.19}$$

where $h_{-i} = h_i$, for i=1,2,...,I-1.

B.2.1 Filter F1

The assumed data rate is 9.6 kbits/sec. and the carrier frequency f_c = 19.2 k Hz. Also, the assumed sampling frequency is $f_s = 16\ f_c$. If the frequency spectrum is divided (sampled) to 32 parts from 0 to f_s then N = 32. Hence the values of H_m, for m=0,1,...,N-1, can be given as follows:-

$$H_m = \begin{cases} 1 & m = 4,28 \\ 0 & \text{elsewhere} \end{cases} \qquad \text{B.20}$$

Now h_n can be calculated from Equation B.17. The number of taps of this filter has been chosen as 43 the I = (43-1)/2=22. Having obtained the values of I and $\{h_n\}$,H(z) can be calculated from Equation B.18 and B.19. The taps (coefficients) of this filter are given in Table B.1a. The roots of this filter are also listed in Table B.1b. Any root which lies outside the unit circle of the z-plane is replaced by a reciprocal of its complex conjugate. An available program calculates the roots of a given filter, looks for roots, that lie outside the unit circle of the z-plane, and replaces them by the reciprocal of their complex conjugate, Tables B.1a, B.1b, and B.1c.

B.2.2 Filter F_2

This filter has the same specifications of filter F_1 except its centre frequency is twice that of filter F_1 or 2x19.2 kHz = 38.4 kHz. Hence, the values of H_m, for m=0,1,...,N-1, are given by

$$H_m = \begin{cases} 1 & m = 8,24 \\ 0 & \text{elsewhere} \end{cases} \qquad \text{B.21}$$

and consequently $\{h_n\}$ can be calculated according to Equation B.17. H(z) for filter F_1 can also be obtained from Equation B.19 when I=22. Tables B.2a, B.2b and B.2c show the coefficients of this filter before and after modification and its roots.

Filter F1 results

Polynomial order 42

Coefficients of polynomial

Real part	Imaginary part
-0.191340E-02	0.000000E+00
0.000000E+00	0.000000E+00
0.240220E-02	0.000000E+00
0.554880E-02	0.000000E+00
0.923480E-02	0.000000E+00
0.126750E-01	0.000000E+00
0.146200E-01	0.000000E+00
0.137000E-01	0.000000E+00
0.889600E-02	0.000000E+00
0.000000E+00	0.000000E+00
-0.120930E-01	0.000000E+00
-0.253840E-01	0.000000E+00
-0.370910E-01	0.000000E+00
-0.442540E-01	0.000000E+00
-0.444620E-01	0.000000E+00
-0.365400E-01	0.000000E+00
-0.209810E-01	0.000000E+00
0.000000E+00	0.000000E+00
0.228280E-01	0.000000E+00
0.432910E-01	0.000000E+00
0.574460E-01	0.000000E+00
0.625000E-01	0.000000E+00
0.574460E-01	0.000000E+00
0.432910E-01	0.000000E+00
0.228280E-01	0.000000E+00
0.000000E+00	0.000000E+00
-0.209810E-01	0.000000E+00
-0.365400E-01	0.000000E+00
-0.444620E-01	0.000000E+00
-0.442540E-01	0.000000E+00
-0.370910E-01	0.000000E+00
-0.253840E-01	0.000000E+00
-0.120930E-01	0.000000E+00
0.000000E+00	0.000000E+00
0.889600E-02	0.000000E+00
0.137000E-01	0.000000E+00
0.146200E-01	0.000000E+00
0.126750E-01	0.000000E+00
0.923480E-02	0.000000E+00
0.554880E-02	0.000000E+00
0.240220E-02	0.000000E+00
0.000000E+00	0.000000E+00
-0.191340E-02	0.000000E+00

Table B.1a

Roots of polynomial

Real part	Imaginary part	Modulus
0.650486E+00	-0.759518E+00	0.100000E+01
0.650486E+00	0.759518E+00	0.100000E+01
-0.997294E+00	-0.735206E-01	0.100000E+01
-0.997294E+00	0.735206E-01	0.100000E+01
0.971495E+00	0.000000E+00	0.971495E+00
-0.313168E+00	0.949698E+00	0.100000E+01
-0.313168E+00	-0.949698E+00	0.100000E+01
0.459379E+00	0.000000E+00	0.459379E+00
-0.689580E+00	0.724210E+00	0.100000E+01
-0.689580E+00	-0.724210E+00	0.100000E+01
0.124459E+00	0.992225E+00	0.100000E+01
0.408370E+00	-0.912816E+00	0.100000E+01
-0.870146E+00	0.492795E+00	0.100000E+01
-0.870146E+00	-0.492795E+00	0.100000E+01
0.408370E+00	0.912816E+00	0.100000E+01
0.124459E+00	-0.992225E+00	0.100000E+01
-0.170033E+00	0.985438E+00	0.100000E+01
0.537795E+00	-0.843076E+00	0.100000E+01
-0.449400E+00	-0.893331E+00	0.100000E+01
0.708461E+00	0.705750E+00	0.100000E+01
-0.975724E+00	0.219003E+00	0.100000E+01
0.995051E+00	-0.993645E-01	0.100000E+01
-0.449400E+00	0.893331E+00	0.100000E+01
-0.170033E+00	-0.985438E+00	0.100000E+01
0.102934E+01	0.000000E+00	0.102934E+01
-0.975724E+00	-0.219003E+00	0.100000E+01
0.269401E+00	0.963028E+00	0.100000E+01
0.269401E+00	-0.963028E+00	0.100000E+01
-0.788450E+00	0.615098E+00	0.100000E+01
0.773141E+00	-0.634234E+00	0.100000E+01
0.537795E+00	0.843076E+00	0.100000E+01
-0.788450E+00	-0.615098E+00	0.100000E+01
-0.575761E+00	0.817618E+00	0.100000E+01
0.708461E+00	-0.705750E+00	0.100000E+01
-0.575761E+00	-0.817618E+00	0.100000E+01
0.773141E+00	0.634234E+00	0.100000E+01
-0.933029E+00	0.359800E+00	0.100000E+01
0.995051E+00	0.993645E-01	0.100000E+01
-0.933029E+00	-0.359800E+00	0.100000E+01
-0.231134E-01	0.999733E+00	0.100000E+01
-0.231134E-01	-0.999733E+00	0.100000E+01
0.217685E+01	0.000000E+00	0.217685E+01

Table B.1b

The polynomial after modification

Real part	Imaginary part
0.687460E-01	0.000000E+00
0.122046E+00	0.000000E+00
0.181635E+00	0.000000E+00
0.233021E+00	0.000000E+00
0.255064E+00	0.000000E+00
0.226036E+00	0.000000E+00
0.131449E+00	0.000000E+00
-0.288867E-01	0.000000E+00
-0.236893E+00	0.000000E+00
-0.457131E+00	0.000000E+00
-0.642994E+00	0.000000E+00
-0.746939E+00	0.000000E+00
-0.732501E+00	0.000000E+00
-0.584676E+00	0.000000E+00
-0.316131E+00	0.000000E+00
0.331779E-01	0.000000E+00
0.402978E+00	0.000000E+00
0.724961E+00	0.000000E+00
0.937638E+00	0.000000E+00
0.999997E+00	0.000000E+00
0.900769E+00	0.000000E+00
0.660896E+00	0.000000E+00
0.328603E+00	0.000000E+00
-0.315960E-01	0.000000E+00
-0.353339E+00	0.000000E+00
-0.582647E+00	0.000000E+00
-0.688556E+00	0.000000E+00
-0.667879E+00	0.000000E+00
-0.543107E+00	0.000000E+00
-0.354652E+00	0.000000E+00
-0.149649E+00	0.000000E+00
0.296472E-01	0.000000E+00
0.154618E+00	0.000000E+00
0.214627E+00	0.000000E+00
0.215961E+00	0.000000E+00
0.176609E+00	0.000000E+00
0.118722E+00	0.000000E+00
0.614522E-01	0.000000E+00
0.164015E-01	0.000000E+00
-0.129527E-01	0.000000E+00
-0.274017E-01	0.000000E+00
-0.243079E-01	0.000000E+00
0.136921E-01	0.000000E+00

Table B.1c

Table B.1 Coefficients, roots and coefficients after modification for Filter F1

Filter F2 results

Polynomial order 42

Coefficients of polynomial

Real part	Imaginary part
-0.353550E-02	0.000000E+00
-0.532110E-02	0.000000E+00
-0.443870E-02	0.000000E+00
0.000000E+00	0.000000E+00
0.706800E-02	0.000000E+00
0.126750E-01	0.000000E+00
0.111900E-01	0.000000E+00
0.000000E+00	0.000000E+00
-0.164380E-01	0.000000E+00
-0.273530E-01	0.000000E+00
-0.223460E-01	0.000000E+00
0.000000E+00	0.000000E+00
0.283890E-01	0.000000E+00
0.442540E-01	0.000000E+00
0.340300E-01	0.000000E+00
0.000000E+00	0.000000E+00
-0.387670E-01	0.000000E+00
-0.575040E-01	0.000000E+00
-0.421810E-01	0.000000E+00
0.000000E+00	0.000000E+00
0.439670E-01	0.000000E+00
0.625000E-01	0.000000E+00
0.439670E-01	0.000000E+00
0.000000E+00	0.000000E+00
-0.421810E-01	0.000000E+00
-0.575040E-01	0.000000E+00
-0.387670E-01	0.000000E+00
0.000000E+00	0.000000E+00
0.340300E-01	0.000000E+00
0.442540E-01	0.000000E+00
0.283890E-01	0.000000E+00
0.000000E+00	0.000000E+00
-0.223460E-01	0.000000E+00
-0.273530E-01	0.000000E+00
-0.164380E-01	0.000000E+00
0.000000E+00	0.000000E+00
0.111900E-01	0.000000E+00
0.126750E-01	0.000000E+00
0.706800E-02	0.000000E+00
0.000000E+00	0.000000E+00
-0.443870E-02	0.000000E+00
-0.532110E-02	0.000000E+00
-0.353550E-02	0.000000E+00

Table B.2a

Roots of polynomial

Real part	Imaginary part	Modulus
-0.997435E+00	0.715751E-01	0.100000E+01
-0.997435E+00	-0.715751E-01	0.100000E+01
0.843388E-01	0.996437E+00	0.100000E+01
0.843388E-01	-0.996437E+00	0.100000E+01
0.975600E+00	0.219556E+00	0.100000E+01
0.975600E+00	-0.219556E+00	0.100000E+01
-0.596339E+00	0.802733E+00	0.100000E+01
-0.596339E+00	-0.802733E+00	0.100000E+01
-0.205643E+00	0.978627E+00	0.100000E+01
-0.205643E+00	-0.978627E+00	0.100000E+01
-0.705002E+00	-0.709205E+00	0.100000E+01
-0.705002E+00	0.709205E+00	0.100000E+01
0.997314E+00	-0.732391E-01	0.100000E+01
0.924949E+00	0.380092E+00	0.100000E+01
0.924949E+00	-0.380092E+00	0.100000E+01
-0.936511E+00	0.350638E+00	0.100000E+01
-0.936511E+00	-0.350638E+00	0.100000E+01
0.348653E+00	0.861003E+00	0.928916E+00
0.348653E+00	-0.861003E+00	0.928916E+00
-0.475242E+00	0.879855E+00	0.100000E+01
-0.475242E+00	-0.879855E+00	0.100000E+01
0.925946E+00	0.451789E+00	0.103029E+01
0.925946E+00	-0.451789E+00	0.103029E+01
-0.876843E+00	0.480776E+00	0.100000E+01
-0.876843E+00	-0.480776E+00	0.100000E+01
0.235099E+00	0.971971E+00	0.100000E+01
0.454669E+00	-0.890660E+00	0.100000E+01
0.454669E+00	0.890660E+00	0.100000E+01
-0.621153E-01	-0.998069E+00	0.100000E+01
-0.976994E+00	0.213265E+00	0.100000E+01
0.997314E+00	0.732391E-01	0.100000E+01
0.235099E+00	-0.971971E+00	0.100000E+01
-0.344189E+00	0.938900E+00	0.100000E+01
-0.976994E+00	-0.213265E+00	0.100000E+01
0.872308E+00	0.425618E+00	0.970604E+00
0.404055E+00	-0.997819E+00	0.107652E+01
-0.799141E+00	0.601143E+00	0.100000E+01
-0.621153E-01	0.998069E+00	0.100000E+01
-0.344189E+00	-0.938900E+00	0.100000E+01
0.872308E+00	-0.425618E+00	0.970604E+00
0.404055E+00	0.997819E+00	0.107652E+01
-0.799141E+00	-0.601143E+00	0.100000E+01

Table B.2b

The polynomial after modification

Real part	Imaginary part
0.711349E-01	0.000000E+00
0.122575E+00	0.000000E+00
0.104450E+00	0.000000E+00
-0.124884E-01	0.000000E+00
-0.186795E+00	0.000000E+00
-0.301317E+00	0.000000E+00
-0.232691E+00	0.000000E+00
0.419894E-01	0.000000E+00
0.387532E+00	0.000000E+00
0.568681E+00	0.000000E+00
0.406641E+00	0.000000E+00
-0.697895E-01	0.000000E+00
-0.599407E+00	0.000000E+00
-0.833462E+00	0.000000E+00
-0.569711E+00	0.000000E+00
0.844665E-01	0.000000E+00
0.748151E+00	0.000000E+00
0.999035E+00	0.000000E+00
0.654766E+00	0.000000E+00
-0.913503E-01	0.000000E+00
-0.784028E+00	0.000000E+00
-0.100000E+01	0.000000E+00
-0.622577E+00	0.000000E+00
0.915252E-01	0.000000E+00
0.693874E+00	0.000000E+00
0.840645E+00	0.000000E+00
0.497760E+00	0.000000E+00
-0.727859E-01	0.000000E+00
-0.511871E+00	0.000000E+00
-0.594441E+00	0.000000E+00
-0.341229E+00	0.000000E+00
0.387116E-01	0.000000E+00
0.307796E+00	0.000000E+00
0.344807E+00	0.000000E+00
0.190175E+00	0.000000E+00
-0.157210E-01	0.000000E+00
-0.141907E+00	0.000000E+00
-0.144944E+00	0.000000E+00
-0.701452E-01	0.000000E+00
0.876473E-02	0.000000E+00
0.512439E-01	0.000000E+00
0.604958E-01	0.000000E+00
0.470064E-01	0.000000E+00

Table B.2c

Table B.2 Coefficients, roots and coefficients after modification for Filter F2

APPENDIX C

Used Tables

C.1 Error Function

The cummulative distribution corresponding to Gaussian probability density is given by

$$P(X \leq x) = F(x) = \int_{-\infty}^{x} \frac{e^{x^2/2\sigma^2}}{\sqrt{2\pi\sigma^2}}\, dx \qquad C.1$$

This is directly related to the error function, tabulated values of which are readily available in mathematical tables. The error function of u [erf(u)] is defined as[4]

$$erf(u) = \frac{2}{\sqrt{\pi}} \int_{o}^{u} e^{-u^2}\, du \qquad C.2$$

$$erf(0) = 0 \qquad C.3$$

$$erf(\infty) = 1 \qquad C.4$$

The complementary error function [erfc(u)] is given by

$$erfc(u) = 1 - erf(u)$$

$$= \frac{2}{\sqrt{\pi}} \int_{u}^{\infty} e^{-u^2}\, du \qquad C.5$$

Table C.1 gives the values of erfc(u). It is possible to relate the integral of Equation C.1 to erfc-function as follows[4]

$$F(x) = \frac{1}{2} \operatorname{erfc}\left(\frac{|x|}{\sqrt{2}\sigma}\right) \qquad C.6$$

erfc(u) is referred to as Q(u) in Chapter 2, Equation 2.28 and 2.29.

$$\operatorname{erfc}(x) = Q(x) = \frac{2}{\sqrt{\pi}} \int_x^{\infty} e^{-u^2} \, du$$

x	Q(x)	x	Q(x)
0.0	1.000	2.0	7.21×10^{-3}
0.2	0.777	2.2	1.86×10^{-3}
0.4	0.572	2.4	6.90×10^{-4}
0.6	0.396	2.6	2.40×10^{-4}
0.8	0.258	2.8	7.90×10^{-5}
1.0	0.157	3.0	2.30×10^{-5}
1.2	8.97×10^{-2}	3.3	3.20×10^{-6}
1.4	4.87×10^{-2}	3.7	1.70×10^{-7}
1.6	2.37×10^{-2}	4.0	1.50×10^{-8}
1.8	1.09×10^{-2}	5.0	1.50×10^{-12}

For larger values of x $Q(x) \cong e^{-x^2}/(x\sqrt{\pi})$

Table C.1 Complementary error function

C.2 Gray Code

Gray Code is used throughout this work to generate data symbols in ranking form such that any two adjacent symbols in the rank are different only in one bit, as in Table C.2. The binary code is converted to Gray code as follows

$$g_1 = b_1$$

$$g_k = b_k + b_{k-1} \qquad \text{Modulo-2} \qquad \text{C.7}$$

where Modulo-2 adder is described in Chapter 2 or it is exclusive -OR. The order of the successive bits from most significant (b_1) to the least significant (b_n) is given by

$$b_1\ b_2\ b_3\ \ldots\ b_n$$

For Gray coded bits

$$g_1\ g_2\ g_3\ \ldots\ g_n$$

Conversion from the Gray code to binary code is easily accomplished by reversing Equation C.7, or

$$b_1 = g_1$$

$$b_k = g_k + b_{k-1} \qquad \text{Modulo-2} \qquad \text{C.8}$$

However Gray coding has been carried out directly in generating symbols used in the computer simulation tests.

Decimal	binary code	Gray code
0	0 0 0 0	0 0 0 0
1	0 0 0 1	0 0 0 1
2	0 0 1 0	0 0 1 1
3	0 0 1 1	0 0 1 0
4	0 1 0 0	0 1 1 0
5	0 1 0 1	0 1 1 1
6	0 1 1 0	0 1 0 1
7	0 1 1 1	0 1 0 0
8	1 0 0 0	1 1 0 0
9	1 0 0 1	1 1 0 1
10	1 0 1 0	1 1 1 1
11	1 0 1 1	1 1 1 0
12	1 1 0 0	1 0 1 0
13	1 1 0 1	1 0 1 1
14	1 1 1 0	1 0 0 1
15	1 1 1 1	1 0 0 0

Table C.2 Decimal-Binary-Gray Code Conversion

APPENDIX D NOISE CORRELATION

D.1 Noise Representations

The band limited noise may be represented by (2-9:22.23)

$$n(t) = n_c\cos(\omega_o t) - n_s(t)\sin(\omega_o t) \qquad D.1$$

where $n_c(t)$ and $n_s(t)$ are the inphase and quadrature components of $n(t)$ respectively. Figure D.1 shows this relation. This representation is frequently used with great convenience in dealing with noise confined to a relatively narrow frequency band in the neighbourhood of $f_o\left(=\frac{\omega_o}{2\pi}\right)$. Likewise $n(t)$, $n_c(t)$ and $n_s(t)$ are stationary random processes that are represented in linear superpositions of the spectral components. Moreover, $n_c(t)$ and $n_s(t)$ have a Gaussian distribution function with zero mean value, and they are uncorrelated. The spectrum of the noise, $n(t)$, extends over the range from $f_o - \frac{B}{2}$ to $f_o + \frac{B}{2}$ Hz, while the specctrum of each of $n_c(t)$ and $n_s(t)$ extends over the range from $-\frac{B}{2}$ to $\frac{B}{2}$ Hz and zero elsewhere, where B is the bandwidth. The power spectral density for $n_c(t)$ and $n_s(t)$ are given by (see Appendix A)

$$G_{n_c}(f) = G_{n_s}(f) = G_n(f - f_o) + G_n(f + f_o) \qquad D.2$$

where $G_n(f)$ is the power spectral density of $n(t)$.

Let a white Gaussian noise (which is represented by $n(t)$) be filtered by a rectangular bandpass filter with $H(f) = 1$ that has a bandwidth of B, the power spectral density is given by

$$G_n(f) = \begin{cases} \frac{N_o}{2} & f_o - \frac{B}{2} \leq |f| \leq f_o + \frac{B}{2} \\ 0 & \text{elsewhere} \end{cases} \qquad \text{D.3}$$

Hence the power spectral density of $n_c(t)$ or $n_s(t)$ can be determined as

$$G_{n_c}(f) = G_{n_s}(f) = G_n(f - f_o) + G_n(f + f_o)$$

$$= \frac{N_o}{2} + \frac{N_o}{2}$$

$$= N_o \qquad |f| \leq \frac{B}{2} \qquad \text{D.4}$$

This means the power spectral density of $n_c(t)$ or $n_s(t)$ is twice that of $n(t)$. Consequently, the power (variance) of $n(t)$ is given by

$$\sigma_n^2 = \int_{-\infty}^{\infty} G_n(f)|H(f)|^2 df$$

$$= \int_{-f_o - \frac{B}{2}}^{-f_o + \frac{B}{2}} G_n(f)df + \int_{f_o - \frac{B}{2}}^{f_o + \frac{B}{2}} G_n(f)df$$

$$= \frac{N_o}{2} B + \frac{N_o}{2} B$$

$$= N_o B \qquad \text{D.5}$$

While that for $n_c(t)$ or $n_s(t)$ is given by

$$\sigma_{n_c}^2 = \sigma_{n_s}^2 = \int_{-\frac{B}{2}}^{\frac{B}{2}} G_{n_c}(f)\, df$$

$$= N_o B \qquad \text{D.6}$$

Therefore, variance of $n_c(t)$ or $n_s(t)$ is equal to the variance of $n(t)$[3-7]

D.2 Noise Correlation in QAM or QPSK System

The noise cmponent of the received signal is given by (Equation 3.20)

$$u(t) = n'(t)*h_R(t) \qquad D.7$$

where $n'(t) = n(t)e^{-j\omega_c t + j\theta}$

$$h_R(t) = c_3(t)*h_4(t)$$

n(t) is a stationary white Gaussian noise with zero mean and two sided-power spectral density of $\frac{1}{2} N_o$, $c_3(t)$ is the impulse response of the equivalent lowpass filter representing the receiver bandpass filter and $h_4(t)$ is the impulse response of the lowpass filters F_{a4} and F_{b4} in a complex form as shown in Figure 3.1. Furthermore, $f_c (= \frac{\omega_c}{2\pi})$ is the carrier frequency and θ is constant. n(t) is bandpass stationary white Gaussian noise with a bandwidth of $\frac{1}{T}$ over the positive frequencies, where $\frac{1}{T}$ is the data rate. It may be expressed as

$$n(t) = n_c(t)\cos(\omega_c t) - n_s(t)\sin(\omega_c t) \qquad D.8$$

where $n_c(t)$ and $n_s(t)$ are lowpass stationary white Gaussian processes each with zero mean and two-sided-power spectral density of N_o over frequency band of $-\frac{1}{2T}$ to $\frac{1}{2T}$ and zero elsewhere. Additionally, for the given $H_3(f)$, the transfer function of the receiver filter whose impulse response is $h_3(t)$, the autocorrelation function of $n_c(t)$ and $n_s(t)$ are equal or

$$R_{n_c}(\tau) = R_{n_s}(\tau) \qquad D.9$$

whereas their cross-correlation is zero, that is

$$R_{n_c, n_s}(\tau) = R_{n_s, n_c}(\tau) = 0 \qquad D.10$$

This means they are uncorrelated. Clearly n(t) can be rewritten as

$$n(t) = \frac{1}{2}[n_c(t) - jn_s(t)]e^{j\omega_c t} + \frac{1}{2}[n_c(t) + jn_s(t)]e^{-j\omega_c t} \qquad D.11$$

Hence

$$n'(t) = n(t)e^{-j(\omega_c t + \phi)}$$

$$= \frac{1}{2}[n_c(t) - jn_s(t)]e^{-j\phi} \qquad D.12$$

the higher frequency terms are eliminated by the lowpass filters F_{a4} and F_{b4} (see Figure 3.1), whose bandwidth is $\frac{1}{2T}$ in the positive frequency. Let

$$u(t) = u_1(t) + j\, u_2(t) \qquad D.13$$

where $u_1(t)$ and $u_2(t)$ are the real and imaginary parts of u(t) respectively. Thus

$$u_1(t) = \frac{1}{2}[n_c(t)*h_R(t)\cos\phi - n_s(t)*h_R(t)\sin\phi] \qquad D.14.a$$

$$u_1(t) = \frac{1}{2}[v_1 + v_2] \qquad D.14.b$$

$$u_2(t) = \frac{1}{2}[n_c(t)*h_R(t)\sin\phi + n_s(t)*h_R(t)\cos\phi] \qquad D.15.a$$

$$u_2(t) = \frac{1}{2}[v_3 + v_4] \qquad D.15.b$$

where
$$\left.\begin{aligned} v_1 &= n_c(t)\cos\phi * h_R(t) \\ v_2 &= -n_s(t)\sin\phi * h_R(t) \\ v_3 &= n_c(t)\sin\phi * h_R(t) \\ v_4 &= n_s(t)\cos\phi * h_R(t) \end{aligned}\right| \qquad D.16$$

Therefore the autocorrelation functions of $u_1(t)$ and $u_2(t)$ are given, respectively, by

$$R_{u1}(\tau) = \frac{1}{4}[R_{v1}(\tau) + R_{v2}(\tau) + R_{v1,v2}(\tau) + R_{v2,v1}(\tau)] \qquad D.17$$

$$R_{u2}(\tau) = \frac{1}{4}[R_{v3}(\tau) + R_{v4}(\tau) + R_{v3,v4}(\tau) + R_{v4,v3}(\tau)] \qquad D.18$$

and the cross-correlation function of $u_1(t)$ and $u_2(t)$ is given by

$$R_{u1,u2}(\tau) = \frac{1}{4}[R_{v1,v3}(\tau) + R_{v1,v4}(\tau) + R_{v2,v3}(\tau) + R_{v2,v4}(\tau)] \qquad D.19$$

Since $n_c(t)$ and $n_s(t)$ are uncorrelated, then the cross-correlation functions

$$\left.\begin{aligned} R_{v1,v2}(\tau) = R_{v2,v1}(\tau) = R_{v3,v4}(\tau) = R_{v4,v3}(\tau) = 0 \\ R_{v1,v4}(\tau) = R_{v4,v1}(\tau) = R_{v2,v3}(\tau) = R_{v3,v2}(\tau) = 0 \end{aligned}\right| \qquad D.20$$

The Fourier transform of $h_R(t)$ is $H_R(f)$, hence

$$R_{v1}(\tau) = R_{v3}(\tau) = \int_{-\frac{1}{2T}}^{\frac{1}{2T}} N_o |H_R(f)|^2 e^{j\omega\tau} df \qquad D.21$$

$$R_{v2}(\tau) = R_{v4}(\tau) = \int_{-\frac{1}{2T}}^{\frac{1}{2T}} N_o |H_R(f)|^2 e^{j\omega\tau} df \qquad D.22$$

and

$$R_{v1,v3}(\tau) = R_{v2,v4}(\tau) = \int_{-\frac{1}{2T}}^{\frac{1}{2T}} N_o |H_R(f)|^2 e^{j\omega\tau} df \qquad D.23$$

By appropriate substituting of Equations D.20-D.23 into Equations D.17-D.19, then this leads to

$$R_{u1}(\tau) = \frac{N_o}{2} \int_{-\frac{1}{2T}}^{\frac{1}{2T}} |H_R(f)|^2 e^{j\omega\tau} df \qquad D.24$$

$$R_{u2}(\tau) = \frac{N_o}{2} \int_{-\frac{1}{2T}}^{\frac{1}{2T}} |H_R(f)|^2 e^{j\omega\tau} df \qquad D.25$$

$$R_{u1,u2}(\tau) = \frac{N_o}{2} \int_{-\frac{1}{2T}}^{\frac{1}{2T}} |H_R(f)|^2 e^{j\omega\tau} df \qquad D.26$$

It is also possible to prove that (see ref.18)

$$R_{u1,u2}(-\tau) = - R_{u1,u2}(\tau) \qquad D.27$$

and, consequently,

$$R_{u2,u1}(\tau) = R_{u1,u2}(-\tau) = - R_{u1,u2}(\tau) \qquad D.28$$

The autocorrelation function of the complex valued u(t) is given by

$$\begin{aligned} R_u(\tau) &= E[u^*(t).u(t+\tau)] \\ &= R_{u1}(\tau) + R_{u2}(\tau) + j[R_{u1,u2}(\tau) - R_{u2,u1}(\tau)] \\ &= 2R_u(\tau) + j2R_{u1,u2}(\tau) \\ &= N_o \int_{-\frac{1}{2T}}^{\frac{1}{2T}} |H_R(f)|^2 e^{j\omega\tau} df \end{aligned} \qquad D.29$$

where u*(t) is the complex conjugate of u(t). Clearly, the autocorrelation function of each of the real and imaginary parts of u(t) is given by half the real part of $R_u(\tau)$, whereas the cross-correlation function of these parts is given by half the imaginary part of $R_u(\tau)$. Furthermore, if $R_{u1,u2}(\tau) = 0$ then $u_1(t)$ and $u_2(t)$ are uncorrelated.

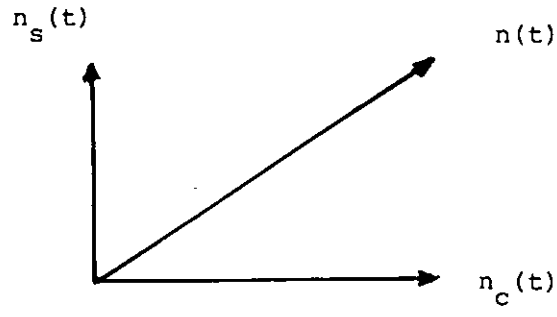

Fig. D.1 Noise representation in a complex-coordinate

APPENDIX E

TRANSMISSION PATH LOSSES IN MICROWAVE COMMUNICATION

The field strength in the vicinity of a mobile station vary rapidly with the time which gives an indication of a highly variable structure of the received signal, because of the existance of multipath between the transmitter and the receiver of the microwave mobile communications. As the vehicle carrying mobile unit moves through the service area, the received signal envelope, phase and frequency fluctuate rapidly due to multipath propagation and interference[9-12,19,21,72-86]. These fluctuations result in a received signal with a Rayleigh probability density function[10,11,72-75]. However, the path losses in a microwave communication system, for a stationary station, are briefly discussed here for better understanding of the corresponding losses in mobile radio communications.

E.1 Propagation and path losses in microwave radio

The transmitter antenna radiates ultra-high frequency (UHF) electromagnetic (microwave) which travels in a straight line until it reaches the receiver antenna. For this reason, it is called line-of-sight radio propagation and hence is greatly influenced by obstructions and multipath fading[10,11,44-71].

One of the simplest forms of propagation loss is that due to free-space, which is normally called free-space loss, L_f (in dB). In practice, the

free-space loss is modified by the presence of the earth and imperfections of the atmosphere. Let p_t (in Watts) be the power which is radiated by an isotropic antenna[43], then the power density (W/m^2) is given by

$$P_D = \frac{P_t}{\text{surface area}} = \frac{P_t}{4\pi R^2} \quad W/m^2 \qquad E.1$$

where R (in metres) is the radius of a sphere centred on the position of the radiated antenna. If an isotropic aerial is placed anywhere on the surface of this sphere with an effective aperture (collecting area) A, then the received signal power is given by[10,11,43,71]

$$P_r = P_t \frac{A}{4\pi R^2} \; W \qquad E.2$$

where $A = \lambda^2/4\pi$ for an isotropic antenna and λ is the wave-length (in metres). Knowing that the isotropic antenna power gain is unity (G = 1 or 0 dB), the free-space loss can be defined as

$$\begin{aligned} L_f &= 10 \log_{10} \left(\frac{P_t}{P_r}\right) && dB \\ &= 20 \log_{10} (4\pi R/\lambda) && dB \\ &= 22 + 20 \log_{10}(R/\lambda) && dB \\ &= -147.5 + 20 \log_{10} R + 20 \log_{10} f_c && dB \end{aligned} \qquad E.3$$

[12]

where f_c is the radiated signal carrier frequency in Hz and R is the distance between the transmitter and receiver antennas, in metres. Hence, the free-space loss depends on the applied frequency and on

the distance separating the two antennas. Some examples are shown in Table E.1 for a distance of 10 Km.

Over a flat and smooth area, it is very important to adjust the height of the receiver and transmitter antennas as well as the distance separating them in order to avoid a spherical earth loss[10,11,25,28-42]. When the earth curvature obstructs the direct line-of-sight this will cause loss which is called a smooth spherical earth loss.

The obstruction (diffraction) loss is, however, due to an obstacle that blocks the direct line-of-sight [10,11,25,26,33]. Therefore, the path profile must be investigated before installation of the microwave communication systems, so as to compromise for minimum loss and look for best settlement. As a matter of practice, the tip of the obstacle must be outside the first Fresnel zone[25,40,41], otherwise the attenuation should be calculated in accordance with Knife-Edge diffraction method [10,11,33]. This is called controlling obstruction[10,11,33]. Consequently, the radius of the first Fresnel zone is given by[25,40,41]

$$R_f = \left(\frac{D_1 D_2 \lambda}{D}\right)^{\frac{1}{2}} \qquad \text{E.4}$$

where λ is the wavelength of the radiated signal, $D = D_1 + D_2$ is the path length, D_1 and D_2 are the distances between the obstruction and each of the two antennas of the transmitter and the receiver, as shown in Figure 3.4. The units of R_f are in meters when D, D_1, D_2 and λ are

in metres. The ratio of R/R_f ought to be less than unity[25] for good performance, where R is the minimum distance between the tip of the knife edge obstacle and the lower boundary of the first Fresnel zone.

The field strength of a diffracted radio wave associated with a knife edge can be expressed, according to electromagnetic theory, by[10,11]

$$\frac{E}{E_o} = Fe^{j\Delta} \qquad \text{E.5}$$

where E_o and E are the free-space electromagnetic fields for direct line-of-sight and the obstructed one, respectively, F is the diffraction coefficient, Δ is the phase difference between the direct path wave and the diffracted wave, and $j = \sqrt{-1}$ [10,11,42]. The loss due to diffraction is given by

$$L_r = 20 \log_{10} F \qquad \text{E.6}$$

where

$$F = \frac{2S + 1}{\sqrt{8} \sin(\Delta + \frac{\pi}{4})} \qquad \text{E.7}$$

$$\Delta = \tan^{-1}\left(\frac{2S+1}{2C+1}\right) - \frac{\pi}{4} \qquad \text{E.8}$$

and C and S are the Fresnel integrals that are formulated by

$$C = \int_o^v \cos\left(\frac{\pi}{2} x^2\right) dx \qquad \text{E.9}$$

$$S = \int_{o}^{v} \sin(\frac{\pi}{2} x^2)\, dx \qquad E.10$$

where v is defined as

$$v = -h \left(\frac{2}{\lambda} \left(\frac{1}{D_1} + \frac{1}{D_2}\right)\right)^{\frac{1}{2}} \qquad E.11$$

where $h = R - R_f$, see Figure 3.4. Moreover v is a dimensionless parameter. The approximate solution to Equation E.7 , which includes terms associated with Fresnel integral, is given by Lee[10], such as:-

i) $\theta L_r = 0$ dB $\qquad v \geq 1$

ii) $1L_r = 20 \log_{10} (0.5 + 0.62\, v)$ dB $\qquad 0 \leq v \leq 1$

iii) $2L_r = 20 \log_{10} (0.5e^{0.95v})$ dB $\qquad -1 \leq v \leq 0$

iv) $3L_r = 20 \log_{10} (0.4 - (0.1184 - (0.1v + 0.38)^2)^{\frac{1}{2}})$ dB $\qquad -2.4 \leq v \leq -1$

v) $4L_r = 20 \log(\frac{0.225}{v})$ dB $\qquad v \leq -2.4$

These equations simplify the computation process. However, it is possible to use Figure E.1 (from ref. 10), by projection methods to obtain the diffraction loss, when v is calculated according to Equation F.11. Clearly, when the tip of the knife-edge is above line-of-sight h is positive ($R > R_f$) and hence v is negative, while, when h is negative ($R < R_f$) then the tip of the knife-edge obstacle is below the line-of-sight and, consequently, v is positive, as that illustrated in Figure 3.4.

As the path length is increased, more reflected waves will be created and will cause indirect paths. This phenomenon introduces the concept of the multipath propagation, in stationary microwave communications, that cause plane earth loss. Figure 3.2 shows an example of a reflected wave, A complex analysis[11,28,32], for a plane surface (flat earth) has shown that the field intensity of the reflected wave is given by

$$E_r = \Gamma E_o e^{j\Psi} \qquad \text{E.12}$$

Where E_o is the field intensity of the received signal through the direct path Γ is the reflection coefficient of the ground and Ψ is the phase difference between the direct path wave and the reflected wave.

The reflection coefficient Γ depends on the angle of incidence, θ, the polarization of the wave and the reflector (ground) characteristics, Γ is given by

$$\Gamma = \frac{\sin\theta - \Omega}{\sin\theta + \Omega} \qquad \text{E.13}$$

where $\Omega = (\varepsilon_o - \cos^2\theta)^{\frac{1}{2}} / \varepsilon_o$ for vertical polarization

$\Omega = (\varepsilon_o - \cos^2\theta)^{\frac{1}{2}}$ for horizontal polarization

$\dot{\varepsilon}_o = \varepsilon - j60\sigma\lambda$

ε = dielectric constant of the reflector (ground) relative to unity in the free-space

σ = the conductivity of the reflector(earth) in mhos/m

$j = \sqrt{-1}$

and λ = wavelength in m

When D, the distance between the two antenna, is much greater than $5\,h_1h_2$ (or $D >> 5h_1h_2$) then

$$\psi = 4\pi \frac{h_1h_2}{\lambda D} \qquad \text{E.14}$$

Therefore, the received field strength is now the vector sum of the direct path and the reflected path (or paths), thus

$$E = E_o + \Gamma E_o e^{j\Psi}$$

$$= E_o (1 + \Gamma e^{j\psi}) \qquad \text{E.15}$$

Then, the received power is now given by

$$P_r = P_t \frac{\lambda}{4\pi D} g_t g_r \lambda \qquad \text{E.16}$$

where $\lambda' = (1 + 2|\Gamma| \cos\psi + |\Gamma|^2)$, $|x|$ is the modules value of x, g_t and g_r are the transmitter and receiver antennas gain ($g_t = g_r = 1$ for isotropic antennas). However, the received signal power may be given by

$$P_r = (P_t + G_t + G_r) - (L_f + L_r + L_\phi + L_c) \text{ dB} \qquad \text{E.17}$$

where $P_t = 10 \log_{10}(p_t)$ dB transmitted power

$G_t = 10 \log_{10}(g_t)$ dB transmitter antenna power gain

$G_r = 10 \log_{10}(g_r)$ dB receiver antenna power gain

L_f = $20 \log_2(\frac{\lambda}{4\pi D})$ dB free-space loss

L_r = diffraction loss in dB (Equation E.6)

L_ϕ = $10 \log_{10}(\phi)$ dB reflection loss

L_c = feeders loss in dB

Furthermore, it is possible to improve the channel performance by making use of the reflected wave to be inphase by adjusting the antenna's height (Equation 3.42) so that $0 \leq \cos\psi \leq 1$. Consequently, if the direct path wave is picked-up by an antenna and the reflected one by another antenna and are then combined by a suitable combing method, this leads to the concept of space diversity[10,11, 35] as shown in Figure 3.3.

f_c(MHz)	λ (meter)	L_f (dB)
1	300.0	42.5
50	6.0	86.5
100	3.0	92.5
500	0.6	106.5
900	0.333	111.6
1000	0.3	112.5

Table E.1 Typical free-space loss for a separation distance of 10 Km between the transmitter and receiver antennas

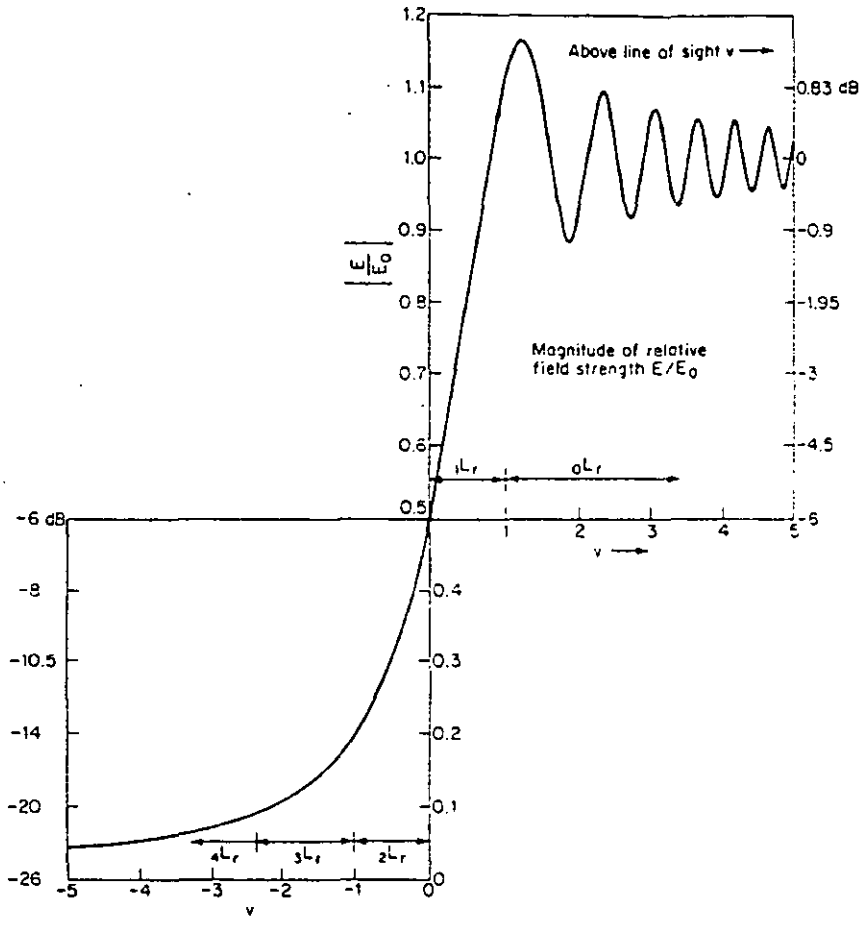

Fig. E.1 Magnitude of relative field strength E/E_o due diffraction loss

[from Ref. 10]

APPENDIX G

DIGITAL PHASE LOCK-LOOP MODELS ANALOGY

Before introducing the stabilised DPLL as a development of stabilised digital control system, it is necessary to introduce the available model in the literature[198,199]. This model is shown in Figure G.1 whose loop filter transfer function is, in general, given by[171-183,198,199]

$$F_{Nh}(z) = \sum_{n=1}^{N} \frac{C_n}{(1-z^{-1})^{n-1}} \qquad G.1$$

where N is the order of the required DPLL and C_n is constant. Hence the loop filter for first and second order DPLL's are given respectively by

$$F_{1h}(z) = 1 \qquad G.2$$

$$F_{2h}(z) = 1 + \frac{\alpha z}{z-1} \qquad G.3$$

where α is constant. Only the second order DPLL is considered here whose transfer function is given by[198]

$$P_{2h} = \frac{\beta(z-1) + \beta\alpha}{(z-1)^2 + \beta(z-1) + \alpha\beta} \qquad G.4$$

where β is the loop gain. Generally, the condition of stability is when all the roots of the characteristic equation

$$(z-1)^2 + \beta(z-1) + \alpha\beta = 0 \qquad G.5$$

must lie within the unit circle of the z-plane. The fulfilment of the stability condition is, therefore, when[198]

$$0 < \beta < \frac{4}{\alpha+2} \qquad G.6$$

Also, when the frequency offset is less than the sampling frequency, then α and β can be chosen such that $\alpha < 1$ and $\beta < 1$, for an optimum system and good tracking performance[198]. Furthermore, it is necessary to achieve lowpass filtering action through the selection of the values of α and β.

However the DPLL transfer function is related to LF and VCO transfer functions as follows

$$P_h(z) = \frac{\beta z^{-1} F(z)G(z)}{1 + \beta z^{-1} F(z)G(z)} \qquad G.7$$

Hence, the difference between this model and the model whose transfer function is given by Equation 5.9 (Chapter 5), is the numerator of Equation G.7 contains extra delay element (z^{-1}). In other words this model contains the delay element in its open loop transfer function and not in the feedback path.

Finally this model is found unlikely to be applicable in mobile radio systems. Moreover, this model is based on trial-and-error method. Nevertheless, the trial-and-error method requires longer time to select the values of the two parameters, α and β, seeking a stable system. Also, only one loop filter is associated with this model. While in the system, that is studied in Chapter 5, any filter can be used and requires less time in looking for stability.

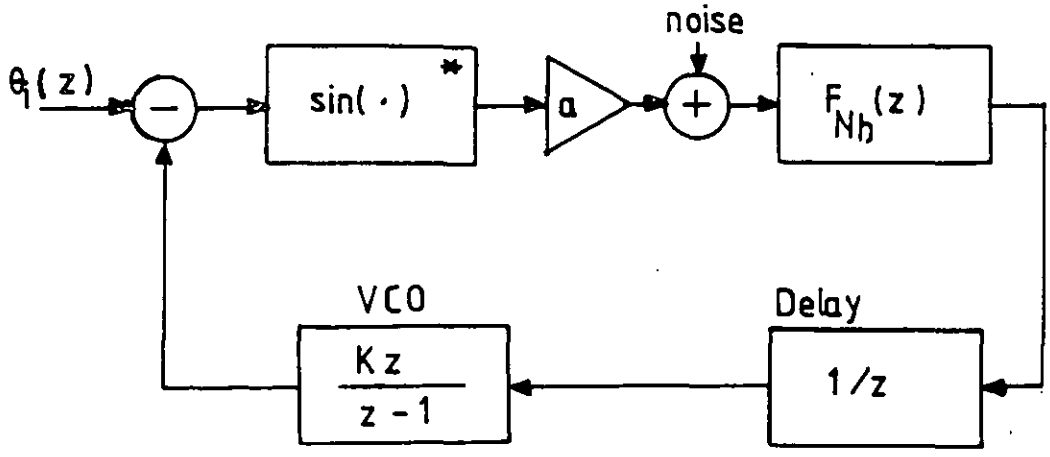

Fig. G.1 DPLL available in the literature

APPENDIX H

STABILISATION OF FEEDBACK SYSTEM

H.1 The closed-loop Characteristic Equation

The principle of the plant, which is represented by the transfer function G(z), is to calculate the stepwise, u_i, based on a finite number of error measurements (e_i, e_{i-1}, ..., e_{i-g}) and probably on the past value of the controller output (u_{i-1}, u_{i-2}, ...) where i is the time index such that $u_i = u(iT)$ and e_i and $e_i = e(iT)$, ... etc. This situation is illustrated in Figure H.1. If a control algorithm in the form of linear difference equation with constant coefficients is employed, then the entire system can be represented by a z-domain transfer function. Therefore, the relation for the error sensor is given by

$$E(z) = X(z) - Y(z) \qquad \text{H.1}$$

and for the controller is given by

$$U(z) = D(z)E(z) \qquad \text{H.2}$$

while that for the plant is given by

$$Y(z) = G(z)U(z) \qquad \text{H.3}$$

Substitution of Equation H.1 into Equation H.2 yields

$$U(z) = D(z)[X(z) - Y(z)] \qquad \text{H.4}$$

The closed-loop transfer function is given by the ratio of the system output to the input, and can be obtained by substituting Equation H.4 into Equation H.3 or [167-169]

$$M(z) = \frac{Y(z)}{X(z)} = \frac{G(z)D(z)}{1 + G(z)D(z)} \qquad H.5$$

The quantity $1 + G(z)D(z)$, which is a rational function of z, is called the closed-loop characteristic equation. The roots location of this equation in the z-plane determine the dynamic character of the closed-loop. If one or more of these roots lie outside the unit circle in the z-plane, the closed-loop system is unstable.[167-169]

Finally, the order of the digital control system [M(z)] equal to the sum of the plant [G(z)] order plus the controller [D(z)] order.

The plant will be considered hereafter as a simple digital integrator, which will be used as voltage controlled oscillator (VCO) in case of the phaselocked loop application. The function of this plant (integrator) depends on the past value of the output plus the current value of the input, that is

$$y_i = y_{i-1} + u_i \qquad H.6$$

Accordingly, by applying z-transform, the transfer function of the plant can be given, irrespective of the sampling rate, by

$$G(z) = \frac{Y(z)}{U(z)} = \frac{z}{z - 1} \qquad H.7$$

Also, the controller is considered as a recursive lowpass digital filter. This filter should be designed to accommodate the maximum possible frequency shift of the received signal (carrier). In a mobile radio environment the expected maximum Doppler frequency shift, for a vehicle moving with speed of 75 MPH, is ± 100 Hz [Chapter 3]. Hence, the filter bandwidth is 100 Hz, while the whole system will be sampled at the data rate (i.e. 9.6 kHz).

To avoid aliasing error, the sampling frequency of the required digital filter must be equal to or greater than Nyquist rate, which is twice the maximum input frequency. In this case, the sampling frequency is well above the Nyquist rate.

Under this assumption, the maximum cut-off frequency of the digital lowpass filter, which is to be used as a controller, can be regarded as 100 Hz and the sampling frequency as 9.6 kHz. First and second order Butterworth lowpass filters have been designed by using bilinear z-transform method[103-106] and a second order Chebyshev lowpass filter has been chosen using Impulse-invariant design method for comparison, (see Appendix B). The transfer function of the three filters can be written in general as

$$D_k(z) = \frac{\alpha_o + \alpha_1 z^{-1} + \alpha_2 z^{-2}}{1 + \beta_1 z^{-1} + \beta_2 z^{-2}} \qquad \text{H.8}$$

where the values of k and the corresponding α_o, α_1, α_3, β_1 and β_2 are given in Table H.1. Now, by substituting Equation H.7 and Equation H.8

into Equation H.5 three different systems can be obtained, that are given by

$$M_k(z) = \frac{c_o + c_1 z^{-1} + c_2 z^{-2}}{1 + d_1 z^{-1} + d_2 z^{-2} + d_3 z^{-3}} \qquad \text{H.9}$$

where the values of k and the corresponding c_{f-1} and d_f, for f = 1 to 3 are given in Table H.2.

All these systems should pass the stability tests that will include the following:-

i) Time-response test

ii) Characteristic equation root locus

iii) Frequency-response test.

The stability is the most important consideration when designing a feedback system. Indeed, all the present day researches in control are concerned with stability. That is not to say the methods for determining stability do not exist, on the contrary, many methods do exist. Unfortunately, they only deal with certain aspects of stability. For a linear system and even for a nonlinear system, it is not always possible to determine analytically for what ranges of relevant parameters the system remains stable[166].

H.2 Stability tests

Since the output of a digital control system is usually a function of time, it is necessary to evaluate the performance of the system

in the time domain. However, when the discrete-time state equation is used, the output of the system is measured only at the sampling instance. Depending on the sampling period and its relation to the time constants of the system, the discrete-time representation may or may not be accurate. In other words, there may be a large discrepancy between the sampled output signal of the digital control system, y(iT), and the continuous output of an identical continuous-data control system used for the same purpose, y(t). Hence,the former may be a valid representation of the system behaviour[169].

The steady state error, which is the difference between the unit step and the final state of the output, can be determined by applying the final value theorem[167-169], when a unit-step function is used as an input signal (or when $X(z) = \frac{z}{1 - z}$). From Equations H.1 and H.5, the error signal is related to the input as

$$E(z) = \frac{X(z)}{1 + G(z)\ D(z)} \qquad \text{H.10}$$

Hence, the steady state can be obtained as

$$e_{ss} = \lim_{k \to \infty} e(kT) = \lim_{z \to 1} (1 - z^{-1}) E(z)$$

$$= \lim_{z \to 1} \frac{1}{1 + G(z)D(z)}$$

$$= 0 \qquad \text{H.11}$$

This means that the relevant system is capable of tracking a step input signal without any steady state error.

In the time response test, the output signal is measured for appropriate number of samples, when a unit-step is applied to the input,[167-170] or when $x(iT) = u_s(iT)$ (Figure H.1), where

$$u_s(iT) = \begin{cases} 1 \text{ for } i \geq 0 \\ 0 \text{ for } i < 0 \end{cases} \qquad \text{H.12}$$

The time-response tests are carried out by computer simulation and the corresponding results are shown in Figures H.2 to 4, for different values of the new damping factor. The new damping factor (ε) is inserted in the controller (filter) transfer function in order not to change the function of the plant (VCO, for example). From Equation H.8, the designed filters transfer function become, after the insertion of the new damping factor, as

$$D'_k(z) = g_u \frac{\alpha_o + \varepsilon\alpha_1 z^{-1} + \varepsilon\alpha_2 z^{-2}}{1 + \varepsilon\beta_1 z^{-1} + \varepsilon\beta z^{-2}}$$

$$= \frac{a_o + a_1 z^{-1} + a_2 z^{-2}}{1 + b_1 z^{-1} + b_2 z^{-2}} \qquad \text{H.13}$$

where g_u is the unity gain factor which is obtained when $\lim_{z \to 1} D'_k(z) = 1$ which leads to

$$g_{uk} = \frac{1 + \varepsilon\beta_1 + \varepsilon\beta_2}{\alpha_o + \varepsilon\alpha_1 + \varepsilon\alpha_2} \qquad \text{H.14}$$

and $k = 1, 2, 3$. Equation H.14 defines the relationship between the unity gain factor and the new damping factor and $g_u = 0$ when $\varepsilon = \varepsilon_o$. Therefore ε_o confines the boundary limit of the damping factor as

$$0 \leq \varepsilon < \varepsilon_o \qquad \text{H.15}$$

beyond this limit the close loop system becomes unstable.

One of the most important requirements in the performance of a feedback system is its stability[166-185]. Many classical textbooks on digital or continuous control (feedback) system describe in great detail the stability methods such as Routh-Hurwitz criterion, Nyquist criterion, roots-locus plot, Bode plot, Liapunou's direct method, Schur-Cohn criterion and Jury's criterion[166-170]. It has been established elsewhere[167-169] that a linear digital control system is stable if all the roots of the characteristic equation lie inside the unit circle in the z-plane. However, computer programs for numerical and graphical representation techniques are readily available and more accurate. (Appendix K).

Since the time responses of all systems under consideration damp very quickly when $\varepsilon = 0.5$, then this value may be recommended in the tests of the system performance in noise (Chapters 5 and 6). The characteristic equations become:-

For System 1

$$1 - 0.9532\ z^{-1} + 0.345745\ z^{-2} = 0 \qquad \text{H.16}$$

For System 2

$$1 - 1.9540\ z^{-1} + 1.4100\ z^{-2} - 0.4560\ z^{-3} = 0 \qquad \text{H.17}$$

and for System 3

$$1 - 1.9944\ z^{-1} + 0.4916\ z^{-2} - 0.4972\ z^{-3} = 0 \qquad \text{H.18}$$

Table H.3 shows the roots of all above equations that are clearly inside the unit circle of the z-plane.

The insertion of the new damping factor, so far, results in a very good advantage in the time domain as well as in the poles-zero-configuration, of course within the provided boundary (Equation H.15). Therefore, the insertion of the new damping factor must not have an adverse effect on the system bandwidth. Accordingly, it is necessary to investigate the frequency response (Bode plot[167-170]). The frequency response diagram is a plot of the amplitude (in decibels, dB) and the phase (in degrees) of the close-loop transfer function as a function of frequency. By setting $z = e^{j\omega T} = \exp(j\omega T)$ in the transfer function M(z), which obtained by substituting Equations H.7 and H.14 into Equation H.5 , when $\epsilon = 0.5$, and letting the frequency vary from 0 to a very high value, then

$$M(f) = M(e^{j\omega T}) = M(z)\Big|_{z=e^{j\omega T}} \qquad \text{H.19}$$

where $j = \sqrt{-1}$, $\omega = 2\pi f$, f is the frequency and T is the duration of the sampling period (in seconds). The result of computer simulation tests are shown in Figures H.5 to 7 by using

$$M = 20 \log_{10} |M(f)| \qquad H.20$$

where $|x|$ is the modulus of x.

All the systems discussed here are applied in the digital phase locked loop DPLL techniques (Chapter 5) and only the second order system is employed in the feedback channel estimator (Chapter 6). Testing the system in environment such as mobile radio, gives an indication that the system is capable of tracking the input signal fluctuations. Also, it is possible to use damping factor directly in the z-domain, rather than going to and fro between the s-plane and z-plane. Furthermore, when a system is designed as stable in s-plane, it may not be stable after transforming it to z-plane (169).

k	α_o	α_1	α_2	β_1	β_2	filter
1	0.0317	0.0317	0	-0.9366	0	1st order Butt
2	1.02321×10^{-3}	2.04642×10^{-3}	1.02321×10^{-3}	-1.9075	0.9119	2nd order Butt.
3	1.0075	-1.002	0.0	-1.9887	0.9944	2nd order Cheb.

Table H.1 The orders and coefficients of the used filters

k	c_o	c_1	c_2	b_1	b_2	b_3
1	0.0307	0.0307	0	-1.8464	0.9078	0
2	1.0222×10^{-3}	2.0443×10^{-3}	1.0222×10^{-3}	-2.9045	2.8162	-0.9110
3	0.5019	-0.4990	0	-1.9841	-1.4860	-0.4953

Table H.2 The coefficient of the digital control systems whose corresponding filters are given in Table H.1

System	Roots
1	-0.4766 ± j0.3444
2	1.0 -0.477 ± j0.478
3	-1.0 -0.4972 ± j0.4999

Table H.3 Root of the charactreristic equations of feedback control systems when $\varepsilon = 0.5$

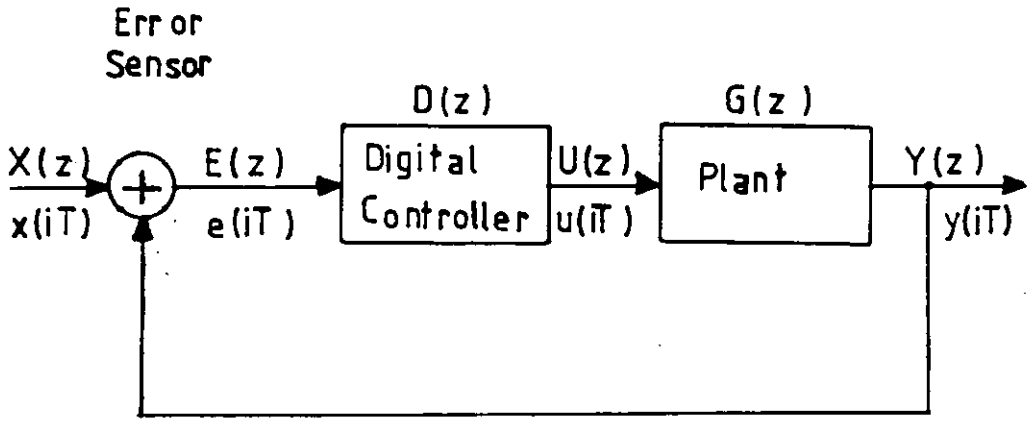

Fig. H.1 Digital Control System Algorithm

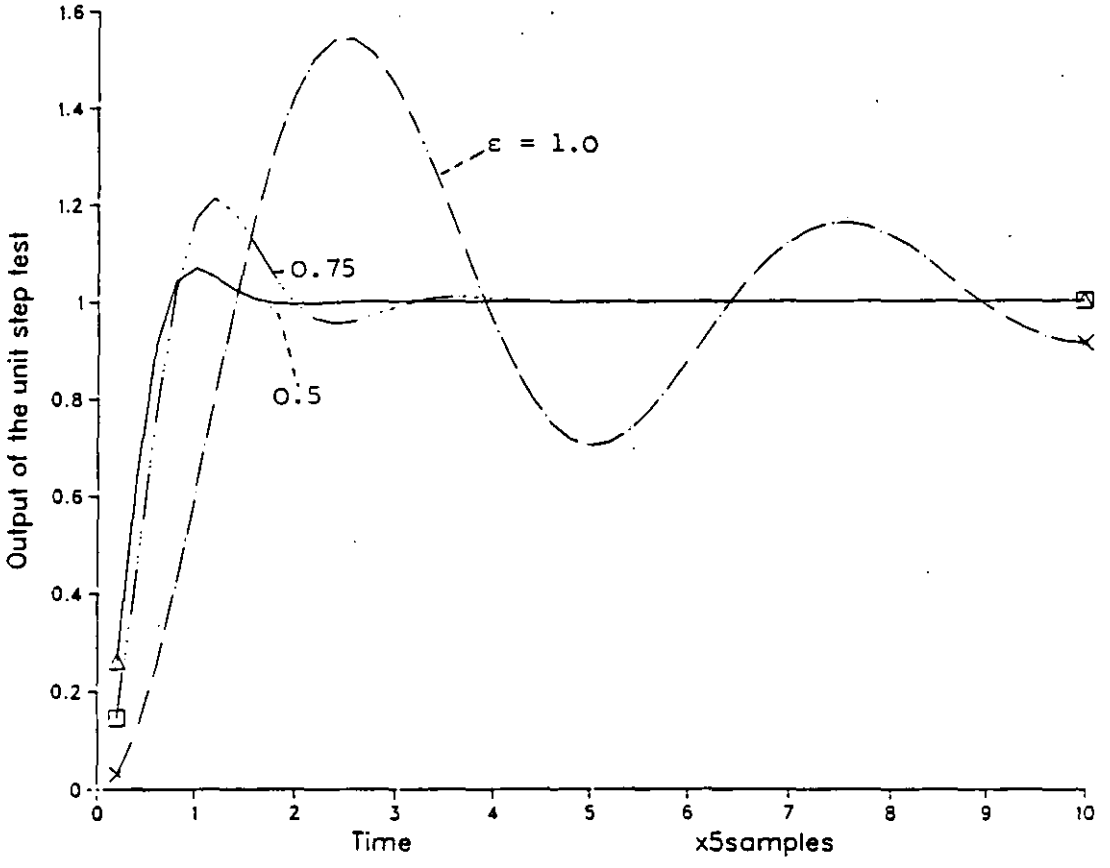

Fig.H.2 Time response for system 1

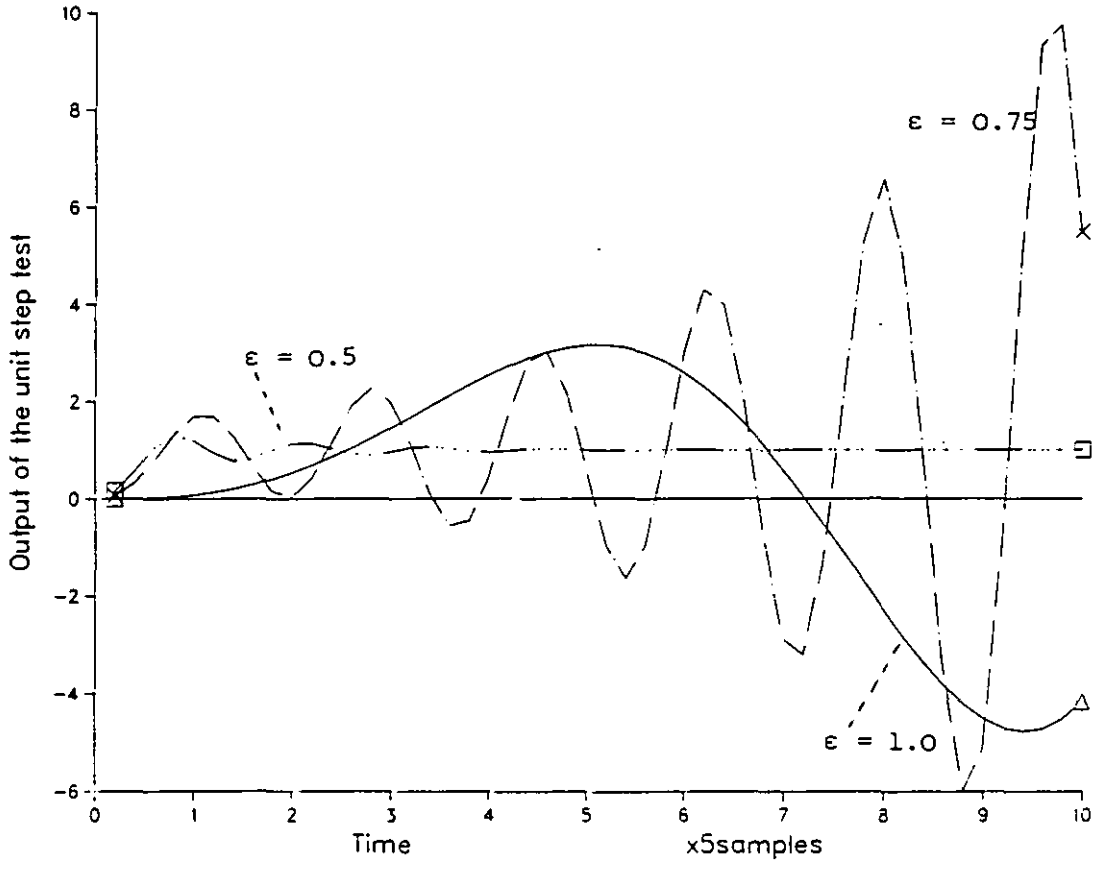

Fig.H.3 Time response for system 2

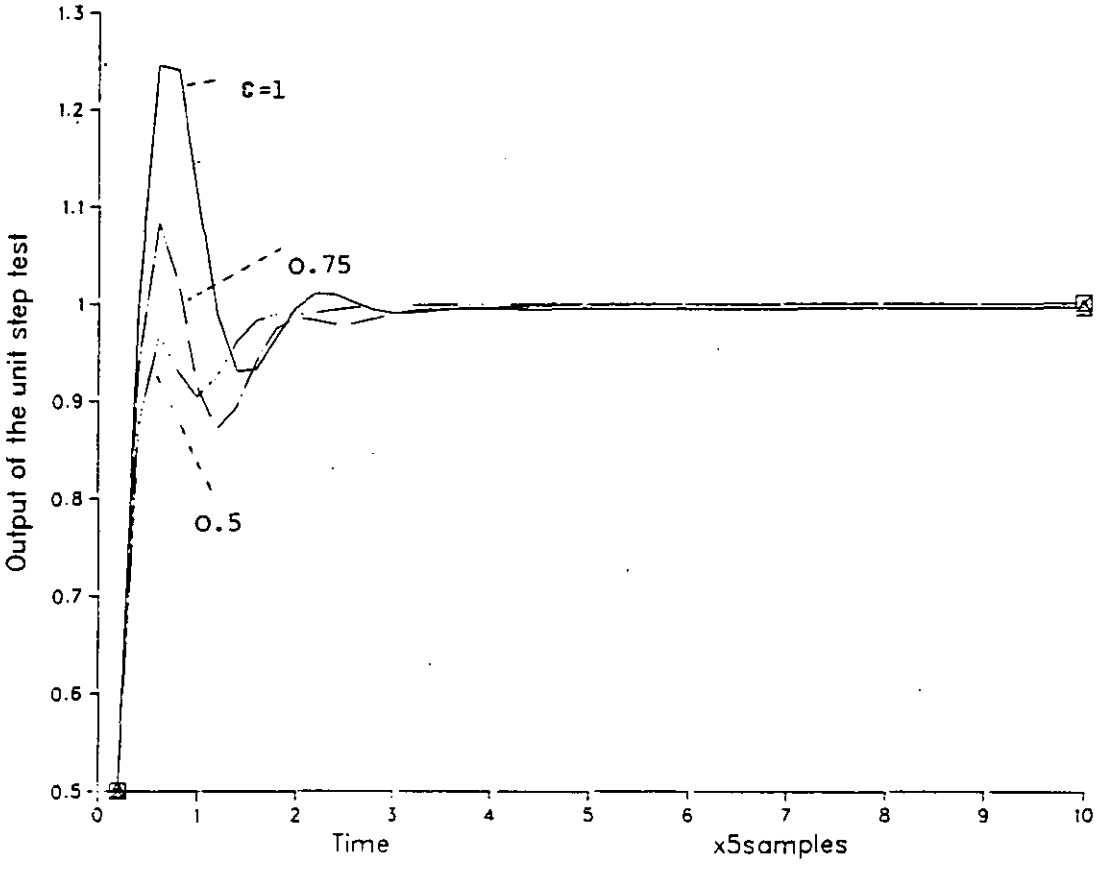

Fig.H.4 Time response for system 3

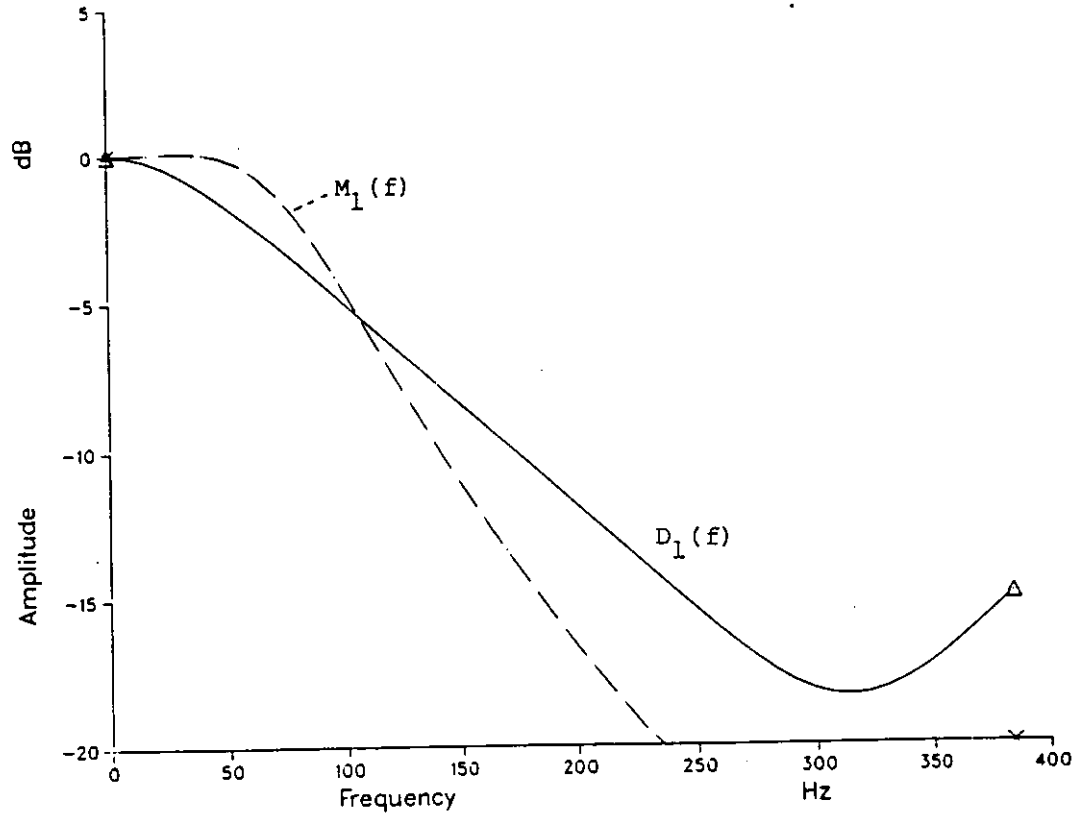

a

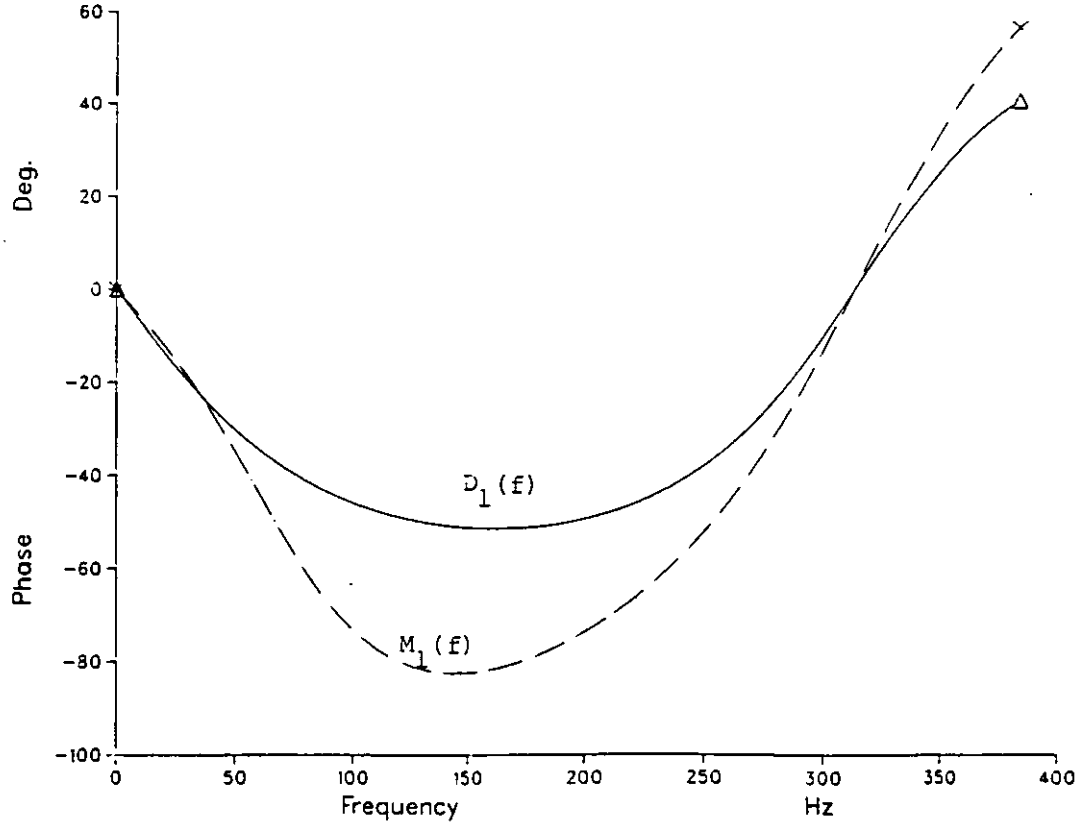

b

Figure H.5 Frequency response for system 1 when $\varepsilon = 0.5$

a - amplitude b - phase

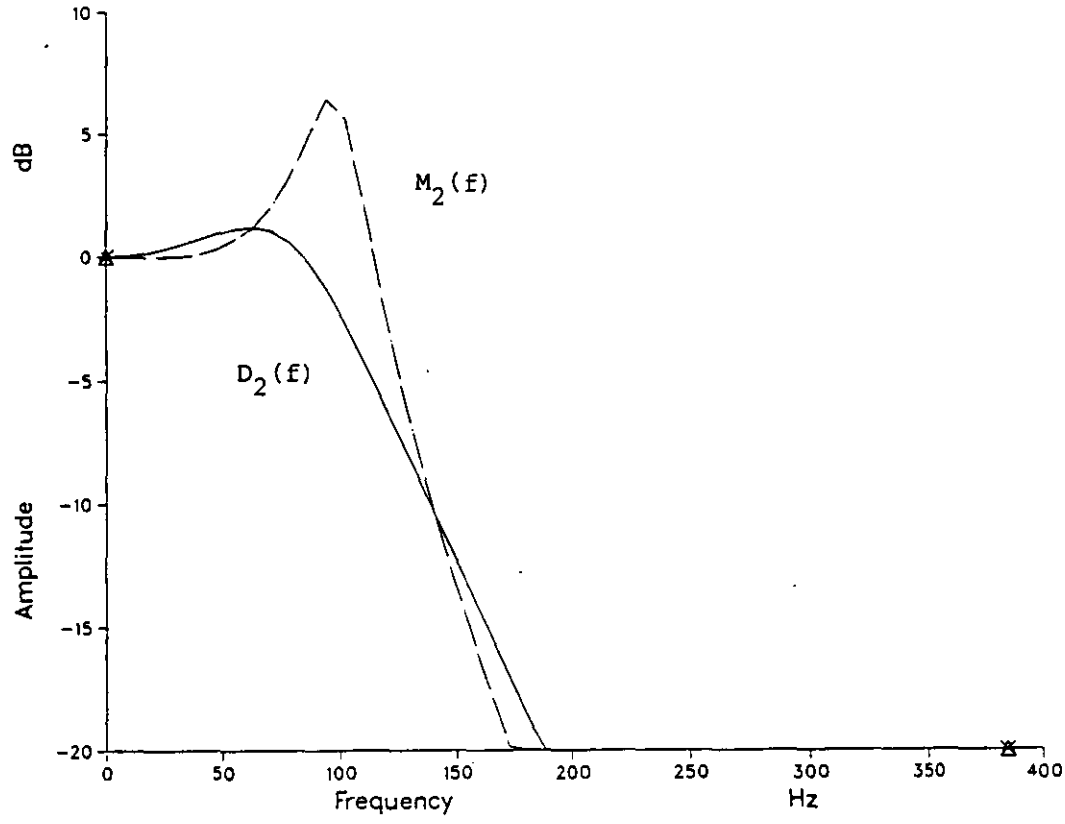

a

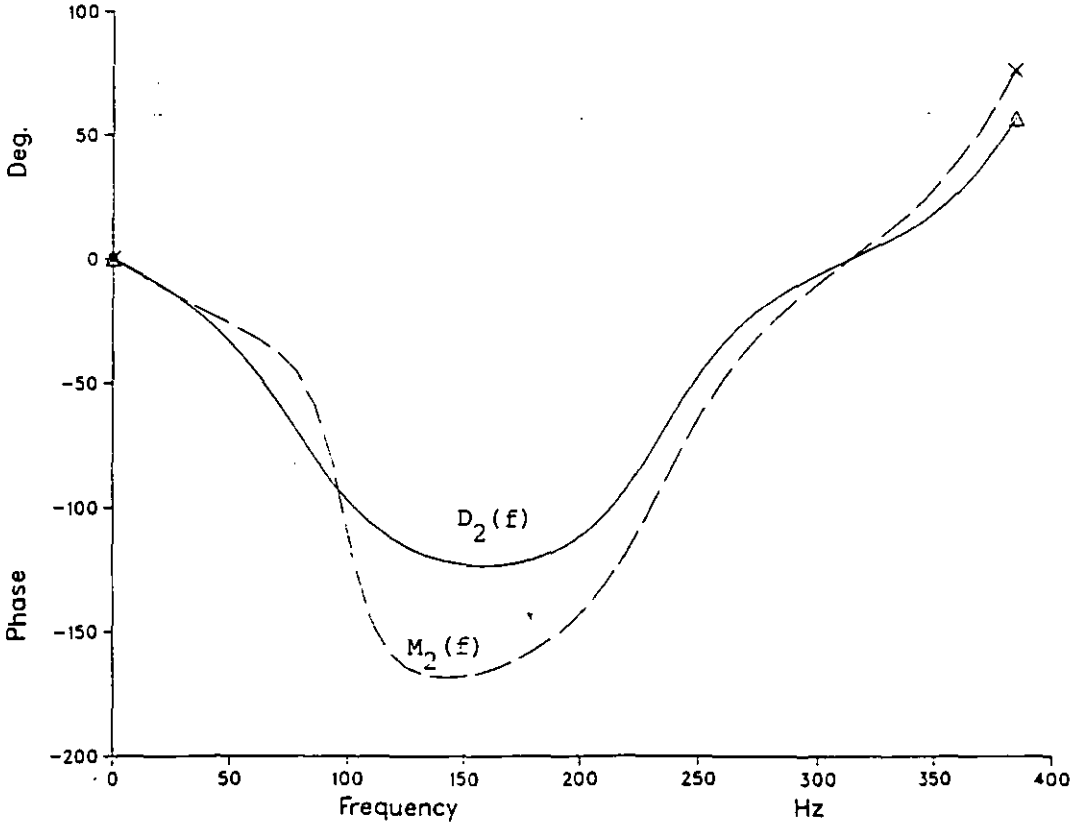

b

Fig. H.6 Frequency response for system 2 when $\varepsilon = 0.5$

a - amplitude b - phase

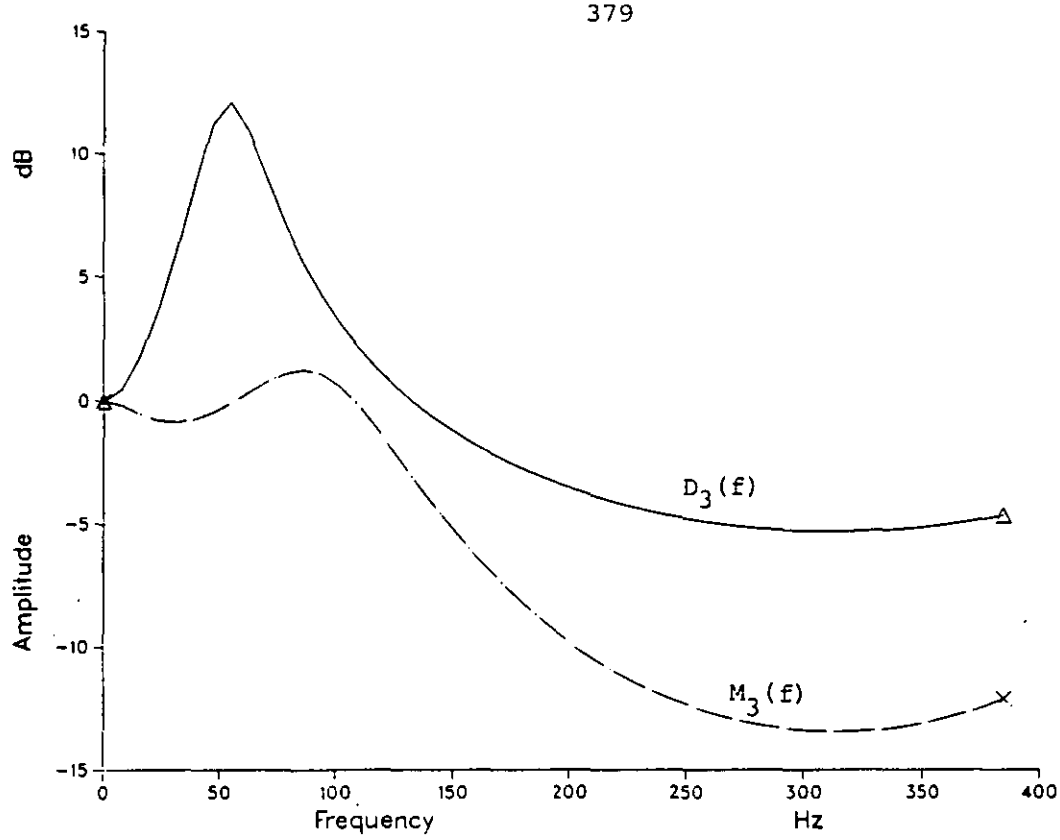

a

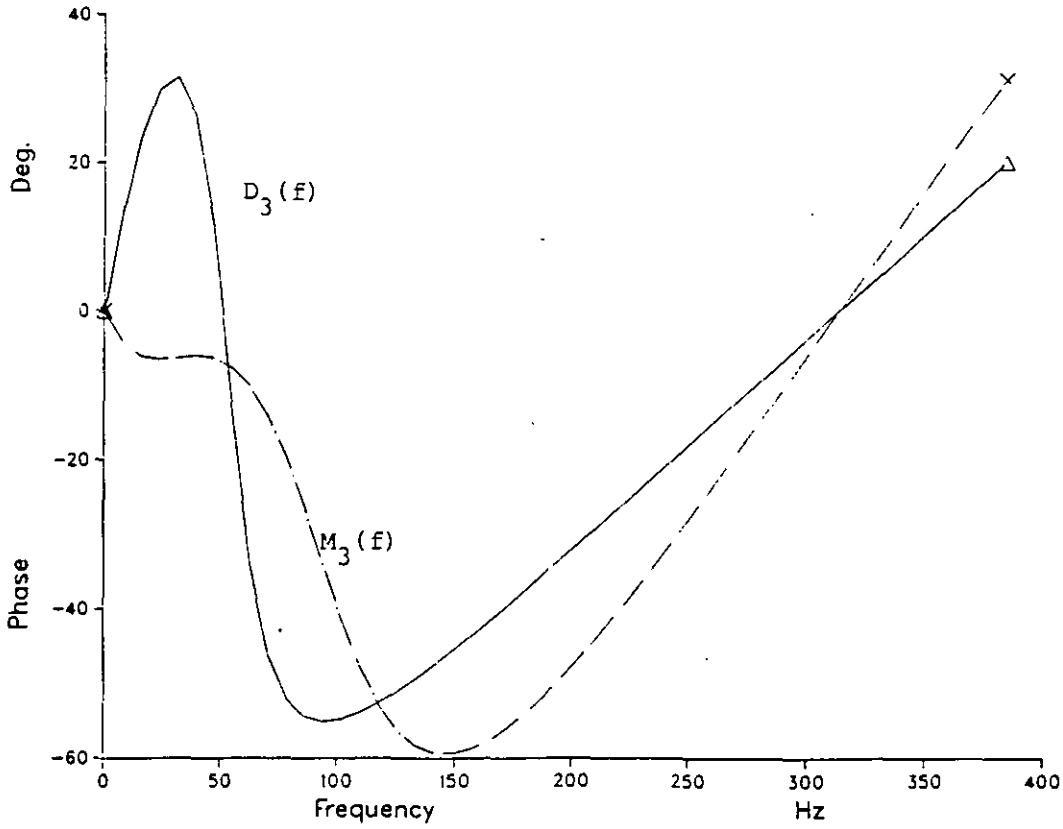

b

Fig. 4.7 Frequency response for system 3 when $\varepsilon = 0.5$

a - amplitude b - phase

APPENDIX I

CARRIER RECOVERY TECHNIQUES

I.1 Unmodulated carrier synchronisation

The unmodulated carrier, such as pilot tone, has to be transmitted within the same channel and at the same time in order to ensure the regenerated carrier can have, as close as possible, the same phase and frequency fluctuation as that of the received signal[191,192]. Moverover, any separation between the received signal spectrum and the pilot tone, especially in mobile radio environment, will result in irreducible error in the received data.

However, the requirement of the carrier recovery of unmodulated tone in the presence of a white Gaussian noise is a bandpass filter (BPF) or a phaselocked loop (PLL), which rejects as possible of the noise components outside its bandwidth as shown in Figure I.1. Let r(t) be the received signal, that is given by

$$r(t) = a(t)e^{j\theta(t)} \qquad \text{I.1}$$

where a(t) is the received signal envelope which may be given by

$$a(t) = ((1 + n_1(t)^2 + n_2(t)^2)^{\frac{1}{2}} \qquad \text{I.2}$$

where $n_1(t)$ and $n_2(t)$ are the inphase and quadrature components of the

additive noise each process zero mean and same variance, $j = \sqrt{-1}$ and $\theta(t)$ is the received signal phase. It is merely a matter of convenience to refer that the inphase and quadrature components of the noise and their statistical properties, jointly, with respect to the signal phase are not affected by the rotation of the coordinates. Also, by assuming that the transfer function of the BPF (or PLL) is symmetric about f_o, the central frequency, and the lowpass equivalent impulse response is h(t), then the output is given by

$$r'(t) = \int_{-\infty}^{\infty} h(\tau) r(t-\tau) d\tau \qquad \text{I.3}$$

where h(t) is assumed to be complex-valued. Then r'(t) can be rewritten as

$$r'(t) = a'(t) e^{j\theta'(t)} \qquad \text{I.4}$$

where a'(t) and $\theta'(t)$ are the envelope and phase of the output signal respectively. Thus, the phase error e(t) is given by

$$e(t) = \theta'(t) - \theta(t)$$

$$= \tan^{-1}\left(\frac{\mathrm{Im}(r'(t) r^*(t))}{\mathrm{Re}(r'(t) r^*(t))} \right) \qquad \text{I.5}$$

where $r^*(t)$ is the complex conjugate of r(t), Im(x) and Re(x) refer to the imaginary and real parts of the complex-valued x. In case of time-invariant channel and high signal-to-noise ratio, the phase error is relatively small so that $\tan^{-1}(x) = x$. The gain of the BPF (or PLL) is always regarded as unity in the center of its passband. Therefore, the variance of the phase jitter can be calculated as

$$P_{var} = 2N_o \int_{-\infty}^{\infty} |H(f)|^2 \, df$$

$$= 2N_o B \qquad \text{I.6}$$

where B is the two-sided equivalent noise bandwidth of BPF (or PLL) that is given by

$$B = \int_{-\infty}^{\infty} |H(f)|^2 \, df \qquad \text{I.7}$$

N_o is the noise power spectral density and $|H(f)|$ is the modulus of H(f) which is the BPF (or PLL) transfer function.

The result obtained in Equation I.6 represents a phase variance of point-to-point communication of stationary stations where the only impairment is the additive noise and probably long normal fading. While in mobile radio environment, the received signal suffers from Rayleigh fading, so it has rapidly faded envelope and rapidly fluctuated phase and time delay with respect to their means[10]. In such circumstances the PLL will no more cope with the signal unless it is provided with similar to hard limiter/discrimator or tanlock techniques[181,182]. Furthermore, the Rayleigh fading cannot be avoided by introducing high signal-to-noise ratio since it is independent on it[12]. However, in this case Equation I.5 can be determined according to the vector diagram, that is shown in Figure I.2, as

$$e(t) = \tan^{-1} \left(\frac{n_2(t)}{a(t) + n_1(t)} \right) \qquad \text{I.8}$$

where a(t) is the amplitude of the received signal before the addition of the noise, $n_1(t)$ and $n_2(t)$ are the inphase and quadrature noise

components that are uncorrelated with zero mean and power spectral density $\frac{1}{2} N_o$. Moreover, a(t) is affected by Rayleigh fading through the transmission path. The statistical nature of the noise components are not affected by the rotation of the coordinates even in mobile radio communication. It is eventually clear from Figure I.2 that all vectors rotate in the same angular speed $(\omega_c \pm \omega_d)$, where ω_c and ω_d are the carrier and Doppler shift angular frequencies respectively. The bandwidth of the required BPF is, now, as wide as twice the Doppler frequency at least. It is, however, difficult to analyse Equation I.8 in such an environment, but it is likely to assume at high signal-to-noise ratio $\tan^{-1}x = x$ for small value of x. Accoding to this assumption the following inequality is valid

$$\int_{-\infty}^{\infty} |a(t)|^2 \, dt >> \sigma^2 \qquad \text{I.9}$$

where σ^2 is the noise variance. Also, average power at input of the transmission path is equal to the average power at its output taken for a very long time (see Chapter 5). Therefore, the mean square value of the signal amplitude at input and output of the BPF approaches unity. Consequently, the result of these assumptions leads, hopefully, to Equation I.6.

In both cases described above, for carrier recovery of unmodulated signal, an ideal channel has been assumed. Also, the minimum bandwidth of the required BPF (or PLL) is, for example, twice the maximum Doppler frequency (10-12). Nevertheless, any bandwidth reduction beyond this limit leads to:-

i) Inability to track unstable received signal such as in mobile radio enviroment.

ii) Distort the symmetry condition, that has been assumed as necessary to obtain the result of equation I.6.

The expression of the phase jitter variance in terms of signal-to-noise ratio (ψ), for data transmission is given by[2,170, 199]

$$P_{var} = BT/2\psi \qquad I.10$$

where T is the sample duration.

I.2 Carrier Recovery for a modulated signal

In the case of a carrier modulated by zero-mean signal, such as digital data, the received signal plus noise can be expressed as[2]

$$r(t) = (a(t) + n(t))e^{j\theta(t)} \qquad \text{I.11}$$

where

$$a(t) = \int_{i=-\infty}^{\infty} s_i \, y(t - iT)\, dt \qquad \text{I.12}$$

$j = \sqrt{-1}$, $\theta(t)$ covers the received signal phase and/or frequency, s_i is the data sequence and $y(t)$ the baseband channel impulse response. Moreover, $n(t)$ is the additive noise which is given by

$$n(t) = n_i(t) + j\, n_2(t) \qquad \text{I.13}$$

where $n_1(t)$ and $n_2(t)$ are statistically independent Gaussian noise components that process zero mean and the same variance with two-sided power spectral density of $\frac{1}{2} N_o$ (1,109). The baseband signal (a(t)) does not possess a carrier component, its mean value is zero, and, of course, its mean square value is given by

$$E\,[a^2\,(t)] = \int_{-\infty}^{\infty} a^2(t)\, dt \qquad \text{I.14}$$

where E[x] is the expectation process of x. The transmission path together with the filtering processes and linear modulator at the transmitter, and filtering processes and linear demodulator at the receiver form the baseband channel. This channel has a Rayleigh distribution function in mobile radio communication (Chapter 3).

Different methods are available for generating a reference carrier from a suppressed carrier received signal, one of them is discussed here.

I.2.1 Squaring method

The method is employed in carrier recovery where a pulse amplitude modulated signal with suppressed carrier (PAM) or a phase-shift-keyed (PSK) signal is used. The popular carrier-phase recovery circuit is shown in Figure I.3, that consist of two band pass filters A(f) and B(f), squaring device and frequency dividing by 2 circuits. The filter A(f) is the receiver bandpass filter whose significant properties has been discussed in Chapter 3. The received signal is squared to remove the modulation, the resultant signal, which is double frequency term, is tracked by a bandpass filter B(f) (or a phase-locked loop or otherwise a combination of them[12,197,198]). The bandwidth of filter B(f) is 4 x maximum Doppler frequency in mobile radio environment[12].

The reference carrier can be obtained by passing r'(t) through an infinite-gain clipper[2,12,201,202], or through zero threshold comparator that can remove the amplitude fluctuations. The square-waveform at the output of the clipper (or comparator) can derive a frequency devider circuit, such as D-type flip-flop, which halves the frequency and the phase [2,201,202]. Therefore, the phase error is given by

$$e(t) = \frac{1}{2} \tan^{-1}\left(\frac{I_m(r'(t)\ (r^*(t))^2)}{R_e(r'(t)\ (r^*(t))^2)} \right)$$

$$= \theta'(t) - \theta(t) \qquad \text{I.15}$$

where, in this case, $r^*(t)$ is the complex-conjugate of $r(t)$,

$$r'(t) = \int_{-\infty}^{\infty} b(\tau) r^2 (t-\tau) d\tau \qquad \text{I.16}$$

and $b(t)$ is the impulse response of the equivalent lowpass of the bandpass filter whose transfer function is $B(f)$. The data sequence s_i (in Equation I.12) can equally likely have any of the two possible values ± 1. By assuming the channel is ideal with zero intersymbol interference, then for high signal to noise ratio $\tan^{-1}(x) = x$. Hence the variance of the phase jitter is given by[2,170,199]

$$P_{var} = ((2N_o)^2 + 2\ N_o) \int_{-\infty}^{\infty} |H(f)|^2\ df$$

$$= 2\ N_o B(1 + 2N_o) \qquad \text{I.17}$$

where B is the noise equivalent bandwidth of the bandpass filter (or PLL) whose transfer function is $B(f)$.

The application is assumed here for a digital data transmission at a rate of $1/T$ symbols per second. The minimum (Nyquist) bandwidth for a signal of such nature, assuming double-sideband modulation of the carrier, is $\frac{1}{T}$ Hz. Therefore, the signal-to-noise ratio can be given as $\psi = T/4N_o$, and Equation I.17 becomes

$$P_{var} = (BT/2\psi) S^{-1} \qquad \text{I.18}$$

where

$$S = 1/(1 - \frac{1}{2\psi}) \qquad \text{I.19}$$

and is called the squaring loss. The difference between Equation I.18 and Equation I.10 is the factor S, where at high signal-to-noise ratio S approach 1 and the same result can be obtained from the two equations.

Fig. I.1 Carrier recovery system of unmodulated carrier

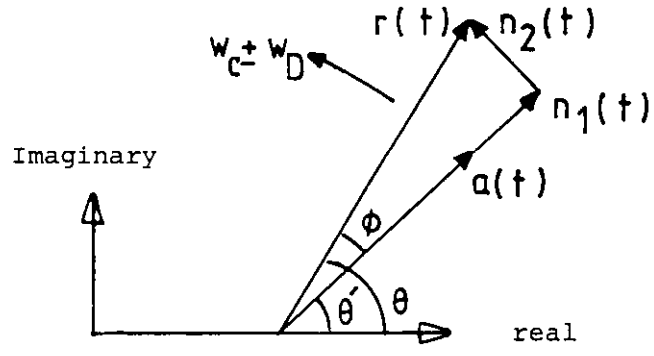

Fig. I.2 Vector diagram

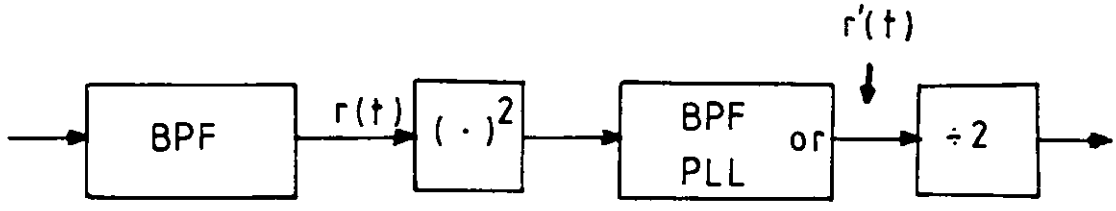

Fig. I.3 Squaring/filtering/dividing by 2 carrier recovery system

APPENDIX J

MATHEMATICAL ANALYSIS OF CHANNEL ESTIMATORS

J.1 FFCE Step-Size

The FFCE has been presented in Chapter 6. It is necessary here to induce the step-size by which the estimator controls its output. The estimator generates the error signal by subtracting the estimated signal r'_i from the received signal (Equation 6.8) or

$$e_i = r_i - r'_i \qquad \text{J.1}$$

(neglecting any delay required by the detector), where

$$r_i = \sum_{\ell=0}^{L-1} s_{i-\ell} y_{i,\ell} + \omega_i \qquad \text{J.2}$$

and

$$r'_i = \sum_{\ell=0}^{L-1} s'_{i-\ell}\, y'_{i-1,\ell} \qquad \text{J.3}$$

All parameters used here are defined in Chapter 6. The step-size needs to be added to Y'_{i-1} to give Y'_i the estimate of Y_i is given by

$$\Delta_{i,\ell} = be_i\, (s'_{i-\ell})^* \quad \text{for } \ell=0,\ 1,\ ..,\ L-1 \qquad \text{J.4}$$

$$= be_i (S'_i)^*$$

where

$$S'_i = [s'_i \quad s'_{i-1} \; s'_{i-2} \quad \cdots \; s'_{i-L+1}] \qquad \text{J.5}$$

and $(x)^*$ means the complex-conjugate of x. Thus

$$y'_{i,\ell} = y'_{i-1,\ell} + \Delta_{i,\ell} \qquad \text{for } \ell=0,1, \ldots,L-1 \qquad \text{J.6}$$

In order to analyse the operation of FFCE, it is necessary to expand and analyse $\Delta_{i,\ell}$, by using Equation J.1 to J.3, as

$$\Delta_{i,0} = b[\sum_{\ell=0}^{L-1} s_{i-\ell} \, y_{i,\ell} + \omega_i - \sum_{\ell=0}^{L-1} s'_{i-1} \; y'_{i-1,\ell}](s'_i)^*$$

$$= b|s'_i|^2 \; (y_{i,0} - y'_{i-1,0}) + u_{i,0} + \omega'_{i,0} \qquad \text{J.7}$$

where, in general, $s'_{i-\ell} = s_{i-\ell}$ from the basic assumption of Chapter 6, $|s_i|$ is the modulus of s_i,

$$\omega'_{i,0} = b(s'_i)^* \, \omega_i \qquad \text{J.8}$$

is the noise component in $y'_{i,0}$, and

$$u_{i,0} = b(s'_i)^* \sum_{\ell=1}^{L-1} (s_{i-\ell} \, y_{i,\ell} - s'_{i-} \; y'_{i-1,\ell}) \qquad \text{J.9}$$

is the intersymbol interference error signal component.

Similarly

$$\Delta_{i,1} = b|s'_{i-1}|^2 \ (Y_{i,1} - y'_{i-1,1}) + u_{i,1} + \omega'_{i,1} \qquad \text{J.10}$$

$$\omega'_{i,1} = b(s'_{i-1})^* \ \omega_i \qquad \text{J.11}$$

and

$$u_{i,1} = b(s'_{i-1})^* \ [s_i y_0 - s'_i \ y'_{i-1,0} + \sum_{\ell=2}^{L-1} (s_{i-\ell} y_{i,\ell} - s'_{i-\ell} y'_{i-1,\ell})] \qquad \text{J.12}$$

For further analysis, the other components can be derived as

$$\Delta_{i,k} = b|s'_{i-k}|^2 (y_{i,k} - y'_{i-1,k}) + u_{i,k} + \omega'_{i,k} \qquad \text{J.13}$$

$$\omega'_{i,k} = b(s'_{i-k})^* \ \omega_i \qquad \text{J.14}$$

and

$$u_{i,k} = b(s'_{i-k})^* \ [\sum_{\ell=0}^{L-1} (s_{i-\ell} \ y_{i,\ell} - s'_{i-\ell} \ y'_{i-1,\ell})$$

$$-[(s_{i-k} \ y_{i,k} - s'_{i-k} \ y'_{i-1,k})] \qquad \text{J.15}$$

where k = 2,3, ..., L-1. The last three equations represent the general solution, when

$$k = 0,1, \ldots, L-1 \qquad \text{J.16}$$

Clearly, from EquationsJ.7 to J.15, the major impairments are the noise and the intersymbol interference error signal components. In case of a constant envelope signal such as (4 or 8-level PSK) $|s_{i-k}|^2 = |s'_{i-k}|^2 = c$, where c is constant for all values of i and k. Then the value of b can be selected such that

$$0 < b \leq \frac{1}{c} \qquad \text{J.17}$$

But, in case of 16-points (or more) QAM signal it is, however, necessary to multiply by the reciprocal of s'_{i-k} to obtain the corresponding estimate $y'_{i,k}$ and not by $(s'_{i-k})^*$, for k = 0,1,..., L-1. Evidently, from Equation J.14 and J.15, multiplication by $(s'_{i-k})^*$ would increase the noise and the intersymbol interference error signals, while multiplying by the reciprocal of (dividing by) s'_{i-k} might reduce the effect of the impairments. By neglecting the noise and intersymbol interference error signals then

$$y'_{i,\ell} = y'_{i-1,\ell} + a(y_{i,\ell} - y'_{i-1,\ell}) \quad \text{for } \ell = 0,1, \ldots, L-1 \qquad \text{J.18}$$

or

$$Y'_i = Y'_{i-1} + a(Y_i - Y'_{i-1}) \qquad \text{J.19}$$

where a is the step-size factor given by

$$a = bc \leq 1 \qquad \text{J.20}$$

and it is constant.

J.2 Feedback Channel Estimator (FBCE)

By, also, neglecting the delay required by the detector, the feedback estimator obtains for each sample r_{i+L} a "raw" estimate ψ_i of Y_i which is used to update the stored estimate Y'_{i-1}. When $Y'_{i-1} \cong Y_i$ there is negligible noise and $\psi_i \cong Y_i$, where $\cong$ means approximately equal. Let P_i be the (L+1)x(L+1) matrix given by[203,205]

$$P_i = \begin{vmatrix} s_i & s_{i+1} & s_{i+2} & \cdots & s_{i+L} \\ s_{i-1} & s_i & s_{i+1} & \cdots & s_{i+L-1} \\ s_{i-2} & s_{i-1} & s_i & \cdots & s_{i+L-2} \\ \cdot & \cdot & \cdot & & \cdot \\ \cdot & \cdot & \cdot & & \cdot \\ s_{i-L} & s_{i-L+1} & s_{i-L+2} & \cdots & s_i \end{vmatrix} \qquad \text{J.21}$$

and let D_i, E_i and F_i be the (L+1)x(L+1) matrices all obtained from P_i and are given as follows

(diagonal matrix)

$$D_i = \begin{vmatrix} s_i & 0 & 0 & \cdots & 0 \\ 0 & s_i & 0 & \cdots & 0 \\ 0 & 0 & s_i & \cdots & 0 \\ \cdot & \cdot & \cdot & & \cdot \\ \cdot & \cdot & \cdot & & \cdot \\ 0 & 0 & 0 & \cdots & s_i \end{vmatrix} \qquad \text{J.22}$$

(Upper triangular matrix)

$$E_i = \begin{vmatrix} 0 & s_{i+1} & s_{i+2} & \cdots & s_{i+L} \\ 0 & 0 & a_{i+1} & \cdots & s_{i+L-1} \\ 0 & 0 & 0 & \cdots & . \\ . & . & . & & . \\ . & . & . & & . \\ 0 & 0 & 0 & \cdots & 0 \end{vmatrix} \qquad \text{J.23}$$

(Lower triangular matrix)

$$F_i = \begin{vmatrix} 0 & 0 & 0 & \cdots & 0 \\ s_{i-1} & 0 & 0 & \cdots & 0 \\ s_{i-2} & s_{i-1} & 0 & \cdots & 0 \\ . & & & & . \\ . & & & & . \\ s_{i-L} & s_{i-L+1} & s_{i-L+2} & & 0 \end{vmatrix} \qquad \text{J.24}$$

Clearly

$$P_i = D_i + E_i + F_i \qquad \text{J.25}$$

and D_i is nonsingular as long as $s_i \neq 0$. Now, suppose that

$$R_i = [r_i \; r_{i+1} \; r_{i+2} \cdots r_{i+L}] \qquad \text{J.26}$$

and

$$W_i = [w_i \; w_{i+1} \; w_{i+2} \cdots w_{i+L}] \qquad \text{J.27}$$

then

$$R_i = P_i Y_i + W_i$$

$$= (D_i + E_i + F_i) Y_i + W_i \qquad \text{J.28}$$

The essential procedure of the estimator is to make use of one or more of previously obtained stored estimates of Y_i, together with a knowledge of E_i and F_i originated from the $\{s_i'\}$ which are assumed to be correctly detected to form an estimate B_i of $(E_i + F_i) Y_i$. The estimator then subtracts B_i from R_i to give

$$A_i = R_i - B_i$$

$$= D_i Y_i + (E_i + E_i) Y_i - B_i + W_i \qquad \text{J.29}$$

By multiplying Equation J.29 by D_i^{-1} to give the row estimate

$$\Psi_i = A_i D^{-1}$$

$$= Y_i + [(E_i + F_i) Y_i - B_i] D_i^{-1} + W_i D_i^{-1} \qquad \text{J.30}$$

From the definition of D_i, D_i^{-1} is, also, a diagonal matrix with each element along the main diagonal equal to the reciprocal of the corresponding diagonal elements of the original matrix D_i. Now,if

$$B_i \cong (E_i + F_i) Y_i \qquad \text{J.31}$$

then

$$\psi_i \cong Y_i + W_i D_i^{-1} \qquad \text{J.32}$$

The components of Ψ_i are used to update Y'_{i-1} the stored estimate of Y_{i-1} to give

$$Y'_i = (1-b)Y'_{i-1} + b\,\Psi_i$$

$$= Y'_{i-1} + b(\Psi_i - Y'_{i-1}) \qquad \text{J.33}$$

This equation is identical to Equation J.19 for FFCE. The factor b, in Equation J.33, represents the step-size of the estimator on the provision $0 < b << 1$. b is assumed constant, but it is not necessarily so[203,205 Champter 6]. However, the smaller the value of b, the smaller is the effect of the additive noise on Y'_i but the slower the rate of response of Y'_i to changes of Y_i[205]. The estimator generates the error vector G_i such that

$$G_i = \Psi_i - Y'_{i-1} \qquad \text{J.34a}$$

$$= [g_{i,0}\ \ g_{i,1}\ \ g_{i,2} \cdots g_{i,L}] \qquad \text{J.34b}$$

and adds bG_i to Y'_{i-1} to give Y'_i.

The important differences between this estimator (FBCE) and the feed-forward estimator (FFCE) are:

i) The delay, of LT seconds, required by FBCE to obtain Y_i on the receipt of r_{i+L}, while FFCE can give an estimation of Y'_i directly, or more precisely, possible before one element duration delay (T),

with simple prediction techniques. In mobile radio communication, any delay degrades the performance of either estimator. Knowing that the detection delay is neglected, including it would make the system inferior, in case of FBCE.

ii) At the same time the FFCE deteriorates by the existence of the interfering error (described above and is neglected in Equations J.18 and J.19), while FBCE substracts it, as that is clear from Equations J.29 to J.32.

The FBCE just described can be implemented in many different methods [109, 203, 205], and is based on nonlinear (decision) feedback filter shown in Figure 6.3. The complexity of the two FBCE estimates presented elsewhere[205] require a number of multiplication processes of $\frac{1}{2}(L + 1)(L + 2) + 2L+1$ for estimator 1 and $4L + 2$ for Estimator 2.

J.3 Modifications of FBCE

The FBCE, described in Section J.2, requires a delay of LT seconds which degrades its performance (severly in case of mobile radio communications), while the FFCE degrades by the existence of the intersymbol interference error signal components. Where L is the number of components in the sampled impulse response of the channel and T is the duration in seconds. Any one of them would be optimum if its degradation could be deducted.

The system about to be introduced uses the power of the FBCE in reducing the intersymbol interference error signal components $\{u_{i,k}\}$ (given by Equation J.15 in case of FFCE) and no delay is required here. Let X_i be the L-component row vector given by

$$X_i = [x_{i,0} \quad x_{i,1} \quad x_{i,2} \cdots \quad x_{i,L-1}] \qquad \text{J.35}$$

whose k^{th} component is given by

$$x_{i,k} = r'_i - s'_{i-k}\, y'_{i-1,k} \qquad \text{J.36}$$

where r'_i is the estimated signal given by Eqaution J.3. Also, let Z_i be a (LxL) diagronal matrix given by

$$Z_i = \begin{vmatrix} z_{i,0} & 0 & 0 & \cdots & 0 \\ 0 & z_{i,1} & 0 & \cdots & 0 \\ 0 & 0 & z_{i,2} & \cdots & 0 \\ \cdot & \cdot & \cdot & & \cdot \\ \cdot & \cdot & \cdot & & \cdot \\ \cdot & \cdot & \cdot & & \cdot \\ 0 & 0 & 0 & & z_{i,L-1} \end{vmatrix} \qquad \text{J.37}$$

whose k^{th} row component is given by

$$z_{i,k} = r_i - x_{i,k} \qquad \text{J.38}$$

where r_i is the received signal given by J.2. The row estimate ψ_i of Y'_i can be obtained as

$$\psi_i = (S'_i)^{-1} Z_i \qquad \text{J.39}$$

where $(S'_i)^{-1}$ is L-component row vector derived from S'_i, Equation J.5, by taking the reciprocal of the corresponding elements of S'_i. The components of ψ_i are used to update Y'_{i-1} the stored estimate of Y_{i-1} to give

$$\begin{aligned} Y'_i &= (1-b)\, Y'_{i-1} + b\psi_i \\ &= Y'_{i-1} + b\,(\psi_i - Y'_{i-1}) \end{aligned} \qquad \text{J.40}$$

where $0 < b < 1$. The analysis of Equation J.39 gives the same result that defined by Equation J.32 which is now

$$\psi_i \cong Y_i + W_i\, D_i^{-1} \qquad \text{J.41}$$

where

$$D^{-1} = \begin{vmatrix} s'^{-1}_i & 0 & 0 & \cdots & 0 \\ 0 & s'^{-1}_{i-1} & 0 & \cdots & 0 \\ 0 & 0 & s'^{-1}_{i-2} & \cdots & 0 \\ \vdots & \vdots & \vdots & & \vdots \\ 0 & 0 & 0 & & s'^{-1}_{i-L+1} \end{vmatrix} \qquad \text{J.42}$$

Hence, the difference between ψ_i in Equation J.23 and ψ_i defined by Equation J.32 lies in the derivation of D_i^{-1}. D_i^{-1} in this case, Equation J.42, contains already detected symbols, while D_i^{-1} in Equation J.32 (which is obtained by taking the reciprocal of the corresponding elements of D_i that has been derived from P_i in Equation J.21) contains symbols which are still not yet detected.

This estimator needs L feedback filters each having (L-1) coefficients (tap gain), all are taken from estimated sampled impulse response of the channel (estimator outputs). The general form of these filters is defined by Equation J.36. Therefore, the number of multiplication processes employed in this estimator is (L+1)L. However, it is possible to use two L-coefficient filters arranged in such away by a suitable designing method to give a complete operation with 4L multiplication processes.

The system is further developed by using a dynamic feedforward filter, feedback control system and static feedforward filter. The significance of these systems are discussed in Section 6.4. The whole operation can be analysed as follows:-

The output signal from the dynamic digital filter is given by

$$\phi'_i = r_i - \sum_{\ell=1}^{L-1} s'_{i-\ell}\, y'_{i-1,\ell} \qquad \text{J.43}$$

The equation is multiplied by $(s'_i)^{-1}$, thus

$$\phi_i = \phi'_i (s'_i)^{-1}$$

$$= y_{i,0} + (s'_i)^{-1} \sum_{\ell=1}^{L-1} (s_{i-\ell}\, y_{i,\ell} - s'_{i-\ell}\, y'_{i-1,\ell}) + w_i (s'_i)^{-1} \qquad \text{J.44}$$

This signal is fed to the digital control system and its output becomes

$$q'_i = \phi_i * c_i \qquad \text{J.45}$$

where * means convolution process and c_i is sampled impulse response of the digital control system (see Equations 6.12 to 6.14). The sequence obtained from equation J.45 is arranged in (LxL) component diagonal matrix given by

$$Q'_i = \begin{vmatrix} q'_i & 0 & 0 & \cdots & 0 \\ 0 & q'_{i-1} & 0 & \cdots & 0 \\ 0 & 0 & q'_{i-2} & \cdots & 0 \\ \vdots & \vdots & \vdots & & \vdots \\ 0 & 0 & 0 & & q'_{i-L+1} \end{vmatrix} \qquad \text{J.46}$$

Finally, the row estimate ψ_i can be given by

$$\psi_i = H_o Q'_i \qquad \text{J.47}$$

The components of ψ_i are used to update Y'_{i-1} according to Equation J.40.

APPENDIX K

List of Computer Programs

```
c     This program calculates the roots of a polynomial using the
c     available Subroutine(C02ADF). Then, it looks for roots with
c     values greater than 1 (or outside the unit circle of the z-
c     plane) and changes them with reciprocal of their complex-
c     conjugates. Rearranges the new (modified) polynomial.
      integer t,nin,nout,ifail,n,nn,nof
      real title(7)
      double precision ar(60),ac(60),rez(60),imz(60),pq(60),
     ,yr(2),yim(2),r1r(60),r1im(60),r2r(60),r2im(60),sr(60),sim(60),
     ,pi,x01aaf,x02aaf,p1,a1p1,p15,zero,tol
      data p1/0.1e0/,a1p1/1.1e0/,p15/0.15e0/,zero/0.0e0/
      open(2,file='rsdft1',status='old',form='formatted',access=
     ''sequential')
      data nin /5/,nout /6/
      open(nout,file='FilterF1')
      print*,'Please give a title to the polynomial'
      print*,'Please input ; expo ;to avoid over/under flow'
      read (nin,99999) title
c     write (nout,99998) (title(i),i=1,6)
      pi=p1*x01aaf(p1)
      tol=x02aaf(p1)
c     write (nout,99995)
20    t=0
      rez(1)=p15
      imz(1)=zero
      ifail=1
      print*,'State howmany coefficients are there in the polynomial'
      read (nin,99997) n
      if(n.le.0) go to 280
      nn=n-1
      print*,'Then give the value of each coefficient'
      print*,'Real part          Imaginary part'
c     read*, (ar(i),ac(i),i=1,n)
      read (2,*) (ar(i),ac(i),i=1,n)
      read(2,*)bcz
      write (nout,99998) (title(i),i=1,6)
      write (nout,99995)
      write (nout,99991)nn
      do 40 i=1,n
40    write (nout,99994) ar(i),ac(i)
      write (nout,99990)
60    nof=n-1
      call c02adf(ar,ac,n,rez,imz,tol,ifail)
      if(ifail.ne.0) go to 140
80    i=nof+1
100   i=i-1
      if(i.lt.n) go to 120
      if(abs(rez(i)).lt.1.0e-8) rez(i)=0.0
      if(abs(imz(i)).lt.1.0e-8) imz(i)=0.0
      pq(i)=sqrt(rez(i)**2+imz(i)**2)
      write (nout,99994) rez(i),imz(i),pq(i)
      go to 100
120   if(n.ne.1) go to 60
      go to 180
140   write (nout,99993)ifail
      if(t.eq.20.or.ifail.ne.2) go to 160
      t=t+1
      rez(1)=rez(1)*a1p1*cos(float(t)*pi)-imz(1)*a1p1*
     *sin(float(t)*pi)
      imz(1)=rez(1)*a1p1*sin(float(t)*pi)+imz(1)*a1p1*
```

```
     *cos(float(t)*pi)
      go to 80
160   n=n-1
      write (nout,99992) n
180   write (nout,99989)
      do 200 k=1,nn
      if(pq(k).gt.1.)then
      rez(k)=rez(k)/pq(k)**2
      imz(k)=imz(k)/pq(k)**2
      endif
200   continue
      do 220 k=1,nn+1
      sr(k)=0.0
      sim(k)=0.0
      r1r(k)=0.0
      r1im(k)=0.0
      r2r(k)=0.0
      r2im(k)=0.0
220   r2im(k)=0.0
      sr(1)=1.0
      yr(1)=1.0
      yim(1)=0.0
      do 260 k=1,nn
      k1=k+1
      yr(2)=-rez(k)
      yim(2)=-imz(k)
      do 240 l=1,k1
      l1=l+1
      r1r(l)=yr(1)*sr(l)-yim(1)*sim(l)
      r1im(l)=yr(1)*sim(l)+yim(1)*sr(l)
      r2r(l1)=yr(2)*sr(l)-yim(2)*sim(l)
240   r2im(l1)=yr(2)*sim(l)+yim(2)*sr(l)
      do 260 l=1,k1
      sr(l)=r1r(l)+r2r(l)
260   sim(l)=r1im(l)+r2im(l)
      do 270 ik=1,nn+1
      if(abs(sr(ik)).lt.1.0e-8) sr(ik)=0.0
      if(abs(sim(ik)).lt.1.0e-8) sim(ik)=0.0
      sr(ik)=sr(ik)/bcz
      sim(ik)=sim(ik)/bcz
270   write (nout,99988) sr(ik),sim(ik)
      go to 20
280   stop
99999 format(6a4,1a3)
99998 format(4(1x/),1h,5a4,1a3,7hresults/1x)
99997 format(i2)
99996 format(1x,f10.7,7x,f10.7)
99995 format(1x//1x)
99994 format(1h,3(e13.6,2x))
99993 format(1h,12hError number,i3)
99992 format(1h,13hProgram fail,4x,10hPoly order,i3)
99991 format(17h0Polynomial order,i6/1h0,20hCoefficients of poly,
     ,6hnomial/1h0,3x,9hReal part,4x,14hImaginary part/)
99990 format(20h0Roots of polynomial/1h0,3x,9hReal part,4x,
     ,14hImaginary part,4x,7hModulus/)
99989 format(34h0The polynomail after modification/,1h0,3x,
     ,9hReal part,4x,14hImaginary part)
99988 format(1h,2(e13.6,2x))
      end
```

```
/*JOB SAM1B,EUELSM,ST=MFX,C=S,TI=1280,
/* PW=SEHR
FTN5,DB=0/PMD,L=0.
LIBRARY,PROCLIB.
NAG(FTN5).
LGO.
####S
      PROGRAM Q4AM
C     THIS PROGRAM SIMULATES THE 4-LEVEL QAM SYSTEM . NEAR-MAXIMUM
C     LIKELIHOOD DETECTOR, KNOWN AS SYSTEM S1D1, IS COMPARED WITH
C     NON-LINEAR EQUALIZER. THE CHANNEL IS SUBJECTED TO A RAYLEIGH
C     FADING IN MOBILE RADIO ENVIRONMENT.
C
C     EXPLANATION OF IMPORTANT COMPLEX-VALUED PARAMETERS:
C     REAL PART IMAGINARY PART          DETAILS
C     _________ _______________ ____________________________________
C     Y1        Y2              NONFADED CHANNEL IMPULSE RESPONSE
C     YR        YIM             FADED CHANNEL IMPULSE RESPONSE
C     Q1        Q2              RAYLEIGH FADING SIMULATOR OUTPUT
C                               SIGNAL
C     SR        SIM             TRANSMITTED DATA SYMBOL
C     R1        R2              THE RECEIVED SIGNAL
C     V1        V2              THE ADDITIVE GAUSSIAN NOISE
C     ____________________________________________________________
C
C     EXPLANATION OF SOME OTHER PARAMETERS
C     C1: ASSOCIATED COST WITH EACH VECTOR
C     P : STANDERD DEVIATION OF THE NOISE
C     IQ: SEED INTEGER NUMBER
C     SN: SIGNAL-TO-NOISE RATIO IN dB
C     ERM: BIT ERROR RATE IN S1D1
C     ERE: BIT ERROR RATE IN NLEQ
C     KK: NUMBER OF BIT PER SYMBOL
C
      DIMENSION
     * MA(2),IS(2),ISS(2),JS(2,2,2),JR(2,2,2),ISE(2),ISM(2),
     * SIM(-4:38),SR(-4:38),MXIM(-4:38),MXR(-4:38),JIS(2,-4:38),
     * WQ1(6),WQ2(6),RAY1(2),RAY2(2),AH(5),BH(5),MRT(4,4),
     * C1(4,-4:38),Q1(-4:38),Q2(-4:38),MMT(4,4),
     * Y1(4),Y2(4),YR(4,38),YIM(4,38),TC1(4,4),
     * ERM(22),SN(22),ERE(22)
      DIMENSION
     * XRC(4),XRC1(4,4),XIC(4),XIC1(4,4),CCC(4),CC1(16),MJR(4)
     *,XR(4,-4:38),XIM(4,-4:38),MM(4,-4:38),MR(4,-4:38),MJI(4)
     *,NXER(-4:38),NXEI(-4:38),KMNV(4),NKV(4)
     * ,FQ1(0:4),FQ2(0:4),FDQ1(4),FDQ2(4)
      DIMENSION INMS(2),IENS(2),JMS(0:3,2)
      OPEN(1,FILE='OUTPUT')
      DATA JS/1,1,-1,-1,1,-1,1,-1/,
     *  JR/-1,-1,1,1,-1,1,-1,1/
      DATA JMS/0,0,1,1,0,1,0,1/
C
C     IMPULSE RESPONSE OF THE NONFADING CHANNEL
C     DATA Y1/1.0,0.222579,-0.11086,0.538306E-2/
C     DATA Y2/0.0,-0.218666,-0.981492E-1,0.646351E-2/
      DATA Y1/1.0,0.552991,0.559095E-1,-0.395242E-2/
      DATA Y2/0.0,-0.101986,-0.100619,-0.875349E-2/
C     DATA Y1/1.0,0.0,0.0,0.0/
C     DATA Y2/0.0,0.0,0.0,0.0/
C
```

```
C       FIFTH ORDER LOWPASS BESSEL DIGITAL FILTER COEFFICIENTS
C
        DATA AH/0.959,-0.574,0.362,-0.1054,0.0131/
        DATA BH/0.7502,-0.63015,0.28443,-6.54E-2,6.24E-3/
C
C       DATA NOUT/1/
C
        iq=38
        II=22
        I1=0
        KK=2
C      KK MUST NOT EXCEED THE VALUE OF 2
        FD=100
        KJ1=38
C
C       THE VALUE OF FD=100,50 OR 25 HZ AND THERE IS ESPECIAL
C       TREATMENT WHEN FD=75 HZ
C
        JJ=1+INT(10E4/KJ1)
        MFD=INT(100/(FD-0.005))
C       MFD=3
        JJ=INT(JJ/MFD)
        LL=4
        LM=4
        M4=16
        PI=4.*ATAN(1.0)
C
C       INITIALIZE NAG-ROUTINES (G05DAF AND G05DDF) WITH SEED INTEGER
C
        CALL G05CBF(IQ)
        NUMBER=0
        DO 1 INM=1,2
        DO 1 MNI=1,2
        NUMBER=NUMBER+1
        MJR(NUMBER)=JS(INM,MNI,1)
1       MJI(NUMBER)=JS(INM,MNI,2)
C
C       INITIALIZE ALL PARAMERTERS FOR EACH VALUE OF THE SNR
C       (SIGNAL-TO-NOISE RATIO)
C
        DO 300 I=1,II
        DO 3 IO=-4,LL
        JIS(1,IO)=-1
        JIS(2,IO)=-1
        Q1(IO)=1.0
        Q2(IO)=0.0
        NXER(IO)=1
        NXEI(IO)=1
        SR(IO)=1.0
        SIM(IO)=1.0
        MXR(IO)=1
        MXIM(IO)=1
        DO 3 MV=1,LM
        C1(MV,IO)=1.0e6
        C1(1,IO)=0
        MR(MV,IO)=1
        MM(MV,IO)=1
        XR(MV,IO)=1.0
3       XIM(MV,IO)=1.0
        QF11=1.0
```

```
      QF21=0.0
      RAY1(2)=1.0
      RAY2(2)=0.0
      DO 4 KQ=2,6
      FQ1(KQ-2)=1.0
      FQ2(KQ-2)=0.0
      WQ1(KQ)=1.0
4     WQ2(KQ)=0.0
C
C
      WP=-0.05*(17.0+1.5*(I-1))
      P=1.414*10.**WP
      IEE=0
      IEM=0
      IE=0
      ICR=0
      LD2=0
      NIM2=0
      NIE2=0
      TSP=0.0
      TNP=0.0
C
C     GENERATE A BLOCK OF DATA SYMBOLS FOR EACH SAMPLE OF THE
C     RAYLEIGH FADING SIMULATOR OUTPUT. LINEAR INTERPOLATION
C     METHOD IS USED TO GENERATE Q1 AND Q2

C
      DO 250 J=1,JJ
C
C     GENERATE TWO NOISE RANDOM VARIABLES AS INPUTS TO THE
C     FIFTH ORDER LOWPASS BESSEL DIGITAL FILTER
C
      QF1=G05DDF(0.0,1.0)
      DFQ1=(QF1-QF11)/MFD
      QF2=G05DDF(0.0,1.0)
      DFQ2=(QF2-QF21)/MFD
C
C     SPECIAL TREATMENT WHEN FD=75 HZ
C
C     DO 20 KF=1,MFD
C     FQ1(KF)=G05DDF(0.0,1.0)
C     FQ2(KF)=G05DDF(0.0,1.0)
C20   CONTINUE
C     DO 25 KF=1,MFD
C     KF1=KF-1
C     FDQ1(KF)=FQ1(KF1)+0.25*(4-KF)*(FQ1(KF)-FQ1(KF1))
C25   FDQ2(KF)=FQ2(KF1)+0.25*(4-KF)*(FQ2(KF)-FQ2(KF1))
C
C     SAMPLE THE INPUT SIGNAL OF THE FILTER
C
      DO 200 NFD=1,MFD
C
C     FIFTH ORDER LOPASS BESSEL DIGITAL FILTER
C
      DO 31 KQ=1,5
      KQ1=KQ+1
      WQ1(KQ)=WQ1(KQ1)
31    WQ2(KQ)=WQ2(KQ1)
      RAY1(1)=RAY1(2)
      RAY2(1)=RAY2(2)
```

```
      WQ1(6)=QF11+DFQ1*NFD
      WQ2(6)=QF21+DFQ2*NFD
C     WQ1(6)=FDQ1(NFD)
C     WQ2(6)=FDQ2(NFD)
      RAY1(2)=0.0
      RAY2(2)=0.0
      DO 33 KQ=1,5
      KQ1=6-KQ
      WQ1(6)=WQ1(6)+BH(KQ)*WQ1(KQ1)
33    WQ2(6)=WQ2(6)+BH(KQ)*WQ2(KQ1)
      DO 35 KQ=1,5
      KQ1=7-KQ
      RAY1(2)=RAY1(2)+AH(KQ)*WQ1(KQ1)
35    RAY2(2)=RAY2(2)+AH(KQ)*WQ2(KQ1)
      DRQ1=(RAY1(2)-RAY1(1))/KJ1
      DRQ2=(RAY2(2)-RAY2(1))/KJ1
C
      DO 100 J1=1,KJ1
      J11=J1-1
C
C      DATA GENERATION AS BIT BY BIT RANDOMLY
C
      DO 40 K=1,KK
      SS=G05DAF(-1.0,1.0)
      IS(K)=INT(SIGN(1.05,SS))
      JIS(K,J1)=IS(K)
      MA(K)=(1+IS(K))/2
40    CONTINUE
C
C      DIFFERENTIAL ENCODING AND DATA MAPPING TO GENERATE SYMBOLS
C
C     L1=1+MA(1)
C     L2=1+MA(2)
      LD1=MA(2)+2*MA(1)
      LD1=LD1-LD2
      IF(LD1.LT.0)LD1=LD1+4
      LD2=LD1
      L1=1+JMS(LD1,1)
      L2=1+JMS(LD1,2)
      SR(J1)=JS(L1,L2,1)
      SIM(J1)=JS(L1,L2,2)
C
C      LINEAR INTERPOLATION IN RAYLEIGH FADING SIMULATION
C
      Q1(J1)=RAY1(1)+J1*DRQ1
      Q2(J1)=RAY2(1)+J1*DRQ2
C     Q1(J1)=1.0
C     Q2(J1)=0.0
C
C     CALCULATE THE TRANSMITTED SIGNAL POWER
C
      PR=(SR(J1)*Q1(J1)-SIM(J1)*Q2(J1))**2
      PIM=(SR(J1)*Q2(J1)+SIM(J1)*Q1(J1))**2
      TSP=TSP+PR+PIM
C
C     RAYLEIGH FADING CHANNEL
C
      DO 50 L=1,LL
      L1=J1-L+1
      YR(L,J1)=Y1(L)*Q1(L1)-Y2(L)*Q2(L1)
```

```
50      YIM(L,J1)=Y1(L)*Q2(L1)+Y2(L)*Q1(L1)
C
C       START-UP TRANSMISSION
C
        R1=0.0
        R2=0.0
        DO 60 L=1,LL
        L1=J1-L+1
        R1=R1+YR(L,J1)*SR(L1)-YIM(L,J1)*SIM(L1)
60      R2=R2+YR(L,J1)*SIM(L1)+YIM(L,J1)*SR(L1)
C
C       ADDITIVE GAUSSIAN NOISE WITH 0 MEAN AND VARIANCE P**2
C
        V1=G05DDF(0.0,P)
        V2=G05DDF(0.0,P)
C
C       CALCULATE NOISE POWER
C
        TNP=TNP+V1*V1+V2*V2
        R1=R1+V1
        R2=R2+V2
C
C       DETECTION PROCESSES
C
C       FIRST...NONLINEAR EQUELISER (NLEQ)
C
        XRE=0.0
        XIE=0.0
        DO 65 L=2,LL
        L1=J1-L+1
        XRE=XRE+YR(L,J1)*NXER(L1)-YIM(L,J1)*NXEI(L1)
65      XIE=XIE+YR(L,J1)*NXEI(L1)+YIM(L,J1)*NXER(L1)
        ERX=R1-XRE
        EIX=R2-XIE
        YY=SQRT(YR(1,J1)**2+YIM(1,J1)**2)
        IF(YY.LT.0.01)YY=0.01
        XER=(YR(1,J1)*ERX+YIM(1,J1)*EIX)/YY
        XEI=(YR(1,J1)*EIX-YIM(1,J1)*ERX)/YY
        NXER(J1)=INT(SIGN(1.05,XER))
        NXEI(J1)=INT(SIGN(1.07,XEI))
C
C        THE NEAR MAXIMUM-LIKELIHOOD DETECTOR (S1D1)
C       ---------------------------------------------
C
C       CACULATE THE INTERSYMBOL INTERFERENCE FOR EACH OF THE M STORED
C       VECTORS. ALSO SUBTRACT THE LOWEST MINIMUM COST FROM THE OTHER
C       MINIMUM COSTS AND GIVE ZERO VALUE TO THE LOWEST COST.
C       EXPAND THE M STORED VECTORS TO 4M VECTORS AND CALCULATE THE
C       COST FOR EACH EXPANDED VECTOR.
C       SELECT M VECTORS ASSOSIATED WITH MINIMUM COST.
C       DISCARD THE NONSELECTED VECTORS BY SETTING THEIR COSTS TO VERY
C       HIGH VALUE.
C       STORE THE SELECTED VECTORS IN TEMPORARY STORES, SO THAT
C       NONE OF THEM COULD BE SELECTED MORE THAN ONCE, AND RETRIEVE
C       THEM WITH A RANKING METHOD SO THAT THE VECTOR ASSOCIATED WITH
C       THE LOWEST MINIMUM COST TAKES THE FIRST POSITION IN THE RANK.
C       TAKE THE FIRST COMPONENT OF THE FIRST VECTOR IN THE RANK TO
C       BE THE DETECTED DATA SYMBOL.
C
        MNK=0
```

```
      CXZ=C1(1,J11)
      DO 71 MV=1,LM
      C1(MV,J11)=C1(MV,J11)-CXZ
      XRC(MV)=0.0
      XIC(MV)=0.0
      DO 70 L=2,LL
      L1=J1-L+1
      XRC(MV)=XRC(MV)+YR(L,J1)*MR(MV,L1)-YIM(L,J1)*MM(MV,L1)
70    XIC(MV)=XIC(MV)+YR(L,J1)*MM(MV,L1)+YIM(L,J1)*MR(MV,L1)
      DO 71 NV=1,LM
      MNK=MNK+1
      XRC1(MV,NV)=YR(1,J1)*MJR(NV)-YIM(1,J1)*MJI(NV)
      XRC1(MV,NV)=R1-XRC(MV)-XRC1(MV,NV)
      XIC1(MV,NV)=YR(1,J1)*MJI(NV)+YIM(1,J1)*MJR(NV)
      XIC1(MV,NV)=R2-XIC(MV)-XIC1(MV,NV)
      CC1(MNK)=C1(MV,J11)+XRC1(MV,NV)**2+XIC1(MV,NV)**2
71    CONTINUE
      DO 80 KV=1,LM
      CCC(KV)=1.0E6
      DO 75 MNK=1,M4
75    CCC(KV)=AMIN1(CCC(KV),CC1(MNK))
      MNK=0
      DO 77 MV=1,LM
      DO 77 NV=1,LM
      MNK=MNK+1
      ACC1=ABS(CCC(KV)-CC1(MNK))
      IF(ACC1.LT.1.0E-9)THEN
      KMN1=MNK
      KMNV(KV)=MV
      NKV(KV)=NV
      ENDIF
77    CONTINUE
      DO 80 MV=1,LM
      KMN1=KMN1+4*(MV-1)
      IF(KMN1.GT.M4) KMN1=KMN1-M4
      CC1(KMN1)=1.0E6
80    CONTINUE
      DO 85 KV=1,LM
      DO 85 L=2,LL
      L1=J1-L+1
      MRT(KV,L)=MR(KMNV(KV),L1)
      MMT(KV,L)=MM(KMNV(KV),L1)
85    TC1(KV,L)=C1(KMNV(KV),L1)
      DO 90 KV=1,LM
      DO 90 L=2,LL
      L1=J1-L+1
      MR(KV,L1)=MRT(KV,L)
      MM(KV,L1)=MMT(KV,L)
90    C1(KV,L1)=TC1(KV,L)
      DO 95 KV=1,LM
      C1(KV,J1)=CCC(KV)
      MR(KV,J1)=MJR(NKV(KV))
95    MM(KV,J1)=MJI(NKV(KV))
      MMR=MR(1,J1-LL)
      MMI=MM(1,J1-LL)
C
C     MAPPING BACK THE SYMBOLS TO REGENERATE THE TRANSMITTED BITS
C
      LM1=(3-MMR)/2
      LM2=(3-MMI)/2
```

```
      L5=(3-NXER(J1))/2
      L6=(3-NXEI(J1))/2
C
C     DIFFERENTIAL DECODING
C
      DO 97 N=1,KK
      INMS(N)=(1+JR(LM1,LM2,N))/2
97    IENS(N)=(1+JR(L5,L6,N))/2
      NIM1=INMS(2)+2*INMS(1)
      LM1=NIM1+NIM2
      NIM2=NIM1
      IF(LM1.GT.3)LM1=LM1-4
      NIE1=IENS(2)+2*IENS(1)
      LE1=NIE1+NIE2
      NIE2=NIE1
      IF(LE1.GT.3)LE1=LE1-4
C
C     BIT ERROR CALCULATIONS
C
      ICR=ICR+1
      DO 100 N=1,KK
C     ISM(N)=JR(LM1,LM2,N)
      ISM(N)=2*JMS(LM1,N)-1
      ISNM=ISM(N)-JIS(N,J1-LL)
      IF(ISNM.NE.0) IEM=IEM+1
C     ISE(N)=JR(L5,L6,N)
      ISE(N)=2*JMS(LE1,N)-1
      ISIE=ISE(N)-IS(N)
      IF(ISIE.NE.0) IEE=IEE+1
100   CONTINUE
C
C     STORE THE REQUIRED INFORMATION TO INITIALIZE NEXT
C     BLOCK OF DATA.
C
      KJL1=KJ1-LL+1
      DO 200 M=KJL1,KJ1
      M1=M-KJ1
      Q1(M1)=Q1(M)
      Q2(M1)=Q2(M)
      MXR(M1)=MXR(M)
      MXIM(M1)=MXIM(M)
      JIS(1,M1)=JIS(1,M)
      JIS(2,M1)=JIS(2,M)
      NXER(M1)=NXER(M)
      NXEI(M1)=NXEI(M)
      SR(M1)=SR(M)
      SIM(M1)=SIM(M)
      DO 200 MV=1,LM
      C1(MV,M1)=C1(MV,M)
      MR(MV,M1)=MR(MV,M)
      MM(MV,M1)=MM(MV,M)
      XR(MV,M1)=XR(MV,M)
200   XIM(MV,M1)=XIM(MV,M)
      QF11=QF1
      QF21=QF2
      FQ1(0)=FQ1(MFD)
      FQ2(0)=FQ2(MFD)
250   CONTINUE
C
C      CALCULATE BIT ERROR RATE
```

```
C
      TOTAL=FLOAT(KK*ICR)
      ERM(I)=FLOAT(IEM)/TOTAL
      ERE(I)=FLOAT(IEE)/TOTAL
C
C     CALCULATE SIGNAL-TO-NOISE RATIO (SNR) IN dB
C
      SN(I)=10.0*LOG10(TSP/TNP)
300   CONTINUE
      WRITE(1,9997)
      WRITE(1,9999)(SN(I),ERM(I),I=1,II)
      WRITE(1,9998)
      WRITE(1,9999)(SN(I),ERE(I),I=1,II)
      STOP
9997  FORMAT(4X,'NMLD RESULTS')
9998  FORMAT(4X,'EQUALISER RESULTS')
9999  FORMAT(1X,2(F12.8,8X))
      END
####S
```

```
/*JOB SAM8WC,EUELSM,ST=MFX,C=S,TI=1280,
/* PW=SEHR
FTN5,DB=0/PMD,L=0.
LIBRARY,PROCLIB.
NAG(FTN5).
LGO.
####S
      PROGRAM QPSK
C     THIS PROGRAM SIMULATES THE 4-LEVEL PSK SYSTEM . NEAR-MAXIMUM
C     LIKELIHOOD DETECTOR, KNOWN AS SYSTEM S2D3, IS COMPARED WITH
C     NON-LINEAR EQUALIZER. THE CHANNEL IS SUBJECTED TO A RAYLEIGH
C     FADING IN MOBILE RADIO ENVIRONMENT.
C
C     EXPLANATION OF IMPORTANT COMPLEX-VALUED PARAMETERS:
C     REAL PART IMAGINARY PART          DETAILS
C     _________ _________________ ____________________________________
C     Y1        Y2                NONFADED CHANNEL IMPULSE RESPONSE
C     YR        YIM               FADED CHANNEL IMPULSE RESPONSE
C     Q1        Q2                RAYLEIGH FADING SIMULATOR OUTPUT
C                                 SIGNAL
C     SR        SIM               TRANSMITTED DATA SYMBOL
C     R1        R2                THE RECEIVED SIGNAL
C     V1        V2                THE ADDITIVE GAUSSIAN NOISE
C     ____________________________________________________________
C
C     EXPLANATION OF SOME OTHER PARAMETERS
C     C1: ASSOCIATED COST WITH EACH VECTOR
C     P : STANDERD DEVIATION OF THE NOISE
C     IQ: SEED INTEGER NUMBER
C     SN: SIGNAL-TO-NOISE RATIO IN dB
C     ERM: BIT ERROR RATE IN S2D3
C     ERE: BIT ERROR RATE IN NLEQ
C     KK: NUMBER OF BIT PER SYMBOL
C
C      IMPLICIT DOUBLE PRECISION (A-H,O-Z)
C
      DIMENSION
     * MA(2),IS(2),ISE(2),ISM(2),FQ1(0:4),FQ2(0:4),FDQ1(4),FDQ2(4),
     * SIM(-4:38),SR(-4:38),MXIM(-4:38),MXR(-4:38),JIS(2,-4:38),
     * WQ1(6),WQ2(6),RAY1(2),RAY2(2),AH(5),BH(5),
     * C1(4,-4:38),Q1(-4:38),Q2(-4:38),KMNV(4),NKV(4),
     * Y1(4),Y2(4),YR(4,38),YIM(4,38),
     * ERM(22),SN(22),ERE(22),JSR(4,2),IB(2,2)
      DIMENSION
     C XRC(4),XRC1(4,4),XIC(4),XIC1(4,4),CCC(4),CC1(16)
     *,XR(4,-4:38),XIM(4,-4:38),MM(4,-4:38),MR(4,-4:38)
     *,NXER(-4:38),NXEI(-4:38),LB(0:38),KBM(0:38),KBD(0:38)
     *,KBE(0:38),MRT(4,4),MMT(4,4),TC1(4,4)
      OPEN(1,FILE='OUTPUT')
      DATA JSR/1,-1,-1,1,1,1,-1,-1/,IB/0,1,3,2/
C
C     IMPULSE RESPONSE OF THE NONFADED CHANNELS
C
C
C     RECTANGULAR SHAPED RESPONSE
      DATA Y1/1.0,0.222579,-0.11086,0.538306E-2/
      DATA Y2/0.0,-0.218666,-0.981492E-1,0.646351E-2/
C     RAISED-COSINE SHAPED RESPONSE
C     DATA Y1/1.0,0.552991,0.559095E-1,-0.395242E-2/
C     DATA Y2/0.0,-0.101986,-0.100619,-0.875349E-2/
```

```
C       DATA Y1/1.0,0.0,0.0,0.0/
C       DATA Y2/0.0,0.0,0.0,0.0/
C
C       FIFTH ORDER LOWPASS BESSEL FILTER COEFFICIENTS
C
        DATA AH/0.959,-0.574,0.362,-0.1054,0.0131/
        DATA BH/0.7502,-0.63015,0.28443,-6.54E-2,6.24E-3/
C
        IQ=38
        II=22
        KK=2
C      KK MUST NOT EXCEED THE VALUE OF 2
        LL=4
        LM=4
        M4=16
C
C       THE VALUE OF FD=100,50, OR 25Hz, AND THERE IS ESPECIAL TREATMENT
C       WHEN FD=75Hz.
        FD=25
        KJ1=38
        KJL1=KJ1-LL+1
        JJ=1+INT(10E4/KJ1)
        MFD=INT(100/(FD-0.005))
C       THE VALUE OF MFD=3 WHEN FD=75 Hz
C       MFD=3
        JJ=INT(JJ/MFD)
        PI=4.*ATAN(1.0)
C       BIT RATE =19.2 KBITS/S.
C       SYMBOL RATE =9.6 KBAUDS/S.
C
C       INITIALIZE NAG-ROUTINES (G05DAF AND G05DDF) WITH SEED INTEGER IQ
C
        CALL G05CBF(IQ)
C
C       THE MAIN LOOP
C
C       INITIALIZE ALL PARAMETERS FOR EACH VALUE OF THE SIGNAL-TO-NOISE-
C       RATIO (SNR)
C
        DO 300 I=1,II
        DO 3 IO=-4,LL
        Q1(IO)=1.0
        Q2(IO)=0.0
        JIS(1,IO)=1
        JIS(2,IO)=1
        NXER(IO)=1
        NXEI(IO)=1
        SR(IO)=1.0
        SIM(IO)=1.0
        MXR(IO)=1
        MXIM(IO)=1
        DO 3 MV=1,LM
        C1(MV,IO)=1.0E6
        C1(1,IO)=0
        MR(MV,IO)=1
        MM(MV,IO)=1
        XR(MV,IO)=1.0
3       XIM(MV,IO)=1.0
        LB(0)=0
        KBM(0)=0
```

```
      KBD(0)=0
      KBE(0)=0
      QF11=1.0
      QF21=0.0
      RAY1(2)=1.0
      RAY2(2)=0.0
      DO 4 KQ=2,6
      FQ1(KQ-2)=1.0
      FQ2(KQ-2)=0.0
      WQ1(KQ)=1.0
4     WQ2(KQ)=0.0
      WP=-0.05*(17.0+1.8*(I-1))
      P=1.414*10.0**WP
      IEE=0
      IEM=0
      IE=0
      COUN=0
      TSP=0.0
      TNP=0.0
C
C     GENERATE A BLOCK OF DATA SYMBOLS FOR EACH SAMPLE OF THE
C     RAYLEIGH FADING SIMULATOR OUTPUT. LINEAR INTERPOLATION METHOD IS
C     USED TO GENERATE Q1 AND Q2 (THE REAL AND IMAGIMARY VALUES OF Q)
C
      DO 250 J=1,JJ
C
C     GENERATE TWO NOISE RAMDOM VARIABLES AS INPUTS TO THE
C     FIFTH ORDER LOWPASS BESSEL FILTER
C
      QF1=G05DDF(0.0,1.0)
      DFQ1=(QF1-QF11)/MFD
      QF2=G05DDF(0.0,1.0)
      DFQ2=(QF2-QF21)/MFD
C
C     ESPECIAL TREATMENT WHEN FD=75 Hz
C
C     DO 20 KF=1,MFD
C     FQ1(KF)=G05DDF(0.0,1.0)
C     FQ2(KF)=G05DDF(0.0,1.0)
C20   CONTINUE
C     DO 25 KF=1,MFD
C     KF1=KF-1
C     FDQ1(KF)=FQ1(KF1)+0.25*(4-KF)*(FQ1(KF)-FQ1(KF1))
C25   FDQ2(KF)=FQ2(KF1)+0.25*(4-KF)*(FQ2(KF)-FQ2(KF1))
C
C     SAMPLE THE INPUT SIGNAL OF THE FILTER
C
      DO 200 NFD=1,MFD
C
C     FIFTH ORDER LOWPASS BESSEL FILTER
C
      DO 31 KQ=1,5
      KQ1=KQ+1
      WQ1(KQ)=WQ1(KQ1)
31    WQ2(KQ)=WQ2(KQ1)
      RAY1(1)=RAY1(2)
      RAY2(1)=RAY2(2)
      WQ1(6)=QF11+DFQ1*NFD
      WQ2(6)=QF21+DFQ2*NFD
C     WQ1(6)=FDQ1(NFD)
```

```
C       WQ2(6)=FDQ2(NFD)
        RAY1(2)=0.0
        RAY2(2)=0.0
        DO 33 KQ=1,5
        KQ1=6-KQ
        WQ1(6)=WQ1(6)+BH(KQ)*WQ1(KQ1)
33      WQ2(6)=WQ2(6)+BH(KQ)*WQ2(KQ1)
        DO 35 KQ=1,5
        KQ1=7-KQ
        RAY1(2)=RAY1(2)+AH(KQ)*WQ1(KQ1)
35      RAY2(2)=RAY2(2)+AH(KQ)*WQ2(KQ1)
        DRQ1=(RAY1(2)-RAY1(1))/KJ1
        DRQ2=(RAY2(2)-RAY2(1))/KJ1
C
        DO 100 J1=1,KJ1
        J11=J1-1
C
C       DATA GENERATION AS BIT BY BIT RANDOMLY
C
        DO 40 K=1,KK
        SS=G05DAF(-1.0,1.0)
        IS(K)=INT(SIGN(1.05,SS))
        JIS(K,J1)=IS(K)
        MA(K)=(1+IS(K))/2
40      CONTINUE
C
C       DIFFERENTIAL ENCODING AND DATA MAPPING TO GENERATE SYMBOLS
C
        L1=(3-IS(1))/2
        L2=(3-IS(2))/2
        LB(J1)=IB(L1,L2)-LB(J11)
        IF(LB(J1).LT.0) LB(J1)=LB(J1)+4
        L3=LB(J1)+1
C       L3=IB(L1,L2)+1
        SR(J1)=JSR(L3,1)
        SIM(J1)=JSR(L3,2)
C
C       LINEAR INTERPOLATION IN (RAYLEIGH FADING SIMULATION)
C
        Q1(J1)=RAY1(1)+J1*DRQ1
        Q2(J1)=RAY2(1)+J1*DRQ2
C       Q1(J1)=1.0
C       Q2(J1)=0.0
C
C       CALCULATE THE TRANSMITTED SIGNAL POWER
C
        PR=(SR(J1)*Q1(J1)-SIM(J1)*Q2(J1))**2
        PIM=(SR(J1)*Q2(J1)+SIM(J1)*Q1(J1))**2
        TSP=TSP+PR+PIM
C
C       RAYLEIGH FADING CHANNEL
C
        DO 50 L=1,LL
        L1=J1-L+1
        YR(L,J1)=Y1(L)*Q1(L1)-Y2(L)*Q2(L1)
50      YIM(L,J1)=Y1(L)*Q2(L1)+Y2(L)*Q1(L1)
C
C       START-UP TRANSMISSION
C
        R1=0.0
```

```
      R2=0.0
      DO 60 L=1,LL
      L1=J1-L+1
      R1=R1+YR(L,J1)*SR(L1)-YIM(L,J1)*SIM(L1)
60    R2=R2+YR(L,J1)*SIM(L1)+YIM(L,J1)*SR(L1)
C
C     ADDITIVE GAUSSIAN NOISE WITH 0 MEAN AND VARIANCE P**2
C
      V1=G05DDF(0.0,P)
      V2=G05DDF(0.0,P)
C
C     CALCULATE THE ADDITIVE NOISE POWER
C
      TNP=TNP+V1*V1+V2*V2
C
C
      R1=R1+V1
      R2=R2+V2
C
C     DETECTION PROCESSES
C
C     FIRST...NONLINEAR EQUELISER (NLEQ)
C
      XRE=0.0
      XIE=0.0
      DO 65 L=2,LL
      L1=J1-L+1
      XRE=XRE+YR(L,J1)*NXER(L1)-YIM(L,J1)*NXEI(L1)
65    XIE=XIE+YR(L,J1)*NXEI(L1)+YIM(L,J1)*NXER(L1)
      ERX=R1-XRE
      EIX=R2-XIE
      YY=SQRT(YR(1,J1)**2+YIM(1,J1)**2)
      IF(YY.LT.0.01)YY=0.01
      XER=(YR(1,J1)*ERX+YIM(1,J1)*EIX)/YY
      XEI=(YR(1,J1)*EIX-YIM(1,J1)*ERX)/YY
      NXER(J1)=INT(SIGN(1.05,XER))
      NXEI(J1)=INT(SIGN(1.07,XEI))
C
C     THE NEAR MAXIMUM-LIKELIHOOD DETECTOR (S2D3)
C     ___________________________________________
C
C     CACULATE THE INTERSYMBOL INTERFERENCE FOR EACH OF THE M STORED
C     VECTORS. ALSO SUBTRACT THE LOWEST MINIMUM COST FROM THE OTHER
C     MINIMUM COSTS AND GIVE ZERO VALUE TO THE LOWEST COST.
C     EXPAND THE M STORED VECTORS TO 4M VECTORS AND CALCULATE THE
C     COST FOR EACH EXPANDED VECTOR.
C     SELECT M VECTORS ASSOSIATED WITH MINIMUM COST.
C     DISCARD THE NONSELECTED VECTORS BY SETTING THEIR COSTS TO VERY
C     HIGH VALUE.
C     STORE THE SELECTED VECTORS IN TEMPORARY STORES, SO THAT
C     NONE OF THEM COULD BE SELECTED MORE THAN ONCE, AND RETRIEVE
C     THEM WITH A RANKING METHOD SO THAT THE VECTOR ASSOCIATED WITH
C     THE LOWEST MINIMUM COST TAKES THE FIRST POSITION IN THE RANK.
C     TAKE THE FIRST COMPONENT OF THE FIRST VECTOR IN THE RANK TO
C     BE THE DETECTED DATA SYMBOL.
C
      MNK=0
      CXZ=C1(1,J11)
      DO 71 MV=1,LM
      C1(MV,J11)=C1(MV,J11)-CXZ
```

```
      XRC(MV)=0.0
      XIC(MV)=0.0
      DO 70 L=2,LL
      L1=J1-L+1
      XRC(MV)=XRC(MV)+YR(L,J1)*MR(MV,L1)-YIM(L,J1)*MM(MV,L1)
70    XIC(MV)=XIC(MV)+YR(L,J1)*MM(MV,L1)+YIM(L,J1)*MR(MV,L1)
      DO 71 NV=1,LM
      MNK=MNK+1
      XRC1(MV,NV)=YR(1,J1)*JSR(NV,1)-YIM(1,J1)*JSR(NV,2)
      XRC1(MV,NV)=R1-XRC(MV)-XRC1(MV,NV)
      XIC1(MV,NV)=YR(1,J1)*JSR(NV,2)+YIM(1,J1)*JSR(NV,1)
      XIC1(MV,NV)=R2-XIC(MV)-XIC1(MV,NV)
      CC1(MNK)=C1(MV,J11)+XRC1(MV,NV)**2+XIC1(MV,NV)**2
71    CONTINUE
      DO 80 KV=1,LM
      CCC(KV)=1.0E6
      DO 75 MNK=1,M4
75    CCC(KV)=AMIN1(CCC(KV),CC1(MNK))
      MNK=0
      DO 77 MV=1,LM
      DO 77 NV=1,LM
      MNK=MNK+1
      ACC1=ABS(CCC(KV)-CC1(MNK))
      IF(ACC1.LT.1.0E-9)THEN
      KMN1=MNK
      KMNV(KV)=MV
      NKV(KV)=NV
      ENDIF
77    CONTINUE
      DO 80 MV=1,LM
      KMN1=KMN1+4*(MV-1)
      IF(KMN1.GT.M4) KMN1=KMN1-M4
      CC1(KMN1)=1.0E6
80    CONTINUE
      DO 85 KV=1,LM
      DO 85 L=2,LL
      L1=J1-L+1
      MRT(KV,L)=MR(KMNV(KV),L1)
      MMT(KV,L)=MM(KMNV(KV),L1)
85    TC1(KV,L)=C1(KMNV(KV),L1)
      DO 90 KV=1,LM
      DO 90 L=2,LL
      L1=J1-L+1
      MR(KV,L1)=MRT(KV,L)
      MM(KV,L1)=MMT(KV,L)
90    C1(KV,L1)=TC1(KV,L)
      DO 95 KV=1,LM
      C1(KV,J1)=CCC(KV)
      MR(KV,J1)=JSR(NKV(KV),1)
95    MM(KV,J1)=JSR(NKV(KV),2)
      MMR=MR(1,J1-LL)
      MMI=MM(1,J1-LL)
C
C     MAPPING BACK THE SYMBOLS TO REGENERATE THE TRANSMITTED BITS
C
      LD1=(3-MMR)/2
      LD2=(3-MMI)/2
C
C     DIFFERENTIAL DECODING FOR S2D3
C
```

```
      KBD(J1)=IB(LD1,LD2)
      LBBD=KBD(J1)+KBD(J11)
      IF(LBBD.GE.4) LBBD=LBBD-4
      LBBD=LBBD+1
C     LBBD=IB(LD1,LD2)+1
      LE1=(3-NXER(J1))/2
      LE2=(3-NXEI(J1))/2
C
C     DIFFERENTIAL DECODING FOR NLEQ
C
      KBE(J1)=IB(LE1,LE2)
      LBBE=KBE(J1)+KBE(J11)
      IF(LBBE.GE.4) LBBE=LBBE-4
      LBBE=LBBE+1
C     LBBE=IB(LE1,LE2)+1
C
C     BITS ERROR CALCULATIONS
C
      COUN=COUN+1
      DO 100 N=1,KK
      ISM(N)=JSR(LBBD,N)
      ISE(N)=JSR(LBBE,N)
C     WRITE (NOUT,99) ISM(N),JIS(N,J1-LL),IS(N),J1
C99   FORMAT(2X,4(I4,6X))
      ISNM=ISM(N)-JIS(N,J1-LL)
      IF(ISNM.NE.0) IEM=IEM+1
      ISIE=ISE(N)-IS(N)
      IF(ISIE.NE.0) IEE=IEE+1
100   CONTINUE
C
C     STORE THE REQUIRED INFORMATION TO INITIALIZE THE NEXT
C     BLOCK OF DATA
C
      LB(0)=LB(KJ1)
      KBD(0)=KBD(KJ1)
      KBM(0)=KBM(KJ1)
      KBE(0)=KBE(KJ1)
      DO 200 M=KJL1,KJ1
      M1=M-KJ1
      Q1(M1)=Q1(M)
      Q2(M1)=Q2(M)
      MXR(M1)=MXR(M)
      MXIM(M1)=MXIM(M)
      JIS(1,M1)=JIS(1,M)
      JIS(2,M1)=JIS(2,M)
      NXER(M1)=NXER(M)
      NXEI(M1)=NXEI(M)
      SR(M1)=SR(M)
      SIM(M1)=SIM(M)
      DO 200 MV=1,LM
      C1(MV,M1)=C1(MV,M)
      MR(MV,M1)=MR(MV,M)
      MM(MV,M1)=MM(MV,M)
      XR(MV,M1)=XR(MV,M)
200   XIM(MV,M1)=XIM(MV,M)
      QF11=QF1
      QF21=QF2
      FQ1(0)=FQ1(MFD)
      FQ2(0)=FQ2(MFD)
250   CONTINUE
```

```
      TOTAL=2.0*COUN
C
C     CALCULATE BIT ERROR RATE
C
      ERM(I)=FLOAT(IEM)/TOTAL
      ERE(I)=FLOAT(IEE)/TOTAL
C
C     CALCULATE SIGNAL-TO-NOISE-RATIO (SNR) IN dB
C
      SN(I)=10.0*LOG10(TSP/TNP)
300   CONTINUE
      WRITE(1,9997)
      WRITE(1,9999)(SN(I),ERM(I),I=1,II)
      WRITE(1,9998)
      WRITE(1,9999)(SN(I),ERE(I),I=1,II)
      STOP
9997  FORMAT(4X,'NMLD RESULTS')
9998  FORMAT(4X,'EQUALISER RESULTS')
9999  FORMAT(1X,2(F12.8,7X))
      END
####S
```

```
/*JOB SAM6D,EUELSM,ST=MFX,C=S,TI=1280,
/* PW=SEHR
FTN5,DB=0/PMD,L=0.
LIBRARY,PROCLIB.
NAG(FTN5).
LGO.
####S
      PROGRAM PSK8
C     THIS PROGRAM SIMULATES THE 8-LEVEL PSK SYSTEM . NEAR-MAXIMUM
C     LIKELIHOOD DETECTOR, KNOWN AS SYSTEM S3D3, IS COMPARED WITH
C     NON-LINEAR EQUALIZER. THE CHANNEL IS SUBJECTED TO A RAYLEIGH
C     FADING IN MOBILE RADIO ENVIRONMENT.
C
C     EXPLANATION OF IMPORTANT COMPLEX-VALUED PARAMETERS:
C     REAL PART IMAGINARY PART          DETAILS
C     _________ _________________ _____________________________________
C     Y1        Y2                NONFADED CHANNEL IMPULSE RESPONSE
C     YR        YIM               FADED CHANNEL IMPULSE RESPONSE
C     Q1        Q2                RAYLEIGH FADING SIMULATOR OUTPUT
C                                 SIGNAL
C     SR        SIM               TRANSMITTED DATA SYMBOL
C     R1        R2                THE RECEIVED SIGNAL
C     V1        V2                THE ADDITIVE GAUSSIAN NOISE
C     ____________________________________________________________________
C
C     EXPLANATION OF SOME OTHER PARAMETERS
C     C1: ASSOCIATED COST WITH EACH VECTOR
C     P : STANDERD DEVIATION OF THE NOISE
C     IQ: SEED INTEGER NUMBER
C     SN: SIGNAL-TO-NOISE RATIO IN dB
C     ERM: BIT ERROR RATE IN S3D3
C     ERE: BIT ERROR RATE IN NLEQ
C     KK: NUMBER OF BIT PER SYMBOL
C
      DIMENSION
     * MA(3),IS(3),ISD(3),ISE(3),ISM(3),TXR(4,4),TXI(4,4),TC1(4,4),
     * SIM(-4:38),SR(-4:38),ERN(22),SN(22),ERE(22),JIS(3,-4:38),
     * WQ1(6),WQ2(6),RAY1(2),RAY2(2),AH(5),BH(5),C1(4,-4:38),
     * Y1(4),Y2(4),YR(4,38),YIM(4,38),Q1(-4:38),Q2(-4:38)
     * ,FQ1(0:3),FQ2(0:3),FDQ1(3),FDQ2(3)
      DIMENSION
     * XRC(4),XRC1(4,0:7),XIC(4),XIC1(4,0:7),CCC(4),CC1(64)
     *,XR(4,-4:38),XI(4,-4:38),NML(4,-4:38),PHO(8)
     *,BXER(-4:38),BXEI(-4:38),LB(0:38),KBM(0:38),KBD(0:38),
     ,KBE(0:38),JSR(0:7,3),IB(0:7),KMNV(4),NKV(4)
      OPEN(1,FILE='OUTPUT')
      DATA JSR/-1,-1,-1,1,1,1,1,-1,-1,-1,1,1,-1,-1,1,1,
     ,-1,1,1,1,1,-1,-1,-1/,IB/0,1,7,2,5,4,6,3/
C
C     IMPULSE RESPONSE OF THE CHANNEL
C
      DATA Y1/1.0,0.222579,-0.11086,0.538306E-2/
      DATA Y2/0.0,-0.218666,-0.981492E-1,0.646351E-2/
C     DATA Y1/1.0,0.552991,0.559095E-1,-0.395242E-2/
C     DATA Y2/0.0,-0.101986,-0.100619,-0.875349E-2/
C     DATA Y1/1.0,0.0,0.0,0.0/
C     DATA Y2/0.0,0.0,0.0,0.0/
C
C
C     FIFTH ORDER LOWPASS BESSEL FILTER COEFFICIENTS
```

```
C
      DATA AH/0.959,-0.574,0.362,-0.1054,0.0131/
      DATA BH/0.7502,-0.63015,0.28443,-6.54E-2,6.24E-3/
C     DATA NOUT/1/
      IQ=38
      II=7
      II1=1
      I1=0
      KK=3
C     KK MUST NOT EXCEED THE VALUE OF 3
      LL=4
C
C     THE VALUE OF FD=100,50 OR25 HZ AND THERE IS ESPECIAL
C     TREATMENT WHEN FD=75 HZ
C
      FD=25
      KJ1=38
      KJL1=KJ1-LL+1
      JJ=1+INT(15E4/KJ1)
      MFD=INT(100/(FD-0.005))
C     MFD=3
      JJ=INT(JJ/MFD)
      M8=32
      LM=4
      PI=4.*ATAN(1.0)
      VL=1/SIN(PI/8)
      DO 1 L8=1,8
1     PHO(L8)=PI*((L8-1)*2+1)/8
C
C     BIT RATE =28.8 KBITS/S.
C     SYMBOL RATE =9.6 KBAUDS/S.
C
C     INITIALIZE NAG-ROUTINES (G05DAF AND G05DDF) WITH SEED INTEGER
C
      CALL G05CBF(IQ)
C
C     INITIALIZE ALL PARAMETERS FOR EACH VALUE OF THE SNR
C
      DO 300 I=II1,II
      DO 3 IO=-4,LL
      JIS(1,IO)=-1
      JIS(2,IO)=-1
      JIS(3,IO)=-1
      Q1(IO)=1.0
      Q2(IO)=0.0
      SR(IO)=VL
      SIM(IO)=0.0
      BXER(IO)=VL
      BXEI(IO)=0.0
      DO 3 MV=1,LM
      C1(MV,IO)=1.0E6
      C1(1,IO)=0
      NML(MV,IO)=0
      XR(MV,IO)=VL
3     XI(MV,IO)=0.0
      LB(0)=0
      KBM(0)=0
      KBD(0)=0
      KBE(0)=0
      QF11=1.0
```

```
      QF21=0.0
      RAY1(2)=1.0
      RAY2(2)=0.0
      DO 4 KQ=2,6
      FQ1(KQ-2)=1.0
      FQ2(KQ-2)=0.0
      WQ1(KQ)=1.0
4     WQ2(KQ)=0.0
      WP=-0.05*(20.0+1.55*(I-1))
      P=2.613*10.0**WP
      IEE=0
      IEM=0
      IE=0
      TSP=0.0
      TNP=0.0
      ICR=0
C
C     GENERATE A BLOCK OF DATA SYMBOLS FOR EACH OF THE
C     RAYLEIGH FADING SIMULATOR OUTPUT. LINEAR INTERPOLATION
C     METHOD USED TO GENERATE Q1 AND Q2
C
      DO 250 J=1,JJ
C
C     GENERATE TWO RANDOM VARIABLES AS INPUTS TO THE
C     FIFTH ORDER LOWPASS BESSEL DIGITAL FILTER
C
      QF1=G05DDF(0.0,1.0)
      DFQ1=(QF1-QF11)/MFD
      QF2=G05DDF(0.0,1.0)
      DFQ2=(QF2-QF21)/MFD
C     DO 20 KF=1,MFD
C
C     SPECIAL TREATMENT WHEN FD=75 HZ
C
C     FQ1(KF)=G05DDF(0.0,1.0)
C     FQ2(KF)=G05DDF(0.0,1.0)
C20    CONTINUE
C     DO 25 KF=1,MFD
C     KF1=KF-1
C     FDQ1(KF)=FQ1(KF1)+0.25*(4-KF)*(FQ1(KF)-FQ1(KF1))
C25   FDQ2(KF)=FQ2(KF1)+0.25*(4-KF)*(FQ2(KF)-FQ2(KF1))
C
C     SAMPLING THE INPUT SIGNAL OF THE FILTER
C
      DO 200 NFD=1,MFD
C
C     FIFTH ORDER LOWPASS BESSEL DIGITAL FILTER
C
      DO 31 KQ=1,5
      KQ1=KQ+1
      WQ1(KQ)=WQ1(KQ1)
31    WQ2(KQ)=WQ2(KQ1)
      RAY1(1)=RAY1(2)
      RAY2(1)=RAY2(2)
      WQ1(6)=QF11+DFQ1*NFD
      WQ2(6)=QF21+DFQ2*NFD
C     WQ1(6)=FDQ1(NFD)
C     WQ2(6)=FDQ2(NFD)
      RAY1(2)=0.0
      RAY2(2)=0.0
```

```
      DO 33 KQ=1,5
      KQ1=6-KQ
      WQ1(6)=WQ1(6)+BH(KQ)*WQ1(KQ1)
33    WQ2(6)=WQ2(6)+BH(KQ)*WQ2(KQ1)
      DO 35 KQ=1,5
      KQ1=7-KQ
      RAY1(2)=RAY1(2)+AH(KQ)*WQ1(KQ1)
35    RAY2(2)=RAY2(2)+AH(KQ)*WQ2(KQ1)
      DRQ1=(RAY1(2)-RAY1(1))/KJ1
      DRQ2=(RAY2(2)-RAY2(1))/KJ1
C
C
      DO 100 J1=1,KJ1
      J11=J1-1
C
C       DATA GENERATION
C
      DO 40 K=1,KK
      SS=G05DAF(-1.0,1.0)
      IS(K)=INT(SIGN(1.05,SS))
      JIS(K,J1)=IS(K)
      MA(K)=(1+IS(K))/2
40    CONTINUE
C
C       DATA MAPPING
C
      L8=4*MA(1)+2*MA(2)+MA(3)
C     PL8=0.25*IB(L8)*PI
C
C     DIFFERENTIAL ENCODING
C
      LB(J1)=IB(L8)-LB(J11)
      IF(LB(J1).LT.0) LB(J1)=LB(J1)+8
      PL8=0.25*LB(J1)*PI
      SR(J1)=VL*COS(PL8)
      SIM(J1)=VL*SIN(PL8)
C
C       LINEAR INTERPOLATION IN RAYLEIGH FADING SIMULATION
C
C
      Q1(J1)=RAY1(1)+J1*DRQ1
      Q2(J1)=RAY2(1)+J1*DRQ2
C     Q1(J1)=1.0
C     Q2(J1)=0.0
C
C     CALCULATE THE TANSMITTED SIGNAL POWER
C
      PR=(SR(J1)*Q1(J1)-SIM(J1)*Q2(J1))**2
      PIM=(SR(J1)*Q2(J1)+SIM(J1)*Q1(J1))**2
      TSP=TSP+PR+PIM
C
C     RAYLEIGH FADING CHANNEL
C
      DO 50 L=1,LL
      L1=J1-L+1
      YR(L,J1)=Y1(L)*Q1(L1)-Y2(L)*Q2(L1)
50    YIM(L,J1)=Y1(L)*Q2(L1)+Y2(L)*Q1(L1)
C
C     START-UP TRANSMISSION
C
```

```
      R1=0.0
      R2=0.0
      DO 60 L=1,LL
      L1=J1-L+1
      R1=R1+YR(L,J1)*SR(L1)-YIM(L,J1)*SIM(L1)
60    R2=R2+YR(L,J1)*SIM(L1)+YIM(L,J1)*SR(L1)
C
C     ADDITIVE GAUSSIAN NOISE WITH ZERO MEAN AND VARIANCE P**2
C
      V1=G05DDF(0.0,P)
      V2=G05DDF(0.0,P)
C
C     CALCULATE THE ADDITIVE NOISE POWER
C
      TNP=TNP+V1*V1+V2*V2
      R1=R1+V1
      R2=R2+V2
C
C     DETECTION PROCESSES
C
C     FIRST...NONLINEAR EQUELISER (NLEQ)
C
      XRE=0.0
      XIE=0.0
      DO 65 L=2,LL
      L1=J1-L+1
      XRE=XRE+YR(L,J1)*BXER(L1)-YIM(L,J1)*BXEI(L1)
65    XIE=XIE+YR(L,J1)*BXEI(L1)+YIM(L,J1)*BXER(L1)
      ERX=R1-XRE
      EIX=R2-XIE
      YY=YR(1,J1)**2+YIM(1,J1)**2
      IF(YY.LT.0.01) YY=0.01
      XER=(YR(1,J1)*ERX+YIM(1,J1)*EIX)/YY
      XEI=(YR(1,J1)*EIX-YIM(1,J1)*ERX)/YY
      PH=ATAN2(XEI,XER)
      IF(PH.LT.0.0) PH=2*PI+PH
      IPH=INT(PH/PH0(1))
      NPH=INT(PH/PH0(8))
      KBE(J1)=INT((IPH+1)/2)-8*NPH
C     PE8=0.25*KBE(J1)*PI
      BXER(J1)=VL*COS(PH)
      BXEI(J1)=VL*SIN(PH)
C
C
C      THE NEAR MAXIUM-LIKELIHOOD DETECTOR (S3D3)
C     ------------------------------------------
C
C     CACULATE THE INTERSYMBOL INTERFERENCE FOR EACH OF THE M STORED
C     VECTORS. ALSO SUBTRACT THE LOWEST MINIMUM COST FROM THE OTHER
C     MINIMUM COSTS AND GIVE ZERO VALUE TO THE LOWEST COST.
C     EXPAND THE M STORED VECTORS TO 4M VECTORS AND CALCULATE THE
C     COST FOR EACH EXPANDED VECTOR.
C     SELECT M VECTORS ASSOSIATED WITH MINIMUM COST.
C     DISCARD THE NONSELECTED VECTORS BY SETTING THEIR COSTS TO VERY
C     HIGH VALUE.
C     STORE THE SELECTED VECTORS IN TEMPORARY STORES, SO THAT
C     NONE OF THEM COULD BE SELECTED MORE THAN ONCE, AND RETRIEVE
C     THEM WITH A RANKING METHOD SO THAT THE VECTOR ASSOCIATED WITH
C     THE LOWEST MINIMUM COST TAKES THE FIRST POSITION IN THE RANK.
C     TAKE THE FIRST COMPONENT OF THE FIRST VECTOR IN THE RANK TO
```

```
C       BE THE DETECTED DATA SYMBOL.
C
        MNK=0
        CXZ=C1(1,J11)
        DO 71 MV=1,LM
        C1(MV,J11)=C1(MV,J11)-CXZ
        XRC(MV)=0.0
        XIC(MV)=0.0
        DO 70 L=2,LL
        L1=J1-L+1
        XRC(MV)=XRC(MV)+YR(L,J1)*XR(MV,L1)-YIM(L,J1)*XI(MV,L1)
70      XIC(MV)=XIC(MV)+YR(L,J1)*XI(MV,L1)+YIM(L,J1)*XR(MV,L1)
C
C
        DO 71 K8=0,7,1
        MNK=MNK+1
        P8=0.25*K8*PI
        XRC1(MV,K8)=YR(1,J1)*COS(P8)-YIM(1,J1)*SIN(P8)
        XRC1(MV,K8)=R1-XRC(MV)-VL*XRC1(MV,K8)
        XIC1(MV,K8)=YIM(1,J1)*COS(P8)+YR(1,J1)*SIN(P8)
        XIC1(MV,K8)=R2-XIC(MV)-VL*XIC1(MV,K8)
71      CC1(MNK)=C1(MV,J11)+XRC1(MV,K8)**2+XIC1(MV,K8)**2
        DO 80 KV=1,LM
        CCC(KV)=1.0E6
        DO 75 MNK=1,M8
75      CCC(KV)=AMIN1(CCC(KV),CC1(MNK))
        MNK=1
77      ACC1=ABS(CCC(KV)-CC1(MNK))
        IF(ACC1-1.0E-9)79,79,78
78      MNK=MNK+1
        GO TO 77
79      MNK1=MNK
        KMNV(KV)=1+INT(0.125*(MNK-0.3))
        NKV(KV)=MNK+8*(1-KMNV(KV))-1
        DO 80 MV=1,LM
        MNK1=MNK1+8*(MV-1)
        IF(MNK1.GT.M8) MNK1=MNK1-M8
        CC1(MNK1)=1.0E6
80      CONTINUE
        DO 85 KV=1,LM
        DO 85 L=2,LL
        L1=J1-L+1
        TXR(KV,L)=XR(KMNV(KV),L1)
        TXI(KV,L)=XI(KMNV(KV),L1)
85      TC1(KV,L)=C1(KMNV(KV),L1)
        DO 90 KV=1,LM
        DO 90 L=2,LL
        L1=J1-L+1
        XR(KV,L1)=TXR(KV,L)
        XI(KV,L1)=TXI(KV,L)
90      C1(KV,L1)=TC1(KV,L)
        DO 95 KV=1,LM
        C1(KV,J1)=CCC(KV)
        NML(KV,J1)=NKV(KV)
        PM8=0.25*NML(KV,J1)*PI
        XR(KV,J1)=VL*COS(PM8)
95      XI(KV,J1)=VL*SIN(PM8)
        KBM(J1)=NML(1,J1-LL)
C
C       MAPPING BACK THE SYMBOLS TO REGENERATE THE TRANSMITTED BITS
```

```
C       AND DIFFERENTIAL DECODING
C
        L8E=KBE(J1)+KBE(J11)
        IF(L8E.GE.8) L8E=L8E-8
C       L8E=KBE(J1)
        LMN=KBM(J1)+KBM(J11)
        IF(LMN.GE.8) LMN=LMN-8
C       LMN=KBM(J1)
C
C       BIT ERROR CALCULATIONS
C
        ICR=ICR+1
        DO 100 N=1,KK
        ISE(N)=JSR(L8E,N)
        ISM(N)=JSR(LMN,N)
        ISNM=ISM(N)-JIS(N,J1-LL)
        IF(ISNM.NE.0) IEM=IEM+1
        ISIE=ISE(N)-IS(N)
        IF(ISIE.NE.0) IEE=IEE+1
100     CONTINUE
C
C       STORE THE REQUIRED INFORMATION TO INITIALIZE THE NEXT
C       BLOCK OF DATA
C
        LB(0)=LB(KJ1)
        KBD(0)=KBD(KJ1)
        KBM(0)=KBM(KJ1)
        KBE(0)=KBE(KJ1)
        DO 200 M=KJL1,KJ1
        M1=M-KJ1
        Q1(M1)=Q1(M)
        Q2(M1)=Q2(M)
        JIS(1,M1)=JIS(1,M)
        JIS(2,M1)=JIS(2,M)
        JIS(3,M1)=JIS(3,M)
        BXER(M1)=BXER(M)
        BXEI(M1)=BXEI(M)
        SR(M1)=SR(M)
        SIM(M1)=SIM(M)
        DO 200 MV=1,LM
        C1(MV,M1)=C1(MV,M)
        NML(MV,M1)=NML(MV,M)
        XR(MV,M1)=XR(MV,M)
200     XI(MV,M1)=XI(MV,M)
        QF11=QF1
        QF21=QF2
        FQ1(0)=FQ1(MFD)
        FQ2(0)=FQ2(MFD)
250     CONTINUE
C
C       BIT ERROR RATE CALCULATIONS
C
        TOTAL=FLOAT(KK*ICR)
        ERN(I)=FLOAT(IEM)/TOTAL
        ERE(I)=FLOAT(IEE)/TOTAL
C
C       SIGNAL-TO-NOISE RATIO (SNR IN dB) CALCULATIONS
C
        SN(I)=10.0*LOG10(TSP/TNP)
300     CONTINUE
```

```
      WRITE(1,9997)
      WRITE(1,9999)(SN(I),ERN(I),I=1,II)
      WRITE(1,9998)
      WRITE(1,9999)(SN(I),ERE(I),I=1,II)
      STOP
9997  FORMAT(4X,'NMLD RESULTS')
9998  FORMAT(4X,'EQUALISER RESULTS')
9999  FORMAT(1X,2(F12.8,7X))
      END
####S
```

```
/*JOB SAM4A1,EUELSM,ST=MFX,C=S,TI=1280,
/* PW=SEHR
FTN5,DB=0/PMD,L=0.
LIBRARY,PROCLIB.
NAG(FTN5).
LGO.
####S
      PROGRAM QAM16
C     THIS PROGRAM SIMULATES THE 16-LEVEL QAM SYSTEM . NEAR-MAXIMUM
C     LIKELIHOOD DETECTORS, KNOWN AS S4D1 AND S4D2, ARE COMPARED WITH
C     NON-LINEAR EQUALIZER. THE CHANNEL IS SUBJECTED TO A RAYLEIGH
C     FADING IN MOBILE RADIO ENVIRONMENT.
C
C     EXPLANATION OF IMPORTANT COMPLEX-VALUED PARAMETERS:
C     REAL PART IMAGINARY PART          DETAILS
C     ---------- ------------------ ------------------------------------
C     Y1         Y2                 NONFADED CHANNEL IMPULSE RESPONSE
C     YR         YIM                FADED CHANNEL IMPULSE RESPONSE
C     Q1         Q2                 RAYLEIGH FADING SIMULATOR OUTPUT
C                                   SIGNAL
C     SR         SIM                TRANSMITTED DATA SYMBOL
C     R1         R2                 THE RECEIVED SIGNAL
C     V1         V2                 THE ADDITIVE GAUSSIAN NOISE
C     ------------------------------------------------------------------
C
C     EXPLANATION OF SOME OTHER PARAMETERS
C     C1: ASSOCIATED COST WITH EACH VECTOR
C     P : STANDERD DEVIATION OF THE NOISE
C     IQ: SEED INTEGER NUMBER
C     KK: NUMBER OF BIT PER SYMBOL
C
      DIMENSION
     * MA(4),IS(4,-4:38),ISD(4),ISE(4),ISM(4),NS(0:3,0:3,2),
     * SIM(-4:38),SR(-4:38),MXIM(-4:38),MXR(-4:38),JR(0:3,0:3,4),
     * WQ1(6),WQ2(6),RAY1(2),RAY2(2),AH(5),BH(5),CC2(64),
     * C1(4,-4:38),Q1(-4:38),Q2(-4:38),NXER(-4:38),NXEI(-4:38),
     * Y1(4),Y2(4),YR(4,0:38),YIM(4,0:38),XRC2(4,16),XIC2(4,16),
     * ENML(2,44),ERE(44),SN(44),NXR(38),NXI(38),ISA(4),ISN(4)
      DIMENSION
     * XRC(4),CXR(4),CXI(4),XIC(4),MM(4,-4:38),MR(4,-4:38)
     *,XRC1(4,4),XIC1(4,4),CC1(16),CCC(4),JJS(2,4),MJR(16),MJI(16)
     *,XR(4,-4:38),XIM(4,-4:38),NR(4,-4:38),NI(4,-4:38),C2(4,-4:38)
     *,KMNV(4),NKV(4),MRT(4,4),MMT(4,4),TC1(4,4)
     *,FQ1(0:4),FQ2(0:4),FDQ1(4),FDQ2(4),KD(2,0:3)
       DATA NS/-1,-1,1,1,-1,-1,1,1,-3,-3,3,3,-3,-3,3,3,-1,1,-1,1,
     , -3,3,-3,3,-1,1,-1,1,-3,3,-3,3/
       DATA JR/1,1,-1,-1,1,1,-1,-1,1,1,-1,-1,1,1,-1,-1,1,1,1,1,1,1,
     , 1,1,-1,-1,-1,-1,-1,-1,-1,-1,1,-1,-1,1,1,-1,-1,1,1,-1,-1,1,1,
     ,-1,-1,1,1,1,1,1,-1,-1,-1,-1,-1,-1,-1,-1,1,1,1,1/
       DATA JJS/1,1,1,-1,-1,1,-1,-1/
       DATA KD/-1,-1,-1,1,1,-1,1,1/
C     OPEN(UNIT=1,FILE='Q16AM4P',FORM='FORMATTED')
      OPEN(1,FILE='OUTPUT')
C
C     IMPULSE RESPONSE OF THE NONFADED CHANNELS
C
C     DATA Y1/1.0,0.222579,-0.11086,0.538306E-2/
C     DATA Y2/0.0,-0.218666,-0.981492E-1,0.646351E-2/
      DATA Y1/1.0,0.552991,0.559095E-1,-0.395242E-2/
      DATA Y2/0.0,-0.101986,-0.100619,-0.875349E-2/
```

```
C       DATA Y1/1.0,0.0,0.0,0.0/
C       DATA Y2/0.0,0.0,0.0,0.0/
        DATA AH/0.959,-0.574,0.362,-0.1054,0.0131/
C
C       FIFTH ORDER LOWPASS BESSEL FILTER COEFFICIENTS
C
        DATA BH/0.7502,-0.63015,0.28443,-6.54E-2,6.24E-3/
C       DATA NOUT/1/
C
        IQ=38
        II=22
        I1=0
        KK=4
C      KK MUST NOT EXCEED THE VALUE OF 4
        LL=4
        M4=16
        M16=64
        LM=4
C
C       THE VALUE OF FD=100,50 OR 25 AND THERE IS SPECIAL
C       TREATMENT WHEN FD=75 HZ
C
        FD=100
        KJ1=38
        KJL1=KJ1-LL+1
        JJ=1+INT(50000/KJ1)
        MFD=INT(100/(FD-0.005))
C       MFD=3
        JJ=INT(JJ/MFD)
C
        PI=4.*ATAN(1.0)
C       F=38.4E3
C       BIT RATE =9.6 KBITS/S.
C       SYMBOL RATE =4.8 KBAUDS/S.
        NUMBER=0
        DO 1 INM=0,3,1
        DO 1 MNI=0,3,1
        NUMBER=NUMBER+1
        MJR(NUMBER)=NS(INM,MNI,1)
1       MJI(NUMBER)=NS(INM,MNI,2)
C
C       INITIALIZE NAG-ROUTINES (G05DAF AND G05DDF) WITH SEED INTEGER
C
        CALL G05CBF(IQ)
C       THE MAIN LOOP
C
C       INITIALIZE ALL PARAMETERS FOR EACH VALUE OF THE SNR
C
        DO 300 I=1,II
        DO 3 IO=-4,LL
        Q1(IO)=1.0
        Q2(IO)=0.0
        SR(IO)=1.0
        SIM(IO)=1.0
        NXER(IO)=1
        NXEI(IO)=1
        MXR(IO)=1
        MXIM(IO)=1
        DO 3 MV=1,LM
        IS(MV,IO)=JR(1,1,MV)
```

```
      NR(MV,IO)=1
      NI(MV,IO)=1
      MR(MV,IO)=1
      MM(MV,IO)=1
      C1(MV,IO)=1.0e6
      C1(1,IO)=0.0
      C2(MV,IO)=1.0e6
      C2(1,IO)=0.0
      XR(MV,IO)=1.0
3     XIM(MV,IO)=1.0
      QF11=1.0
      QF21=0.0
      RAY1(2)=1.0
      RAY2(2)=0.0
      DO 4 KQ=2,6
      FQ1(KQ-2)=1.0
      FQ2(KQ-2)=0.0
      WQ1(KQ)=1.0
4     WQ2(KQ)=0.0
      WP=-0.05*(23.0+2.0*(I-1))
      P=3.162279*10.0**WP
      LI3=0
      LNO3=0
      LMO3=0
      LEO3=0
      IEE=0
      IEM=0
      IEN=0
      ICR=0
      TSP=0.0
      TNP=0.0
C
C     GENERATE A BLOCK OF DATA SYMBOLS FOR EACH SAMPLE OF THE
C     RAYLEIGH FADING SIMULATOR OUTPUT. LINEAR INTERPOLATION
C     METHOD USED TOGENERATE Q1 AND Q2
C
      DO 250 J=1,JJ
C
C     GENERATE TWO NOISE RANDOM VARIABLES AS INPUTS TO THE
C     FIFTH ORDER LOWPASS BESSEL DIGITAL FILTER
C
      QF1=G05DDF(0.0,1.0)
      DFQ1=(QF1-QF11)/MFD
      QF2=G05DDF(0.0,1.0)
      DFQ2=(QF2-QF21)/MFD
C     DO 20 KF=1,MFD
C     FQ1(KF)=G05DDF(0.0,1.0)
C     FQ2(KF)=G05DDF(0.0,1.0)
C20   CONTINUE
C     DO 25 KF=1,MFD
C     KF1=KF-1
C     FDQ1(KF)=FQ1(KF1)+0.25*(4-KF)*(FQ1(KF)-FQ1(KF1))
C25   FDQ2(KF)=FQ2(KF1)+0.25*(4-KF)*(FQ2(KF)-FQ2(KF1))
C
C     SAMPLING THE INPUT SIGNAL OF THE FILTER
C
      DO 200 NFD=1,MFD
C
C     5TH ORDER BESSEL FILTER IN RAYLEIGH FADING SIMULATOR
C
```

```
      DO 31 KQ=1,5
      KQ1=KQ+1
      WQ1(KQ)=WQ1(KQ1)
31    WQ2(KQ)=WQ2(KQ1)
      RAY1(1)=RAY1(2)
      RAY2(1)=RAY2(2)
      WQ1(6)=QF11+DFQ1*NFD
      WQ2(6)=QF21+DFQ2*NFD
C     WQ1(6)=FDQ1(NFD)
C     WQ2(6)=FDQ2(NFD)
      RAY1(2)=0.0
      RAY2(2)=0.0
      DO 33 KQ=1,5
      KQ1=6-KQ
      WQ1(6)=WQ1(6)+BH(KQ)*WQ1(KQ1)
33    WQ2(6)=WQ2(6)+BH(KQ)*WQ2(KQ1)
      DO 35 KQ=1,5
      KQ1=7-KQ
      RAY1(2)=RAY1(2)+AH(KQ)*WQ1(KQ1)
35    RAY2(2)=RAY2(2)+AH(KQ)*WQ2(KQ1)
      DRQ1=(RAY1(2)-RAY1(1))/KJ1
      DRQ2=(RAY2(2)-RAY2(1))/KJ1
C
      DO 110 J1=1,KJ1
      J11=J1-1
C
C      DATA GENERATION
C
      DO 40 K=1,KK
      SS=G05DAF(-1.0,1.0)
      IS(K,J1)=INT(SIGN(1.05,SS))
      MA(K)=(1+IS(K,J1))/2
40    CONTINUE
C
C      DIFFERENTIAL ENCODING AND DATA MAPPING TO GENERATE SYMBOLS
C
      LI1=MA(2)+2*MA(1)
      LAMA=LI1
      LI1=LI1-LI3
      IF(LI1.LT.0)LI1=LI1+4
      LI3=LI1
      LI2=MA(4)+2*MA(3)
      SR(J1)=NS(LI1,LI2,1)
      SIM(J1)=NS(LI1,LI2,2)
C
C      LINEAR INTERPOLATION IN RAYLEIGH FADING SIMULATION
C
      Q1(J1)=RAY1(1)+J1*DRQ1
      Q2(J1)=RAY2(1)+J1*DRQ2
C     Q1(J1)=1.0
C     Q2(J1)=0.0
C
C     SIGNAL POWER CALCULATIONS
C
      PR=(SR(J1)*Q1(J1)-SIM(J1)*Q2(J1))**2
      PIM=(SR(J1)*Q2(J1)+SIM(J1)*Q1(J1))**2
      TSP=TSP+PR+PIM
C
C     RAYLEIGH FADING CHENNAL
C
```

```
      DO 50 L=1,LL
      L1=J1-L+1
      YR(L,J1)=Q1(L1)*Y1(L)+Q2(L1)*Y2(L)
50    YIM(L,J1)=Q1(L1)*Y2(L)-Q2(L1)*Y1(L)
C
C     START-UP TRANSMISSION
C
      R1=0.0
      R2=0.0
      DO 55 L=1,LL
      L1=J1-L+1
      R1=R1+YR(L,J1)*SR(L1)-YIM(L,J1)*SIM(L1)
55    R2=R2+YR(L,J1)*SIM(L1)+YIM(L,J1)*SR(L1)
C     TSP=TSP+R1**2+R2**2
C
C     ADDITIVE GAUSSIAN NOISE WITH ZERO MEAN AND VARIANCE P**2
C
      V1=G05DDF(0.0,P)
      V2=G05DDF(0.0,P)
C
C     NOISE POWER CALCULATIONS
C
      TNP=TNP+V1**2+V2**2
      R1=R1+V1
      R2=R2+V2
C
C     DETECTION PROCESSES
C
C     NONLINEAR EQUALISER (NLEQ)
C
      XRE=0.0
      XIE=0.0
      DO 60 L=2,LL
      L1=J1-L+1
      XRE=XRE+YR(L,J1)*NXER(L1)-YIM(L,J1)*NXEI(L1)
60    XIE=XIE+YR(L,J1)*NXEI(L1)+YIM(L,J1)*NXER(L1)
      ERX=R1-XRE
      EIX=R2-XIE
      YY=YR(1,J1)**2+YIM(1,J1)**2
      IF(YY.LT.0.01) YY=0.01
      XER=(YR(1,J1)*ERX+YIM(1,J1)*EIX)/YY
      XEI=(YR(1,J1)*EIX-YIM(1,J1)*ERX)/YY
      IF(XER.LT.-2.0) THEN
      NXER(J1)=-3
      ELSE IF(XER.GT.-2.0.AND.XER.LT.0.0) THEN
      NXER(J1)=-1
      ELSE IF(XER.GT.2.0) THEN
      NXER(J1)=3
      ELSE
      NXER(J1)=1
      ENDIF
      IF(XEI.LT.-2.0) THEN
      NXEI(J1)=-3
      ELSE IF(XEI.GT.-2.0.AND.XEI.LT.0.0) THEN
      NXEI(J1)=-1
      ELSE IF(XEI.GT.2.0) THEN
      NXEI(J1)=3
      ELSE
      NXEI(J1)=1
      ENDIF
```

```
C
C       THE NEAR MAXIMUM-LIKELIHOOD DETECTORS {S4D1 AND S4D2}
C       ------------------------------------------------------
C
C       CACULATE THE INTERSYMBOL INTERFERENCE FOR EACH OF THE STORED
C       VECTORS. ALSO SUBTRACT THE LOWEST MINIMUM COST FROM THE OTHER
C       MINIMUM COSTS AND GIVE ZERO VALUE TO THE LOWEST COST.
C       EXPAND THE STORED VECTORS  AND CALCULATE THE
C       COST FOR EACH EXPANDED VECTOR.
C       SELECT ALL VECTORS ASSOSIATED WITH MINIMUM COST.
C       DISCARD THE NONSELECTED VECTORS BY SETTING THEIR COSTS TO VERY
C       HIGH VALUE.
C       STORE THE SELECTED VECTORS IN TEMPORARY STORES, SO THAT
C       NONE OF THEM COULD BE SELECTED MORE THAN ONCE, AND RETRIEVE
C       THEM WITH A RANKING METHOD SO THAT THE VECTOR ASSOCIATED WITH
C       THE LOWEST MINIMUM COST TAKES THE FIRST POSITION IN THE RANK.
C       TAKE THE FIRST COMPONENT OF THE FIRST VECTOR IN THE RANK TO
C       BE THE DETECTED DATA SYMBOL.
C
C        SYSTEM S4D1
C
        MNK=0
        CXZ1=C1(1,J11)
        CXZ2=C2(1,J11)
        DO 65 MV=1,LM
        C1(MV,J11)=C1(MV,J11)-CXZ1
        C2(MV,J11)=C2(MV,J11)-CXZ2
        CXR(MV)=0.0
        CXI(MV)=0.0
        XRC(MV)=0.0
        XIC(MV)=0.0
C
C       CALCULATE THE VALUES OF {Z} FOR S4D1 AND S4D2
C
        DO 63 L=2,LL
        L1=J1-L+1
        CXR(MV)=CXR(MV)+YR(L,J1)*NR(MV,L1)-YIM(L,J1)*NI(MV,L1)
        CXI(MV)=CXI(MV)+YR(L,J1)*NI(MV,L1)+YIM(L,J1)*NR(MV,L1)
        XRC(MV)=XRC(MV)+YR(L,J1)*MR(MV,L1)-YIM(L,J1)*MM(MV,L1)
63      XIC(MV)=XIC(MV)+YR(L,J1)*MM(MV,L1)+YIM(L,J1)*MR(MV,L1)
        DO 65 NV=1,M4
        MNK=MNK+1
        XRC2(MV,NV)=MJR(NV)*YR(1,J1)-MJI(NV)*YIM(1,J1)
        XRC2(MV,NV)=R1-CXR(MV)-XRC2(MV,NV)
        XIC2(MV,NV)=MJI(NV)*YR(1,J1)+MJR(NV)*YIM(1,J1)
        XIC2(MV,NV)=R2-CXI(MV)-XIC2(MV,NV)
65      CC2(MNK)=C2(MV,J11)+XRC2(MV,NV)**2+XIC2(MV,NV)**2
C
C       SELECT THE VECTORS WITH MINIMUM COST AND DISCARD THE
C       NONSELECTED VECTORS
C
        DO 70 KV=1,LM
        CCC(KV)=1.0E6
        DO 66 MNK=1,M16
66      CCC(KV)=AMIN1(CCC(KV),CC2(MNK))
        MNK=1
67      ACC1=ABS(CCC(KV)-CC2(MNK))
        IF(ACC1-1.0E-9)69,69,68
68      MNK=MNK+1
        GO TO 67
```

```
69      KMN1=MNK
        KMNV(KV)=1+INT(0.0625*(MNK-0.5))
        NKV(KV)=MNK+16*(1-KMNV(KV))
        DO 70 MV=1,LM
        KMN1=KMN1+16*(MV-1)
        IF(KMN1.GT.M16) KMN1=KMN1-M16
        CC2(KMN1)=1.0E6
70      CONTINUE
C
C       TRANSFER THE SELECTED VECTORS {P} BACK TO VECTORS {Q} BY
C       RANKING METHOD
C
        DO 72 KV=1,LM
        DO 72 L=2,LL
        L1=J1-L+1
        MRT(KV,L)=NR(KMNV(KV),L1)
        MMT(KV,L)=NI(KMNV(KV),L1)
72      TC1(KV,L)=C2(KMNV(KV),L1)
        DO 73 KV=1,LM
        DO 73 L=2,LL
        L1=J1-L+1
        NR(KV,L1)=MRT(KV,L)
        NI(KV,L1)=MMT(KV,L)
73      C2(KV,L1)=TC1(KV,L)
        DO 74 KV=1,LM
        C2(KV,J1)=CCC(KV)
        NR(KV,J1)=MJR(NKV(KV))
74      NI(KV,J1)=MJI(NKV(KV))
C
C       SELECT THE FIRST COMPONENT AS THE DETECTED DATA SYMBOL
C
        NNR=NR(1,J1-LL)
        NNI=NI(1,J1-LL)
C
C       SYSTEM S4D2
C
        MNK=0
C
C       {Z} IS ALREADY DETERMINED FOR S4D2 . GIVE DIFFERENT VALUES
C       OF {+-2+-j2} TO THE LAST COMPONENTS AND CALCULATE THE COSTS
C
        DO 80 MV=1,LM
        DO 80 NV=1,LM
        MNK=MNK+1
        XRC1(MV,NV)=JJS(1,NV)*YR(1,J1)-JJS(2,NV)*YIM(1,J1)
        XRC1(MV,NV)=R1-XRC(MV)-2*XRC1(MV,NV)
        XIC1(MV,NV)=JJS(2,NV)*YR(1,J1)+JJS(1,NV)*YIM(1,J1)
        XIC1(MV,NV)=R2-XIC(MV)-2*XIC1(MV,NV)
80      CC1(MNK)=C1(MV,J11)+XRC1(MV,NV)**2+XIC1(MV,NV)**2
        DO 87 KV=1,LM
        CCC(KV)=1.0E6
        DO 82 MNK=1,M4
82      CCC(KV)=AMIN1(CCC(KV),CC1(MNK))
        MNK=1
83      ACC1=ABS(CCC(KV)-CC1(MNK))
        IF(ACC1-1.0E-9)86,86,85
85      MNK=MNK+1
        GO TO 83
86      KMN1=MNK
        KMNV(KV)=1+INT(0.25*(MNK-0.5))
```

```
      NKV(KV)=MNK+4*(1-KMNV(KV))
      DO 87 MV=1,LM
      KMN1=KMN1+4*(MV-1)
      IF(KMN1.GT.M4) KMN1=KMN1-M4
      CC1(KMN1)=1.0E6
87    CONTINUE
      MNK=0
      DO 88 MV=1,LM
      MR(MV,J1)=2*JJS(1,NKV(MV))
      MM(MV,J1)=2*JJS(2,NKV(MV))
C
C     ADD TO THE SELECTED VALUE OF THE LAST COMPONENTS 4 DIFFERENT
C     VALUES {+-1+-j}
C
      DO 88 NV=1,LM
      MNK=MNK+1
      KUR=MR(MV,J1)+JJS(1,NV)
      KUI=MM(MV,J1)+JJS(2,NV)
      XRC1(MV,NV)=R1-XRC(MV)-KUR*YR(1,J1)+KUI*YIM(1,J1)
      XIC1(MV,NV)=R2-XIC(MV)-KUI*YR(1,J1)-KUR*YIM(1,J1)
88    CC1(MNK)=C1(MV,J11)+XRC1(MV,NV)**2+XIC1(MV,NV)**2
C
C     SELECT THE VECTORS WITH MINIMUM COST AND DISCARD THE
C     NONSELECTED VECTORS
C
      DO 93 KV=1,LM
      CCC(KV)=1.0E6
      DO 89 MNK=1,M4
89    CCC(KV)=AMIN1(CCC(KV),CC1(MNK))
      MNK=1
90    ACC2=ABS(CCC(KV)-CC1(MNK))
      IF(ACC2-1.0E-9)92,92,91
91    MNK=MNK+1
      GO TO 90
92    KMN1=MNK
      KMNV(KV)=1+INT(0.25*(MNK-0.5))
      NKV(KV)=MNK+4*(1-KMNV(KV))
      DO 93 MV=1,LM
      KMN1=KMN1+4*(MV-1)
      IF(KMN1.GT.M4) KMN1=KMN1-M4
      CC1(KMN1)=1.0E6
93    CONTINUE
C
C     TRANSFER THE SELECTED VECTORS {P} BACK TO VECTORS {Q} BY
C     RANKING METHOD
C
      DO 94 KV=1,LM
      DO 94 L=2,LL
      L1=J1-L+1
      MRT(KV,L)=MR(KMNV(KV),L1)
      MMT(KV,L)=MM(KMNV(KV),L1)
94    TC1(KV,L)=C1(KMNV(KV),L1)
      DO 96 KV=1,LM
      DO 96 L=2,LL
      L1=J1-L+1
      MR(KV,L1)=MRT(KV,L)
      MM(KV,L1)=MMT(KV,L)
96    C1(KV,L1)=TC1(KV,L)
      DO 97 KV=1,LM
      C1(KV,J1)=CCC(KV)
```

```
      MR(KV,J1)=MR(KV,J1)+JJS(1,NKV(KV))
97    MM(KV,J1)=MM(KV,J1)+JJS(2,NKV(KV))
C
C     SELECT THE FIRST COMPONENT AS THE DETECTED DATA SYMBOL
C
      MMR=MR(1,J1-LL)
      MMI=MM(1,J1-LL)
C
C      MAPPING BACK THE RECEIVED SYMBOL TO REGENERATE THE TRANSMITTED
C      BITS
C
      LN1=(3-NNR)/2
      LN2=(3-NNI)/2
      LM1=(3-MMR)/2
      LM2=(3-MMI)/2
      LE1=(3-NXER(J1))/2
      LE2=(3-NXEI(J1))/2
C
C     DIFFERENTIAL DECODING
C
      ICR=ICR+1
      DO 100 N=1,KK
      ISN(N)=JR(LN1,LN2,N)
      ISM(N)=JR(LM1,LM2,N)
      ISE(N)=JR(LE1,LE2,N)
100   CONTINUE
      DO 101 N=1,2
      ISN(N)=(ISN(N)+1)/2
      ISM(N)=(ISM(N)+1)/2
101   ISE(N)=(ISE(N)+1)/2
      L1N=ISN(2)+2*ISN(1)
      LN1=L1N+LNO3
      LNO3=L1N
      IF(LN1.GT.3)LN1=LN1-4
      L1M=ISM(2)+2*ISM(1)
      LM1=L1M+LMO3
      LMO3=L1M
      IF(LM1.GT.3)LM1=LM1-4
      L1E=ISE(2)+2*ISE(1)
      LE1=L1E+LEO3
      LEO3=L1E
      IF(LE1.GT.3)LE1=LE1-4
      DO 105 N=1,2
      ISN(N)=KD(N,LN1)
      ISM(N)=KD(N,LM1)
105   ISE(N)=KD(N,LE1)
C
C     BIT ERROR CALCULATION
C
      DO 110 N=1,KK
      ISNS=ISN(N)-IS(N,J1-LL)
      IF(ISNS.NE.0) IEN=IEN+1
      ISNM=ISM(N)-IS(N,J1-LL)
      IF(ISNM.NE.0) IEM=IEM+1
      ISIE=ISE(N)-IS(N,J1)
      IF(ISIE.NE.0) IEE=IEE+1
110   CONTINUE
C
C     STORE THE REQUIRED INFORMATION TO INITIALIZE THE NEXT
C     BLOCK OF DATA
```

```
C
      DO 200 M=KJL1,KJ1
      M1=M-KJ1
      Q1(M1)=Q1(M)
      Q2(M1)=Q2(M)
      MXR(M1)=MXR(M)
      MXIM(M1)=MXIM(M)
      NXER(M1)=NXER(M)
      NXEI(M1)=NXEI(M)
      SR(M1)=SR(M)
      SIM(M1)=SIM(M)
      DO 199 MV=1,LM
      IS(MV,M1)=IS(MV,M)
      C1(MV,M1)=C1(MV,M)
      C2(MV,M1)=C2(MV,M)
      NI(MV,M1)=NI(MV,M)
      NR(MV,M1)=NR(MV,M)
      MM(MV,M1)=MM(MV,M)
      MR(MV,M1)=MR(MV,M)
      XR(MV,M1)=XR(MV,M)
199   XIM(MV,M1)=XIM(MV,M)
200   CONTINUE
      QF11=QF1
      QF21=QF2
      FQ1(0)=FQ1(MFD)
      FQ2(0)=FQ2(MFD)
250   CONTINUE
C
C     BIT ERROR RATE CALCULATION
C
      TOTAL=FLOAT(KK*ICR)
      ENML(1,I)=FLOAT(IEN)/TOTAL
      ENML(2,I)=FLOAT(IEM)/TOTAL
      ERE(I)=FLOAT(IEE)/TOTAL
      IF(TNP.EQ.0.0) TNP=1.0E-5
C
C     SNR IN dB CALCULATION
C
      SN(I)=10.0*LOG10(TSP/TNP)
300   CONTINUE
      WRITE(1,9996)
      WRITE(1,9999) (SN(I),ENML(1,I),I=1,II)
      WRITE(1,9997)
      WRITE(1,9999) (SN(I),ENML(2,I),I=1,II)
      WRITE(1,9998)
      WRITE(1,9999) (SN(I),ERE(I),I=1,II)
      STOP
9996  FORMAT(4X,'NMLD SYSTEM 1 RESULTS')
9997  FORMAT(4X,'NMLD SYSTEM 2 RESULTS')
9998  FORMAT(4X,'EQUALISER RESULTS')
9999  FORMAT(1X,2(F12.8,8X))
      END
####S
```

```
ts1pll.fortran -nhe -ppl 72 -pl 60 -no_vertsp -ind 8
      C/*JOB JOBA1,EUELSM,ST=MFY,C=S,TI=1280,
      C/* PW=SEHR
      CFTN5,DB=0/PMD,L=0.
      CLIBRARY,PROCLIB.
      CNAG(FTN5).
      CLGO.
      C####S
            PROGRAM TS1PLL
      C
      C     THIS PROGRAM SIMULATES DIGITAL PHASE LOCKED-LOOPS (DPLL'S)
      C     USING 4-LEVEL PSK OR QAM SIGNAL. THE ASSUMED CHANNEL IS
      C     SUBJECTED TO A RAYLEIGH FADING.
      C
      C
            DOUBLE PRECISION P,G05DAF,G05DDF
            DIMENSION IS(2),IB(2,2),JSR(4,2)
            DIMENSION SR(-21:38),SIM(-21:38)
            DIMENSION WQ1(6),WQ2(6),RAY1(2),RAY2(2),AH(5),BH(5)
            DIMENSION Q1(-21:38),Q2(-21:38),QQ(-21:38)
            DIMENSION RR1(-21:38),RR2(-21:38),R1M1(-21:38),R1M2(-21:38)
            DIMENSION R2M1(-21:38),R2M2(-21:38),R3M1(-21:38)
            DIMENSION R3M2(-21:38),R4M1(-21:38),R4M2(-21:38)
            DIMENSION Y1(4),Y2(4),YR(4,38),YIM(4,38),YER(4,38),YEI(4,38)
            DIMENSION V1PLL(22),V2PLL(22),V3PLLB(22),V4PLLC(22),SN(22)
            DATA JSR/1,-1,-1,1,1,1,-1,-1/,IB/0,1,3,2/
      C
            DATA Y1/1.0,0.222579,-0.11086,0.538306E-2/
            DATA Y2/0.0,-0.218666,-0.981492E-1,0.646351E-2/
      C     DATA Y1/1.0,0.552991,0.559095E-1,-0.395242E-2/
      C     DATA Y2/0.0,-0.101986,-0.100619,-0.875349E-2/
      C
            DATA AH/0.959,-0.574,0.362,-0.1054,0.0131/
            DATA BH/0.7502,-0.63015,0.28443,-6.54E-2,6.24E-3/
      C
            OPEN(1,FILE='OUTPUT')
            IQ=30
            II=21
            KK=2
      C     KK MUST NOT EXCEED THE VALUE OF 2
            LL=4
            KJ1=38
      C     KJL1=KJ1-LL+1
            KJL1=KJ1-20
            JJ=INT(11400/KJ1)
            FD=100
            MFD=INT(100/(FD-0.005))
            JJ=INT(JJ/MFD)
            ND=0
      C
            PI=4.*ATAN(1.0)
            PI2=2*PI
      C     BIT RATE =19.2 KBITS/S.
      C     SYMBOL RATE =9.6 KBAUDS/S.
      C
      C     INITIALIZE NAG-ROUTINES (G05DAF AND G05DDF) WITH SEED INTEGER
      C
            CALL G05CBF(IQ)
      C
      C     THE MAIN LOOP
      C
```

```
      DO 300 I=1,II
      DO 3 IO=-20,LL
      Q1(IO)=1.0
      Q2(IO)=0.0
      QQ(IO)=1.0
      SR(IO)=1.0
      SIM(IO)=1.0
      R1M1(IO)=0.0
      R1M2(IO)=0.0
      DO 2 L=1,LL
      R1M1(IO)=R1M1(IO)+Y1(L)*SR(IO)-Y2(L)*SIM(IO)
2     R1M2(IO)=R1M2(IO)+Y1(L)*SIM(IO)+Y2(L)*SR(IO)
      R2M1(IO)=R1M1(IO)
      R2M2(IO)=R1M2(IO)
      R3M1(IO)=R1M1(IO)
      R3M2(IO)=R1M2(IO)
      R4M1(IO)=R1M1(IO)
      R4M2(IO)=R1M2(IO)
      RR1(IO)=R1M1(IO)
3     RR2(IO)=R1M2(IO)
      QF11=1.0
      QF21=0.0
      RAY1(2)=1.0
      RAY2(2)=0.0
      DO 4 KQ=2,6
      WQ1(KQ)=1.0
4     WQ2(KQ)=0.0
C     ND=I-1
      THQ=6.0*(I-1)-60.0
      THQ1=PI*THQ/180
      DD=1.0/(ND+1)
      DD1=1.0-DD
C     WP=-0.05*(10.0+1.8*(I-1))
      WP=-0.05*33.5
      P=1.414*10.0**WP
      ICR=0
      TSP=0.0
      TNP=0.0
      EEE1=0.0
      EEE2=0.0
      EEE3=0.0
      EEE4=0.0
      C1R=1.0
      C1I=0.0
      C2R=1.0
      C2I=0.0
      C3R=1.0
      C3I=0.0
      C4R=1.0
      C4I=0.0
      TH1=0.0
      TH2=0.0
      TH3=0.0
      TH4=0.0
      EP1=0.0
      EP2=0.0
      EP3=0.0
      EP4=0.0
      PH1I2=0.0
      PH1H2=0.0
```

```
      PH2I3=0.0
      PH1I3=0.0
      PH2H3=0.0
      PH1H3=0.0
      PH1I4=0.0
      PH2H4=0.0
      PH1H4=0.0
C
C     RAYLEIGH FADING SIMULATOR
C
      DO 250 J=1,JJ
      QF1=G05DDF(0.0D0,1.0D0)
      DQF1=(QF1-QF11)/MFD
      QF2=G05DDF(0.0D0,1.0D0)
      DQF2=(QF2-QF21)/MFD
      DO 200 NFD=1,MFD
      DO 31 KQ=1,5
      KQ1=KQ+1
      WQ1(KQ)=WQ1(KQ1)
31    WQ2(KQ)=WQ2(KQ1)
      RAY1(1)=RAY1(2)
      RAY2(1)=RAY2(2)
      WQ1(6)=QF11+DQF1*NFD
      WQ2(6)=QF21+DQF2*NFD
      RAY1(2)=0.0
      RAY2(2)=0.0
      DO 33 KQ=1,5
      KQ1=6-KQ
      WQ1(6)=WQ1(6)+BH(KQ)*WQ1(KQ1)
33    WQ2(6)=WQ2(6)+BH(KQ)*WQ2(KQ1)
      DO 35 KQ=1,5
      KQ1=7-KQ
      RAY1(2)=RAY1(2)+AH(KQ)*WQ1(KQ1)
35    RAY2(2)=RAY2(2)+AH(KQ)*WQ2(KQ1)
      DRQ1=(RAY1(2)-RAY1(1))/KJ1
      DRQ2=(RAY2(2)-RAY2(1))/KJ1
      DO 100 J1=1,KJ1
      J11=J1-1
      DO 40 K=1,KK
C
C     DATA GENERATION
C
      SS=G05DAF(-1.0D0,1.0D0)
40    IS(K)=INT(SIGN(1.03,SS))
      L1=(3-IS(1))/2
      L2=(3-IS(2))/2
      L3=IB(L1,L2)+1
      SR(J1)=JSR(L3,1)
      SIM(J1)=JSR(L3,2)
C     SR(J1)=1.0
C     SIM(J1)=1.0
C
C      LINEAR INTERPOLATION IN RAYLEIGH FADING SIMULATION
C
C     Q1(J1)=RAY1(1)+J1*DRQ1
C     Q2(J1)=RAY2(1)+J1*DRQ2
      Q1(J1)=COS(THQ1)
      Q2(J1)=SIN(THQ1)
C     Q1(J1)=1.0
C     Q2(J1)=0.0
```

```
      QQ(J1)=SQRT(Q1(J1)**2+Q2(J1)**2)
      PCY1=Q1(J1)/QQ(J1)
      PCY2=Q2(J1)/QQ(J1)
      PR=(SR(J1)*Q1(J1)-SIM(J1)*Q2(J1))**2
      PIM=(SR(J1)*Q2(J1)+SIM(J1)*Q1(J1))**2
      TSP=TSP+PR+PIM
C
C     RAYLEIGH FADING CHANNEL
C
      DO 50 L=1,LL
      L1=J1-L+1
      YER(L,J1)=Y1(L)*QQ(L1)
      YEI(L,J1)=Y2(L)*QQ(L1)
      YR(L,J1)=Y1(L)*Q1(L1)-Y2(L)*Q2(L1)
50    YIM(L,J1)=Y1(L)*Q2(L1)+Y2(L)*Q1(L1)
      R1=0.0
      R2=0.0
      RR1(J1)=0.0
      RR2(J1)=0.0
      DO 60 L=1,LL
      L1=J1-L+1
      RR1(J1)=RR1(J1)+YER(L,J1)*SR(L1)-YEI(L,J1)*SIM(L1)
      RR2(J1)=RR2(J1)+YER(L,J1)*SIM(L1)+YEI(L,J1)*SR(L1)
      R1=R1+YR(L,J1)*SR(L1)-YIM(L,J1)*SIM(L1)
60    R2=R2+YR(L,J1)*SIM(L1)+YIM(L,J1)*SR(L1)
C
C     ADDITIVE GAUSSIAN NOISE WITH ZERO MEAN AND VARIANCE P**2
C
      V1=G05DDF(0.0D0,P)
      V2=G05DDF(0.0D0,P)
      TNP=TNP+V1*V1+V2*V2
      R1=R1+V1
      R2=R2+V2
C
C     PHASE DETECTION
C
      JD=J1-ND
      R1M1(J1)=C1R*R1+C1I*R2
      R1M2(J1)=C1R*R2-C1I*R1
      R1R1=RR1(JD)*R1M1(JD)+RR2(JD)*R1M2(JD)
      R1R2=RR1(JD)*R1M2(JD)-RR2(JD)*R1M1(JD)
      R1M=SQRT(R1R1**2+R1R2**2)
      IF(R1M.LT.0.001) R1M=0.001
      R1R1=R1R1/R1M
      R1R2=R1R2/R1M
      R2M1(J1)=C2R*R1+C2I*R2
      R2M2(J1)=C2R*R2-C2I*R1
      R2R1=RR1(JD)*R2M1(JD)+RR2(JD)*R2M2(JD)
      R2R2=RR1(JD)*R2M2(JD)-RR2(JD)*R2M1(JD)
      R2M=SQRT(R2R1**2+R2R2**2)
      IF(R2M.LT.0.001) R2M=0.001
      R2R1=R2R1/R2M
      R2R2=R2R2/R2M
      R3M1(J1)=C3R*R1+C3I*R2
      R3M2(J1)=C3R*R2-C3I*R1
      R3R1=RR1(JD)*R3M1(JD)+RR2(JD)*R3M2(JD)
      R3R2=RR1(JD)*R3M2(JD)-RR2(JD)*R3M1(JD)
      R3M=SQRT(R3R1**2+R3R2**2)
      IF(R3M.LT.0.001) R3M=0.001
      R3R1=R3R1/R3M
```

```
      R3R2=R3R2/R3M
      R4M1(J1)=C4R*R1+C4I*R2
      R4M2(J1)=C4R*R2-C4I*R1
      R4R1=RR1(JD)*R4M1(JD)+RR2(JD)*R4M2(JD)
      R4R2=RR1(JD)*R4M2(JD)-RR2(JD)*R4M1(JD)
      R4M=SQRT(R4R1**2+R4R2**2)
      IF(R4M.LT.0.001) R4M=0.001
      R4R1=R4R1/R4M
      R4R2=R4R2/R4M
C     FIRST ORDER PLL F(Z)=0.1
C     PHI1=0.1*ATAN2(R1R2,R1R1)
      PHI1=0.1*R1R2
      EEE1=EEE1+PHI1
C     TH1=TH1+PHI1
C     IF(TH1.GT.PI2) TH1=TH1-PI2
C     EP1=DD1*EP1+DD*TH1
C     C1R=COS(EP1)
C     C1I=SIN(EP1)
C     EEE1=EEE1+(C1R*PCY2-C1I*PCY1)**2
C     IF(EEE1.GT.ICR) EEE1=ICR
C
C     SECOND ORDER DPLL2B BY USING FIRST ORDER BUTTERWORTH
C     LOWPASS FILTER WITH E=0.5
C     PHI2=ATAN2(R2R2,R2R1)
      PHI2=R2R2
      PHH2=0.2617012*PHI2+0.130851*PH1I2+0.2148938*PH1H2
      PH1I2=PHI2
      PH1H2=PHH2
      EEE2=EEE2+PHH2
C     TH2=TH2+PHH2
C     IF(TH2.GT.PI2) TH2=TH2-PI2
C     EP2=DD1*EP2+DD*TH2
C     C2R=COS(EP2)
C     C2I=SIN(EP2)
C     EEE2=EEE2+(C2R*PCY2-C2I*PCY1)**2
C     IF(EEE2.GT.ICR) EEE2=ICR
C
C     THIRD ORDER DPLL3B BY USING SECOND ORDER BUTTERWORTH
C     LOWPASS FILTER WITH E=0.5
C
C     PHI3=ATAN2(R3R2,R3R1)
      PHI3=R3R2
      PHH3=0.1672348*(PHI3+PH1I3+0.5*PH2I3)
      PHH3=PHH3+0.6270156*PH1H3-0.4631895*PH2H3
      PH2I3=PH1I3
      PH1I3=PHI3
      PH2H3=PH1H3
      PH1H3=PHH3
      EEE3=EEE3+PHH3
C     TH3=TH3+PHH3
C     IF(TH3.GT.PI2) TH3=TH3-PI2
C     EP3=DD1*EP3+DD*TH3
C     C3R=COS(EP3)
C     C3I=SIN(EP3)
C     EEE3=EEE3+(C3R*PCY2-C3I*PCY1)**2
C     IF(EEE3.GT.ICR) EEE3=ICR
C     THIRD ORDER DPLL3C BY USING SECOND ORDER CHEBYSHEV
C     LOWPASS FILTER WITH E=0.5
C
C     PHI4=ATAN2(R4R2,R4R1)
```

```
      PHI4=R4R2
      PHH4=0.501884*PHI4-0.249537*PH1I4
      PHH4=PHH4+0.742974*PH1H4-0.247663*PH2H4
      PH1I4=PHI4
      PH2H4=PH1H4
      PH1H4=PHH4
      EEE4=EEE4+PHH4
C     TH4=TH4+PHH4
C     IF(TH4.GT.PI2) TH4=TH4-PI2
C     EP4=DD1*EP4+DD*TH4
C     C4R=COS(EP4)
C     C4I=SIN(EP4)
C     EEE4=EEE4+(C4R*PCY2-C4I*PCY1)**2
C     IF(EEE4.GT.ICR) EEE4=ICR
      ICR=ICR+1
100   CONTINUE
C
C     STORE ALL THE REQUIRED INFORMATION TO INITIALIZE THE NEXT
C     BLOCK OF DATA
C
      DO 200 M=KJL1,KJ1
      M1=M-KJ1
      Q1(M1)=Q1(M)
      Q2(M1)=Q2(M)
      QQ(M1)=QQ(M)
      R1M1(M1)=R1M1(M)
      R1M2(M1)=R1M2(M)
      R2M1(M1)=R2M1(M)
      R2M2(M1)=R2M2(M)
      R3M1(M1)=R3M1(M)
      R3M2(M1)=R3M2(M)
      R4M1(M1)=R4M1(M)
      R4M2(M1)=R4M2(M)
      RR1(M1)=RR1(M)
      RR2(M1)=RR2(M)
200   CONTINUE
      QF11=QF1
      QF21=QF2
250   CONTINUE
C
C
C     V1PLL(I)=10.0*LOG10(EEE1/ICR)
C     V2PLL(I)=10.0*LOG10(EEE2/ICR)
C     V3PLLB(I)=10.0*LOG10(EEE3/ICR)
C     V4PLLC(I)=10.0*LOG10(EEE4/ICR)
      V1PLL(I)=EEE1/ICR
      V2PLL(I)=EEE2/ICR
      V3PLLB(I)=EEE3/ICR
      V4PLLC(I)=EEE4/ICR
      SN(I)=10.0*LOG10(TSP/TNP)
      SNR=SN(I)
      SN(I)=THQ
300   CONTINUE
      PRINT*,'SNR=',SNR,'        DB'
      WRITE(6,9995)
      WRITE(6,9999)(SN(I),V1PLL(I),I=1,II)
      WRITE(6,9996)
      WRITE(6,9999)(SN(I),V2PLL(I),I=1,II)
      WRITE(6,9997)
      WRITE(6,9999)(SN(I),V3PLLB(I),I=1,II)
```

```
      WRITE(6,9998)
      WRITE(6,9999)(SN(I),V4PLLC(I),I=1,II)
      STOP
9995  FORMAT(3X,'STNR DB',7X,'V1PLL')
9996  FORMAT(3X,'STR DB',7X,'V2PLL')
9997  FORMAT(3X,'STNR DB',7X,'V3PLLB')
9998  FORMAT(3X,'STNR DB',7X,'V4PLLC')
9999  FORMAT(1X,2(F12.7,5X))
      END
C####S
```

```
C/*JOB YFFE4,EUELSM,ST=MFY,C=S,TI=1280,
C/* PW=SEHR
CFTN5,DB=0/PMD,L=0.
CLIBRARY,PROCLIB.
CNAG(FTN5).
CLGO.
C####S
C       PROGRAM FFCE
C       THIS PROGRAM SIMULATES FEEDFORWARD CHANNEL ESTIMATOR WHICH
C       CAN BE USED WITH 4-LEVEL PSK OR QAM SIGNAL. THE ASSUMED CHANNEL
C       IS SUBJECTED TO A RAYLEIGH FADING.
C
C       EXPLANATION OF IMPORTANT COMPLEX-VALUED PARAMETERS:
C       REAL PART IMAGINARY PART            DETAILS
C       ---------- ---------------- ----------------------------------
C       Y1         Y2               NONFADED CHANNEL IMPULSE RESPONSE
C       YR         YIM              FADED CHANNEL IMPULSE RESPONSE
C       Q1         Q2               RAYLEIGH FADING SIMULATOR OUTPUT
C                                   SIGNAL
C       SR         SIM              TRANSMITTED DATA SYMBOL
C       R1         R2               THE RECEIVED SIGNAL
C       V1         V2               THE ADDITIVE GAUSSIAN NOISE
C       ------------------------------------------------------------
C
C       EXPLANATION OF SOME OTHER PARAMETERS
C       C1: ASSOCIATED COST WITH EACH VECTOR
C       P : STANDERD DEVIATION OF THE NOISE
C       IQ: SEED INTEGER NUMBER
C       KK: NUMBER OF BIT PER SYMBOL
        DOUBLE PRECISION P,CC,G05DAF,G05DDF
C
        DIMENSION MA(2),IS(2),JS(2,2,2)
        DIMENSION SR(-21:38),SIM(-21:38),Q1(-21:38),Q2(-21:38)
        DIMENSION WQ1(6),WQ2(6),RAY1(2),RAY2(2),AH(5),BH(5)
        DIMENSION Y1(4),Y2(4),YR(4,38),YIM(4,38)
        DIMENSION EY1(4,-21:38),EY2(4,-21:38)
        DIMENSION E1Y(4,-21:38),E2Y(4,-21:38)
        DIMENSION EY1N(4,-21:38),EY2N(4,-21:38)
        DIMENSION X1Y1(4,-21:38),X1Y2(4,-21:38)
        DIMENSION ER(22),SN(22),EEY(4)
        DIMENSION FD(4)
C
C
C       OPEN(1,FILE='OUTPUT')
C       OPEN(1,FILE='Y3FFE',STATUS='NEW',FORM='FORMATTED',ACCESS=
C     1'SEQUENTIAL')
        DATA JS/1,1,-1,-1,1,-1,1,-1/
C
C       IMPULSE RESPONSE OF THE CHANNEL
C
C       DATA Y1/1.0,0.222579,-0.11086,0.538306E-2/
C       DATA Y2/0.0,-0.218666,-0.981492E-1,0.646351E-2/
        DATA Y1/1.0,0.552991,0.559095E-1,-0.395242E-2/
        DATA Y2/0.0,-0.101986,-0.100619,-0.875349E-2/
C
C       FIFTH ORDER LOWPASS BESSEL FILTER COEFFICIENTS
C
        DATA AH/0.959,-0.574,0.362,-0.1054,0.0131/
        DATA BH/0.7502,-0.63015,0.28443,-6.54E-2,6.24E-3/
C
```

```
C
      DATA NOUT/1/
C
      IQ=30
      II=21
      II=1
      KK=2
C     KK MUST NOT EXCEED THE VALUE OF 2
      KJ1=38
      MST=KJ1-20
      JJ=INT(38000/KJ1)
      JJ=2
      FD(1)=100
      FD(2)=50
      FD(3)=25
      FD(4)=10
      LL=4
      ND=1
      DD=1.0/ND
      DD1=1-DD
      WRITE (NOUT,998)
      PI=4.*ATAN(1.0)
      BBB=0.70
      BB=0.09
C
C
c
C     INITIALIZE NAG-ROUTINES (G05DAF AND G05DDF) WITH SEED INTEGER
C
      CALL G05CBF(IQ)
      WP=-0.625
C     WP=-2.0
      P=1.414*10**WP
      DO 333 KFD=1,4
      WRITE(NOUT,999)JJ,FD(KFD)
      WRITE(NOUT,998)
      MFD=INT(100/(FD(KFD)-0.005))
C     JJ=INT(JJ/MFD)
C
C     START THE MAIN LOOP
C
      DO 300 I=1,II
C
C     INITIALIZE ALL PARAMETERS FOR EACH VALUE OF SNR
C
C     BB=1.0E-2*(I-1)
C     BB=0.04+0.002*(I-1)
C     BBB=0.05*I+0.05
      DO 1 IO=-21,LL
      SR(IO)=1.0
      SIM(IO)=1.0
      Q1(IO)=1.0
      Q2(IO)=0.0
      DO 1 MV=1,4
C     E1Y(MV,IO)=Y1(MV)
C     E2Y(MV,IO)=Y2(MV)
C     EY1(MV,IO)=Y1(MV)
C     EY2(MV,IO)=Y2(MV)
C     EY1N(MV,IO)=Y1(MV)
C     EY2N(MV,IO)=Y2(MV)
```

```
      E1Y(MV,IO)=0.0
      E2Y(MV,IO)=0.0
      EY1(MV,IO)=0.0
      EY2(MV,IO)=0.0
      EY1N(MV,IO)=0.0
      EY2N(MV,IO)=0.0
      X1Y1(MV,IO)=0.0
1     X1Y2(MV,IO)=0.0
      QF11=1.0
      QF21=0.0
      RAY1(2)=1.0
      RAY2(2)=0.0
      DO 4 KQ=2,6
      WQ1(KQ)=1.0
4     WQ2(KQ)=0.0
      DO 6 L=1,LL
6     EEY(L)=0.0
      II1=I-1
C     ND=I
C     DD=1.0/ND
C     DD1=1-DD
C     WP=-0.625,-1.625,-3.125,FOR SNR=10,30,60
C     WP=-0.625
C     WP=-0.05*(12.5+1.5*II1)
C     P=1.414*10**WP
      IE=0
      TSP=0.0
      TNP=0.0
      ICR=0
C
C     GENERATE A BLOCK OF DATA SYMBOLS FOR EACH SAMPLE OF THE
C     RAYLEIGH FADING SIMULATOR OUTPUT. LINEAR INTERPOLATION
C     METHOD USED TO GENERATE Q1 AND Q2
C
      DO 250 J=1,JJ
C
C     GENERATE TWO NOISE RANDOM VARIABLES AS INPUTS TO THE
C     FIFTH ORDER LOWPASS BESSEL DIGITAL FILTER
C
      QF1=G05DDF(0.0D0,1.0D0)
      DFQ1=(QF1-QF11)/MFD
      QF2=G05DDF(0.0D0,1.0D0)
      DFQ2=(QF1-QF21)/MFD
C
C     SELECT FADING RATE AND SAMPLE THE INPUT SIGNAL TO THE FILTER
C
      DO 200 NFD=1,MFD
C
C     FIFTH ORDER LOWPASS BESSE FILTER
C
      DO 31 KQ=1,5
      KQ1=KQ+1
      WQ1(KQ)=WQ1(KQ1)
31    WQ2(KQ)=WQ2(KQ1)
      RAY1(1)=RAY1(2)
      RAY2(1)=RAY2(2)
      WQ1(6)=QF11+DFQ1*NFD
      WQ2(6)=QF21+DFQ2*NFD
      RAY1(2)=0.0
      RAY2(2)=0.0
```

```
      DO 33 KQ=1,5
      KQ1=6-KQ
      WQ1(6)=WQ1(6)+BH(KQ)*WQ1(KQ1)
33    WQ2(6)=WQ2(6)+BH(KQ)*WQ2(KQ1)
      DO 35 KQ=1,5
      KQ1=7-KQ
      RAY1(2)=RAY1(2)+AH(KQ)*WQ1(KQ1)
35    RAY2(2)=RAY2(2)+AH(KQ)*WQ2(KQ1)
      DRQ1=(RAY1(2)-RAY1(1))/KJ1
      DRQ2=(RAY2(2)-RAY2(1))/KJ1
C
      DO 100 J1=1,KJ1
      JJ1=J1-1
      JD=J1-ND
C
C       DATA GENERATION
C
      DO 40 K=1,KK
      SS=G05DAF(-1.0D0,1.0D0)
      IS(K)=INT(SIGN(1.05,SS))
      MA(K)=(1+IS(K))/2
40    CONTINUE
C
C       DATA MAPPING TO GENERATE SYMBOLS
C
      L1=1+MA(1)
      L2=1+MA(2)
      SR(J1)=JS(L1,L2,1)
      SIM(J1)=JS(L1,L2,2)
C
C       LINEAR INTERPOLATION IN RAYLEIGH FADING SIMULATION
C
      Q1(J1)=RAY1(1)+J1*DRQ1
      Q2(J1)=RAY2(1)+J1*DRQ2
C     Q1(J1)=SQRT(Q1(J1)**2+Q2(J1)**2)
C     Q1(J1)=1.0
C     Q1(J1)=0.0
C     QQ=SQRT(Q1(J1)**2+Q2(J1)**2)
C     Q1(J1)=Q1(J1)/QQ
C     Q2(J1)=Q2(J1)/QQ
C
C     SIGNAL POWER CALCULATION
C
      PR=(SR(J1)*Q1(J1)-SIM(J1)*Q2(J1))**2
      PIM=(SR(J1)*Q2(J1)+SIM(J1)*Q1(J1))**2
      TSP=TSP+PR+PIM
C
C     RAYLEIGH FADING CHANNEL
C
      DO 50 L=1,LL
      L1=J1-L+1
      YR(L,J1)=Y1(L)*Q1(L1)-Y2(L)*Q2(L1)
50    YIM(L,J1)=Y1(L)*Q2(L1)+Y2(L)*Q1(L1)
      R1=0.0
      R2=0.0
      RF1=0.0
      RF2=0.0
      DO 60 L=1,LL
      L1=J1-L+1
      RF1=RF1+EY1(L,JJ1)*SR(L1)-EY2(L,JJ1)*SIM(L1)
```

```
      RF2=RF2+EY1(L,JJ1)*SIM(L1)+EY2(L,JJ1)*SR(L1)
      R1=R1+YR(L,J1)*SR(L1)-YIM(L,J1)*SIM(L1)
60    R2=R2+YR(L,J1)*SIM(L1)+YIM(L,J1)*SR(L1)
C
C     ADDITIVE GAUSSIAN NOISE WITH ZERO MEAN AND VARIANCE P**2
C
      V1=G05DDF(0.0,P)
      V2=G05DDF(0.0,P)
C
C     NOISE POWER CALCULATION
C
      TNP=TNP+V1**2+V2**2
      R1=R1+V1
      R2=R2+V2
C
C     ESTIMATION AND PREDICTION PROCESSES
C
      ERT1=R1-RF1
      ERT2=R2-RF2
      DO 80 L=1,LL
      L1=J1-L+1
      ER1=(SR(L1)*ERT1+SIM(L1)*ERT2)*BB
      ER2=(SR(L1)*ERT2-SIM(L1)*ERT1)*BB
      E1Y(L,J1)=E1Y(L,JJ1)+ER1
      E2Y(L,J1)=E2Y(L,JJ1)+ER2
      EX1=E1Y(L,J1)-EY1(L,JJ1)
      EX2=E2Y(L,J1)-EY2(L,JJ1)
      X1Y1(L,J1)=X1Y1(L,JJ1)+(1-BBB)**2*EX1
      X1Y2(L,J1)=X1Y2(L,JJ1)+(1-BBB)**2*EX2
      EY1(L,J1)=EY1(L,JJ1)+X1Y1(L,J1)+(1-BBB**2)*EX1
      EY2(L,J1)=EY2(L,JJ1)+X1Y2(L,J1)+(1-BBB**2)*EX2
      EY1N(L,J1)=EY1(L,J1)+(ND-1)*X1Y1(L,J1)
      EY2N(L,J1)=EY2(L,J1)+(ND-1)*X1Y2(L,J1)
80    CONTINUE
C
C     MEAN SQUARE ERROR CALCULATION
C
      YYEE=0.0
      DO 90 L=1,LL
C     IF(ICR.LT.1000) EEY(L)=0.0
      EYEY=(EY1N(L,JD)-YR(L,JD))**2
     +    +(EY2N(L,JD)-YIM(L,JD))**2
      YYEE=YYEE+EYEY
C     EEY(L)=EEY(L)+0.5*EYEY
      EEY(L)=EEY(L)+EYEY
      IF(EEY(L).GT.10000.0) GO TO 250
90    CONTINUE
      IF(YYEE.LT.1.0E-4)YYEE=1.0E-4
      YYEE=10.0*LOG10(YYEE)
      WRITE(NOUT,1000)ICR,YYEE
C     PRINT*,'ICR,',ICR,'      EEYY=',YYEE
      ICR=ICR+1
100   CONTINUE
C
C     STORE THE REQUIRED INFORMATION TO INITIALIZE THE NEXT
C     BLOCK OF DATA
C
      DO 200 LM=MST,KJ1
      LM1=LM-KJ1
      Q1(LM1)=Q1(LM)
```

```
        Q2(LM1)=Q2(LM)
        SR(LM1)=SR(LM)
        SIM(LM1)=SIM(LM)
        DO 200 MV=1,4
        EY1(MV,LM1)=EY1(MV,LM)
        EY2(MV,LM1)=EY2(MV,LM)
        E1Y(MV,LM1)=E1Y(MV,LM)
        E2Y(MV,LM1)=E2Y(MV,LM)
        EY1N(MV,LM1)=EY1N(MV,LM)
        EY2N(MV,LM1)=EY2N(MV,LM)
        X1Y1(MV,LM1)=X1Y1(MV,LM)
200     X1Y2(MV,LM1)=X1Y2(MV,LM)
        QF11=QF1
        QF21=QF2
250     CONTINUE
C
C
        ER(I)=0.0
        ICR=1000
        DO 299 L=1,LL
C299    ER(I)=ER(I)+0.25*EEY(L)/ICR
299     ER(I)=ER(I)+EEY(L)/ICR
C       ER(I)=10.0*LOG10(ER(I))
        IF(TNP.EQ.0.0)TNP=1.0E-5
        IF(TSP.EQ.0.0)TSP=1.0E-5
        TSNP=TSP/TNP
C       SSNN=10.0*LOG10(TSP/TNP)
        SSNN=10.0*LOG10(TSNP)
C       SSNN=10.0*(LOG10(TSP)-LOG10(TNP))
C       PRINT*,'SNR=',SSNN
C       SN(I)=SSNN
C       SN(I)=BB
        SN(I)=ND
C       SN(I)=BBB
C       SN(I)=FLOAT(ICR)
C300    WRITE (NOUT,999) SN(I),ER(I)
300     CONTINUE
333     CONTINUE
        STOP
998     FORMAT(1X,'ERROR RATE',9X,'ERROR COUNTER',4X,'STN_RATIO_DB')
999     FORMAT(1X,2(F16.8,6X))
1000    FORMAT(1X,I4,6X,F16.8)
        END
C####S
```

```
C/*JOB YFBE4,EUELSM,ST=MFY,C=S,TI=1280,
C/* PW=SEHR
CFTN5,DB=0/PMD,L=0.
CLIBRARY,PROCLIB.
CNAG(FTN5).
CLGO.
C####S
C       PROGRAM MFBCE
C
C       PROGRAM TO SIMULATE THE MODIFIED FEEDBACK CHANNEL ESTIMATOR
C       USING 4-LEVEL PSK OR QAM SIGNAL. THE ASSUMED CHANNEL IS
C       SUBJECTED TO RAYLEIGH FADING.
C
C       EXPLANATION OF IMPORTANT COMPLEX-VALUED PARAMETERS:
C       REAL PART IMAGINARY PART            DETAILS
C
C       Y1        Y2                NONFADED CHANNEL IMPULSE RESPONSE
C       YR        YIM               FADED CHANNEL IMPULSE RESPONSE
C       Q1        Q2                RAYLEIGH FADING SIMULATOR OUTPUT
C                                   SIGNAL
C       SR        SIM               TRANSMITTED DATA SYMBOL
C       R1        R2                THE RECEIVED SIGNAL
C       V1        V2                THE ADDITIVE GAUSSIAN NOISE
C       ------------------------------------------------------------
C
C       EXPLANATION OF SOME OTHER PARAMETERS
C       C1: ASSOCIATED COST WITH EACH VECTOR
C       P : STANDERD DEVIATION OF THE NOISE
C       IQ: SEED INTEGER NUMBER
C       KK: NUMBER OF BIT PER SYMBOL
        DOUBLE PRECISION P,CC,G05DAF,G05DDF
C
        DIMENSION MA(2),IS(2),JS(2,2,2)
        DIMENSION SR(-21:38),SIM(-21:38),Q1(-21:38),Q2(-21:38)
        DIMENSION WQ1(6),WQ2(6),RAY1(2),RAY2(2),AH(5),BH(5)
        DIMENSION Y1(4),Y2(4),YR(4,38),YIM(4,38)
        DIMENSION EU1(4,-21:38),EU2(4,-21:38)
        DIMENSION EU1N(4,-21:38),EU2N(4,-21:38)
        DIMENSION YB1(4,-21:38),YB2(4,-21:38)
        DIMENSION Z1Y1(4,-21:38),Z1Y2(4,-21:38)
        DIMENSION XYR(4,-21:38),XYI(4,-21:38)
        DIMENSION ER(22),SN(22),EEU(4)
        DIMENSION FD(4)
C       OPEN(1,FILE='OUTPUT')
C       OPEN(1,FILE='Y2FBE',STATUS='NEW',FORM='FORMATTED',ACCESS=
C    1'SEQUENTIAL')
        DATA JS/1,1,-1,-1,1,-1,1,-1/
C
C       IMPULSE RESPONSE OF THE CHANNELS
C
C       DATA Y1/1.0,0.222579,-0.11086,0.538306E-2/
C       DATA Y2/0.0,-0.218666,-0.981492E-1,0.646351E-2/
        DATA Y1/1.0,0.552991,0.559095E-1,-0.395242E-2/
        DATA Y2/0.0,-0.101986,-0.100619,-0.875349E-2/
C
C       COEFFICIENTS OF THE FIFTH ORDER BESSEL LOWPASS DIGITAL FILTER
C
        DATA AH/0.959,-0.574,0.362,-0.1054,0.0131/
        DATA BH/0.7502,-0.63015,0.28443,-6.54E-2,6.24E-3/
        DATA NOUT/1/
```

```
C
      IQ=30
      II=21
      II=1
      KK=2
C     KK MUST NOT EXCEED THE VALUE OF 2
      KJ1=38
      JJ=INT(38000/KJ1)
      JJ=2
      LL=4
      ND=1
      DD=1.0/ND
      DD1=1-DD
      WRITE (NOUT,998)
      PI=4.*ATAN(1.0)
      F=9.6E3
C     BIT RATE =19.2 KBITS/S.
C     SYMBOL RATE =9.6 KBAUDS/S.
      FD(1)=100
      FD(2)=50
      FD(3)=25
      FD(4)=10
       BBX=0.8
C      BBX=0.85
C      BBX=0.9
C      BBX=0.95
       BB=0.50
C      BB=0.45
C      BB=0.175
C      BB=0.125
C      BB=0.025
       BB1=1-BB
C
C     INITIALIZE NAG-ROUTINES (G05DAF AND G05DDF) WITH SEED INTEGER
C
      CALL G05CBF(IQ)
      WP=-0.625
C     WP=-2.0
      P=1.414*10**WP
      DO 333 KFD=1,4
      WRITE(NOUT,999)JJ,FD(KFD)
      WRITE(NOUT,998)
      MFD=INT(100/(FD(KFD)-0.005))
C     JJ=INT(JJ/MFD)
      DO 300 I=1,II
C
C     INITIALIZE ALL PARAMETERS FOR EACH VALUE OF THE SNR
C
C     BB=2.5E-2*(I-1)
C     BB1=1-BB
C     BBX=0.05*I+0.05
      DO 1 IO=-21,LL
      SR(IO)=1.0
      SIM(IO)=1.0
      Q1(IO)=1.0
      Q2(IO)=0.0
      DO 1 MV=1,4
C     EU1(MV,IO)=Y1(MV)
C     EU2(MV,IO)=Y2(MV)
C     EU1N(MV,IO)=Y1(MV)
```

```
C       EU2N(MV,IO)=Y2(MV)
C       YB1(MV,IO)=Y1(MV)
C       YB2(MV,IO)=Y2(MV)
        EU1(MV,IO)=0.0
        EU2(MV,IO)=0.0
        EU1N(MV,IO)=0.0
        EU2N(MV,IO)=0.0
        YB1(MV,IO)=0.0
        YB2(MV,IO)=0.0
        Z1Y1(MV,IO)=0.0
        Z1Y2(MV,IO)=0.0
        XYR(MV,IO)=0.0
        XYI(MV,IO)=0.0
1       CONTINUE
        QF11=1.0
        QF21=0.0
        RAY1(2)=1.0
        RAY2(2)=0.0
        DO 4 KQ=2,6
        WQ1(KQ)=1.0
4       WQ2(KQ)=0.0
        DO 6 L=1,LL
6       EEU(L)=0.0
        II1=I-1
        ND=I
        DD=1.0/ND
        DD1=1-DD
C       WP=-0.625,-1.625,-3.125 FOR SNR OF 10,30,60 DB
C       WP=-0.625
C       WP=-0.05*(12.5+1.5*II1)
C       P=1.414*10**WP
        IE=0
        TSP=0.0
        TNP=0.0
        ICR=0
C
C       GENERATE A BLOCK OF DATA SYMBOLS FOR EACH SAMPLE OF THE
C       RAYLEIGH FADING SIMULATOR OUTPUT. LINEAR INTERPOLATION
C       USED TO GENERATE Q1 AND Q2.
C
        DO 250 J=1,JJ
C
C       GENERATE TWO NOISE RANDOM VARIABLES AS INPUTS TO THE
C       FIFTH ORDER LOWPASS BESSEL FILTER
C
        QF1=G05DDF(0.0D0,1.0D0)
        DFQ1=(QF1-QF11)/MFD
        QF2=G05DDF(0.0D0,1.0D0)
        DFQ2=(QF2-QF21)/MFD
C
C       SELECT FADING RATE AND SAMPLE THE INPUT SIGNAL TO THE FILTER
C
        DO 200 NFD=1,MFD
C
C       FIFTH ORDER LOWPASS BESSEL FILTER
C
        DO 31 KQ=1,5
        KQ1=KQ+1
        WQ1(KQ)=WQ1(KQ1)
31      WQ2(KQ)=WQ2(KQ1)
```

```
      RAY1(1)=RAY1(2)
      RAY2(1)=RAY2(2)
      WQ1(6)=QF11+DFQ1*NFD
      WQ2(6)=QF21+DFQ2*NFD
      RAY1(2)=0.0
      RAY2(2)=0.0
      DO 33 KQ=1,5
      KQ1=6-KQ
      WQ1(6)=WQ1(6)+BH(KQ)*WQ1(KQ1)
33    WQ2(6)=WQ2(6)+BH(KQ)*WQ2(KQ1)
      DO 35 KQ=1,5
      KQ1=7-KQ
      RAY1(2)=RAY1(2)+AH(KQ)*WQ1(KQ1)
35    RAY2(2)=RAY2(2)+AH(KQ)*WQ2(KQ1)
      DRQ1=(RAY1(2)-RAY1(1))/KJ1
      DRQ2=(RAY2(2)-RAY2(1))/KJ1
      DO 100 J1=1,KJ1
      JJ1=J1-1
      JD=J1-ND
C
C       DATA GENERATION
C
      DO 40 K=1,KK
      SS=G05DAF(-1.0D0,1.0D0)
      IS(K)=INT(SIGN(1.05,SS))
      MA(K)=(1+IS(K))/2
40    CONTINUE
C
C       DATA MAPPING
C
      L1=1+MA(1)
      L2=1+MA(2)
      SR(J1)=JS(L1,L2,1)
      SIM(J1)=JS(L1,L2,2)
C
C       LINEAR INTERPOLATION IN RAYLEIGH FADING SIMULATION
C
      Q1(J1)=RAY1(1)+J1*DRQ1
      Q2(J1)=RAY2(1)+J1*DRQ2
C     Q1(J1)=1.0
C     Q2(J1)=0.0
C     QQ=SQRT(Q1(J1)**2+Q2(J1)**2)
C     Q1(J1)=Q1(J1)/QQ
C     Q2(J1)=Q2(J1)/QQ
      PR=(SR(J1)*Q1(J1)-SIM(J1)*Q2(J1))**2
C
C     SIGNAL POWER CALCULATION
C
      PIM=(SR(J1)*Q2(J1)+SIM(J1)*Q1(J1))**2
      TSP=TSP+PR+PIM
C
C     RAYLEIGH FADING CHANNEL
C
      DO 50 L=1,LL
      L1=J1-L+1
      YR(L,J1)=Y1(L)*Q1(L1)-Y2(L)*Q2(L1)
50    YIM(L,J1)=Y1(L)*Q2(L1)+Y2(L)*Q1(L1)
C
C
      R1=0.0
```

```
      R2=0.0
      DO 60 L=1,LL
      L1=J1-L+1
      R1=R1+YR(L,J1)*SR(L1)-YIM(L,J1)*SIM(L1)
60    R2=R2+YR(L,J1)*SIM(L1)+YIM(L,J1)*SR(L1)
C
C     ADDITIVE GAUSSIAN NOISE WITH ZERO MEAN AND VARIANCE P**2
C
      V1=G05DDF(0.0,P)
      V2=G05DDF(0.0,P)
C
C     NOISE POWER CALCULATION
C
      TNP=TNP+V1**2+V2**2
      R1=R1+V1
      R2=R2+V2
C
C     ESTIMATION AND PREDICTION PROCESSES
C
      RB1=0.0
      RB2=0.0
      DO 70 L=2,LL
      L1=J1-L+1
      RB1=RB1+EU1(L,JJ1)*SR(L1)-EU2(L,JJ1)*SIM(L1)
70    RB2=RB2+EU1(L,JJ1)*SIM(L1)+EU2(L,JJ1)*SR(L1)
C
C
      ER1T=R1-RB1
      ER2T=R2-RB2
C
C
      Z1Y1(4,J1)=0.5*(SR(J1)*ER1T+SIM(J1)*ER2T)
      Z1Y2(4,J1)=0.5*(SR(J1)*ER2T-SIM(J1)*ER1T)
      Z1Y1(1,J1)=Z1Y1(4,J1)-Z1Y1(2,JJ1)
      Z1Y1(3,J1)=0.2617012*Z1Y1(1,J1)+0.130851*
     *Z1Y1(1,JJ1)+0.2148938*Z1Y1(3,JJ1)
      Z1Y1(2,J1)=Z1Y1(2,JJ1)+Z1Y1(3,J1)
      Z1Y2(1,J1)=Z1Y2(4,J1)-Z1Y2(2,JJ1)
      Z1Y2(3,J1)=0.2617012*Z1Y2(1,J1)+0.130851*
     *Z1Y2(1,JJ1)+0.2148938*Z1Y2(3,JJ1)
      Z1Y2(2,J1)=Z1Y2(2,JJ1)+Z1Y2(3,J1)
C
C
      DO 80 L=1,LL
      L1=J1-L+1
      YB1(L,J1)=BB1*YB1(L,JJ1)+
     +BB*(Z1Y1(2,L1)*Y1(L)-Z1Y2(2,L1)*Y2(L))
      YB2(L,J1)=BB1*YB2(L,JJ1)+
     +BB*(Z1Y1(2,L1)*Y2(L)+Z1Y2(2,L1)*Y1(L))
      EXY1=YB1(L,J1)-EU1(L,JJ1)
      EXY2=YB2(L,J1)-EU2(L,JJ1)
      XYR(L,J1)=XYR(L,JJ1)+EXY1*(1-BBX)**2
      XYI(L,J1)=XYI(L,JJ1)+EXY2*(1-BBX)**2
      EU1(L,J1)=EU1(L,JJ1)+XYR(L,J1)+EXY1*(1-BBX**2)
      EU2(L,J1)=EU2(L,JJ1)+XYI(L,J1)+EXY2*(1-BBX**2)
      EU1N(L,J1)=EU1(L,J1)+(ND-1)*XYR(L,J1)
      EU2N(L,J1)=EU2(L,J1)+(ND-1)*XYI(L,J1)
80    CONTINUE
C
C     MEAN SQUARE ERROR CALCULATION
```

```
C
      UUEE=0.0
      DO 90 L=1,LL
C     IF(ICR.LT.1000)EEU(L)=0.0
      EUEU=(EU1N(L,JD)-YR(L,J1))**2
     +    +(EU2N(L,JD)-YIM(L,JD))**2
      UUEE=UUEE+EUEU
C     EEU(L)=EEU(L)+0.5*EUEU
      EEU(L)=EEU(L)+EUEU
      IF(EEU(L).GT.10000.0) GO TO 250
90    CONTINUE
      IF(UUEE.LT.1.0E-4)UUEE=1.0E-4
      UUEE=10.0*LOG10(UUEE)
      WRITE(NOUT,1000)ICR,UUEE
      ICR=ICR+1
100   CONTINUE
C
C     STORE THE REQUIRED INFORMATION TO INITIALIZE THE NEXT
C     BLOCK OF DATA
C
      KJL1=KJ1-20
      DO 200 M=KJL1,KJ1
      M1=M-KJ1
      Q1(M1)=Q1(M)
      Q2(M1)=Q2(M)
      SR(M1)=SR(M)
      SIM(M1)=SIM(M)
      DO 200 MV=1,4
      EU1(MV,M1)=EU1(MV,M)
      EU2(MV,M1)=EU2(MV,M)
      EU1N(MV,M1)=EU1N(MV,M)
      EU2N(MV,M1)=EU2N(MV,M)
      Z1Y1(MV,M1)=Z1Y1(MV,M)
      Z1Y2(MV,M1)=Z1Y2(MV,M)
      XYR(MV,M1)=XYR(MV,M)
      XYI(MV,M1)=XYI(MV,M)
      YB1(MV,M1)=YB1(MV,M)
200   YB2(MV,M1)=YB2(MV,M)
      QF11=QF1
      QF21=QF2
250   CONTINUE
C
C
C     ER(I)=FLOAT(IE)/FLOAT(KK*ICR)
      SSNN=10.0*LOG10(TSP/TNP)
      ICR=1000
C     PRINT*,'SNR=',SSNN
      ER(I)=0.0
      DO 299 L=1,LL
C299  ER(I)=ER(I)+0.25*EEU(L)/ICR
299   ER(I)=ER(I)+EEU(L)/ICR
      IF(ER(I).LT.1.0E-8) ER(I)=1.0E-8
C     ER(I)=10.0*LOG10(ER(I))
C     SN(I)=SSNN
      SN(I)=ND
C     SN(I)=BB
C     SN(I)=FLOAT(I)
C     SN(I)=BBX
C     SN(I)=FLOAT(ICR)
300   WRITE (NOUT,999) SN(I),ER(I)
```

```
333     CONTINUE
        STOP
998     FORMAT(1X,'ERROR RATE',9X,'ERROR COUNTER',4X,'SNR_RATIO_DB')
999     FORMAT(1X,2(F16.8,6X))
1000    FORMAT(1X,I3,6X,F16.8)
        END
C####S
```

```
/*JOB SA4DV,EUELSM,ST=MFX,C=S,TI=1280,
/* PW=SEHR
FTN5,DB=0/PMD,L=0.
LIBRARY,PROCLIB.
NAG(FTN5).
LGO.
####S
       PROGRAM Q4PSDIV
C      THIS PROGRAM SIMULATES THE 4-LEVEL PSK SIGNAL WITH USE OF
C      SPACE DIVERSITY IN MOBILE RADIO ENVIRONMENT. NEAR-MAXIMUM
C      LIKELIHOOD DETECTOR,KNOWN AS SYSTEM S2D3, IS COMPARED WITH
C      NONLINEAR EQUALISER UNDER NOISY AND RAYLEIGH FADING
C      CONDITIONS.
C
C       EXPLANATION OF IMPORTANT COMPLEX-VALUED PARAMETERS:
C       REAL PART IMAGINARY PART            DETAILS
C
C       Y1          Y2                NONFADED CHANNEL IMPULSE RESPONSE
C       YR          YIM               FADED CHANNEL IMPULSE RESPONSE
C       Q1          Q2                RAYLEIGH FADING SIMULATOR OUTPUT
C                                     SIGNAL
C       SR          SIM               TRANSMITTED DATA SYMBOL
C       R1          R2                THE RECEIVED SIGNAL
C       V1          V2                THE ADDITIVE WHITE GAUSSIAN NOISE
C
C
C       EXPLANATION OF SOME OTHER PARAMETERS
C       C1: ASSOCIATED COST WITH EACH VECTOR
C       P : STANDERD DEVIATION OF THE NOISE
C       IQ: SEED INTEGER NUMBER
C       SN: SIGNAL-TO-NOISE RATIO IN dB
C       ERM: BIT ERROR RATE IN S2D3
C       ERE: BIT ERROR RATE IN NLEQ
C       KK: NUMBER OF BIT PER SYMBOL
C
C      DOUBLE PRECISION P,G05DDF,G05DAF
C
C
       DIMENSION MA(2),IS(2),ISM(2),ISE(2),JSR(4,2),IB(2,2)
       DIMENSION SIM(-4:38),SR(-4:38),JIS(2,-4:38)
       DIMENSION WQ1(2,6),WQ2(2,6),RAY1(2,2),RAY2(2,2),AH(5),BH(5)
       DIMENSION FQ1(2,0:4),FQ2(2,0:4),FDQ1(2,4),FDQ2(2,4)
       DIMENSION QF11(2),QF21(2),QF1(2),QF2(2),DFQ1(2),DFQ2(2)
       DIMENSION DRQ1(2),DRQ2(2),Q1(2,-4:38),Q2(2,-4:38)
       DIMENSION EQ1(-4:38),EQ2(-4:38),QQ(2,-4:38)
       DIMENSION Y1(4),Y2(4),YR(2,4,38),YIM(2,4,38)
       DIMENSION RY1(4),RY2(4),YB1(4),YB2(4),XY1(4),XY2(4)
       DIMENSION UY1(4),UY2(4),RY1N(4,-4:38),RY2N(4,-4:38)
       DIMENSION UY1M(4),UY2M(4)
       DIMENSION YQ1(2,4,38),YQ2(2,4,38),C1R(2),C1I(2)
       DIMENSION ATT(2,2),TTA(2,2),THTA(2)
       DIMENSION RA(2),RB(2),RC(2),RD(2)
       DIMENSION CHO1(2),CHO2(2),CHI1(2),CHI2(2)
       DIMENSION C1(4,-4:38),CC1(16),CCC(4)
       DIMENSION XRC(4),XRC1(4,4),XIC(4),XIC1(4,4)
       DIMENSION KMNV(4),NKV(4),MRT(4,4),MMT(4,4),TC1(4,4)
       DIMENSION MM(4,-4:38),MR(4,-4:38),NXER(-4:38),NXEI(-4:38)
       DIMENSION LB(0:38),KBM(0:38),KBD(0:38),KBE(0:38)
       DIMENSION SN(22),ERM(22),ERE(22)
        OPEN(1,FILE='OUTPUT')
```

```
      DATA JSR/1,-1,-1,1,1,1,-1,-1/,IB/0,1,3,2/
C
C     IMPULSE RESPONSE OF THE NONFADED CHANNELS
C
C
C     RECTANGULAR SHAPED RESPONSE
      DATA Y1/1.0,0.222579,-0.11086,0.538306E-2/
      DATA Y2/0.0,-0.218666,-0.981492E-1,0.646351E-2/
C     RAISED-COSINE SHAPED RESPONSE
C     DATA Y1/1.0,0.552991,0.559095E-1,-0.395242E-2/
C     DATA Y2/0.0,-0.101986,-0.100619,-0.875349E-2/
C     DATA Y1/1.0,0.0,0.0,0.0/
C     DATA Y2/0.0,0.0,0.0,0.0/
C
C     FIFTH ORDER LOWPASS BESSEL FILTER COEFFICIENTS
C
      DATA AH/0.959,-0.574,0.362,-0.1054,0.0131/
      DATA BH/0.7502,-0.63015,0.28443,-6.54E-2,6.24E-3/
      DATA GI1/0.2617012/,GI2/0.1308506/,GI3/0.2148938/
      DATA BB/0.5/,BB1/0.5/,BBB/0.8/
      DATA NOUT/1/
      IQ=38
      II=22
      KK=2
C     KK MUST NOT EXCEED THE VALUE OF 2
      LL=4
      LM=4
      M4=16
C
C     THE VALUE OF FD=100,50, OR 25Hz, AND THERE IS ESPECIAL TREATMENT
C     WHEN FD=75Hz.
      FD=25
      KJ1=38
      KJL1=KJ1-LL+1
      JJ=1+INT(10E4/KJ1)
      MFD=INT(100/(FD-0.005))
      ND=1
C     THE VALUE OF MFD=3 WHEN FD=75 Hz
C     MFD=3
      JJ=INT(JJ/MFD)
      PI=4.*ATAN(1.0)
      PI2=2*PI
      B1B=(1-BBB)**2
      B2B=1-BBB**2
C     BIT RATE =19.2 KBITS/S.
C     SYMBOL RATE =9.6 KBAUDS/S.
C
C     INITIALIZE NAG-ROUTINES (G05DAF AND G05DDF) WITH SEED INTEGER IQ
C
      CALL G05CBF(IQ)
C
C     THE MAIN LOOP
C
C     INITIALIZE ALL PARAMETERS FOR EACH VALUE OF THE SIGNAL-TO-NOISE-
C     RATIO (SNR)
C
      DO 300 I=1,II
      DO 3 IO=-4,LL
      DO 1 IDV=1,2
      Q1(IDV,IO)=1.0
```

```
      Q2(IDV,IO)=0.0
      QQ(IDV,IO)=1.0
1     JIS(IDV,IO)=1
      NXER(IO)=1
      NXEI(IO)=1
      SR(IO)=1.0
      SIM(IO)=1.0
      EQ1(IO)=1.0
      EQ2(IO)=0.0
      DO 3 MV=1,LM
      C1(MV,IO)=1.0E6
      C1(1,IO)=0
      MR(MV,IO)=1
      MM(MV,IO)=1
      RY1N(MV,IO)=Y1(MV)
      RY2N(MV,IO)=Y2(MV)
3     CONTINUE
      LB(0)=0
      KBM(0)=0
      KBD(0)=0
      KBE(0)=0
      CHO1(1)=0.0
      CHO2(1)=0.0
      CHI1(1)=0.0
      CHI2(1)=0.0
      DO 4 IDV=1,2
      QF11(IDV)=1.0
      QF21(IDV)=0.0
      RAY1(IDV,2)=1.0
      RAY2(IDV,2)=0.0
      THTA(IDV)=0.0
      TTA(IDV,1)=0.0
      ATT(IDV,1)=0.0
      C1R(IDV)=1.0
      C1I(IDV)=0.0
      DO 4 KQ=2,6
      FQ1(IDV,KQ-2)=1.0
      FQ2(IDV,KQ-2)=0.0
      WQ1(IDV,KQ)=1.0
4     WQ2(IDV,KQ)=0.0
      DO 5 L=1,LL
      UY1(L)=Y1(L)
      UY2(L)=Y2(L)
      RY1(L)=Y1(L)
      RY2(L)=Y2(L)
      YB1(L)=Y1(L)
      YB2(L)=Y2(L)
      XY1(L)=0.0
5     XY2(L)=0.0
      WP=-0.05*(17.0+1.8*(I-1))
      P=1.414*10.0**WP
      IEE=0
      IEM=0
      IE=0
      COUN=0
      TSP=0.0
      TNP=0.0
C
C     GENERATE A BLOCK OF DATA SYMBOLS FOR EACH SAMPLE OF THE
C     RAYLEIGH FADING SIMULATOR OUTPUT. LINEAR INTERPOLATION METHOD IS
```

```
C       USED TO GENERATE Q1 AND Q2 (THE REAL AND IMAGIMARY VALUES OF Q)
C
        DO 250 J=1,JJ
C
C       GENERATE TWO NOISE RAMDOM VARIABLES AS INPUTS TO THE
C       FIFTH ORDER LOWPASS BESSEL FILTER
C
        DO 25 IDV=1,2
        QF1(IDV)=G05DDF(0.0,1.0)
        DFQ1(IDV)=(QF1(IDV)-QF11(IDV))/MFD
        QF2(IDV)=G05DDF(0.0,1.0)
        DFQ2(IDV)=(QF2(IDV)-QF21(IDV))/MFD
C
C       SPECIAL TREATMENT WHEN FD=75 Hz
C
C       DO 20 KF=1,MFD
C       FQ1(IDV,KF)=G05DDF(0.0,1.0)
C       FQ2(IDV,KF)=G05DDF(0.0,1.0)
C20     CONTINUE
C       DO 25 KF=1,MFD
C       KF1=KF-1
C       FDQ1(IDV,KF)=FQ1(IDV,KF1)+0.25*(4-KF)*(FQ1(IDV,KF)-FQ1(IDV,KF1))
C       FDQ2(IDV,KF)=FQ2(IDV,KF1)+0.25*(4-KF)*(FQ2(IDV,KF)-FQ2(IDV,KF1))
25      CONTINUE
C
C       SAMPLE THE INPUT SIGNAL OF THE FILTER
C
        DO 200 NFD=1,MFD
C
C       FIFTH ORDER LOWPASS BESSEL FILTER
C
        DO 37 IDV=1,2
        DO 31 KQ=1,5
        KQ1=KQ+1
        WQ1(IDV,KQ)=WQ1(IDV,KQ1)
31      WQ2(IDV,KQ)=WQ2(IDV,KQ1)
        RAY1(IDV,1)=RAY1(IDV,2)
        RAY2(IDV,1)=RAY2(IDV,2)
        WQ1(IDV,6)=QF11(IDV)+DFQ1(IDV)*NFD
        WQ2(IDV,6)=QF21(IDV)+DFQ2(IDV)*NFD
C       WQ1(IDV,6)=FDQ1(IDV,NFD)
C       WQ2(IDV,6)=FDQ2(IDV,NFD)
        RAY1(IDV,2)=0.0
        RAY2(IDV,2)=0.0
        DO 33 KQ=1,5
        KQ1=6-KQ
        WQ1(IDV,6)=WQ1(IDV,6)+BH(KQ)*WQ1(IDV,KQ1)
33      WQ2(IDV,6)=WQ2(IDV,6)+BH(KQ)*WQ2(IDV,KQ1)
        DO 35 KQ=1,5
        KQ1=7-KQ
        RAY1(IDV,2)=RAY1(IDV,2)+AH(KQ)*WQ1(IDV,KQ1)
35      RAY2(IDV,2)=RAY2(IDV,2)+AH(KQ)*WQ2(IDV,KQ1)
        DRQ1(IDV)=(RAY1(IDV,2)-RAY1(IDV,1))/KJ1
        DRQ2(IDV)=(RAY2(IDV,2)-RAY2(IDV,1))/KJ1
37      CONTINUE
C
        DO 150 J1=1,KJ1
        J11=J1-1
        JD=J1-ND
C
```

```
C       DATA GENERATION AS BIT BY BIT RANDOMLY
C
        DO 40 K=1,KK
        SS=G05DAF(-1.0,1.0)
        IS(K)=INT(SIGN(1.05,SS))
        JIS(K,J1)=IS(K)
        MA(K)=(1+IS(K))/2
40      CONTINUE
C
C       DIFFERENTIAL ENCODING AND DATA MAPPING TO GENERATE SYMBOLS
C
        L1=(3-IS(1))/2
        L2=(3-IS(2))/2
        LB(J1)=IB(L1,L2)-LB(J11)
        IF(LB(J1).LT.0) LB(J1)=LB(J1)+4
        L3=LB(J1)+1
C       L3=IB(L1,L2)+1
        SR(J1)=JSR(L3,1)
        SIM(J1)=JSR(L3,2)
C
C       LINEAR INTERPOLATION IN (RAYLEIGH FADING SIMULATION)
C
        DO 60 IDV=1,2
        Q1(IDV,J1)=RAY1(IDV,1)+J1*DRQ1(IDV)
        Q2(IDV,J1)=RAY2(IDV,1)+J1*DRQ2(IDV)
C       Q1(IDV,J1)=1.0
C       Q2(IDV,J1)=0.0
        QQ(IDV,J1)=SQRT(Q1(IDV,J1)**2+Q2(IDV,J1)**2)
C
C       CALCULATE THE TRANSMITTED SIGNAL POWER
C
        PR=(SR(J1)*Q1(IDV,J1)-SIM(J1)*Q2(IDV,J1))**2
        PIM=(SR(J1)*Q2(IDV,J1)+SIM(J1)*Q1(IDV,J1))**2
        TSP=TSP+PR+PIM
C
C       RAYLEIGH FADING CHANNEL
C
        DO 50 L=1,LL
        L1=J1-L+1
        YQ1(IDV,L,J1)=Y1(L)*QQ(IDV,L1)
        YQ2(IDV,L,J1)=Y2(L)*QQ(IDV,L1)
        YR(IDV,L,J1)=Y1(L)*Q1(IDV,L1)-Y2(L)*Q2(IDV,L1)
50      YIM(IDV,L,J1)=Y1(L)*Q2(IDV,L1)+Y2(L)*Q1(IDV,L1)
C
C       START-UP TRANSMISSION
C
        RA(IDV)=0.0
        RB(IDV)=0.0
        RC(IDV)=0.0
        RD(IDV)=0.0
        DO 55 L=1,LL
        L1=J1-L+1
        RC(IDV)=RC(IDV)+YQ1(IDV,L,J1)*SR(L1)-YQ2(IDV,L,J1)*SIM(L1)
        RD(IDV)=RD(IDV)+YQ1(IDV,L,J1)*SIM(L1)+YQ2(IDV,L,J1)*SR(L1)
        RA(IDV)=RA(IDV)+YR(IDV,L,J1)*SR(L1)-YIM(IDV,L,J1)*SIM(L1)
55      RB(IDV)=RB(IDV)+YR(IDV,L,J1)*SIM(L1)+YIM(IDV,L,J1)*SR(L1)
C
C
C       ADDITIVE GAUSSIAN NOISE WITH 0 MEAN AND VERIANCE P**2
C
```

```
      V1=G05DDF(0.0,P)
      V2=G05DDF(0.0,P)
C
C     CALCULATE THE ADDITIVE NOISE POWER
C
      TNP=TNP+V1*V1+V2*V2
C
C
      RA(IDV)=RA(IDV)+V1
      RB(IDV)=RB(IDV)+V2
C     C1R(IDV)=1.0
C     C1I(IDV)=0.0
C
C     DEMODULATION PROCESSES
C
      R1R1=C1R(IDV)*RA(IDV)+C1I(IDV)*RB(IDV)
      R2R1=C1R(IDV)*RB(IDV)-C1I(IDV)*RA(IDV)
      RA(IDV)=R1R1
      RB(IDV)=R2R1
60    CONTINUE
C
C     COPHASE COMBINER OPERATION
C
      R1=RA(1)+RA(2)
      R2=RB(1)+RB(2)
      DO 63 L=1,LL
      UY1M(L)=RY1N(L,J1-LL)
      UY2M(L)=RY2N(L,J1-LL)
      UY1(L)=RY1(L)
      UY2(L)=RY2(L)
C     UY1(L)=YQ1(1,L,J1)+YQ1(2,L,J1)
C     UY2(L)=YQ2(1,L,J1)+YQ2(2,L,J1)
C     UY1(L)=YR(1,L,J1)+YR(2,L,J1)
C     UY2(L)=YIM(1,L,J1)+YIM(2,L,J1)
C     UY1M(L)=UY1(L)
C     UY2M(L)=UY2(L)
63    CONTINUE
C
C     DETECTION PROCESSES
C
C     FIRST...NONLINEAR EQUELISER (NLEQ)
C
      XRE=0.0
      XIE=0.0
      DO 65 L=2,LL
      L1=J1-L+1
      XRE=XRE+UY1(L)*NXER(L1)-UY2(L)*NXEI(L1)
65    XIE=XIE+UY1(L)*NXEI(L1)+UY2(L)*NXER(L1)
      ERX=R1-XRE
      EIX=R2-XIE
      YY=SQRT(RY1(1)**2+RY2(1)**2)
      IF(YY.LT.0.01)YY=0.01
      XER=(UY1(1)*ERX+UY2(1)*EIX)/YY
      XEI=(UY1(1)*EIX-UY2(1)*ERX)/YY
      NXER(J1)=INT(SIGN(1.05,XER))
      NXEI(J1)=INT(SIGN(1.07,XEI))
C
C     THE NEAR MAXIMUM-LIKELIHOOD DETECTOR (S2D3)
C     ___________________________________________
C
```

```
C       CACULATE THE INTERSYMBOL INTERFERENCE FOR EACH OF THE M STORED
C       VECTORS. ALSO SUBTRACT THE LOWEST MINIMUM COST FROM THE OTHER
C       MINIMUM COSTS AND GIVE ZERO VALUE TO THE LOWEST COST.
C       EXPAND THE M STORED VECTORS TO 4M VECTORS AND CALCULATE THE
C       COST FOR EACH EXPANDED VECTOR.
C       SELECT M VECTORS ASSOSIATED WITH MINIMUM COST.
C       DISCARD THE NONSELECTED VECTORS BY SETTING THEIR COSTS TO VERY
C       HIGH VALUE.
C       STORE THE SELECTED VECTORS IN TEMPORARY STORES, SO THAT
C       NONE OF THEM COULD BE SELECTED MORE THAN ONCE, AND RETRIEVE
C       THEM WITH A RANKING METHOD SO THAT THE VECTOR ASSOCIATED WITH
C       THE LOWEST MINIMUM COST TAKES THE FIRST POSITION IN THE RANK.
C       TAKE THE FIRST COMPONENT OF THE FIRST VECTOR IN THE RANK TO
C       BE THE DETECTED DATA SYMBOL.
C
        MNK=0
        CXZ=C1(1,J11)
        DO 71 MV=1,LM
        C1(MV,J11)=C1(MV,J11)-CXZ
        XRC(MV)=0.0
        XIC(MV)=0.0
        DO 70 L=2,LL
        L1=J1-L+1
        XRC(MV)=XRC(MV)+UY1M(L)*MR(MV,L1)-UY2M(L)*MM(MV,L1)
70      XIC(MV)=XIC(MV)+UY1M(L)*MM(MV,L1)+UY2M(L)*MR(MV,L1)
        DO 71 NV=1,LM
        MNK=MNK+1
        XRC1(MV,NV)=UY1M(1)*JSR(NV,1)-UY2M(1)*JSR(NV,2)
        XRC1(MV,NV)=R1-XRC(MV)-XRC1(MV,NV)
        XIC1(MV,NV)=UY1M(1)*JSR(NV,2)+UY2M(1)*JSR(NV,1)
        XIC1(MV,NV)=R2-XIC(MV)-XIC1(MV,NV)
        CC1(MNK)=C1(MV,J11)+XRC1(MV,NV)**2+XIC1(MV,NV)**2
71      CONTINUE
        DO 80 KV=1,LM
        CCC(KV)=1.0E6
        DO 75 MNK=1,M4
75      CCC(KV)=AMIN1(CCC(KV),CC1(MNK))
        MNK=0
        DO 77 MV=1,LM
        DO 77 NV=1,LM
        MNK=MNK+1
        ACC1=ABS(CCC(KV)-CC1(MNK))
        IF(ACC1.LT.1.0E-9)THEN
        KMN1=MNK
        KMNV(KV)=MV
        NKV(KV)=NV
        ENDIF
77      CONTINUE
        DO 80 MV=1,LM
        KMN1=KMN1+4*(MV-1)
        IF(KMN1.GT.M4) KMN1=KMN1-M4
        CC1(KMN1)=1.0E6
80      CONTINUE
        DO 85 KV=1,LM
        DO 85 L=2,LL
        L1=J1-L+1
        MRT(KV,L)=MR(KMNV(KV),L1)
        MMT(KV,L)=MM(KMNV(KV),L1)
85      TC1(KV,L)=C1(KMNV(KV),L1)
        DO 90 KV=1,LM
```

```
      DO 90 L=2,LL
      L1=J1-L+1
      MR(KV,L1)=MRT(KV,L)
      MM(KV,L1)=MMT(KV,L)
90    C1(KV,L1)=TC1(KV,L)
      DO 95 KV=1,LM
      C1(KV,J1)=CCC(KV)
      MR(KV,J1)=JSR(NKV(KV),1)
95    MM(KV,J1)=JSR(NKV(KV),2)
      MMR=MR(1,J1-LL)
      MMI=MM(1,J1-LL)
C
C     CHANNEL ESTIMATION USING MFBCE
C
      RC1=0.0
      RC2=0.0
      DO 97 L=2,LL
      L1=J1-L+1
      RC1=RC1+RY1(L)*SR(L1)-RY2(L)*SIM(L1)
97    RC2=RC2+RY1(L)*SIM(L1)+RY2(L)*SR(L1)
      ET1=R1-RC1
      ET2=R2-RC2
      ETT=0.5*(SR(J1)*ET1+SIM(J1)*ET2)
      ET2=0.5*(SR(J1)*ET2-SIM(J1)*ET1)
      CHI1(2)=ETT-EQ1(J11)
      CHI2(2)=ET2-EQ2(J11)
      CHO1(2)=GI1*CHI1(2)+GI2*CHI1(1)+GI3*CHO1(1)
      CHO2(2)=GI1*CHI2(2)+GI2*CHI2(1)+GI3*CHO2(1)
      CHI1(1)=CHI1(2)
      CHI2(1)=CHI2(2)
      CHO1(1)=CHO1(2)
      CHO2(1)=CHO2(2)
      EQ1(J1)=EQ1(J11)+CHO1(2)
      EQ2(J1)=EQ2(J11)+CHO2(2)
      DO 99 L=1,LL
      L1=J1-L+1
      YB1(L)=BB1*YB1(L)+BB*(EQ1(L1)*Y1(L)-EQ2(L1)*Y2(L))
      YB2(L)=BB1*YB2(L)+BB*(EQ1(L1)*Y2(L)+EQ2(L1)*Y1(L))
      DXY1=YB1(L)-RY1(L)
      DXY2=YB2(L)-RY2(L)
      XY1(L)=XY1(L)+DXY1*B1B
      XY2(L)=XY2(L)+DXY2*B1B
      RY1(L)=RY1(L)+XY1(L)+DXY1*B2B
      RY2(L)=RY2(L)+XY2(L)+DXY2*B2B
      RY1N(L,J1)=RY1(L)+3*XY1(L)
      RY2N(L,J1)=RY2(L)+3*XY2(L)
99    CONTINUE
C
C     CARRIER SYNCHRONISATION USING DA-DPLL
C
      JD=J1-ND
      DO 100 IDV=1,2
      RCR1=RC(IDV)*RA(IDV)+RD(IDV)*RB(IDV)
      RCR2=RC(IDV)*RB(IDV)-RD(IDV)*RA(IDV)
      IF(RCR1.LT.0.001)RCR1=0.001
      TTA(IDV,2)=ATAN2(RCR2,RCR1)
      ATT(IDV,2)=GI1*TTA(IDV,2)+GI2*TTA(IDV,1)+GI3*ATT(IDV,1)
      TTA(IDV,1)=TTA(IDV,2)
      ATT(IDV,1)=ATT(IDV,2)
      THTA(IDV)=THTA(IDV)+ATT(IDV,2)
```

```
      IF(THTA(IDV).GT.PI2)THTA(IDV)=THTA(IDV)-PI2
      C1R(IDV)=COS(THTA(IDV))
      C1I(IDV)=SIN(THTA(IDV))
100   CONTINUE
C
C     MAPPING BACK THE SYMBOLS TO REGENERATE THE TRANSMITTED BITS
C
      LD1=(3-MMR)/2
      LD2=(3-MMI)/2
C
C     DIFFERENTIAL DECODING FOR S2D3
C
      KBD(J1)=IB(LD1,LD2)
      LBBD=KBD(J1)+KBD(J11)
      IF(LBBD.GE.4) LBBD=LBBD-4
      LBBD=LBBD+1
C     LBBD=IB(LD1,LD2)+1
      LE1=(3-NXER(J1))/2
      LE2=(3-NXEI(J1))/2
C
C     DIFFERENTIAL DECODING FOR NLEQ
C
      KBE(J1)=IB(LE1,LE2)
      LBBE=KBE(J1)+KBE(J11)
      IF(LBBE.GE.4) LBBE=LBBE-4
      LBBE=LBBE+1
C     LBBE=IB(LE1,LE2)+1
C
C     BITS ERROR CALCULATIONS
C
      COUN=COUN+1
      DO 150 N=1,KK
      ISM(N)=JSR(LBBD,N)
      ISE(N)=JSR(LBBE,N)
C     WRITE (NOUT,147) ISM(N),JIS(N,J1),IS(N),J1
C147  FORMAT(2X,4(I4,6X))
      ISNM=ISM(N)-JIS(N,J1-LL)
      IF(ISNM.NE.0) IEM=IEM+1
      ISIE=ISE(N)-IS(N)
      IF(ISIE.NE.0) IEE=IEE+1
150   CONTINUE
C
C     STORE THE REQUIRED INFORMATION TO INITIALIZE THE NEXT
C     BLOCK OF DATA
C
      LB(0)=LB(KJ1)
      KBD(0)=KBD(KJ1)
      KBM(0)=KBM(KJ1)
      KBE(0)=KBE(KJ1)
      DO 200 M=KJL1,KJ1
      M1=M-KJ1
      DO 170 IDV=1,2
      Q1(IDV,M1)=Q1(IDV,M)
      Q2(IDV,M1)=Q2(IDV,M)
      QQ(IDV,M1)=QQ(IDV,M)
170   JIS(IDV,M1)=JIS(IDV,M)
      EQ1(M1)=EQ1(M)
      EQ2(M1)=EQ2(M)
      NXER(M1)=NXER(M)
      NXEI(M1)=NXEI(M)
```

```
        SR(M1)=SR(M)
        SIM(M1)=SIM(M)
        DO 200 MV=1,LM
        C1(MV,M1)=C1(MV,M)
        MR(MV,M1)=MR(MV,M)
        MM(MV,M1)=MM(MV,M)
        RY1N(MV,M1)=RY1N(MV,M)
        RY2N(MV,M1)=RY2N(MV,M)
200     CONTINUE
        DO 250 IDV=1,2
        QF11(IDV)=QF1(IDV)
        QF21(IDV)=QF2(IDV)
        FQ1(IDV,0)=FQ1(IDV,MFD)
        FQ2(IDV,0)=FQ2(IDV,MFD)
250     CONTINUE
C
C
        TOTAL=2.0*COUN
C
C       CALCULATE BIT ERROR RATE
C
        ERM(I)=FLOAT(IEM)/TOTAL
        ERE(I)=FLOAT(IEE)/TOTAL
C
C       CALCULATE SIGNAL-TO-NOISE-RATIO (SNR) IN dB
C
        SN(I)=10.0*LOG10(TSP/TNP)
C       WRITE(6,9999)SN(I),ERM(I)
300     CONTINUE
        WRITE(NOUT,9997)
        WRITE(NOUT,9999)(SN(I),ERM(I),I=1,II)
        WRITE(NOUT,9998)
        WRITE(NOUT,9999)(SN(I),ERE(I),I=1,II)
        STOP
9997    FORMAT(4X,'NMLD RESULTS')
9998    FORMAT(4X,'EQUALISER RESULTS')
9999    FORMAT(1X,2(F12.8,7X))
        END
####S
```

```
/*JOB JOBF3,EUELSM,ST=MFY,C=S,TI=1280,
/* PW=SAM1
FTN5,DB=O/PMD,L=0.
LIBRARY,PROCLIB.
NAG(FTN5).
LGO.
####S
      PROGRAM CRS12
C
C     THIS PROGRAM SIMULATES A RECEIVER EMPLOYING CRS2 DESCRIBED
C     IN CHAPTERS 5 AND 8 (SEE FIGURE 8.3) WITH USE OF SPACE
C     DIVERSITY. ALSO,THIS PROGRAM CAN BE MODIFIED TO SIMULATE
C     THE FUNCTION OF A RECEIVER EMPLOYING CRS1 (FIGURE 8.2).
C     IN EITHER CASE THE SIMULATION IS CARREID OUT TO DETERMINE
C     THE SYSTEM TOLERACE TO ADDITIVE WHITE GAUSSIAN NOISE
C     UNDER RAYLEIGH FADING CONDITIONS.
C
C
C
       DIMENSION
     * QW2(2,6)),RAY1(2,-1:2),RAY2(2,-1:2),QW1(2,6),AH(5),BH(5),
     * Q1(2),Q2(2),Q1Q(2),Q2Q(2),QQ1(2),QQ2(2),DQ1(2),DQ2(2)
     *,WQ1(2),OBS(2),LOBS(2),CRC(2)
     *,WQ2(2),DELTA1(2),DELTA2(2),IZO(2),IDZ(2),IZ1(2),AAA(2),
     * HK1(16),HK2(16),HK3(16),
     * TX1(2,-15:32),TX2(2,-15:32),TX3(2,-15:32)
     * ,CV(2,-15:32),CV1(2,-15:32),CV2(2,-15:32)
     * ,IZ2(2,-15:32),IZ21(2,-15:32),IZ22(2,-15:32)
     * ,XY(2),XYS(2),XYC(2)
     * ,IS(-5:38),ISS(-5:38)
       DIMENSION
     * U(2,-5:38)
     * ,XX(2,-15:32),XX1(2,-15:32),XX2(2,-15:32),XX3(2,-15:32)
     * ,HH1(16),HH2(16),HH3(16)
     * ,HF1(16),HF2(16),HF3(16)
     * ,XZA(2,-15:32),XZB(2,-15:32),XZC(2,-15:32)
     * ,IZ11(2,-15:32),IZ12(2,-15:32),IZ13(2,-15:32)
C      DOUBLE PRECISION PI,G05DAF,G05DDF,P
     1 ,XC(2,-15:32),XC1(2,-15:32),XC2(2,-15:32),XX4(2,-15:32)
     1 ,XS(2,-15:32),XS1(2,-15:32),XS2(2,-15:32)
     2 ,XDATA(16),ZDATA(16),TDAT(16),TXDA(16),CDA(16),SDA(16)
       DATA NOUT/6/
C
C      COEFFICIENTS OF FIFTH ORDER BESSEL DIGITAL FILTER
C
       DATA AH/0.959,-0.574,0.362,-0.1054,0.0131/
       DATA BH/0.7502,-0.63015,0.28443,-6.54E-2,6.24E-3/
C
C      COEFFICIENTS OF FILTER F1
C
       DATA HH1/6.87478946E-2,0.122048137,0.181637437,0.233023051,
     ,0.255064314,0.226035515,0.131445974,-2.88917152E-2,-0.23689837,
     ,-0.457137063,-0.642999058,-0.746939,-0.732501942,-0.584670595,
     ,-0.316122069,3.31861899E-2/
       DATA HH2/0.402987096,0.724967173,0.937638785,1.0,0.900762414,
     ,0.660885885,0.328592937,-3.16052633E-2,-0.353344241,-0.582647344,
     ,-0.688551413,-0.667872734,-0.543098055,-0.354642889,-0.149642855,
     ,2.9650692E-2/
       DATA HH3/0.154619515,0.214625427,0.215957761,0.176605779,
     , 0.118719364,6.14500994E-2,1.64002915E-2,-1.29527908E-2,
```

```
     ,-2.7401233E-2,-2.43069181E-2,1.36916244E-2,0.0,0.0,0.0,0.0,0.0,0.0/
C
C        COEFFICIENTS OF FILTER F2
C
         DATA HF1/7.1134886E-2,0.122574656,0.104450198,-1.24884406E-2
     ,,-0.18679452,-0.301316707,-0.23269146,4.19893582E-2,0.387532189
     ,,0.568680733,0.406640442,-6.97895119E-2,-0.599406735,-0.83345901
     ,,-0.569711477,8.44662749E-2/
         DATA HF2/0.74815405,0.999032566,0.654766037,-8.8789142E-2
     ,,-0.784027373,-1.0,-0.62257679,9.15249897E-2,0.693873864
     ,,0.840643628,0.497759962,-7.27859267E-2,-0.51187099,-0.59444152
     ,,-0.341229069,3.87116049E-2/
         DATA HF3/0.307795672,0.344807153,1.9017485E-2,-1.57210232E-2
     ,,-0.141906984,-0.144944444,-7.01451863E-2,8.76474271E-2,
     ,5.12439358E-2,6.04958102E-2,4.70064306E-2,0.0,0.0,0.0,0.0,0.0,0.0/
C
C      INITIALISATION OF ALL REQUIRED PARAMETERS
C
       DATA XDATA/0.44119,0.75916,0.96155,1.01755,0.91865,0.67988,
     ,0.33761,-0.05605,-0.44119,-0.75916,-0.96155,-1.01755,
     ,-0.91865,-0.67988,-0.33761,0.05605/
         DATA CDA/0.42339,0.51496,0.0,-0.68972,-0.88027,-0.4605,0.0
     ,,-0.03793,-0.4221,-0.51339,0.0,0.68762,0.87759,0.45909,0.0,
     ,0.03781/
         DATA SDA/0.0,0.51496,0.92207,0.68972,0.0,-0.4605,-0.32328,
     ,0.03793,0.0,-0.51339,-0.91926,-0.68762,0.0,0.45909
     ,,0.32229,-0.03781/
         DATA ZDATA/0.50612,0.14895,-0.2368,-0.42312,-0.30112,0.0575
     ,,0.44388,0.62865,0.50427,0.1484,-0.23593,-0.42157,-0.3,
     ,0.05728,0.44224,0.62633/
         DATA TDAT/5.82596,3.18687,-1.34212,-5.10799,-5.90474,-3.26565
     ,,1.26334,5.02921,5.82596,3.18687,-1.34212,-5.10799,-5.90474,
     ,-3.26565,1.26334,5.02921/
         DATA TXDA/0.43777,0.03389,0.10518,0.61363,1.26141,1.67113,
     ,1.60831,1.0905,0.43777,0.03389,0.10518,0.61363,1.26141,
     ,1.67113,1.60831,1.0905/
         OPEN (1,FILE='OUTPUT')
         WRITE (NOUT,500)
C
C    THE INPUT DATA FOR THE PROGRAM
C
C
         PI=4.0*ATAN(1.0)
         P2I=2*PI
C        V=60.0
C        F IS THE DATA RATE IN C/S
         F=9.6E3
C        FC IS THE CARRIER FREQUENCY IN HZ
         FC=19.2E3
         FNC=0.5*FC/F
         AUNC=2*PI*FNC
         KC=2
         KC1=38
         KC2=16
         KC3=2*KC2
         KTH=1
        DT=1.0/KC2
        T=-1.*KC2*DT
        ISOLD=1
        GAIN1=5.13
```

```
      GAIN2=1.0
      ROOT2=SQRT(2.0)
      OOR2=1./ROOT2
      OSGA=0.05
      OSGA1=1.0-OSGA
C
C
      CALL G05CBF(33)
      DO 100 MZ=1,2
      LOBS(MZ)=1
      Q1Q(MZ)=1.0
      Q2Q(MZ)=0.0
      WQ1(MZ)=1.0
      WQ2(MZ)=0.0
      DO 100 K=1,2
      K1=1-K
      QW1(MZ,K1)=GAIN1
      QW2(MZ,K1)=0.0
      QW11(MZ,K1)=GAIN1
      QW12(MZ,K1)=GAIN1
      QW21(MZ,K1)=0.0
      QW22(MZ,K1)=0.0
      RAY1(MZ,K1)=1.0
      RAY2(MZ,K1)=0.0
100   CONTINUE
C
      DO 120 M=1,KC2
      M1=M-KC2
      M2=1+INT((M+1)/8)
      M3=INT((M)/4)
C     THC=2*PI*FC*T/F
      THC=PI*FC*T/F
      DO 119 MZ=1,2
      XX(MZ,M1)=XDATA(M)
      XX1(MZ,M1)=XDATA(M)
      XX2(MZ,M1)=XDATA(M)
      XX3(MZ,M1)=XDATA(M)
      XX4(MZ,M1)=XDATA(M)
      XC(MZ,M1)=CDA(M)
      XC1(MZ,M1)=CDA(M)
      XC2(MZ,M1)=CDA(M)
      XS(MZ,M1)=SDA(M)
      XS1(MZ,M1)=SDA(M)
      XS2(MZ,M1)=SDA(M)
      TX1(MZ,M1)=ZDATA(M)
      TX2(MZ,M1)=ZDATA(M)
      TX3(MZ,M1)=ZDATA(M)
      IZ2(MZ,M1)=(-1)**M2
      IZ21(MZ,M1)=(-1)**M2
      IZ22(MZ,M1)=(-1)**M2
      IZ11(MZ,M1)=(-1)**M3
      IZ12(MZ,M1)=(-1)**M3
      IZ13(MZ,M1)=(-1)**M3
      CV(MZ,M1)=COS(THC)
      CV1(MZ,M1)=CV(MZ,M1)
119   CV2(MZ,M1)=CV1(MZ,M1)
120   T=T+DT
      ISA=-1
      ISA0=-1
      ISA1=1
```

```
      ISB1=1
C
C
      DO 125 JS=-3,0,1
      IS(JS)=1
      ISS(JS)=1
      DO 125 MZ=1,2
125   U(MZ,JS)=1.0
C
C     THE IMPULSE RESPONSE OF THE CHANNEL HAS BEEN CALCULATED TO BE
C     Y1=1.0
C     Y2=0.315
C     Y3=1.0715E-3
C
      IZ2(1,0)=-1
      IZ2(2,0)=-1
      DO 400 L=1,5,2
      VP=-0.05*(3.5+1.3*(L-1))
      P=10**VP
      IE=0
      ICOUN=0
      TSP=0.0
      TNP=0.0
      WNC1=0.0
      WNC2=0.0
C
C     C
      DO 392 LI=1,395
      DO 240 I=1,KC
      IK1=I-1
      IK2=I-2
C     FIFTH ORDER LOWPASS BESSEL FILTER
C
      DO 130 MZ=1,2
      DO 31 KQ=1,5
      KQ1=KQ+1
      WQ1(MZ,KQ)=WQ1(MZ,KQ1)
31    WQ2(MZ,KQ)=WQ2(MZ,KQ1)
      RAY1(MZ,IK1)=RAY1(MZ,I)
      RAY2(MZ,IK1)=RAY2(MZ,I)
      WQ1(MZ,6)=G05DDF(0.0,1.0)
      WQ2(MZ,6)=G05DDF(0.0,1.0)
      RAY1(MZ,I)=0.0
      RAY2(MZ,I)=0.0
      DO 33 KQ=1,5
      KQ1=6-KQ
      WQ1(MZ,6)=WQ1(MZ,6)+BH(KQ)*WQ1(MZ,KQ1)
33    WQ2(MZ,6)=WQ2(MZ,6)+BH(KQ)*WQ2(MZ,KQ1)
      DO 35 KQ=1,5
      KQ1=7-KQ
      RAY1(MZ,I)=RAY1(MZ,I)+AH(KQ)*WQ1(MZ,KQ1)
35    RAY2(MZ,I)=RAY2(MZ,I)+AH(KQ)*WQ2(MZ,KQ1)
      DELTA1(MZ)=(RAY1(MZ,I)-RAY1(MZ,IK1))/KJ1
      DELTA2(MZ)=(RAY2(MZ,I)-RAY2(MZ,IK1))/KJ1
130   CONTINUE
C
C
      DO 230 I1=1,KC1
      DO 140 MZ=1,2
      QQ1(MZ)=RAY1(MZ,IK1)+I1*DELTA1(MZ)
```

```
      DQ1(MZ)=(QQ1(MZ)-Q1Q(MZ))/KC3
      QQ2(MZ)=RAY2(MZ,IK1)+I1*DELTA2(MZ)
140   DQ2(MZ)=(QQ2(MZ)-Q2Q(MZ))/KC3
      ISS(I1)=ISA0
C
C     BITS GENERATION AND DIFFERENTIAL CODING
C
      SS=G05DAF(-1.0,1.0)
      ISA0=INT(SIGN(1.05,SS))
      ISA=ISA0*ISA1
      ISA1=ISA
C
C     RESET THE INTEGRATOR
C
      RS1=0.0
      RS2=0.0
      OBS(1)=0.0
      OBS(2)=0.0
      DO 210 IRF=1,KC3
      IRF1=IRF-KC2
      THS=0.5*(1.0+ISA)*PI
      Q1(1)=Q1Q(1)+DQ1(1)*IRF
      Q1(2)=Q1Q(2)+DQ1(2)*IRF
      IF(Q1(1).EQ.0.0) Q1(1)=0.1E-5
      IF(Q1(2).EQ.0.0) Q1(2)=0.1E-5
      Q2(1)=Q2Q(1)+DQ2(1)*IRF
      Q2(2)=Q2Q(2)+DQ2(2)*IRF
      THQ1=ATAN(Q2(1)/Q1(1))+0.5*(1.0-(Q1(1)/ABS(Q1(1))))*PI
      THQ2=ATAN(Q2(2)/Q1(2))+0.5*(1.0-(Q1(2)/ABS(Q1(2))))*PI
      A1Q=SQRT(Q1(1)**2+Q2(1)**2)
      A2Q=SQRT(Q1(2)**2+Q2(2)**2)
      WGN1=WNC1
      WGN2=WNC2
      WNC1=G05DDF(0.0,P)
      WNC2=G05DDF(0.0,P)
C
C     NOISE POWER CALCULATION
C
      TNP=TNP+0.5*(WNC1**2+WNC2**2)
      THC=AUNC*T
      LJ=INT(THC/P2I)
      THC=THC-LJ*P2I
      THLO=2*THC
C
C     LOCAL OSCILLATOR SIGNAL
C
      OSCLO=COS(THLO)
      PHIT1=THC+THS+THQ1
      PHIT2=THC+THS+THQ2
C
C     LINEAR MODULATION AND CHANNEL FADING
C
      CV(1,IRF)=A1Q*COS(PHIT1)
      CV(2,IRF)=A2Q*COS(PHIT2)
C
C     SIGNAL POWER CALCULATION
C
      TSP=TSP+0.5*(CV(1,IRF)**2+CV(2,IRF)**2)
      CV(1,IRF)=CV(1,IRF)+WGN1
      CV(2,IRF)=CV(2,IRF)+WGN2
```

```
      DO 200 MZ=1,2
      CV1(MZ,IRF)=CV(MZ,IRF1)
      CV2(MZ,IRF)=CV1(MZ,IRF1)
      XC(MZ,IRF)=0.0
      DO 149 IH=1,KC2
C
C     RECEIVER FILTER F1
C
      IH1=IRF-IH+1
      XC(MZ,IRF)=XC(MZ,IRF)+0.09*CV(MZ,IH1)*HH1(IH)
      XC(MZ,IRF)=XC(MZ,IRF)+0.09*CV1(MZ,IH1)*HH2(IH)
149   XC(MZ,IRF)=XC(MZ,IRF)+0.09*CV2(MZ,IH1)*HH3(IH)
      XX(MZ,IRF)=XC(MZ,IRF)
      XX1(MZ,IRF)=XX(MZ,IRF1)
      XX2(MZ,IRF)=XX1(MZ,IRF1)
      XX3(MZ,IRF)=XX2(MZ,IRF1)
      XX4(MZ,IRF)=XX3(MZ,IRF1)
      XS(MZ,IRF)=XC(MZ,IRF)*SIN(THLO)
      XS1(MZ,IRF)=XS(MZ,IRF1)
      XS2(MZ,IRF)=XS1(MZ,IRF1)
      XC(MZ,IRF)=XC(MZ,IRF)*OSCLO
      XC1(MZ,IRF)=XC(MZ,IRF1)
      XC2(MZ,IRF)=XC1(MZ,IRF1)
      XYC(MZ)=0.0
      XYS(MZ)=0.0
      DO 159 IH=1,KC2
      IH1=IRF-IH+1
      XYS(MZ)=XYS(MZ)-XS(MZ,IH1)*HH1(IH)
      XYS(MZ)=XYS(MZ)-XS1(MZ,IH1)*HH2(IH)
      XYS(MZ)=XYS(MZ)-XS2(MZ,IH1)*HH3(IH)
      XYC(MZ)=XYC(MZ)-XC(MZ,IH1)*HH1(IH)
      XYC(MZ)=XYC(MZ)-XC1(MZ,IH1)*HH2(IH)
159   XYC(MZ)=XYC(MZ)-XC2(MZ,IH1)*HH3(IH)
C
C     SQUARING IS CARRIED OUT BY THIS FORMULA
C     COS(2X)=COS**(X)-SIN**(X)
C
      XY(MZ)=XYC(MZ)**2-XYS(MZ)**2
C
C     HARD LIMITER
C
      IF(XY(MZ).LT.0.0) THEN
      IZ11(MZ,IRF)=-1
      ELSE
      IZ11(MZ,IRF)=1
      ENDIF
      IZ12(MZ,IRF)=IZ11(MZ,IRF1)
      IZ13(MZ,IRF)=IZ12(MZ,IRF1)
      XZA(MZ,IRF)=0.0
      DO 179 IH=1,KC2
      IH1=IRF-IH+1
      XZA(MZ,IRF)=XZA(MZ,IRF)+6.25E-2*IZ11(MZ,IH1)*HF1(IH)
      XZA(MZ,IRF)=XZA(MZ,IRF)+6.25E-2*IZ12(MZ,IH1)*HF2(IH)
179   XZA(MZ,IRF)=XZA(MZ,IRF)+6.25E-2*IZ13(MZ,IH1)*HF3(IH)
      XZB(MZ,IRF)=XZA(MZ,IRF1)
      XZC(MZ,IRF)=XZB(MZ,IRF1)
C
C     FREQUENCY DIVIDING BY 2
C
      IF(XZA(MZ,IRF).LT.0.0) THEN
```

```
      IZ1(MZ)=-1
      ELSE
      IZ1(MZ)=1
      ENDIF
      IDZ(MZ)=IZ1(MZ)-IZ0(MZ)
      IF(IDZ(MZ).EQ.2)THEN
      IZ2(MZ,IRF)=-IZ2(MZ,IRF-1)
      ELSE
      IZ2(MZ,IRF)=IZ2(MZ,IRF-1)
      ENDIF
      IZ2(MZ,IRF)=IZ2(MZ,IRF)*LOBS(MZ)
      IZ21(MZ,IRF)=IZ2(MZ,IRF1)
      IZ22(MZ,IRF)=IZ21(MZ,IRF1)
      TX1(MZ,IRF)=0.0
      DO 189 IH=1,KC2
      IH1=IRF-IH+1
      TX1(MZ,IRF)=TX1(MZ,IRF)+0.09*IZ2(MZ,IH1)*HH1(IH)
      TX1(MZ,IRF)=TX1(MZ,IRF)+0.09*IZ21(MZ,IH1)*HH2(IH)
189   TX1(MZ,IRF)=TX1(MZ,IRF)+0.09*IZ22(MZ,IH1)*HH3(IH)
      TX1(MZ,IRF)=TX1(MZ,IRF)*XX3(MZ,IRF-14)
      TX2(MZ,IRF)=TX1(MZ,IRF1)
      TX3(MZ,IRF)=TX2(MZ,IRF1)
      AAA(MZ)=0.0
      DO 199 IH=1,KC2
      IH1=IRF-IH+1
      AAA(MZ)=AAA(MZ)+6.25E-2*TX1(MZ,IH1)*HF1(IH)
      AAA(MZ)=AAA(MZ)+6.25E-2*TX2(MZ,IH1)*HF2(IH)
199   AAA(MZ)=AAA(MZ)+6.25E-2*TX3(MZ,IH1)*HF3(IH)
200   CONTINUE
C     ,,JJR1,JJR2
      IZ0(1)=IZ1(1)
      IZ0(2)=IZ1(2)
C
C     DEMODULATION AND TIME INTEGRAL
C
      RS1=RS1+AAA(1)*OSCLO
      RS2=RS2+AAA(2)*OSCLO
210   T=T+DT
C
C     PAHSE OBSERVATION LOGIC
C
      RSRS=ABS(RS1)-ABS(RS2)
      RRSS=RS1*RS2
      IF(RRSS) 211,211,214
 211  IF(RSRS) 212,213,213
 212  IRS1=IRS1+1
      IRS2=0
      GO TO 215
 213  IRS1=0
      IRS2=IRS2+1
      GO TO 215
 214  IRS1=0
      IRS2=0
      GO TO 215
 215  CONTINUE
      IF(IRS1.EQ.5) IZ2(1,KC3)=-IZ2(1,KC3)
      IF(IRS2.EQ.5) IZ2(2,KC3)=-IZ2(2,KC3)
      IF(OBS(1).LT.0.0) THEN
      LOBS(1)=-1
      ELSE
```

```
      LOBS(1)=1
      ENDIF
      IF(OBS(2).LT.0.0) THEN
      LOBS(2)=-1
      ELSE
      LOBS(2)=1
      ENDIF
C
C     COMBINING AND THRESHOLD DETECTION
C
      RS=0.5*(RS1+RS2)
      IF(RS.LT.0.0)THEN
      ISB=1
      ELSE
      ISB=-1
      ENDIF
      IS(I1)=ISB*ISB1
      ISB1=ISB
      ICOUN=ICOUN+1
C
C     ERRORS CALCULATION
C
      ISSA=IS(I1)-ISS(I1-2)
      IF(ISSA.NE.0) IE=IE+1
C
C     STORE THE REQUIRED INFORMATION TO INITIALIZE THE NEXT
C     BLOCK OF DATA
C
C     THQ2=DTHQ
      Q1Q(1)=QQ1(1)
      Q1Q(2)=QQ1(2)
      Q2Q(1)=QQ2(1)
      Q2Q(2)=QQ2(2)
      DO 230 MZ=1,2
      DO 229 IG=1,KC2
      IG1=KC3-IG+1
      IG2=IG1-KC3
      IZ11(MZ,IG2)=IZ11(MZ,IG1)
      IZ12(MZ,IG2)=IZ12(MZ,IG1)
      IZ13(MZ,IG2)=IZ13(MZ,IG1)
      IZ2(MZ,IG2)=IZ2(MZ,IG1)
      IZ21(MZ,IG2)=IZ21(MZ,IG1)
      IZ22(MZ,IG2)=IZ22(MZ,IG1)
      XZA(MZ,IG2)=XZA(MZ,IG1)
      XZB(MZ,IG2)=XZB(MZ,IG1)
      XZC(MZ,IG2)=XZC(MZ,IG1)
      TX1(MZ,IG2)=TX1(MZ,IG1)
      TX2(MZ,IG2)=TX2(MZ,IG1)
      TX3(MZ,IG2)=TX3(MZ,IG1)
      CV(MZ,IG2)=CV(MZ,IG1)
      CV1(MZ,IG2)=CV1(MZ,IG1)
      CV2(MZ,IG2)=CV2(MZ,IG1)
      XC(MZ,IG2)=XC(MZ,IG1)
      XC1(MZ,IG2)=XC1(MZ,IG1)
      XC2(MZ,IG2)=XC2(MZ,IG1)
      XS(MZ,IG2)=XS(MZ,IG1)
      XS1(MZ,IG2)=XS1(MZ,IG1)
      XS2(MZ,IG2)=XS2(MZ,IG1)
      XX4(MZ,IG2)=XX4(MZ,IG1)
      XX3(MZ,IG2)=XX3(MZ,IG1)
```

```
      XX(MZ,IG2)=XX(MZ,IG1)
      XX1(MZ,IG2)=XX1(MZ,IG1)
229   XX2(MZ,IG2)=XX2(MZ,IG1)
230   CONTINUE
C
      DO 240 JSS=1,3
      JSS1=KC1-JSS+1
      JSS2=JSS1-KC1
      ISS(JSS2)=ISS(JSS1)
      IS(JSS2)=IS(JSS1)
      DO 240 MZ=1,2
      U(MZ,JSS2)=U(MZ,JSS1)
240   CONTINUE
C
C
      DO 300 MZ=1,2
      DO 299 JK=1,2
      JK1=JK-2
      QW1(MZ,JK1)=QW1(MZ,JK)
      QW12(MZ,JK1)=QW12(MZ,JK)
      QW11(MZ,JK1)=QW11(MZ,JK)
      QW2(MZ,JK1)=QW2(MZ,JK)
      QW21(MZ,JK1)=QW21(MZ,JK)
      QW22(MZ,JK1)=QW22(MZ,JK)
      RAY1(MZ,JK1)=RAY1(MZ,JK)
299   RAY2(MZ,JK1)=RAY2(MZ,JK)
300   CONTINUE
C
      ER=FLOAT(IE)/FLOAT(ICOUN)
      SN=10.0*LOG10(TSP/TNP)
400   WRITE (1,600) ER,IE,SN,(L+1)/2
      STOP
C420  FORMAT(1H ,6(I3,4X))
440   FORMAT(1X,'TX=',I4,6X,'RX=',I4,6X,'I=',I3,6X,'RS1=',F10.5,
     ,6X,'RS2=',F10.5)
C460  FORMAT(1X,'C1=',I3,6X,'C2=',I3,6X,'TS1=',F10.5,6X,'TS2=',F10.5,6

C     , 'XY2=',F10.5)
500   FORMAT(1X,'ERROR RATE',9X,'ERROR COUNTER',4X,'SNR-DB')
600   FORMAT(1X,F10.8,9X,I6,11X,F10.5,4X,I2)
      END
####S
```

REFERENCES

1. Clark, A.P., "Principle of digital data transmission", Pench Press, Ltd., London 1983.
2. Feher, K., "Digital communication satellite/earth station engineering" Prentice-Hall, Inc, 1983.
3. Schwartz, M., "Information, transmission, modulation, and noise" McGraw Hill, 1980.
4. Taub, H., and Schilling, D.L., "Principles of communication systems", McGraw Hill, 1971.
5. Proakis, J.G., "Digital communications", McGraw Hill, 1983.
6. Coates, R.F.W., "Modern Communication systems", McMillan Press Ltd., 1975.
7. Stremler, F.G., "Introduction to communication systems", Addison-Wesley Publishing Co., Inc., Philippines 1977.
8. Oppenheim, A.V., Willsky, A.S., with Young, I.T.,"Signal and Systems" Prentice-Hall, Inc. 1985.
9. Clark, A.P., "Digital modems for land mobile radio",IEE PRO, Vol. 132, Pt. F, No.5, Aug. 1985, pp 348-362.
10. Lee, W.C.Y., "Mobile communication engineering", McGraw-Hill, 1982.
11. Jakes, Jr., W.C., "Microwave mobile communication", John Wiley & Sons, 1974.
12. Bateman, A.J., and McGeehan, J.D., "Date transmission over UHF fading mobile radio channels", IEE PRO, Vol. 131, Pt. F., No. 4, July 1984, pp. 364-374.
13. Maseng, T., "Digital phase modulated (DPM) signal", IEEE Trans. Comm. Vol. 33, No. 9, Sept. 1985, pp. 911-918.
14. Korn, I., "New method for computation of error probability in PSK system with interference", IEE PRO, Vol. 132, Pt. F., No.6, Oct. 1985., pp. 461-465.
15. Ausin, D.F., Chang, M.U., Harwood, D.F. and Maslov, R.A., "QPSK, Staggered QPSK, and MSK-A comparative evaluation", IEEE Trans. Comm. Vol. 31, No.2, Feb. 1985, pp. 171-182.
16. Metzger, K., and Valentin, R., "An analysis ofsensitivity of digital modulation techniques to frequency-selective fading", IEEE Trans. Comm. Vol. 33, No.9, Sept. 1985, pp. 986-992.
17. Li, L., and Milstein, L.B., "Rejection of CW interference in QPSK system using decision feedback filters", IEEE Trans. Comm., Vol. 31, No. 4, 1983, pp. 473-483.
18. Najdi, H.Y., "Digital data transmission over noise channel", PhD Thesis, Loughborough University of Technology, Loughborough, Leics. England, 1983.
19. Clark, A.P., "Modelling of digital communication system", Arab School of Science and Technology, Damascus, Syria, "Mathematical Modelling and Application", Damascus, April 1986.
20. Foschin, G.J., and Salz, J., "Digital communication over fading channels", Bell Sys. Tech. J., Vol. 62, No. 2, Feb. 1983, pp. 429-456.
21. Suzuki, H., Yamao, Y., Kikuchi, H., "A single-chip MSK coherent demodulation for mobile radio Transmission", IEEE Trans. Veh. Tech., Vol.VT-34, No. 4, Nov. 1985, pp. 157-168.

22. Popoulis, A., "Probability, ramdon variable and stochastic process", McGraw-Hill, 1984.
23. Connor, F.R., "Noise", Edward Arnold, 1982.
24. Bajpai, A.C., Mustoe, L.R., and Walker, D., "Advanced engineering mathematics", John Wiley & Sons, Ltd., 1983.
25. Vigants, A., "Microwave radio obstruction fading", Bell Sys. Tech. J., Vol. 60, No. 6, July/Aug. 1981, pp. 785-801.
26. Schiavone, J.A., "Prediction of positive refractivity gradients for line-of-sight microwave radio path", Bell Sys. Tech. J., Vol. 60, No. 6, July/Aug. 1981, pp. 803-822.
27. Loew, K., "Boundaries between radio cells-influence of building and vegetation", IEE, PRO, Vol. 132, Pt. F, No. 5, Aug. 1985, pp. 321-325.
28. Norton, K.A. "The propagation of radio wave over the surface of the earth in the upper atmosphere", Part 1, IRE PRO, Vol. 24, Octo. 1936, p. 1367.
29. Norton, K.A., "The propagation of radio wave over surface of the earth in the upper atmosphere", Part 2, IRE PRO, Vol. 25, Sept. 1937, p. 1203.
30. Norton, K.A., "The calculation of ground wave field intensivity over a finitely conducting spherical earth", IRE PRO, Vol. 63, Dec. 1941, p.63.
31. Bullington, K., "Radio propagation at frequencies above 30 megacycles", IRE PRO, Vol. 35, Oct. 1947, p. 1122.
32. Bullington, K., "Radio propagation fundamental", Bell Sys. Tech., J. Vol. 36, May 1957, p. 593.
33. Jones, D.S., "The theory of electromagnetism", McMillan, 1964.
34. Vigants, A., and Pursley, M.V., "Transmission Unavailability of frequency-diversity protected microwave FM radio system caused by multi-path fading", Bell Sys. Tech., J., Vol. 58, No. 8, Oct. 1979, pp. 1779-1796.
35. Vigants, A., "Space-diversity engineering", Bell Sys. Tech. J., Vol. 54, No. 1, Jan. 1975, pp. 103-142.
36. Barnett, W.T., "Microwave line-of-sight propagation with and without frequency diversity", Bell Sys. Tech. J., Vol. 49, No. 8, Oct. 1970, pp. 1827-1871.
37. Barnett, W.T., "Multipath propagation at 4, 6 and 11 GHz", Bell Sys. Tech. J., Vol. 51, No.2, Feb. 1972, pp. 321-361.
38. Lin, S.H., "Statistical behaviour of deep fade of diversity signal", IEEE Trans. Comm. Vol. 20, No. 6, Dec. 1972, pp. 1100-1107.
39. Chen, W.Y.S., "Estimated outage in long-haul radio relay systems with protection switching", Bell Sys. Tech. J., Vol. 50, No. 4, April 1971, pp. 1455-1485.
40. Livingston, D.C., "The physic of microwave propagation", Prentice-Hall, 1970.
41. White, R.F., "Engineering considerations for microwave communications systems", Lenkurt Electronic Co., 1970.
42. Anderson, L.J., and Trolese, L.G., "Simplified method for computing knife-edge diffraction in the shadow region", IEEE Trans. Anten. Prop., July 1958, pp. 281-286.
43. Connor, F.R., "Antennas", Edward Arnold 1981.
44. Egli, J.J., "Radio propagation above 40 MC over irregular terrain", IRE PRO, Vol. 45., Oct. 1957, pp. 1383-1391.
45. Rice, P.L., "Transmission loss predictions for tropspheric communication circuits", NBS Tech. Note 101, NTIS Acc., No. AD687820 and AD687821, Vol. 1967.

46. Longley, A.G., and Price, P.L., "Prediction of tropospheric radio transmission loss over irregular terrain, a computer method, 1968", ESSA Tech. Rep. ERL-79-ITS67, NTIS, Acc., No. 676874, 1968.
47. Okumura, Y., Ohmori, E., Kawano., T., and Fukuda, K., "Field strength and its variability in VHF and UHF land-mobile radio service", Rev. Elec. Comm. Lab., Vol. 16, Nos. 9 and 10, Sept.-Oct. 1968, pp. 825-837.
48. Edwards, R.E., and Durkin, J., "Computer prediction of service areas for v.h.f. mobile radio network", PRO, Ins. Elec. Eng., Vol. 116, No.9 Sept. 1968, pp. 1493-1500.
49. Reasoner, R.K., and Longley, A.G., "Comparison of propagation measurment with predicted values in the 20 to 10000 MHz range", ESSA Tech. Rep. ERL 148-ITS97, NTIS Acc., No. AC703579, 1970.
50. Murphy, J.P., "Statistical propagation model for irregular terrain paths between transportable and mobile antennas", AGARD Conf. Proc., No. 70, 1970, pp. 49/1-20.
51. Baris, A.P.. "Radio wave propagation over irregular terrain in the 76- to -9200 MHz frequency range", IEEE Tran. Veh., Vol. VT20, No.2, Feb. 1971, pp. 41-62.
52. Blomquist, A., and Ladell, L., "Prediction and calculation of transmission loss in different types of terrain", NATO ACARD Conf., Pub. Cp. 144, Res. Inst. Nat. Defense, Dep. 3, S.10450, Stockholm 80, Sweden, pp. 32/1-17, 1974.
53. Dadson, C.E., Durkin, J., and Martin, R.E., "Computer prediction of field strength in the planning of radio systems", IEEE Trans Veh. Tech. Vol. VT24, No. 1, Jan. 1975, pp. 1-8.
54. Durkin, J., "Computer prediction of service areas for VHF and UHF land mobile radio services", IEEE Trans. Veh. Tech., Vol. VT-26, No. 4, Nov. 1977, pp. 323-327.
55. Allsebrook, K., and Parsons, J.D., "Mobile radio propagation in British cities at frequencies in the VHF and UHF bands", IEEE Trans. Veh. Tech., Vol. VT-26, No. 4, Nov. 1977, pp. 313-323.
56. Bullington, K., "Radio propagation for vehicular communication", IEEE Trans. Veh. Tech., Vol. VT-26, No. 4, Nov. 1977, pp. 295-308.
57. Lustgarten, M.N. and Madison, J.A., "An empirical propagation model (EMP-73)", IEEE Trans, Electromagn. Comp., Vol. EMC-19, No. 3, 1979, pp. 301-309.
58. Kessler, W.J., and Wiggins, M.J., "A simplified method for calculating UHF base-to-mobile statistical converge contours over irregular terrain", 27th IEEE Veh. Tech. Conf., 1977, pp. 227-236.
59. Palmer, F.H., "The CRC VHF/UHF propagation prediction program description and comparison with field measurements", AGARD Conf. Proc., No. 238, 1978, pp. 49/1-15.
60. Ott., G.D., and Plitkins, "Urban path-loss characteristics at 820 MHz" IEEE Trans. Veh. Tech., Vol. VT-27, No. 4, Nov. 1978, pp. 189-197.
61. Longley, A.G., "Radio propagation in urban areas" OT Rep. 78-144 NTIS, 1978.
62. Palmer, F.H., "VHF/UHF path-loss calculations using terrain profiles deduced from a digital topographic data base", AGARD Conf. Pro., No.269, 1979, pp. 26/1-11.
63. MacDonald, V.H., "The cellular concept", Bell Sys. Tech. J., Vol, 58, No. 1, Jan. 1979, pp. 15-42.
64. Warford, D.J., "Complementary use of computer predictions and radio survey measurements in the base station area coverage engineering", IERE Conf. Proc., No. 44, 1979, pp. 51-58.

65. Dadson, C.E., "Radio network and radio link surveys derived by computer from a terrain data base", AGARD Conf. Proc., No. 269, 1979, pp. 25/1-17.
66. Hata, M., "Empirical formula for propagation loss in land mobile radio services", IEEE Trans. Veh. Tech., Vol.VT 29, No. 3, 1980, pp. 317-325.
67. Parsons, J.D., Ibrahim, M.F., and Samuel,R.J., "Median signal strength prediction for mobile radio propagation in London", Elec. Lett., Vol. 16, No. 5, 1980, pp. 172-173.
68. Ibrahim, M.F., and Parson, J.D., "Urban mobile radio propagation at 900 MHz", Elec. Lett., Vol. 18, No. 3, 1982, pp. 113-115.
69. Akeyama, A., Nagatsu, T., and Ebine, Y., "Mobile radio propagation characteristic and radio zone design method in local cities, "Rev. Elec. Comm. Lab. Vol. 30, No. 2, 1982, pp. 308-317.
70. Aurand, J.F., and Post, R.E., "A comparison of prediction methods for 800 MHz mobile radio propagation", IEEE Trans. Veh. Tech., Vol. VT.34. No. 4, Nov. 1985, pp. 149-153.
71. Delsile, G.Y., Lefevre, J.P., Lecours, M., and Chouinard, J.Y., "Propagation loss prediction: A comparative study with application to the mobile radio channel", IEEE Trans. Veh. Tech., Vol. VT34, No.2, May 1985, pp. 86-96.
72. Aulin, T., "A modified model for fading signal at a mobile radio channel", IEEE Trans. Veh. Tech., Vol. VT-28, No. 3, Aug. 1979, pp. 182-203.
73. Rice, S.O., "Mathematical analysis of random noise", Bell Sys. Tech. J. Vol. 23, July 1944, pp. 282-332.
74. Rice, S.O., "Mathematical analysis of random noise", Bell Sys. Tech. J., Vol. 24, Jan. 1945, pp. 146-156.
75. Rice, S.O., "Statistical properties of a sine wave plus random noise", Bell Sys. Tech. J., Vol. 27, Jan. 1948, pp. 109-157.
76. Ossanna, J. F., "A model for mobile radio fading due to building reflection: Theoretical and experimental waveform power spectra", Bell Sys. Tech. J., Vol. 43, Nov. 1964, pp. 2935-2971.
77. Gans, M.J., "A power-spectral theory of propagation in the mobile radio environment", IEEE Trans. Veh. Tech., Vol. VT-21, Feb. 1972, pp. 27-38.
78. Greenstein, L.J. and Czekau, B.A., "Modeling multipath fading responses using multitone probing signal and polynomial approximation", Bell Sys. Tech. J., Vol. 60m No.2, Feb. 1981, pp. 193-214.
79. Ream, N., "Simulation of Rayleigh fading by digital generation of amplitude and phase", The Radio and Electronic Eng., Vol. 48, No. 11, Nov. 1978, pp. 567-572.
80. Rallphs, J.D., and Sladen, F.M.F., "An h.f. channel simulator using a new Rayleigh fading method", The Radio and Electronic Eng., Vol. 46, No. 12, Dec. 1976, pp. 579-587.
81. Clarke, R.H., "A statistical theory of mobile radio reception", Bell Sys. Tech. H., Vol. 47, July/Aug. 1968, pp. 957-1000.
82. Arredondo, G.H., and Walker, E.H., "A multipath fading simulator for mobile radio", IEEE Trans. Comm., Vol. 21, No. 11, Nov. 1973.
83. Bajwa, A.S., "UHF wideband statistical model and simulation of mobile radio multipath propagation effects", IEE PRO, Vol. 132, Pt. F., No.5, Aug. 1985, pp. 327-333.
84. Arnold, H.W., and Bodtmann, W.F., "A hybrid multichannel hardware simulator for frequency-selective mobile radio paths", IEEE Trans. Comm., Vol. 31, No. 3, March 1983, pp. 370,377.
85. Lerenz, R.W., and Gebbruch, H.J., "Bit error distribution in digital mobile radio communication: Comparison between field measurements and fading simulation", IEE PRO, Vol. 132, Pt. F., No.5, Aug. 1985, pp. 343-347.

86. Hughes, C.J., and Appleby, M.S., "Definition of a cellular mobile radio system", IEE PRO, Vol. 132, Pt. F., No.5, Aug. 1985, pp. 416-424.
87. Geraniotis, E.A., and Pursley, M.B., "Performance of noncoherent direct-sequence spread spectrum communication over specular multipath fading channels", IEEE Trans. Comm., Vol. 34, No. 3, March 1986, pp. 219-226.
88. Lee, W.C.Y., "Estimate of local average power of a mobile radio signal", IEEE Trans. Veh. Tech., Vol. VT-34, No. 1, Feb. 1985, pp. 22-27.
89. Gilbert, E.N., "Energy reception for mobile radio", Bell Sys. Tech. J. Vol. 44, Oct. 1965, pp. 1779-1803.
90. Schmid, H.F., "A prediction model for multipath propagation of pulse signal at VHF and UHF over irregular terrain", IEEE Trans. Anten. Prop., March 1970, pp. 253-258.
91. Turin, G.L., "Communication through noisy, random multipath channels", IRE Conu. Rec., Pt. 4, 1956, pp. 154-166.
92. Turin, G.L., "A statistical model for urban multipath propagation", IEEE TRans. Veh. Tech., Vol. VT-21, Feb. 1972, pp. 1-9.
93. Lee, W.C.Y., "Theoretical and experimental study of the properties of the signal from an energy density mobile antenna", IEEE Trans. Veh. Tech., Vol. VT-16, Oct. 1967, pp. 121-128.
94. Smith, J.D., "A multipath fading simulator for mobile radio IEEE Trans. Veh. Tech., Vol. VT-24, Nov. 1975, pp. 39-40.
95. Hashimi, H., "Simulation of the urban radio propagation channel", IEEE Trans. Veh. Tech., Vol. VT-28, Aug. 1979, pp. 213-223.
96. Caples, E.L., Massad, K.E., and Minor, T.R., "A UHF channel simulator for digital mobile radio", IEEE Trans. Veh. Tech., Vol. VT-29, May 1980, pp. 281-289.
97. Suzuki, H., "A statistical model for urban radio propagation", IEEE Trans. Comm., Vol. 25, No. 7, July 1977, pp. 673-680.
98. Rustako, Jr., A.J., Woodworth, C.B., Roman, R.S., and Hoffman, H.H., "A laboratory simulation facility for multipath fading microwave radio channel", AT&T Tech. J., Vol. 64, No. 10, Dec. 1985, pp. 2281-2319.
99. Brigham, E.O., "The fast fourier transform", Prentice-Hall Inc., 1974.
100. CCIR, "Fading of radio signals received via the ionosphere", XIIIth Plenary Assembly CCIR, Vol. VI, Report No. 266-3, Geneva, 1974.
101. Fink, D.G., "Electronics engineer's handbook", McGraw-Hill, Inc. 1975.
102. Rabiner, L.K. and Gold, B., "Theory and application of digital signal processing", Prentice-Hall, 1975.
103. Antoniou, A., "Digital filters: Analysis and design", McGraw-Hill Inc., 1979.
104. Oppenheim, A.V., and Schafer, R.W., "Digital signal processing", Prentice-Hall, 1975.
105. Bozic, S.M., "Digital and Kalman filtering", Edward Arnold, 1979.
106. Terrell, T.J., "Introduction to digital filters", MacMillan Press Ltd., 1980.
107. Angelo, Jr., E.J., "A tutorial introduction to digital filtering", Bell Sys. Tech. J., Vol. 60, No. 7, Sept. 1981, pp. 1499-1540.
108. Nyquist, H., "Certain topics in telegraph transmission theory", AIEE Trans., Vol. 47, April 1928, pp. 617-644.
109. Clark, A.P., "Advanced data transmission systems", Pentach Press, Ltd. 1977.
110. Luky, R.W., and Weldon, E.J., "Principles of data communication", McGraw-Hill, 1968.

111. Papoulis, A., "Circuits and systems a modern approach", Holt Rinehart and Winston Inc., 1980.
112. French, R.C. "The effect of fading and shadowing on channel reuse in mobile radio", IEEE Trans. Tech. Vol. VT-28,No.3, Aug.1979. pp. 171-181.
113. Wong, W.C., Steele, R., Glance, B., Horn, D.,"Time diversity with adaptive error detection to combat Rayleigh fading in digital mobile radio", IEEE Trans. Comm. Vol. 31, No. 3, March 1983, pp. 378-387.
114. Stjernvall, J.E., and Uddenfeldt, J., "Gaussian MSK with different modulators and channel coding for mobile telephony", IEEE/Elsevier Science Publishers, B.V.,(North-Holland) 1984, pp. 1219-1222.
115. Halpern, S., "Reuse partitioning in cellular system", Bell. Labs.
116. Muammar, R., and Gupta, S.C., "Co-channel interference in high capacity mobile radio systems", IEEE Trans. Comm. Vol. 30, Aug. 1982, pp. 1973-1978.
117. Gupta, S.C. Viswanthan, R., and Muammar, R., "Land mobile radio system: A tutorial exposition", IEEE Comm. Magazine, Vol 23., No. 6, June 1985, pp. 34-45
118. Sundberg, C.E., "Alternative cell configurations for mobile digital mobile radio system", Bell Sys. Tech. J. Vol., 62, No.7, Sept. 1983, pp. 2037-2064.
119. Cox, D.C., "Cochannel interference consideration in frequency reuse small coverage area radio system", IEEE Trans. Comm., Vol. 30, No. 1, Jan. 1982, pp. 135-142.
120. Sundberg, C.E., "On continuous phase modulation in cellular digital mobile radio system", Bell Sys. Tech.J., Vol. 62, No.7, Sept. 1983, pp. 2067-2089.
121. Fluhr, Z.C., and Porter, P.T., "Control architecture", Bell Sys. Tech. J., Vol. 58, No. 1, Jan. 1979, pp. 43-69.
122. Arredondo, G.A., Feggeler, J.C., and Smith, J.I., "Voice and data transmission", Bell Sys. Tech. J., Vol. 58, No. 1,Jān.1979, pp. 97-122.
123. Steele, R. and Prabhu, V.K., "High user density digital cellular mobile radio systems", IEE PRO, Vol. 132, Pt. F., No. 5, Aug. 1985, pp. 396-404.
124. Nojima, T., and Konno, T., "Cuber predistortion linearizer for relay equipment in 800 MHz band land mobile telephone system", IEEE Trans. Veh., Tech., Vol. VT-34, No.4, Nov. 1985, pp. 169-177.
125. Kuramoto, M., Hirade, K., and Sakamoto, M., "Design concept of new high-capacity land mobile communication", IEEE/Elsevier Science Publishers B.V. (North-Holland) 1984, pp. 1188-1191.
126. Parsons, J.D., Henze, M., Ratcliff, P.A. and Withers, M.J., "Diversity techniques for mobile radio reception", Radio & Elect. Eng., Vol. 45, 1975, pp. 357-367.
127. Daikoku, K., and Ohdate, H., "Optimal design for cellular mobile systems", IEEE Trans. Veh. Tech., Vol. VT-34, No.1, Feb. 1985, pp. 3-12.
128. Murota, K., "Spectrum efficiency of GMSK land mobile radio", IEEE Trans. Veh. Tech., Vol. VT-34, No. 2, May 1985, pp. 69-75.
129. Eklundh, B., "Channel utilization and blocking probability in a cellular mobile telephone system with directed retry", IEEE Trans Comm. Vol. 34, No. 4, April 1986, pp. 329-337.
130. Adachi, F., Feeney, M.T., Williamson, A.G., and Parsons, J.D. "Cross-correlation between the envelopes of 900 MHz signals received at a mobile radio base station site", IEE PRO. Vol. 133, Pt. F, No. 6, Oct. 1986, pp. 506-512.
131. Jesch, L.T., "Measured vehicular antenna performance", IEEE Trans. Veh. Tech., Vol. 34, No. 2, May 1985, pp. 97-107.

132. Cox, C.D., Murray, R.R., and Norris, A.W., "Antenna high dependance of 800 MHz attenuation measured in houses", IEEE Trans. Veh., Vol. 34, No. 2, May 1985, pp. 108-115.
133. Davis, B.R., and Bonger, R.E., "Propagation at 500 MHz for mobile radio", IEE PRO. Vol . 132, Pt. F., No. 5, Aug. 1985, pp. 307-320.
134. Muilwijk, D., "On spectrum efficiency of radio transmission schemes for cellular mobile ratio", IEEE/Elsevier Science Publishers, B.V. (North-Holland), 1984, pp. 1199-1206.
135. Henry, P.S., and Glance, B.S., "A new approach to high-capacity digital mobile radio", Bell Sys. Tech. J., Vol. 60, Oct. 1981, pp. 1891-1905.
136. Yeh, Y.S., and Reudink, D.O., "Efficient spectrum utilization for mobile radio system using space diversity", IEEE Trans. Comm., Vol. 30, March 1982, pp. 447-455.
137. Forney, G.D., "Maximum likelihood sequence estimation of digital sequences in the presence of intersymbol interference", IEEE Trans. Inf. T., Vol. 1-18, No. 3, May 1972, pp. 363-378.
138. Forney, G.D., "The Viterbi Algorithm", Proc. IEEE, Vol. 61, No. 3, March 1973, pp. 268-278.
139. Qureshi, S.U.H., and Newhall, E.E., "An adaptive receiver for data transmission over time-dispersive channels", IEEE Trans. Inf. T., Vol. 19, No. 4, July 1973, pp. 448-467.
140. Fredricsson, S.A., "Joint optimization of transmitter and receiver filter in digital PAM systems with a Viterbi detector", IEEE Trans. Inf. T., Vol. IT-22, No. 2, March 1976, pp. 200-210.
141. Mclane, P.J., "A residual intersymbol interference error bound for trancated state Viterbi detectors", IEEE Trans. Inf. T., Vol. IT-26. No. 5, Sept. 1980, pp. 548-553.
142. Acampora, A.S., "Analysis of maximum likelihood estimation performance quadrature amplitude modulation", Bell Sys. Tech. J., Vol. 60, No.6, July/Aug. 1981, pp. 1259-1262.
143. Zervos, N., Pasupathy, S. and Venetsanopoulas, A., "Low complexity maximum likelihood equalizer", IEEE/Elsevier Science Publishers B.V. (North-Holland), 1984, pp. 1259-1262.
144. Hayes, J.F., Cover, T.M., and Riera, J.B., "Optimal sequence detection and optimal symbol-by-symbol detection: Similar algorithm", IEEE Trans. Comm., Vol. 30, No. 1, Jan. 1982, pp. 152-157.
145. Abend, K., and Fritchman, B.D., "Statistical detection for communication channels with intersymbol interference", Proc. IEEE, Vol. 58, No. 5, May 1970, pp. 779-785.
146. Foschini, G.J., "A reduced state variant of maximum likelihood sequence detection attaining optimum performance for high signal-to-noise ratios", IEEE Trans. Inf. T., Vol. IT-23, Sept. 1977, pp. 605-509.
147. Clark, A.P., "Equalizers for digital modem", Pentech Press, 1985,
148. Clark, A.P., Lee, L.H. and Marshall, R.S., "Developments of conventional nonlinear equalizer", IEE. PRO. Pt. F., Vol. 12o, No. 2, April 1982, pp. 85-94.
149. Clark, A.P., "Adaptive detection with intersymbol interference cancellation for distorted digital signals", IEEE Trans. Comm., Vol. 20, June 1972, pp. 350-361.
150. Gersho, A., and Lim, T.L., "Adaptive cancellation of intersymbol interference for data transmission", Bell Sys. Tech. J., Vol. 60, No. 11, Jan. 1981, pp. 1997-2021.

151. Clark, A.P., and Harvey, J.D., "Detection processes for distorted binary signals", The Radio and Elect. Engineer., Vol. 46, No. 11, Nov. 1976, pp. 533-542.
152. Clark, A.P., Harvey, J.D., and Driscoll, J.P., "Near-maximum-likelihood detection processes for distorted digital signals", The Radio and Elect. Engineer, Vol. 48, No.6., June 1978, pp. 301-309.
153. Clark, A.P., and Harvey, J.D., "Detection of distorted q.a.m. signals" Electronic Circuits and Sytems, April 1977, Vol. 1, No. 3, pp. 103-109.
154. Clark, A.P., Kwong, C.P., and Harvey, J.D., "Detection processes for severely distorted digital signals", Electronic Circuit and Systems, Vol. 3, No. 1, 1979, pp. 27-36.
155. Clark, A.P., and Fairfield, M.J., "Detection processes for a 9600 bit/s modem", The Radio and Electronic Engineer, Vol. 51, No. 9, Sept. 1981, pp. 455-465.
156. Clark, A.P. "Distance measures for near-maximum-likelihood detection processes", IEE PRO, Vol. 128, Pt. F, No. 3, May 1981, pp. 114-122.
157. Clark, A.P., and Asghar, S.M., "Detection of digital signals transmitted over a known time-varying channel", IEE PRO, Vol. 128, Pt. F, June 1981, pp. 167-174.
158. Clark, A.P., "Equalisation and detection technqiues", Presented at IEE Collq., A Review of Modem Techniques, London, England, Jan. 14th, 1981.
159. Clark, A.P., Ip, S.F.A., and Soon, C.W., "Pseudo-binary detection processes for a 9600 bit/s modem", IEE PRO, Vol. 129, Pt. F, No. 5, Oct. 1982, pp. 305-314.
160. Clark, A.P., Najdi, H.Y., and Fairfield, M.J., "Data transmission at 19.2 kbit/s over telephone circuits", The Radio and Elect. Engineering, Vol. 53, No. 4, April 1983, pp. 157-166.
161. Clark, A.P., and Hau, S.F., "Adaptive adjustment of receiver for distorted digital signals", IEE PRO, Vol. 131, Pt. F., No. 5, Aug. 1984, pp. 526-536.
162. Clark, A.P., and Clayden, M., "The pseudobinary Viterbi detector", IEE PRO., Vol. 131, Pt. F., No. 2, April, 1984, pp. 208-218.
163. Ser, W., and Clark, A.P., "Near-maximum likelihood detectors for binary signals,", IEE PRO., Vol. 132, Pt. F, No. 6, Oct. 1985, pp. 485-490.
164. Clark, A.P., Abdulah, S.N., Jayasinghe, S.G., and Sun, K.H., "Pseudobinary and pseudoquaternary detection processes for linearly distorted multilevel QAM signals", IEEE Trans. Comm. Vol., 33, No.7, July, 1985, pp. 639-645.
165. Clark, A.P., "Near-maximum likelihood detection processes", Jordan Int. Elec. and Elec. Eng. Conf., April 28 - May 1, 1985, Amman-Jordan.
166. Burghes, D.N. and Graham, A., "Introduction to control theory including optimal control", Ellis Horwood Ltd., 1980
167. Jaccqout, R.G., "Modern digital system", Marcell Dekker, Ltd., 1981.
168. Katz, P., "Digital control using microprocessors", Prentice Hall International, 1981.
169. Kuo, B.C. "Digital control system", Holt, Rinhart and Winston Inc. 1980.
170. Gardener, F.M., "Phaselocked technqiues", John Wiley and Son Inc. 1979.
171. Gill, G.S. and Gupta, S.C.,"First-order discrete phase-locked loop with applications to demodulation of angle modulated carrier", IEEE Trans. Comm. Vol. 20, June 1972, pp. 454-462.
172. Gill, G.S., a dn Gupta, S.C., "On high order discrete phase-locked loop", IEEE Trans. Aerosp. and Elec. Sys. Vol. AES-8, No.5, Sept. 1972, pp.615-623.
173. Weinberg, A., and Liu, B., "Discrete time analysis of nonuniform sampling first- and second-ord. digital phaselocked loops", IEEE Trans Comm. Vol. 22, Feb. 1974, pp. 123-137.

174. Gupta, S.C., "Phaselocked loop", Proc. IEEE, Vol. 63, Feb. 1975, pp.291-306.
175. Chie, C.M., "Mathematical analysis between first-order digital and analogue phase-locked loop", IEEE Trans. Comm., Vol. 26, June 1978, pp. 860-865.
176. Lindsey, W.C., and Chie, C.M., "Acquisition behaviour of a first-order digital phase locked loop", IEEE Trans. Comm. Vol. 26, No.9, Sept. 1978, pp. 1364-1370.
177. D'Andrea, A.N., and Russo, F., "A binary quantized digital phase-locked loop: A graphical analysis", IEEE Trans. Comm. Vol. 26, No. 9, Sept. 1978, 1355-1364.
178. Osborne, H.C., "Stability analysis of an N^{th} power digital phase-locked loop, Part I: First-order DPLL", IEEE Trans. Comm., Vol. 28, Aug. 1980, pp. 1343-1354.
179. Osborne, H,C., "Stability analysis of an N^{th} power digital phase-locked Part II: second- and third-order DPLL's", IEEE Trans. Comm. Vol. 28, Aug. 1980, pp. 1355-1364.
180. D'Andrea, A.N. and Russo, F., "Multilevel quantized DPLL behaviour with phase- and frequency step plus noise input", IEEE Trans. Comm., Vol. 28, No. 8, Aug. 1980, pp. 1373-1382.
181. Lee, J.C. and Un, C.K., "Performance analysis of digital Tanlock Loop" IEEE Trans. Comm. Vol. 30, No. 10, Oct. 1982, pp 2398-2411.
182. Kim, H.J., Un, C.K. and Lee, J.C., "The N-phase digital Tanlock loop for tracking suppressed-carrier N-ary PSK signals", IEEE Trans. Comm., Vol. 33, No. 9, Sept. 1985, pp. 904-910.
183. Moridi,S. and Sari, H., "Analysis of four decision-feedback carrier recovery loops in the presence of intersymbol interference", IEEE Trans. Comm., Vol. 33, No. 6, June 1985, pp. 543-530.
184. Mastuo, Y., and Namiki, J., "Carrier recovery system for arbitrarily mapped APK signals", IEEE Trans. Comm., Vol. No. 10, Oct. 1982, pp. 2385-2390.
185. Simon, M.K., "The false lock performance of costas loops with hard limited inphase channel", IEEE Trans. Comm., Vol. 26, No. 1, Jan. 1978 pp 23-34.
186. Simon, M.K., "Optimum receiver structures for phase multiplexed modulations" IEEE Trans. Comm., Vol. 26, No. 6, June 1978, pp. 865-872.
187. Simon, M.K., and Woo, K.T., "Alias lock behaviour of sampled-data Costas loops", IEEE Trans. Comm., Vol. 28, No. 8, Aug. 1980, pp. 1315-1325.
188. Shimamura, T., "On false-locked phenomena in carrier Tracking loops" IEEE Trans. Comm., Vol. 28, No. 8, Aug. 1980, pp. 1326-1344.
189. Kleinberg, S.T. and Chang, H., "Sideband false-lock performance of squaring,fourth-power, and quadriphase Costas loops for NRZ data signal", IEEE Trans Comm., Vol. 28, No. 8., Aug. 1980, pp. 1335-1342.
190. Sladen, J.P.H., and McGeehan, J.P., "The performance of combined feed-forward A.G.C. and phase locked A.F.C., in a single-baseband mobile radio receiver", IEE PRO, Vol. 131, Pt. F, No. 5, Aug. 1984, pp. 437-441.
191. Bateman, A.J., Lightfoot, G., Lymer, A., and McGeehan, J.P., "Speech and data communication over 942 MHz TAB and TTIB single sideband mobile radio system incorporating feedforward signal regeneration", IEEE Trans. Veh. Tech., Vol. CT-34, No. 1, Feb. 1985, pp. 13-21.
192. Bateman, A.J., and McGeehan, J.P., "Coherent demodulation of pilot tone single sideband with phase-locked TTIB/FFSR processing", IEE PRO, Vol. 132, Pt. F, No. 5, Aug. 1985, pp. 363-365.

193. McGeehan, J.P., and Bateman, A.J., "Simple simultaneous carrier and bit synchronisation system for narrowband data transmission", IEE PRO, Vol. 132, Pt. F., No. 2, April 1985, pp. 69-72.
194. McGeehan, J.P., and Sladen, J.P.H., "The tracking performance of a narrowband phase-locked loop in the mobile multipath environment", IEE PRC.,Vol. 132, Pt. F., No. 2, April, 1985, pp. 73-76.
195. Bateman, A.J. and McGeehan, J.P., "Data transmission over UHF fading mobile radio channel", IEE PRO., Vol. 131, Pt. F., No. 4, July 1984 pp. 364-374.
196. Elnoubi, S.M. and Gupta, S.C., "Performance of first-order digital phase-locked loops in mobile radio channels", IEEE Trans. Comm. Vol. 33, No. 5, May 1985, pp. 450-456.
197. Thorpe, J.P., and Mclane, P.J., "A hybrid phase/data Viterbi demodulator for encoded CPFSK modulation", IEEE Trans. Comm.,Vol. 33, No. 6, June, 1985, pp. 535-542.
198. Franks, L.E., "Carrier and bit synchronization in data communication: A tutorial review", IEEE Trans. Comm., Vol. 28, No. 8, Aug. 1980, pp. 1107-1121.
199 Harvey, J.D., "Synchronisation of a synchronous modem", Science Research Council Report No. GR/A/1200.7, Dec, 1980.
200. McVerry, F., "High speed data transmission over HF radio link", PhD Thesis, Dept. of Elec. and Electronic Eng.,Loughborough University of Technology, 1982.
201. Berlin, H.M., "Design of Op-Amp circuit with experiments", Howard W. Sams, and Co. Inc., USA, 1981.
202. Millman, J. and Halikias, C.C., "Integrated electronics: Analog and digital circuit and system", McGraw Hill, 1972.
203. Harun, R., "Techniques of channel estimation for HF radio link", PhD Thesis, Dept. of Elec. and Electronic Eng., Loughborough University of Technology, England. 1984
204. Clark, A.P., and McVerry, F., "Channel estimation for an HF radio link", IEE PRO, Vol. 128, Pt. F., No. 1, Feb. 1981, pp. 33-42.
205. Clark, A.P., Kwong, C.P., and McVerry, F., "Estimation of the sampled impulse response of a channel", Signal Processing 2, 1980, pp. 39-53.
206. Clark, A.P., and Harun, R., "Assessment of Kalman-filter channel estimators for an HF radio link", IEE PRO. Vol. 133, Pt. F., No. 6. Oct. 1986, pp. 513-521.